PLASTICS IN THE ENVIRONMENT: UNDERSTANDING IMPACTS AND IDENTIFYING SOLUTIONS

EDITED BY: Montserrat Filella, Hans Peter Heinrich Arp and Andrew Turner
PUBLISHED IN: Frontiers in Environmental Science and Frontiers in Marine Science

frontiers Research Topics

ISSN 1664-8714
ISBN 978-2-88971-048-5
DOI 10.3389/978-2-88971-048-5

About Frontiers

Frontiers is more than just an open-access publisher of scholarly articles: it is a pioneering approach to the world of academia, radically improving the way scholarly research is managed. The grand vision of Frontiers is a world where all people have an equal opportunity to seek, share and generate knowledge. Frontiers provides immediate and permanent online open access to all its publications, but this alone is not enough to realize our grand goals.

Frontiers Journal Series

The Frontiers Journal Series is a multi-tier and interdisciplinary set of open-access, online journals, promising a paradigm shift from the current review, selection and dissemination processes in academic publishing. All Frontiers journals are driven by researchers for researchers; therefore, they constitute a service to the scholarly community. At the same time, the Frontiers Journal Series operates on a revolutionary invention, the tiered publishing system, initially addressing specific communities of scholars, and gradually climbing up to broader public understanding, thus serving the interests of the lay society, too.

Dedication to Quality

Each Frontiers article is a landmark of the highest quality, thanks to genuinely collaborative interactions between authors and review editors, who include some of the world's best academicians. Research must be certified by peers before entering a stream of knowledge that may eventually reach the public - and shape society; therefore, Frontiers only applies the most rigorous and unbiased reviews.
Frontiers revolutionizes research publishing by freely delivering the most outstanding research, evaluated with no bias from both the academic and social point of view. By applying the most advanced information technologies, Frontiers is catapulting scholarly publishing into a new generation.

What are Frontiers Research Topics?

Frontiers Research Topics are very popular trademarks of the Frontiers Journals Series: they are collections of at least ten articles, all centered on a particular subject. With their unique mix of varied contributions from Original Research to Review Articles, Frontiers Research Topics unify the most influential researchers, the latest key findings and historical advances in a hot research area! Find out more on how to host your own Frontiers Research Topic or contribute to one as an author by contacting the Frontiers Editorial Office: frontiersin.org/about/contact

PLASTICS IN THE ENVIRONMENT: UNDERSTANDING IMPACTS AND IDENTIFYING SOLUTIONS

Topic Editors:
Montserrat Filella, Université de Genève, Switzerland
Hans Peter Heinrich Arp, Norwegian Geotechnical Institute, Norway
Andrew Turner, University of Plymouth, United Kingdom

Citation: Filella, M., Arp, H. P. H., Turner, A., eds. (2021). Plastics in the Environment: Understanding Impacts and Identifying Solutions. Lausanne: Frontiers Media SA. doi: 10.3389/978-2-88971-048-5

Table of Contents

frontiers in Environmental Science

EDITORIAL
published: 24 May 2021
doi: 10.3389/fenvs.2021.699971

Editorial: Plastics in the Environment: Understanding Impacts and Identifying Solutions

Montserrat Filella[1]*, *Andrew Turner*[2] and *Hans Peter H. Arp*[3,4]

[1]Department F.-A. Forel, University of Geneva, Geneva, Switzerland, [2]School of Geography, Earth and Environmental Sciences, University of Plymouth, Plymouth, United Kingdom, [3]Norwegian Geotechnical Institute, Oslo, Norway, [4]Norwegian University of Science and Technology, Trondheim, Norway

Keywords: plastics, environment, impacts, pollution, effects

Editorial on the Research Topic

Plastics in the Environment: Understanding Impacts and Identifying Solutions

Plastics are one of the most widely used materials in the world which society will always be dependent on. This dependency has been clearly highlighted by the requirements for hygiene and protection during the recent global COVID pandemic (Adyel, 2020; Prata et al., 2020). Plastics are broadly integrated into today's lifestyle and are present in almost all consumer and industrial sectors and their production continues to increase (Geyer et al., 2017). Unfortunately, one of the characteristics of plastics that make them so useful—their durability—also ensures that they persist in the environment for very long periods of time. Additionally, and because of their low cost, many plastic objects have long been perceived as disposable. The consequence of this, coupled with the difficulty in developing effective waste management strategies, has been the ubiquitous contamination of the entire planet by plastic debris.

Even if proposed global actions to recycle more plastic or prevent the export of plastic waste to countries with poorly developed waste infrastructure through the Basel Convention are implemented, plastic emissions are expected to increase for the foreseeable future unless significant breakthroughs in plastic design or waste management are realized (Lau et al., 2020). Increasing emissions also imply that exposure to plastic pollution and its degradation products, like microplastics, nanoplastics, plastic additives, and other chemical leachates, will continue to increase. Such an accumulating plastic cocktail can result in complex and unpredictable impacts, including those on ecological processes (Rillig et al., 2021) or the global carbon cycle (Zhu, 2021).

Although the problem of plastic pollution was recognised several decades ago, research on plastics lost to the environment and their environmental and health impacts is now an extremely dynamic field involving a great deal of funding, support and effort. As an attempt to find solutions, there have been calls to integrate and introduce more biodegradable or recyclable plastics into the market in order to shift towards more sustainable supply chains. There is also some debate about which solutions make the most sense practically and economically, although it is likely that a combination of approaches may be required. An additional concern centres around the additives used in plastics, many of which are endocrine disrupting substances or otherwise harmful to the environment if released from the material. Chemical regulators, and particularly those in Europe, have become increasing active to make plastics safer and more recyclable, but clearly plastics are complex and diverse materials and understanding their complete life cycle and the (eco)toxicological implications of their extensive use and management is a highly justified, albeit difficult, task.

OPEN ACCESS

Edited and reviewed by:
Oladele Ogunseitan, University of California, Irvine, United States

***Correspondence:**
Montserrat Filella
montserrat.filella@unige.ch

Specialty section:
This article was submitted to Toxicology, Pollution and the Environment, a section of the journal Frontiers in Environmental Science

Received: *24 April 2021*
Accepted: *05 May 2021*
Published: *24 May 2021*

Citation:
Filella M, Turner A and Arp HPH (2021) Editorial: Plastics in the Environment: Understanding Impacts and Identifying Solutions. Front. Environ. Sci. 9:699971. doi: 10.3389/fenvs.2021.699971

A global, transdisciplinary problem requires a global, transdisciplinary response. Accordingly, the contributions in this Research Topic in Frontiers in Environmental and Marine Science: "Plastics in the Environment: Understanding Impacts and Identifying Solutions" cover a wide variety of aspects of plastic research and embrace a diversity of environment types, climates and habitats over a broad geographical extent (Europe, Asia, Africa, and the Arctic).

The importance of efficient but robust and comparable monitoring and detection methods is a key component of the Research Topic, and areas covered in this respect include the potential for remote sensing of litter using drones (Escobar-Sánchez et al.), the requirement for representative subsampling (Brandt et al.) and a critical review of techniques used to isolate microplastics from geogenic and biogenic material by chemical digestion (Pfeiffer and Fischer).

In many contributions, both contemporary and historical plastics are used to study environmental sources and distributions or to model transport and fate. For example, the general leakage of plastic to the environment and its subsequent distribution is explored using international, empirical data and its relation to drivers such as population density and land use (Schuyler et al.), while records of microplastics in marine sediments, ice cores and peat archives are used to attempt to unravel historical uses of plastics (Bancone et al.). Historical, aerial records of coastlines have also been combined with assessments of soil profiles, vegetation characteristics and type, and abundance of litter in a novel study examining the roles that plastics play in shaping coastal landscapes and habitats (Bastesen et al.). On beaches, emphasis is placed on the implications of quantifying plastic particles on a mass vs. number basis and considering both surface and buried debris (Ryan et al.), while in surface and subsurface seawater inputs of microplastics are calculated from urban runoff and waste water treatment plants (Schernewski et al.).

The weathering of plastics in the environment is considered in contributions that examine the fragmentation of expanded polystyrene into nano-sized particles by thermo-oxidation and hydrodynamic turbulence (Mattsson et al.) and that characterise microbial communities on conventional and biodegradable plastics in alpine and polar soils (Rüthi et al.). The impacts of both the fragmentation and aggregation of microplastics are also studied in the context of the feeding behaviour of freshwater zooplankton (Drago et al.). Further up the food chain, microplastics are profiled in long-lived marine animals (Meaza et al.) and are measured in a variety of animals, including commercially important pelagic fish (Bakir et al.; Haave et al.), with all studies linking observations to potential impacts on human exposure and health.

This eclectic collection of articles illustrates the wide diversity of environmental problems that arise from the mismanagement of plastics, and the many difficulties and challenges that scientists, managers, regulators, and stakeholders face in reducing or solving these problems. The transdisciplinarity of the subjects should also serve to inform scientists of the many and varied techniques and approaches that are currently available to guide future research towards understanding the diverse impacts of-and identifying the complex solutions to-plastic pollution.

AUTHOR CONTRIBUTIONS

All authors listed have made a substantial, direct, and intellectual contribution to the work and approved it for publication.

REFERENCES

Adyel, T. M. (2020). Accumulation of Plastic Waste During COVID-19. *Science* 369, 1314–1315. doi:10.1126/science.abd9925

Geyer, R., Jambeck, J. R., and Law, K. L. (2017). Production, Use, and Fate of All Plastics Ever Made. *Sci. Adv.* 3, e1700782. doi:10.1126/sciadv.1700782

Lau, W. W. Y., Shiran, Y., Bailey, R. M., Cook, E., Stuchtey, M. R., Koskella, J., et al. (2020). Evaluating Scenarios toward Zero Plastic Pollution. *Science* 369, 1455–1461. doi:10.1126/science.aba9475

Prata, J. C., Silva, A. L. P., Walker, T. R., Duarte, A. C., and Rocha-Santos, T. (2020). COVID-19 Pandemic Repercussions on the Use and Management of Plastics. *Environ. Sci. Technol.* 54, 7760–7765. doi:10.1021/acs.est.0c02178

Rillig, M. C., Kim, S. W., Kim, T.-Y., and Waldman, W. R. (2021). The Global Plastic Toxicity Debt. *Environ. Sci. Technol.* 55 (5), 2717–2719. doi:10.1021/acs.est.0c07781

Zhu, X. (2021). The Plastic Cycle - an Unknown Branch of the Carbon Cycle. *Front. Mar. Sci.* 7, 609243. doi:10.3389/fmars.2020.609243

Conflict of Interest: The authors declare that the research was conducted in the absence of any commercial or financial relationships that could be construed as a potential conflict of interest.

frontiers in Environmental Science

ORIGINAL RESEARCH
published: 24 September 2020
doi: 10.3389/fenvs.2020.562263

The "Plastisphere" of Biodegradable Plastics Is Characterized by Specific Microbial Taxa of Alpine and Arctic Soils

*Joel Rüthi[1,2], Damian Bölsterli[1], Lucrezia Pardi-Comensoli[3], Ivano Brunner[1] and Beat Frey[1]**

[1] Forest Soils and Biogeochemistry, Swiss Federal Institute for Forest, Snow and Landscape Research (WSL), Birmensdorf, Switzerland, [2] Institute of Biogeochemistry and Pollutant Dynamics, Swiss Federal Institute of Technology, ETH Zürich, Zurich, Switzerland, [3] Laboratory for Mechanical Systems Engineering, Swiss Federal Laboratories for Materials Science and Technology (EMPA), Dübendorf, Switzerland

Plastic pollution poses a threat to terrestrial ecosystems, even impacting soils from remote alpine and arctic areas. Biodegradable plastics are a promising solution to prevent long-term accumulation of plastic litter. However, little is known about the decomposition of biodegradable plastics in soils from alpine and polar ecosystems or the microorganisms involved in the process. Plastics in aquatic environments have previously been shown to form a microbial community on the surface of the plastic distinct from that in the surrounding water, constituting the so-called "plastisphere." Comparable studies in terrestrial environments are scarce. Here, we aimed to characterize the plastisphere microbiome of three types of plastics differing in their biodegradability in soil using DNA metabarcoding. Polylactic acid (PLA), polybutylene adipate terephthalate (PBAT), and polyethylene (PE) were buried in two different soils, from the Swiss Alps and from Northern Greenland, at 15°C for 8 weeks. While physico-chemical characteristics of the polymers only showed minor (PLA, PBAT) or no (PE) changes after incubation, a considerably lower α-diversity was observed on the plastic surfaces and prominent shifts occurred in the bacterial and fungal community structures between the plastisphere and the adjacent bulk soil not affected by the plastic. Effects on the plastisphere microbiome increased with greater biodegradability of the plastics, from PE to PLA. Copiotrophic taxa within the phyla Proteobacteria and Actinobacteria benefitted the most from plastic input. Especially taxa with a known potential to degrade xenobiotics, including Burkholderiales, Caulobacterales, *Pseudomonas*, *Rhodococcus*, and *Streptomyces*, thrived in the plastisphere of the Alpine and Arctic soils. In addition, Saccharimonadales (superphylum Patescibacteria) was identified as a key taxon associated with PLA. The association of Saccharibacteria with plastic has not been reported before, and pursuing this finding further may shed light on the lifestyle of this obscure candidate phylum. Plastic addition affected fungal taxa to a lesser extent since only few fungal genera such as *Phlebia* and *Alternaria*

OPEN ACCESS

Edited by:
Montserrat Filella, Université de Genève, Switzerland

Reviewed by:
Cristina Silva Pereira, New University of Lisbon, Portugal
Ciro Sannino, University of Perugia, Italy

***Correspondence:**
Beat Frey
beat.frey@wsl.ch

Specialty section:
This article was submitted to Toxicology, Pollution and the Environment, a section of the journal Frontiers in Environmental Science

Received: *14 May 2020*
Accepted: *28 August 2020*
Published: *24 September 2020*

Citation:
Rüthi J, Bölsterli D, Pardi-Comensoli L, Brunner I and Frey B (2020) The "Plastisphere" of Biodegradable Plastics Is Characterized by Specific Microbial Taxa of Alpine and Arctic Soils. Front. Environ. Sci. 8:562263. doi: 10.3389/fenvs.2020.562263

were increased on the plastisphere. Our findings suggest that the soil microbiome can be strongly influenced by plastic pollution in terrestrial cryoenvironments. Further research is required to fully understand microbial colonization on plastic surfaces and the biodegradation of plastic in soils.

Keywords: alpine soil, arctic soil, biodegradation, bioplastics, microbiome, plastisphere, Saccharimonadales

INTRODUCTION

Plastic pollution is a threat to ecosystems all over the globe, with clear implications for animals like birds, marine mammals and fish (Secretariat of the Convention of Biological Diversity, 2016; Thiel et al., 2018). Additionally, plastic pollution potentially causes food safety problems (Wright and Kelly, 2017; Smith et al., 2018), leads to developmental, reproductive and metabolic disorders in invertebrates through the uptake of nano-sized particles (Shen et al., 2019), and even contributes to the spread of pathogens and antibiotic resistance by serving as a raft for microorganisms (Keswani et al., 2016; Laganà et al., 2019). Most of the attention in research is paid to plastic debris in oceans, while knowledge about the occurrence, fate and potential hazards of landfill waste is scarce and its impact is likely underestimated considerably (de Souza Machado et al., 2018). Yet, some studies have examined the quantity of synthetic polymers in terrestrial ecosystems (Piehl et al., 2018; Scheurer and Bigalke, 2018; Zhang and Liu, 2018) and have documented detrimental effects of plastics in soils on earthworms (Huerta Lwanga et al., 2016) and microorganisms (Wang et al., 2016), as well as implications for agricultural productivity (Rillig et al., 2019). It is estimated that the amount of plastic released into terrestrial environments is 4–23 times higher than into marine environments (Horton et al., 2017). Plastics can reach habitats not only by direct littering and transport through rivers and oceans, but also by transport through the atmosphere and deposition in pristine regions such as alpine and Arctic environments (Allen et al., 2019). Plastic pollution has even been reported in remote areas of the Swiss Alps and the Arctic (Ambrosini et al., 2019; Bergmann et al., 2019).

A possible way to deal with the plastic pollution in the environment is to develop biodegradable plastics. However, they make up only around 1% of the total plastic currently being produced (PlasticsEurope, 2018). In addition, very little is known about the fate of biodegradable plastics in terms of microbial colonization and their degradability, in particular in soils from cold environments since new materials are usually tested for decomposition at temperatures above 20°C (Briassoulis and Dejean, 2010). In one study on the microbial degradation of plastic in temperate, marine sediment, there were no signs of biodegradation for both polyethylene (PE) and biodegradable carrier bags after a 3-month incubation at 10°C (Nauendorf et al., 2016). A second study showed a weight loss of 37% for biodegradable plastic bags incubated in agricultural soil in the lab for 3 months at 25°C (Accinelli et al., 2012). However, in the same study samples incubated in the field under natural conditions were far less prone to biodegradation. Given that the rate of biodegradation of plastics, besides of intrinsic material parameters, largely depends on external factors like temperature, moisture, and UV radiation (O'Brine and Thompson, 2010; Wilkes and Aristilde, 2017), biodegradation in soils of cold regions is assumed to be rather slow. The resident microbiome might be another critical parameter determining the biodegradability of plastics in soils. The composition of the soil microbiome strongly depends on various climatic and soil variables (Fierer, 2017). Alpine and Arctic soils are low in carbon and nitrogen content, and knowledge of their microbial communities is limited (Frasson et al., 2015; Frey et al., 2016; Malard and Pearce, 2018; Adamczyk et al., 2019; Pontes et al., 2020; Pushkareva et al., 2020). Plastic deposition may introduce a carbon and energy source into oligotrophic soils, possibly leading to profound changes in the soil microbiome and its functions in alpine and Arctic ecosystems. However, it has not been investigated whether the enzymatic ability to degrade plastics is pervasive in all soils or whether, especially in remote soils that have only recently been affected by pollution, plastic-degrading microorganisms are lacking.

The term "plastisphere" was introduced to describe the diverse microbial community influenced by plastic surfaces, analogous to the rhizosphere surrounding plant roots (Zettler et al., 2013; Amaral-Zettler et al., 2020). Since then, researchers have analyzed the composition of this novel habitat in many studies from aquatic environments and have shown that the plastisphere selects for particular microbial communities that differ from those in the surrounding environment (De Tender et al., 2015; Oberbeckmann et al., 2018; Ogonowski et al., 2018; Kirstein et al., 2019) and from communities on other inert surfaces like glass (Kirstein et al., 2018). However, data about the plastisphere microbiome in terrestrial ecosystems are scarce, and to our knowledge plastic-colonizing microbes in soils from cold environments have not previously been studied with culture-independent approaches to cover the entire microbial community on the plastic surface.

In the present mesocosm experiment, we buried pieces of three different plastic types in two different top soils, from the Swiss Alps and from Northern Greenland, at 15°C for 8 weeks. We used polylactic acid (PLA), polybutylene adipate terephthalate (PBAT), and PE, plastics that vary in their biodegradability. We characterized the plastisphere microbiome of the three types of plastics using soil DNA metabarcoding. We aimed to determine: (1) whether different polymer types are colonized by different microbial communities; (2) whether the plastisphere microbiome is different in the two soils; and (3) whether the plastisphere microbial communities can be linked to the biodegradability of the tested plastics. We hypothesized that the plastic material would determine the associated plastisphere microbiome, and that shifts in the plastisphere microbial

Abbreviations: CA, contact angle; CI, carbonyl index; PAHs, polyaromatic hydrocarbons; PBAT, polybutylene adipate terephthalate; PE, polyethylene; PLA, polylactic acid.

communities compared to in bulk soil would be smallest in PE, which has the lowest biodegradability.

MATERIALS AND METHODS

Plastic Types

Three different types of plastic were used in the experiments. The first specimen, purchased at Coop AG (Basel, Switzerland), was a compostable plastic bag made of Ecovio, a plastic blend primarily made of PLA. The second specimen was an agricultural mulch foil, purchased at Oeremansplastic (Genderen, Netherlands), made of PBAT. While PLA is made of renewable plant sources, PBAT is fabricated from fossil fuels. The third specimen was a common non-biodegradable waste bag made of low-density PE, purchased from TopPac (Schwarzenbach, Switzerland). The exact composition of the plastics was not known, as they are commercially available products. The plastics were chosen based on their different expected biodegradabilities, ranging from high biodegradability (PLA) to medium biodegradability (PBAT) to very low biodegradability (PE). The plastic surfaces were not sterilized to avoid chemical changes of the polymers. However, we surveyed the surfaces of non-incubated plastic pieces for the presence of indigenous microorganisms by plating 4 × 4 cm pieces of plastic on R2A (Carl Roth GmbH + Co., Karlsruhe, Germany) and LB (Merck KGaA, Darmstadt, Germany) agar plates and were only able to obtain 0–2 colonies per piece of plastic.

Soils Used for Incubation

We used two different top soils (0–10 soil depth), one from an alpine and one from an Arctic environment. The alpine soil was collected on the northwestern flank of "Muot da Barba Peider" (Barba Peider) in the eastern Swiss Alps at 2979 m a.s.l. (Frey et al., 2016). The Arctic soil was sampled in Villum at Station Nord in Northern Greenland. The coordinates, soil characteristics and climatic parameters of the two soils used are given in **Table 1**. We sampled three independent locations (field replications) for each soil type and replicated them in the mesocosm experiment (see below). Soils were transported in cold boxes to the laboratory and stored in closed plastic bags at 4°C in the dark until the start of the incubation experiment (less than 3 months).

TABLE 1 | Physico-chemical and site characteristics of soils used in the microcosm experiment.

Properties	Barba Peider	Villum
C [%]	0.14 ± 0.01*	2.47 ± 2.30*
N [%]	<0.02	0.25 ± 0.14*
pH [H_2O]	6.5 ± 0.1*	6.9 ± 0.3*
Sand [%]	80.5	88.9
Silt [%]	15.9	7.7
Clay [%]	3.6	3.4
Mean annual soil temperature [°C]	−1.8	−5.4
Minimal soil temperature [°C]	−13.5	−16.3
Maximal soil temperature [°C]	21.3	21.7
Annual precipitation [mm]	1500	188
Elevation [m a.s.l.]	2979	24
Vegetation	Sparsely vegetated (*Poa*, *Cerastium*, *Jacobea*)	Crusts and sporadic *Saxifraga arctica*
Coordinates	46°49′ 59.75″ N, 9° 93′ 14.30″ W	81° 36′ 5.26″ N, 16° 39′ 43.31″ W

**Values represent means ± standard deviations (n = 9 for C and N, n = 3 for pH).*

Experimental Set-Up

Half of the soil collected from each site was autoclaved (1× at 120°C for 20 min) to produce sterile controls for detecting possible abiotic degradation of the plastics. Sterilization of the investigated soils was confirmed by the lack of cultivable microorganisms. Incubation mesocosms were then prepared using 100 ml beaker glasses containing approximately 80 g of soil, with three replicates for each soil origin (Barba Peider, Villum), treatment (natural soil, autoclaved control) and plastic type (PLA, PBAT, PE) (36 beakers in total). Prior to incubation, the plastic pieces (4 × 4 cm) were quickly submerged in a soil suspension for 1 min to ensure contact of the indigenous microbial community of the respective soil with the plastic surface. The suspension was prepared by shaking 10 g of the corresponding soil in 40 ml of sterile dH_2O for 60 min. Plastic pieces for sterile controls were submerged in sterile dH_2O instead of the suspension. The beaker glasses were covered by parafilm and incubated at 15°C in the dark for 8 weeks. The incubation temperature represents the maximum temperature in the topsoils at both sites during snow-free season. The moisture content was determined gravimetrically and balanced once a week by adding sterile dH_2O.

At the end of the incubation experiment, samples were prepared for further processing. Bulk soil was collected from a distance of >2 cm to the incubated plastic sample. For the plastisphere samples, small soil particles adherent to the plastic piece were manually scratched off and added to the extraction tube. In addition, 4−5 small pieces of plastic (1 × 2 mm) were added to the extraction tube. For bulk soil samples approximately 250 mg fresh weight was used for DNA extraction, while for plastisphere samples only 100 mg fresh weight could be used due to the low mass of soil adherent to the plastic surfaces. Samples were added into extraction tubes and were frozen at −20°C until DNA extraction was performed. Small pieces of plastic (1 × 2 mm) were added to 5 ml Falcon tubes containing sterile tap water for cultivation of microorganisms. The remaining material from each plastic piece was rinsed with sterile dH_2O to provide a clean surface and dried at 35°C for 4 days prior to the physico-chemical analysis.

Cultivation of Microorganisms

The 5 ml Falcon tubes containing the plastic pieces were shaken with a vortex for 10 min at half speed. The resulting cell suspensions were serially diluted 1:10, 1:100, and 1:1000 in sterile tap water. All dilutions were plated in duplicate on R2A agar plates (Carl Roth GmbH + Co., Karlsruhe, Germany). The agar plates were incubated at 15°C for 2 months and growing colonies were picked once a week with a sterile tooth pick. Strains were phylogenetically characterized by sanger Sequencing as recently

outlined (Lapanje et al., 2012; Brunner et al., 2018). Briefly, the 16S rDNA (bacteria) and ITS (fungi) regions of isolated organisms were amplified by colony PCR. For bacteria universal primers 27F (Heuer et al., 1997) and 907R (Muyzer et al., 1995) were used. For fungi, primers ITS1 and ITS4 (White et al., 1990) were used. PCR products were sent to Macrogen B.V. (Amsterdam, Netherlands) for sequencing. Retrieved sequences were trimmed to the high quality portion and closest related sequences were searched on the NCBI nucleotide database with the blastn algorithm and default parameters.

Light Microscopy of Plastic Surfaces

Washed plastic pieces were analyzed with a VHX-500f digital microscope (Keyence International, Mechelen, Belgium). Images were acquired with a 5× and a 50× magnification.

Physico-Chemical Analysis

Fourier-transform infrared spectroscopy (FTIR) was performed with a Tensor 27 spectrometer (Bruker, Billerica, MA, United States). Spectra were obtained with a diamond Attenuated Total Reflectance (ATR) crystal plate. For each sample, 32 scans were recorded with wavelengths in the range of 4000–650 cm^{-1} for the analysis of Barba Peider soil and 4000–320 cm^{-1} for Villum soil. The scans were recorded with a spectral resolution of 4 cm^{-1}, and the resulting spectra averaged. OPUS software (Winterthur, Switzerland) was used to collect and correct the data (baseline correction). As a standard, three measurements per replicate were performed. Carbonyl indices were used to evaluate the degradation of plastics by semi-quantitative data. The indices were calculated with the OPUS software (Winterthur, Switzerland) using the height of the peaks (K algorithm). With this technique it is possible to calculate the ratio between C = O and C-H chemical bonds ($A_{C=O}/A_{C-H}$). Depending on the plastic type, different wavelengths were chosen for the carbonyl index calculations ($CI_{PLA} = A_{1713}/A_{1456}$; $CI_{PBAT} = A_{1713}/A_{729}$). No carbonyl index calculations were possible for PE because no C = O bonds were detected in the incubated samples.

Contact angle analysis was used to determine the wettability of plastic surfaces by measuring the contact angle of a sitting drop. For this purpose a Drop Shape Analyzer DSA30 (Krüss, Hamburg, Germany) was used. A 2 µl drop of distilled water was placed on the plastic surface, and the contact angle was determined using the Krüss Advance software package with the Ellipse fitting method. The contact angle was measured ten times per drop at three different locations per replicate. The values obtained for the ten drops per location were averaged in advance to statistical analysis. This method was applied for all plastic types. Cleaned specimens from the mesocosm experiments were compared to plastic controls without prior incubation in the soils and to the controls incubated in sterilized soil.

DNA Extraction, PCR Amplification, and Illumina MiSeq Sequencing

DNA extraction was performed with the DNeasy PowerSoil kit (Qiagen, Hilden, Germany) according to the manufacturer's protocol. DNA was quantified using the Qubit™ high-sensitivity assay for double stranded DNA (Thermo Fisher Scientific, Waltham, MA, United States). DNA concentrations for sterile controls were below the detection limit. The V3–V4 region of the prokaryotic small-subunit (16S) rRNA gene (bacteria and archaea) and the internal transcribed spacer region 2 (ITS2) of the eukaryotic (fungal groups and some groups of protists and green algae) ribosomal operon were PCR amplified from 5 ng of DNA template, using primers and conditions previously described (Frey et al., 2016). PCRs of individual samples were run in duplicate, pooled, and purified using Agencourt Ampure XP (Beckman Coulter). Prokaryotic and fungal amplicon pools were sent to the Génome Québec Innovation Centre at McGill University (Montreal, QC, Canada) for barcoding using the Fluidigm Access Array technology (Fluidigm) and paired-end sequencing on the Illumina MiSeq v3 platform (Illumina Inc., San Diego, CA, United States).

Sequence Quality Control, OTU Clustering, and Taxonomic Assignments

Quality filtering, OTU clustering, and assignment were conducted similarly to methods described previously (Frey et al., 2016; Luláková et al., 2019) using a customized pipeline based on UPARSE (Edgar, 2013). Briefly, paired-end reads were merged using the fastq_mergepairs algorithm (Edgar and Flyvbjerg, 2015), filtering for sequences with a minimum length of 300 bp ($16S_{V3V4}$) or 200 bp (ITS2) and a minimum overlap of 50 bp. PCR primers were removed using Cutadapt (Martin, 2011) allowing for a maximum of one mismatch in the forward and reverse primer. Next, reads were quality filtered using the USEARCH fastq_filter function, discarding reads with an expected error of one or greater. De-replicated sequences were clustered into OTUs at 97% sequence identity using the cluster_otu function. The clustering step includes an "on the fly" chimera removal algorithm. The OTU centroid sequences were then filtered for the presence of ribosomal signatures using Metaxa2 (Bengtsson-Palme et al., 2015) or ITSx (Bengtsson-Palme et al., 2013). Subsequently, sequences were mapped back on the OTU centroid sequences and taxonomic classification was conducted using a naïve Bayesian classifier (Wang et al., 2007) implemented in Mothur (Schloss et al., 2009) with a minimum bootstrap support of 0.6. Prokaryotic $16S_{V3V4}$ sequences were queried against the SILVA v132 database (Quast et al., 2013), whereas eukaryotic ITS2 sequences were queried against the fungal ITS database UNITE v8.0 (Nilsson et al., 2019). Prokaryotic sequences identified as originating from organelles (chloroplast, mitochondria), as well as eukaryotic sequences identified as originating from soil animals (metazoa) or plants (viridiplantae) were not included in the analyses. Raw sequences were deposited in the NCBI Sequence Read Archive under the accession number PRJNA630025.

Statistical Analyses

Results from all statistical tests performed in this study were considered significant at $P < 0.05$ unless indicated otherwise. Unless indicated otherwise, all figures were created with the ggplot2 package (Wickham, 2016) implemented in R Development Core Team (2008). Differences in contact angle and carbonyl index data were assessed using factorial ANOVA

and Tukey's HSD *post hoc* test, implemented in R. OTU richness (S_{obs}) and Shannon index (H') were retrieved with the *estimate_richness* function implemented in the phyloseq package in R (McMurdie and Holmes, 2013). Differences in soil S_{obs} and H' data were assessed using factorial ANOVAs and paired *t*-tests implemented in StatView, 2nd edition (SAS Institute Inc., Cary, NC, United States).

Principal coordinate analysis (PCoA) of microbial β-diversity was performed using the *ordinate* function based on Bray-Curtis dissimilarities and plotted using the *plot_ordination* function, both implemented in the phyloseq package in R (McMurdie and Holmes, 2013). Differences in β-diversity were tested by permutational multivariate analysis of variance (Anderson, 2001) and pairwise PERMANOVA functions in PRIMER version 7 (Clarke and Gorley, 2006) based on 10^5 permutations (Hartmann et al., 2017). For the pairwise tests, the Monte Carlo approximated level of significance [*P*(MC)] was determined.

Relative abundances of the most abundant taxa were assessed in R by agglomerating OTUs on phylum and order levels using the *tax_glom* function implemented in the phyloseq package (McMurdie and Holmes, 2013), normalizing the abundances using the function *normalise_data* from the microbiomeSeq package (Ssekagiri, 2020) and using the function *aggregate_top_taxa* implemented in the microbiome package in R (Lahti and Shetty, 2019). Differences in relative abundance of the most abundant taxa were assessed using factorial ANOVAs and Tukey's HSD *post hoc* tests implemented in R. Relative abundances of taxa were plotted using the function *plot_taxa* implemented in the microbiomeSeq package (Ssekagiri, 2020).

Differential abundance analysis was performed using the *differential_abundance* function implemented in the microbiomeSeq package in R (Ssekagiri, 2020). First, the analysis was carried out using OTUs as a taxonomic classifier. In a second analysis, OTUs were aggregated to the next highest classifiable taxonomic rank for bacteria (mostly genus). For fungi, only sequences classifiable to the genus level were considered in the second analysis. In order to assess which OTUs/taxa were significantly affected by plastic type, we calculated $\log_2$-fold changes relative to the bulk samples using DESeq2 (Love et al., 2014). OTUs and taxa were considered significantly different (Wald test) between plastisphere and bulk soil samples if the false discovery rate (adjusted *P*) was < 0.05.

RESULTS

Physico-Chemical Measurements of Polymer Degradation

After 8 weeks of incubation in the Alpine (Barba Peider) or Arctic (Villum) soil, no clear signs of degradation were observed in any of the three plastic types (PLA, PBAT, and PE). However, PLA incubated in natural soil was covered with white stains, some of which appeared cloudy and others mycelium-like (**Supplementary Figure 1**).

Carbonyl indices of PLA and PBAT were significantly affected by both incubation and soil type without interactions (**Table 2a**). The contact angle of PBAT was significantly affected by incubation, soil type and their interactions, whereas PE was not influenced by incubation or soil type. In contrast, PLA was affected by soil type and interactions between incubation and soil type (**Table 2a**).

In Barba Peider soil, the contact angle of PLA incubated in natural-soil was significantly different than that incubated in sterile soil (**Table 2b**). However, neither of these incubated PLAs differed from the non-incubated PLA regarding contact angle. For PLA in Villum soil, only the difference between the carbonyl index of sterile-soil incubated and non-incubated plastics was statistically significant. However, the carbonyl index of PLA incubated in natural soil was very similar to that of the sterile-soil incubated samples but lower than the non-incubated PLA ($P = 0.059$).

In Barba Peider soil, the carbonyl index and the contact angle of PBAT from the 8-week incubation in natural soil were significantly different from the non-incubated sample, as well as from PBAT incubated in sterile soil (**Table 2b**). In contrast, the carbonyl index of natural-soil and sterile-soil incubated samples in Villum soil was significantly different from non-incubated PBAT, but no difference was detected between natural-soil and sterile-soil incubated PBAT. No difference was detected for the contact angle of non-incubated, sterile-soil incubated and natural-soil incubated PBAT.

Polymer-Dependent Microbiome

Sequencing of Barba Peider samples yielded a total of 1,169,088 (64,949 ± 4,606 per sample; mean ± standard error) prokaryotic $16S_{V3V4}$ and 335,637 (18,647 ± 394) eukaryotic ITS2 high-quality sequences that were clustered into 2,360 and 334 OTUs, respectively. Samples from Villum yielded a total of 412,004 (22,889 ± 851 per sample) prokaryotic $16S_{V3V4}$ and 1,007,107 (55,950 ± 3,404) eukaryotic ITS2 high-quality sequences that were clustered into 2,918 and 280 OTUs, respectively.

Bacterial and Fungal α-Diversity

We estimated the prokaryotic and fungal α-diversity of plastisphere and bulk soil samples in Barba Peider and Villum soils by analyzing the observed OTU richness (S_{obs}) and Shannon indices (H'). ANOVA of plastisphere and bulk soil samples showed significant differences for all α-diversity measures except for prokaryotic S_{obs} in Barba Peider soil (**Table 3a**). By pairwise comparisons of plastisphere and bulk soil of each plastic and soil type, we observed a significant reduction in prokaryotic H' in both soils in the PLA plastisphere when compared with the bulk soil (**Table 3b**). Similar trends were observed for S_{obs} (**Figure 1**). In addition, prokaryotic S_{obs} was significantly lower in the PE plastisphere when compared with the bulk soil in the Villum samples. Fungal α-diversity was significantly lower in the PLA plastisphere than in the bulk soil in samples from Barba Peider, and the same trend was true for Villum samples (**Figure 2**). Fungal α-diversity was lower in the plastisphere of PBAT compared with the bulk soil in the Villum samples, but no such effects of PBAT were found for Barba Peider samples. Furthermore, fungal S_{obs} of the plastisphere of PE was lower compared with the bulk soil in Villum samples.

TABLE 2 | Physico-chemical characterization of plastics before and after an 8-week incubation in autoclaved (sterile) and natural (non-sterile) soil from Barba Peider or Villum.

(a)

Plastic type	Carbonyl index (CI)			Contact angle (CA)		
	Inc.	Soil	Inc. × Soil	Inc.	Soil	Inc. × Soil
PLA	3.65*	30.1***	1.19^{ns}	$3.13^{(ns)}$	10.8**	8.04**
PBAT	30.3***	38.9***	2.25^{ns}	9.67***	5.55*	11.2**
PE	NA	NA	NA	1.76^{ns}	$3.02^{(ns)}$	1.63^{ns}

(b)

Plastic type	Measure	Soil	non-incubated	Barba Peider		Villum	
				Incubation	*P*	Incubation	*P*
PLA	Carbonyl index	Sterile	8.25 ± 0.14	8.41 ± 0.32	0.995	7.60 ± 0.17	**0.005**
		Natural	8.25 ± 0.14	8.28 ± 0.49	1.00	7.74 ± 0.18	*0.059*
					1.00		0.995
	Contact angle	Sterile	89.6 ± 6.9	104.2 ± 9.4	0.286	80.7 ± 12.8	0.540
		Natural	89.6 ± 6.9	83.0 ± 5.8	0.846	78.9 ± 4.8	0.298
					0.016		1.00
PBAT	Carbonyl index	Sterile	1.26 ± 0.01	1.26 ± 0.01	1.00	1.16 ± 0.02	**<0.001**
		Natural	1.26 ± 0.01	1.18 ± 0.05	**<0.001**	1.11 ± 0.04	**<0.001**
					0.012		0.104
	Contact angle	Sterile	107.2 ± 9.1	108.7 ± 1.1	1.00	100.4 ± 6.2	0.883
		Natural	107.2 ± 9.1	82.8 ± 13.9	**<0.001**	99.3 ± 5.9	0.789
					0.005		1.00
PE	Carbonyl index	Sterile	NA	NA	–	NA	–
		Natural	NA	NA	–	NA	–
	Contact angle	Sterile	87.8 ± 14.0	96.2 ± 10.7	0.907	95.9 ± 5.5	0.703
		Natural	87.8 ± 14.0	88.6 ± 8.2	1.00	97.5 ± 6.9	0.495
					0.923		1.00

*(a) Effects of the type of incubation (non-incubated, incubated in sterile soil, and incubated in natural soil), soil origin (Barba Peider and Villum), and the interaction between the two variables based on analysis of variance (ANOVA). F-values are given and asterisks indicate significant differences, with ***$P < 0.001$, **$P < 0.01$, *$P < 0.05$, $^{(ns)}P < 0.1$, and $^{ns}P > 0.1$. (b) Results of pairwise comparisons (Tukey HSD tests) between non-incubated plastics and those incubated in sterile or natural soil. P-values ($P < 0.05$ in bold; $0.1 > P > 0.05$ in italics) and means ± standard deviations are given. P-values in the third row of each comparison indicate significance of differences between incubated sterile and natural soils. The comparison of non-incubated and sterile incubated soils indicates the abiotic effect of soils on plastics, the comparison of non-incubated and natural incubated soils indicates the combination of abiotic and microbial factors affecting the plastics, and the comparison of sterile and natural incubated soils indicates the microbial component of degradation. NA, Not applicable, Inc., incubation.*

Bacterial and Fungal β-Diversity

Principal coordinate analysis and permutational analysis of variance (PERMANOVA) revealed that microbial community structures in the PLA plastisphere microbiome were significantly distinct from the microbial communities in the bulk soil from both sampling sites (**Figure 3** and **Table 4**). In addition, PBAT plastisphere microbial community structures were significantly distinct from the microbiome in the bulk soil in Villum samples, but this was not true for samples from Barba Peider. In contrast, PE plastisphere community structures did not differ significantly from the bulk soil in samples from both sites. Bulk soil in samples with the different plastic types did not differ significantly regarding community structures (data not shown).

"Plastisphere Taxa"

Relative Abundances of Microbial Taxa

The search for taxa at the phylum and order level that are affected by the plastics revealed that most community structural changes occurred in the PLA plastisphere at both taxonomic levels and in both soils (**Figure 4**, **Table 5**, and **Supplementary Figure 2**). Bacterial phyla that increased in relative abundance in the plastisphere of PLA were Actinobacteria, Proteobacteria and Patescibacteria in Barba Peider and only Patescibacteria in Villum. Mainly Acidobacteria, Chloroflexi, Gemmatimonadetes, Planctomycetes, and Nitrospirae decreased in relative abundance in the PLA plastisphere in both soils. β-Proteobacteriales, Rhizobiales, and Saccharimonadales (superphylum Patescibacteria) increased in abundance in the plastisphere of Barba Peider, whereas in Villum only the latter was enriched. Archaea were not affected by any of the plastic types. Fungal phyla and orders were largely unaffected by PLA (**Table 5** and **Supplementary Figures 3**, **4**). The only changes in the plastisphere of PLA in Barba Peider soil were a decrease in the phylum Mortierellomycota and an increase in the order Thelebolales. The only phyla enriched in the

TABLE 3 | α-diversity of prokaryotes and fungi in the plastisphere and bulk soil of Barba Peider and Villum soils.

(a)

Main test	Barba Peider				Villum			
	Richness (S_{obs})		Shannon (H')		Richness (S_{obs})		Shannon (H')	
	F	P	F	P	F	P	F	P
Prokaryotes	1.8	0.196	5.9	**0.006**	11.2	**<0.001**	35.8	**<0.001**
Fungi	23.3	**<0.001**	8.9	**<0.001**	30.1	**<0.001**	12.7	**<0.001**

(b)

Pairwise test	t	P	t	P	t	P	t	P
Prokaryotes								
PLA	−3.8	*0.062*	−4.3	*0.050*	−3.9	*0.059*	−7.3	**0.018**
PBAT	0.3	0.786	−2.1	0.165	−2.2	0.162	−2.1	0.168
PE	0.2	0.838	−1.8	0.213	−6.5	**0.023**	−2.9	0.102
Fungi								
PLA	−31.2	**0.001**	−8.4	**0.014**	−3.9	*0.060*	−3.8	*0.063*
PBAT	−0.7	0.580	−1.7	0.24	−7.1	**0.020**	−6.9	**0.020**
PE	−3.0	*0.097*	1.4	0.289	−11.2	**0.008**	−1.3	0.314

*(a) Differences between plastisphere and bulk soil samples using analysis of variance (ANOVA). F- and P-values ($P < 0.05$ in bold; $0.1 > P > 0.05$ in italics) of the observed species richness and the Shannon diversity are given. (b) Pairwise comparisons between the plastisphere and bulk soil of each plastic type using paired t-tests. P- and t-values for S_{obs} and H' are presented. Negative t-values indicate smaller means in the plastisphere compared with the bulk soil. α-diversity for prokaryotes and fungi are shown in **Figures 1**, **2**, respectively.*

plastisphere of PBAT were Proteobacteria in Villum soil and Mortierellomycota in Barba Peider soil (**Table 5** and **Supplementary Figures 2**, **3**). In Villum, only the orders β-Proteobacteriales and Rhizobiales were significantly increased in relative abundance in the plastisphere of PBAT, whereas only Helotiales were favored in Barba Peider (**Figure 4**, **Table 5**, and **Supplementary Figure 3**). In the PE plastisphere of both soils, the only significant increase in relative abundance was observed for Actinobacteria and the associated order of Propionibacteriales (**Figure 4**, **Table 5**, and **Supplementary Figure 2**).

Specific "Plastisphere Taxa"

Differential abundance analysis was performed by comparing total abundances of OTUs in plastisphere and bulk soil samples. The number of differentially abundant OTUs for both prokaryotes and fungi in both soils was highest for PLA, followed by PBAT and lastly PE (**Supplementary Table 1**). Whereas more bacterial OTUs showed positive $\log_2$-fold changes in the plastisphere compared with bulk soils, a larger portion of the fungal OTUs in Villum soil showed negative $\log_2$-fold changes in the plastisphere compared with bulk soils.

A repetition of the differential abundance analysis with OTUs aggregated to the lowest classifiable taxonomic level (mostly genus) revealed the bacterial taxa most strongly affected by the different plastics, as shown in **Figures 5**–**7**. Most taxa with significant $\log_2$-fold changes belonged to the phyla Proteobacteria and Actinobacteria, and only few exceptions were identified (Bacteroidetes, Verrucomicrobia, and Patescibacteria). No archaeal taxa were significantly influenced by the plastics.

Bacteria

Most taxa with positive $\log_2$-fold changes in the plastisphere of PLA compared with bulk soils belonged to the phyla Actinobacteria and Proteobacteria, and a few belonged to Bacteroidetes, Patescibacteria, and Verrucomicrobia. *Nocardia* and *Saccharimonadales* exhibited positive log2-fold changes in the plastisphere of both soils. Several genera increased substantially in the plastisphere of PLA in Barba Peider soil, where Actinobacteria (e.g., *Streptacidiphilus*, *Catenulispora*), Proteobacteria (e.g., *Collimonas*, *Rhizobiaceae*, *Variovorax*, *Pseudomonas*) and Verrucomicrobia (*Luteolibacter*) dominated (**Figure 5A**). Furthermore, strong positive $\log_2$-fold changes in the PLA plastisphere of Villum soil compared with bulk soils were observed for genera of Actinobacteria (e.g., *Nocardioides, Streptomyces*), *Proteobacteria* (e.g., *Caulobacter*, *Brevundimonas*, *Sphingorhabdus*), and Bacteroidetes (e.g., *Dyadobacter*, *Ohtaekwangia*) (**Figure 5B**).

Taxa with positive $\log_2$-fold changes in the plastisphere of PBAT, as with PLA, belong to Actinobacteria and Proteobacteria, with a few belonging to Bacteroidetes and Verrucomicrobia. Positive $\log_2$-fold changes on PBAT in both soils were observed for *Nocardia*. Furthermore, genera within Actinobacteria (e.g., *Rhodococcus*, *Umezawaea*), Proteobacteria (e.g., *Collimonas*, *Pseudomonas*, *Variovorax*, *Mesorhizobium*), Bacteroidetes (*Sediminibacterium*) and others had positive $\log_2$-fold changes in the PBAT plastisphere of

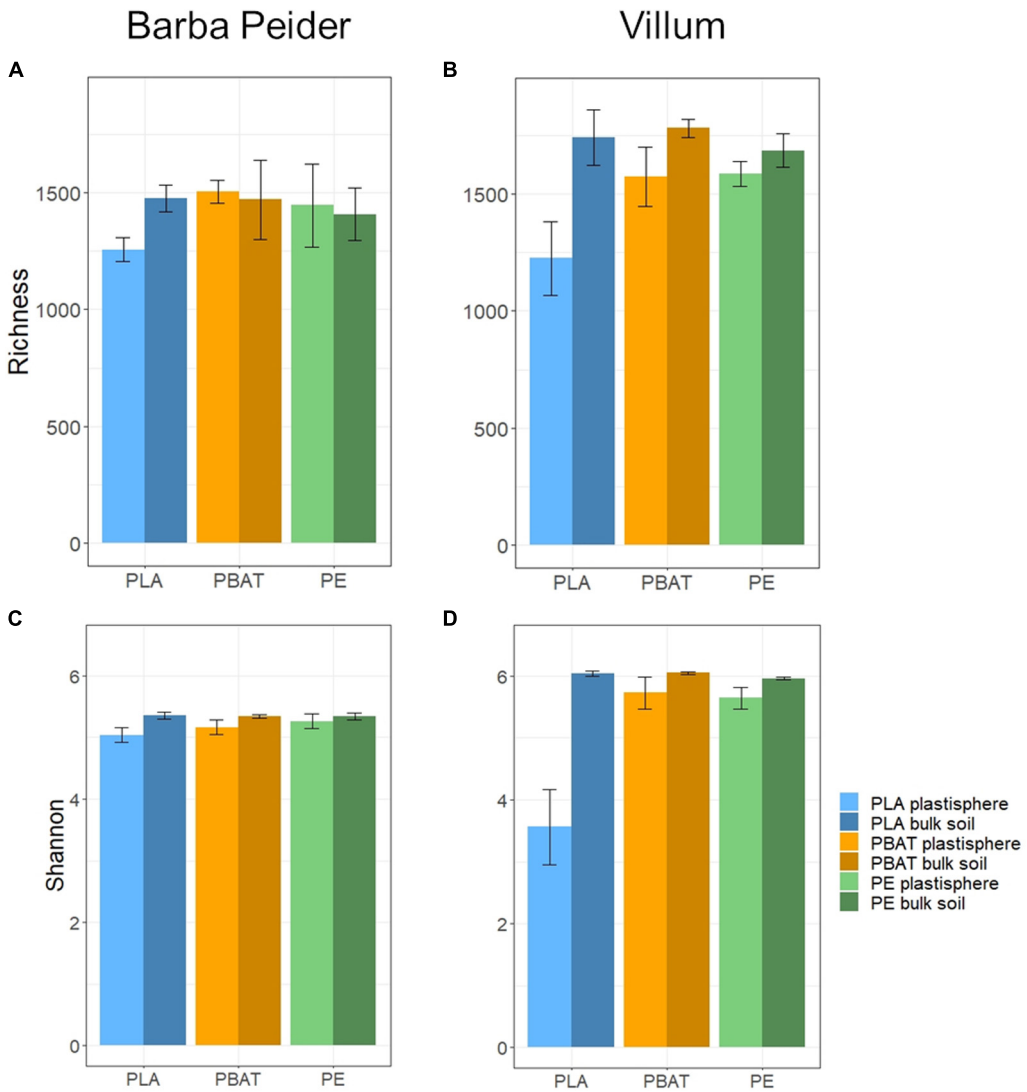

FIGURE 1 | Prokaryotic α-diversity (mean ± sd; $n = 3$) of plastisphere and bulk soil samples showing observed richness **(A,B)** and Shannon Index **(C,D)** in Barba Peider (Swiss Alps) **(A,C)** and Villum (Northern Greenland) **(B,D)** soil.

Barba Peider soil (**Figure 6A**). Genera of Actinobacteria (e.g., *Actinocorallia*, *Streptomyces*) and Proteobacteria (e.g., *Aquabacterium*, *Acidovorax*, *Caulobacter*, *Brevundimonas*) showed positive $\log_2$-fold changes on the PBAT surface of Villum soils (**Figure 6B**).

Mostly genera of the phyla Actinobacteria and Proteobacteria showed positive $\log_2$-fold changes in the plastisphere of PE. The genera *Nocardia* and *Nocardioides* (Actinobacteria) had positive $\log_2$-fold changes on PE in both soils. In addition, *Rhodococcus* (Actinobacteria) showed a positive $\log_2$-fold change in the plastisphere of PE in Barba Peider soil (**Figure 7A**), and *Streptomyces*, *Aeromicrobium* (Actinobacteria), *Aquabacterium*, *Brevundimonas*, *Sphingorhabdus* and *Solimonas* (Proteobacteria) had positive $\log_2$-fold changes on PE in Villum soil (**Figure 7B**).

Fungi

Even though the proportion of differentially abundant fungal OTUs in Villum soil was very high (**Supplementary Table 1**), most of the found OTUs were non-classifiable at low taxonomic ranks. Of the fungal OTUs in Villum soil, 43% were, e.g., only classifiable to the phylum level. Only fungi classifiable to the genus level were included in the subsequent analysis (36% of OTUs in Villum soil) (**Supplementary Figures 5–7**). Fungi with differential abundances in the plastisphere compared with the bulk soils mostly belonged to Ascomycota, with the exception of the plastisphere of PE in Villum soil, where more fungal taxa showing an increase belonged to Basidiomycota.

Generally, observed effects were much stronger in Villum than in Barba Peider soil for PLA. In Barba Peider soil, the genera *Oidiodendron* and *Kabatiella* had the greatest positive

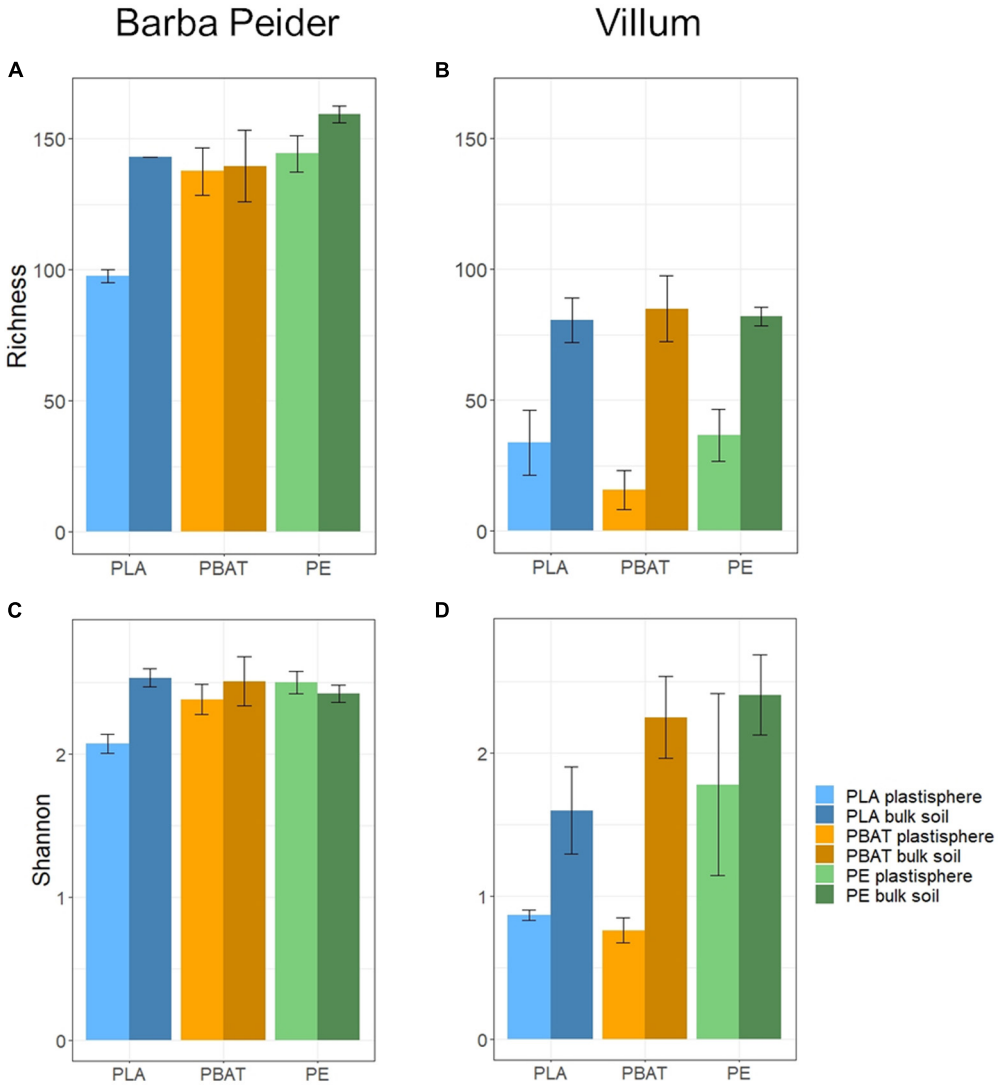

FIGURE 2 | Fungal α-diversity (mean ± sd; $n = 3$) of plastisphere and bulk soil samples showing observed richness **(A,B)** and Shannon Index **(C,D)** in Barba Peider (Swiss Alps) **(A,C)** and Villum (Northern Greenland) **(B,D)** soil.

log_2-fold changes in the plastisphere of PLA (**Supplementary Figure 5A**). In Villum soil, we found positive log_2-fold changes for *Mycosphaerella*, *Alternaria* and *Mycoarthris* in the plastisphere of PLA (**Supplementary Figure 5B**).

The only classifiable genus showing a positive log_2-fold change in the plastisphere of PBAT in Barba Peider soil was *Trichocladium* (**Supplementary Figure 6A**). Whereas the genus *Pseudogymnoascus* had the greatest positive log_2-fold change in the plastisphere of PBAT in Villum soil, it exhibited a negative log_2-fold change on the PLA surface in Barba Peider soil (**Supplementary Figure 6**). Many fungal genera were found to have negative log_2-fold changes especially in the plastisphere of PBAT in Villum soil (**Supplementary Figure 6B**).

The fungal genus *Mycena* was found to be strongly increased in abundance in the plastisphere of PE in Villum soil (**Supplementary Figure 7**). However, the enrichment of *Mycena* was only observed in one of the three replicates, and the genus was additionally not detected in the bulk soil samples. Other genera with significant positive log_2-fold changes in the PE plastisphere in Villum soil belonged to Basidiomycota (i.e., *Phlebia* and *Tricholoma*) or Ascomycota (i.e., *Aspergillus* and *Colletotrichum*) (**Supplementary Figure 7**). No significant differences between the plastisphere of PE and the bulk soil in Barba Peider samples were found.

Cultivable "Plastisphere" Strains

Eighty bacterial and 14 fungal strains were isolated from the plastic surfaces (**Supplementary Table 2**). Bacterial isolates belonged to 28 different genera within the phyla Actinobacteria, Bacteroidetes and Proteobacteria. Fungal isolates belonged to four different genera within the phyla

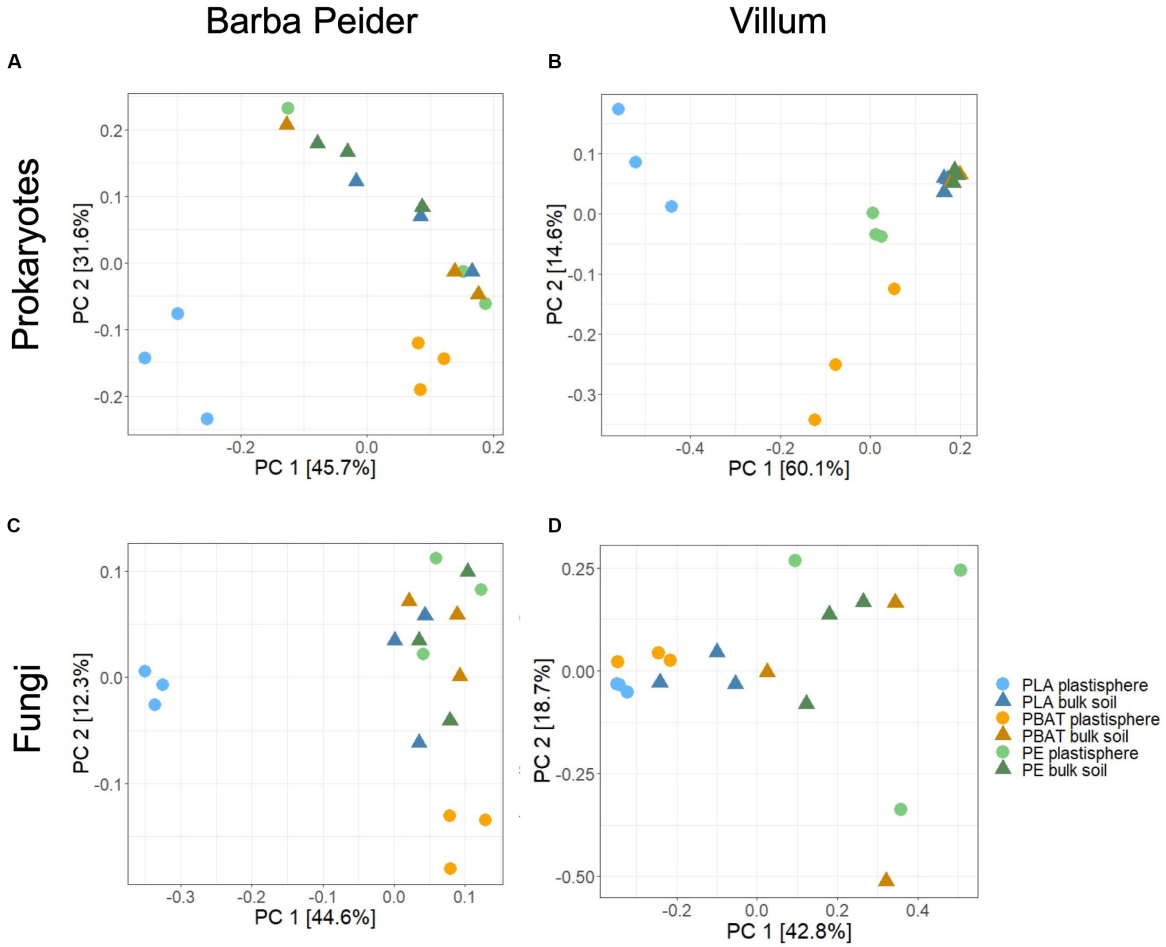

FIGURE 3 | Differences in β-diversity between plastisphere and bulk soil samples of the three plastic types, visualized by principal coordinate analysis (PCoA) based on Bray-Curtis dissimilarities. The variance explained by each PC axis is given in parentheses, and quantitative statistical results based on PERMANOVA are provided in **Table 4**. Results are displayed for prokaryotes **(A,B)** and fungi **(C,D)** in Barba Peider (Swiss Alps) **(A,C)** and Villum (Northern Greenland) **(B,D)** soils.

Ascomycota and Mortierellomycota. A large part of the cultivated microorganisms (i.e., *Streptomyces*, *Rhodococcus*, *Pseudomonas*, *Variovorax* and *Pseudogymnoascus*) were found to be increased on the plastisphere by differential abundance analysis.

DISCUSSION

In the present study, we linked FTIR and contact angle measurements of plastics incubated in soils with shifts in the resident microbiome. To our knowledge, this is the first experimental study comparing the effects of different plastic types on the plastisphere microbiome in alpine and Arctic soils. Increasing plastic pollution in these regions due to increased human activities highlights the need for pollution control and clean-up suitable for cold regions. The biotechnological potential of terrestrial cryoenvironments is strongly linked to patterns of taxonomical and functional diversity. Microorganisms in cold environments are known to harbor special adaptations, and particular types of genes are only in these environments present (Shi et al., 2015; da Silva et al., 2017). Our findings suggest that plastic debris provides a habitat for complex microbial assemblages that differ from those in bulk soil. The observed effects of the plastic on the microbiome were strongly dependent on the biodegradability of the plastics and were most pronounced for PLA, followed by PBAT and lastly PE.

Physico-Chemical Measurements of Polymer Degradation

Overall, analyses of the biodegradable (PLA and PBAT) and non-biodegradable (PE) plastics showed no or only weak signs of degradation after 8 weeks (initial stage of degradation) of incubation in Alpine (Barba Peider) and Arctic (Villum) soils at 15°C. The contact angle and FTIR analyses confirmed that PE is almost non-biodegradable. FTIR data allow to conclude that no oxidation of the PE occurred. Oxidation of the C-C backbone of PE is considered an important

TABLE 4 | Changes in prokaryotic and fungal community structures in the plastisphere.

	Barba Peider				Villum			
	Prokaryotes		Fungi		Prokaryotes		Fungi	
Main test	***Pseudo F***	***P***	***Pseudo F***	***P***	***Pseudo F***	***P***	***Pseudo F***	***P***
	3.665	**<0.001**	3.259	**<0.001**	4.314	**<0.001**	3.383	**<0.001**
Pairwise test	**t**	***P* (MC)**	***t***	***P* (MC)**	***t***	***P* (MC)**	***t***	***P* (MC)**
PLA	2.758	**0.008**	2.538	**0.013**	2.914	**0.007**	1.798	**0.050**
PBAT	1.731	*0.056*	1.381	0.145	1.852	**0.045**	2.533	**0.017**
PE	1.235	0.226	1.276	0.207	1.688	*0.058*	1.207	0.263

Pseudo F- and P-values (P < 0.05 in bold; 0.1 > P > 0.05 in italics) for the differences between plastisphere and bulk soil samples and the three plastic types regarding prokaryotic and fungal β-diversity were assessed by permutational analysis of variance (PERMANOVA) in the main test. Pairwise PERMANOVA tests were performed for pairs of plastisphere and bulk soil samples of each plastic type, and the Monte Carlo approximated level of significance [P(MC)] was determined.

requirement for the biological degradation and assimilation of non-hydrolyzable plastics (O'Brine and Thompson, 2010; Kumar Sen and Raut, 2015).

In contrast, results for PBAT in Barba Peider soil suggested that chemical and physical changes on the polymer surface occurred due to microbial activity in this soil, as the plastic pieces incubated in natural soil differed from those incubated in sterile soil and from non-incubated pieces. On the other hand, the findings for Villum soil suggest that chemical changes occurred in the PBAT pieces as a result of unknown abiotic factors.

Notably, for the contact angle of PLA in Barba Peider soil, we observed a higher value for the sterile-soil incubated plastic relative to the non-incubated pieces and a lower angle for the natural-soil incubated plastic. Even though these results seem contradictory at first glance, the observation might be explained by opposing effects caused by abiotic degradation and microbial colonization of PLA (i.e., higher hydrophilicity of the surface due to biofilm formation). This circumstance might lead to diverging results in the physico-chemical analysis of the plastic pieces depending on the context (i.e., incubation duration). Our results demonstrate that degradation of PLA is partly abiotically driven. Abiotic degradation of PLA involves a temperature and moisture dependent chemical hydrolysis reaction (Karamanlioglu et al., 2017). It was previously shown that abiotic processes in PLA degradation (i.e., breaking down to a low molecular weight) precede microbial degradation and result in a material that is more accessible to microorganisms (Castro-Aguirre et al., 2017). The measured carbonyl indices of PLA incubated in sterile Villum soil provide further evidence that both abiotic and microbial degradation are affecting the breakdown of PLA at low temperatures.

The low level of plastic degradation observed in our study might be due to the short incubation period (8 weeks) and relatively low incubation temperature (15°C), an overall low microbial activity, or a lack of specific plastic-degrading microorganisms. Earlier soil burial experiments showed little biodegradation of PLA when incubated at 25°C for 120 days (Kamiya et al., 2007) or at 0–30°C for 1 year (Shogren et al., 2003). Another study showed little degradation of PLA after a 1-year incubation in compost and soil at 25°C, but significant degradation in compost at 45°C after only 3 weeks of incubation (Karamanlioglu and Robson, 2013). Low temperatures and a lack of sunlight, as in our experimental set-up, potentially prevent abiotic degradation that could stimulate further microbial degradation (Singh and Sharma, 2008; Castro-Aguirre et al., 2017). Nonetheless, we detected small differences between non-incubated, sterile-soil incubated and natural-soil incubated biodegradable plastics by FTIR and contact angle measurements. It would be interesting to test different incubation temperatures and durations to investigate whether greater degrees of degradation could be achieved.

The optimal temperature for biodegradation in cold terrestrial environments remains unknown, as fast biodegradation is mostly reached at considerably higher temperatures like in industrial compost, whereas microorganisms in Arctic and alpine soils are adapted to low temperatures. Furthermore, other techniques such as respirometric measurements could be applied to better differentiate between abiotic and microbial degradation of plastics (Castro-Aguirre et al., 2017). Respirometric measurements and the analysis of more than one time-point could be possible approaches to elucidate the interplay between abiotic and biotic factors taking place in the plastisphere.

Plastics Decrease Diversity and Alter Microbial Community Structures

The two soils showed many similarities regarding the effects of plastics on microbial α-diversity. Overall, the microbial diversity was lower in the plastisphere than in bulk soil, in particular with PLA. While the PLA plastisphere clearly was most prone to changes in bacterial α-diversity in both soils, the results for fungi were less consistent. Even though effects of PLA were similar in the two soils, the fungal community in Villum soil was by far more affected by PBAT and PE. Moreover, PCoA and PERMANOVA revealed clear shifts in the microbial community structures that took place in the plastisphere of the various plastics.

TABLE 5 | Changes in the relative abundance of prokaryotic and fungal phyla and orders in the plastisphere.

	Barba Peider				Villum			
Taxa	**Main test (*F*)**	**PLA**	**PBAT**	**PE**	**Main test (*F*)**	**PLA**	**PBAT**	**PE**
Bacteria:								
Phyla								
Acidobacteria	31.5***	↓***	– ns	– ns	33.1***	↓***	↓**	↓*
Actinobacteria	39.8***	↑***	– ns	↑***	22.2***	– ns	– ns	↑***
Bacteroidetes	4.5*	– ns	– ns	– ns	0.4ns	– ns	– ns	– ns
Chlamydiae	3.4*	– ns	– ns	– ns	2.8(ns)	– ns	– ns	– ns
Chloroflexi	7.3**	↓**	– ns	– ns	13.1***	↓***	↓*	– ns
Gemmatimonadetes	31.7***	↓***	↓*	↓**	27.8***	↓***	↓**	– ns
Patescibacteria	34.7***	↑*	– ns	– ns	48.4***	↑***	– ns	– ns
Planctomycetes	22.4***	↓***	↓**	– ns	59.8***	↓***	↓**	↓***
Proteobacteria	40.0***	↑***	– ns	– ns	7.3**	– ns	↑**	– ns
Verrucomicrobia	6.0**	– ns	↓(ns)	– ns	17.7***	↓***	– ns	– ns
Nitrospirae	5.4**	↓*	– ns	– ns	32.8***	↓***	↓**	↓**
Orders								
β-Proteobacteriales[1]	51.3***	↑***	– ns	– ns	8.7**	↓(ns)	↑*	– ns
Chitinophagales	3.7*	– ns	– ns	– ns	4.3*	↓*	– ns	– ns
Chthoniobacterales	4.9*	↓(ns)	– ns	– ns	17.7***	↓***	– ns	– ns
Gemmatales	8.8**	↓**	↓*	– ns	54.3***	↓***	↓**	↓***
Gemmatimonadales	32.9***	↓***	↓*	↓**	29.1***	↓***	↓**	– ns
Ktedonobacterales	5.6**	↓(ns)	– ns	– ns	NA	NA	NA	NA
Parcubacteria	31.3***	↓***	– ns	– ns	6.2**	– ns	– ns	– ns
Pirellulales	12.8***	– ns	↓(ns)	↓**	54.1***	↓***	↓***	↓**
Planctomycetales	9.5***	↓**	↓(ns)	↓*	7.8**	– ns	– ns	– ns
Propionibacteriales	18.2***	– ns	– ns	↑***	15.9***	↑(ns)	– ns	↑***
Pyrinomonadales	14.6***	↓***	– ns	↓*	29.1***	↓***	↓**	↓**
Rhizobiales	73.6***	↑***	– ns	– ns	8.7**	– ns	↑**	– ns
Saccharimonadales	26.5***	↑***	– ns	– ns	57.1***	↑***	– ns	– ns
Solibacterales	22.1***	↓***	– ns	– ns	88.9***	↓***	↓***	↓***
Subgroup 6[2]	11.6***	↓(ns)	↓**	– ns	28.0***	↓***	↓**	– ns
Tepidisphaerales	21.4***	↓***	↓(ns)	– ns	20.5***	↓***	↓**	↓*
Fungi:								
Phyla								
Ascomycota	4.9*	– ns	– ns	– ns	1.4ns	– ns	– ns	– ns
Basidiomycota	4.6*	– ns	– ns	– ns	0.9ns	– ns	– ns	– ns
Mortierellomycota	18.3***	↓**	↑**	↑(ns)	4.6*	– ns	– ns	– ns
Orders								
Cystofilobasidiales	1.2ns	– ns	– ns	– ns	NA	NA	NA	NA
Helotiales	5.0*	– ns	↑*	– ns	2.2ns	– ns	– ns	– ns
Pleosporales	1.2ns	– ns	– ns	– ns	1.5ns	– ns	– ns	– ns
Thelebolales	50.8***	↑***	– ns	– ns	17.7***	– ns	↑**	– ns

*The ten most abundant bacterial phyla and orders were taken for each soil separately, resulting in a total of 11 phyla and 16 orders analyzed. The same procedure was applied to the three most abundant fungal phyla and orders, resulting in a total of three phyla and four orders. ANOVA was performed to determine the effect of plastic on the relative abundance of the selected taxa. F-values and statistical significances of the main effect are given in the first column for Barba Peider and for Villum. Tukey HSD tests were performed for the pairwise testing of plastisphere and bulk soil of each plastic type. The direction of change and statistical significances are given in columns two to four for each soil. ↑ represents a higher relative abundance of a taxon in the plastisphere in comparison to the respective bulk soil, while ↓ represents the opposite. No direction of change was analyzed for non-significant results. Asterisks indicate significant differences, with ***$P < 0.001$, **$P < 0.01$, *$P < 0.05$, (ns)$P < 0.1$, and ns$P > 0.1$; NA, not applicable. The relative abundances of the analyzed bacterial orders are visualized in* ***Figure 4****, and bacterial phyla and fungal taxa are shown in* ***Supplementary Figures 2–5****. [1]Silva database version v132 has changed β-Proteobacteria to the order β-Proteobacteriales (which include Burkholderiales) within the γ-Proteobacteria. [2]Acidobacterial subgroup 6.*

Parallel to the changes in α-diversity, we observed pronounced shifts in the microbial community structures with PLA and moderate changes with PBAT, whereas PE had no effect in either soil. Based on our hypothesis concerning the degree of biodegradability of the different plastics, we expected to find the largest changes in microbial community structures in the plastisphere of PLA and little change for PE; this was confirmed with our DNA metabarcoding. In general,

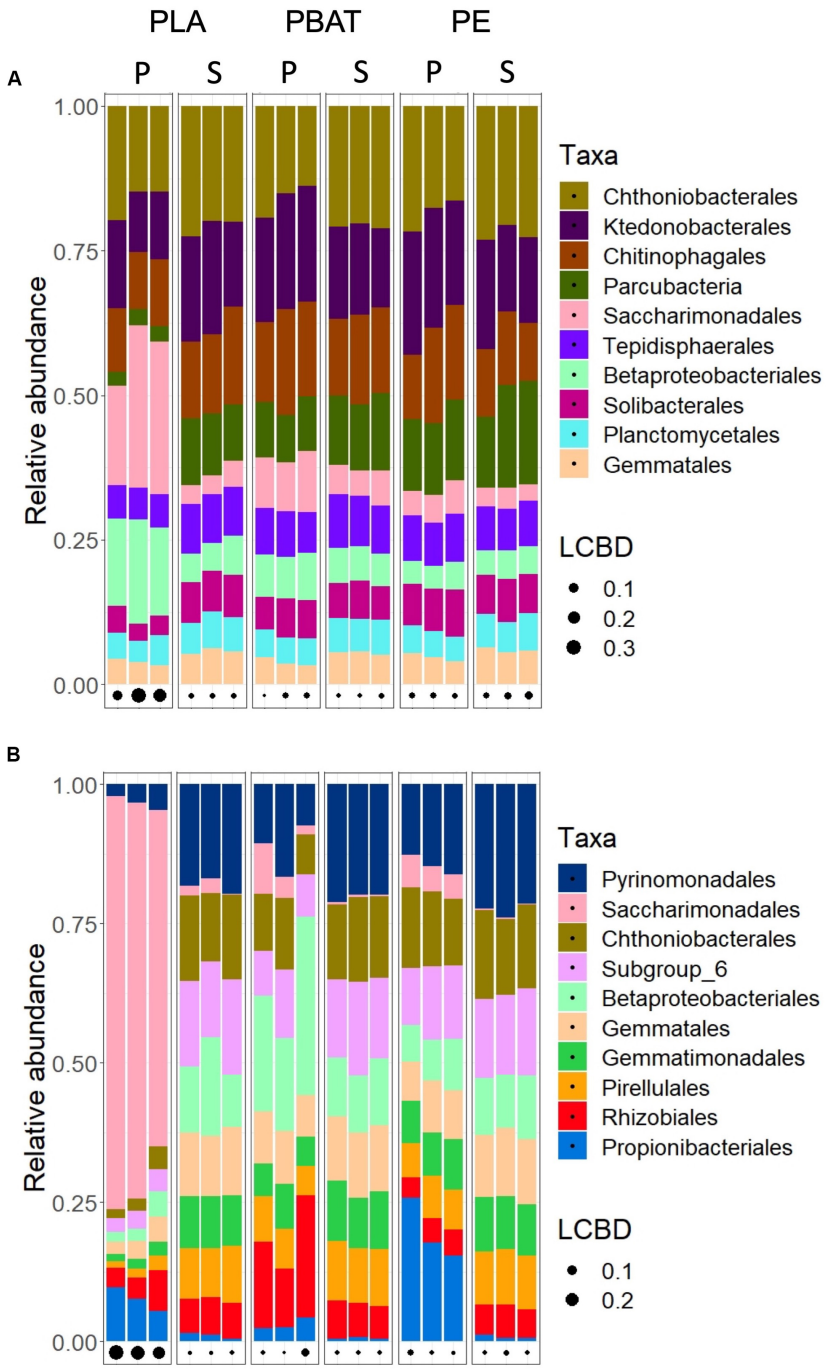

FIGURE 4 | Relative abundance of the ten most abundant bacterial orders in the plastisphere (P) and bulk soil (S) of Barba Peider (Swiss Alps) **(A)** and Villum (Northern Greenland) **(B)** soils. The three replicates for each habitat are shown as separate columns. LCBD, local contribution to β-diversity.

it seems that the microbial community in Villum soil is more affected by plastic addition than that in Barba Peider soil. The different C and N content, and resulting higher initial microbial biomass in Villum soil could be a possible reason for these findings. In support of this explanation, Kamiya et al. (2007) found that several bioplastics were more prone to biodegradation in a soil with more organic matter than in one with little organic matter. To improve our understanding on the biodegradation of plastics in cold environments, soils with different characteristics, e.g., varying in C, N and organic matter content, should be tested. Moreover, analyzing the plastisphere at different time-points might demonstrate if the colonization and degradation of the plastics occurs along with a succession of taxa, or if initial

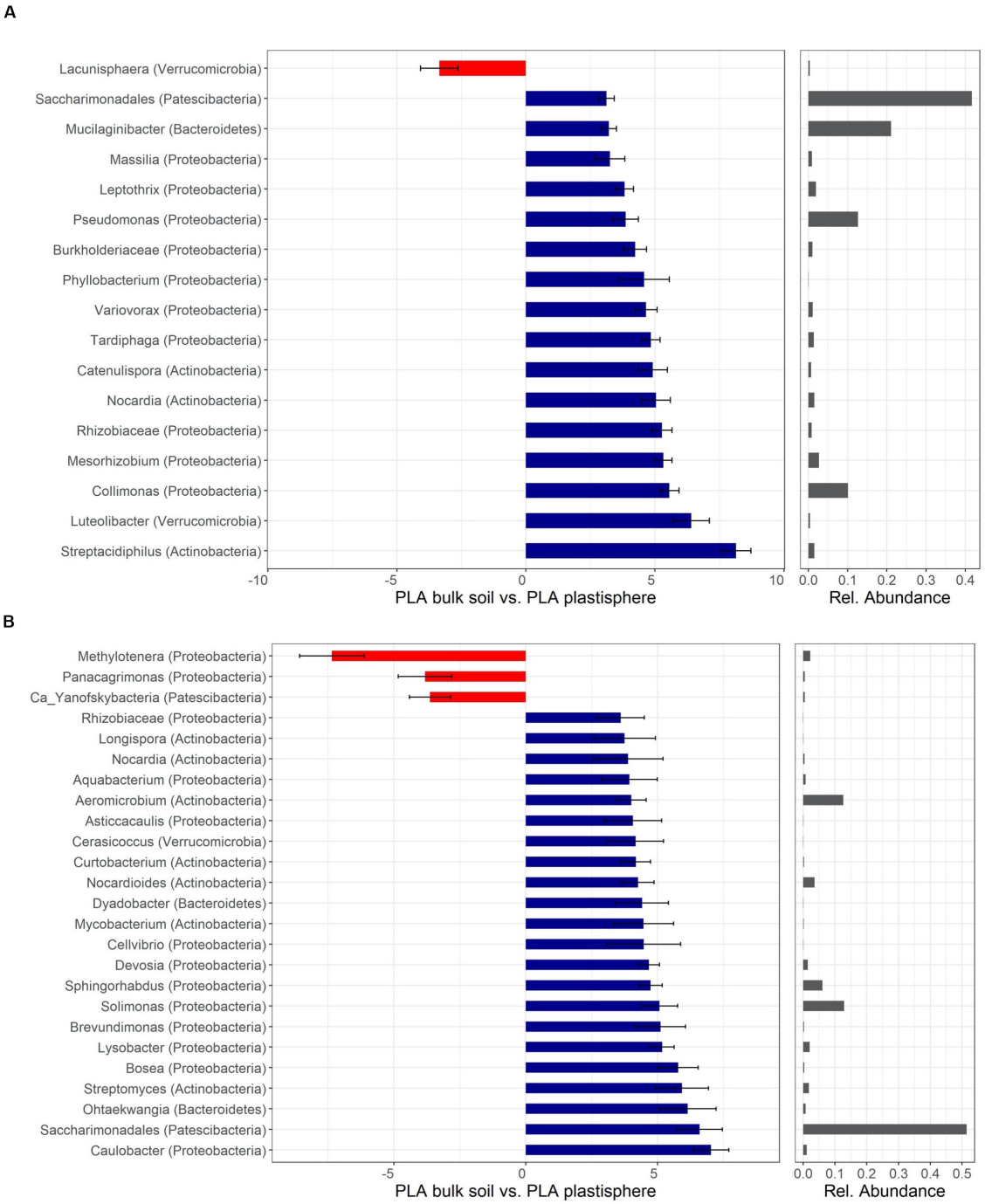

FIGURE 5 | Differentially abundant taxa of PLA in Barba Peider (Swiss Alps) **(A)** and Villum (Northern Greenland) **(B)** soil. Taxa are classified to the lowest possible taxonomic level. Values on the *X*-axis in the left panels show the differential abundances in the plastisphere and bulk soil as $\log_2$-fold changes. Only significant taxa ($P < 0.05$) with $\log_2$-fold changes >3 for panel **(A)** and >3.5 for panel **(B)** are shown. Note that the scales in the *x*-axis in panels **(A,B)** are different. Positive values indicate a higher occurrence in the plastisphere, whereas negative values indicate a higher occurrence in the bulk soil. Names in brackets specify the phylum the taxa belong to. Values in the right panels indicate the abundances of specific taxa relative to the taxa shown in the figure. Ca, candidatus.

microbial colonizers remain unchanged with time and at later degradation stages.

Reduced observed richness on the surface of plastics incubated in soil for 90 days was previously reported by Huang et al. (2019). A decrease in α-diversity on plastic substrates compared with in the surroundings after only 2 weeks was previously reported in a study from a marine environment (Ogonowski et al., 2018). Most other experiments in marine environments documented higher

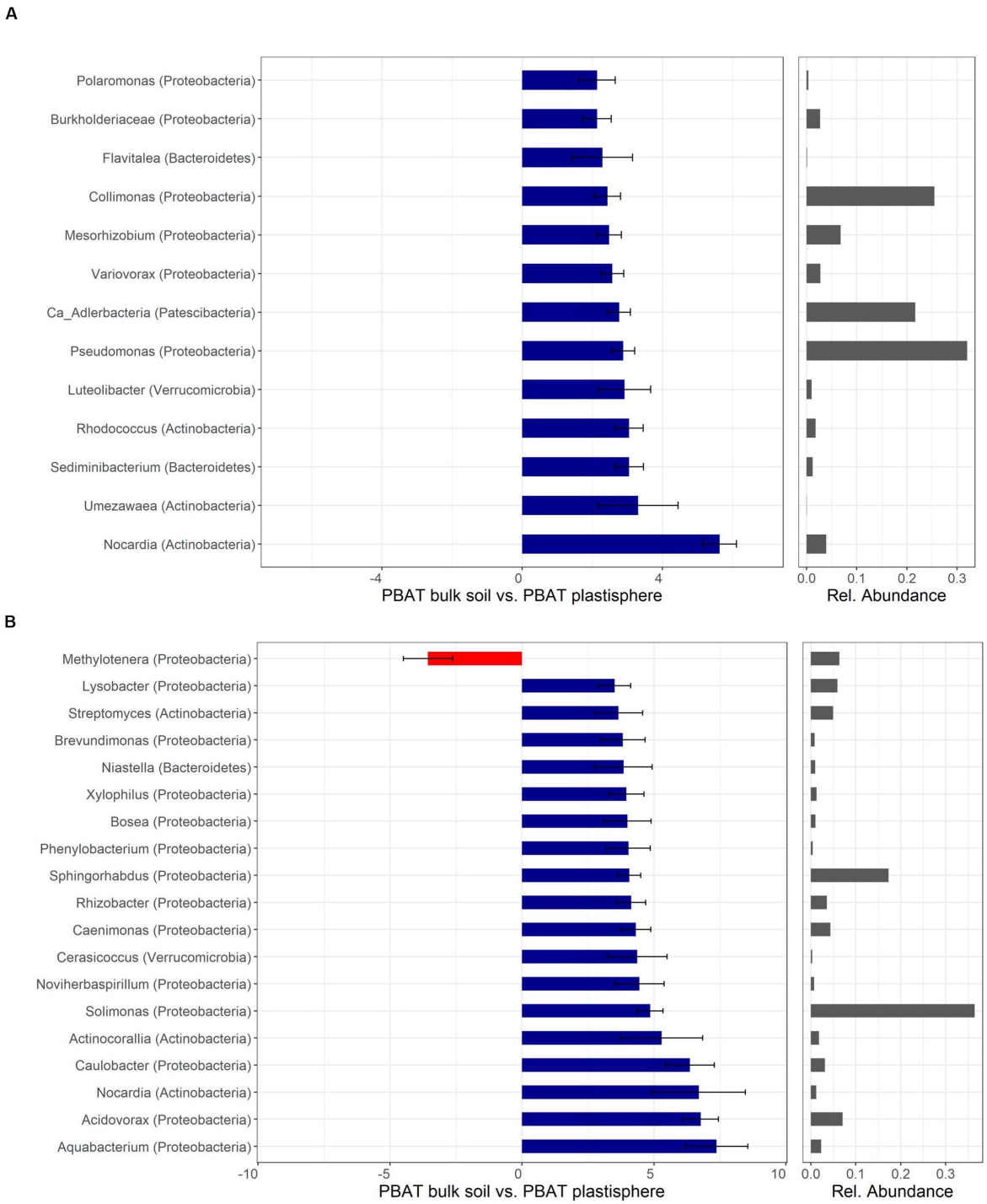

FIGURE 6 | Differentially abundant taxa of PBAT in Barba Peider (Swiss Alps) **(A)** and Villum (Northern Greenland) **(B)** soil. Taxa are classified to the lowest possible taxonomic level. Values on the *X*-axis in the left panels show the differential abundances in the plastisphere and bulk soil as $\log_2$-fold changes. Only significant taxa ($P < 0.05$) with $\log_2$-fold changes >2 **(A)** and >3.5 **(B)** are shown. Note that the scales in the *x*-axis in panels **(A,B)** are different. Positive values indicate a higher occurrence in the plastisphere, whereas negative values indicate a higher occurrence in the bulk soil. Names in brackets specify the phylum the taxa belong to. Values in the right panels indicate the abundances of specific taxa relative to the taxa shown in the figure. Ca, candidatus.

α-diversity on plastics than in the sea water (Zettler et al., 2013; Debroas et al., 2017; Dussud et al., 2018). De Tender et al. (2015) showed that only a very small set of OTUs in their marine study belonged to a core plastisphere microbiome present in all samples with an abundance of at least 0.01%, providing evidence that plastisphere microbiomes are very diverse even among marine

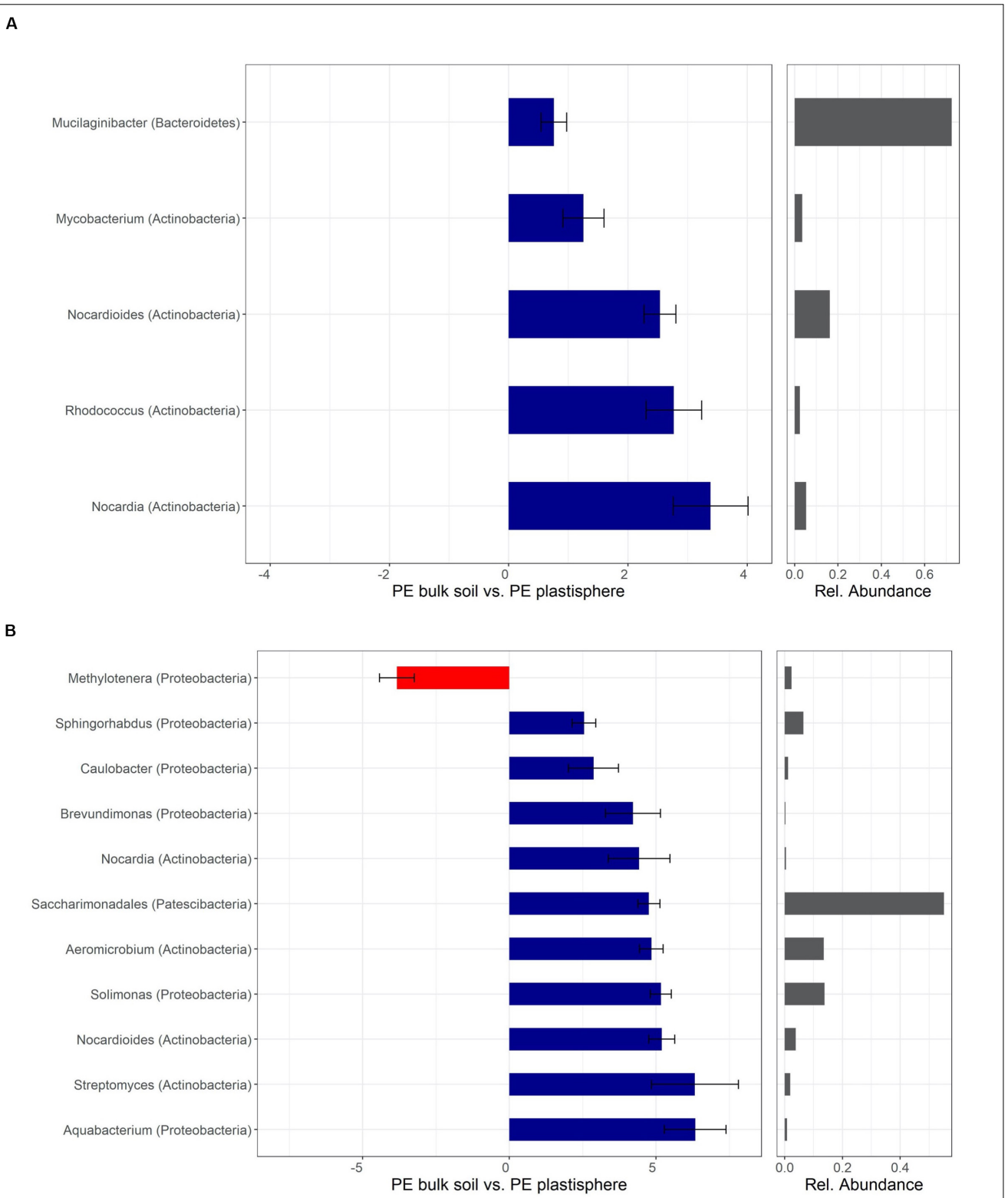

FIGURE 7 | Differentially abundant taxa of PE in Barba Peider (Swiss Alps) **(A)** and Villum (Northern Greenland) **(B)** soil. Taxa are classified to the lowest possible taxonomic level. Values on the *X*-axis in the left panels show the differential abundances in the plastisphere and bulk soil as $\log_2$-fold changes. Only significant taxa ($P < 0.05$) with $\log_2$-fold changes >2.5 are shown. Note that the scales in the *x*-axis in panels **(A,B)** are different. Positive values indicate a higher occurrence in the plastisphere, whereas negative values indicate a higher occurrence in the bulk soil. Names in brackets specify the phylum the taxa belong to. Values in the right panels indicate the abundances of specific taxa relative to the taxa shown in the figure.

environments. However, studies in aquatic and soil environments are difficult to compare (Bryant et al., 2016; Oberbeckmann et al., 2016; Kirstein et al., 2018). While plastic floating in water is in contact with a large number of different organisms over time and can serve as a raft for them (Oberbeckmann et al., 2016; Brunner et al., 2018), plastic substrates in soil are relatively immobile and stay permanently in contact with the inhabiting soil microbes, which are strongly adsorbed at soil surfaces (i.e., clay) (Jiang et al., 2007). There are several conceivable reasons for the reduction in the observed richness. By gaining access to a new energy and carbon source, they might outcompete other microbes not able to metabolize this carbon source in this specific niche (Dini-Andreote et al., 2015). This growth advantage can lead to the decline of other taxa, a phenomenon named "competitive exclusion" (Hibbing et al., 2010). Secondly, plastic addition can change the microenvironment of the soils by releasing potentially harmful compounds (Atuanya et al., 2016), changing the pH, or creating a barrier for water, oxygen, and nutrients (Bandopadhyay et al., 2018).

Plastic-Dependent Microbiome

Relative Abundances of Microbial Taxa

Overall, the microbial communities of the plastisphere and bulk soil were characterized by taxonomic groups commonly observed in Arctic and alpine soils (Frey et al., 2016; Rime et al., 2016; Donhauser and Frey, 2018; Malard and Pearce, 2018). Only few phyla of this endemic microbiome showed an altered relative abundance in the plastisphere. Plastic addition might have little influence on the relative abundances of fungi if higher taxonomic ranks, for example phyla, are regarded. However, this interpretation might be misleading regarding the investigated soils, as the phylum Ascomycota is very dominant in these soils. Therefore, a plastic-induced selection for Ascomycota, as reported elsewhere (Muroi et al., 2016), cannot be detected by solely comparing relative abundances at the phylum level. The relative abundances of high-ranking bacterial taxa shared many similarities among the two soils. Only few phyla and orders seemed to be competitive in the plastisphere of PLA and PBAT. Especially Actinobacteria, Proteobacteria, and Patescibacteria seemed to profit from the plastisphere environment. While Proteobacteria increased in relative abundance on PLA in Barba Peider soil, it showed growth advantages on PBAT in Villum soil. Actinobacteria benefitted from PE in both soils, as well as from PLA in Barba Peider soil. Patescibacteria strongly increased in relative abundance in the PLA plastisphere in Villum soil and also profited from this plastic type in Barba Peider soil. Only little research has dealt with the colonization and biodegradation of plastics in soils so far. In one study, the effect of PBAT on the microbial community was analyzed by genetic profiling (DGGE), and Ascomycota were found to profit from the plastic, while the bacterial community did not change considerably (Muroi et al., 2016). Whereas this earlier study analyzed the long-term effects of plastic addition on a whole agricultural field, we investigated the region in proximity to single plastic pieces. A spatial limitation of the effects caused by plastic in soil might be one reason we observed more pronounced effects on the bacterial community than reported previously. Other studies investigated the microbial community changes on PE microplastics and PLA/PHB (poly(3-hydroxybutyrate)) blend foils in laboratory incubation experiments (Jeszeová et al., 2018; Huang et al., 2019). Consistent with our findings, Huang et al. (2019) detected a significant increase in Actinobacteria on the plastic surface, and Jeszeová et al. (2018) found significant changes in the microbial community structure of PLA/PHB foil, i.e., increased numbers of *Streptomyces* and *Rhodococcus*.

Members of the Proteobacteria are physiologically and ecologically extremely diverse but are key players in C and N cycling. In particular, members of the Burkholderiales within Proteobacteria thrived in the plastisphere of both soils. Actinobacteria are ubiquitous and frequently saprophytic organisms able to degrade recalcitrant C sources. They play a vital role in the C cycle in the soil (Ventura et al., 2007; Bull, 2011; Rosenberg et al., 2014; Mohammadipanah and Wink, 2016). The ability to decompose recalcitrant compounds is an important trait in oligotrophic soil environments when more readily available substrates are rather limited. Furthermore, many members of the Actinobacteria are capable of spore formation and filamentous growth, which facilitates survival under low soil moisture (Wolf et al., 2013). With these capabilities, Actinobacteria are known to compete well under oligotrophic conditions. In contrast, Acidobacteria (i.e., subgroup Gp6) decreased in the plastisphere of all polymers. While the broad metabolic potential of Actinobacteria and Proteobacteria is widely known, it was surprising to find Patescibacteria and the associated order Saccharimonadales accumulating in the plastisphere.

Bacterial Key Taxa Associated With Plastics

Since different subgroups within a phylum can show ambiguous responses to polymer addition, we identified specific "*plastisphere taxa*" at lower taxonomic levels. Several actinobacterial taxa, such as *Rhodococcus*, *Nocardia* and *Streptomyces*, increased in the plastisphere in our study. Cultivated strains of these genera isolated from the incubated plastics yield further evidence for their presence on the plastic surfaces and complement our DNA metabarcoding data. Actinobacteria are, in general, promising candidates for biodegradation of all kinds of plastics, including PLA, PBAT, and strikingly even PE. Butbunchu and Pathom-Aree (2019) summarized the known abilities of Actinobacteria to degrade PLA. Interestingly, PLA biodegradation has been demonstrated for only a very limited number of actinobacterial families, and biodegradation by cold-adapted Actinobacteria has not yet been reported. PBAT degradation has so far only been shown for two thermophilic *Thermomonospora fusca* strains (Kleeberg et al., 1998). Other researchers reported that various isolated strains, including *Rhodococcus* spp., *Streptomyces* spp. and *Nocardia*, were associated with the biodegradation of PE (Kumar Sen and Raut, 2015; Pathak and Navneet, 2017). However, we have to consider that in most studies examining PE degradation, pretreated polymers or commercial products bearing additives have been used.

Most of the plastic-associated taxa within the Proteobacteria in our tested soils belong to a small number of orders, such as Burkholderiales, Caulobacterales, Rhizobiales and

a few γ-Proteobacteria. Members of these orders were also found among the isolated strains obtained from the incubated plastics. Especially *Pseudomonas* is well known for its broad metabolic capabilities, and various strains of the genus are associated with the degradation of PLA, PBAT, PE, and many other plastics (Wallace et al., 2017; Wilkes and Aristilde, 2017; Bubpachat et al., 2018). Burkholderiales possess a broad range of enzymes able to degrade polyaromatic hydrocarbons (PAHs), which include important soil pollutants (Pérez-Pantoja et al., 2012). *Aquabacterium* was first isolated from biofilms of a drinking water system (Kalmbach et al., 1999), and a species of the genus was shown to degrade oil (Pham et al., 2015). Strains of the genus *Variovorax* hold highly diverse catabolic capabilities, including the degradation of 3,3'-Thiodipropionic acid (TDP), an additive widely used to stabilize polymers, as well as dimethyl terephthalate and vinyl chloride, two other chemicals used in plastic production (Satola et al., 2013; Wilson et al., 2016). *Collimonas* comprises chitinolytic species shown to degrade xenobiotics (Leveau et al., 2010); however, the genus has not been linked to plastic degradation yet. Species of the genera *Acidovorax* and *Leptothrix* are able to degrade the bioplastic poly(tetramethylene succinate)-co-adipate (PBSA) (Uchida et al., 2000; Nakajima-Kambe et al., 2009b). Additionally, the *Leptothrix* strain has been shown to degrade PLA (Nakajima-Kambe et al., 2009a). In our study, *Leptothrix* was increased in the PLA plastisphere of Barba Peider soil.

In a recent study, Rhizobiales were recognized as important taxon present on plastics floating in the North Atlantic garbage patch (Debroas et al., 2017). *Mesorhizobium* spp. have been shown to be associated with anaerobic PLA degradation (Yagi et al., 2014). *Sphingorhabdus*, a genus of the order Sphingomonadales, has been found to be able to degrade oil (Jeong et al., 2016). *Caulobacter crescentus* is a model laboratory organism that has been extensively studied concerning the process of the attachment of bacterial cells to surfaces and the formation of biofilms (Entcheva-Dimitrov and Spormann, 2004). In addition, *Caulobacter* spp. have been shown to degrade PAHs including pyrene and phenantrene (Chang et al., 2014; Al-Thukair and Malik, 2016). A *Brevundimonas* species has been reported to degrade the biodegradable plastic poly(ε-caprolactone) (Nawaz et al., 2015).

We found members of the Saccharimonadales to be the major "plastisphere taxa" in both soils. To our knowledge, this is the first report of Saccharimonadales within the Patescibacteria superphylum thriving in the plastisphere. Very little is known about the ecology of Saccharimonadales, which belongs to the candidate phylum Saccharibacteria (formerly TM7), and knowledge almost exclusively stems from genomic data. Saccharibacteria have been shown to possess very small genomes and cell sizes, and they have therefore been proposed to live in symbiosis with other microorganisms depending on co-metabolism (Lemos et al., 2019). Further, Lemos et al. (2019) stated that the majority of unique genes found in nearly complete genomes of two Saccharibacteria are of unknown function, underlining the knowledge gaps existing regarding this bacterial order. Several genes involved in the catabolism of complex C sources were identified in TM7 strain RAAC3 and other Saccharibacteria (Kantor et al., 2013; Starr et al., 2018). In addition, some Saccharibacteria were shown to take up oleic acid and to possess lipase and other exoenzymatic activities (Kindaichi et al., 2016). Interestingly, many Saccharibacteria seem to possess a D−lactate dehydrogenase−like protein acting in the conversion of pyruvate into lactate in a fermentation pathway (Lemos et al., 2019). Our data implicate that lactate, the monomer of PLA, might be used as a C source instead of being only a final waste product in the metabolism of some Saccharibacteria. Furthermore, metagenomic data indicate that representatives of the phylum are able to degrade a variety of polymers (Kantor et al., 2013; Starr et al., 2018). However, the involvement of Saccharibacteria in the degradation of PLA is speculative and needs to be addressed in future studies.

In our study, some taxa within the Bacteroidetes (i.e., *Sediminibacterium*, *Dyadobacter*, *Ohtaekwangia*) increased in the plastisphere. *Sediminibacterium* was previously shown to degrade vinylchloride (Wilson et al., 2016). This chemical is the monomer of an important plastic, namely polyvinylchloride (PVC). *Dyadobacter* and *Ohtaekwangia*, which both increased significantly in the plastisphere of PLA in Villum soil, were previously identified as potential biodegraders of xenobiotic pollutants (Willumsen et al., 2005; Tejeda-Agredano et al., 2013; Bao et al., 2020).

As far as we know, the only link between Verrucomicrobia and plastics in earlier investigations was made in a study where Verrucomicrobia subdivision 1 was shown to be associated with polyethylene terephthalate (PET) in a marine environment, whereas subdivision 4 was rather found in the surrounding water (Oberbeckmann et al., 2016). Our results partly fit with this observation, as we found *Luteolibacter* (subdivision 1) to be increased in the proximity of plastic and *Lacunisphaera* (subdivision 4) increased in the bulk soil. However, *Cerasicoccus* (subdivision 4) was augmented in the plastisphere as well, which contrasts with the previous findings.

Fungal Key Taxa Associated With Plastics

Oidiodendron spp., found to be enriched in the plastisphere of PLA in Barba Peider soil, are closely related to the dominant *Pseudogymnoascus* and are found on a great variety of substrates, including wood, peat and human hair (Rice and Currah, 2005). The genus has been shown to possess the ability to degrade a broad spectrum of substrates, e.g., cellulose and lignin (Rice and Currah, 2005).

The genus *Alternaria*, found to be increased in the plastisphere of PLA in Villum soil, comprises saprobic and endophytic species and is known to cause serious disease in plants (Woudenberg et al., 2013). The genera *Alternaria* and *Pseudogymnoascus* (synonym *Geomyces*) were previously linked to polyurethane degradation (Loredo-Treviño et al., 2012). *Mycosphaerella*, another genus that increased in the plastisphere of PLA in Villum soil, likewise comprises plant pathogenic species. Species of this

genus have been shown to produce a wide variety of polymer-degrading enzymes involved in the break-down of plant cell walls (Douaiher et al., 2007).

Phlebia, a basidiomycetous genus found to be increased in the plastisphere of PE in Villum soil, is known to possess enzymes for lignin decomposition (Kantelinen et al., 1989) and has been linked to the biodegradation of PAHs (Mori et al., 2003). In our experiment, *Mycena* showed the largest growth advantage of all fungi in the plastisphere of all plastics in both soils. However, the strong increase in abundance was only observed in one replicate. Due to the lack of consistency, these results have to be interpreted with caution. Like *Phlebia*, *Mycena* has been linked to PAH degradation (Winquist et al., 2014).

CONCLUSION

As far as we know, this is the first report on the plastisphere microbiome of different plastic types (biodegradable and non-biodegradable) in terrestrial cryoenvironments using DNA metabarcoding. We found clear differences between microbial consortia on plastics and the surrounding environment, as previously reported in marine environments. Our findings suggest that plastic debris form a habitat for complex microbial assemblages with lifestyles and possibly metabolic pathways distinct from those of the microbial communities in bulk soil.

Even though degradation in our mesocosm experiment was slight, we detected pronounced shifts in bacterial and fungal α-diversity and community structures in the plastisphere compared with values in adjacent soils not affected by the plastics. Our results supported our hypothesis that the effects were larger on biodegradable (PLA, PBAT) than non-biodegradable plastics (PE).

Interestingly, members of only a few phyla (Actinobacteria, Proteobacteria, and Patescibacteria) were found to benefit from the plastics in both soils. Similarly, the key microbial taxa associated with plastics were similar in the two soils (Barba Peider and Villum). Plastic addition affected fungal taxa to a lesser extent, and we have not found any common taxa that reacted similarly in both soils. However, it is noteworthy that some genera (i.e., *Mycena* and *Plebia*) were increased on PE in the Villum. We found several candidate taxa in the plastisphere with known potential to biodegrade xenobiotics, e.g., Burkholderiales, *Pseudomonas*, *Caulobacter*, *Rhodococcus*, *Nocardia* and *Streptomyces* indicating the potential of cold-adapted microorganisms to degrade bioplastics. Plastic degraders from terrestrial cryoenvironments are thus conceivable but further investigations with single isolates or consortia of microorganisms degrading plastics needs to be performed.

In addition to identifying many organisms that are already prominently published in the context of plastics and especially their biodegradation, we found members of the Saccharimonadales to be the major "plastisphere taxa." To our knowledge, this is the first report of Saccharimonadales within the Patescibacteria superphylum thriving in the plastisphere. Further research is needed to evaluate their occurrence in the plastisphere of other soils from cold or temperate environments, to find traits responsible for their thriving on the PLA surface, and to analyze if they potentially even degrade PLA.

Increased human activities in the Arctic and the Alps demand environment-friendly processes for pollution control and clean-up, suitable for cold regions. Microorganisms from terrestrial cryoenvironments harbor great biotechnological potential, as they are known to possess special adaptations to cold temperatures. Major knowledge gaps still exist about the microbial life in the plastisphere, especially in terrestrial cryoenvironments. The expansive geographical dimensions of these environments point to their global importance, and we plead for further clarification of existing ambiguities. Our findings highlight that correct waste management is crucial not only for non-biodegradable but also for biodegradable plastics in order to protect environments all over the world against this serious threat.

DATA AVAILABILITY STATEMENT

The datasets presented in this study can be found in online repositories. The names of the repository/repositories and accession number(s) can be found below: https://www.ncbi.nlm.nih.gov/, PRJNA630025.

AUTHOR CONTRIBUTIONS

JR, BF, and IB designed the study. JR and DB performed the experiment. JR, LP-C, and DB participated in data analysis. JR wrote the manuscript with the help of BF and IB. All authors contributed to the article and approved the submitted version.

FUNDING

This study was partly funded by the Swiss National Science Foundation (SNSF) under the grant IZLSZ2_170941, the Swiss Polar Institute (SPI), and the BNP Paribas Swiss Foundation.

ACKNOWLEDGMENTS

We thank C. Perez-Mon for providing soils from Villum Research Station and Muot da Barba Peider; B. Stierli for laboratory assistance; R. Köchli for completing soil analyses; and S. Gunz and A. Dharmarajah for providing advice in data analysis. We acknowledge the Genetic Diversity Centre (GDC) of the ETH Zürich and the contribution of scientists at the McGill University and Génome Québec Innovation Center in Montreal, Canada for performing Illumina MiSeq sequencing. We also thank M. Dawes for her valuable contribution to the editing of this article.

SUPPLEMENTARY MATERIAL

The Supplementary Material for this article can be found online at: https://www.frontiersin.org/articles/10.3389/fenvs.2020.562263/full#supplementary-material

SUPPLEMENTARY DATA SHEET 1 | Supplementary Tables S1, S2.

SUPPLEMENTARY DATA SHEET 2 | Supplementary Figures S1–S7.

SUPPLEMENTARY DATA SHEET 3 | List of significant ($q > 0.05$) differently abundant (log2-fold change) bacterial and fungal OTUs in the plastisphere compared to bulk soils.

SUPPLEMENTARY DATA SHEET 4 | List of significant ($q > 0.05$) differently abundant (log2-fold change) bacterial and fungal genera in the plastisphere compared to bulk soils.

SUPPLEMENTARY DATA SHEET 5 | 16S rDNA sequences of isolated bacterial and fungal strains from the plastisphere.

REFERENCES

Accinelli, C., Saccà, M. L., Mencarelli, M., and Vicari, A. (2012). Deterioration of bioplastic carrier bags in the environment and assessment of a new recycling alternative. *Chemosphere* 89, 136–143. doi: 10.1016/j.chemosphere.2012.05.028

Adamczyk, M., Hagedorn, F., Wipf, S., Donhauser, J., Vittoz, P., Rixen, C., et al. (2019). The soil microbiome of Gloria Mountain summits in the Swiss Alps. *Front. Microbiol.* 10:1080. doi: 10.3389/fmicb.2019.01080

Allen, S., Allen, D., Phoenix, V. R., Le Roux, G., Durántez Jiménez, P., Simonneau, A., et al. (2019). Atmospheric transport and deposition of microplastics in a remote mountain catchment. *Nat. Geosci.* 12, 339–344. doi: 10.1038/s41561-019-0335-5

Al-Thukair, A. A., and Malik, K. (2016). Pyrene metabolism by the novel bacterial strains *Burkholderia fungorum* (T3A13001) and *Caulobacter* sp (T2A12002) isolated from an oil-polluted site in the Arabian Gulf. *Int. Biodeter. Biodegr.* 110, 32–37. doi: 10.1016/j.ibiod.2016.02.005

Amaral-Zettler, L. A., Zettler, E. R., and Mincer, T. J. (2020). Ecology of the plastisphere. *Nat. Rev. Microbiol.* 18, 139–151. doi: 10.1038/s41579-019-0308-0

Ambrosini, R., Azzoni, R. S., Pittino, F., Diolaiuti, G., Franzetti, A., and Parolini, M. (2019). First evidence of microplastic contamination in the supraglacial debris of an alpine glacier. *Environ. Pollut.* 253, 297–301. doi: 10.1016/j.envpol.2019.07.005

Anderson, M. J. (2001). Non-parametric MANOVA. *Aust. Ecol.* 26, 32–46. doi: 10.1111/j.1442-9993.2001.01070.pp.x

Atuanya, E., Udochukwu, U., and Dave-Omoregie, A. (2016). Bioavailability and toxicity of plastic contaminants to soil and soil bacteria. *Br. Microbiol. Res. J.* 13, 1–8. doi: 10.9734/bmrj/2016/25128

Bandopadhyay, S., Martin-closas, L., and Pelacho, A. M. (2018). Biodegradable plastic mulch films: impacts on soil microbial communities and ecosystem functions. *Front. Microbiol.* 9:819. doi: 10.3389/fmicb.2018.00819

Bao, H., Wang, J., Zhang, H., Li, J., Li, H., and Wu, F. (2020). Effects of biochar and organic substrates on biodegradation of polycyclic aromatic hydrocarbons and microbial community structure in PAHs-contaminated soils. *J. Hazard. Mater.* 385:121595. doi: 10.1016/j.jhazmat.2019.121595

Bengtsson-Palme, J., Hartmann, M., Eriksson, K. M., Pal, C., Thorell, K., Larsson, D. G. J., et al. (2015). metaxa2: improved identification and taxonomic classification of small and large subunit rRNA in metagenomic data. *Mol. Ecol. Resour.* 15, 1403–1414. doi: 10.1111/1755-0998.12399

Bengtsson-Palme, J., Ryberg, M., Hartmann, M., Branco, S., Wang, Z., Godhe, A., et al. (2013). Improved software detection and extraction of ITS1 and ITS2 from ribosomal ITS sequences of fungi and other eukaryotes for analysis of environmental sequencing data. *Methods Ecol. Evol.* 4, 914–919. doi: 10.1111/2041-210X.12073

Bergmann, M., Mützel, S., Primpke, S., Tekman, M. B., Trachsel, J., and Gerdts, G. (2019). White and wonderful? Microplastics prevail in snow from the Alps to the Arctic. *Sci. Adv.* 5, 1–11. doi: 10.1126/sciadv.aax1157

Briassoulis, D., and Dejean, C. (2010). Critical review of norms and standards for biodegradable agricultural plastics part I. Biodegradation in soil. *J. Polym. Environ.* 18, 384–400. doi: 10.1007/s10924-010-0168-1

Brunner, I., Fischer, M., Rüthi, J., Stierli, B., and Frey, B. (2018). Ability of fungi isolated from plastic debris floating in the shoreline of a lake to degrade plastics. *PLoS One* 13:e0202047. doi: 10.1371/journal.pone.0202047

Bryant, J. A., Clemente, T. M., Viviani, D. A., Fong, A. A., Thomas, K. A., Kemp, P., et al. (2016). Diversity and activity of communities inhabiting plastic debris in the north Pacific gyre. *mSystems* 1, 1–19. doi: 10.1128/msystems.00024-16

Bubpachat, T., Sombatsompop, N., and Prapagdee, B. (2018). Isolation and role of polylactic acid-degrading bacteria on degrading enzymes productions and PLA biodegradability at mesophilic conditions. *Polym. Degrad. Stabil.* 152, 75–85. doi: 10.1016/j.polymdegradstab.2018.03.023

Bull, A. T. (2011). "Actinobacteria of the extremobiosphere," in *Extremophiles Handbook*, ed. K. Horikoshi (Tokyo: Springer), 1203–1240. doi: 10.1007/978-4-431-53898-1_58

Butbunchu, N., and Pathom-Aree, W. (2019). Actinobacteria as promising candidate for polylactic acid type bioplastic degradation. *Front. Microbiol.* 10:2834. doi: 10.3389/fmicb.2019.02834

Castro-Aguirre, E., Auras, R., Selke, S., Rubino, M., and Marsh, T. (2017). Insights on the aerobic biodegradation of polymers by analysis of evolved carbon dioxide in simulated composting conditions. *Polym. Degrad. Stabil.* 137, 251–271. doi: 10.1016/j.polymdegradstab.2017.01.017

Chang, Y. T., Hung, C. H., and Chou, H. L. (2014). Effects of polyethoxylate lauryl ether (Brij 35) addition on phenanthrene biodegradation in a soil/water system. *J. Environ. Sci. Heal. A* 49, 1672–1684. doi: 10.1080/10934529.2014.951228

Clarke, K., and Gorley, R. (2006). *PRIMER v6Q15: User Manual/Tutorial*. PRIMER-E (Plymouth: Plymouth Routines in Multivariate Ecological Research).

da Silva, A. C., Rachid, C. T. C. C., de Jesus, H. E., Rosado, A. S., and Peixoto, R. S. (2017). Predicting the biotechnological potential of bacteria isolated from Antarctic soils, including the rhizosphere of vascular plants. *Polar Biol.* 40, 1393–1407. doi: 10.1007/s00300-016-2065-0

de Souza Machado, A. A., Kloas, W., Zarfl, C., Hempel, S., and Rillig, M. C. (2018). Microplastics as an emerging threat to terrestrial ecosystems. *Glob. Chang. Biol.* 24, 1405–1416. doi: 10.1111/gcb.14020

De Tender, C. A., Devriese, L. I., Haegeman, A., Maes, S., Ruttink, T., and Dawyndt, P. (2015). Bacterial community profiling of plastic litter in the Belgian part of the North Sea. *Environ. Sci. Technol.* 49, 9629–9638. doi: 10.1021/acs.est.5b01093

Debroas, D., Mone, A., and Ter Halle, A. (2017). Plastics in the North Atlantic garbage patch: a boat-microbe for hitchhikers and plastic degraders. *Sci. Total Environ.* 599–600, 1222–1232. doi: 10.1016/j.scitotenv.2017.05.059

Dini-Andreote, F., Stegen, J. C., Van Elsas, J. D., and Salles, J. F. (2015). Disentangling mechanisms that mediate the balance between stochastic and deterministic processes in microbial succession. *PNAS* 112, E1326–E1332. doi: 10.1073/pnas.1414261112

Donhauser, J., and Frey, B. (2018). Alpine soil microbial ecology in a changing world. *FEMS Microbiol. Ecol.* 94, 1–31. doi: 10.1093/femsec/fiy099

Douaiher, M. N., Nowak, E., Dumortier, V., Durand, R., Reignault, P., and Halama, P. (2007). Mycosphaerella graminicola produces a range of cell wall-degrading enzyme activities in vitro that vary with the carbon source. *Eur. J. Plant Pathol.* 117, 71–79. doi: 10.1007/s10658-006-9073-9

Dussud, C., Meistertzheim, A. L., Conan, P., Pujo-Pay, M., George, M., Fabre, P., et al. (2018). Evidence of niche partitioning among bacteria living on plastics, organic particles and surrounding seawaters. *Environ. Pollut.* 236, 807–816. doi: 10.1016/j.envpol.2017.12.027

Edgar, R. C. (2013). UPARSE: highly accurate OTU sequences from microbial amplicon reads. *Nat. Methods* 10, 996–998. doi: 10.1038/nmeth.2604

Edgar, R. C., and Flyvbjerg, H. (2015). Error filtering, pair assembly and error correction for next-generation sequencing reads. *Bioinformatics* 31, 3476–3482. doi: 10.1093/bioinformatics/btv401

Entcheva-Dimitrov, P., and Spormann, A. M. (2004). Dynamics and control of biofilms of the oligotrophic bacterium *Caulobacter crescentus*. *J. Bacteriol.* 186, 8254–8266. doi: 10.1128/JB.186.24.8254-8266.2004

Fierer, N. (2017). Embracing the unknown: disentangling the complexities of the soil microbiome. *Nat. Rev. Microbiol.* 15, 579–590. doi: 10.1038/nrmicro.2017.87

Frasson, D., Udovièiæ, M., Frey, B., Lapanje, A., Zhang, D. C., Margesin, R., et al. (2015). *Glaciimonas alpina* sp. nov. isolated from alpine glaciers and reclassification of glaciimonas immobilis Cr9-12 as the type strain of glaciimonas alpina sp. nov. *Int. J. Syst. Evol. Microbiol.* 65, 1779–1785. doi: 10.1099/ijs.0.000174

Frey, B., Rime, T., Phillips, M., Stierli, B., Hajdas, I., Widmer, F., et al. (2016). Microbial diversity in European alpine permafrost and active layers. *FEMS Microbiol. Ecol.* 92:fiw018. doi: 10.1093/femsec/fiw018

Hartmann, M., Brunner, I., Hagedorn, F., Bardgett, R. D., Stierli, B., Herzog, C., et al. (2017). A decade of irrigation transforms the soil microbiome of a semi-arid pine forest. *Mol. Ecol.* 26, 1190–1206. doi: 10.1111/mec.13995

Heuer, H., Krsek, M., Baker, P., Smalla, K., and Wellington, E. M. (1997). Analysis of actinomycete communities by specific amplification of genes encoding 16S rRNA and gel-electrophoretic separation in denaturing gradients. *Appl. Environ. Microbiol.* 63, 3233–3241. doi: 10.1128/aem.63.8.3233-3241.1997

Hibbing, M. E., Fuqua, C., Parsek, M. R., and Peterson, S. B. (2010). Bacterial competition: surviving and thriving in the microbial jungle. *Nat. Rev. Microbiol.* 8, 15–25. doi: 10.1038/nrmicro2259

Horton, A. A., Walton, A., Spurgeon, D. J., Lahive, E., and Svendsen, C. (2017). Microplastics in freshwater and terrestrial environments: evaluating the current understanding to identify the knowledge gaps and future research priorities. *Sci. Total Environ.* 586, 127–141. doi: 10.1016/j.scitotenv.2017.01.190

Huang, Y., Zhao, Y., Wang, J., Zhang, M., Jia, W., and Qin, X. (2019). LDPE microplastic films alter microbial community composition and enzymatic activities in soil. *Environ. Pollut.* 254:112983. doi: 10.1016/j.envpol.2019.112983

Huerta Lwanga, E., Gertsen, H., Gooren, H., Peters, P., Salánki, T., Van Der Ploeg, M., et al. (2016). Microplastics in the terrestrial ecosystem: implications for *Lumbricus terrestris* (Oligochaeta, Lumbricidae). *Environ. Sci. Technol.* 50, 2685–2691. doi: 10.1021/acs.est.5b05478

Jeong, H. I., Jin, H. M., and Jeon, C. O. (2016). Complete genome sequence of Sphingorhabdus sp. M41, a versatile hydrocarbon degrader, isolated from crude oil-contaminated costal sediment. *J. Biotechnol.* 227, 41–42. doi: 10.1016/j.jbiotec.2016.04.016

Jeszeová, L., Puškárová, A., Bučková, M., Kraková, L., Grivalský, T., Danko, M., et al. (2018). Microbial communities responsible for the degradation of poly(lactic acid)/poly(3-hydroxybutyrate) blend mulches in soil burial respirometric tests. *World J. Microbiol. Biotechnol.* 34:101. doi: 10.1007/s11274-018-2483-y

Jiang, D., Huang, Q., Cai, P., Rong, X., and Chen, W. (2007). Adsorption of *Pseudomonas* putida on clay minerals and iron oxide. *Colloids Surf. B* 54, 217–221. doi: 10.1016/j.colsurfb.2006.10.030

Kalmbach, S., Manz, W., Wecke, J., and Szewzyk, U. (1999). Aquabacterium gen. nov., with description of *Aquabacterium citratiphilum* sp. nov., *Aquabacterium parvum* sp. nov. and *Aquabacterium commune* sp. nov., three in situ dominant bacterial species from the Berlin drinking water system. *Int. J. Syst. Bacteriol.* 49, 769–777. doi: 10.1099/00207713-49-2-769

Kamiya, M., Asakawa, S., and Kimura, M. (2007). Molecular analysis of fungal communities of biodegradable plastics in two Japanese soils. *Soil Sci. Plant Nutr.* 53, 568–574. doi: 10.1111/j.1747-0765.2007.00169.x

Kantelinen, A., Hatakka, A., and Viikari, L. (1989). Production of lignin peroxidase and laccase by *Phlebia radiata*. *Appl. Microbiol. Biotechnol.* 31, 234–239.

Kantor, R. S., Wrighton, K. C., Handley, K. M., Sharon, I., Hug, L. A., Castelle, C. J., et al. (2013). Small genomes and sparse metabolisms of sediment-associated bacteria from four candidate phyla. *mBio* 4:e00708-13. doi: 10.1128/mBio.00708-13

Karamanlioglu, M., Preziosi, R., and Geoffrey D. R. (2017). Abiotic and biotic environmental degradation of the bioplastic polymer poly(lactic acid): a review. *Polym. Degrad. Stabil.* 137, 122–130. doi: 10.1016/j.polymdegradstab.2017.01.009

Karamanlioglu, M., and Robson, G. D. (2013). The influence of biotic and abiotic factors on the rate of degradation of poly(lactic) acid (PLA) coupons buried in compost and soil. *Polym. Degrad. Stabil.* 98, 2063–2071. doi: 10.1016/j.polymdegradstab.2013.07.004

Keswani, A., Oliver, D. M., Gutierrez, T., and Quilliam, R. S. (2016). Microbial hitchhikers on marine plastic debris: human exposure risks at bathing waters and beach environments. *Mar. Environ. Res.* 118, 10–19. doi: 10.1016/j.marenvres.2016.04.006

Kindaichi, T., Yamaoka, S., Uehara, R., Ozaki, N., Ohashi, A., Albertsen, M., et al. (2016). Phylogenetic diversity and ecophysiology of Candidate phylum Saccharibacteria in activated sludge. *FEMS Microbiol. Ecol.* 92, 1–11. doi: 10.1093/femsec/fiw078

Kirstein, I. V., Wichels, A., Gullans, E., Krohne, G., and Gerdts, G. (2019). The plastisphere – uncovering tightly attached plastic "specific" microorganisms. *PLoS One* 14:e215859. doi: 10.1371/journal.pone.0215859

Kirstein, I. V., Wichels, A., Krohne, G., and Gerdts, G. (2018). Mature biofilm communities on synthetic polymers in seawater – specific or general? *Mar. Environ. Res.* 142, 147–154. doi: 10.1016/j.marenvres.2018.09.028

Kleeberg, I., Hetz, C., Kroppenstedt, R. M., Müller, R. J., and Deckwer, W. D. (1998). Biodegradation of aliphatic-aromatic copolyesters by *Thermomonospora fusca* and other thermophilic compost isolates. *Appl. Environ. Microbiol.* 64, 1731–1735. doi: 10.1128/aem.64.5.1731-1735.1998

Kumar Sen, S., and Raut, S. (2015). Microbial degradation of low density polyethylene (LDPE): a review. *J. Environ. Chem. Eng.* 3, 462–473. doi: 10.1016/j.jece.2015.01.003

Laganà, P., Caruso, G., Corsi, I., Bergami, E., Venuti, V., Majolino, D., et al. (2019). Do plastics serve as a possible vector for the spread of antibiotic resistance? First insights from bacteria associated to a polystyrene piece from King George Island (Antarctica). *Int. J. Hyg. Environ. Health* 222, 89–100. doi: 10.1016/j.ijheh.2018.08.009

Lahti, L., and Shetty, S. (2019). *Microbiome R Package (1.8.0)*. Available online at: http://microbiome.github.io (accessed March 4, 2020).

Lapanje, A., Wimmersberger, C., Furrer, G., Brunner, I., and Frey, B. (2012). Pattern of elemental release during the granite dissolution can be changed by aerobic heterotrophic bacterial strains isolated from *Damma glacier* (Central Alps) deglaciated granite. *Microbial. Ecol.* 63, 865–882. doi: 10.1007/s00248-011-9976-7

Lemos, L. N., Medeiros, J. D., Dini-Andreote, F., Fernandes, G. R., Varani, A. M., Oliveira, G., et al. (2019). Genomic signatures and co-occurrence patterns of the ultra-small Saccharimonadia (phylum CPR/Patescibacteria) suggest a symbiotic lifestyle. *Mol. Ecol.* 28, 4259–4271. doi: 10.1111/mec.15208

Leveau, J. H. J., Uroz, S., and de Boer, W. (2010). The bacterial genus *Collimonas*: mycophagy, weathering and other adaptive solutions to life in oligotrophic soil environments. *Environ. Microbiol.* 12, 281–292. doi: 10.1111/j.1462-2920.2009.02010.x

Loredo-Treviño, A., Gutiérrez-Sánchez, G., Rodríguez-Herrera, R., and Aguilar, C. N. (2012). Microbial enzymes involved in polyurethane biodegradation: a review. *J. Polym. Environ.* 20, 258–265. doi: 10.1007/s10924-011-0390-5

Love, M. I., Huber, W., and Anders, S. (2014). Moderated estimation of fold change and dispersion for RNA-seq data with DESeq2. *Genome Biol.* 15, 1–21. doi: 10.1186/s13059-014-0550-8

Luláková, P., Perez-Mon, C., Šantrůčková, H., Ruethi, J., and Frey, B. (2019). High-alpine permafrost and active-layer soil microbiomes differ in their response to elevated temperatures. *Front. Microbiol.* 10:668. doi: 10.3389/fmicb.2019.00668

Malard, L. A., and Pearce, D. A. (2018). Microbial diversity and biogeography in Arctic soils. *Environ. Microbiol. Rep.* 10, 611–625. doi: 10.1111/1758-2229.12680

Martin, M. (2011). Cutadapt removes adapter sequences from high-throughput sequencing reads. *EMBnet J.* 17, 10. doi: 10.14806/ej.17.1.200

McMurdie, P. J., and Holmes, S. (2013). Phyloseq: an R package for reproducible interactive analysis and graphics of microbiome census data. *PLoS One* 8:e0061217. doi: 10.1371/journal.pone.0061217

Mohammadipanah, F., and Wink, J. (2016). Actinobacteria from arid and desert habitats: diversity and biological activity. *Front. Microbiol.* 6:1541. doi: 10.3389/fmicb.2015.01541

Mori, T., Kitano, S., and Kondo, R. (2003). Biodegradation of chloronaphthalenes and polycyclic aromatic hydrocarbons by the white-rot fungus *Phlebia lindtneri*. *Appl. Microbiol. Biotechnol.* 61, 380–383. doi: 10.1007/s00253-003-1253-3

Muroi, F., Tachibana, Y., Kobayashi, Y., Sakurai, T., and Kasuya, K. I. (2016). Influences of poly(butylene adipate-co-terephthalate) on soil microbiota and plant growth. *Polym. Degrad. Stabil.* 129, 338–346. doi: 10.1016/j.polymdegradstab.2016.05.018

Muyzer, G., Teske, A., Wirsen, C. O., and Jannasch, H. W. (1995). Phylogenetic relationships of Thiomicrospiraspecies and their identification in deep-sea

hydrothermal vent samples by denaturing gradient gel electrophoresis of 16S rDNA fragments. *Arch. Microbiol.* 164, 165–172. doi: 10.1007/BF02529967

Nakajima-Kambe, T., Ichihashi, F., Matsuzoe, R., Kato, S., and Shintani, N. (2009a). Degradation of aliphatic-aromatic copolyesters by bacteria that can degrade aliphatic polyesters. *Polym. Degrad. Stabil.* 94, 1901–1905. doi: 10.1016/j.polymdegradstab.2009.08.006

Nakajima-Kambe, T., Toyoshima, K., Saito, C., Takaguchi, H., Akutsu-Shigeno, Y., Sato, M., et al. (2009b). Rapid monomerization of poly(butylene succinate)-co-(butylene adipate) by *Leptothrix* sp. *J. Biosci. Bioeng.* 108, 513–516. doi: 10.1016/j.jbiosc.2009.05.018

Nauendorf, A., Krause, S., Bigalke, N. K., Gorb, E. V., Gorb, S. N., Haeckel, M., et al. (2016). Microbial colonization and degradation of polyethylene and biodegradable plastic bags in temperate fine-grained organic-rich marine sediments. *Mar. Pollut. Bull.* 103, 168–178. doi: 10.1016/j.marpolbul.2015.12.024

Nawaz, A., Hasan, F., and Shah, A. A. (2015). Degradation of poly(ε-caprolactone) (PCL) by a newly isolated Brevundimonas sp. strain MRL-AN1 from soil. *FEMS Microbiol. Lett.* 362, 1–7. doi: 10.1093/femsle/fnu004

Nilsson, R. H., Larsson, K. H., Taylor, A. F. S., Bengtsson-Palme, J., Jeppesen, T. S., Schigel, D., et al. (2019). The UNITE database for molecular identification of fungi: handling dark taxa and parallel taxonomic classifications. *Nucleic Acids Res.* 47, D259–D264. doi: 10.1093/nar/gky1022

Oberbeckmann, S., Kreikemeyer, B., and Labrenz, M. (2018). Environmental factors support the formation of specific bacterial assemblages on microplastics. *Front. Microbiol.* 8:2709. doi: 10.3389/fmicb.2017.02709

Oberbeckmann, S., Osborn, A. M., and Duhaime, M. B. (2016). Microbes on a bottle: substrate, season and geography influence community composition of microbes colonizing marine plastic debris. *PLoS One* 11:e159289. doi: 10.1371/journal.pone.0159289

O'Brine, T., and Thompson, R. C. (2010). Degradation of plastic carrier bags in the marine environment. *Mar. Pollut. Bull.* 60, 2279–2283. doi: 10.1016/j.marpolbul.2010.08.005

Ogonowski, M., Motiei, A., Ininbergs, K., Hell, E., Gerdes, Z., Udekwu, K. I., et al. (2018). Evidence for selective bacterial community structuring on microplastics. *Environ. Microbiol.* 20, 2796–2808. doi: 10.1111/1462-2920.14120

Pathak, V. M., and Navneet. (2017). Review on the current status of polymer degradation: a microbial approach. *Bioresour. Bioprocess* 4:15. doi: 10.1186/s40643-017-0145-9

Pérez-Pantoja, D., Donoso, R., Agulló, L., Córdova, M., Seeger, M., Pieper, D. H., et al. (2012). Genomic analysis of the potential for aromatic compounds biodegradation in Burkholderiales. *Environ. Microbiol.* 14, 1091–1117. doi: 10.1111/j.1462-2920.2011.02613.x

Pham, V. H. T., Jeong, S. W., and Kim, J. (2015). *Aquabacterium olei* sp. nov., an oil-degrading bacterium isolated from oil-contaminated soil. *Int. J. Syst. Evol. Microbiol.* 65, 3597–3602. doi: 10.1099/ijsem.0.000458

Piehl, S., Leibner, A., Löder, M. G. J., Dris, R., Bogner, C., and Laforsch, C. (2018). Identification and quantification of macro- and microplastics on an agricultural farmland. *Sci. Rep.* 8:17950. doi: 10.1038/s41598-018-36172-y

PlasticsEurope. (2018). *Plastics - The facts 2017*. Brussels: PlasticsEurope.

Pontes, A., Ruethi, J., Frey, B., Aires, A., Thomas, A., Overy, D., et al. (2020). *Cryolevonia* gen. nov. and *Cryolevonia schafbergensis* sp. nov., a cryophilic yeast from ancient permafrost and melted sea ice. *Int. J. Syst. Evol. Microbiol.* 70, 2334–2338. doi: 10.1099/ijsem.0.004040

Pushkareva, E., Eckhardt, K. U., Hotter, V., Frossard, A., Leinweber, P., Frey, B., et al. (2020). Chemical composition of soil organic matter and potential enzyme activity in the topsoil along a moisture gradient in the High Arctic (Svalbard). *Geoderma* 368, 114304. doi: 10.1016/j.geoderma.2020.114304

Quast, C., Pruesse, E., Yilmaz, P., Gerken, J., Schweer, T., Yarza, P., et al. (2013). The SILVA ribosomal RNA gene database project: improved data processing and web-based tools. *Nucleic Acids Res.* 41, 590–596. doi: 10.1093/nar/gks1219

R Development Core Team (2008). *R: A Language and Environment for Statistical Computing. (3.6.2)*. Vienna: R Foundation for Statistical Computing.

Rice, A. V., and Currah, R. S. (2005). Oidiodendron: a survey of the named species and related anamorphs of Myxotrichum. *Stud. Mycol.* 53, 83–120. doi: 10.3114/sim.53.1.83

Rillig, M. C., Lehmann, A., de Souza Machado, A. A., and Yang, G. (2019). Microplastic effects on plants. *New Phytol.* 223, 1066–1070. doi: 10.1111/nph.15794

Rime, T., Hartmann, M., and Frey, B. (2016). Potential sources of microbial colonizers in an initial soil ecosystem after retreat of an alpine glacier. *ISME J.* 10, 1625–1641. doi: 10.1038/ismej.2015.238

Rosenberg, E., DeLong, E. F., Lory, S., Stackebrandt, E., and Thompson, F. (2014). *The Prokaryotes: Actinobacteria*. Berlin: Springer.

Satola, B., Wübbeler, J. H., and Steinbüchel, A. (2013). Metabolic characteristics of the species Variovorax paradoxus. *Appl. Microbiol. Biot.* 97, 541–560. doi: 10.1007/s00253-012-4585-z

Scheurer, M., and Bigalke, M. (2018). Microplastics in Swiss Floodplain soils. *Environ. Sci. Technol.* 52, 3591–3598. doi: 10.1021/acs.est.7b06003

Schloss, P. D., Westcott, S. L., Ryabin, T., Hall, J. R., Hartmann, M., Hollister, E. B., et al. (2009). Introducing mothur: open-source, platform-independent, community-supported software for describing and comparing microbial communities. *Appl. Environ. Microbiol.* 75, 7537–7541. doi: 10.1128/AEM.01541-09

Secretariat of the Convention of Biological Diversity (2016). *Marine Debris: Understanding, Preventing and Mitigating the Significant Adverse Impacts on Marine and Coastal Biodiversity. CBD Technical Series* (Vol. 83). Montreal, QC: Convention of Biological Diversity, doi: 10.1080/14888386.2007.9712830

Shen, M., Zhang, Y., Zhu, Y., Song, B., Zeng, G., Hu, D., et al. (2019). Recent advances in toxicological research of nanoplastics in the environment: a review. *Environ. Pollut.* 252, 511–521. doi: 10.1016/j.envpol.2019.05.102

Shi, Y., Grogan, P., Sun, H., Xiong, J., Yang, Y., Zhou, J., et al. (2015). Multi-scale variability analysis reveals the importance of spatial distance in shaping Arctic soil microbial functional communities. *Soil Biol. Biochem.* 86, 126–134. doi: 10.1016/j.soilbio.2015.03.028

Shogren, R. L., Doane, W. M., Garlotta, D., Lawton, J. W., and Willett, J. L. (2003). Biodegradation of starch/polylactic acid/poly(hydroxyester-ether) composite bars in soil. *Polym. Degrad. Stabil.* 79, 405–411. doi: 10.1016/S0141-3910(02)00356-7

Singh, B., and Sharma, N. (2008). Mechanistic implications of plastic degradation. *Polym. Degrad. Stabil.* 93, 561–584. doi: 10.1016/j.polymdegradstab.2007.11.008

Smith, M., Love, D. C., Rochman, C. M., and Neff, R. A. (2018). Microplastics in seafood and the implications for human health. *Curr. Environ. Health Rep.* 5, 375–386. doi: 10.1007/s40572-018-0206-z

Ssekagiri, A. (2020). *microbiomeSeq: Microbial Community Analysis in an Environmental Context (0.1)*. Available online at: http://www.github.com/umerijaz/microbiomeSeq (accessed March 4, 2020).

Starr, E. P., Shi, S., Blazewicz, S. J., Probst, A. J., Herman, D. J., Firestone, M. K., et al. (2018). Stable isotope informed genome-resolved metagenomics reveals that *Saccharibacteria* carbon. *Microbiome* 6:122.

Tejeda-Agredano, M. C., Gallego, S., Vila, J., Grifoll, M., Ortega-Calvo, J. J., and Cantos, M. (2013). Influence of the sunflower rhizosphere on the biodegradation of PAHs in soil. *Soil Biol. Biochem.* 57, 830–840. doi: 10.1016/j.soilbio.2012.08.008

Thiel, M., Luna-Jorquera, G., álvarez-Varas, R., Gallardo, C., Hinojosa, I. A., Luna, N., et al. (2018). Impacts of marine plastic pollution from continental coasts to subtropical gyres-fish, seabirds, and other vertebrates in the SE Pacific. *Front. Mar. Sci.* 5:238. doi: 10.3389/fmars.2018.00238

Uchida, H., Nakajima-Kambe, T., Shigeno-Akutsu, Y., Nomura, N., Tokiwa, Y., and Nakahara, T. (2000). Properties of a bacterium which degrades solid poly(tetramethylene succinate)-co-adipate, a biodegradable plastic. *FEMS Microbiol. Lett.* 189, 25–29. doi: 10.1016/S0378-1097(00)00246-9

Ventura, M., Canchaya, C., Tauch, A., Chandra, G., Fitzgerald, G. F., Chater, K. F., et al. (2007). Genomics of actinobacteria: tracing the evolutionary history of an ancient phylum. *Microbiol. Mol. Biol. Rev.* 71, 495–548. doi: 10.1128/mmbr.00005-07

Wallace, P. W., Haernvall, K., Ribitsch, D., Zitzenbacher, S., Schittmayer, M., Steinkellner, G., et al. (2017). PpEst is a novel PBAT degrading polyesterase identified by proteomic screening of *Pseudomonas* pseudoalcaligenes. *Appl. Microbiol. Biotechnol.* 101, 2291–2303. doi: 10.1007/s00253-016-7992-8

Wang, J., Lv, S., Zhang, M., Chen, G., Zhu, T., Zhang, S., et al. (2016). Effects of plastic film residues on occurrence of phthalates and microbial activity in soils. *Chemosphere* 151, 171–177. doi: 10.1016/j.chemosphere.2016.02.076

Wang, Q., Garrity, G. M., Tiedje, J. M., and Cole, J. R. (2007). Naïve Bayesian classifier for rapid assignment of rRNA sequences into the new bacterial taxonomy. *Appl. Environ. Microbiol.* 73, 5261–5267. doi: 10.1128/AEM.00062-07

White, T., Bruns, T., Lee, S., and Taylor, J. (1990). "Amplification and direct sequencing of fungal ribosomal RNA genes for phylogenetics," in *PCR Protocols: A Guide to Meth- Ods and Applications*, eds M. Innis, D. Gelfand, J. Sninsko, and T. White (San Diego, CA: Academic Press), 315–322.

Wickham, H. (2016). *ggplot2: Elegant Graphics for Data Analysis* (3.2.1). New York, NY: Springer-Verlag.

Wilkes, R. A., and Aristilde, L. (2017). Degradation and metabolism of synthetic plastics and associated products by *Pseudomonas* sp.: capabilities and challenges. *J. Appl. Microbiol.* 123, 582–593. doi: 10.1111/jam.13472

Willumsen, P. A., Johansen, J. E., Karlson, U., and Hansen, B. M. (2005). Isolation and taxonomic affiliation of N-heterocyclic aromatic hydrocarbon-transforming bacteria. *Appl. Microbiol. Biotechnol.* 67, 420–428. doi: 10.1007/s00253-004-1799-8

Wilson, F. P., Liu, X., Mattes, T. E., and Cupples, A. M. (2016). *Nocardioides, Sediminibacterium, Aquabacterium, Variovorax*, and *Pseudomonas* linked to carbon uptake during aerobic vinyl chloride biodegradation. *Environ. Sci. Pollut. Res. Int* 23, 19062–19070. doi: 10.1007/s11356-016-7099-x

Winquist, E., Björklöf, K., Schultz, E., Räsänen, M., Salonen, K., Anasonye, F., et al. (2014). Bioremediation of PAH-contaminated soil with fungi - From laboratory to field scale. *Int. Biodeter. Biodegr.* 86, 238–247. doi: 10.1016/j.ibiod.2013.09.012

Wolf, A. B., Vos, M., De Boer, W., and Kowalchuk, G. A. (2013). Impact of matric potential and pore size distribution on growth dynamics of filamentous and non-filamentous soil bacteria. *PLoS One* 8:e83661. doi: 10.1371/journal.pone.0083661

Woudenberg, J. H. C., Groenewald, J. Z., Binder, M., and Crous, P. W. (2013). Alternaria redefined. *Stud. Mycol.* 75, 171–212. doi: 10.3114/sim0015

Wright, S. L., and Kelly, F. J. (2017). Plastic and human health: a micro issue? *Environ. Sci. Technol.* 51, 6634–6647. doi: 10.1021/acs.est.7b00423

Yagi, H., Ninomiya, F., Funabashi, M., and Kunioka, M. (2014). Mesophilic anaerobic biodegradation test and analysis of eubacteria and archaea involved in anaerobic biodegradation of four specified biodegradable polyesters. *Polym. Degrad. Stabil.* 110, 278–283. doi: 10.1016/j.polymdegradstab.2014.08.031

Zettler, E. R., Mincer, T. J., and Amaral-Zettler, L. A. (2013). Life in the "plastisphere": microbial communities on plastic marine debris. *Environ. Sci. Technol.* 47, 7137–7146. doi: 10.1021/es401288x

Zhang, G. S., and Liu, Y. F. (2018). The distribution of microplastics in soil aggregate fractions in southwestern China. *Sci. Total Environ.* 642, 12–20. doi: 10.1016/j.scitotenv.2018.06.004

Conflict of Interest: The authors declare that the research was conducted in the absence of any commercial or financial relationships that could be construed as a potential conflict of interest.

frontiers in Environmental Science

SYSTEMATIC REVIEW
published: 24 September 2020
doi: 10.3389/fenvs.2020.574008

The Paleoecology of Microplastic Contamination

*Chiara E. P. Bancone[1], Simon D. Turner[1], Juliana A. Ivar do Sul[2] and Neil L. Rose[1]**

[1] Department of Geography, Environmental Change Research Centre, University College London, London, United Kingdom, [2] Leibniz Institute for Baltic Sea Research, Rostock, Germany

While the ubiquity and rising abundance of microplastic contamination is becoming increasingly well-known, there is very little empirical data for the scale of their historical inputs to the environment. For many pollutants, where long-term monitoring is absent, paleoecological approaches (the use of naturally-accumulating archives to assess temporal trends) have been widely applied to determine such historical patterns, but to date this has been undertaken only very rarely for microplastics, despite the enormous potential to identify the scale and extent of inputs as well as rates of change. In this paper, we briefly assess the long-term monitoring and paleoecological microplastic literature before considering the advantages and disadvantages of various natural archives (including lake and marine sediments, ice cores and peat archives) as a means to determine historical microplastic records, as well as the range of challenges facing those attempting to extract microplastics from them. We also outline some of the major considerations in chemical, physical and biological taphonomic processes for microplastics as these are critical to the correct interpretation of microplastic paleoecological records but are currently rarely considered. Finally, we assess the usefulness of microplastic paleoecological records as a stratigraphic tool, both as a means to provide potential chronological information, as well as a possible marker for the proposed Anthropocene Epoch.

Keywords: Anthropocene, anthropogenic particles, chemostratigraphic units, ice cores, peats, sediment cores, taphonomy

OPEN ACCESS

Edited by:
Hans Peter Heinrich Arp, Norwegian Geotechnical Institute, Norway

Reviewed by:
Clare Alexandra Wilson, University of Stirling, United Kingdom
Saija Maarit Saarni, University of Helsinki, Finland

****Correspondence:***
Neil L. Rose
n.rose@ucl.ac.uk

Specialty section:
This article was submitted to Toxicology, Pollution and the Environment, a section of the journal Frontiers in Environmental Science

Received: *18 June 2020*
Accepted: *14 August 2020*
Published: *24 September 2020*

Citation:
Bancone CEP, Turner SD, Ivar do Sul JA and Rose NL (2020) The Paleoecology of Microplastic Contamination. Front. Environ. Sci. 8:574008. doi: 10.3389/fenvs.2020.574008

RESEARCH HIGHLIGHTS

- The concept of paleoecology is explored from a microplastic context
- Dated natural archives provide reliable microplastic temporal records
- Taphonomic processes influence microplastic transport and accumulation
- Microplastic/polymers have utility as stratigraphic markers in sediments
- Methodological standardization is required in microplastic paleoecology.

INTRODUCTION

Microplastics are now considered ubiquitous in the environment. They have been recorded in polar ice (Obbard et al., 2014), within amphipods in the deepest ocean trenches (Jamieson et al., 2017), and in the atmosphere and sediments of remote mountain lakes (Free et al., 2014; Allen et al., 2019). They have been recorded in high concentrations in fresh- and ocean surface waters, in a

wide range of biota and terrestrial soils and therefore represent evidence of diverse anthropogenic contamination sources on a global scale.

Although there is currently no standardized definition, microplastics are generally understood to be solid, insoluble, polymeric or co-polymeric materials either created (primary microplastics) or fragmented (secondary) to a size of below 5 mm. There have been a number of proposals calling for standardization of terminology but even these have different classifications. Hartmann et al. (2019) suggested a size-range of 1–1,000 μm while Frias and Nash (2019) proposed 1 μ m to 5 mm, and the European Chemical Agency, 1 nm−5 mm (ECHA, European Chemicals Agency, 2019) for intentional (i.e., primary) microplastics. Within these size-bounds the term encompasses a wide range of polymers to which a further variety of additives including plasticizers, flame retardants and stabilizers may have been added, as well as a broad range of morphologies from fibers and fragments to beads, films and foams and all imaginable colors (Rochman et al., 2019). Furthermore, these particles may adsorb contaminants including persistent organic pollutants and trace metals and provide a transfer mechanism for attached microbiota. Such contaminant adsorption may be enhanced during environmental weathering as surface areas increase (Teuten et al., 2009). Clearly, microplastics cannot be considered a single contaminant but rather a "diverse contaminant suite" (Rochman et al., 2019) and this raises considerable challenges in their extraction and analysis from within environmental compartments. However, while many of the properties of microplastics are wide-ranging, physical and chemical durability are commonplace. These properties, plus the dramatic increase in plastic production in recent decades, reaching more than 359 million tons in 2018 (Plastics Europe, 2019) (**Figure 1**), have resulted in their global ubiquity and preservation.

The majority of microplastics studies have been undertaken in the oceans with far fewer in freshwater, terrestrial and atmospheric systems (Meng et al., 2020). However, although there is now considerable information on the distribution of macro- and microplastic abundance in ocean surface waters and shorelines, and rapidly increasing knowledge on chemical and morphological classes, there remains very little information on temporal changes. For example, the rates at which microplastic inputs to aquatic and terrestrial systems are increasing is very poorly understood even though this would provide valuable insights into the potential exposure to biota. The relative novelty of microplastics as an environmental contaminant has so far precluded any long-term monitoring of concentrations and even for macroplastics such data are sparse.

Where such long-term data have been absent, paleoecological approaches, the use of naturally accumulating archives to provide historical data of varying resolution and longevity, have been widely used to assess physical, biological and chemical change. However, this has only recently started to be applied to microplastics. As a result, the science of microplastic paleoecology is in its infancy and studies to date are generally limited to producing historical profiles from individual sites and comparing these against broad-scale, plastic production data. However, the development of paleoecology tells us that there are considerable challenges to the interpretation of the records stored in natural archives and that such comparisons may come to be viewed as rather simplistic. These challenges are not only those of using standardized and comparable techniques and units between studies, although these remain for microplastics, but also issues around taphonomy, i.e., the processes affecting how microplastics of varying provenance are transported to, and buried within, the selected archive location. Future paleoecological studies involving microplastics will certainly have to consider these issues. The aims of this paper, therefore, are 4-fold: (i) to assess the current status of microplastic paleoecology and highlight gaps in knowledge; (ii) to consider the advantages and disadvantages of common natural archives for determining microplastic records; (iii) to use paleoecological knowledge to highlight some of the issues and uncertainties that will need to be considered for future microplastic records to be interpreted in a more robust way; and (iv) in the light of these issues, consider how microplastic paleoecological records may be used chronologically as a stratigraphic marker, e.g., for the proposed Anthropocene Epoch (Zalasiewicz et al., 2016).

LONG-TERM RECORDS OF MACRO- AND MICROPLASTICS

With the rapid increase in global plastic production and the input of debris into the oceans it might be expected that increasing trends in macroplastics would be observed throughout the world, but data indicate that trends are far more ambiguous. At the HAUSGARTEN deep-sea observatory (located at 79°N 4°E; 2,500 m below the ocean surface), litter densities increased from 3,635 to 7,710 km^{-2} between 2004 and 2011, and especially since 2007, with plastics remaining the dominant litter-type throughout (Bergmann and Klages, 2012). However, on shores around Antarctic islands, abundances in plastic accumulation between 1990 and 2006 were similar and may even have declined (Barnes et al., 2009). In Hawaii, debris densities showed considerable inter-annual variability between 1990 and 2006 but no directional trend, while in the UK, debris increased steadily from 1994 (Barnes et al., 2009). In South Africa, trends in the number of plastic bottles increased between 1984 and 2005 on beaches with no cleaning programmes but stayed much the same where those programmes existed. By contrast, numbers of plastic bottle lids increased in both locations, thought to be due to their small size, i.e., that they might be overlooked by beach-cleaning teams (Ryan et al., 2009). The monitoring of plastic on the floor of the North Sea has been undertaken since 1992 and also shows considerable variation in spatial litter densities (for example, between 0 and 1835 km^{-2} in 2011). Here, no clear difference was observed between near-shore and off-shore areas (Maes et al., 2018) and while 63% of all sampling trawls over the 25 years contained plastic, there was no significant trend through the monitoring period. However, trends in specific litter categories such as plastic sheeting (including packaging) and "fishing-related" debris (including fishing line, cable ties, straps, and crates) did show statistically significant increases while plastic bags were the only category to show a negative

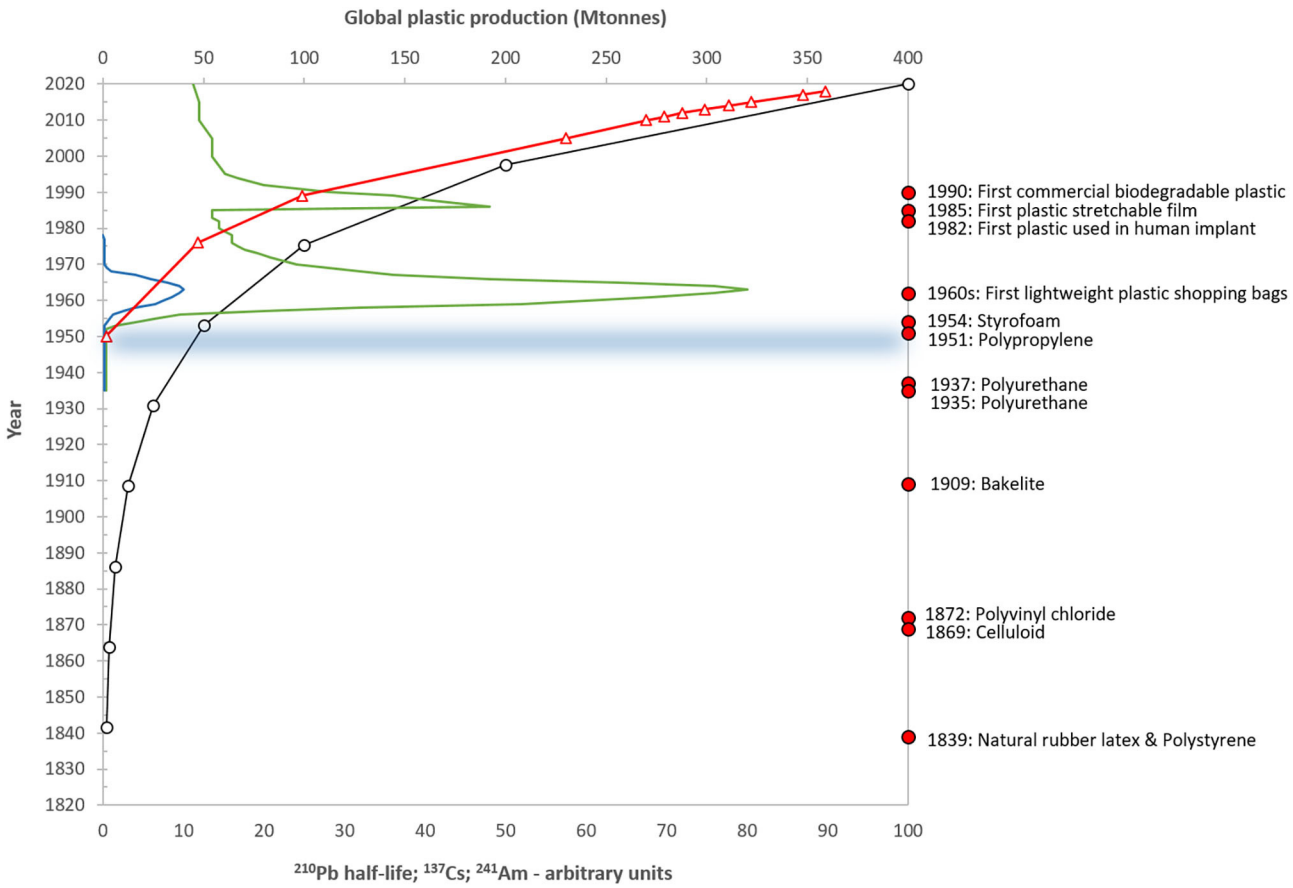

FIGURE 1 | Schematic diagram showing the timescales of radiometric dating techniques for natural archives, including the decay of the natural isotope ^{210}Pb (half-life 22.23 years; open circles); the 1963 nuclear weapons bomb-testing peaks of ^{137}Cs (green line) and ^{241}Am (blue line); and the Chernobyl reactor accident in 1986 (^{137}Cs). The global production of plastics in millions of tons is also shown (red triangles) (data from Plastics Europe, 2012, 2016, 2019) along with selected moments in plastic production history (taken from Crawford and Quinn, 2016) and the start of the proposed Anthropocene Epoch in circa. 1950 (horizontal line).

trend, considered to be due to the implementation of a plastic bag charge in some regions around the North Sea (Maes et al., 2018).

While shore-line monitoring data appear to show no consistent temporal trends in macroplastic accumulation after the 1990s (Barnes and Milner, 2005; Barnes et al., 2009), the occurrence of plastics associated with wildlife does. For example, the percentage of kittiwake (*Rissa tridactyla*) nests in Denmark containing plastic debris increased from 39 to 57% between 1992 and 2005 (Hartwig et al., 2007), while the number of seals in California entangled in plastic debris and the percentage of prions (*Pachyptila* spp.) reported with plastics in their stomachs have largely shown steady growth since these records began (Ryan et al., 2009). More recently, a 60-year time-series (1957–2016) of marine plastics in the North Atlantic based on records of entanglement by trawls of the Continuous Plankton Recorder has shown a marked increase in macroplastic abundance especially since the 1990s (Ostle et al., 2019). Unfortunately, for microplastics, no similar long-term datasets exist and, in the absence of monitoring, paleoecological approaches, using the accumulation of natural archives such as lake and marine sediments, ice cores and peat sequences, are one of the only ways to assess temporal trends in the environment.

THE VALUE OF CONTAMINANT PALEOECOLOGY

The paleoecological approach has been used to observe temporal trends for a wide-range of contaminants in many areas around the world including trace metals (Yang et al., 2010), fly-ash particles (Rose, 2015) and a large number of different organic chemicals such as organochlorine pesticides (Muir et al., 1995; Lin et al., 2012), brominated flame retardants (Yang et al., 2016), and pharmaceuticals (Kerrigan et al., 2018).

Paleoecology uses the properties of undisturbed natural archives and the law of superposition to observe and record environmental change over a broad range of historical scales from annual (Gajewski et al., 1997; Kinder et al., 2019) to millennial (Meyers and Lallier-Vergès, 1999). For lake systems, where the majority of this work has been undertaken, benthic sediments provide a means to determine the changes occurring

both within the lake and its catchment as well as atmospheric deposition from local, regional and long-range sources. Lake sediments include not just records of contaminants and other stressors, but also the preservation of a broad range of biological remains from single-celled algae, such as diatoms, to invertebrates (e.g., chironomid head capsules; mollusc shells), plant pollen and macro-fossils (seeds, spores) to fish-scales. As a result, these natural archives contain a record of both stressors and biological response and so are powerful tools in exploring environmental change. However, while they can clearly show directions of change, i.e., increases or decreases in contaminant concentrations or changes in the abundance of different species, it is the use of dating techniques to provide robust chronologies that allows rates of change to be determined. For the microplastic time period (i.e., since c. 1950) (**Figure 1**) such chronological approaches are mainly radiometric (e.g., ^{210}Pb, ^{137}Cs, ^{241}Am) and these can provide accurate dates to a sub-decadal resolution or better. Other approaches to sediment dating such as the counting of annual varves are clearly better than this but are only rarely present.

Microplastic concentrations have been reported in a number of environmental archives including lake (Imhof et al., 2013; Fischer et al., 2016; Vaughan et al., 2017), river (Klein et al., 2015; Hurley et al., 2018a; Peng et al., 2018), deep-sea and coastal sediments (Claessens et al., 2011; Van Cauwenberghe et al., 2013; Nor and Obbard, 2014; Woodall et al., 2014), as well as soils (Scheurer and Bigalke, 2018) and ice (Obbard et al., 2014; Peeken et al., 2018) and so there is clearly considerable potential. However, very few studies have considered using these records to observe changes in microplastic abundance and type through time and even fewer have also employed chronological techniques.

In 2011, Claessens et al. presented microplastic concentrations in beach sediments from four different depths from Groenendijk-Bad, Belgium showing an increase from 54.7 ± 8.7 to 156.2 ± 6.3 particles kg^{-1} dry sediment between 1993–96 and 2005–08. However, these dates were not derived from direct chronological measurements but rather from annual local deposition rates produced from coast-line maps. Similarly, Matsuguma et al. (2017) reported changing concentrations of microplastics in sediments from a range of locations in Asia and Africa including Tokyo Bay, the moat of the Imperial Palace in Tokyo, the Gulf of Thailand, the Straits of Johor in Malaysia and Durban Bay, South Africa. For most of these sites, microplastic concentrations were compared within just two or three sediment depths and, although they were not dated, the particles were allocated to a polymer-type by Fourier-Transform Infra-Red spectrometry (FT-IR) thereby providing information on changing sources at different, albeit unspecified, times. A more detailed profile (six undated sediment levels) were analyzed from a canal in Tokyo Bay. In Lake Ontario, Corcoran et al. (2015) reported increases in microplastic concentrations in surficial sediments (0–8 cm depth, no microplastics found below 8 cm). Although these sediment cores were also not directly dated, comparison with sediment accumulation rates from cores taken elsewhere indicated that the first presence of microplastics probably occurred between 1977 and 1997.

Very few studies have so far undertaken the analysis of microplastics on directly dated sediment cores. In 2019, Turner et al. reported on microplastic concentrations from a ^{210}Pb-dated sediment core taken from an urban lake in north London, UK. Here, an increase in microplastic concentrations (number kg^{-1} dry sediment) and accumulation rates (number m^{-2} yr^{-1}) was evident after the late-1950s and these were analyzed by Raman spectroscopy to reveal that the main polymer-type was polystyrene, while polyacrylonitrile and polyvinyl chloride fibers were also prevalent. Then, just a few months later, Brandon et al. (2019) presented microplastic accumulation rates for a varved marine sediment core collected from 580 m water depth in the Santa Barbara Basin, off the coast of California. Although polymer data through time were not reported, the microplastic accumulation rates showed an excellent agreement with trends in global plastic production, and increased rates, especially from the 1970s onwards, were driven mainly by microplastic fibers and fragments. Most recently, two further studies have been produced, both from China. First, Dong et al. (2020) produced a microplastics profile from Donghu in Wuhan, Hubei Province. Here, fibers were the only microplastic-type found to be present but their increasing concentrations, through the lake sediment record since 1960, showed a very good agreement with global synthetic fiber production. Second, Xue et al. (2020) produced a microplastic concentration profile from a sediment core taken from the Beibu Gulf in south China and found that peak concentrations occurred in the 1930s, although a presence of microplastics was recorded throughout the core, including basal sediments dated to c.1897. The presence of microplastics in these early sediments was attributed to bioturbation by burrowing invertebrates such as "peanut" worms (*Sipunculus nudus*) and lugworms (*Arenicola marina*). Clearly, such disturbances need to be taken into consideration when selecting both coring locations as well as appropriate cores for analysis, otherwise interpretation of temporal trends is exceptionally difficult or impossible. As these few studies show, there is enormous untapped potential for exploring natural archives to provide temporal trends and accumulation rates of microplastics in a range of environments. These can provide information on increasing risk to biotic, including human, health as well as providing their own chronological information. However, the derivation of robust microplastic data from these records also presents considerable analytical and interpretative challenges.

MICROPLASTIC PALEOECOLOGY IN DIFFERENT NATURAL ARCHIVES

A wide range of natural archives have been used to provide temporal records of environmental change including freshwater and marine sediments, ice cores, peat sequences, speleothems, tree-rings, corals, whale ear wax plugs and faunal (e.g., bird, bat) middens. More intermittent records have also been compiled from teeth, antlers and bird eggs as well as from herbaria and museum specimens. Not all of these archives have been used for microplastic records and a number would not be

appropriate. Here, we consider only the more commonly used paleoarchives (**Table 1**).

Marine Sediments

As concentrations of microplastic contamination in deep-sea sediments from the Atlantic Ocean, Mediterranean Sea and Indian Ocean have been found to be up to four orders of magnitude higher than in surface waters, these profundal areas (more than 300 million km^2) are likely to be a global sink for microplastic debris (Woodall et al., 2014). For example, Tekman et al. (2020) found that Arctic Ocean sediments contained microplastic concentrations 16,000 times higher than in the water column. Less disturbed than shallow waters and less exposed to storm water discharge, waves, tides, currents, landslides and dredging (Mulder et al., 2011), deep-sea sediments have a great potential for reconstructing the deposition histories of microplastic contamination. Marine sediment records have shown a close correlation between increasing worldwide plastic production and microplastic concentrations (Brandon et al., 2019) while comparisons between different locations may be applied to transport models in order to extrapolate microplastic distributions and to predict potential "hot-spots" of plastic deposition, as has already been successfully undertaken for surface waters (Law et al., 2010; Pagter et al., 2018).

The distribution and preservation of contaminants in marine sediment cores is determined by site-specific factors such as sedimentation rate and bioturbation (Johannessen and Macdonald, 2012; Outridge and Wang, 2015) and the mechanisms by which microplastics reach and deposit on the sea floor are still poorly understood (Gregory, 2009). If floating microplastic particles become denser due to heavy biofouling they may sink and be deposited as "marine snow" (Zhao et al., 2017; Porter et al., 2018). This comprises microaggregates of phytoplankton, organic matter and clay particles held together by extracellular polymeric material and sinking rates in marine systems range from 1 to 368 m d^{-1} (Alldredge and Silver, 1988). Therefore, deposition to some deep-sea locations may only occur several years after the microplastic particles originally entered the marine environment (Van Cauwenberghe et al., 2013). As a consequence, some deep-sea depositional systems characterized by very slow sedimentation rates are not likely to offer a high-resolution stratigraphy over short timescales. Very low deposition rates might compromise the possibility of estimating deposition and microplastic concentrations, even in undisturbed sediments, except on longer timescales. A potential solution to this issue might be to collect benthic samples from areas where overlying surface waters are highly productive, facilitating the sinking of microplastics to the seafloor via biofouling, ingestion, and formation of fecal pellets and enhancing sedimentation rates (Brandon et al., 2019).

Another factor affecting distribution of microplastics within marine sediments is bioturbation. This process of sediment reworking by living organisms (e.g., by lug-worms, *Arenicola spp*., which can live up to 70 cm below the sediment surface) (Claessens et al., 2011) alters sediment stratigraphies and can occur during or after deposition (Mulder et al., 2011). As a result, upper sediment layers potentially containing microplastics, could be partially or totally homogenized compromising the true temporal record (Claessens et al., 2011). To avoid such disturbance, areas of anerobic bottom water or low-oxygen marine basins should be chosen for sample collection. This minimizes the possibility of bioturbation and increases the likelihood of collecting undisturbed sediments containing continuous temporal microplastic records (Brandon et al., 2019).

Finally, while undisturbed deep-sea marine sediment cores may represent an excellent archive for analyzing long-term historical trends of microplastic accumulation, the provenance of microplastics depositing there is difficult to reliably predict as they may cover a very large source area. Almost all microplastics ending up in deep-sea sediments will have originated from sites located on the continental margin (Van Cauwenberghe et al., 2013) and ocean circulation dynamics will control both their vertical and horizontal transfer from these coastal regions to deeper areas where they ultimately sink (Galgani et al., 1995, 1996; Van Cauwenberghe et al., 2013; Woodall et al., 2014). The heterogeneity of microplastic abundances in sediments is a result of different densities, buoyancies and residence times in the water which are further affected by factors including wave-mixing, fragmentation and biofouling (Galloway et al., 2017; Erni-Cassola et al., 2019) as well as a wide range of potential sources (Woodall et al., 2014; Tekman et al., 2020). Consequently, while marine archives, collected from appropriate locations, may provide a useful tool for understanding long-term historical trends in microplastic contamination they are unlikely to be able to provide information on the precise origin of the microplastic debris accumulated there (Woodall et al., 2014; Tekman et al., 2020).

Lake Sediments

As with marine environments, lake sediments are likely to be a final sink for both low-density positively-buoyant and high-density negatively-buoyant microplastics (Barnes et al., 2009). Many synthetic polymers with densities less than that of water, such as polyethylene and polypropylene, will be buoyant as they enter a lake and will only deposit to benthic habitats once their density has increased due to biofouling (Andrady, 2011; Woodall et al., 2014), the "fecal express" (Cole et al., 2013; Setälä et al., 2014; Zalasiewicz et al., 2016) or via the adsorption of particulate matter to plastic surfaces (Frias et al., 2016). Although data are more sparse for freshwaters than for marine systems, these processes are likely to result in the substantial accumulation of microplastics in lake sediments (Woodall et al., 2014; Tekman et al., 2020) and research shows that microplastic concentrations in freshwaters and their sediments are comparable to those in marine environments (Corcoran et al., 2015; Ballent et al., 2016; Klein et al., 2018). Furthermore, as observed by Dong et al. (2020) and Turner et al. (2019), down-core variations in microplastic abundance and polymer-type can be observed in lake sediments and may reflect changes in plastic production and usage, providing a temporal perspective to our understanding of microplastic inputs to lakes which has, to date, been underexplored.

Although contaminant deposition in lake sediments is controlled by factors including lake hydrology and bathymetry,

TABLE 1 | Strengths and weaknesses of the principal natural archives for microplastic records.

Archive	Strengths	Weaknesses
Lake sediments (also ponds and reservoirs)	• Spatial distribution: there are an estimated 300+ million lakes worldwide (Downing et al., 2006) • Accumulation rate allows sub-decadal to annual resolution for microplastic records (e.g., laminae and varves) • Typically low-level bioturbation, especially in anerobic basins • Generally easy to sample from boats or from ice surfaces • Well-defined hydrological catchments	• Sediment focusing (movement of sediments down slope to profundal areas) • Variable accumulation rates requires independent dating • Small-scale bioturbation causes smoothing of records • Potential for anthropogenic disturbance, especially in urban and lowland lakes
Marine sediments	• Potentially around 70% of the Earth's surface available for sampling • Lack of disturbance of deep-water sediments • Shallow waters can be easy to sample	• Deep-water sediments have very low accumulation rates reducing resolution of microplastic records • Deep-water sediments are difficult to obtain • Shallow coastal waters may be highly dynamic leading to disturbance • May have significant bioturbation • "Catchment" for deposited microplastics is very large and potentially variable
Peats	• No "sediment" focusing issues • Exclusively atmospheric inputs • Good spatial distribution • Generally easy to sample • Accumulation rate allows sub-decadal to annual resolution	• Accumulation rates vary as peat grows and decays • Poor consolidation of most recent material • Bioturbation from plant roots may alter microplastic records
Ice cores	• No focusing problems • High accumulation rates allow sub-annual resolution • No bioturbation • Exclusively atmospheric inputs	• Distribution of sampling sites is spatially limited • Low microplastic concentrations (remote sites; rapid accumulation rates) • Handling/storage/transport of frozen samples from remote locations needs great care • Requires ultraclean laboratories • Loss of recent ice records from ice-cap melting and glacial retreat

the small size and restricted, well-defined catchments when compared to oceans are likely to enable a better differentiation of local and regional hydrological pathways, and regional to global inputs from atmospheric sources (Fischer et al., 2016). Hence, catchment-scale microplastic assessments are possible for freshwater systems which are not possible for ocean sediments where microplastics from long-range transport from multiple catchments, sink and are deposited (Hidalgo-Ruz et al., 2012; Hardesty et al., 2017). As only an estimated 5% of the more than 350 million tons of plastic waste generated each year are directly discharged into the oceans (Xiong et al., 2018), lake sediments are not only generally more accessible for sampling than their marine equivalents, but are also closer to vast terrestrial sources. Furthermore, given that overall lacustrine sedimentation rates are typically an order of magnitude (or more) higher than in marine systems, where sedimentation rates of 1–10 cm Ka^{-1} are common, lake sediments are also likely to offer a good microplastic stratigraphy with high temporal resolution over relatively short timescales (Scholz, 2001).

As in marine environments, where organic aggregates influence the fate and sinking of microplastics, biofilm coverings and combinations of microplastics with organic matter also increase settling rates and accelerate the transport of microplastics to freshwater sediments (Möhlenkamp et al., 2018; Porter et al., 2018). Nutrient enrichment, particularly common in shallow lakes, can result in high primary productivity, increasing biofouling processes and accelerating microplastic deposition and burial (Kaiser et al., 2017). Furthermore, increasing microplastic stress has the potential to lower the resilience of shallow lake food-webs, increasing the probability of abrupt changes (Kong and Koelmans, 2019) and as a result shallow lakes are likely to be priority systems when assessing temporal trends in microplastic contamination.

Shallow waters tend to be better mixed by wind and water currents resulting in a more homogenous distribution of microplastics. By contrast, microplastic deposition in deeper lakes may be affected by lake stratification, resulting in the generation of a thermocline and waters of differing densities. Sinking microplastic particles which have densities similar to that of the epilimnion are likely to remain within this layer and accumulate at the thermocline (Fischer et al., 2016). As a result, the presence of a thermocline might play a key role in microplastic transport and retention within the water column (Zobkov et al., 2019) while seasonal stratification and mixing may affect microplastic sedimentation rates and distribution in sediments. The same may also be true for other aquatic systems where stratification occurs.

Bioturbation by benthic fauna also influences lake sediment microplastic stratigraphies. Tubificid worm bioturbation, for example, is associated with sediment reworking and the production of burrows (Brinkhurst et al., 1972; McCall and Fisher, 1980). In lake sediments, biological mixing of sediments is generally less significant than in marine habitats because of anoxic bottom waters or less active benthic communities (Robbins, 1978; Appleby, 2001), and careful site selection can pre-empt many potential issues. However, human disturbance of

the sediment record is likely a greater issue for many freshwater records than for marine sites, especially for urban lakes. Here, even where sampling points are selected far from the shore there remains a higher potential for disturbance from a range of anthropogenic impacts, including dredging, construction and a wide range of catchment activities. These may result in an altered distribution of contaminants within sediments as well as compromised accumulation and chronologies (Dong et al., 2020). Although urban, shallow water systems can be difficult ones from which to recover undisturbed sediment cores, when they are obtained, they can provide valuable records of microplastic pollution as well as a wide range of other anthropogenic contaminants over the recent historical period (Turner et al., 2019; Dong et al., 2020).

Ice Cores

Ice cores extracted from Antarctic and Greenland ice sheets and from high altitude glaciers can provide important historical records of human activities (Gabrielli and Vallelonga, 2015). Aerially transported debris and contaminants deposited onto the surface are retained and accumulate as ice layers form (Lovett and Kinsman, 1990; Lei and Wania, 2004). Although, to our knowledge, no published research has yet produced microplastic temporal trends and accumulation rates in dated ice cores, due to their high accumulation rates they have the potential to provide very detailed paleo-environmental information on microplastic deposition especially for regions where other archives may be less available (Gabrielli and Vallelonga, 2015). While polar ice core records might be sufficiently remote from anthropogenic sources to provide reconstructions of hemispheric and global atmospheric contamination (McConnell and Edwards, 2008; McConnell et al., 2014), lower-latitude/high-altitude ice cores (i.e., alpine cores) are likely to be more indicative of regional pollution (Eichler et al., 2012; Gabrieli and Barbante, 2014; Uglietti et al., 2015; Beaudon et al., 2017).

Ice cores have been drilled worldwide since the 1950s in order to determine the history of atmospheric pollutants such as lead and mercury as well as other trace metals, organic compounds, radioactive species and black carbon (Gabrielli and Vallelonga, 2015; Gabrielli et al., 2020). Indeed, the major changes occurring in the chemical composition of the atmosphere since the beginning of the Anthropocene are well-recorded in ice cores extracted from polar regions and high-altitude glaciers (Gabrielli and Vallelonga, 2015). As most of these contaminants have been found everywhere from the Northern Hemisphere to Antarctica, it is likely that there are no glaciers or ice sheets where atmospherically-transported anthropogenic contaminants cannot be detected (Gabrielli and Vallelonga, 2015). Therefore, as microplastics are now largely considered to be both ubiquitous and atmospherically transported, ice core studies are also likely to provide archive information on microplastic fallout over the past 80 years.

The efficiency of snow at scavenging contaminants from the atmosphere combined with the high rates of snow accumulation at high-latitudes and altitudes provide the possibility of recovering long records of microplastics, characterized by a high temporal resolution (Hong et al., 2009; Gabrielli et al., 2020), especially where ice stratigraphy is continuous, and reworking processes at the surface such as wind erosion, re-deposition and summer melting are limited (Schotterer et al., 2004). Ice core chronologies may be produced by counting annual ice-layers, using the seasonal variability of stable isotopes and soluble ions, and/or the concentration profiles of seasonal species. Lead-210 may also be used for dating the more recent period (e.g., post-1900) (Döscher et al., 1996) and all these methods may be supplemented by the use of independent stratigraphic markers. These are typically chemical or particulate signals in the ice which identify major events, such as volcanic eruptions, aeolian dust deposits or, previously, atmospheric nuclear tests (Barbante et al., 2004; Gabrielli and Vallelonga, 2015).

Assessing the abundance of microplastics trapped in ice would not only provide an understanding of accumulation and dynamics of atmospheric microplastics but also the potential consequences associated with these contaminants being released back into the environment due to global warming and progressive ice melting (Obbard et al., 2014). The preservation and continuity of ice stratigraphy is critical to the use of ice cores as paleo-environmental archives (Schotterer et al., 2004). Increasing climate warming leads to summer melting, percolation and refreezing which alter depositional sequences and cause the loss of valuable historical information (Gabrielli and Vallelonga, 2015). However, even where ice sequences remain extant, the volume of meltwater available from each layer may limit their use in generating high resolution microplastics records and it is likely that to ensure reliable historical information, ice core records will need to be replicated with inevitable increases in fieldwork and analytical procedure costs (Jouzel et al., 1989).

Peat Sequences

Peatlands represent 3% of the continental area, covering ∼5 million km^2 of the Earth's surface (Gore, 1983). They are characterized by water at, or near the surface, anoxic conditions and specific vegetation, the decay of which leads to the formation and accumulation of the peat as well as to characteristic acidic conditions (Charman, 2002; Hansson et al., 2015). As a consequence, peats have low density, a high organic matter content (Lennartz and Liu, 2019) and a high porosity which facilitates water and solute movement (Quinton et al., 2009; Rezanezhad et al., 2016). Peatlands are defined as ombrotrophic only when their surface layers are supplied with nutrients by atmospheric sources, such as aerosols, rain, snow, fog and dust and are completely hydraulically isolated from groundwater (Damman, 1986; Shotyk, 1996).

Ombrotrophic peats record atmospheric inputs more directly than other continental archives such as lake sediments (Hansson et al., 2015) and are therefore important stores of historical information of both natural changes and human activities (Martínez-Cortizas and Weiss, 2002). Together with ice cores, ombrotrophic peat cores are the only archives which exclusively record atmospheric deposition at high resolution (De Vleeschouwer et al., 2010), but peats have the additional advantages of having a wider global distribution, being generally more accessible and easier to sample (Hansson et al., 2015).

As a result, peats have been widely used to analyze historical changes in the atmospheric deposition of many trace metals including Pb, Ni, Cu, Zn, Hg, Co, and Cd, to produce high-resolution multi-metal chronologies (Martínez-Cortizas et al., 1999; Nieminen et al., 2002; Rausch et al., 2005; Allan et al., 2013). These have been cross-validated with other natural archives, including lake sediments, ice, and herbaria samples (Renberg et al., 2001; Hansson et al., 2015). However, as with ice cores, to our knowledge, no microplastic peat records have yet been published.

Peat cores are likely to be valuable archives of microplastic atmospheric fallout. As they tend to have higher accumulation rates than those of marine and many lake sediments (Gałuszka et al., 2017), peat cores are likely to provide a high-resolution history of microplastic atmospheric contamination and accumulation in the environment, covering a wide range of spatial scales from local to global (Martínez-Cortizas and Weiss, 2002). However, due to local variations in topography and vegetation, which might affect the retention efficiency of microplastic deposition, multiple cores at different sites are likely to be required (Bindler et al., 2004; Allan et al., 2013; Souter and Watmough, 2016). Furthermore, in order to directly relate microplastic concentrations in peat cores to atmospheric deposition, coring locations should be selected to minimize post-depositional remobilization (Martínez-Cortizas and Weiss, 2002). While major disturbance from human activities, such as peatland drainage for agricultural practices may be avoided in this way (Holden et al., 2006) post-depositional remobilization of microplastics as a result of historical and contemporary root growth may be more difficult to avoid (Laiho et al., 2014). Although no records of microplastics in dated peat cores have yet been published, peatlands are likely to have a great potential as a sink for microplastic atmospheric fallout as their high porosity should enhance retention and accumulation of microplastics deposited to surface layers. Furthermore, as peatlands are often located in transition zones connecting soils with aquatic systems (e.g., coastal wetlands), they may also act as a source of microplastics to adjacent systems (Lennartz and Liu, 2019). Therefore, assessing microplastic contamination in peatlands might not only help determine high-resolution spatial and temporal patterns of deposition, but also lead to a better understanding of the potential for microplastic exchange between ecosystem compartments.

ANALYTICAL CHALLENGES FOR MICROPLASTIC PALEOECOLOGY

While there is still no fully agreed definition for microplastics, a further concern is the difficulty in making comparisons between studies due to the lack of standardization in analytical techniques. Full comparability will only be possible when units of abundance, methodologies for extraction and identification are standardized and harmonized. While such problems have been reported elsewhere, these issues will also be key to comparisons between paleoecological studies. Therefore, although a detailed analysis is beyond the scope of this current paper, we briefly highlight the main issues here.

Standardization of Extraction Methodology

Microplastic extraction from solid matrices, such as sediments, is usually performed by density separation, agitating the sample in saturated salt solutions (Crawford and Quinn, 2016). The higher the density of these solutions, the more polymers may be separated. However, the medium for density separation varies widely across studies from 1.0 to 1.2 g cm^{-3} for sodium chloride (NaCl) up to 2.1 g cm^{-3} for aqueous solutions of sodium polytungstate (Käppler et al., 2016; Turner et al., 2019). Other solutions, including sodium iodide (NaI), zinc chloride ($ZnCl_2$) (Van Cauwenberghe et al., 2015) and zinc bromide ($ZnBr_2$) (Quinn et al., 2017), have intermediate densities normally ranging between 1.6 and 1.8 gcm^{-3}. This wide range of solutions and densities, coupled with differences in methodologies between laboratories, results in the reporting of both different total concentrations and polymer assemblages. This makes comparisons between studies challenging and a move toward standardization of extraction techniques is required.

A further challenge for the extraction of microplastics from many lake sediment cores, and certainly for future studies involving peats, is the removal of organic material and this may be by chemical or enzymatic means (Li et al., 2018). Many studies have used hydrogen peroxide (H_2O_2) at different strengths (10–35%), temperatures and time intervals (Nuelle et al., 2014; Erni-Cassola et al., 2017; Li et al., 2018; Mai et al., 2018; Prata et al., 2019) while alternative approaches use acid (Avio et al., 2015; Dehaut et al., 2016) or alkaline digestions (Dehaut et al., 2016; Hurley et al., 2018b). While degradation of some polymer types has been observed following these chemical extractions (Nuelle et al., 2014; Dehaut et al., 2016), Fenton's reagent, an oxidant involving H_2O_2 in the presence of a ferrous catalyst (Fe^{2+}) at room temperature, does not appear to affect plastic polymers (Hurley et al., 2018b). Enzymatic approaches appear to be an effective technique when applied to small samples (i.e., biological tissues), but are expensive for large samples with high organic matter content and potentially require a range of enzymes to digest different organic compounds (Hurley et al., 2018b).

Microplastic Identification

While many studies, especially earlier ones, have used visual sorting only, this may lead to a great under- or over-estimation of microplastic contamination and the use of spectroscopic approaches such as infra-red (IR) or Raman analysis greatly increases reliability (Hidalgo-Ruz et al., 2012; Eriksen et al., 2013; Mendoza and Balcer, 2019). However, a major challenge for microplastic paleoecology when using spectroscopic methods is that reference databases (Zarfl, 2019) typically only include "virgin" plastics and these do not easily match those from environmentally exposed, degraded and aged materials. Spectra from polymers at different stages of degradation, or containing additives which are not recognized by commercial plastic libraries, need to be included in reference databases for environmental analyses (Ribeiro-Claro et al., 2017; Silva et al., 2018; Zarfl, 2019). Primpke et al. (2020) have begun this by developing free semi-automated software that allows the matching of FT-IR spectra with a library collected from degraded microplastics.

Validation

Validation of microplastic extraction methods is a fundamental step that is currently often neglected (Zhao et al., 2018). Recovery tests involving spiked microplastics in environmental samples, preferably including different colors, sizes, composition and densities, should be included with extractions in order to estimate recovery efficiencies and confidence intervals for the methodology employed. Furthermore, as spectroscopic techniques are time consuming, it is common practice to analyze either a proportion (10–20%) of the total particles visually identified as potential microplastics (Mendoza and Balcer, 2019) or a fractional area (25%) of a final filter when visual sorting has not been performed (Mintenig et al., 2017; Redondo-Hasselerharm et al., 2018). However, as total numbers of identified plastic polymers vary considerably between studies, the proportions of particle numbers or filter areas analyzed should be reported in order to aid comparison while a sufficiently high proportion needs to be analyzed to provide statistical significance.

Units of Measurement

Studies on microplastic contamination use a wide range of different units for microplastic quantification and show very heterogeneous concentrations, which may differ by several orders of magnitude (Klein et al., 2018). Some units may over-represent sample size, leading to an exponential increase in values when upscaling calculated microplastic densities to larger volumes or areas (Mendoza and Balcer, 2019). For paleoecological studies, this may be less of an issue but standardization is still required. For natural archives such as sediments and peats the numbers of particles per unit dry weight (dw), expressed either in g or kg is proposed (Ng and Obbard, 2006). Furthermore, the use of reliably dated archives allows the calculation of microplastic accumulation rates or "fluxes," as well as concentrations, and the two should both be reported together whenever possible. The use of fluxes takes into account variation in archive accumulation rates within a sequence that may increase or decrease concentrations and, for microplastics, should be reported in units of numbers of particles per area and time e.g., n m^{-2} yr^{-1} (e.g., Brandon et al., 2019; Turner et al., 2019). This results in more comparable data, both in input rates through time within a single archive, but also between sites.

For ice cores, microplastic concentrations could be reported as number of particles/L of filtered, melted ice as often used for smaller volume water samples (Mendoza and Balcer, 2019). Additional information on concentrations of size-classes and polymer-types should be given where possible (Koelmans et al., 2019; Mendoza and Balcer, 2019). These are important as differing approaches to methodology and identification affect lower-size detection limits as well as the polymer assemblage extracted.

Contamination

The control of contamination is fundamental to the accurate analysis of microplastics in environmental samples particularly where concentrations are expected to be very low, either due to isolation from emission sources or where rapid accumulation rates dilute inputs. For example, a combination of these factors might be expected to occur for ice cores in polar regions. For paleoecological studies, the potential contamination of older samples is especially important not only because microplastic concentrations are at their lowest, but also because a first presence may be used to provide stratigraphic information (see below).

To prevent contamination from plastic core tubes, the outer 1 cm of each sediment layer can be removed during extrusion (Matsuguma et al., 2017). The use of aluminum tubes may avoid this core-trimming, although their lack of transparency can be problematic with regard to assessing the quality and quantity of the retained material. Similarly, the outer layers of ice cores, which could be contaminated during drilling, may be removed mechanically in order to obtain a "clean inner core" (Candelone et al., 1994).

In the field, all available measures must be taken to minimize contamination, for example by sampling upwind of other activities, the use of nitrile gloves while handling cores, the avoidance of plastic equipment as much as possible and the use of exposed filters during coring activities to determine airborne contamination during sample collection (Kanhai et al., 2020). As contamination can also occur during sample processing, it is extremely important to avoid the use of plastic tools whenever possible during subsampling. For example, aluminum extrusion heads may be used together with metal implements to slice the core into layers. For ice cores, all analytical procedures must take place in ultraclean laboratories, where work areas and equipment must be washed with filtered Milli-Q water between the processing of different core subsections (Barbante et al., 2004; Kanhai et al., 2020). Methodological blanks should be included regularly to detect potential contamination during the processing of sediment or melted ice samples, and clean filters left on work areas to check airborne contamination (Kanhai et al., 2020). Cotton, instead of synthetic, laboratory coats should be worn during sample processing, but attention should also be paid to potential self-contamination from synthetic clothes during sample collection. Scopetani et al. (2020) found that 23% of fibers detected in environmental samples produced FT-IR spectra matching the cotton worn by personnel during sampling. Higher numbers of fibers were found in samples where collection was associated with higher physical effort and movement, and longer exposure to air. To help eliminate these contaminants from further consideration, it may be useful to create a library of FT-IR spectra for fibers collected from laboratory coats and clothing worn during fieldwork, as well as fragments of any plastic tools used during field and laboratory activities. Comparison of the spectra obtained from plastic particles in samples against those in the spectra library could then help identify whether contamination has occurred.

THE TAPHONOMY OF MICROPLASTICS

Microplastics have now joined the ranks of the numerous stratigraphic indicators of human activity stored in natural archives. Like other anthropogenic paleoecological signatures,

their final occurrence in depositional settings are a result of a myriad of human and natural processes, related to their production, utility, composition and transport to burial. However, unlike more classical paleoecological indicators that are used to interpret human activity (e.g., pollen, diatoms, invertebrate micro-remains, charcoal) our understanding of how ecological and environmental processes influence the final record of microplastics in natural archives is still to be determined. Though the potential historical occurrence and environmental abundance of plastics has been assessed by collation of development, production and usage data (Zalasiewicz et al., 2016) the release of plastic waste into the environment has not been systematically monitored. If we are to expand the use of sedimentary microplastics as a reliable archive of plastic use and waste emission, as well as apportion sources, we need to consider environmental transport and depositional factors that determine or skew the accumulating record.

The study of plant, animal and human paleoecology deals with the issues of representation, bias and differential preservation through the study of taphonomy. With a few exceptions, the majority of fossil assemblages are understood to have been intensely modified by taphonomic processes (Benton and Harper, 1997). Taphonomic processes affecting microplastics are therefore in conflict with the uniformitarian assumption that a microplastic record in an environmental archive faithfully represents its historical record of production and disposal. Without a greater understanding of taphonomic processes, microplastic sequences extracted from sediments, peats and ice cores will provide a distorted, even biased, historical narrative of the changing abundance and composition of plastic waste in the environment. Conversely, along with other fossils, the presence of microplastics and their taphonomic data add to our understanding of sedimentary processes operating in depositional environments.

The principal taphonomic considerations for microplastics is the interplay of (i) their high resistance to environmental influences, leading to extremely low degradation and long residence times (Klein et al., 2018) and (ii) the compositional and structural mixture of polymers released into the environment. A difference in the age of the sediment sample and the age of "death" (or release of fossil material to be preserved) is usually to be expected. For benthic or planktonic lifeforms and atmospherically transported materials, this time difference may be relatively small following transport through the atmosphere and /or water-column. With greater distances, or time taken to reach a depositional setting, materials have a greater potential for temporary storage and being re-worked *en route*, resulting in their eventual burial with sediments inconsistent with the age of that "fossil." Producing a robust interpretation of past environments from a fossil record is therefore complex. Even for a traditional paleoecological discipline such as pollen analysis, that has been used globally and intensively for many decades, it is only comparatively recently that vegetation reconstruction from fossil records has become more quantifiable and objective (Davis, 2000).

Working in parallel to processes of death/release and time/distance to burial is the resistance of fossils to degradation. Less resistant forms will not survive being transported, stored and reworked, often leading to a bias in more resistant, transportable or locally dominant forms in sediment sequences e.g., *Pinus* pollen grains (Wiltshire, 2006). Paleolithic stone tools provide a good example of durable man-made materials that can upset the normal rules of stratigraphic succession. Lithic remains create more complex scenarios due to their durability and survive being eroded and transported from primary to secondary contexts (Barham et al., 2015; Archer et al., 2020). Similarly, although information can be obtained from analysis of durable stone tools and their contexts, what we know about prehistoric human life is greatly enhanced when exceptional preservation allows remains such as wood and other organic remains to survive, e.g., Neanderthal string (Knight et al., 2019; Hardy et al., 2020). For stone tools and microplastics alike, the same consequences of distance from source, durability, reworking and movement from primary to secondary contexts apply to correctly interpreting their depositional assemblage.

Although we have a well-documented history of plastic invention and usage, it will be many decades before early-mid twentieth century plastics can be ruled out from occurring in contemporary basins due to reworking of "natural" (soils, floodplain sediments) or anthropogenic archives, e.g., eroding coastal landfills (Brand et al., 2018). This lag not only provides the potential for older microplastics to recur, but also blurs the first occurrence in sequences due to the rapidity of polymer inventions. This is further exacerbated by the time taken to generate microplastics from macroplastic debris ether *in situ* or *en route*. This is discussed more fully below. Hence, in poorly dated, slowly accumulating stratigraphic sequences downstream of urban areas, a potential technological chronostratigraphy of plastics may well be lost.

Taphonomic Processes Affecting Microplastic Particles

Although self-selective due to the density and form of particles capable of becoming airborne, the atmosphere allows minimal delay between the production, usage and transport of microplastics to their deposition in archives. Microplastic fibers and dust-sized particles may be transported over at least regional, and possibly global, scales (Dris et al., 2016; Bergmann et al., 2019) while larger micro- and macroplastics may be dragged, saltated or become airborne only if wind and landscape conditions allow (Zylstra, 2013; Dris et al., 2016; Šilc et al., 2018; Rezaei et al., 2019). With less catchment influence, remote, atmospherically-dominated sites have long provided essential global and regional paleoecological data (Birks, 2019), however, for microplastics even here more proximal contamination has been found to be significant (Free et al., 2014; Zhang et al., 2016; Miller et al., 2017). Quantifying long-range atmospherically-transported vs. local hydrological plastic inputs is a challenge but detailed statistical analysis of morphometry and composition may have the potential to differentiate between sources at remote sites or those isolated from wastewater inputs.

Microplastics moving toward depositional archives via rivers, glaciers and air currents are an agglomeration from multiple spatial and temporal sources, mirroring natural sedimentary

particles. Like sediments, microplastics enter from both point and diffuse sources, or are created by the breakdown of larger plastic particles also being transported, and therefore occur as bedload, in suspension and at the near-surface (buoyant) depending on their density and shape (Morritt et al., 2014; Horton et al., 2017; Kooi et al., 2018). Microplastic particles within bedload have a higher potential for temporary in-channel sediment storage when flow velocities decrease, whereas buoyant particles during high-flow events have a greater potential of being transported into low-flow, vegetated areas (Yao et al., 2019). Buoyant, lower density plastics are also affected by wind-wave conditions; sometimes oblique to bedload flow paths, e.g., in estuaries (Browne et al., 2010) and therefore may be circulated for longer, while other materials sink (Lebreton et al., 2019). Microplastics are also added during flow by repeated chemical and structural degradation of macroplastics during transport, e.g., UV and physical degradation of river plastics trapped by obstructions (Williams and Simmons, 1996), although quantification of this process contributing to the total pool of microplastic remains limited (Castro-Jiménez et al., 2019). During flow downstream, microplastics move between bedload and suspension (Hurley et al., 2018a) depending on flow rates and, when conditions allow, may be temporarily stored (Tibbetts et al., 2018).

Even within depositional settings microplastic assemblages continue to be spatially and temporally complex, due to the interaction of physical, chemical and biological factors affecting their burial. The route to burial is not straightforward for any particulate entering a depositional environment; they are rarely homogenous sinks, with internal flows connecting areas of higher and lower rates of deposition. The controlling factors of density and durability that control the distribution of plastics in environmental flows continue, but upon entering lentic, low energy settings, physical degradation is reduced, and chemical and biological processes can take precedence.

The boundaries between high and low energy conditions do not often occur abruptly, and are usually connected by transitional environments, such as floodplains, deep water channels (Kane et al., 2020), estuaries, shorelines and coasts. Both micro- and macroplastics in these settings continue to be re-worked, temporarily stored and released, contributing to the overall amount of microplastics in the environment. The common occurrence of considerably aged plastics in coastal systems; "*Plastic bottle washes up looking 'almost new' after nearly 50 years at sea*" (Lyons, 2018); "*Crisp packet from the 60s found washed up on beach*" (Byrne, 2019) and "*Plastic bag found in Sunshine Coast waterway could be up to 40 years old and it's just the tip of the iceberg*" (Mapstone, 2019); highlight the ability of plastics to remain in these transitional environments for considerable periods of time (years to multiple decades). Plastics identified by production dates as many years/decades old in scientific surveys of buried, surface and buoyant plastics (Hoffmann and Reicherter, 2014; Sander, 2016; Lebreton et al., 2018) support the idea of a long-term build-up of anachronistic microplastics now found in depositional settings. Modeling of transport and removal of buoyant plastic from the surface ocean predicts that most of the plastic mass that has entered the marine environment since the 1950s has not disappeared by degradation, but is stranded or settled on its way to offshore waters, possibly slowly circulating between coastal environments with repeated episodes of beaching, fouling, defouling and resurfacing (Lebreton et al., 2019). This "accumulation and slow release" loop will likely have occurred at different scales, since the mid-twentieth century at the margins of depositional basins globally. The implication of this is that without independent dating of individual particles, a paleoecological assemblage of microplastics in a sediment sequence is best considered as time cumulative. Aside from the stratigraphic "first occurrence" of invented plastics (see below), microplastic types and volumes occurring in stratigraphic intervals should be considered anachronistic. It is now perhaps too simplistic to continue comparing global production of plastic data (Plastics Europe, 2016; Geyer et al., 2017) against the abundance of fragments found in monitoring and sediment studies (Thompson et al., 2004; Claessens et al., 2011; Willis et al., 2017; Brandon et al., 2019) without considering that microplastic totals within defined time slices also contain historical releases.

Physical models using microplastic size, composition and density have made significant improvements to our understanding of microplastics in the environment; revealing non-steady state transport and long-term cycling between storage and release and mechanisms to explain the preponderance of types of plastic waste in certain locations. The highly efficient, spatially restricted sorting of macroplastic waste by size and composition is evident at channel margins, strandlines and beaches globally. Subtle changes in shape (e.g., handedness of sneakers as flotsam), may direct their orientation to wind/currents and their shoreline accumulation (Ebbesmeyer and Scigliano, 2009). There is a paucity of data describing how subtle differences in form (e.g., spherical vs. film) and polymer composition affect the spatial variability of microplastics found in depositional settings, but sorting by wind and water currents clearly occurs (Corcoran et al., 2015; Fischer et al., 2016; Su et al., 2016; Vaughan et al., 2017; Yao et al., 2019) as well as entrainment with sediment matrices of similar density and size (Pietrelli et al., 2017; Haave et al., 2019).

Biological Taphonomy

The interaction of plastic waste with organisms in the environment has long been recognized, with studies of plastic ingestion and entanglement of seabirds and cetaceans, elevating global plastic waste to the forefront of conservation concerns. Understanding the impact of plastics on organisms has therefore been a driving cause for microplastic research, due to detrimental effects of ingestion and potential ontogenic accumulation of plastic-associated chemicals. Due to their durability, microplastic particles have a high potential for circulating through trophic levels. However, how much of an effect biological processes have on the final stratigraphic record of microplastics is little understood, but from studies of the interaction of organisms and plastics in the environment, we can identify likely taphonomic factors.

As soon as plastic waste is emitted, biological activity is intrinsic to its alteration and accumulation. In low energy

environments, biological processes can become central, determining capture, sinking, burial and re-working (see sections above on aquatic archives) (**Figure 2**). Plastic surfaces are quickly (hours to days) colonized in aquatic environments by a diverse microbial community dependent on location, season and substrate (i.e., type of plastic) (Amaral-Zettler et al., 2020). Biofilm formation and algal colonization change surface chemistry characteristics, influencing UV and chemical degradation, while biofilm-induced particle clumping leads to enhanced sinking rates (Michels et al., 2018). The sorting effects of preferential biofilm development on some plastics are conveyed to higher trophic levels by consumption of biofilms and microplastics by invertebrates, e.g., rasping and grazing by gastropods (Weinstein et al., 2016; Vosshage et al., 2018). Physical and chemical predilection of biofilm formation on some plastics compared with those durable to microbial degradation drives a sorting gradient to separate polymers (Amaral-Zettler et al., 2020); sustaining continued transport and distribution in some while enhancing clustering and sinking in others.

Primary production in the form of vegetation growth is effective at capturing plastics at the periphery of depositional basins. Films and fibers may be tangled in stems and branches intercepting flow (i.e., the "Christmas tree effect"; Williams and Simmons, 1996) and sorting plastics across the range of capture and energy conditions found in freshwater and coastal wetlands (Ivar do Sul et al., 2014; Li et al., 2019; Yao et al., 2019; Helcoski et al., 2020). Variability in growth rate, stand-density, water-level changes from flooding or tidal regime affect microplastic capture and hence abundance, leading to spatial and temporal variability of microplastics accumulated over time, irrespective or additional to emission inputs.

Microplastic accumulation by primary trophic levels is followed by secondary consumption by invertebrates in the water column (plankton) as well as by detritivores and filter-feeders in benthic habitats. Due to the basin-scale volumes of water and suspended material able to be processed over time by plankton and benthic invertebrates, any selection of microplastics due to feeding strategy, will have a taphonomic effect on what reaches the sediment surface by sinking or benthic incorporation of fecal matter. How much of an effect particular feeding strategies or abundance of filter feeders have had on historical microplastic accumulation is poorly understood and ingestion studies have typically used concentrations far higher than realistic environmental levels (e.g., Katija et al., 2017; Scherer et al., 2017). Measurements of microplastic concentrations in zooplankton indicate that concentrations of ingested plastic is a positive function of available plastic and inversely related to particle size (Desforges et al., 2015) but more experimental work (Aljaibachi et al., 2020; Redondo-Hasselerharm et al., 2020), comparative monitoring, and sediment studies from areas with contrasting zooplankton and benthic ecosystems are clearly required (Su et al., 2016; Naidu et al., 2018).

Feeding strategies, trophic level and existing environmental concentrations continue to determine microplastic ingestion in higher organisms. Selective feeding, based on size and color (Martí et al., 2020), by planktonic fish will have a measurable effect as will non-selective feeding e.g., benthic fish at the sediment water-interface (Sanchez et al., 2014; Baldwin et al., 2020). Increased longevity (multiple years to decades) and trophic position of wildfowl increases their potential to incorporate microplastics from multiple sources and vectoring to the sediment via feces (Reynolds and Ryan, 2018).

Finally, as observed for other contaminants including a range of trace metals (Brimble et al., 2009), biovector transport may be an additional transport mechanism by which microplastics are transferred between environments. Microplastics accumulated by anadramous fish such as salmon, feeding in the oceans over periods of years, may be transferred to terrestrial headwaters as the fish return to spawn and then die. Similarly, seabirds feeding at sea, will accumulate microplastics themselves or transfer them to chicks, in which they are accumulated or released via feces to the coastal terrestrial environment. Furthermore, seabirds transfer macroplastic to terrestrial environments by collecting marine plastic debris and using it as nesting material and the same has been observed in freshwaters (e.g., Vaughan et al., 2017). A Northern gannet (*Morus bassanus*) colony of 40,000 birds on Grassholm, in Wales, UK, included a mean of 470 g of plastic debris in each nest resulting in an estimated colony total of more than 18 tons (Votier et al., 2011). Although biological activity is ubiquitous in depositional settings (**Figure 2**) and the interaction with plastics and microplastics is easily conceived, our lack of basic knowledge regarding biological processes and their interaction with chemical and physical factors on microplastic deposition, currently limits our understanding of organism bias on the paleoecology of plastics.

MICROPLASTICS AS STRATIGRAPHIC MARKERS

Given the issues surrounding anachronistic microplastics in the environment as a result of differing taphonomies, as well as the various strengths and weaknesses of natural archives from which they might be extracted, there is a need to consider the role of microplastics as stratigraphic markers. In particular, it has been suggested that they may play a role in defining the start of the proposed Anthropocene Epoch, even though chronologically constrained historical records of microplastics are currently remarkably sparse.

The current internationally agreed method for defining chronostratigraphic boundaries is via selection of a Global Boundary Stratotype Section and Point (GSSP) as a physical reference level for a geological time boundary. The process of deciding on a lower boundary of the Anthropocene is complex and requires an initial selection of a primary marker and, ideally, auxiliary markers that support a global correlation (Waters et al., 2018). Different from any geological unit previously determined, the Anthropocene hinges more on effects than on cause (Zalasiewicz et al., 2019). This is particularly relevant for microplastics since these materials may be considered not only as environmental pollutants, but also as contributors to the character of recent (post mid-twentieth century) strata (i.e., plastic-rich sediments) (Zalasiewicz et al., 2016). Furthermore, in contrast to some other organic and inorganic pollutants that

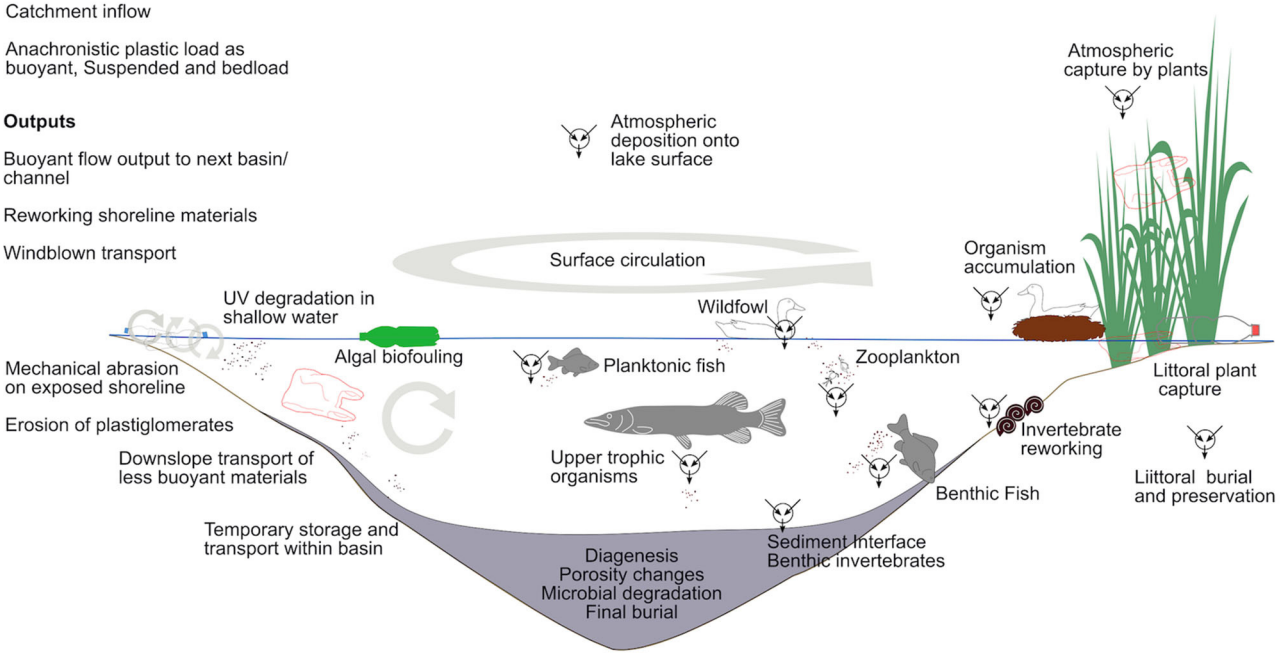

FIGURE 2 | Indirect transport of microplastics to a simple aquatic basin and sediment sequence. Plastic waste is transported to and broken down by interacting physical, chemical, and biological processes.

are also considered as potential markers of the Anthropocene (i.e., PAHs, metals), microplastics (or their constituent plastic polymers) have the advantage of being exclusively anthropogenic in nature, which means there are no naturally occurring background levels in the environment.

When compared to macroplastics, microplastics have a greater potential to spread and be distributed over wider areas, which makes them potentially globally correlatable within sedimentary layers. Therefore, they have a greater potential to become auxiliary markers for the Anthropocene boundary. However, microplastics have yet to be identified within some natural archives and, as described above, this may not be straightforward. In general, independent of the environmental matrix (water, sediment, biota), identifying microplastic in the small size ranges (particularly $<100\,\mu m$) that will be transported over longer distances, is particularly challenging and requires care to extract particles and avoid external contamination (Turner et al., 2019; Enders et al., 2020). In addition, the characteristics of the archives themselves will add a layer of complexity and challenge to their stratigraphic interpretation.

In the Anthropocene context, archives need to be varved, or accurately dated and undisturbed, to allow reliable correlations between microplastic (or polymer) concentrations or fluxes and create a reliable microplastic deposition profile. Specific polymers (or occasionally entire plastic objects; Zalasiewicz et al., 2016) are potentially correlatable since they were invented, produced and discarded at different times. For example, when considering the most prevalent polymers (i.e., PE, PP, PVC, PET, and PS; Geyer et al., 2017) there are sometimes decadal gaps between their first creation and their subsequent production at large scales (Andrady and Neal, 2009), when they may be expected to be found in deep marine sediment layers for the first time. On the other hand, relatively modern polymer types are expected to be found only in more recent sediment layers, which will accumulate all polymer types currently in use (**Figure 3**) as well as older microplastics delayed *en route* to the same depositional environment. Therefore, while the increasing abundance of microplastic particles in natural archives over the last <70 years may indicate Anthropocene-related strata (see Abundance zone 2 in **Figure 3**), it is the first presence of polymer-types in stratigraphic layers (see Abundance zone 1 in **Figure 3**) which may potentially provide a physical reference marker for the onset of the Anthropocene Epoch.

Microplastics in the environment occur with a wide range of shapes (Frias and Nash, 2019). Microbeads, originating mainly from cosmetic and personal products such as exfoliants and toothpastes, are expected to occur in differing abundances and accumulate in sediments at significantly different times in the developed northern hemisphere when compared to the less developed and less populated southern hemisphere. Therefore, microbeads may be irregularly distributed, which makes this specific particle-type less suitable as a globally synchronous stratigraphic marker. By contrast, fibers appear to be ubiquitous over a range of habitats (Dris et al., 2016; Bergmann et al., 2019) and are also expected to occur in sediments in a more synchronous way on a global scale, independent of sources. Fibers are incredibly mobile, often being the only microplastic particle identified in lake sediments and especially where atmospheric

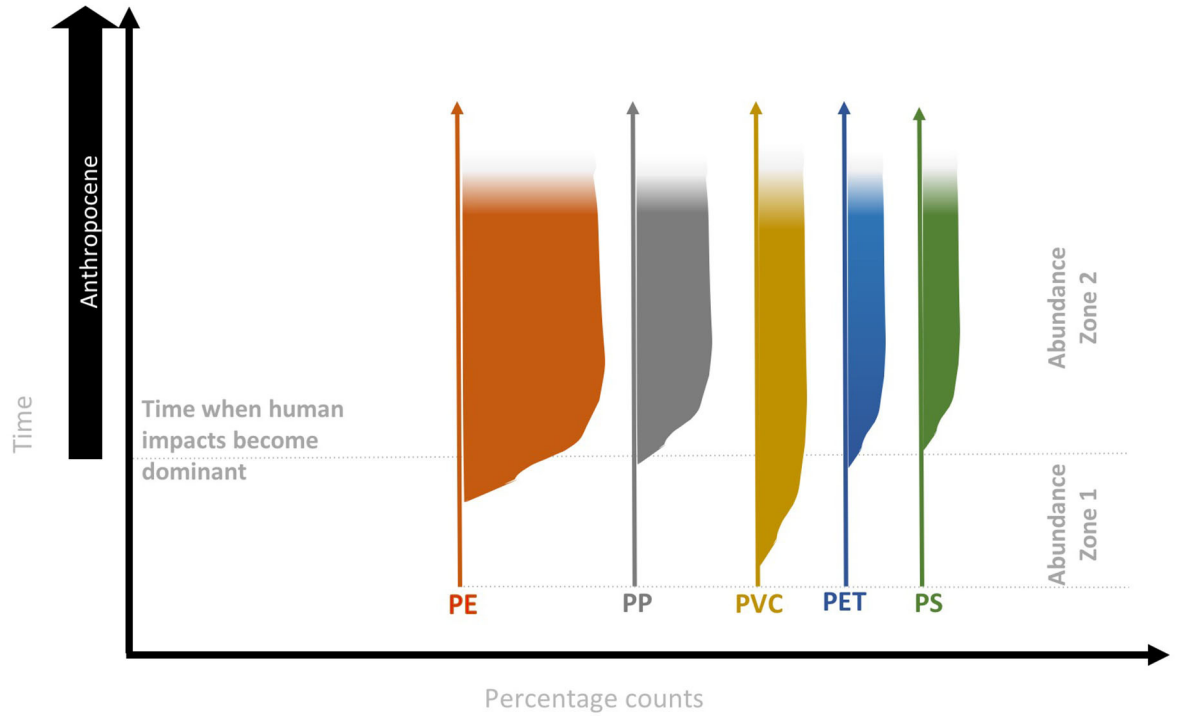

FIGURE 3 | Microplastic potential abundance zones and their utility for defining the Anthropocene. Abundant zones are based on the relative percentages of individual polymer species (herein represented by production rates of PE, PP, PVC, PE, and PS) and can potentially be used to characterize the Anthropocene strata. Original figures and complete discussion on the biostratigraphy of the Anthropocene are published in Barnosky (2014).

deposition is the main route of microplastic accumulation. Hence, abundances of microplastic forms, rather than total concentrations may have greater stratigraphic utility.

The Preservation of the Microplastic Record

Microplastics comprise hundreds of different polymer-types (Andrady, 2011) but they all have long polymeric chains that are composed mostly of carbon (e.g., polypropylene (PP) and polyethylene (PE) are >90% carbon-based) (Rillig, 2018). These high-molecular-weight organic chains resemble the long polymeric chains in persistent organic fossils such as wood, spores, pollen and graptolites (Zalasiewicz et al., 2016). Therefore, even if microplastic particles themselves do not endure, these polymers are expected to be preserved in sediments as trace technofossils. Although many studies imply that plastic longevity in the environment is at the scale of "centuries to millennia" under specific environmental conditions (Gregory and Andrady, 2003), these are often based on short-term laboratory experiments and should be interpreted with caution. What is clearer is that solar ultraviolet (UV) light is by far the main driver of plastic fragmentation, while the absence of UV light combined with low temperatures and a lack of oxygen may facilitate microplastic preservation in the deposited sediments. Deep ocean sediments may therefore offer the best conditions for long-term preservation and this is another key criterion in the selection of an appropriate stratigraphic marker for the Anthropocene.

Microplastic polymer types or "species" such as PE or PP in natural archives, may be able to fulfill a role similar to that played by fossils in specific biostratigraphic units. Within these units, fossils help to establish the relative age of specific strata at different locations (Barnosky, 2014). As stratigraphic markers, microplastics or polymers could be used as, not bio-, but chemostratigraphic units and therefore as a means to correlate between strata, be this indicative of the Anthropocene or other time periods (Ivar do Sul and Labrenz, 2020). The long polymeric chain N-acetylglucosamine, a derivative of glucose considered to be a component of chitin, is known to be preserved in graptolite fossils for 500 million years. However, while plastic polymers are clearly long-lived on human time-scales, knowledge of their potential fossilization and final preservation remains lacking. While natural examples suggest that such chemical preservation may seem likely, it is less clear whether microplastic particles themselves could be preserved as permanent casts and molds in lithified rocks (Leinfelder and Ivar do Sul, 2019) over such vast time-scales as occurs for biological micro-fossils.

CONCLUDING REMARKS

Rapidly increasing knowledge on the distribution of microplastics across a broad range of environments suggests

that, to all practical extents, they are likely to be ubiquitous. In particular, microplastic fibers are easily transported through the atmosphere and as a result, it may be expected that a range of natural archives from lake and marine sediments to ice and peat cores would contain historical records of their deposition. Therefore, although no microplastic records have yet been published for peats and ice cores, it seems probable that microplastic fibers will offer the best opportunity as a global stratigraphic marker.

As with other environmental contaminants, the paleoecological records of microplastics will be invaluable in determining the scale and extent of contamination at a range of geographical and temporal scales. They will allow directions of change (increasing or decreasing inputs) to be assessed as well as the rates at which that change is occurring. However, while there is considerable potential, data remain sparse and much remains to be done to explore these records and their possible role as stratigraphic markers.

What is clear is that the science of microplastic paleoecology is currently still in its infancy. Microplastics were not mentioned within the "50 priority research questions in paleoecology" produced only a few years ago (Seddon et al., 2014) and while such data are now being generated, little attention is currently being paid to the complexities of their interpretation. In particular the taphonomy of microplastics, i.e., the processes affecting their transport to, and deposition within, natural archives needs to be understood. This will allow a better understanding of microplastic records and their use, while conversely allowing microplastic records to contribute to our knowledge of depositional processes. Paleoecology has a rich history of interpreting temporal data and many lessons for the interpretation of microplastics in natural archives may well be learned from these more established techniques.

DATA AVAILABILITY STATEMENT

The original contributions generated for the study are included in the article/supplementary material, further inquiries can be directed to the corresponding author/s.

AUTHOR CONTRIBUTIONS

All authors conceived, wrote, edited, and reviewed this manuscript.

ACKNOWLEDGMENTS

CB acknowledged the support of the Natural Environment Research Council as part of the London NERC DTP (Grant no. NE/L002485/1). This paper contributes to the research of the Anthropocene Working Group (AWG), which is a working group of the Sub-commission on Quaternary Stratigraphy of the International Commission on Stratigraphy.

REFERENCES

Aljaibachi, R., Laird, W. B., Stevens, F., and Callaghan, A. (2020). Impacts of polystyrene microplastics on *Daphnia magna*: a laboratory and a mesocosm study. *Sci. Total Environ*. 705:135800. doi: 10.1016/j.scitotenv.2019.135800

Allan, M., Le Roux, G., De Vleeschouwer, F., Bindler, R., Blaauw, M., Piotrowska, N., et al. (2013). High-resolution reconstruction of atmospheric deposition of trace metals and metalloids since AD 1400 recorded by ombrotrophic peat cores in Hautes-Fagnes, Belgium. *Environ. Pollut.* 178, 381–394. doi: 10.1016/j.envpol.2013.03.018

Alldredge, A. L., and Silver, M. W. (1988). Characteristics, dynamics and significance of marine snow. *Progr. Oceanogr.* 20, 41–82. doi: 10.1016/0079-6611(88)90053-5

Allen, S., Allen, D., Phoenix, V. R., Le Roux, G., Jiménez, P. D., Simonneau, A., et al. (2019). Atmospheric transport and deposition of microplastics in a remote mountain catchment. *Nat. Geogr*. 12, 339–344. doi: 10.1038/s41561-019-0335-5

Amaral-Zettler, L. A., Zettler, E. R., and Mincer, T. J. (2020). Ecology of the plastisphere. *Nat. Rev. Microbiol.* 18, 139–151. doi: 10.1038/s41579-019-0308-0

Andrady, A. L. (2011). Microplastics in the marine environment. *Mar. Pollut. Bull.* 62, 1596–1605. doi: 10.1016/j.marpolbul.2011.05.030

Andrady, A. L., and Neal, M. A. (2009). Applications and societal benefits of plastics. *Philos. Trans. R. Soc. Lond. B Biol. Sci.* 364, 1977–1984. doi: 10.1098/rstb.2008.0304

Appleby, P. (2001). "Chronostratrigraphic techniques in Recent Sediments" in *Tracking Environmental Change Using Lake Sediments - Volume 1: Basin Analysis, Coring, and Chronological Techniques*, eds W. Last and J. P. Smol (Dordrecht: Kluwer Academic Publishers), 171–203.

Archer, W., Aldeias, V., and McPherron, S. P. (2020). What is '*in situ*'? A reply to Harmand et al. 2015. *J. Hum. Evol.* 142:102740. doi: 10.1016/j.jhevol.2020.102740

Avio, C. G., Gorbi, S., and Regoli, F. (2015). Experimental development of a new protocol for extraction and characterization of microplastics in fish tissues: first observations in commercial species from Adriatic Sea. *Mar. Environ. Res.* 111, 18–26. doi: 10.1016/j.marenvres.2015.06.014

Baldwin, A. K., Spanjer, A. R., Rosen, M. R., and Thom, T. (2020). Microplastics in Lake Mead national recreation area, USA: occurrence and biological uptake. *PLoS ONE* 15:e0228896. doi: 10.1371/journal.pone.0228896

Ballent, A., Corcoran, P. L., Madden, O., Helm, P. A., and Longstaffe, F. J. (2016). Sources and sinks of microplastics in Canadian Lake Ontario nearshore, tributary and beach sediments. *Mar. Pollut. Bull.* 110, 383–395. doi: 10.1016/j.marpolbul.2016.06.037

Barbante, C., Schwikowski, M., Döring, T., Gäggeler, H. W., Schotterer, U., Tobler, L., et al. (2004). Historical record of European emissions of heavy metals to the atmosphere since the 1650s from Alpine snow/ice cores drilled near Monte Rosa. *Environ. Sci. Technol.* 38, 4085–4090. doi: 10.1021/es049759r

Barham, L., Tooth, S., Duller, G. A. T., Plater, A. J., and Turner, S. (2015). Excavations at Site C North, Kalambo Falls, Zambia: new insights into the mode 2/3 transition in South-Central Africa. *J. African Archaeol.* 13, 187–214. doi: 10.3213/2191-5784-10270

Barnes, D. K., Galgani, F., Thompson, R. C., and Barlaz, M. (2009). Accumulation and fragmentation of plastic debris in global environments. *Philos. Trans. R. Soc. B Biol. Sci.* 364, 1985–1998. doi: 10.1098/rstb.2008.0205

Barnes, D. K. A., and Milner, P. (2005). Drifting plastic and its consequences for sessile organism dispersal in the Atlantic Ocean. *Mar. Biol.* 146, 815–825. doi: 10.1007/s00227-004-1474-8

Barnosky, A. (2014). "Palaeontological evidence for defining the Anthropocene," in *A Stratigraphical Basis for the Anthropocene,* eds C. N Waters, J. A. Zalasiewicz, M. Williams, M. A. Ellis, and A. M. Snelling (London: Geological Society, Special Publications), 149–165.

Beaudon, E., Gabrielli, P., Sierra-Hernández, M. R., Wegner, A., and Thompson, L. G. (2017). Central Tibetan Plateau atmospheric trace metals contamination: a 500-year record from the Puruogangri ice core. *Sci. Total Environ*. 601–602, 1349–1363. doi: 10.1016/j.scitotenv.2017.05.195

Benton, M., and Harper, D. (1997). *Basic Palaeontology*. Harlow: Addison Wesley Longman.

Bergmann, M., and Klages, M. (2012). Increase of litter at the Arctic deep-sea observatory HAUSGARTEN. *Mar. Pollut. Bull.* 64, 2734–2741. doi: 10.1016/j.marpolbul.2012.09.018

Bergmann, M., Mützel, S., Primpke, S., Tekman, M. B., Trachsel, J., and Gerdts, G. (2019). White and wonderful? Microplastics prevail in snow from the Alps to the Arctic. *Sci. Adv.* 5:eaax1157. doi: 10.1126/sciadv.aax1157

Bindler, R., Klarqvist, M., Klaminder, J., and Förster, J. (2004). Does within-bog spatial variability of mercury and lead constrain reconstructions of absolute deposition rates from single peat records? The example of Store Moss, Sweden. *Glob. Biogeochem. Cycles* 18:GB3020. doi: 10.1029/2004GB002270

Birks, H. J. B. (2019). Contributions of quaternary botany to modern ecology and biogeography. *Plant Ecol. Divers.* 12, 189–385. doi: 10.1080/17550874.2019.1646831

Brand, J. H., Spencer, K. L., O'shea, F. T., and Lindsay, J. E. (2018). Potential pollution risks of historic landfills on low-lying coasts and estuaries. *Wiley Interdisc. Rev. Water* 5:e1264. doi: 10.1002/wat2.1264

Brandon, J. A., Jones, W., and Ohman, M. D. (2019). Multidecadal increase in plastic particles in coastal ocean sediments. *Sci. Adv.* 5:eaax0587. doi: 10.1126/sciadv.aax0587

Brimble, S. K., Foster, K. L., Mallory, M. L., Macdonald, R. W., Smol, J. P., and Blais, J. M. (2009). High arctic ponds receiving biotransported nutrients from a nearby seabird colony are also subject to potentially toxic loadings of arsenic, cadmium and zinc. *Environ. Toxicol. Chem.* 28, 2426–2433. doi: 10.1897/09-235.1

Brinkhurst, R. O., Chua, K. E., and Kaushik, N. K. (1972). Interspecific interactions and selective feeding by tubificid oligocheates. *Limnology* 17, 122–133. doi: 10.4319/lo.1972.17.1.0122

Browne, M. A., Galloway, T. S., and Thompson, R. C. (2010). Spatial patterns of plastic debris along estuarine shorelines. *Environ. Sci. Technol.* 44, 3404–3409. doi: 10.1021/es903784e

Byrne, P. (2019). '*Crisp Packet From the 60s Found Washed Up on Beach Highlights Plastic Risk to Sea*' *The Mirror*. Available online at: https://www.mirror.co.uk/news/uk-news/crisp-packet-60s-found-washed-18935596 (accessed June 16, 2020).

Candelone, J. P., Hong, S., and Boutron, C. F. (1994). An improved method for decontaminating polar snow and ice cores for heavy metal analysis. *Anal. Chim. Acta* 299, 9–16. doi: 10.1016/0003-2670(94)00327-0

Castro-Jiménez, J., González-Fernández, D., Fornier, M., Schmidt, N., and Sempere, R. (2019). Macro-litter in surface waters from the Rhone River: plastic pollution and loading to the NW Mediterranean Sea. *Mar. Pollut. Bull.* 146, 60–66. doi: 10.1016/j.marpolbul.2019.05.067

Charman, D. (2002). *Peatlands and Environmental Change*. Chichester: John Wiley & Sons Ltd.

Claessens, M., De Meester, S., Van Landuyt, L., De Clerck, K., and Janssen, C. R. (2011). Occurrence and distribution of microplastics in marine sediments along the Belgian coast. *Mar. Pollut. Bull.* 62, 2199–2204. doi: 10.1016/j.marpolbul.2011.06.030

Cole, M., Lindeque, P., Fileman, E., Halsband, C., Goodhead, R., Moger, J., et al. (2013). Microplastic ingestion by zooplankton. *Environ. Sci. Technol.* 47, 6646–6655. doi: 10.1021/es400663f

Corcoran, P. L., Norris, T., Ceccanese, T., Walzak, M. J., Helm, P. A., and Marvin, C. H. (2015). Hidden plastics of Lake Ontario, Canada and their potential preservation in the sediment record. *Environ. Pollut.* 204, 17–25. doi: 10.1016/j.envpol.2015.04.009

Crawford, C. B., and Quinn, B. (2016). *Microplastic Pollutants*. Amsterdam: Elsevier Science.

Damman, A. W. (1986). Hydrology, development, and biogeochemistry of ombrogenous peat bogs with special reference to nutrient relocation in a western Newfoundland bog. *Can. J. Bot.* 64, 384–394. doi: 10.1139/b86-055

Davis, M. B. (2000). Palynology after Y2K—understanding the source area of pollen in sediments. *Annu. Rev. Earth Planet. Sci.* 28, 1–18. doi: 10.1146/annurev.earth.28.1.1

De Vleeschouwer, F., Le Roux, G., and Shotyk, W. (2010). Peat as an archive of atmospheric pollution and environmental change: a case study of lead in Europe. *PAGES Mag.* 18, 20–22. doi: 10.22498/pages.18.1.20

Dehaut, A., Cassone, A. L., Frère, L., Hermabessiere, L., Himber, C., Rinnert, E., et al. (2016). Microplastics in seafood: Benchmark protocol for their extraction and characterization. *Environ. Pollut.* 215, 223–233. doi: 10.1016/j.envpol.2016.05.018

Desforges, J. P. W., Galbraith, M., and Ross, P. S. (2015). Ingestion of microplastics by zooplankton in the northeast pacific ocean. *Arch. Environ. Contam. Toxicol.* 69, 320–330. doi: 10.1007/s00244-015-0172-5

Dong, M., Luo, Z., Jiang, Q., Xing, X., Zhang, Q., and Sun, Y. (2020). The rapid increases in microplastics in urban lake sediments. *Sci. Rep.* 10:848. doi: 10.1038/s41598-020-57933-8

Döscher, A., Gäggeler, H. W., Schotterer, U., and Schwikowski, M. (1996). A historical record of ammonium concentrations from a glacier in the Alps. *Geophys. Res. Lett.* 23, 2741–2744. doi: 10.1029/96GL02615

Downing, J. A., Prairie, Y. T., Cole, J. J., Duarte, C. M., Tranvik, L. J., Striegl, R. G., et al. (2006). The global abundance and size distribution of lakes, ponds, and impoundments. *Limnol. Oceanogr.* 51, 2388–2397. doi: 10.4319/lo.2006.51.5.2388

Dris, R., Gasperi, J., Saad, M., Mirande, C., and Tassin, B. (2016). Synthetic fibers in atmospheric fallout: a source of microplastics in the environment? *Mar. Pollut. Bull.* 104, 290–293. doi: 10.1016/j.marpolbul.2016.01.006

Ebbesmeyer, C., and Scigliano, E. (2009). *Flotsametrics and the Floating World: How One Man's Obsession with Runaway Sneakers and Rubber Ducks Revolutionized Ocean Science*. London: Collins.

ECHA, European Chemicals Agency (2019). *ANNEX XV. Restriction Report Proposal for a Restriction. Intentionally Added Microplastics*. Available online at: https://echa.europa.eu/documents/10162/05bd96e3-b969-0a7c-c6d0-441182893720 (accessed June 3, 2020).

Eichler, A., Tobler, L., Eyrikh, S., Gramlich, G., Malygina, N., Papina, T., et al. (2012). Three centuries of Eastern European and Altai lead emissions recorded in a Belukha ice core. *Environ. Sci. Technol.* 46, 4323–4330. doi: 10.1021/es2039954

Enders, K., Lenz, R., Ivar do Sul, J. A., Tagg, A. S., and Labrenz, M. (2020). When every particle matters: a QuEChERS approach to extract microplastics from environmental samples. *Methods X* 7:100784. doi: 10.1016/j.mex.2020.100784

Eriksen, M., Mason, S., Wilson, S., Box, C., Zellers, A., Edwards, W., et al. (2013). Microplastic pollution in the surface waters of the Laurentian Great Lakes. *Mar. Pollut. Bull.* 77, 177–182. doi: 10.1016/j.marpolbul.2013.10.007

Erni-Cassola, G., Gibson, M. I., Thompson, R. C., and Christie-Oleza, J. A. (2017). Lost, but found with Nile red: a novel method for detecting and quantifying small microplastics (1 mm to 20 μm) in environmental samples. *Environ. Sci. Technol.* 51, 13641–13648. doi: 10.1021/acs.est.7b04512

Erni-Cassola, G., Zadjelovic, V., Gibson, M. I., and Christie-Oleza, J. A. (2019). Distribution of plastic polymer types in the marine environment: a meta-analysis. *J. Haz. Mat.* 369, 691–698. doi: 10.1016/j.jhazmat.2019.02.067

Fischer, E. K., Paglialonga, L., Czech, E., and Tamminga, M. (2016). Microplastic pollution in lakes and lake shoreline sediments – a case study on Lake Bolsena and Lake Chiusi (central Italy). *Environ. Pollut.* 213, 648–657. doi: 10.1016/j.envpol.2016.03.012

Free, C. M., Jensen, O. P., Mason, S. A., Eriksen, M., Williamson, N. J., and Boldgiv, B. (2014). High-levels of microplastic pollution in a large, remote, mountain lake. *Mar. Pollut. Bull.* 85, 156–163. doi: 10.1016/j.marpolbul.2014.06.001

Frias, J. P. G. L., Gago, J., Otero, V., and Sobral, P. (2016). Microplastics in coastal sediments from Southern Portuguese shelf waters. *Mar. Environ. Res.* 114, 24–30. doi: 10.1016/j.marenvres.2015.12.006

Frias, J. P. G. L., and Nash, R. (2019). Microplastics: finding a consensus on the definition. *Mar. Pollut. Bull.* 138, 145–147. doi: 10.1016/j.marpolbul.2018.11.022

Gabrieli, J., and Barbante, C. (2014). The Alps in the age of the Anthropocene: the impact of human activities on the cryosphere recorded in the Colle Gnifetti glacier. *Rend. Lincei.* 25, 71–83. doi: 10.1007/s12210-014-0292-2

Gabrielli, P., and Vallelonga, P. (2015). "Contaminant records in ice cores," *in Environmental Contaminants. Developments in Paleoenvironmental Research*, Vol. 18, eds J. Blais, M. Rosen, and J. Smol (Dordrecht: Spriger), 393–430.

Gabrielli, P., Wegner, A., Sierra-Hernández, M. R., Beaudon, E., Davis, M., Barker, J. D., et al. (2020). Early atmospheric contamination on the top of the Himalayas since the onset of the European Industrial Revolution. *Proc. Natl. Acad. Sci. U.S.A.* 117, 3967–3973. doi: 10.1073/pnas.1910485117

Gajewski, K., Hamilton, P. B., and McNeely, R. (1997). A high resolution proxy-climate record from an arctic lake with annually-laminated sediments on Devon Island, Nunavut, Canada. *J. Paleolimnol.* 17, 215–225. doi: 10.1023/A:1007984617675

Galgani, F., Burgeot, T., Bocquene, G., Vincent, F., Leaute, J. P., Labastie, J., et al. (1995). Distribution and abundance of debris on the continental shelf of the Bay of Biscay and in Seine Bay. *Mar. Pollut. Bull.* 30, 58–62. doi: 10.1016/0025-326X(94)00101-E

Galgani, F., Souplet, A., and Cadiou, Y. (1996). Accumulation of debris on the deep sea floor off the French Mediterranean coast. *Mar. Ecol. Progr. Ser.* 142, 225–234. doi: 10.3354/meps142225

Galloway, T. S., Cole, M., and Lewis, C. (2017). Interactions of microplastic debris throughout the marine ecosystem. *Nat. Ecol. Evol.* 1, 1–8. doi: 10.1038/s41559-017-0116

Gałuszka, A., Migaszewski, Z. M., and Namieśnik, J. (2017). The role of analytical chemistry in the study of the Anthropocene. *Trends Anal. Chem.* 97, 146–152. doi: 10.1016/j.trac.2017.08.017

Geyer, R., Jambeck, J. R., and Law, K. L. (2017). Production, use, and fate of all plastics ever made. *Sci. Adv.* 3:e1700782. doi: 10.1126/sciadv.1700782

Gore, A. J. P. (1983). *Ecosystems of the World—Mires: Swamps, Bog, Fen, and Moor.* Amsterdam; Oxford; New York, NY: Elsevier.

Gregory, M. R. (2009). Environmental implications of plastic debris in marine settings–entanglement, ingestion, smothering, hangers-on, hitch-hiking and alien invasions. *Philos. Trans. R. Soc. Lond. B Biol. Sci.* 364, 2013–2025. doi: 10.1098/rstb.2008.0265

Gregory, M. R., and Andrady, A. L. (2003). "Plastics in the marine environment," in *Plastics and the Environment,* ed A. L. Andrady (New Jersey NJ: John Wiley and Sons), 379–400.

Haave, M., Lorenz, C., Primpke, S., and Gerdts, G. (2019). Different stories told by small and large microplastics in sediment - first report of microplastic concentrations in an urban recipient in Norway. *Mar. Pollut. Bull.* 141, 501–513. doi: 10.1016/j.marpolbul.2019.02.015

Hansson, S. V., Bindler, R., and De Vleeschouwer, F. (2015). "Using peat records as natural archives of past atmospheric metal deposition," in *Environmental Contaminants. Developments in Paleoenvironmental Research,* Vol. 18, eds J. Blais, M. Rosen, and J. Smol (Dordrecht: Springer), 35–60.

Hardesty, B. D., Harari, J., Isobe, A., Lebreton, L., Maximenko, N., Potemra, J., et al. (2017). Using numerical model simulations to improve the understanding of micro-plastic distribution and pathways in the marine environment. *Front. Mar. Sci.* 4:30. doi: 10.3389/fmars.2017.00030

Hardy, B. L., Moncel, M. H., Kerfant, C., Lebon, M., Bellot-Gurlet, L., and Mélard, N. (2020). Direct evidence of Neanderthal fibre technology and its cognitive and behavioral implications. *Scient. Rep.* 10:8167. doi: 10.1038/s41598-020-65143-5

Hartmann, N. B., Hüffer, T., Thompson, R. C., Hassellöv, M., Verschoor, A., Daugaard, A. E., et al. (2019). Are we speaking the same language? Recommendations for a definition and categorization framework for plastic debris. *Environ. Sci. Technol.* 53, 1039–1047. doi: 10.1021/acs.est.8b05297

Hartwig, E., Clemens, T., and Heckroth, M. (2007). Plastic debris as nesting material in a Kittiwake-(*Rissa tridactyla*)-colony at the Jammerbugt, Northwest Denmark. *Mar. Pollut. Bull.* 54, 595–597. doi: 10.1016/j.marpolbul.2007.01.027

Helcoski, R., Yonkos, L. T., Sanchez, A., and Baldwin, A. H. (2020). Wetland soil microplastics are negatively related to vegetation cover and stem density. *Environ. Pollut.* 256:113391. doi: 10.1016/j.envpol.2019.113391

Hidalgo-Ruz, V., Gutow, L., Thompson, R. C., and Thiel, M. (2012). Microplastics in the marine environment: a review of the methods used for identification and quantification. *Environ. Sci. Technol.* 46, 3060–3075. doi: 10.1021/es2031505

Hoffmann, G., and Reicherter, K. (2014). Reconstructing Anthropocene extreme flood events by using litter deposits. *Glob. Planet. Change* 122, 23–28. doi: 10.1016/j.gloplacha.2014.07.012

Holden, J., Chapman, P. J., Lane, S. N., and Brookes, C. (2006). "Impacts of artificial drainage of peatlands on runoff production and water quality," in *Peatlands: Evolution and Records of Environmental and Climate Changes,* eds I. P. Martini, A. M. Cortizas, and W. Chesworth (Oxford: Elsevier B.V.), 501–528.

Hong, S., Lee, K., Hou, S., Hur, S. D., Ren, J., Burn, L. J., et al. (2009). An 800-year record of atmospheric As, Mo, Sn, and Sb in central Asia in high-altitude ice cores from Mt. Qomolangma (Everest), Himalayas. *Environ. Sci. Technol.* 43, 8060–8065. doi: 10.1021/es901685u

Horton, A. A., Svendsen, C., Williams, R. J., Spurgeon, D. J., and Lahive, E. (2017). Large microplastic particles in sediments of tributaries of the River Thames, UK – abundance, sources and methods for effective quantification. *Mar. Pollut. Bull.* 114, 218–226. doi: 10.1016/j.marpolbul.2016.09.004

Hurley, R., Woodward, J., and Rothwell, J. J. (2018a). Microplastic contamination of river beds significantly reduced by catchment-wide flooding. *Nat. Geosci.* 11, 251–257. doi: 10.1038/s41561-018-0080-1

Hurley, R. R., Lusher, A. L., Olsen, M., and Nizzetto, L. (2018b). Validation of a method for extracting microplastics from complex, organic-rich, environmental matrices. *Environ. Sci. Technol.* 52, 7409–7417. doi: 10.1021/acs.est.8b01517

Imhof, H. K., Ivleva, N. P., Schmid, J., Niessner, R., and Laforsch, C. (2013). Contamination of beach sediments of a subalpine lake with microplastic particles. *Curr. Biol.* 23, R867–R868. doi: 10.1016/j.cub.2013.09.001

Ivar do Sul, J. A., Costa, M. F., Silva-Cavalcanti, J. S., and Araújo, M. C. B. (2014). Plastic debris retention and exportation by a mangrove forest patch. *Mar. Pollut. Bull.* 78, 252–257. doi: 10.1016/j.marpolbul.2013.11.011

Ivar do Sul, J. A., and Labrenz, M. (2020). "Microplastics into the anthropocene: rise and fall of the human footprint," in *Handbook of Microplastics in the Environment*, eds T. Rocha-Santos, M. Costa, and C. Mouneyrac (Springer). doi: 10.1007/978-3-030-10618-8

Jamieson, A. J., Malkocs, T., Piertney, S. B., Fujii, T., and Zhang, Z. (2017). Bioaccumulation of persistent organic pollutants in the deepest ocean fauna. *Nat. Ecol. Evol.* 1, 1–4. doi: 10.1038/s41559-016-0051

Johannessen, S. C., and Macdonald, R. W. (2012). There is no 1954 in that core! Interpreting sedimentation rates and contaminant trends in marine sediment cores. *Mar. Pollut. Bull.* 64, 675–678. doi: 10.1016/j.marpolbul.2012.01.026

Jouzel, J., Raisbeck, G., Benoist, J. P., Yiou, F., Lorius, C., Raynaud, D., et al. (1989). A comparison of deep Antarctic ice cores and their implications for climate between 65,000 and 15,000 years ago. *Quat. Res.* 31, 135–150. doi: 10.1016/0033-5894(89)90003-3

Kaiser, D., Kowalski, N., and Waniek, J. J. (2017). Effects of biofouling on the sinking behavior of microplastics. *Environ. Res. Lett.* 12:124003. doi: 10.1088/1748-9326/aa8e8b

Kane, I. A., Clare, M. A., Miramontes, E., Wogelius, R., Rothwell, J. J., Garreau, P., et al. (2020). Seafloor microplastic hotspots controlled by deep-sea circulation. *Science* 368, 1140–1145. doi: 10.1126/science.aba5899

Kanhai, L. D. K., Katarina, G., Krumpen, T., and Thompson, R. C. (2020). Microplastics in sea ice and seawater beneath ice floes from the Arctic Ocean. *Sci. Rep.* 10:5004. doi: 10.1038/s41598-020-61948-6

Käppler, A., Fischer, D., Oberbeckmann, S., Schernewski, G., Labrenz, M., Eichhorn, K. J., et al. (2016). Analysis of environmental microplastics by vibrational microspectroscopy: FTIR, Raman or both? *Anal. Bioanal. Chem.* 408, 8377–8391. doi: 10.1007/s00216-016-9956-3

Katija, K., Choy, C. A., Sherlock, R. E., Sherman, A. D., and Robison, B. H. (2017). From the surface to the seafloor: how giant larvaceans transport microplastics into the deep sea. *Sci. Adv.* 3:e1700715. doi: 10.1126/sciadv.1700715

Kerrigan, J. F., Sandberg, K. D., Engstrom, D. R., La Para, T. M., and Arnold, W. A. (2018). Sedimentary record of antibiotic accumulation in Minnesota Lakes. *Sci. Tot. Environ.* 621, 970–979. doi: 10.1016/j.scitotenv.2017.10.130

Kinder, M., Tylmann, W., Bubak, I., Fiłoc, M., Gasiorowski, M., Kupryjanowicz, M., et al. (2019). Holocene history of human impacts inferred from annually laminated sediments in Lake Szurpiły, northeast Poland. *J. Paleolimnol.* 61, 419–435. doi: 10.1007/s10933-019-00068-2

Klein, S., Dimzon, I. K., Eubeler, J., and Knepper, T. P. (2018). "Analysis, occurrence, and degradation of microplastics in the aqueous environment," in *Freshwater Microplastics: Emerging Environmental Contaminants?* eds M. Wagner and S. Lambert (Cham: Springer Open), 51–67.

Klein, S., Worch, E., and Knepper, T. P. (2015). Occurrence and spatial distribution of microplastics in river shore sediments of the Rhine-Main area in Germany. *Environ. Sci. Technol.* 49, 6070–6076. doi: 10.1021/acs.est.5b00492

Knight, M., Ballantyne, R., Robinson Zeki, I., and Gibson, D. (2019). The must farm pile-dwelling settlement. *Antiquity* 93, 645–663. doi: 10.15184/aqy.2019.38

Koelmans, A. A., Nor, N. H. M., Hermsen, E., Kooi, M., Mintenig, S. M., and De France, J. (2019). Microplastics in freshwaters and drinking water: Critical review and assessment of data quality. *Water Res.* 155, 410–422. doi: 10.1016/j.watres.2019.02.054

Kong, X., and Koelmans, A. A. (2019). Modeling decreased resilience of shallow lake ecosystems toward eutrophication due to microplastic ingestion across the food web. *Environ. Sci. Technol.* 53, 13822–13831. doi: 10.1021/acs.est.9b03905

Kooi, M., Besseling, E., Kroeze, C., Van Wezel, A. P., and Koelmans, A. A. (2018). "Modeling the fate and transport of plastic debris in freshwaters: Review and Guidance," in *Freshwater Microplastics*: *Emerging Environmental Contaminants?* eds M. Wagner and S. Lambert (Cham: Springer Open), 125–152.

Laiho, R., Bhuiyan, R., Straková, P., Mäkiranta, P., Badorek, T., and Penttilä, T. (2014). Modified ingrowth core method plus infrared calibration models for estimating fine root production in peatlands. *Plant Soil* 385, 311–327. doi: 10.1007/s11104-014-2225-3

Law, K. L., Morét-Ferguson, S., Maximenko, N. A., Proskurowski, G., Peacock, E. E., Hafner, J., et al. (2010). Plastic accumulation in the North Atlantic subtropical gyre. *Science* 329, 1185–1188. doi: 10.1126/science.1192321

Lebreton, L., Egger, M., and Slat, B. (2019). A global mass budget for positively buoyant macroplastic debris in the ocean. *Sci. Rep.* 9:12922. doi: 10.1038/s41598-019-49413-5

Lebreton, L., Slat, B., Ferrari, F., Sainte-Rose, B., Aitken, J., Marthouse, R., et al. (2018). Evidence that the Great Pacific Garbage Patch is rapidly accumulating plastic. *Sci. Rep.* 8:4666. doi: 10.1038/s41598-018-22939-w

Lei, Y. D., and Wania, F. (2004). Is rain or snow a more efficient scavenger of organic chemicals? *Atmos. Environ.* 38, 3557–3571. doi: 10.1016/j.atmosenv.2004.03.039

Leinfelder, R., and Ivar do Sul, J. A. (2019). "The stratigraphy of plastics and their preservation in geological records," in *The Anthropocene as a Geological Time Unit: A Guide to the Scientific Evidence and Current Debate*, eds J. A. Zalasiewicz, C. N. Waters, M. Williams, and C. P. Summerhayes (Cambridge: Cambridge University Press), 147–155.

Lennartz, B., and Liu, H. (2019). Hydraulic functions of peat soils and ecosystem service. *Front. Environ. Sci.* 7:92. doi: 10.3389/fenvs.2019.00092

Li, J., Liu, H., and Chen, J. P. (2018). Microplastics in freshwater systems: a review on occurrence, environmental effects, and methods for microplastics detection. *Water Res.* 137, 362–374. doi: 10.1016/j.watres.2017.12.056

Li, R., Zhang, L., Xue, B., and Wang, Y. (2019). Abundance and characteristics of microplastics in the mangrove sediment of the semi-enclosed Maowei Sea of the south China sea: New implications for location, rhizosphere, and sediment compositions. *Environ. Pollut.* 244, 685–692. doi: 10.1016/j.envpol.2018.10.089

Lin, T., Hu, L., Shi, X., Li, Y., Guo, Z., and Zhang, G. (2012). Distribution and sources of organochlorine pesticides in sediments of the coastal East China Sea. *Mar. Pollut. Bull.* 64, 1549–1555. doi: 10.1016/j.marpolbul.2012.05.021

Lovett, G. M., and Kinsman, J. D. (1990). Atmospheric pollutant deposition to high-elevation ecosystems. *Atmos. Environ. Part A Gen. Top.* 24, 2767–2786. doi: 10.1016/0960-1686(90)90164-I

Lyons, K. (2018, October 9) 'Plastic bottle washes up looking 'almost new' after nearly 50 years at sea'. *The Guardian*. Available onlilne at: https://www.theguardian.com/environment/2018/oct/09/plastic-bottle-washes-up-looking-almost-new-after-nearly-50-years-at-sea (accessed June 16, 2020).

Maes, T., Barry, J., Leslie, H. A., Vethaak, A. D., Nicolaus, E. E. M., Law, R. J., et al. (2018). Below the surface: Twenty-five years of seafloor litter monitoring in coastal seas of North West Europe (1992–2017). *Sci. Total Environ.* 630, 790–798. doi: 10.1016/j.scitotenv.2018.02.245

Mai, L., Bao, L. J., Shi, L., Wong, C. S., and Zeng, E. Y. (2018). A review of methods for measuring microplastics in aquatic environments. *Environ. Sci. Poll. Res.* 25, 11319–11332. doi: 10.1007/s11356-018-1692-0

Mapstone, T. (2019, June 12). "Plastic bag found in Sunshine Coast waterway could be up to 40 years old and it's just the tip of the iceberg". *ABC News*. Available online at: https://www.abc.net.au/news/2019-06-13/40-year-old-plastic-bag-found-in-waterway/11197892 (accessed June 16, 2020).

Martí, E., Martin, C., Galli, M., Echevarría, F., Duarte, C. M., and Cózar, A. (2020). The colours of the ocean plastics. *Environ. Sci. Technol.* 54, 6594–6601. doi: 10.1021/acs.est.9b06400

Martínez-Cortizas, A., Pontevedra-Pombal, X., Garcia-Rodeja, E., Novoa-Munoz, J. C., and Shotyk, W. (1999). Mercury in a Spanish peat bog: archive of climate change and atmospheric metal deposition. *Science* 284, 939–942. doi: 10.1126/science.284.5416.939

Martínez-Cortizas, A., and Weiss, D. (2002). Peat bog archives of atmospheric metal deposition. *Sci. Tot. Environ.* 292, 1–5. doi: 10.1016/S0048-9697(02)00024-4

Matsuguma, Y., Takada, H., Kumata, H., Kanke, H., Sakurai, S., Suzuki, T., et al. (2017). Microplastics in sediment cores from Asia and Africa as indicators of temporal trends in plastic pollution. *Arch. Environ. Contam. Toxicol.* 73, 230–239. doi: 10.1007/s00244-017-0414-9

McCall, P. L., and Fisher, J. B. (1980). "Effects of tubificid oligochaetes on physical and chemical properties of lake Erie sediments," in *Aquatic Oligochaete Biology*, eds R. O. Brinkhurst and D. G. Cook (Boston, MA: Springer), 253–317.

McConnell, J. R., and Edwards, R. (2008). Coal burning leaves toxic heavy metal legacy in the Arctic. *Proc. Natl. Acad. Sci. U.S.A.* 105, 12140–12144. doi: 10.1073/pnas.0803564105

McConnell, J. R., Maselli, O. J., Sigl, M., Vallelonga, P., Neumann, T., Anschütz, H., et al. (2014). Antarctic-wide array of high-resolution ice core records reveals pervasive lead pollution began in 1889 and persists today. *Sci. Rep.* 4:5848. doi: 10.1038/srep05848

Mendoza, L. M. R., and Balcer, M. (2019). Microplastics in freshwater environments: a review of quantification assessment. *Trends Anal. Chem.* 113, 402–408. doi: 10.1016/j.trac.2018.10.020

Meng, Y., Kelly, F. J., and Wright, S. L. (2020). Advances and challenges of microplastic pollution in freshwater ecosystems: a UK perspective. *Environ. Pollut.* 256:113445. doi: 10.1016/j.envpol.2019.113445

Meyers, P. A., and Lallier-Vergès, E. (1999). Lacustrine sedimentary organic matter records of Late Quaternary paleoclimates. *J. Paleolimnol.* 21, 345–372. doi: 10.1023/A:1008073732192

Michels, J., Stippkugel, A., Lenz, M., Wirtz, K., and Engel, A. (2018). Rapid aggregation of biofilm-covered microplastics with marine biogenic particles. *Proc. R. Soc. B.* 285:20181203. doi: 10.1098/rspb.2018.1203

Miller, R. Z., Watts, A. J. R., Winslow, B. O., Galloway, T. S., and Barrows, A. P. W. (2017). Mountains to the sea: river study of plastic and non-plastic microfiber pollution in the northeast USA. *Mar. Pollut. Bull.* 124, 245–251. doi: 10.1016/j.marpolbul.2017.07.028

Mintenig, S. M., Int-Veen, I., Löder, M. G., Primpke, S., and Gerdts, G. (2017). Identification of microplastic in effluents of waste water treatment plants using focal plane array-based micro-Fourier-transform infrared imaging. *Water Res.* 108, 365–372. doi: 10.1016/j.watres.2016.11.015

Möhlenkamp, P., Purser, A., and Thomsen, L. (2018). Plastic microbeads: an experimental study of their hydrodynamic behaviour, vertical transport and resuspension in phytoplankton and sediment aggregates. *Elem. Sci. Anth.* 6:61. doi: 10.1525/elementa.317

Morritt, D., Stefanoudis, P. V., Pearce, D., Crimmen, O. A., and Clark, P. F. (2014). Plastic in the Thames: a river runs through it. *Mar. Pollut. Bull.* 78, 196–200. doi: 10.1016/j.marpolbul.2013.10.035

Muir, D. C. G., Grift, N. P., Lockhart, W. L., Wilkinson, P., Billeck, B. N., and Brunskill, G. J. (1995). Spatial trends and historical profiles of organochlorine pesticides in Arctic lake sediments. *Sci. Total Environ.* 160–161, 447–457. doi: 10.1016/0048-9697(95)04378-E

Mulder, T., Hüneke, H., and Van Loon, A. J. (2011). "Progress in deep-sea sedimentology," in *Developments in Sedimentology*, eds H. Hüneke and T. Mulder (Amsterdam: Elsevier), 1–24.

Naidu, S. A., Ranga Rao, V., and Ramu, K. (2018). Microplastics in the benthic invertebrates from the coastal waters of Kochi, Southeastern Arabian Sea. *Environ. Geochem. Health* 40, 1377–1383. doi: 10.1007/s10653-017-0062-z

Ng, K. L., and Obbard, J. P. (2006). Prevalence of microplastics in Singapore's coastal marine environment. *Mar. Pollut. Bull.* 52, 761–767. doi: 10.1016/j.marpolbul.2005.11.017

Nieminen, T. M., Ukonmaanaho, L., and Shotyk, W. (2002). Enrichment of Cu, Ni, Zn, Pb and as in an ombrotrophic peat bog near a Cu–Ni smelter in Southwest Finland. *Sci. Total Environ.* 292, 81–89. doi: 10.1016/S0048-9697(02)00028-1

Nor, N. H. M., and Obbard, J. P. (2014). Microplastics in Singapore's coastal mangrove ecosystems. *Mar. Pollut. Bull.* 79, 278–283. doi: 10.1016/j.marpolbul.2013.11.025

Nuelle, M. T., Dekiff, J. H., Remy, D., and Fries, E. (2014). A new analytical approach for monitoring microplastics in marine sediments. *Environ. Pollut.* 184, 161–169. doi: 10.1016/j.envpol.2013.07.027

Obbard, R. W., Sadri, S., Wong, Y. Q., Khitun, A. A., Baker, I., and Thompson, R. C. (2014). Global warming releases microplastic legacy frozen in Arctic Sea ice. *Earth's Fut.* 2, 315–320. doi: 10.1002/2014EF000240

Ostle, C., Thompson, R. C., Broughton, D., Gregory, L., Wootton, M., and Johns, D. G. (2019). The rise in ocean plastics evidenced from a 60-year time series. *Nat. Commun.* 10:1622. doi: 10.1038/s41467-019-09506-1

Outridge, P. M., and Wang, F. (2015). "The stability of metal profiles in freshwater and marine sediments," in *Environmental contaminants. Developments in Paleoenvironmental Research*, Vol. 18, eds J. Blais, M. Rosen, and J. Smol (Dordrecht: Springer), 35–60.

Pagter, E., Frias, J., and Nash, R. (2018). Microplastics in galway bay: a comparison of sampling and separation methods. *Mar. Pollut. Bull.* 135, 932–940. doi: 10.1016/j.marpolbul.2018.08.013

Peeken, I., Primpke, S., Beyer, B., Gütermann, J., Katlein, C., Krumpen, T., et al. (2018). Arctic sea ice is an important temporal sink and means of transport for microplastic. *Nat. Commun.* 9:1505. doi: 10.1038/s41467-018-03825-5

Peng, G., Xu, P., Zhu, B., Bai, M., and Li, D. (2018). Microplastics in freshwater river sediments in Shanghai, China: a case study of risk assessment in mega-cities. *Environ. Pollut.* 234, 448–456. doi: 10.1016/j.envpol.2017.11.034

Pietrelli, L., Di Gennaro, A., Menegoni, P., Lecce, F., Poeta, G., Acosta, A. T. R., et al. (2017). Pervasive plastisphere: first record of plastics in egagropiles (*Posidonia* spheroids). *Environ. Pollut.* 229, 1032–1036. doi: 10.1016/j.envpol.2017.07.098

Plastics Europe (2012). *Plastics—The Facts 2012: An Analysis of European Plastics Production, Demand and Waste Data for 2011.* Available online at: https://www.plasticseurope.org/download_file/force/1687/181 (accessed June 17, 2020).

Plastics Europe (2016). *Plastics—The Facts 2016: An Analysis of European Plastics Production, Demand and Waste Data.* Available online at: https://www.plasticseurope.org/application/files/4315/1310/4805/plastic-the-fact-2016.pdf (accessed June 15, 2020).

Plastics Europe (2019). *Plastics – The Facts 2019: An Analysis of European Plastics Production, Demand and Waste Data.* Available online at: https://www.plasticseurope.org/download_file/force/3183/181 (accessed June 15, 2020).

Porter, A., Lyons, B. P., Galloway, T. S., and Lewis, C. (2018). Role of marine snows in microplastic fate and bioavailability. *Environ. Sci. Technol.* 52, 7111–7119. doi: 10.1021/acs.est.8b01000

Prata, J. C., da Costa, J. P., Duarte, A. C., and Rocha-Santos, T. (2019). Methods for sampling and detection of microplastics in water and sediment: a critical review. *Trends Anal. Chem.* 110, 150–159. doi: 10.1016/j.trac.2018.10.029

Primpke, S., Cross, R. K., Mintenig, S. M., Simon, M., Vianello, A., Gerdts, G., et al. (2020). EXPRESS: toward the systematic identification of microplastics in the environment: evaluation of a new independent software tool (siMPle) for spectroscopic analysis. *Appl. Spectrosc.* 3702820917760. doi: 10.1177/0003702820917760

Quinn, B., Murphy, F., and Ewins, C. (2017). Validation of density separation for the rapid recovery of microplastics from sediment. *Anal. Meth.* 9, 1491–1498. doi: 10.1039/C6AY02542K

Quinton, W., Elliot, T., Price, J., Rezanezhad, F., and Heck, R. (2009). Measuring physical and hydraulic properties of peat from X-ray tomography. *Geoderma* 153, 269–277. doi: 10.1016/j.geoderma.2009.08.010

Rausch, N., Nieminen, T., Ukonmaanaho, L., Le Roux, G., Krachler, M., Cheburkin, A. K., et al. (2005). Comparison of atmospheric deposition of copper, nickel, cobalt, zinc, and cadmium recorded by Finnish peat cores with monitoring data and emission records. *Environ. Sci. Technol.* 39, 5989–5998. doi: 10.1021/es050260m

Redondo-Hasselerharm, P. E., Falahudin, D., Peeters, E. T., and Koelmans, A. A. (2018). Microplastic effect thresholds for freshwater benthic macroinvertebrates. *Environ. Sci. Technol.* 52, 2278–2286. doi: 10.1021/acs.est.7b05367

Redondo-Hasselerharm, P. E., Gort, G., Peeters, E. T. H. M., and Koelmans, A. A. (2020). Nano- and microplastics affect the composition of freshwater benthic communities in the long term. *Sci. Adv.* 6:eaay4054. doi: 10.1126/sciadv.aay4054

Renberg, I., Bindler, R., and Brännvall, M.-L. (2001). Using the historical atmospheric lead-deposition record as a chronological marker in sediment deposits in Europe. *Holocene* 11, 511–516. doi: 10.1191/095968301680223468

Reynolds, C., and Ryan, P. G. (2018). Micro-plastic ingestion by waterbirds from contaminated wetlands in South Africa. *Mar. Pollut. Bull.* 126, 330–333. doi: 10.1016/j.marpolbul.2017.11.021

Rezaei, M., Riksen, M. J. P. M., Sirjani, E., Sameni, A., and Geissen, V. (2019). Wind erosion as a driver for transport of light density microplastics. *Sci. Tot. Environ.* 669, 273–281. doi: 10.1016/j.scitotenv.2019.02.382

Rezanezhad, F., Price, J. S., Quinton, W. L., Lennartz, B., Milojevic, T., and Van Cappellen, P. (2016). Structure of peat soils and implications for water storage, flow and solute transport: a review update for geochemists. *Chem. Geol.* 429, 75–84. doi: 10.1016/j.chemgeo.2016.03.010

Ribeiro-Claro, P., Nolasco, M. M., and Araújo, C. (2017). Characterization of microplastics by Raman spectroscopy. *Compr. Anal. Chem.* 75, 119–151. doi: 10.1016/bs.coac.2016.10.001

Rillig, M. C. (2018). Microplastic disguising as soil carbon storage. *Environ. Sci. Technol.* 52, 6079–6080. doi: 10.1021/acs.est.8b02338

Robbins, J. A. (1978). "Geochemical and geophysical applications of radioactive lead," in *The Biogeochemistry of Lead in the Environment*, ed J. O. Nriagu (Amsterdam: Elsevier/North-Holland Biomedical), 285–393.

Rochman, C. M., Brookson, C., Bikker, J., Djuric, N., Earn, A., Bucci, K., et al. (2019). Rethinking microplastics as a diverse contaminant suite. *Environ. Toxicol. Chem.* 38, 703–711. doi: 10.1002/etc.4371

Rose, N. L. (2015). Spheroidal carbonaceous fly-ash particles provide a globally synchronous stratigraphic marker for the Anthropocene. *Environ. Sci. Technol.* 49, 4155–4162. doi: 10.1021/acs.est.5b00543

Ryan, P. G., Moore, C. J., van Franeker, J. A., and Moloney, C. L. (2009). Monitoring the abundance of plastic debris in the marine environment. *Philos. Trans. R. Soc. B. Biol. Sci.* 364, 1999–2012. doi: 10.1098/rstb.2008.0207

Sanchez, W., Bender, C., and Porcher, J.-M. (2014). Wild gudgeons (*Gobio gobio*) from French rivers are contaminated by microplastics: preliminary study and first evidence. *Environ. Res.* 128, 98–100. doi: 10.1016/j.envres.2013.11.004

Sander, L. (2016). Date-prints on stranded macroplastics: inferring the timing and extent of overwash deposition on the Skallingen peninsula, Denmark. *Mar. Pollut. Bull.* 109, 373–377. doi: 10.1016/j.marpolbul.2016.05.051

Scherer, C., Brennholt, N., Reifferscheid, G., and Wagner, M. (2017). Feeding type and development drive the ingestion of microplastics by freshwater invertebrates. *Sci. Rep.* 7:17006. doi: 10.1038/s41598-017-17191-7

Scheurer, M., and Bigalke, M. (2018). Microplastics in swiss floodplain soils. *Environ. Sci. Technol.* 52, 3591–3598. doi: 10.1021/acs.est.7b06003

Scholz, C. A. (2001). "Applications of seismic sequence stratigraphy in lacustrine basins," in *Tracking Environmental Change Using Lake Sediments. Volume 1: Basin Analysis, Coring, and Chronological Techniques,* eds W. M. Last and J. P. Smol (Dordrecht: Kluwer Academic Publishers), 7–22.

Schotterer, U., Stichler, W., and Ginot, P. (2004). "The Influence of post-depositional effects on ice core studies: examples from the Alps, Andes, and Altai," in *Earth Paleoenvironments: Records Preserved in Mid- and Low-Latitude Glaciers.* eds L. Cecil, J. R. DeWayne, L. G. Green Thompson (Dordrecht: Springer), 39–59.

Scopetani, C., Esterhuizen-Londt, M., Chelazzi, D., Cincinelli, A., Setälä, H., and Pflugmacher, S. (2020). Self-contamination from clothing in microplastics research. *Ecotoxicol. Environ. Safety* 189:110036. doi: 10.1016/j.ecoenv.2019.110036

Seddon, A. W. R., Mackay, A. W., Baker, A. G., Birks, H. J. B., Breman, E., Buck, C. E., et al. (2014). Looking forward through the past. Identification of fifty priority research questions in palaeoecology. *J. Ecol.* 102, 256–267. doi: 10.1111/1365-2745.12195

Setälä, O., Fleming-Lehtinen, V., and Lehtiniemi, M. (2014). Ingestion and transfer of microplastics in the planktonic food web. *Environ. Pollut.* 185, 77–83. doi: 10.1016/j.envpol.2013.10.013

Shotyk, W. (1996). Peat bog archives of atmospheric metal deposition: geochemical evaluation of peat profiles, natural variations in metal concentrations, and metal enrichment factors. *Environ. Rev.* 4, 149–183. doi: 10.1139/a96-010

Šilc, U., Küzmič, F., Caković, D., and Stešević, D. (2018). Beach litter along various sand dune habitats in the southern Adriatic (E Mediterranean). *Mar. Pollut. Bull.* 128, 353–360. doi: 10.1016/j.marpolbul.2018.01.045

Silva, A. B., Bastos, A. S., Justino, C. I. L., da Costa, J. P., Duarte, A. C., and Rocha- Santos, T. A. P. (2018). Microplastics in the environment: challenges in analytical chemistry - a review. *Anal. Chim. Acta* 1017, 1–19. doi: 10.1016/j.aca.2018.02.043

Souter, L., and Watmough, S. A. (2016). The impact of drought and air pollution on metal profiles in peat cores. *Sci. Total Environ.* 541, 1031–1040. doi: 10.1016/j.scitotenv.2015.09.137

Su, L., Xue, Y., Li, L., Yang, D., Kolandhasamy, P., Li, D., et al. (2016). Microplastics in Taihu Lake, China. *Environ. Pollut.* 216, 711–719. doi: 10.1016/j.envpol.2016.06.036

Tekman, M. B., Wekerle, C., Lorenz, C., Primpke, S., Hasemann, C., Gerdts, G., et al. (2020). Tying up loose ends of microplastic pollution in the arctic: distribution from the sea surface through the water column to deep-sea sediments at the HAUSGARTEN observatory. *Environ. Sci. Technol.* 54, 4079–4090. doi: 10.1021/acs.est.9b06981

Teuten, E. L., Saquing, J. M., Knappe, D. R. U., Barlaz, M. A., Jonsson, S., Björn, A., et al. (2009). Transport and release of chemicals from plastics to the environment and to wildlife. *Philos. Trans. R. Soc. B Biol. Sci.* 364, 2027–2045. doi: 10.1098/rstb.2008.0284

Thompson, R. C., Olsen, Y., Mitchell, R. P., Davis, A., Rowland, S. J., John, A. W. G., et al. (2004). Lost at sea: where is all the plastic? *Science* 304:838. doi: 10.1126/science.1094559

Tibbetts, J., Krause, S., Lynch, I., and Smith, G. H. S. (2018). Abundance, distribution, and drivers of microplastic contamination in urban river environments. *Water* 10:1597. doi: 10.3390/w10111597

Turner, S. D., Horton, A., Rose, N. L., and Hall, C. J. (2019). A temporal sediment record of microplastics in an urban lake, London, UK. *J. Paleolimnol.* 61, 449–462. doi: 10.1007/s10933-019-00071-7

Uglietti, C., Gabrielli, P., Cooke, C. A., Vallelonga, P., and Thompson, L. G. (2015). Widespread pollution of the South American atmosphere predates the Industrial Revolution by 240 y. *Proc. Natl. Acad. Sci. U.S.A.* 112, 2349–2354. doi: 10.1073/pnas.1421119112

Van Cauwenberghe, L., Devriese, L., Galgani, F., Robbens, J., and Janssen, C. R. (2015). Microplastics in sediments: a review oftechniques, occurrence and effects. *Mar. Environ. Res.* 111, 5–17. doi: 10.1016/j.marenvres.2015.06.007

Van Cauwenberghe, L., Vanreusel, A., Mees, J., and Janssen, C. R. (2013). Microplastic pollution in deep-sea sediments. *Environ. Pollut.* 182, 495–499. doi: 10.1016/j.envpol.2013.08.013

Vaughan, R., Turner, S. D., and Rose, N. L. (2017). Microplastics in the sediments of a UK urban lake. *Environ. Pollut.* 229, 10–18. doi: 10.1016/j.envpol.2017.05.057

Vosshage, A. T. L., Neu, T. R., and Gabel, F. (2018). Plastic alters biofilm quality as food resource of the freshwater gastropod *Radix balthica*. *Environ. Sci. Technol.* 52, 11387–11393. doi: 10.1021/acs.est.8b02470

Votier, S. C., Archibald, K., Morgan, G., and Morgan, L. (2011). The use of plastic debris as nesting material by a colonial seabird and associated entanglement mortality. *Mar. Pollut. Bull.* 62, 168–172. doi: 10.1016/j.marpolbul.2010.11.009

Waters, C. N., Zalasiewicz, J., Summerhayes, C., Fairchild, I. J., Rose, N. L., Loader, N. J., et al. (2018). Global Boundary Stratotype Section and Point (GSSP) for the anthropocene series: where and how to look for potential candidates. *Earth-Sci. Rev.* 178, 379–429. doi: 10.1016/j.earscirev.2017.12.016

Weinstein, J. E., Crocker, B. K., and Gray, A. D. (2016). From macroplastic to microplastic: degradation of high-density polyethylene, polypropylene, and polystyrene in a salt marsh habitat. *Environ. Toxicol. Chem.* 35, 1632–1640. doi: 10.1002/etc.3432

Williams, A. T., and Simmons, S. L. (1996). The degradation of plastic litter in rivers: Implications for beaches. *J. Coast. Conserv.* 2, 63–72. doi: 10.1007/BF02743038

Willis, K. A., Eriksen, R., Wilcox, C., and Hardesty, B. D. (2017). microplastic distribution at different sediment depths in an urban estuary. *Front. Mar. Sci.* 4, 1–8. doi: 10.3389/fmars.2017.00419

Wiltshire, P. E. J. (2006). Consideration of some taphonomic variables of relevance to forensic palynological investigation in the United Kingdom. *Forensic Sci. Int.* 163, 173–182. doi: 10.1016/j.forsciint.2006.07.011

Woodall, L. C., Sanchez-Vidal, A., Canals, M., Paterson, G. L., Coppock, R., Sleight, V., et al. (2014). The deep sea is a major sink for microplastic debris. *R. Soc. Open Sci.* 1:140317. doi: 10.1098/rsos.140317

Xiong, X., Zhang, K., Chen, X., Shi, H., Luo, Z., and Wu, C. (2018). Sources and distribution of microplastics in China's largest inland lake Qinghai Lake. *Environ. Pollut.* 235, 899–906. doi: 10.1016/j.envpol.2017.12.081

Xue, B., Zhang, L., Li, R., Wang, Y., Guo, J., Yu, K., et al. (2020). Underestimated microplastic pollution derived from fishery activities and "Hidden" in deep sediment. *Environ. Sci. Technol.* 54, 2210–2217. doi: 10.1021/acs.est.9b04850

Yang, C., Rose, N. L., Turner, S. D., Yang, H., Goldsmith, B., Losada, S., et al. (2016). Hexabromocyclododecanes, polybrominated diphenyl ethers and polychlorinated biphenyls in radiometrically dated sediment cores from English Lakes, ∼1950 – present. *Sci. Total Environ.* 541, 721–728. doi: 10.1016/j.scitotenv.2015.09.102

Yang, H., Engstrom, D., and Rose, N. L. (2010). Recent changes in atmospheric mercury deposition recorded in the sediments of remote, equatorial lakes in the Rwenzori Mountains, Uganda. *Environ. Sci. Technol.* 44, 6570–6575. doi: 10.1021/es101508p

Yao, W., Di, D., Wang, Z., Liao, Z., Huang, H., Mei, K., et al. (2019). Micro- and macroplastic accumulation in a newly formed *Spartina alterniflora* colonized estuarine saltmarsh in southeast China. *Mar. Pollut. Bull.* 149:110636. doi: 10.1016/j.marpolbul.2019.110636

Zalasiewicz, J., Waters, C. N., Ivar do Sul, J. A., Corcoran, P. L., Barnosky, A. D., Cearreta, A., et al. (2016). The geological cycle of plastics and their use as a stratigraphic indicator of the Anthropocene. *Anthropocene* 13, 4–17. doi: 10.1016/j.ancene.2016.01.002

Zalasiewicz, J. A., Summerhayes, C. P., Head, M. J., Wing, S., Gibbard, P., and Waters, C. N. (2019). "Stratigraphy and the geological time scale," in *The Anthropocene as a Geological Time Unit: A Guide to the Scientific Evidence and Current Debate*, eds J. A. Zalasiewicz, C. N. Waters, M. Williams, and C. P. Summerhayes (Cambridge: Cambridge University Press), 11–30.

Zarfl, C. (2019). Promising techniques and open challenges for microplastic identification and quantification in environmental matrices. *Anal. Bioanal. Chem.* 411, 3743–3756. doi: 10.1007/s00216-019-01763-9

Zhang, K., Su, J., Xiong, X., Wu, X., Wu, C., and Liu, J. (2016). Microplastic pollution of lakeshore sediments from remote lakes in Tibet plateau, China. *Environ. Pollut.* 219, 450–455. doi: 10.1016/j.envpol.2016.05.048

Zhao, S., Danley, M., Ward, J. E., Li, D., and Mincer, T. J. (2017). An approach for extraction, characterization and quantitation of microplastic in natural marine snow using Raman microscopy. *Anal. Met.* 9, 1470–1478. doi: 10.1039/C6AY02302A

Zhao, S., Zhu, L., Gao, L., and Li, D. (2018). "Limitations for microplastic quantification in the ocean and recommendations for improvement and standardization," in *Microplastic Contamination in Aquatic Environments*, ed E. Y. Zeng (Amsterdam: Elsevier), 27–49.

Zobkov, M. B., Esiukova, E. E., Zyubin, A. Y., and Samusev, I. G. (2019). Microplastic content variation in water column: The observations employing a novel sampling tool in stratified Baltic Sea. *Mar. Pollut. Bull.* 138, 193–205. doi: 10.1016/j.marpolbul.2018.11.047

Zylstra, E. R. (2013). Accumulation of wind-dispersed trash in desert environments. *J. Arid Environ.* 89, 13–15. doi: 10.1016/j.jaridenv.2012.10.004

Conflict of Interest: The authors declare that the research was conducted in the absence of any commercial or financial relationships that could be construed as a potential conflict of interest.

frontiers in Marine Science

ORIGINAL RESEARCH
published: 04 November 2020
doi: 10.3389/fmars.2020.574663

Microplastics in Commercially Important Small Pelagic Fish Species From South Africa

Adil Bakir[1], Carl D. van der Lingen[2], Fiona Preston-Whyte[1], Ashok Bali[2], Yonela Geja[2], Jon Barry[1], Yandiswa Mdazuka[3], Gcobani Mooi[3], Denise Doran[1], Freya Tooley[1], Rogan Harmer[1] and Thomas Maes[1,4]*

[1] Centre for Environment, Fisheries and Aquaculture Science, Lowestoft Laboratory, Lowestoft, United Kingdom, [2] Fisheries Management, Department of Environment, Forestry and Fisheries, Cape Town, South Africa, [3] Oceans and Coasts, Department of Environment, Forestry and Fisheries, Cape Town, South Africa, [4] GRID-Arendal, Arendal, Norway

This study documented the levels of microplastics in three commercially important small pelagic fish species in South African waters, namely European anchovy (*Engraulis encrasicolus*), West Coast round herring (*Etrumeus whiteheadi*) and South African sardine (*Sardinops sagax*). Data suggested variation between species with a higher concentration of microplastics for *S. sagax* (mean of 1.58 items individual^{-1}) compared to *Et. whiteheadi* (1.38 items individual^{-1}) and *En. encrasicolus* (1.13 items individual^{-1}). The occurrence of microplastics was also higher for *S. sagax* (72%) and *Et. whiteheadi* (72%) compared to *En. encrasicolus* (57%). Microfibers accounted for 80% of ingested microplastics (the remainder were plastic fragments) with the main ingested polymers being poly(ethylene:propylene:diene) (33% occurrence), polyethylene (20%), polyamide (20%), polyester (20%), and polypropylene (7%). The abundance of ingested items was not significantly correlated with fish caudal length or body weight, and spatial investigation indicated an increase in the abundance of ingested items from the West to the South coast. *Etrumeus whiteheadi* is proposed as a bio-indicator for microplastics for South Africa.

Keywords: commercial small pelagic fish species, *Engraulis encrasicolus* (European anchovy), *Etrumeus whiteheadi* (West Coast round herring), *Sardinops sagax* (South African sardine), marine litter, microplastics

OPEN ACCESS

Edited by:
Andrew Turner,
University of Plymouth,
United Kingdom

Reviewed by:
Periyadan K. Krishnakumar,
King Fahd University of Petroleum & Minerals, Saudi Arabia
Qing Wang,
Yantai Institute of Coastal Zone Research (CAS), China

****Correspondence:***
Adil Bakir
adil.bakir@cefas.co.uk

Specialty section:
This article was submitted to Marine Pollution, a section of the journal Frontiers in Marine Science

Received: *23 June 2020*
Accepted: *07 October 2020*
Published: *04 November 2020*

Citation:
Bakir A, van der Lingen CD, Preston-Whyte F, Bali A, Geja Y, Barry J, Mdazuka Y, Mooi G, Doran D, Tooley F, Harmer R and Maes T (2020) Microplastics in Commercially Important Small Pelagic Fish Species From South Africa. Front. Mar. Sci. 7:574663. doi: 10.3389/fmars.2020.574663

INTRODUCTION

Plastics are valuable resources with numerous societal benefits. Global plastics production was almost 360 million tonnes in 2018, of which 7% was attributed to the Middle East and Africa (PlasticsEurope, 2019). In South Africa in 2015, most plastic consumption was attributed to product packaging (53%), followed by building and construction (13%), and agriculture (9%) (Plastics SA, 2019).

Reduction of marine plastic litter through plastic waste management is the current focus of international efforts (Babayemi et al., 2019). Impacts of marine plastic litter are varied and include ingestion by biota (macro, meso, and microplastics including microfibers) or entanglement/collision [e.g., ghost fishing caused by Abandoned Lost or otherwise Discarded Fishing Gear (ALDFG)]. Plastics can also act as substrate for a wide variety of species increasing their potential for long-range transport (GESAMP, 2020). Microplastics are widespread in the

environment with some known environmental and ecological impacts. Field and laboratory studies have demonstrated the ingestion of microplastics by a large range of marine organisms representing various trophic levels including seabirds, marine mammals, fish and invertebrates (GESAMP, 2015) and detrimental physical effects of microplastics have been reported following ingestion (Wright et al., 2013), including mortality (Maes et al., 2020). There is also evidence that microplastics can act as carriers for harmful sorbed co-contaminants (i.e., hydrophobic organic compounds, additives, pathogens) with the potential for transfer to biota following ingestion (Rochman et al., 2013; Tanaka et al., 2013; Bakir et al., 2014). However, the transfer of sorbed co-contaminants from microplastics to biota may be negligible compared to other routes of exposure (Bakir et al., 2016; Herzke et al., 2016; Koelmans et al., 2016; Lohmann, 2017).

Plastic litter in biota within and off South Africa has been studied on a macro scale in sharks (Cliff et al., 2002), turtles (Ryan et al., 2016a), albatrosses and Southern Ocean fur seals (Ryan et al., 2016b), on a micro scale in fish (Naidoo et al., 2015, 2020b; Ross, 2017; Naidoo and Glassom, 2019) and inland waterbirds (Reynolds and Ryan, 2018). Data on the abundance of microplastics in commercially important fish species for South Africa is, however, limited and there is a need to address this knowledge gap. Small pelagic fish are of particular importance as they occupy a vital place in marine food webs and the fishery for these species is South Africa's largest and second-most valuable (DFFE, 2020). Whilst most of the catch is processed into agri- and aqua-feeds, small pelagic fish are an important source of food with canned sardine (pilchard) being one of the most important basic food items in the diets of South Africans (Isaacs, 2016). Investigation in microplastic contamination in small pelagic fish is therefore required to assess some related ecological impacts as well as understanding the potential for direct uptake via the human diet.

The aim of this study was to investigate the abundance of microplastics in three commercially important South African small pelagic fish species, namely European anchovy (*Engraulis encrasicolus*), West Coast round herring (*Etrumeus whiteheadi*) and South African sardine (*Sardinops sagax*). The main objectives were to (i) apply a proposed approach for the extraction and quantification of microplastics in small pelagic fish, (ii) to investigate interspecific differences in microplastic ingestion, (iii) to identify the main plastic and polymer types ingested by biota, (iv) to investigate spatial variations with the identification of "accumulation zones" of microplastics contamination, and (v) to identify and propose a suitable bio-indicator species for the monitoring of microplastics in South African waters.

MATERIALS AND METHODS

Biota Sampling

Samples of the three small pelagic fish species were collected during the 2019 Pelagic Recruit Survey that covered the inshore shelf along the South African coastline from the Orange River mouth (West Coast) to Mossel Bay (South Coast) in seven geographical areas or strata (A–G; **Figure 1**, Shabangu et al., 2019). Echosounders were used to identify biomass hotspots along survey transects and midwater trawls (nylon net) were used to catch pelagic fish. Trawl composition varied from one to several species, with all three small pelagic species often being caught in a single trawl. Collected biota samples (i.e., intact individuals) were stored intact and frozen (−20°C) in labeled (date and location of capture) plastic bags until ready for dissection.

Chemicals

The chemicals used in this study are listed in **Table 1**.

Quantification of Contamination and Quality Control

Contamination control procedures were followed to reduce contamination of samples. Cotton lab coats were worn to avoid contamination from clothing items. Prior to use, all glassware and dissection kits were cleaned using a laboratory detergent and rinsed using reverse osmosis (RO) water and covered with RO rinsed foil until ready for use. Gastrointestinal tracts (GITs) were removed under a fume cupboard and quickly transferred to RO rinsed 120 mL glass specimen jars covered with RO rinsed foil. Jars were then transferred to a PCR workstation with laminar flow for the addition of chemical solutions. All chemical solutions used in this study were previously filtered using a 47 mm diameter, 0.2 μm regenerated cellulose membrane filter. Contamination monitoring within the laboratory was carried out by using negative and positive controls. Negative controls consisted of blank filters processed in the same way as environmental samples for each batch of samples processed. Positive controls consisted on the spiking of some filters and checking for particle recovery.

Microplastics in Biota

A total of 593 individual fish were processed during this study comprising of 178 *En. encrasicolus*, 188 *Et. whiteheadi* and 227 *S. sagax*, collected from seven stations per species split across the survey strata as shown in **Figure 1**. For strata with a homogeneous population size distribution, the caudal length (equivalent to standard length) and wet body weight were recorded for five individuals per species, per sampling station (thus representing each stratum), and averaged values were used for calculations. Individual fish caudal length (0.1 cm) and wet body weight (0.1 g) were recorded prior to removal of the GITs under a pre-cleaned fume cupboard to avoid ambient contamination. Stomach weight was collected for all individuals. To determine potential health effects from microplastics on sardines, the lengths and weights of all individual fish were measured in strata E and F. The wet weight of the tissues was recorded and each GIT was transferred to a 120 mL glass jar, pre-cleaned with RO water. To compensate for ambient contamination, an empty glass jar was left open inside the fume cupboard, during the time required to dissect one individual as a blank. The number of items in the blank were deducted from the total number of items in fish for the corresponding batch. As the size of *En. encrasicolus* varied greatly across strata, for sites where individuals were too small for dissection

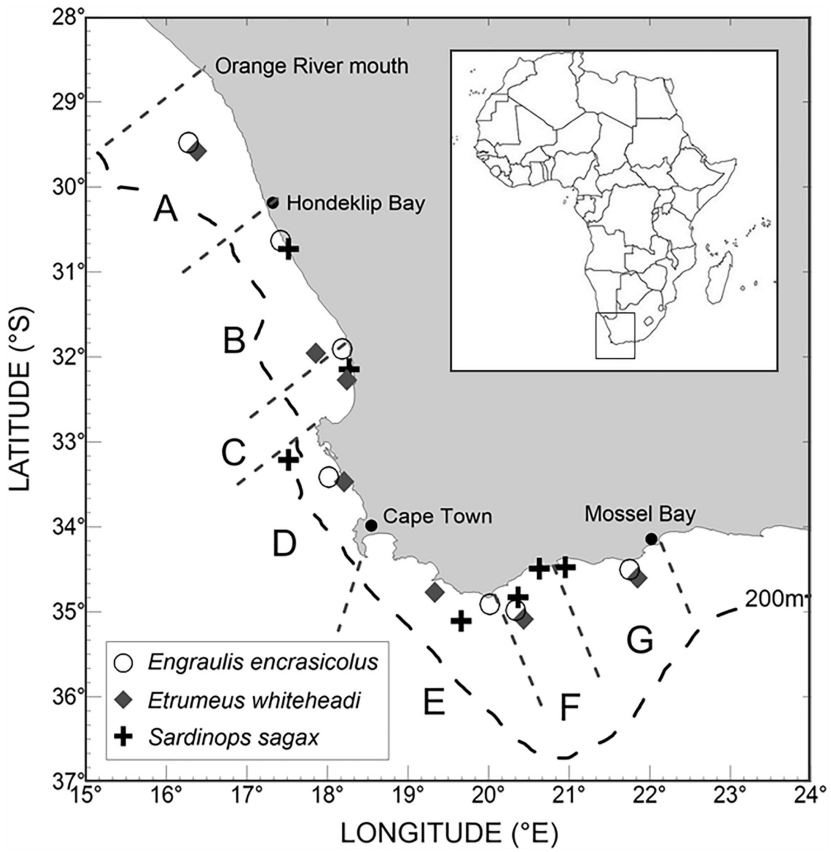

FIGURE 1 | Locations of midwater trawls where biota (small pelagic fishes: white circles for *Engraulis encrasicolus*; gray diamonds for *Etrumeus whiteheadi*; black crosses for *Sardinops sagax*) samples were collected during the 2019 Pelagic Recruit Survey and processed for microplastics. The 200 m depth contour is indicated by the black dashed line and the borders of survey strata A to G by gray dashed lines. Note that sardines were collected from two trawls in stratum F in order to obtain sufficient fish for processing.

TABLE 1 | List of chemicals, manufacturers, and suppliers.

Chemicals	Molecular formula	Manufacturer/supplier	Purity (%)
Potassium hydroxide	KOH	Lasec, South Africa	Analytical Reagent
Sodium hypochlorite	NaClO	Lasec, South Africa	13% active chlorine
Ethanol	C_2H_6O	VWR	95% purity
Nile Red	$C_{20}H_{18}N_2O_2$	VWR	99% purity

(∼5 cm), the outside of the individuals were rinsed with MilliQ water (18.2 M′Ωcm and TOC < 10 ppb) and the head and tail removed. The remaining body was then placed in a glass jar as previously described. A fixed volume of 40 mL of a 30% KOH:NaClO solution was added to each pot in an PCR workstation with laminar flow to avoid particle contamination and each sample was sonicated using a VWR ultrasonic cleaning bath for 5 min (Enders et al., 2017). Each sample was then incubated at 40°C for 24 h before filtration using a pre-rinsed Whatman GF/D filter (2.7 μm porosity). Identification of the extracted microplastics was carried out using the fluorescence tagging of polymers using Nile Red coupled with digital imaging and an automated particle counting method developed at Cefas based on ArcGIS (Maes et al., 2017). As a validation step, each filter was examined under a microscope (VWR Stereo microscope, VisiScope SZT360-6) to remove any false positives from the fluorescence of biological items and to differentiate suspected anthropogenic-origin items into fibers and fragments based on their morphology. For additional quality assessment, a GF/D filter was spiked with a known number of plastic particles to investigate recovery rates using both a visual (digital imaging and microscopy) and an automated particle counting method. Data were corrected from the procedural control (i.e., negative control) to compensate for ambient contamination. A summary of the methods is shown in **Supplementary Figure S1**.

Quality Control and Polymer Identification Using Fourier-Transform Infrared Spectroscopy

Polymer identification of particles was carried out using attenuated total reflection Fourier transform infrared spectroscopy (ATR-FT-IR) with a Thermo Fisher Scientific Nicolet iS5 ATR-FTIR with OMNIC software (version 9.9.473) and by comparison of their IR spectra to a polymer library. ATR-FT-IR has been shown to be a fast and effective tool for the identification of polymers of plastic marine debris, including those ingested by marine organisms (Jung et al., 2018). Due to size limitation using ATR-FT-IR, only particles above ∼250 μm in size were analyzed. In total, 2.3% of particles were selected for polymer identification. Spectra were collected in absorbance mode in the range 4000–400 cm^{-1} at a resolution of 4 cm^{-1}. Polymer identification was verified based on the% match (>70%) against polymer libraries (HR Nicolet Sampler Library, HR Spectra IR Demo and Hummel Polymer Sample Library). Quality control was carried out with the analysis of a polystyrene (PS) and polyethylene (PE) reference material before each batch. Categorization of the extracted particles for quality control is shown in the supporting information section (**Supplementary Figure S3**).

Statistical Analysis

A Poisson log-linear model (**Supplementary Figure S2**) was applied to model the relationships between the number of items $individual^{-1}$ in fish against species, geographic range (strata), and stomach weights using Eq. 1.

$$\log(\mu) = fn(Species,\ Strata,\ Stomach\ weight) \quad (1)$$

where μ is the Poisson mean and *fn (Species, Strata, Stomach weight)* is a linear function of the three potential explanatory variables. We use the link function log (μ) to constrain μ to be positive. Statistical analysis was carried out using R Core Team (2019). Once all combinations of the explanatory variables were fitted into the model, the Akaike Information Criterion (AIC) was used to judge the suitability of the models.

The effect of microplastics on fish health and fitness was investigated using the caudal length to body weight ratio. Symmetric distribution of the ratios suggested Normality and the following linear model was applied using (Eq. 2).

$$Ratio = f(Count,\ Strata) + error \quad (2)$$

where $f(Count,\ Strata)$s a linear *function* of Count and Strata and the error is assumed to be Normally distributed with mean 0 and constant variance.

With further consideration of fish health, a linear regression model was applied to investigate the potential relationship between mean microplastic count, in each species, against the mean weight and mean caudal length of fish, within each geographical location. Finally, a modified bootstrap analysis was applied on results obtained on microplastics abundance to evaluate the optimum sampling sizes for each species for future monitoring (Manly, 2006).

RESULTS

Interspecific Variation

This study confirmed the presence of microplastics in GITs of commercially important small pelagic fish species in South African waters, specifically *En. encrasicolus* (n = 178), *Et. whiteheadi* (n = 188), and *S. sagax* (n = 227). A total of 813 suspected microplastics were detected in 406 fish across all the species out of 593 individuals, representing a 68% occurrence overall. The corresponding total mean concentration of microplastics for biota across all the strata was 1.36 items $individual^{-1}$. The mean occurrence of microplastics was substantially lower for *En. encrasicolus* (57%) as compared to *Et. whiteheadi* and *S. sagax* (each 72%) (**Table 2**).

Mean number of microplastics (mean number of items $individual^{-1}$) ranged from 1.13 items $individual^{-1}$ for *En. encrasicolus* followed by *Et. whiteheadi* and *S. sagax* with 1.38 and 1.58 items $individual^{-1}$, respectively (**Table 2**), and varied between strata (**Figure 2**). The results from the Poisson log-linear model (AIC values) suggested that species, strata and their interaction influence the abundance of microplastics in fish species. This makes inter-comparisons and identification of global trends difficult (**Table 3**). The mean number of items $individual^{-1}$ per species and per stratum is shown in **Figure 2**, along with 95% confidence intervals derived from the fitted log-linear model with the interaction between species and strata. The overall trend, irrespective of species, indicated a slight decrease from stratum A to B followed by a distinct increase in abundance of ingested items to stratum C. The mean number of items $individual^{-1}$ was then generally stable until further increasing in stratum G. For *En. encrasicolus*, the abundance of microplastics was generally constant and linear across strata. This trend was however different for *Et. whiteheadi* and *S. sagax* which showed a gradual increase in the abundance of ingested items from the strata B to G (**Table 2** and **Figure 2**). This interspecific difference was particularly clear for stratum G in which *Et. whitehead* and *S. sagax* ingested substantially higher numbers of microplastic items (means of 1.80 and 2.38 items $individual^{-1}$, respectively) as compared to *En. encrasicolus* (mean of 0.92 items $individual^{-1}$) (**Figure 2**).

The mean number of items per individual was also plotted against mean fish body weight (**Figures 3**, **4**) and mean fish caudal length (**Figures 3**, **5**) for all strata per species to assess whether larger organisms showed a higher ingestion of particles. Linear regression models were applied to derive levels of significance, but the mean number of items $individual^{-1}$ was not significantly linearly related ($p > 0.05$) to fish body weight or to body caudal length for all species under investigation.

Main Microplastic Types and Sources

Fibers and fragments were the most common types of microplastics found for all the species under investigation. Overall, for all the species, fibers represented 80% of the analyzed particles and fragments 20%. This was consistent across species with fibers representing 82, 81, and 76% of the particles analyzed for *En. encrasicolus, Et. whitehead,* and *S. sagax*,

TABLE 2 | Number of individuals studied, number of individuals with micro plastics, % occurrence per strata, and mean number of items individual^{-1} per species [range in ()] for anchovy (*Engraulis encrasicolus*), West Coast round herring (*Etrumeus whiteheadi),* and sardines (*Sardinops sagax*).

Strata	Species	Number of individuals	Number of individuals with microplastics	% occurrence	Mean number of items individual^{-1} (range of number of items in individual)		Fibers vs. fragments (%) per species		Fibers vs. fragments (%) per stratum	
							Fibers	Fragments	Fibers	Fragments
A	***Engraulis encrasicolus***	36	24	67	1.22 (0–4)	1.19	93	7	85	16
	Etrumeus whiteheadi	25	15	60	1.16 (0–6)		76	24		
	Sardinops sagax	0	0	NA	NA			NA		
B	***Engraulis encrasicolus***	25	17	68	1.24 (0–6)	1.04	85	15	73	27
	Etrumeus whiteheadi	24	12	50	0.75 (0–2)		79	21		
	Sardinops sagax	25	14	56	1.12 (0–6)		54	46		
C	***Engraulis encrasicolus***	10	5	50	1.10 (0–5)	1.53	60	40	82	18
	Etrumeus whiteheadi	33	29	88	2.18 (0–7)		96	4		
	Sardinops sagax	50	37	74	1.30 (0–4)		91	9		
D	***Engraulis encrasicolus***	10	6	60	1.50 (0–7)	1.37	92	8	79	21
	Etrumeus whiteheadi	10	5	50	1.10 (0–4)		50	50		
	Sardinops sagax	50	35	70	1.50 (0–7)		96	4		

(Continued)

TABLE 2 | Continued

Strata	Species	Number of individuals	Number of individuals with microplastics	% occurrence	Mean number of items individual^{-1} (range of number of items in individual)		Fibers vs. fragments (%) per species		Fibers vs. fragments (%) per stratum	
							Fibers	Fragments	Fibers	Fragments
E	***Engraulis encrasicolus***	25	16	64	0.96 (0–3)	1.35	71	29	66	34
	Etrumeus whiteheadi	25	18	72	1.20		81	19		
	Sardinops sagax	24	21	88	1.88 (0–4)		47	53		
F	***Engraulis encrasicolus***	47	27	57	0.94 (0–4)	1.26	95	5	86	14
	Etrumeus whiteheadi	46	37	80	1.50 (0–5) (0–6)		93	7		
	Sardinops sagax	49	30	61	1.33 (0–9)		70	30		
G	***Engraulis encrasicolus***	25	12	48	0.92 (0–3)	1.70	77	23	89	11
	Etrumeus whiteheadi	25	20	80	1.80 (0–7)		89	11		
	Sardinops sagax	29	26	90	2.38 (0–7)		100	0		
Total	***Engraulis encrasicolus***	**178**	**102**	**57**	**1.13 (0–7)**	**1.36**	**82**	**18**	**80**	**20**
	Etrumeus whiteheadi	**188**	**136**	**72**	**1.38 (0–7)**		**81**	**19**		
	Sardinops sagax	**227**	**163**	**72**	**1.58 (0–9)**		**76**	**24**		

Bold values were used to highlight total values.

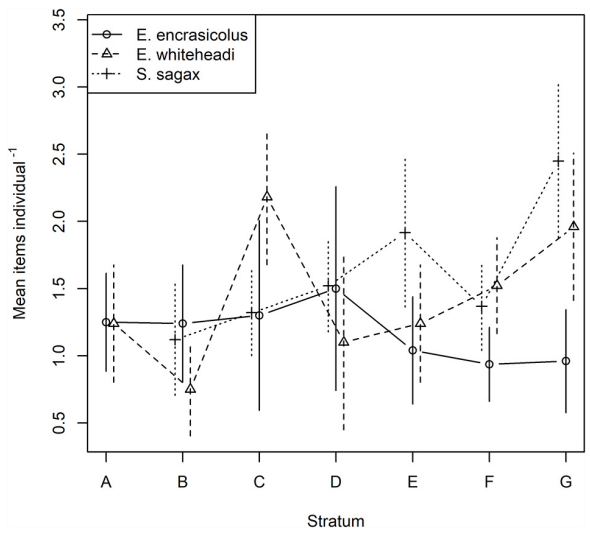

FIGURE 2 | Mean number of items individual^{-1} by stratum for *Engraulis encrasicolus* (n = 178), *Etrumeus whiteheadi* (n = 188), and *Sardinops sagax* (n = 227). Also shown are 95% confidence intervals from the interaction Poisson log-linear model. *S. sagax* was not collected from Stratum A.

TABLE 3 | Summary of AIC values for the Poisson log-linear models in decreasing order of model quality (low values of AIC are best).

Variables in model	AIC
Strata + Species + Strata.Species	1919.9
Strata + Species	1931.2
Strata + Species + Stomach weight	1932.2
Species	1938.2
Species + Stomach weight	1940.2
Strata	1940.8
Stomach weight	1952.6
None	1950.8

respectively (**Table 2**). The most commonly found polymers were poly(ethylene:propylene:diene) (EPDM, 33%), polyethylene (PE, 20%), polyamide (PA, 20%), polyester (PET, 20%), and polypropylene (PP, 7%) (**Supplementary Figure S3**).

DISCUSSION

Uncertainties and Evaluation of Method

The Nile red screening method for microplastics was applied for a fast and cost-effective assessment of the occurrence of microplastics in biota collected in South Africa. This method has recently been used for large-scale mapping of microplastics (Wang et al., 2018). Due to the nature of the project, only small, portable items were used during this study. This included the use of a portable ATR-FTIR for plastic particle validation and polymer identification with a validation step restricted to particles down to about 250 μm in size. No micro-FTIR or Raman spectroscopy was accessible on site and are commonly used for the identification of smaller size particles (Kniggendorf et al., 2019). The presence of false positives has been previously identified as a source of error when applying the Nile red screening method (Maes et al., 2017; Kukkola et al., 2020). Additional steps were therefore required for plastic confirmation and removal of false positives, including visual observation using digital imaging and microscopy.

Interspecific Variation

This study documented and compared levels of microplastics in three small pelagic fish species found off the coast of South Africa, namely *En. encrasicolus, Et. whiteheadi,* and *S. sagax.* All three species are planktivorous but show resource partitioning and feed primarily on different components of the plankton. *Sardinops sagax* are able to retain small particles so phytoplankton (diatoms and dinoflagellates) is on occasion relatively important, but the majority of the dietary intake of this species is via filter-feeding on smaller zooplankton such as poecilostomatoid and small calanoid copepods as well as fish eggs (Van Der Lingen, 2002). Phytoplankton is of less importance to *En. encrasicolus* which primarily particulate-feeds on larger zooplankton such as calanoid copepods and euphausiids (James, 1987). The diet of *Et. whiteheadi* has been reported to consist entirely of zooplankton (euphausiids, large copepods and decapods; Wallace-Fincham, 1987) but it is likely they also eat larval and early juveniles stages of fish (van der Lingen and Miller, 2011).

Given their planktivorous nature and the overlap in size between their natural prey and microplastics, the ingestion of

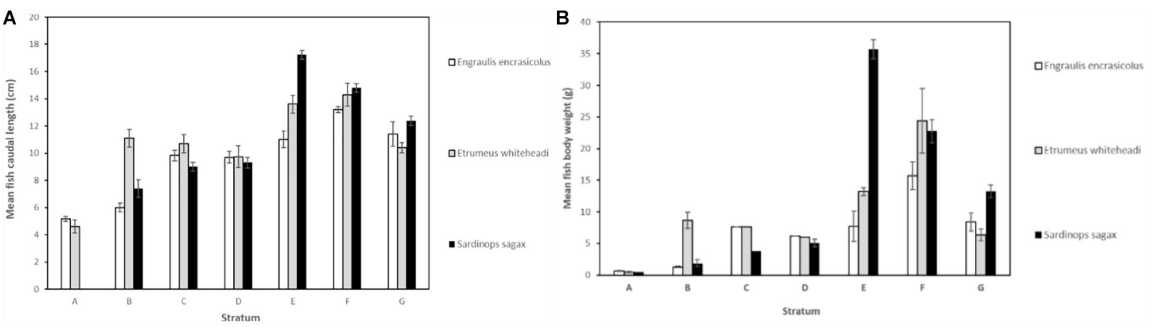

FIGURE 3 | Mean **(A)** fish caudal length (in cm) and **(B)** mean fish body weight (g) (mean ± 95% CI) for *Engraulis encrasicolus* (n = 178), *Etrumeus whiteheadi* (n = 188), and *Sardinops sagax* (n = 227).

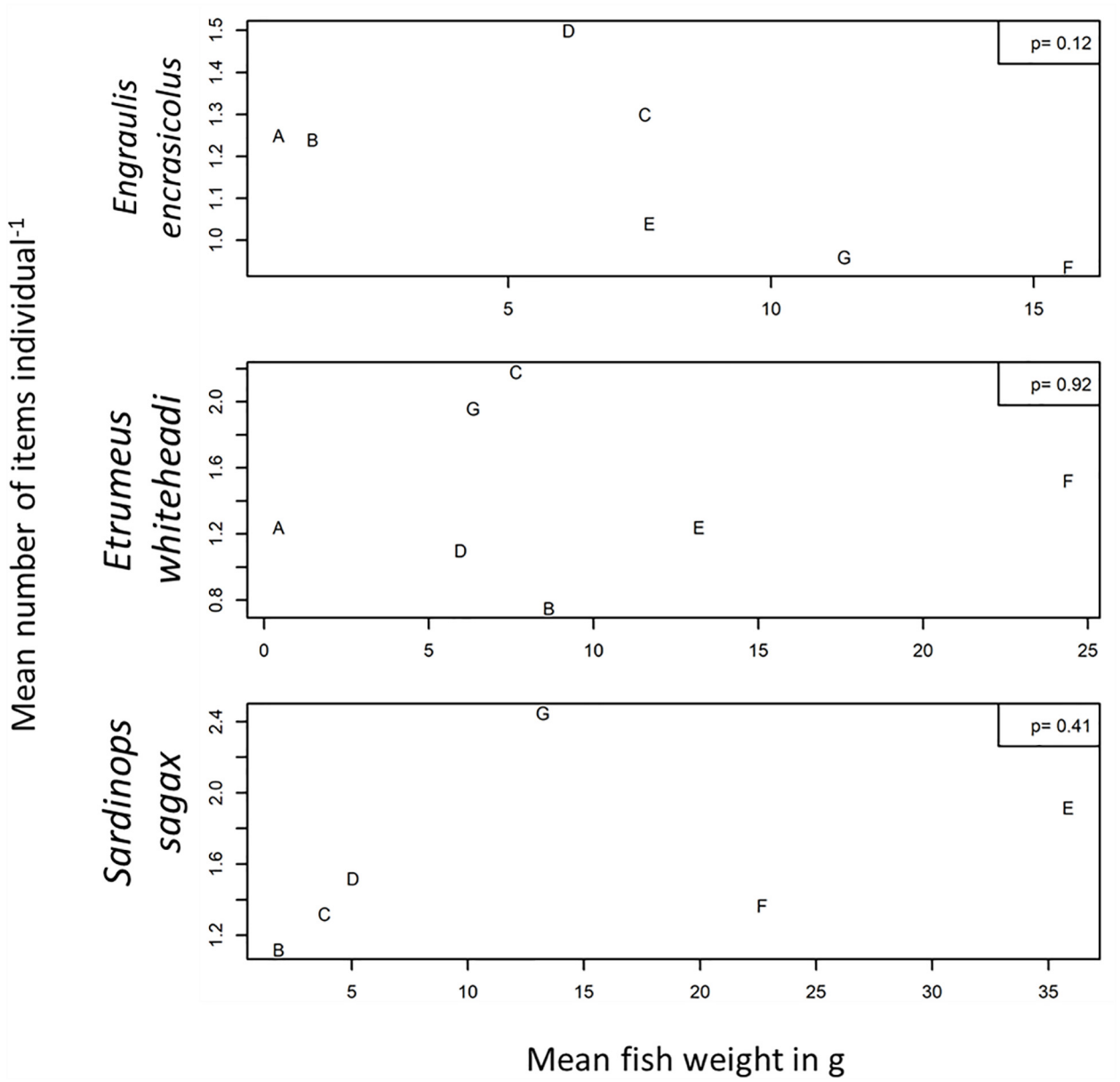

FIGURE 4 | Mean number of items individual^{-1} plotted against mean weight (g^{-1}) for *Engraulis encrasicolus, Etrumeus whiteheadi* and *Sardinops sagax* for each stratum. Also shown are *p*-values for a linear regression model.

microplastics by these small pelagic fish species is predictable. Detailed comparative analysis of diet, feeding morphology and behavior and energetics of sardine and anchovy (van der Lingen et al., 2006), as well as a comparison of nitrogen stable isotope ratios that reflect the trophic position of all three species (van der Lingen and Miller, 2011; Van Der Lingen and Miller, 2014), have demonstrated clear differences in their feeding ecologies in South African waters, suggesting that microplastic ingestion levels may vary between them. Such interspecific differences were indeed observed, with the Poisson log-linear model indicating that species, location (stratum) and their interaction all had significant effects on microplastic abundance in these small pelagic fish species. Overall, *En. encrasicolus* had both the lowest occurrence (57%) and lowest mean abundance (1.13 items individual^{-1}) of microplastics, whereas *Et. whiteheadi* and *S. sagax* had the same occurrence (72%), the mean abundance of microplastics was higher in sardine (1.58 items individual^{-1}) than in round herring (1.38 items individual^{-1}).

The interspecific difference reported here supports the hypothesis of Collard et al. (2017) that planktivorous fish species with the most efficient filtration apparatus will be more likely to ingest microplastics. Those authors determined filtration areas and particle retention thresholds of *En. encrasicolus*, *Clupea harengus,* and *Sardina pilchardus* in European waters

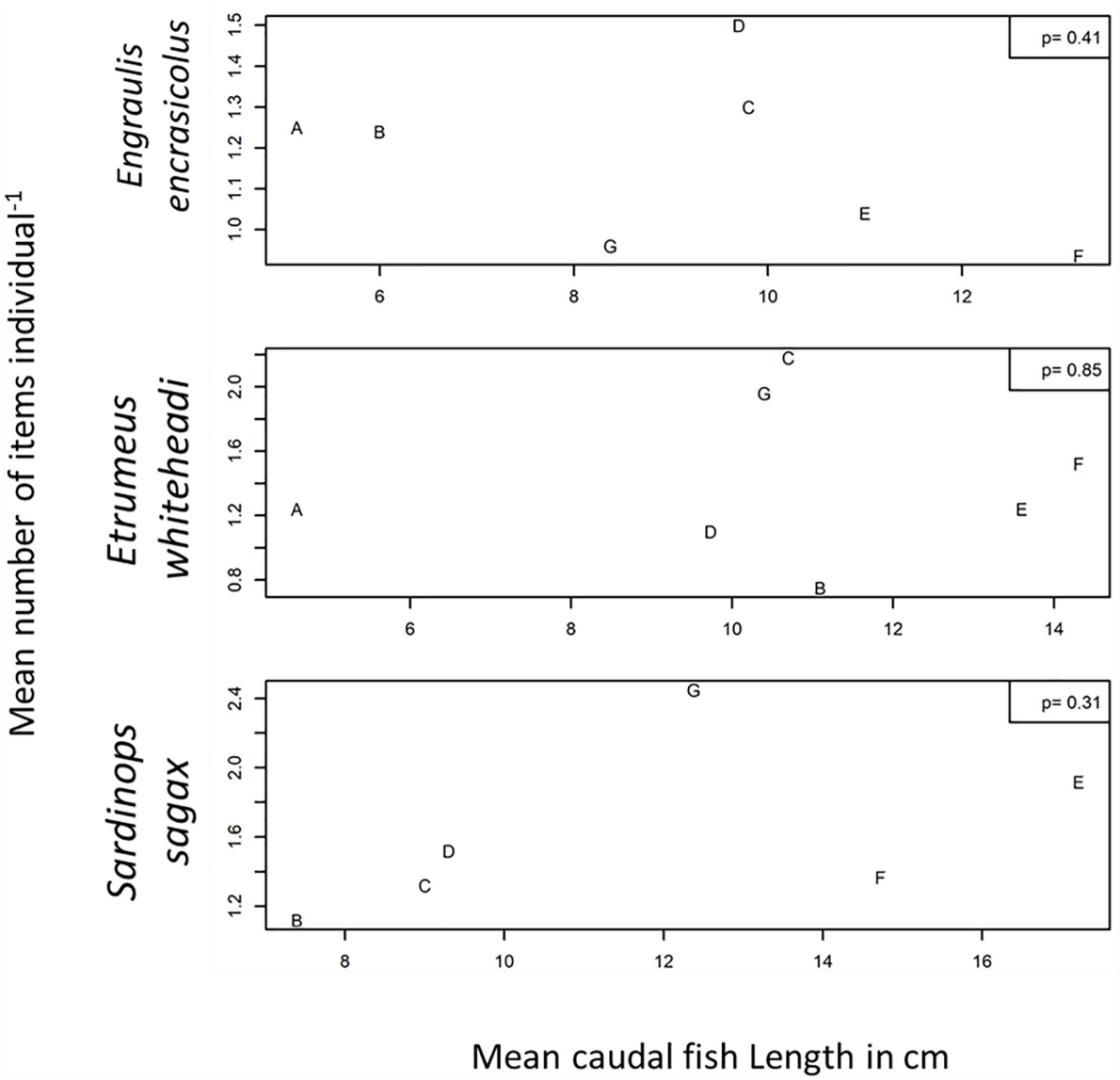

FIGURE 5 | Mean number of items individual^{-1} plotted against mean caudal length (cm) for *Engraulis encrasicolus*, *Etrumeus whiteheadi* and *Sardinops sagax* for each stratum. Also shown are *p*-values for a linear regression model.

and compared these with their anthropogenic particle (including microplastics) levels, and reported that sardine, which had the largest area and closest gill raker spacing, ingested more fibers and smaller fragments than anchovy or herring. *S. sagax* has a markedly smaller gill raker gap than either *En. encrasicolus* or *Et. whiteheadi* in southern African waters (Vorsatz et al., 2015), which provides a plausible mechanism to explain the higher occurrence and abundance of microplastics in sardine compared to the other two species reported here. However, the hypothesis that retention of smaller particles results in increased microplastics ingestion is in contrast to findings by Lopes et al. (2020), who reported that planktivorous species from Alanto-Iberian waters that fed on larger zooplankton prey (*Trachurus trachurus*, *Scomber scombrus,* and *En. encrasicolus*) accumulated more microplastics than those feeding on smaller prey size (*S. pilchardus*, *Sc. colias,* and *Boops boops*), and recommended *T. trachurus* as a suitable bio-indicator species for monitoring microplastics in that ecosystem. While studies on bioaccumulation of microplastics are limited, there is indication that plastic particles can be ingested and transferred in the planktonic food web (Setälä et al., 2014), representing another potential route of uptake by biota.

Data on the occurrence and abundance of microplastics in sardines, anchovies, and round herrings from various studies of the same or similar species, including from South African waters, are listed in **Table 4**. It must be noted that methods used in those studies are not all standardized and that sample sizes vary substantially between them, hence inferences made from

comparing those data are questionable. Nonetheless, we feel that they provide a useful contextualization of our results. Ross (2017) assessed ingestion of microplastics by the same three epipelagic species from the a similar geographical area investigated in this study and reported an overall microplastics occurrence of 67%, which was consistent with the overall 68% occurrence observed in this study using markedly larger sample sizes. In contrast to our findings, however, Ross (2017) found that *En. encrasicolus* had the highest (80%) and *Et. whiteheadi* the lowest (44%) occurrence of microplastics, whereas observations from the two studies for sardine were similar (76% from Ross, 2017 and 72% from this study; **Table 4**). Despite these differences, estimates from both studies for *En. encrasicolus* off South Africa are higher than the median occurrence of 30% calculated from available data for anchovies in the literature (**Table 4**). More strikingly, estimates of microplastic occurrence in *S. sagax* off South Africa are the highest yet reported for this species compared to a median value of 25% from the eight values reported in **Table 4**. We could find no other reports of microplastic occurrence in *Etrumeus* spp. but the median value from Ross's (2017) and this study is 58%.

Our estimate of mean microplastics abundance for *En. encrasicolus* is substantially (< 50%) lower than that estimated by Ross (2017) but is above the median value of 0.48 items individual^{-1} for anchovies listed in **Table 4**, where mean abundance ranges from 0.0 to 4.0 items individual^{-1} across six species from three genera. Similarly, Ross (2017) reported a higher mean microplastics abundance and substantially larger range for *S. sagax* than observed in this study, and abundance values from both studies are the highest yet reported for this species and compare to a median of 0.35 (range 0.0–2.8 items individual^{-1}) across the four species in four genera of sardines reported in **Table 4**. We could find no microplastic abundance data for any other *Etrumeus* species but Sparks and Immelman (2020) reported that *Et. whiteheadi* from a single sample collected in shelf-edge waters off South Africa's South Coast (in Stratum G of this analysis) had a mean abundance of 3.3 (± 0.5 SE) items individual^{-1}, which is somewhat but not substantially higher than the value of 1.80 (± 0.55 95% CI) 2.5 items individual^{-1} estimated for this species in Stratum G in this study.

Main Plastic Types and Sources

Fibers were the main type of ingested items in biota, representing 80% of the extracted items in this study. Microfibers are known to represent a large fraction (>85%) of microplastic debris found along shorelines globally (Carr, 2017). This was in agreement with Ross (2017) who reported that microfibers represented 99% of the items extracted from *En. encrasicolus*, *S. sagax*, *Et. whiteheadi*, *Lampanyctodes hectoris,* and *Maurolicus walvisensis* from the West and South coasts of South Africa. Similarly, Naidoo et al. (2016) reported that plastic fibers were ingested most commonly by *Mugil cephalus* in the Port of Durban off South Africa's East Coast. Naidoo et al. (2020b) also reported that fibers represented 68% of ingested items by juvenile *Oreochromis mossambicus*, *Terapon jarbua*, *Ambassis dussumieri* and *Mugil* spp., within four mangroves also along the East Coast of South Africa, and Sparks and Immelman (2020) that filaments (i.e., fibers) comprised 67% of microplastics ingested by three species of intertidal mussel around Cape Town.

Microfibers can enter the environment from both primary sources (fibers < 5 mm in size) or resulting from the fragmentation of larger items (Henry et al., 2019). Whereas wastewater treatment plants have been previously thought to be a primary source of microfibers in the environment, recent studies have shown that direct input from shedding of fibers, from common fabric and textiles, could represent a much important source (Carr, 2017; Conley et al., 2019). De Villiers (2019) investigated the occurrence of microfibers in river sediments adjacent to South Africa's coastline and reported a significant positive relationship between river sediment, microfiber levels, and the percentage of households in the catchment area that do not have access to piped water. That study also suggested that rivers represent direct vectors for the transport of fibers to the marine environment from rural communities, for whom rivers are the only source of accessible water, from clothes-washing activities. It is however worth noting that natural fibers (cellulose and of animal origin) represent a greater proportion of oceanic fibers (91.8%) as compared to synthetic fibers (8.2%) despite synthetic polymers currently accounting for two-thirds of global fiber production (Suaria et al., 2020).

The main commonly found polymers in biota in our study were poly(ethylene:propylene:diene) (EPDM, 33% occurrence), polyethylene (PE, 20%), polyamide (PA, 20%), polyester (PET, 20%), and polypropylene (PP, 7%) (**Supplementary Figure S3**). While data on the type of polymer found in biota for South Africa is limited these results are consistent with a meta-analysis by Erni-Cassola et al. (2019) that indicated the prevalence of PE, followed by PA, PET, and PP in aquatic environments globally.

Spatial Variation

Significant variation in the occurrence and abundance of microplastics in biota across the different strata were also observed in this study. The ingestion of particles throughout the inshore shelf suggested the widespread occurrence of microplastics in the pelagic environment along the South African coastline, between the Orange River mouth and Mossel Bay, with a significant increase in the number of items per individual in biota from the West to the South coast observed. This study was carried out in the southern Benguela coastal upwelling ecosystem (west of Cape Agulhas; Strata A–E) and the Agulhas Bank temperate shelf ecosystem (east of Cape Agulhas; Strata F and G), and prevailing oceanographic conditions differ between the two (Hutchings et al., 2009). The southern Benguela is characterized by seasonal upwelling that brings cool waters from the depths of the Central South Atlantic to the surface inshore, and warm Agulhas Current water offshore. The Agulhas Bank displays characteristics of both upwelling and temperate shelf ecosystems, and its dynamics are markedly impacted by the Agulhas Current that transports warm, salty water from the Indian Ocean along South Africa's East and South coasts. Because of the differing origins and transport routes of source waters of these two systems it might be expected that microplastics load off the West Coast are lower than those off the South Coast, as suggested by the results of this study.

TABLE 4 | Occurrence and number of items individual^{-1} for anchovies, sardine and round herring reported in the literature from several locations (number of individuals examined indicated where possible; ns: not specified; nd: not determined).

Fish/species		Location	Number of individuals examined	Occurrence (%)	Mean number of items per individual	References
Anchovies	*Coilia ectenes*	Yangtze estuary, China	18	nd	4.0 ± 1.8	Jabeen et al., 2017
	Ctengraulis mysticetus	Pacific Ocean, Columbia	30	3	0.03 ± 0.03 SE	Ory et al., 2018
	Ctengraulis mysticetus	Pacific Ocean, Panama	10	0	0	Ory et al., 2018
	Engraulis encrasicolus	Mediterranean Sea, Spain	ns	nd	1.18 ± 0.40	Ferrer et al., 2016
	Engraulis encrasicolus	Atlantic and Indian oceans, South Africa	25	80	2.68 (1–7)	Ross, 2017
	Engraulis encrasicolus	Atlantic Ocean and Mediterranean Sea (United Kingdom, France, Spain)	20	40	0.85	Collard et al., 2017
	Engraulis encrasicolus	Mediterranean Sea, Spain	>15	14.28	0.48	Compa et al., 2018
	Engraulis encrasicolus	Southern Tyrrhenian Sea	19	nd	0.26	Savoca et al., 2020
	Engraulis encrasicolus	Atlantic Ocean, Portugal	131	79	0.48 median (0.10–0.90 interquartile range)	Lopes et al., 2020
	Engraulis encrasicolus	**Atlantic and Indian oceans, South Africa**	**178**	**57**	**1.13 (0–7)**	**This study**
Sardines	*Engraulis japonicus*	Tokyo Bay	64	nd	2.3 ± 2.5	Tanaka and Takada, 2016
	Engraulis mordax	Pacific Ocean, United States (California)	10	30	0.3 ± 0.5 SD	Rochman et al., 2015
	Engraulis ringens	Pacific Ocean, Chile	76	1.3	0.01 ± 0.01 SE	Ory et al., 2018
	Engraulis ringens	Pacific Ocean, Peru (40)	40	0	0.0	Ory et al., 2018
	Opisthonema libertate	Pacific Ocean, Columbia	40	0	0.0	Ory et al., 2018
	Opisthonema libertate	Pacific Ocean, Ecuador	40	5	0.05 ± 0.04 SE	Ory et al., 2018
	Sardina pilchardus	Atlantic Ocean and Mediterranean Sea (United Kingdom, France, Spain)	20	45	0.55	Collard et al., 2017
	Sardina pilchardus	Mediterranean Sea, Spain	>15	15.24	1.43 ± 0.79	Compa et al., 2018
	Sardina pilchardus	Southern Tyrrhenian Sea	27	nd	0.53	Savoca et al., 2020
	Sardina pilchardus	Atlantic Ocean, Portugal	76	58	0.16 median (0.00–0.53 interquartile range)	Lopes et al., 2020
	Sardinops sagax	Atlantic and Indian oceans, South Africa	25	76	2.8 (1–16)	Ross, 2017
	Sardinops sagax	Pacific Ocean, Chile	7	0	0.0	Ory et al., 2018
	Sardinops sagax	**Atlantic and Indian oceans, South Africa**	**227**	**72**	**1.58 (0–9)**	**This study**
	Strangomera bentincki	Pacific Ocean, Chile	10	0	0.0	Ory et al., 2018
Round herring	*Etrumeus whiteheadi*	West and South coasts, South Africa	25	44	**0.8 (1–3)**	Ross, 2017
	Etrumeus whiteheadi	Indian Ocean, South Africa	15	nd	3.3 ± 0.5	Sparks and Immelman, 2020
	Etrumeus whiteheadi	**West and South coasts, South Africa**	**188**	**69**	**1.38 (0–7)**	**This study**

Bold values were used to highlight data coming from this study as compared to other reported studies from the literature.

TABLE 5 | Recommended criteria for the selection of a bioindicator species for the monitoring of microplastics in biota for SA coastal waters.

Criteria	Biota		
	Engraulis encrasicolus	***Etrumeus whiteheadi***	***Sardinops sagax***
Wide geographical distribution	✓	✓	✓
Representative of a specific monitoring area	✓	✓	✓
Species that are not protected or endangered	✓	✓	✓
Suitable particle retention time within organisms (hours)	4–158[1–3]	4–158[1–3]	4–158[1–3]
Already used as bioindicator/biomonitoring species	✓	×	✓
Ability to ingest and retain small to larger sized particles	<5 mm[1–3]	<5 mm[1–3]	<5 mm[1–3]
Species that can be kept in cages for easy field deployment and collection	×	×	×
Invertebrate species, which require less staff training (cost-effective) for handling than vertebrate species	×	×	×
Perform sampling in a cost-effective manner by synergies with pre-existing programs	✓	✓	✓
Commercially important species with public health implications	✓	✓	✓
Ease of sample preparation and validated analytical protocol using Nile Red polymer fluorescence tagging	✓	✓	✓

[1]*(Ward and Kach, 2009; Catarino et al., 2017).* [2]*(Brett and Grooves, 1979).* [3]*(Nelms et al., 2018).*

Along the South African coastline, macro litter has been observed in higher abundance close to urban centers (Ryan et al., 2009), whereas, micro litter on beach sediments has not been observed to be driven by population demographics, but rather by large scale ocean currents (Nel et al., 2017). Microplastic concentrations are higher in environmental matrices near or in highly populated areas, close to large coastal wastewater treatment plant discharge points, in rivers and harbors, and are affected by seasonal changes in river runoff (Naidoo et al., 2015; Nel et al., 2017; de Villiers, 2018). De Villiers (2019) noted higher microplastic levels in river sediments in KwaZulu-Natal and the Wild Coast (both along the South African East Coast) which are comparable to levels in the sediments of rivers along the Cape South Coast (ca. 20–26°E).

We also found that microplastics abundance was not significantly linearly related with individuals' caudal length or weight, which is in agreement with other studies that reported no correlation between total number of particles per fish and fish mass (Naidoo et al., 2020b) or fish size (Vendel et al., 2017).

Selection and Proposal of a Bioindicator for Microplastics for South African Waters

One of the objectives of this study was to identify and propose a suitable and sustainable indicator species for the monitoring of microplastics in biota for South African waters, with fish considered to be appropriate bio-indicators of larger microplastics (Ryan et al., 2020). A list of criteria for the selection of a suitable bio-indicator for microplastics has been modified from GESAMP (2019) and is presented in **Table 5**. The species used in this study, *En. encrasicolus*, *Et. whiteheadi* and *S. sagax,* fulfilled most of these criteria; in particular, they are widely distributed in shelf waters along the South African coastline (**Supplementary Figure S4**) and are already being collected as part of annual research surveys, indicating that a broad-scale assessment of microplastics could be cost-efficiently integrated into an existing monitoring program.

In consideration of a microplastics bio-indicator and the development of a potential monitoring plan, a bootstrap (Manly, 2006) analysis to generate confidence intervals was carried out to estimate optimum sample size for each species (**Figure 6**). Output from the analysis suggested a sample size of 150 individuals across

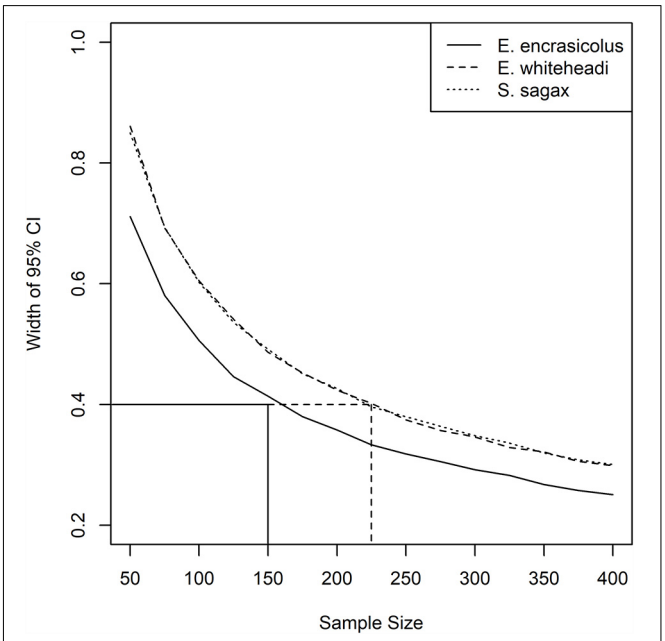

FIGURE 6 | Widths of 95% bootstrapped confidence intervals for sample sizes between 50 and 400, for *Engraulis encrasicolus*, *Etrumeus whiteheadi,* and *Sardinops sagax*. Note that the lines for *Etrumeus whiteheadi* and *Sardinops sagax* are virtually identical.

all strata (22 individuals per stratum) sampled in the 2019 Pelagic Recruit survey for *En. encrasicolus,* and 225 individuals for both *Et. whiteheadi* and *S. sagax* across all strata (32 individuals per stratum), to obtain a precision of 0.4 items of MP per individual, as measured by a 95% confidence interval. Plots for *Et. whiteheadi* and *S. sagax* were similar due to their nearly identical standard deviations of 1.532 and 1.537, respectively. The CI widths for *En. encrasicolus* were also lower due to a lower standard deviation of 1.29 in this study. As mentioned previously, the Poisson log-linear model suggested that the effect of fish species was not similar across strata and the interaction between MP items in the fish species and strata was an important factor to consider (**Supplementary Table S3**). In other words, the pattern of MP abundance across strata was different, depending on the species. Given that the fish in this study were caught together, rather than caught per species, the interaction relationship is unlikely to have been influenced by the sampling technique.

Although fewer *En. encrasicolus* would be required for microplastics assessment to achieve the desired precision, it was clear that both *Et. whiteheadi* and *S. sagax* showed spatial trends in microplastics abundance whereas anchovy did not, suggesting that the former two species might represent more suitable candidates for monitoring programs. *Sardina pilchardus* has already been proposed as a bio-indicator for microplastics for the Mediterranean Sea (Fossi et al., 2018) and the selection of *S. sagax* would allow for global comparisons. However, its suitability in a South African context is under question as the local *S. sagax* population is presently in a depleted state (DFFE, 2020), which could negatively impact sample collection until it recovers. Given this, the present large population size of *Et. whiteheadi*, and the recommendation by Lopes et al. (2020) that planktivorous species that feed on larger zooplankton prey (which this species does) be used as bio-indicator species for monitoring microplastics, we suggest the latter as a suitable regional microplastics bio-indicator specific for South African waters. This despite the lack of knowledge of plastic ingestion by this genus elsewhere which will make global comparisons difficult. The estimate of 225 fish as a required sample size applies to the area covered in the 2019 Pelagic Recruit Survey and would need to be adjusted for other surveys that cover a larger spatial extent.

Potential Impacts on Human Health

The occurrence of microplastics in biota has caused several concerns, ranging from its effects on biodiversity and populations to potential risks to food safety and human health. As fish consumption in South Africa grew by more than 26% between 1994 and 2009, there is potential for the transfer of microplastics from fish to humans following consumption (Naidoo et al., 2020a). It has been suggested by the Food and Agriculture Organization (FAO) that the transfer of sorbed co-contaminants and additives from the ingestion of plastic particles would be negligible due to the low dietary exposure to such contaminants (Lusher et al., 2017). However, the transfer of plastics along the food chain to humans and impacts on human health has been identified as a gap in the understanding of marine plastic pollution in a South African perspective and data on levels of transferral of microplastics from edible aquatic species to humans are currently lacking (Godfrey, 2020; Naidoo et al., 2020a). This gap must be filled in order to make predictive decisions in regard to safety for consumption (Naidoo et al., 2020a).

CONCLUSION

The data presented in this study confirmed the occurrence of microplastics, principally microfibers, in the commercially important small pelagic fishes *En. encrasicolus*, *Et. whiteheadi,* and *S. sagax* in South Africa, with an overall occurrence of 68%. The abundance of microplastics in these fish was impacted by both species and location, as well as the interaction of these two factors, but the overall pattern indicated an increase from the West to the South coast. Microplastic abundance levels in South African anchovy and sardine are above median values for similar species elsewhere but were not correlated with fish biological characteristics in any of the three species examined here. We propose that *Et. whiteheadi* be used as a bio-indicator for microplastics in South African waters and that the collection and processing of this species be included in regular survey programs. Finally, an increase in fish consumption in South Africa suggests potential for the transfer of microplastics to human following consumption with unknown related effects on human health. However, the impacts of microplastics and associated co-contaminants on human health have been suggested to be minor by both the World Health Organization and FAO due to the low dietary exposure to such contaminants.

DATA AVAILABILITY STATEMENT

The datasets presented in this study can be found in online repositories. The names of the repository/repositories and accession number(s) can be found below: 10.14466/CefasDataHub.100.

ETHICS STATEMENT

Ethical review and approval was not required for the animal study because the fish were collected as part of an already existing fisheries survey conducted by the South African Government. Research was conducted on dead fish.

AUTHOR CONTRIBUTIONS

FP-W, TM, CL, and AdB designed and coordinated the study. CL, AsB, and YG collected the samples. AdB, YM, GM, DD, FT, and RH carried out the laboratory work. JB carried out the statistical analysis. AdB and CL wrote the manuscript. All authors contributed to the article and approved the submitted version.

FUNDING

Microplastic sampling and analysis were carried out as part of the Commonwealth Litter Programme (CLiP), implemented by the Centre for Environment, Fisheries and Aquaculture Science (Cefas), funded by the United Kingdom Government's Department for Environment, Food and Rural Affairs (Defra), through Official Development Assistance (ODA) funding.

ACKNOWLEDGMENTS

We gratefully acknowledge the contributions of collaborators from the Department of Environment, Forestry and Fisheries [(DEFF) formerly from the Department of Agriculture, Forestry and Fisheries (DAFF)] involved in sample collection during the Pelagic Recruit Survey, including Janet C. Coetzee (Survey Co-ordinator), Dagmar Merkle, Mzwamadoda Phillips, and Fannie Shabangu (Chief Scientists), and the master, officers, and crew of the *FRS Africana*, as well as collaborators from the Department of Environment, Forestry and Fisheries [(DEFF) formerly from the Department of Environmental Affairs (DEA)], especially Keshnee Pillay and Marco Worship. We would also like to thank Jeroen Van Der Kooij for kindly agreeing to review the final draft of this manuscript.

SUPPLEMENTARY MATERIAL

The Supplementary Material for this article can be found online at: https://www.frontiersin.org/articles/10.3389/fmars.2020.574663/full#supplementary-material

REFERENCES

Babayemi, J. O., Nnorom, I. C., Osibanjo, O., and Weber, R. (2019). Ensuring sustainability in plastics use in Africa: consumption, waste generation, and projections. *Environ. Sci. Eur.* 31:60.

Bakir, A., O'Conner, I. A., Rowland, S. J., and Hendriks, A. J. (2016). Relative importance of microplastics as a pathway for the transfer of hydrophobic organic chemicals to marine life. *Env. Poll.* 219, 56–65. doi: 10.1016/j.envpol.2016.09.046

Bakir, A., Rowland, S. J., and Thompson, R. C. (2014). Enhanced desorption of persistent organic pollutants from microplastics under simulated physiological conditions. *Environ. Pollut.* 185, 16–23. doi: 10.1016/j.envpol.2013.10.007

Brett, J. R., and Grooves, T. D. D. (1979). "Physiology Energetics," in *Fish Physiology*, eds W. S. Hoar, D.J. Randall, and J. R. Brett. New York, NY: Academic Press, 279–352.

Carr, S. A. (2017). Sources and dispersive modes of micro−fibers in the environment. *Integr. Environ. Assess. Manag.* 13, 466–469. doi: 10.1002/ieam.1916

Catarino, A. I., Thompson, R., Sanderson, W., and Henry, T. B. (2017). Development and optimization of a standard method for extraction of microplastics in mussels by enzyme digestion of soft tissues. *Environ. Toxicol. Chem.* 36, 947–951. doi: 10.1002/etc.3608

Cliff, G., Dudley, S. F. J., Ryan, P. G., and Singleton, N. (2002). Large sharks and plastic debris in KwaZulu-Natal. *S. Afr. Mar. Freshw. Res.* 53, 575–581. doi: 10.1071/MF01146

Collard, F., Gilbert, B., Eppe, G., Roos, L., Compère, P., Das, K., et al. (2017). Morphology of the filtration apparatus of three planktivorous fishes and relation with ingested anthropogenic particles. *Mar. Pollut. Bull.* 116, 182–191. doi: 10.1016/j.marpolbul.2016.12.067

Compa, M., Ventero, A., Iglesias, M., and Deudero, S. (2018). Ingestion of microplastics and natural fibres in Sardina pilchardus (Walbaum, 1792) and Engraulis encrasicolus (Linnaeus, 1758) along the Spanish Mediterranean coast. *Mar. Pollut. Bull.* 128, 89–96. doi: 10.1016/j.marpolbul.2018.01.009

Conley, K., Clum, A., Deepe, J., Lane, H., and Beckingham, B. (2019). Wastewater treatment plants as a source of microplastics to an urban estuary: Removal efficiencies and loading per capita over one year. *Water Res. X* 3:100030. doi: 10.1016/j.wroa.2019.100030

R Core Team (2019). *R: A language and environment for statistical computing*. United States: R Core Team.

de Villiers, S. (2018). Quantification of microfibre levels in South Africa's beach sediments, and evaluation of spatial and temporal variability from 2016 to 2017. *Mar. Pollut. Bull.* 135, 481–489. doi: 10.1016/j.marpolbul.2018.07.058

De Villiers, S. (2019). Short communication: Microfibre pollution hotspots in river sediments adjacent to South Africa's coastline. *Water SA* 45, 97–102. doi: 10.4314/wsa.v45i1.11

DFFE (2020). *Status of the South African Marine Fishery Resources 2020*. Cape Town: Department of Forestry Fisheries and Environmental Affairs.

Enders, K., Lenz, R., Beer, S., and Stedmon, C. A. (2017). Extraction of microplastic from biota: Recommended acidic digestion destroys common plastic polymers. *ICES J. Mar. Sci.* 74, 326–331. doi: 10.1093/icesjms/fsw173

Erni-Cassola, G., Zadjelovic, V., Gibson, M. I., and Christie-Oleza, J. A. (2019). Distribution of plastic polymer types in the marine environment; A meta-analysis. *J. Hazard. Mater.* 369, 691–698. doi: 10.1016/j.jhazmat.2019.02.067

Ferrer, M. C., Ventero, A., Iglesias, M., and Deudero, S. (2016). Microplastic ingestion in commercial fish species Boops Boops. Sardina pilchardus and Engraulis Encrasicolus in the Western Mediterranean sea: Medias Survey. *Rapp. Comm. Int. Mer. Medit.* 41:218.

Fossi, M. C., Peda, C., Compa, M., Tsangaris, C., Alomar, C., Claro, F., et al. (2018). Bioindicators for monitoring marine litter ingestion and its impacts on Mediterranean biodiversity. *Environ. Pollut.* 237, 1023–1040. doi: 10.1016/j.envpol.2017.11.019

GESAMP (2015). Sources, fate and effects of microplastics in the marine environment: a global assessment. *Rep. Stud. GESAMP* 90:96. doi: 10.13140/RG.2.1.3803.7925

GESAMP (2019). *Guidelines for the monitoring and assessment of plastic litter in the ocean*. London: GESAMP.

GESAMP (2020). *Proceedings of the GESAMP International Workshop on assessing the risks associated with plastics and microplastics in the marine environment*. London: GESAMP.

Godfrey, L. (2020). Are there gaps in our understanding of marine plastic pollution? *S. Afr. J. Sci.* 116:sajs.2020/8170.

Henry, B., Laitala, K., and Klepp, I. G. (2019). Microfibres from apparel and home textiles: Prospects for including microplastics in environmental sustainability assessment. *Sci. Total Environ.* 652, 483–494. doi: 10.1016/j.scitotenv.2018.10.166

Herzke, D., Anker-Nilssen, T., Nøst, T. H., Götsch, A., Christensen-Dalsgaard, S., Langset, M., et al. (2016). Negligible Impact of Ingested Microplastics on Tissue Concentrations of Persistent Organic Pollutants in Northern Fulmars off Coastal Norway. *Environ. Sci. Technol.* 50, 1924–1933. doi: 10.1021/acs.est.5b04663

Hutchings, L., Van der Lingen, C. D., Shannon, L. J., Crawford, R. J. M., Verheye, H. M. S., Bartholomae, C. H., et al. (2009). The Benguela Current: An ecosystem of four components. *Prog. Oceanogr.* 83, 15–32. doi: 10.1016/j.pocean.2009.07.046

Isaacs, M. (2016). The humble sardine (small pelagics): fish as food or fodder. *Agric. Food Secur.* 5:27.

Jabeen, K., Su, L., Li, J., Yang, D., Tong, C., Mu, J., et al. (2017). Microplastics and mesoplastics in fish from coastal and fresh waters of China. *Environ. Pollut.* 221, 141–149. doi: 10.1016/j.envpol.2016.11.055

James, A. G. (1987). Feeding ecology, diet and field-based studies on feeding selectivity of the Cape anchovy Engraulis capensis Gilchrist. *S. Afr. J. Mar. Sci.* 5, 673–692. doi: 10.2989/025776187784522784

Jung, M. R., Horgen, F. D., Orski, S. V., Rodriguez C, V., Beers, K. L., Balazs, G. H., et al. (2018). Validation of ATR FT-IR to identify polymers of plastic marine debris, including those ingested by marine organisms. *Mar. Pollut. Bull* 127, 704–716. doi: 10.1016/j.marpolbul.2017.12.061

Kniggendorf, A.-K., Wetzel, C., and Roth, B. (2019). Microplastics detection in streaming tap water with Raman spectroscopy. *Sensors* 19:1839. doi: 10.3390/s19081839

Koelmans, A. A., Bakir, A., Burton, G. A., and Janssen, C. R. (2016). Microplastic as a Vector for Chemicals in the Aquatic Environment: Critical Review and Model-Supported Reinterpretation of Empirical Studies. *Environ. Sci. Technol.* 50, 3315–3326. doi: 10.1021/acs.est.5b06069

Kukkola, A. T., Senior, B., Maes, T., Kroger, S., and Ag, M. (2020). *Digging down into the detail: a large-scale study of microplastic abundance in sediment cores from the UK continental shelf*. Cambridge: Academic Press.

Lohmann, R. (2017). Microplastics are not important for the cycling and bioaccumulation of organic pollutants in the oceans—but should microplastics be considered POPs themselves? *Integr. Environ. Assess. Manag.* 13, 460–465. doi: 10.1002/ieam.1914

Lopes, C., Raimundo, J., Caetano, M., and Garrido, S. (2020). Microplastic ingestion and diet composition of planktivorous fish. *Limnol. Oceanogr. Lett.* 5, 103-112.

Lusher, A., Bråte, I. L. N., Hurley, R., Iversen, K., and Olsen, M. (2017). *Testing of methodology for measuring microplastics in blue mussels (Mytilus spp) and sediments, and recommendations for future monitoring of microplastics (R & D-project)*. Report number: 7209-2017.

Maes, T., Jessop, R., Wellner, N., Haupt, K., and Mayes, A. G. (2017). A rapid-screening approach to detect and quantify microplastics based on fluorescent tagging with Nile Red. *Sci. Rep.* 7:44501.

Maes, T., van Diemen, de Jel, J., Vethaak, A. D., Desender, M., Bendall, V. A., et al. (2020). You Are What You Eat, Microplastics in Porbeagle Sharks From the North East Atlantic: Method Development and Analysis in Spiral Valve Content and Tissue. *Front. Mar. Sci*. 7:273.

Manly, B. F. J. (2006). *Randomization, bootstrap and Monte Carlo methods in biology*. Florida, FL: CRC press.

Naidoo, T., and Glassom, D. (2019). Decreased growth and survival in small juvenile fish, after chronic exposure to environmentally relevant concentrations of microplastic. *Mar. Pollut. Bull* 145, 254–259. doi: 10.1016/j.marpolbul.2019.02.037

Naidoo, T., Glassom, D., and Smit, A. J. (2015). Plastic pollution in five urban estuaries of KwaZulu-Natal. *S. Afr. Mar. Pollut. Bull.* 101, 473–480. doi: 10.1016/j.marpolbul.2015.09.044

Naidoo, T., Smit, A. J., and Glassom, D. (2016). Plastic ingestion by estuarine mullet *Mugil cephalus* (Mugilidae) in an urban harbour, KwaZulu-Natal, South Africa. *African J. Mar. Sci.* 38, 145–149. doi: 10.2989/1814232X.2016.1159616

Naidoo, T., Rajkaran, A., and Sershen, N (2020a). Impacts of plastic debris on biota and implications for human health: A South African perspective. *S. Afr. J. Sci.* 116:sajs.2020/7693.

Naidoo, T., Sershen, Thompson, R. C., and Rajkaran, A. (2020b). Quantification and characterisation of microplastics ingested by selected juvenile fish species associated with mangroves in KwaZulu-Natal. *S. Afr. Environ. Pollut.* 257:113635. doi: 10.1016/J.ENVPOL.2019.113635

Nel, H. A., Hean, J. W., Noundou, X. S., and Froneman, P. W. (2017). Do microplastic loads reflect the population demographics along the southern African coastline? *Mar. Pollut. Bull.* 115, 115–119.doi: 10.1016/j.marpolbul.2016.11.056

Nelms, S. E., Galloway, T. S., Godley, B. J., Jarvis, D. S., and Lindeque, P. K. (2018). Investigating microplastic trophic transfer in marine top predators. *Environ. Pollut.* 238, 999–1007. doi: 10.1016/j.envpol.2018.02.016

Ory, N., Chagnon, C., Felix, F., Fernández, C., Ferreira, J. L., Gallardo, C., et al. (2018). Low prevalence of microplastic contamination in planktivorous fish species from the southeast Pacific Ocean. *Mar. Pollut. Bull.* 127, 211–216. doi: 10.1016/j.marpolbul.2017.12.016

Plastics SA (2019). *PlasticsSA-Training brochure*. South Africa: Plastics SA.

PlasticsEurope (2019). *Plastics - the Facts 2019*. London: PlasticsEurope.

Reynolds, C., and Ryan, P. G. (2018). Micro-plastic ingestion by waterbirds from contaminated wetlands in South Africa. *Mar. Pollut. Bull.* 126:330–333. doi: 10.1016/j.marpolbul.2017.11.021

Rochman, C. M., Hoh, E., Kurobe, T., and Teh, S. J. (2013). Ingested plastic transfers hazardous chemicals to fish and induces hepatic stress. *Sci. Rep.* 3:3263. doi: 10.1038/srep03263

Rochman, C. M., Tahir, A., Williams, S. L., Baxa, D. V., Lam, R., Miller, J. T., et al. (2015). Anthropogenic debris in seafood: Plastic debris and fibers from textiles in fish and bivalves sold for human consumption. *Sci. Rep.* 5:14340.

Ross, K. J. (2017). *Ingestion of microplastics by epipelagic and mesopelagic fish in South African waters: A species comparison*. Rondebosch: University of Cape Town.

Ryan, P. G., Cole, G., Spiby, K., Nel, R., Osborne, A., and Perold, V. (2016a). Impacts of plastic ingestion on post-hatchling loggerhead turtles off South Africa. *Mar. Pollut. Bull.* 107, 155–160.doi: 10.1016/j.marpolbul.2016.04.005

Ryan, P. G., de Bruyn, P. J. N., and Bester, M. N. (2016b). Regional differences in plastic ingestion among Southern Ocean fur seals and albatrosses. *Mar. Pollut. Bull.* 104, 207–210.doi: 10.1016/j.marpolbul.2016.01.032

Ryan, P. G., Moore, C. J., Van Franeker, J. A., and Moloney, C. L. (2009). Monitoring the abundance of plastic debris in the marine environment. *Philos. Trans. R. Soc. B Biol. Sci.* 364, 1999–2012. doi: 10.1098/rstb.2008.0207

Ryan, P. G., Pichegru, L., Perold, V., and Moloney, C. L. (2020). Monitoring marine plastics–will we know if we are making a difference? *S. Afr. J. Sci.* 116, 1–9. doi: 10.1002/9781118891230.ch1

Savoca, S., Bottari, T., Fazio, E., Bonsignore, M., Mancuso, M., Luna, G. M., et al. (2020). Plastics occurrence in juveniles of Engraulis encrasicolus and Sardina pilchardus in the Southern Tyrrhenian Sea. *Sci. Total Environ.* 718:137457. doi: 10.1016/j.scitotenv.2020.137457

Setälä, O., Fleming-Lehtinen, V., and Lehtiniemi, M. (2014). Ingestion and transfer of microplastics in the planktonic food web. *Environ. Pollut.* 185, 77–83. doi: 10.1016/j.envpol.2013.10.013

Shabangu, F., Geja, Y., Phillips, M., Merkle, D., and Coetzee, J. (2019). *Results of the 2019 pelagic recruitment survey*. Cape Town: Department ofAgriculture, Forestry and Fisheries.

Sparks, C., and Immelman, S. (2020). Microplastics in offshore fish from the Agulhas Bank. *S. Afr. Mar. Pollut. Bull.* 156:111216. doi: 10.1016/j.marpolbul.2020.111216

Suaria, G., Achtypi, A., Perold, V., Lee, J. R., Pierucci, A., Bornman, T. G., et al. (2020). Microfibers in oceanic surface waters: A global characterization. *Sci. Adv.* 6:eaay8493. doi: 10.1126/sciadv.aay8493

Tanaka, K., and Takada, H. (2016). Microplastic fragments and microbeads in digestive tracts of planktivorous fish from urban coastal waters. *Sci. Rep.* 6:34351.

Tanaka, K., Takada, H., Yamashita, R., Mizukawa, K., Fukuwaka, M., and Watanuki, Y. (2013). Accumulation of plastic-derived chemicals in tissues of seabirds ingesting marine plastics. *Mar. Pollut. Bull.* 69, 219–222. doi: 10.1016/j.marpolbul.2012.12.010

Van Der Lingen, C. D. (2002). Diet of sardine Sardinops sagax in the southern Benguela upwelling ecosystem. *S. Afr. J. Mar. Sci.* 24, 301–316.

van der Lingen, C. D., and Miller, T. W. (2011). "Trophic dynamics of pelagic nekton in the southern Benguela current ecosystem: calibrating trophic models with stable isotope analysis." in *Interdisciplinary Studies on Environmental Chemistry- Marine Environmental Modeling & Analysis*, eds J. Omori, X. Guo, N. Yoshie, N. Fujii, I. Handoh, A. Isobe, et al. (Tokyo: TERRAPUB).

Van Der Lingen, C. D., and Miller, T. W. (2014). Spatial, ontogenetic and interspecific variability in stable isotope ratios of nitrogen and carbon of Merluccius capensis and Merluccius paradoxus off South Africa. *J. Fish Biol.* 85, 456–472. doi: 10.1111/jfb.12436

van der Lingen, C. D., Hutchings, L., and Field, J. G. (2006). Comparative trophodynamics of anchovy Engraulis encrasicolus and sardine Sardinops sagax in the southern Benguela: are species alternations between small pelagic fish trophodynamically mediated? *Afr. J. Mar. Sci.* 28, 465–477. doi: 10.2989/18142320609504199

Vendel, A. L., Bessa, F., Alves, V. E. N., Amorim, A. L. A., Patrício, J., and Palma, A. R. T. (2017). Widespread microplastic ingestion by fish assemblages in

tropical estuaries subjected to anthropogenic pressures. *Mar. Pollut. Bull.* 117, 448–455. doi: 10.1016/j.marpolbul.2017.01.081

Vorsatz, L. D., van der Lingen, C. D., and Gibbons, M. J. (2015). Diet and gill morphology of the East Coast redeye round herring Etrumeus wongratanai off KwaZulu-Natal. *S. Afr. J. Mar. Sci.* 37, 575–581. doi: 10.2989/1814232x.2015.1108933

Wallace-Fincham, B. P. (1987). *The food and feeding of Etrumeus whiteheadi Wongratana 1983, off the Cape Province of South Africa*. Cape Town: University of Cape Town.

Wang, Z., Su, B., Xu, X., Di, D., Huang, H., Mei, K., et al. (2018). Preferential accumulation of small (< 300 μm) microplastics in the sediments of a coastal plain river network in eastern China. *Water Res.* 144, 393–401. doi: 10.1016/j.watres.2018.07.050

Ward, J. E., and Kach, D. J. (2009). Marine aggregates facilitate ingestion of nanoparticles by suspension-feeding bivalves. *Mar. Environ. Res.* 68, 137–142. doi: 10.1016/j.marenvres.2009.05.002

Wright, S. L., Thompson, R. C., and Galloway, T. S. (2013). The physical impacts of microplastics on marine organisms: A review. *Environ. Pollut.* 178, 483–492. doi: 10.1016/j.envpol.2013.02.031

Conflict of Interest: The authors declare that the research was conducted in the absence of any commercial or financial relationships that could be construed as a potential conflict of interest.

frontiers in Marine Science

ORIGINAL RESEARCH
published: 05 November 2020
doi: 10.3389/fmars.2020.575395

Toward Balancing the Budget: Surface Macro-Plastics Dominate the Mass of Particulate Pollution Stranded on Beaches

Peter G. Ryan[1], Eleanor A. Weideman[1], Vonica Perold[1] and Coleen L. Moloney[2]*

[1] FitzPatrick Institute of African Ornithology, DST-NRF Centre of Excellence, University of Cape Town, Cape Town, South Africa, [2] Department of Biological Sciences and Marine Research Institute, University of Cape Town, Cape Town, South Africa

Most studies report the abundance of plastic items in the environment, but mass is an equally important currency for monitoring plastic pollution, particularly given attempts to balance the global plastic budget. We determined the size/mass composition of litter stranded on a remote, infrequently-cleaned sandy beach on the west coast of South Africa. Traditional surveys of superficial macro-litter were augmented by sieved transects for buried macro-litter (8-mm mesh), meso-litter (2-mm mesh) and sediment cores for micro-litter. Aggregating the data across all sampling scales, the total density was $\sim 1.9 \times 10^5$ anthropogenic particulate pollutants per linear meter of beach, 99.7% of which were microfibers (most of which are likely not 'plastic'). Plastics comprised 99.6% of beach macro- and meso-litter by number and 89% by mass. Small items dominated samples numerically, but were trivial relative to larger items in terms of their mass. Buried litter accounted for 86% of macro-plastic items, but only 5% of the mass of macro-plastics, because smaller items are buried more easily than large items. The total density of plastic (~ 1.2 kg·m^{-1}), at least half of which was from fisheries and shipping, is much lower than predicted by global models of plastic leakage from land-based sources. Ongoing degradation of plastic items already in the environment, particularly on beaches, is likely to result in a marked increase in plastic fragments, even if we stop leaking additional plastic. The collection of large items from beaches is a useful stop-gap measure to limit the formation of micro-plastics while we formulate effective steps to prevent plastic leakage into the environment.

Keywords: micro-plastics, macro-plastics, litter density, plastic budget, sampling scale, buried litter, beach cleaning, plastic mitigation

OPEN ACCESS

Edited by:
Hans Peter Heinrich Arp, Norwegian Geotechnical Institute, Norway

Reviewed by:
Tim van Emmerik, Wageningen University & Research, Netherlands
Alicia Herrera, University of Las Palmas de Gran Canaria, Spain

****Correspondence:***
Peter G. Ryan
pryan31@gmail.com

Specialty section:
This article was submitted to Marine Pollution, a section of the journal Frontiers in Marine Science

Received: *23 June 2020*
Accepted: *12 October 2020*
Published: *05 November 2020*

Citation:
Ryan PG, Weideman EA, Perold V and Moloney CL (2020) Toward Balancing the Budget: Surface Macro-Plastics Dominate the Mass of Particulate Pollution Stranded on Beaches. Front. Mar. Sci. 7:575395. doi: 10.3389/fmars.2020.575395

INTRODUCTION

Plastics are a diverse group of synthetic chemicals that have a myriad of uses thanks to their lightness, strength, durability, and insulative and barrier properties. However, these traits combine to make inappropriately discarded plastics a major pollution threat, with a diverse array of environmental impacts (UNEP, 2009). Plastic litter is now ubiquitous in marine systems, where it occurs as floating litter, on the sea floor, suspended in mid-water, buried in sediments and stranded

along coastlines (Bergmann et al., 2015; GESAMP, 2019). There is growing concern about micro-plastics, typically defined as plastic fragments < 5 mm in diameter (Hartmann et al., 2019), which are common constituents in sediments and surface waters (Thompson et al., 2004). Not only are micro-plastics by far the most abundant type of plastic pollution (e.g., Lee et al., 2013; Cózar et al., 2014; Eriksen et al., 2014), but small items probably have a larger impact on marine ecosystems than larger litter items (Barnes et al., 2009; Bergmann et al., 2015). Micro-plastics are ingested by a greater range of organisms than macro-plastic items (Ryan, 2016), and their much greater surface area to volume ratios promote the transfer of persistent organic pollutants and plastic-associated toxins into marine foodwebs (Takada and Karapanagioti, 2018).

Although much of the environmental focus in the last decade has been on micro-plastics, it is clear that, at least among floating plastics, most of the mass is in macro-plastic items. For example, Eriksen et al. (2014) estimated that macro-plastics (>5 mm) accounted for more than 85% of the mass of floating plastic at sea, despite accounting for < 8% of floating items > 0.3 mm. Indeed, the items larger than 200 mm (only 0.2% of floating plastic items) were estimated to be responsible for 75% of the mass of floating plastic. The empirical data for macro-plastics was less robust than for micro-plastics (Eriksen et al., 2014), but the same pattern emerged in a detailed study of the North Pacific 'garbage patch,' where macro-plastics accounted for 92% of the mass of plastics despite comprising only 6% of floating plastic items (Lebreton et al., 2018).

Tracking the mass of plastics is important for understanding the dynamics of plastic litter in marine ecosystems (Ryan et al., 2009, 2020). In particular, it is critical to try to balance the global plastic budget. Jambeck et al. (2015) estimated that in 2010 alone, some 5–12 million tons of plastic leaked into the sea from land-based sources, 20–50 times more than the total estimate of plastic floating at sea (even allowing for the fact that Eriksen et al., 2014 may have underestimated the amount of micro-plastics; van Sebille et al., 2015). Although estimated inputs from rivers (0.5–2.7 million tons per year; Lebreton et al., 2017; Schmidt et al., 2017) are less than the Jambeck et al. (2015) estimate, they are still much greater than at-sea estimates of floating plastic. Even allowing for sinking of polymers that are more dense than seawater (e.g., PET, PVC, PS which comprise some 40% of global plastic production by mass), there is a gross mismatch between the estimate of land-based sources of plastics and what we can account for at sea. One possible explanation for the mismatch is that most plastics entering the sea rapidly fragment and sink to the seafloor (Koelmans et al., 2017). However, most dated items found floating in the North Pacific gyre (Lebreton et al., 2018) are much older than the average 3-year residence time for floating items predicted by Koelmans et al. (2017).

Lebreton et al. (2019) included beached plastic in their model of plastic flux, and were able to balance the global plastic budget if almost all plastic items from land-based sources (96–98%) strand within 1 year of entering the sea, and if only 1% of stranded/seabed macro-plastic is resuspended and returned to coastal surface waters each year. These estimates appear to be quite extreme, but physical models also predict that a high proportion of micro-plastic litter leaking into coastal waters washes ashore (Collins and Hermes, 2019; van Sebille et al., 2020) and coastal surveys suggest that most macro-litter from land-based sources strands close to where it enters the sea (Rech et al., 2014; Willis et al., 2017; Ryan, 2020a). These results suggest that beaches are important sinks for plastic litter, and thus a thorough understanding of the amount of plastic on beaches is central to balancing the global plastic budget.

Beaches are the marine compartment where we have the best information on the abundance and composition of plastic pollution (GESAMP, 2019; Ryan et al., 2020), but there remains considerable confusion about how best to characterize plastics on beaches (Browne et al., 2015). Early studies of beach litter reported the amount per linear meter of beach for both macro (e.g., Dixon and Dixon, 1983; Merrell, 1984) and micro-plastics (Gregory, 1978; Ryan and Moloney, 1990). This makes sense because litter washes up in a linear front and accumulates in a series of strandlines ranging from the most recent wave front, through the last high tide line and a succession of older strandlines to the extreme storm strandline (GESAMP, 2019; Ryan et al., 2020). Lightweight items often blow farther inland until they become trapped by vegetation. All these areas were sampled in traditional beach litter studies, which reported densities per unit length of beach. Density estimates per unit area are greatly influenced by beach width, which plays little role in determining the amount of litter washing ashore. The increasing focus on micro-plastics has seen a shift toward reporting densities per unit area or volume of beach, which is more compatible with the small scale of sampling appropriate for micro-plastics. However, this method largely ignores the systematic variation in litter density across the beach profile (Chubarenko et al., 2018, 2020b), with most studies deliberately targeting the 'main' strandline, usually without any attempt to assess how this relates to other parts of the beach, or even if plastic concentrations are indeed greatest along this strandline. Attempts to extrapolate total litter loads on beaches from area-based density estimates are thus fraught with difficulty, with estimates at best using a stratified approach that acknowledges the predictable structure linked to position on the shoreline (e.g., Lavers and Bond, 2017). The most comprehensive method remains sampling across the width of the beach, as was done in traditional beach litter studies.

Olivelli et al. (2020) highlight the importance of integrating all litter items from the waterline to the backshore vegetation. However, their visual survey approach ignores critical processes within the beach. The pattern of increasing litter item size from the sea to the backshore is a simple consequence of the much greater abundance of small plastic items at sea (which means most items washing ashore are small) and the differential burial of smaller items as you move toward the back of the beach (because smaller items are buried much more rapidly by windblown sand or infiltration than large items; see section "Results"). To date, few studies have sampled buried litter on beaches, even though it may account for a significant proportion of beach litter (Browne et al., 2015). Kusui and Noda (2003) conducted perhaps the best study to date, but it is unclear how comparative their area-based approach is, given sampling at very different scales for differently-sized litter items (100 m^2 quadrats for surface macro-litter and

0.16 m^2 quadrats for buried litter). Also, they only sampled the top 5 cm of the beach, even though micro-plastics occur up to 2 m deep in beaches (Turra et al., 2014; Chubarenko et al., 2018).

Finally, most studies of beach litter focus on only one size class of litter, and thus there is no way to assess the proportion of the total litter load represented by different size fractions. The few studies that have sampled across different size classes have tended to report numbers of items, not mass (e.g., Lee et al., 2013). Only Martins and Sobral (2011) have characterized both numbers and masses of plastics in beaches and reported that micro-plastics (<5 mm) accounted for just over 50% by number but < 5% by mass. However, they only sampled the top 2 cm of sand, and their largest quadrats (2 m × 2 m) were too small to sample megalitter items (>1 m), which account for most of the mass of floating plastic at sea (Lebreton et al., 2018) and require large areas to sample adequately on beaches (OSPAR, 2010).

In this study, we characterize beach plastic and other anthropogenic litter across the full size spectrum from micro to megalitter items. To do so, we pool data from samples collected from the surface and buried to 15–20 cm deep across a range of spatial scales and integrated from the waterline to the backshore dune vegetation. By selecting a remote beach with very few visitors and little if any beach cleaning effort, we provide a snapshot of the plastic load typical of marine inputs, which can be compared to the size distribution of plastics recorded at sea. By reporting the relative contribution of different size classes, we provide the first estimate of the proportion of beach litter mass represented by superficial macro-litter. Such estimates are needed to infer how much plastic is stored in global beaches, although the proportion likely varies with beach type and recent patterns of erosion/deposition as well as cleaning effort.

MATERIALS AND METHODS

Field Sampling

We sampled stranded litter along a 500 m-stretch of open sandy beach near the center of 16 Mile Beach (33.214°S, 18.082°E), a long, remote beach in the West Coast National Park, 85 km north of Cape Town, South Africa (**Supplementary Figure S1**). Like most beaches in the region, it is a dissipative beach with a gently shelving low shore, increasing in slope toward the backshore. The intertidal zone averages around 30–40 m wide, with a further 5–10 m from the spring high tide line to the start of the dune vegetation. The beach lies in the downstream plume of litter emanating from Cape Town (Collins and Hermes, 2019) and is characterized by a mix of local, land-based litter and fishery/marine inputs (Fazey and Ryan, 2016). By sampling 10 km from the north end of the beach, distant from easy access points, we reduced the risk of significant local inputs by beach-goers and loss of items to beachcombers or informal cleaning efforts (cf. Ryan et al., 2009). Prior to 2010, only the ends of the beach were cleaned once or twice per year by volunteers and park staff. The central section was not cleaned, other than informal efforts by members of the public (e.g., selective removal of sought after items like fishing floats). Since 2010, teams employed by the government's 'Working for the Coast' program[1] have cleaned the beach more systematically, and so no surveys of macro-litter were conducted after 2010.

We used four approaches to sample three size classes of litter items. Items large enough to be collected by hand, similar to those removed by manual cleaning efforts (roughly > 10 mm), were picked from the surface of the beach. These traditional surveys of superficial macro-litter were augmented by sieved transects for buried macro-litter (8-mm mesh), meso-litter (2-mm mesh) and sediment cores for micro-litter. Although these mesh sizes do not correspond exactly with the definitions of macro-, meso-, and micro-plastics (e.g., Hartmann et al., 2019) they are close enough that we use these terms as a convenient shorthand to report the results from the different sampling approaches.

Macro- and meso-litter were sampled during the austral summer in March 2010, and meso- and micro-litter were sampled in November 2017. The relative importance of buried versus superficial macro-litter was estimated from eight 1-m wide transects running from the waterline to above the storm strandline. Transects were located 50 m apart. After demarcating each transect, all surface litter was collected from the water line to above the storm strand line (retaining items that straddled the transect boundary if they were more than half in the transect). We then sampled buried litter from the most recent high tide line to above the storm strand line (**Figure 1**). Spades were used to dig up the sand, which was passed through a 1 × 1 m raised sieve with a 8 × 10 mm-mesh (**Supplementary Figure S2**). We sampled two depth strata: first the top 5 cm of sand was sieved, and then sand 5–15 cm deep was sieved. All retained material was sorted to collect macro-litter items, which were returned to the lab for processing (see below). Macro-litter from a further 10 such transects was collected in March 2008, increasing the sample size and providing an indication of inter-year variability in buried litter loads.

In 2010, we augmented the 1-m macro-litter transects with more extensive macro-litter surveys in four 50 m-wide stretches of beach, each bounded by two 1-m macro-litter transects (**Figure 1**). Teams scoured the area from the waterline to the back of the storm strand line and into the adjacent vegetated dune fringe, where wind-blown litter from the beach accumulates. In tandem with each 1-m macro-litter transect we also sampled meso-litter in the top 5 cm of sand in a 0.5-m wide transect with a 2-mm mesh sieve (Ryan et al., 2018). The sand deeper than 5 cm was too wet and coarse to sieve with the fine-meshed sieve. The area of wet sand below the recent high tide line was searched visually for any recently-stranded meso-litter items, which were added to the samples. Litter was collected from the sieved material by searching visually. All remaining material was then poured into a large bucket of seawater to detect any small floating litter that may have been confused with denser particles such as shell fragments. Repeated swirling of the bucket contents detected plastics with densities greater than seawater (because they remain in motion for much longer than more dense shells and stones). Again, all anthropogenic material was returned to the lab for processing.

[1] https://www.environment.gov.za/projectsprogrammes/workingfor_thecoast

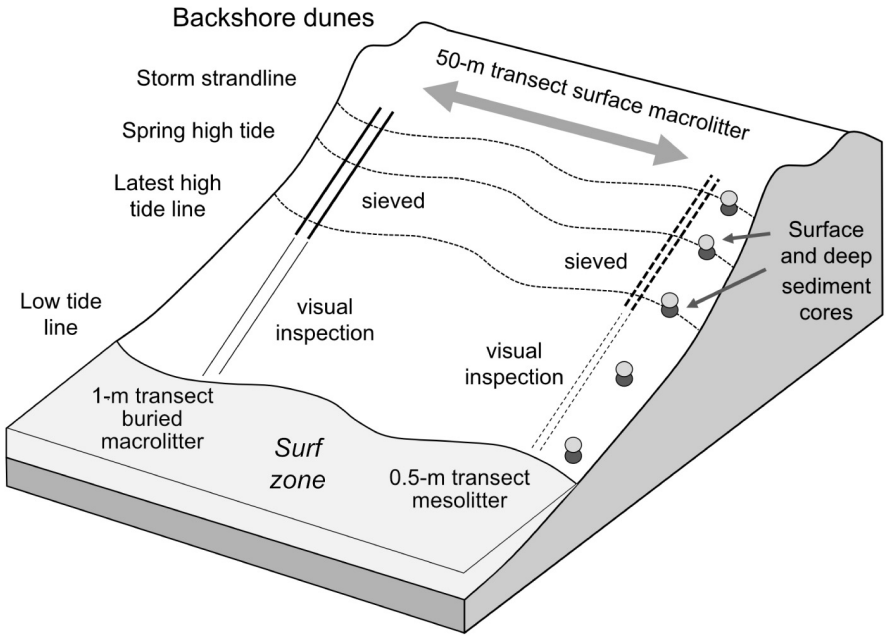

FIGURE 1 | Schematic diagram of sampling protocols, combining 50-m transects for surface macro-litter, 1-m coarse-sieved samples for buried macro-litter, 0.5-m fine sieved samples for meso-plastics, and paired sediment cores (shallow and deep) at five sites across the beach profile for micro-plastics.

In 2017, we sampled micro-plastics at the same site using a series of core samples. A 7-cm diameter metal corer was used to collect surface and deep core samples, each ∼12 cm deep (∼480 cm^3) and comprising 828 ± 81 (SD) g of sand (dry mass). The surface core was removed, and then a second, deeper core taken from immediately beneath the surface core. Each core was stored in a foil tray with a card lid for transport to the laboratory. The paired surface and deep samples were collected at low tide from five locations up the beach profile: at the low shore, mid shore, most recent high tide line, the spring high tide line and storm strand line (**Figure 1**). The distances between each sample site were measured to the nearest 0.5 m. Three such transects were sampled, 50 m apart. The average (± SD) distances between core sites extending up the shore from the low shore were 15.3 ± 1.5 m (low to mid shore), 9.3 ± 0.6 m (mid shore to high tide line), 6.5 ± 1.2 m (high tide to spring high) and 2.5 ± 0.5 m (spring high to storm strandline). Each micro-plastic core transect was paired with a 0.5-m meso-litter sieved transect as conducted in 2010 (see above). These sieved samples were divided into three levels on the shore, linked to the top three coring sites: from the recent high tide line to 1.5 m below the spring high tide line; from there to midway between the spring high and storm strandlines; and from there to 1 m above the storm strandline. Another 0.5-m sieved sample collected in 2015 from the same site (Ryan et al., 2018) was also included to give a total of 12 meso-litter samples.

Sample Processing

All macro- and meso-litter was categorized by material (plastic, glass, wood, paper, metal, etc.) following standard beach survey protocols employed since the 1980s on South African beaches (Ryan and Moloney, 1990). Most macro items were also placed into major categories of use: different types of packaging, other single-use items, fishing and shipping gear, other user items, etc. After cleaning off any sand, large items (>1 kg) were weighed *in situ* with one of a series of spring balances (5–25 kg). All remaining items were removed from the beach, cleaned of sand, dried and weighed on top pan balances. Macro-litter items were weighed to the nearest 0.1 g, meso-litter to the nearest 0.1 mg. Not all macro items were weighed individually; groups of similar items were weighed together (e.g., small ropes, sweet wrappers, etc.), assigning each item the average weight for the group (i.e., mass/n).

In the lab, each micro-litter sand core was dried, weighed to the nearest 0.1 g and then added to 2 L of a saturated salt (NaCl) solution in a well-rinsed 5-L glass beaker (Mathalon and Hill, 2014; Nel and Froneman, 2015). The salt solution was pre-filtered through a 25 μm filter because even the laboratory-grade salt we used contained microfibers. The beaker was stirred vigorously with a metal spoon, covered with metal foil and allowed to settle for 24 h, after which the supernatant was filtered through a 25 μm nylon filter. The filter was examined under a dissecting microscope to collect all visible anthropogenic particles. Fibers were identified as anthropogenic in origin if they were an homogeneous color, had a constant width, if there were no organic or cellular structures visible and if they did not break apart when pulled using tweezers (Hidalgo-Ruz et al., 2012; Horton et al., 2017). All items were measured (approximate length and diameter for fibers; mean length, breadth, and depth for fragments) to the nearest 1 μm using a graticule. The approximate mass of items was inferred from item volume ($l \cdot b \cdot d$ for fragments; $l \cdot \pi \cdot r^2$ for fibers), assuming a mean density of 1.0 $mg \cdot mm^{-3}$ for plastic fragments, 1.2 $mg \cdot mm^{-3}$ for fibers

and 0.016 mg · mm^{-3} for expanded polystyrene (Andrady, 2017). Every attempt was made to reduce the risk of contamination. All lab equipment was covered with metal foil when not in use and thoroughly rinsed with Milli-Q water prior to use. All filters were triple-rinsed with Milli-Q water prior to use. To estimate levels of contamination in the lab, a control filter was exposed whenever a sample was uncovered. Control filters contained 0–3 fibers (average 0.59 ± 1.01 SD, n = 33 controls), with 67% of controls containing 0 fibers. The fiber count from each control filter was subtracted from the matched sample count data (Suaria et al., 2020). Overall, this reduced the number of fibers counted in samples by only 6%. Three core samples were extracted a second time to estimate the proportion of items not recovered during the initial extraction process; only one fiber was recovered during the second extraction, from a sample with 0 fibers on the initial extraction, and may well have been a contaminant.

Data Analysis

The various data sets were combined to estimate the average total number and mass of plastic items per linear meter of beach. To integrate across the full size spectrum of litter sampled, we were perforce obliged to combine data across years, using macro-litter data from 2010, micro-litter data from 2017 and meso-litter data from both years. Although this is not ideal, long-term monitoring at the site [including five-yearly surveys of meso-litter and superficial macro-litter since the 1980s (Ryan and Moloney, 1990) and the buried macro-litter sampling in 2008 and 2010] show limited inter-year variation in litter loads at this beach at least in the last two decades. Data on micro-plastics are more limited, but also suggest relatively little temporal variation (de Villiers, 2018). Ultimately, we consider the biases potentially introduced through combining data collected in two different years to be no greater than those resulting from the extrapolation required to integrate data across sampling scales ranging over 4–5 orders of magnitude (see below). Our results should be seen as more qualitative than quantitative, giving only a crude indication of the relative contribution of the different litter size classes to the number and mass of litter items.

The size of items was scored based on their mass (g), using a log scale ranging across 13 orders of magnitude (from < 0.1 μg to 100 kg). Because not all macro-litter items were weighed individually, and micro-plastic masses were inferred from measurements, the estimates of abundance by size class are indicative rather than precise. Micro-plastic densities from sediment cores were extrapolated based on the average beach width, assuming that the core samples were central within each sample zone. We assumed densities recorded by the low shore cores extended another 5 m down shore and the storm strandline extended another 1 m into the dunes, giving an effective transect of 39.6 m. However, for the spring high tide line, which had an appreciably higher density of microfibers than the recent high tide line, we only applied its density 1.5 m downshore toward the recent high tide line. Given the small size of the cores (7 cm diameter), the extrapolation factors to estimate densities per meter of beach were very large (195–1096, given three replicates per shore stratum). Rather than trying to combine these error terms, we simply report the coefficients of variation (CV) for each sampling approach, to give a rough idea of the confidence in each estimate.

TABLE 1 | The median and maximum masses of litter items sampled at different spatial scales on a beach in the West Coast National Park, South Africa, in 2010 (macro- and meso-litter) and 2017 (micro-litter).

Sample and litter type	Median	Inter-quartile range	Maximum	*n*
50-m macro-litter transects (*n* = 4)				
Macro-plastics	3.0 g	0.6–26.0 g	35000 g	1479
Macro non-plastics	115.0 g	10.0–450 g	2250 g	96
1-m macro-litter transects (*n* = 8)				
Surface macro-plastics	2.0 g	0.4–8.4 g	550 g	107
Surface non-plastics	4.8 g	1.7–61.8 g	182 g	10
Buried macro-plastics (0–5 cm)	0.2 g	0.1–0.5 g	41.5 g	331
Buried macro-plastics (5–15 cm)	0.1 g	0.05–0.3 g	34.2 g	376
Buried non-plastics	0.3 g	0.2–0.7 g	1.5 g	10
0.5-m meso-litter transects (*n* = 8)				
Industrial pellets	21.5 mg	13.0–27.5 mg	94 mg	1332
Expanded polystyrene*	2.0 mg	1.0–7.0 mg	92 mg	115
Other meso-plastics*	10.0 mg	4.0–20.0 mg	195 mg	359
Non-plastics (wax)*	55.9 mg	34.4–77.3 mg	99 mg	2
Micro-plastic sediment cores (*n* = 30)				
Micro-plastic fragments*	12 μg	–		1
Microfibers*	0.1 μg	0.07–0.23 μg	4.9 μg	313

**Right truncated to exclude items > 10 mm (meso-litter samples) and > 2 mm (micro-litter samples).*

Superficial macro-litter density was based on the 50 m beach collections because these samples captured more large, scarce items, as reflected in the greater mass per meter of beach from these samples compared to the 1 m-transects (**Table 1**). The 1-m sieved transects provided data on buried macro-litter and the 0.5-m sieved transects estimated meso-litter in the surface 5 cm. Macro-litter items that would have been captured by the macro sieve (>10 mm) were discarded from the meso- and micro-samples. However, we explored the implications of extrapolating meso-litter from the micro-plastic core samples in the estimate of total litter load.

All size classes of litter were strongly right skewed and so we report median and inter-quartile ranges (IQR) for masses. We used Spearman rank correlations to test for consistent patterns in the abundance and mass of surface versus buried macro-litter, and among samples of macro and meso-litter collected in 2010. Generalized linear models (GLMs; R Core Team, 2019) were used to assess which factors determine the number and length of microfibers in core samples. For the number of microfibers, we fitted the GLM with a negative binomial distribution because the data were over-dispersed; for fiber length, we used a gamma distribution because the data were strongly right-skewed and

TABLE 2 | The abundance and mass of macro-litter per meter of beach in the West Coast National Park, South Africa, in 2010 sampled by four 50 m-transects for surface litter each with two paired 1-m transects for buried litter, and the percentage of surface litter of the total (%S).

Litter type	Number·m^{-1}				Mass (g·m^{-1})			
	Surface	Buried	Total	%S	Surface	Buried	Total	%S
All plastics	7.4	91.7	99.1	7%	1111.5	77.1	1188.7	94%
Bottles	1.3	0.5	1.8	72%	106.5	2.1	108.6	98%
Lids	0.9	5.1	6.0	15%	2.3	4.8	7.1	32%
Straws	0.1	1.6	1.7	6%	0.1	1.8	1.9	3%
Bags, wrappers	1.5	20.5	22.0	7%	6.5	8.4	14.9	44%
Polystyrene	0.7	14.5	15.2	5%	7.1	10.6	17.7	40%
Other packaging	0.5	4.5	5.0	10%	3.0	5.8	8.8	34%
Fishing/shipping	0.9	10.4	11.3	8%	565.1	15.9	581.0	97%
Other user items	0.4	2.5	2.9	15%	418.6	12.6	431.2	97%
Rigid fragments	1.0	32.1	33.1	3%	2.5	15.1	17.6	14%
All non-plastics	0.5	1.0	1.5	32%	142.0	0.5	142.5	100%
Glass	0.2	0.0	0.2	100%	70.8	0.0	70.8	100%
Wood	0.1	0.0	0.1	100%	69.9	0.0	69.9	100%
Metal	0.0	0.0	0.0	100%	0.4	0.0	0.4	100%
Cigarette butts	<0.1	0.5	0.5	4%	<0.1	0.1	0.1	2%
Other non-plastics	0.1	0.5	0.6	17%	0.8	0.4	1.3	67%
Total	7.9	92.7	100.6	8%	1253.5	77.6	1331.1	94%
% plastic	93.9	98.9	98.5		88.7	99.3	89.3	

constrained to lengths > 0. Explanatory variables in both models were shore stratum, sample depth and transect (A–C).

RESULTS

Macro-litter

The patterns detected in the 10 1-m macro-litter transects sampled in 2008 and the eight transects in 2010 were broadly similar in terms of both the number (**Supplementary Table S1**) and mass (**Supplementary Table S2**) of items collected, and so data from the 2 years were pooled. Variance among replicates was moderate; coefficients of variation (CV) were 43% for numbers of items, and 75% for mass of items, with little difference in CVs among depth strata. Surface items comprised only 10.6% of macro-litter items; 41.0% were in the top 5 cm, and 48.4% from 5 to 15 cm deep. Given the greater volume of sand sampled in the deeper stratum (2x surface stratum), the density of buried macro-litter almost halved from the surface 5 to 5–15 cm. Despite the numerical dominance of buried macro-litter, superficial items accounted for 66.1% of the mass of macro-litter, because the mass of surface items was much greater than buried items (**Table 1**). This was reflected in the greater abundance of small litter items among buried litter (e.g., straws, rigid plastic fragments, and cigarette butts), whereas large items such as bottles and pieces of wood were mostly recorded on the surface (**Table 2** and **Supplementary Table S1**).

Most macro-litter items were plastic (97.0%). There was a slight increase in the proportion of plastic items from the surface (93.6%) to buried litter (97.4% for 0–5 cm and 97.5% for 5–15 cm) due to the greater mass (and size) of non-plastic items than plastic items (**Table 1**). However, it was clear that the 1-m transects failed to adequately sample large litter items. In 2010 we therefore collected all superficial macro-litter in four 50-m transects, each paired with two 1-m buried litter transects (one at either end of the 50 m stretch). In total, 1575 macro-litter items weighing 204.6 kg were collected in these 50-m transects. CVs for the four 50-m macro-litter transects were 25% for the number of items and 61% for mass. Surface litter density (7.9 m^{-1}) was half that recorded in paired 1-m transects (14.6 m^{-1}, **Supplementary Table S1**), possibly because search intensity was greater in the smaller 1-m wide transects. However, the density of litter by mass was four times greater (1.03 kg·m^{-1} compared to 0.23 kg·m^{-1} in the 1 m-transects, **Supplementary Table S2**) because 50-m transects captured more large, scarce items. The largest item sampled in the 50-m transects was a 35 kg tangle of polypropylene fishing rope, substantially larger than the largest item in all 18 1-m transects (a 550 g heavy-duty polyethylene bag).

Combining the surface litter data from the 50-m transects with the buried litter data from the paired 1-m transects sampled in 2010, there were just over 100 macro-litter items per meter of beach (**Table 2**). Surface litter comprised less than 10% of the total number of items, but contributed almost 95% to the total mass of litter. There was little difference in the composition or size of buried litter with respect to depth stratum (**Figure 2** and **Supplementary Tables S1, S2**) and so they were pooled in **Table 2**. The mean mass of buried items was relatively constant irrespective of whether they were in the shallow (0.8 g) or deep (0.9 g) stratum. However, the masses of buried items were strongly right skewed (**Figure 2**), and median masses were considerably smaller than the means. Plastics comprised 93.9% of surface macro-litter items and 98.9% of buried macro-litter (**Table 2**). Non-plastic items contributed more in terms of mass than by number of items, especially

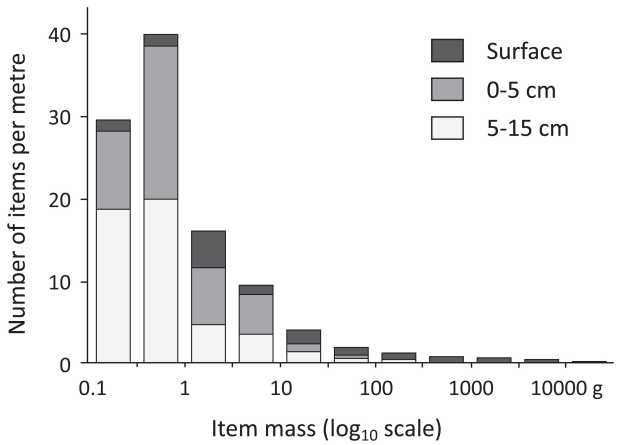

FIGURE 2 | The frequency distribution of the masses of macro-litter items recorded at three depth strata in the beach in the West Coast National Park, South Africa in 2010 (surface litter data from four 50-m cleaned areas, buried data from eight paired 1-m wide sieved transects; items < 0.1 g pooled into the smallest size class).

among superficial macro-litter, but they still only made up 11.3% of the mass in this category (**Table 2**). Buried litter was more than 99% plastic by mass (**Table 2**). The total mass of macro-litter averaged 1.33 kg·m^{-1} of beach, of which plastics contributed 1.19 kg·m^{-1}. Fishing gear and other marine-source litter accounted for 49% of the mass of macro-plastics, and 44% of the mass of all macro-litter.

Meso-litter

The 12 0.5-m transects contained 3437 meso-litter items (69.58 g), of which only two small pieces of paraffin wax (0.1%) were not plastic (**Table 3**). Industrial pellets accounted for 64% of the meso-litter (70% by mass), followed by rigid fragments (19% by number and 20% by mass) and expanded polystyrene (14% by number, 7% by mass). The variation among meso-litter samples was similar to that recorded among macro-litter samples, with overall CVs of 73% for the numbers and 74% for the masses of items collected (**Table 3**). Sampling over three different years did not greatly affect the variation among samples; CVs in 2010, when eight samples were collected ∼50 m apart, were similar: 66% for numbers of items and 69% for mass of items. The largest litter item recorded in a 0.5-m transect was a 224 g glass bottle.

Although we did not subdivide most transects across the beach profile, it was clear that meso-litter items (like macro-litter) were concentrated in a series of strandlines on the high shore, not all of which were evident on the surface. In the three transects sampled in 2017, meso-litter loads peaked around the spring high tide line in two transects, decreasing slightly to the storm strandline, but were much higher at the storm strandline in Transect C (**Supplementary Table S3**). Across all samples, the abundance of meso-litter in the top 5 cm of the beach averaged 573 m^{-1} of beach (444 m^{-1} based only on 2010 transects), roughly 10 times the density of macro-litter to this depth, and five times the abundance of macro-litter to 15 cm depth (**Table 2**). However, the total mass of meso-litter was only 11.6 g m^{-1} of beach (9.1 g m^{-1} based on 2010 samples), which is 0.9% of the mass of macro-litter, and 1% of the mass of macro-plastics.

TABLE 3 | The mean abundance and mass of meso-litter (2–10 mm) per meter of beach in the West Coast National Park, South Africa, based on 12 0.5-m transects sampling the top 5 cm of sand in 2010 (n = 8), 2015 (1) and 2017 (3).

Litter type	Number (range)	CV	Mass g (range)	CV
Industrial pellets	368 (54–762)	69%	8.13 (1.22–18.88)	71%
Rigid fragments	111 (10–296)	73%	2.34 (0.37–6.65)	82%
Flexible fragments	9 (0–38)	121%	0.25 (0.00–1.02)	140%
Expanded polystyrene	80 (0–526)	184%	0.80 (0.00–5.65)	199%
Fibers/monofilament	5 (0–14)	92%	0.06 (0.00–0.33)	166%
Paraffin wax	0.3 (0–2)	234%	0.02 (0.00–0.20)	292%
Total	573 (68–1544)	73%	11.60 (0.80–15.26)	74%

Items larger than 10 mm were excluded as macro-litter. Coefficients of variation (CV) provide a relative measure of variation among samples for each type of item.

Micro-litter

Microfibers were by far the most abundant anthropogenic items in the micro-litter cores. After correcting for fiber contamination, the 30 cores contained 296 microfibers and only one microfragment (<1 mm; **Supplementary Table S3**). Fibers were found in 26 of 30 cores, but there was considerable variation among samples and transects (count CVs among transects = 74–80%). All four cores lacking fibers were found in one transect (C), which contained only 10–15% of the number of fibers in the other two transects (**Supplementary Tables S3, S4**). There was a tendency for microfibers to be more abundant toward the high shore (**Supplementary Table S3**), but the only shore stratum that had a significantly lower density of microfibers was the mid shore (**Supplementary Table S4**). Microfiber density tended to increase with sample depth (**Supplementary Table S3**), particularly on the low-mid shore, although this was not significant given the small number of samples (**Supplementary Table S4**).

The extrapolated abundance of micro-plastics was 188 × 10^3 microfibers and 200 microfragments per meter of beach (**Table 4**). Given the much greater width of the low and mid shore, these two strata accounted for just over half of all microfibers, in stark contrast to larger litter items, which are predominantly found along the high-shore strandlines. Because microfibers were more abundant in the deep cores on the low shore, the extrapolated estimates suggest that there are twice as many fibers per meter of beach in the 12–24 cm depth stratum (128 × 10^3 m^{-1}) than there are in the surface 12 cm (60 × 10^3 m^{-1}).

Median microfiber dimensions were 524 × 14.3 μm (length IQR 421–1016, diameter 13–16 μm). Microfibers tended to be longer in deeper cores at all levels on the shore (**Figure 3** and **Supplementary Table S5**). The estimated masses of individual microfibers ranged from 0.003 to 4.9 μg (**Table 1**). Extrapolating from the dimensions of the fibers measured for each depth and shore stratum, the estimated mass of microfibers per meter of beach was 60 mg (**Table 4**). Because deep cores tended to have longer fibers, the skew in mass with depth was even greater than abundance, with deep cores accounting for 79% of the estimated

TABLE 4 | The proportions of microfibers at different levels on the shoreline and at two depth strata in 2017, expressed in terms of the number and mass of fibers.

Shoreline level	Extrapolated number*			Extrapolated mass*		
	Surface	Deep	Total	Surface	Buried	Total
Storm strand line	14%	7%	9%	4%	1%	1%
Spring high tide line	18%	4%	9%	7%	1%	2%
Recent high tide line	25%	35%	32%	16%	13%	14%
Mid shore	25%	10%	15%	27%	6%	11%
Low shore	18%	44%	36%	46%	78%	72%
Total (m^{-1} beach)	60×10^3	128×10^3	188×10^3	12.4 mg	47.5 mg	59.9 mg
% total	32%	68%		21%	79%	

**Extrapolation factors 195, 238, 836, 1065, and 1096 for the five shore zones from storm strand line to low shore, based on differences in shore widths (see section "Materials and Methods" for details).*

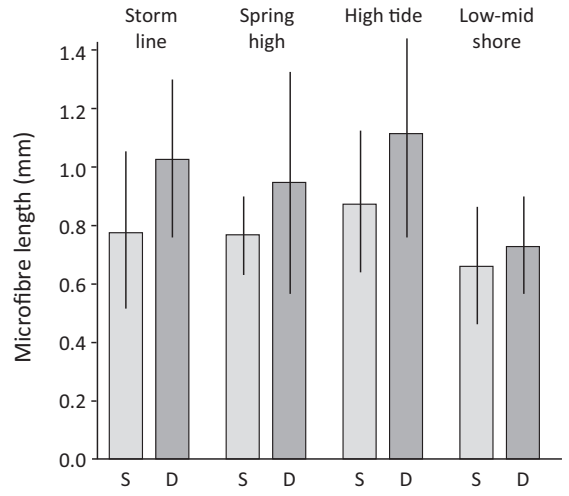

FIGURE 3 | The mean length of microfibers from surface (S, 0–12 cm) and deep (D, 12–24 cm) cores collected at three sites on a beach in the West Coast National Park, South Africa, in 2017. Bars show 95% confidence intervals of the mean.

mass of microfibers, and the low and mid-shore accounting for 84% of the mass (**Table 4**).

Meso- and macro-litter was found in five cores, all from the top two sample strata: six items in two cores from the storm strandline, and nine items from three cores from the spring high tideline. All 15 items were plastic: five macro-plastic fragments (maximum mass 1.63 g) and 10 meso-plastics (three fragments of hard plastic, three industrial pellets, three foamed polystyrene balls and one tiny length of monofilament line). Most (14 of 15) meso- and macro-litter items were found in deep cores, including nine meso-plastics. Extrapolating from these data gives a surface meso-litter density of 2.4×10^2 industrial pellets (5 g) per meter of beach in the surface 12 cm, which is similar to the amounts estimated from the meso-litter sieved transects. However, the deep core meso-litter extrapolates to 1.9×10^3 meso-plastics per meter of beach with a total mass of 48 g, which is substantially more than that estimated from the meso-litter sieved transects.

Spatial Pattern

There were significant correlations between both the number ($r_s = 0.869$, $P < 0.02$) and mass ($r_s = 0.885$, $P < 0.01$) of macro- and meso-litter when we compared the data from the eight paired 1- and 0.5-m transects conducted ∼50 m apart in 2010. Similarly, there were significant correlations between the number and mass of macro-litter items on the surface and buried in the 1-m transects in both 2008 ($r_s = 0.908$, $P < 0.001$ and 0.893, $P < 0.005$, respectively) and 2010 ($r_s = 0.927$ and 0.929, respectively, both $P < 0.005$). These results suggest that there is consistent spatial variation in the density of litter items at a scale of 10s to 100s of meters along the beach. However, the patterns across years were less well-defined. Among all 18 1-m macro-litter transects there were significant relationships between the two depth strata (0–5 and 5–15 cm) in terms of the number ($r_s = 0.609$, $P < 0.01$) and mass of litter items ($r_s = 0.512$, $P < 0.05$), but only a weak correlation between the number of litter items on the surface and buried items ($r_s = 0.423$, one-tailed $P < 0.05$); this relationship was not significant for the mass of litter items ($r_s = 0.333$). There was no evidence of a link between microfiber densities and the paired meso-litter samples; Transect C had significantly fewer fibers than Transects A and B, yet was collected immediately adjacent to the 0.5-m transect with the highest meso-litter load (**Supplementary Table S3**).

The Litter Size-Mass Spectrum

Combining the macro and meso-litter data from 2010 with the micro-litter samples from 2017, the total density is $\sim 1.9 \times 10^5$ anthropogenic particulate pollutants per meter of beach with a total mass of at least 1.45 kg (**Table 5**). All estimates are minima given the sampling limitations listed in **Table 5**. The number of items increases exponentially with decreasing particle size down to a mass of around 10 mg, then there is a large deficit in the numbers of micro-plastics down to around 1 μg, where the numbers of microfibers again fit an exponential model of increasing abundance with decreasing particle size (i.e., a linear trend on the log scale shown in **Figure 4**). The mass-frequency distribution highlights the importance of the small number of megalitter items in determining the total mass of litter (**Figure 4**). Only four items > 10 kg were sampled, yet they contributed the greatest amount of mass of any size class (**Figure 4**).

DISCUSSION

Estimating the relative importance of different litter classes across the full size spectrum required sampling at a range of spatial scales appropriate to capture items ranging from micro (<1 mm) to mega (>1 m), spanning 13 orders of magnitude in mass from < 0.1 μg to 10s of kg (**Figure 4**). The effective length of beach surveyed ranged over five orders of magnitude from 200 m for surface macro-litter to only 0.002 m for micro-plastics (although three core transects represent 0.21 m of beach length, the five cores per transect represent only 0.9% of the beach profile). As expected, the maximum item size captured by each method was directly related to sampling scale (**Figure 5**). With hindsight we should have increased the spatial scale of

TABLE 5 | Estimated numbers and masses of macro-, meso-, and micro-litter per meter of beach in the West Coast National Park, South Africa, combining data from 2010 (macro-litter), 2017 (micro-litter) and both years combined (meso-litter).

Litter type	Number		Mass		Sampling biases
	$n \cdot m^{-1}$	%	$g \cdot m^{-1}$	%	
Macro-plastic – surface	15	<0.1%	1200	83%	Longer length of beach needed for megaplastics
Macro-plastic – buried	200	<0.1%	85	6%	Only sampled to 15 cm; Large items under-represented
Industrial pellets	370	0.1%	10	1%	Only sampled to 5 cm
Other meso/micro-plastics	400	0.2%	5	<1%	Only sampled to 5 cm
Microfibers	188×10^3	99.7%	<0.1	<<1%	Only sampled to 24 cm; Sample < 1% beach profile; Filter mesh 25 μm
Non-plastic litter	5	<0.1%	150	10%	(as macro-plastics above)
Total	1.9×10^5 m^{-1}		1450 g		

Values rounded up given the potential sampling biases listed.

our sampling; had we sampled 10 km of beach for megalitter, the total mass of litter per meter of beach would likely have been appreciably higher. Indeed, when we conducted the 50-m transects for surface macro-litter there was a massive marine floating buffer stranded about 1 km beyond our sampling area that weighed > 100 kg.

Integrating data collected at such a wide range of spatial scales inevitably leads to some gross extrapolation, particularly from the very small micro-plastic cores. There are also numerous methodological challenges to using sieves to characterize the distribution of particle sizes (Filella, 2015). Our replicate samples indicate varying levels of spatial variation in litter loads, with CVs mostly ranging from 25 to 80%. At least some of this variation was the result of consistent, local-scale variation in the abundance of different litter classes, but with little correlation between microfibers that were distributed throughout the shoreline and the larger, more buoyant litter items that were concentrated along high-shore strandlines. We were also obliged to pool data from two different years to obtain a picture of the full size spectrum distribution of litter. Fortunately, the comparisons of macro- and meso-litter densities showed that variation among years was similar to that among spatial replicates collected on the same day. However, when taken together, these factors mean that our estimate of the total amount of anthropogenic beach litter is perforce crude, although it appears to be the first attempt to sample across the full size spectrum of particulate pollutants across the beach profile. The results should be taken as largely indicative given the numerous sampling limitations listed in **Table 5**, but they give some insight into the relative abundance and mass of plastic and other pollutants stranding on a beach with little interference from land-based activities (either littering or cleaning).

Aggregating the data across all sampling scales gave a total density of $\sim 1.9 \times 10^5$ anthropogenic particulate pollutants with a total mass of around 1.45 kg per meter of beach (**Table 5**). These are minimum estimates, because we only sampled the upper 15–20 cm of the beach. Micro-plastics can be mixed down to at least 2 m in beaches (Turra et al., 2014; Chubarenko et al., 2018). To fully explore the abundance of litter items would therefore require appreciably deeper sampling than we performed. The density of macro-litter almost halved (per unit volume) from the top 5 cm of the beach to the deeper stratum sampled in both 2008 and 2010 (5–15 cm, **Supplementary Tables S1, S2**). Extrapolating this rate of decrease suggests that deeper sampling to 1–2 m might increase the total number of items by 30–50%. The impact on mass is less marked, because buried litter is much smaller than surface litter. However, this conclusion might be biased by our relatively shallow sampling. Elsewhere, we have seen bottles, crates and other large litter items buried 2–3 m in old beach sediments exposed by coastal erosion.

We not only failed to dig deep enough, but we also only sampled 18 m of beach for buried macro-litter; had we sampled a few 100 m, we might have found some larger buried litter items as we did when we expanded the search area for surface macro-litter. However, our mismatch between surface and buried litter sampling effort was much less than in the seminal study of buried litter by Kusui and Noda (2003), who sampled roughly 1000 times more area for surface litter ($\sim$500 m^2 per beach) than buried litter (0.48 m^2 per beach). Additional sampling both in terms of depth and spatial extent is needed to adequately characterize buried macro-litter, but the marked difference in item sizes between surface and buried items even within 1-m transects (**Table 1**) indicates that buried litter items are a non-random subset of litter items due to the faster burial of smaller items. We therefore suspect that comprehensive sampling of buried litter is unlikely to more than double the number or mass of macro-litter items.

Microfibers accounted for 99.7% of all particulate pollutants in the study beach. The dominance of microfibers among micro-plastic samples from beaches along the west coast of South Africa is well-known (Nel et al., 2017; de Villiers, 2018). The densities we recorded are slightly lower than those reported by de Villiers (2018) at Yzerfontein, 15 km south of our study site. She counted 47, 52, and 120 fibers$\cdot dm^{-3}$ in sand collected from the top 5 cm at the 'high-level water mark' on three occasions in 2016–2017 (S. de Villiers, pers. comm.). If we double our counts to match the larger sample volume, our three surface counts for the spring high tide line were 6, 40, and 42 fibers$\cdot dm^{-3}$, despite using a finer mesh filter (25 μm) to extract fibers than the 40 μm mesh used by de Villiers (2018). It is thus unlikely that our estimates of microfibers are inflated. However, when we extrapolate across the entire beach profile, the numbers of fibers completely dwarf other particulate litter items. This is partly because of their higher densities than larger litter items, but also because they occur throughout the beach profile, with little evidence of concentration at high shore strandlines.

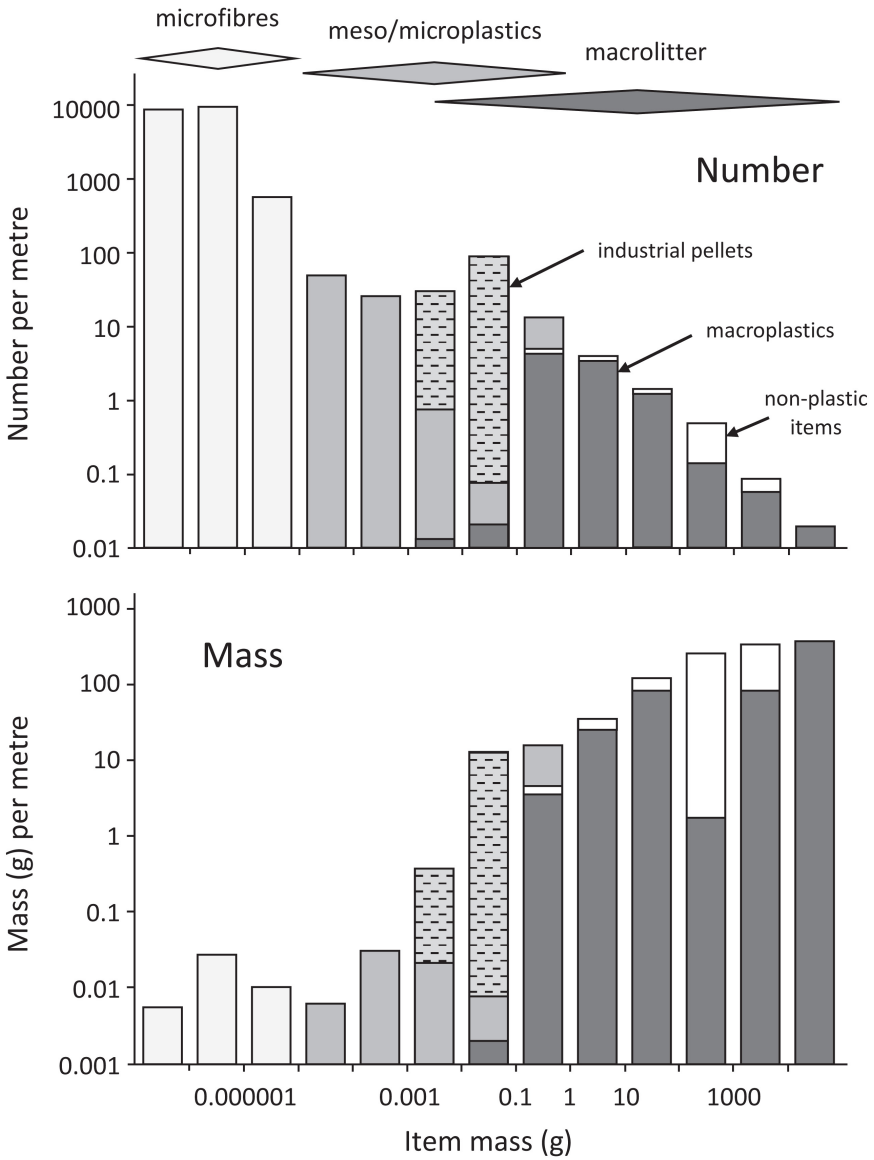

FIGURE 4 | The contributions of macro-, meso, and micro-litter samples to the abundance and mass of plastic litter per meter of beach in the West Coast National Park, South Africa, pooling data from 2010 and 2017. Note log scales on both axes in both panels, but shading within each size class shows the proportional contribution of each litter class. Horizontal dashed lines = industrial pellets; white = non-plastic litter.

This presumably reflects their small size relative to the pore size in sandy beaches, allowing them to infiltrate into beaches (Chubarenko et al., 2020b) and provides another example of how microfibers behave differently in the environment from larger micro-plastic fragments (Suaria et al., 2020).

Previous studies have tended to assume that most, if not all, microfibers found in beaches are synthetic (e.g., Nel et al., 2017; de Villiers, 2018). However, Suaria et al. (2020) found that only 8% of microfibers collected in surface waters at sea are synthetic, and they are probably best treated as a separate class of pollutant to micro-plastics. The fibers in our study (median length 0.52 mm, IQR 0.42–1.02) were roughly half the length of fibers sampled at sea in the Atlantic Ocean (median 1.11 mm, IQR 0.71–1.85, Suaria et al., 2020), which might reflect mechanical degradation in the high-energy beach environment (Chubarenko et al., 2020a). However, the tendency for fibers to be longer in deeper sediments (**Figure 3**) is counter-intuitive and this pattern needs to be confirmed. We clearly need a better understanding of the dynamics of microfibers in natural systems (Suaria et al., 2020), including how fibers are distributed within beaches and their impacts on beach biota. Yet despite their overwhelming numerical dominance, microfibers contribute a vanishingly small amount to the mass of plastic. To put the mass of microfibers in perspective, the total mass of microfibers per meter of beach was roughly the same as 2–3 industrial pellets.

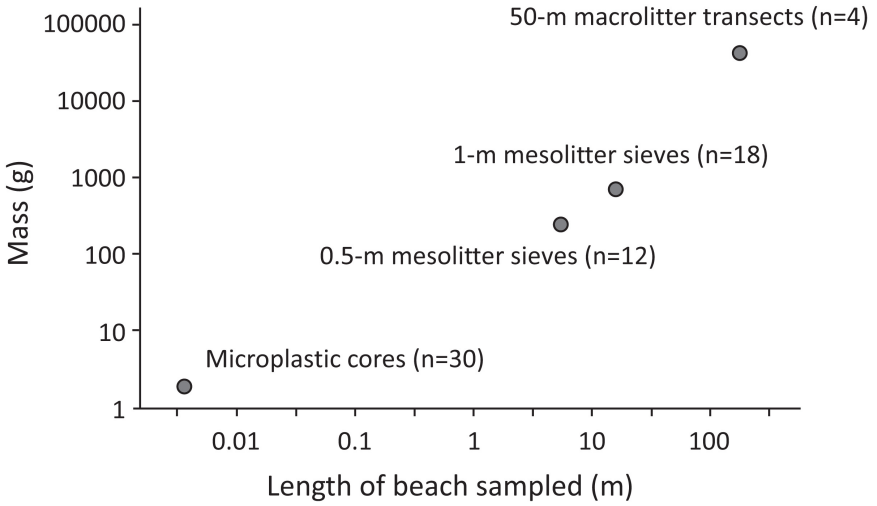

FIGURE 5 | The maximum litter item size (mass) recorded using four different sampling methods to characterize the full size spectrum of litter on a beach in the West Coast National Park, South Africa. Note the $\log_{10}$ scale on both axes.

Excluding microfibers, plastics accounted for 99.5% of the number and ∼90% of the mass of particulate pollutants (**Table 5**). Non-plastic litter was largely confined to macro-litter, yet plastics also dominated this size class (**Table 5**). Some glass and metal might have been overlooked in the smaller size categories, because sieving was restricted to the upper shore, whereas fragments of dense pollutants tend to accumulate lower on the shoreline. However, this bias is likely to be minor, because such non-plastics typically arrive at remote beaches as sealed items (e.g., glass bottles, lightbulbs, aerosol cans), and these items were minor constituents of the larger macro-litter (**Table 2**). No glass or metal fragments were recorded in the visual survey of the low shore, or in the low shore micro-litter cores. Despite representing only 2% of litter items, surface macro-litter accounted for ∼90% of the mass of litter, with much of the remainder contributed by buried macro-litter. The dominance of macro-plastics in terms of the total mass of environmental plastics is thus similar to that recorded for Portuguese beaches (Martins and Sobral, 2011) and for litter floating at sea (Eriksen et al., 2014; Lebreton et al., 2017). This finding suggests that in terms of beaches as potential sinks that might balance the global plastic mass budget, we can largely ignore micro-plastics.

Global inventories of floating plastics have highlighted the paucity of micro-plastic particles (<1 mm) floating at sea, based on the expectation of an exponential increase in abundance with decreasing particle size due to fragmentation of larger plastic items (Cózar et al., 2014; Eriksen et al., 2014). Chubarenko et al. (2018) reported a similar pattern among beach litter, although they found a paucity of larger items, possibly due to mechanical beach cleaning at their study site. Superficial examination of **Figure 4** suggests a similar pattern among beach litter at our study site. The increase in the abundance of litter items is strikingly linear (on a log-log scale) from megalitter down to around 10 mg (roughly 1–2 mm, depending on item shape and thickness), with a paucity of smaller fragments from 10 mg to 1 μg. However, the composition of litter varies considerably across these size ranges. Industrial pellets, which are primary micro-plastics (i.e., manufactured, not the product of fragmentation) account for most of the items in the 10–100 mg size class (**Figure 4**), and flexible packaging is more prevalent among macro-litter (**Table 2**) than meso-litter (**Table 3**). We believe that, at least on our study beach, the exponential increase in abundance with decreasing particle size is largely coincidental. Chubarenko et al. (2020a) show how rates of mechanical degradation on beaches differ among polymer types and with item thickness. The paucity of flexible packaging in the 1–5 mm size range probably reflects its faster degradation than the thicker, rigid plastic items that predominate meso-litter samples (together with industrial pellets). Movement within the beach/sea interface probably also influences the size-frequency distribution (Chubarenko et al., 2020b), with more buoyant rigid and foamed plastics more likely to remain on the upper shore than flexible sheet plastics (Hinata et al., 2017; van Sebille et al., 2020). The paucity of very small micro-plastics (<1 mm) other than microfibers might also reflect a combination of faster degradation and infiltration rates among small particles.

How does the mass of plastic on our study beach compare with the prediction of leakage from land-based sources? Jambeck et al. (2015) estimated that South Africa was the 11^{th} worst country globally in terms of plastic pollution from land-based sources, losing some 90–250 × 10^3 tons of plastic into the sea in 2010. At least 25% of this is thought to come from Cape Town (Collins and Hermes, 2019; Weideman et al., 2020), and the study beach lies in the main downstream stranding plume for litter emanating from Cape Town's Table Bay (Collins and Hermes, 2019). Oceanographic models suggest that ∼20% of litter in Table Bay strands along the 140 km of coast between Cape Town and Cape Columbine (Collins and Hermes, 2019). This is a minimum estimate, because the models were seeded with litter 8–10 km offshore, whereas much litter entering coastal waters

from rivers and storm drains strands close to their source without dispersing offshore (Rech et al., 2014; Willis et al., 2017). If the global model estimate is correct, we'd expect to see an annual stranding rate of 30–90 $kg{\cdot}m^{-1}$, 20–60 times more than the total standing stock of plastic on the study beach. However, almost half of the mass of litter at the study beach comes from fishing and other marine activities, and some of the general rubbish is also dumped illegally from ships (Ryan et al., 2019). Even at heavily polluted urban beaches in Cape Town, extrapolated daily litter accumulation rates are only 0.4–16 $kg{\cdot}m^{-1}{\cdot}year^{-1}$ (Chitaka and von Blottnitz, 2019). Perhaps the most likely explanation for the large discrepancy between the standing stock of beach litter and the global estimate of land-based leakage is that the latter is grossly inflated (Ryan, 2020b). Both direct measures of marine inputs (Weideman et al., 2020) and refined estimates of solid waste budgets (Verster and Bouwman, 2020) indicate that Jambeck et al. (2015) overestimate solid waste leakage from South Africa by roughly an order of magnitude. This concurs with recent direct measures of river inputs (Castro-Jiménez et al., 2019; Schöneich-Argent et al., 2020; Vriend et al., 2020) being several orders of magnitude less than those predicted by global models (Lebreton et al., 2017; Schmidt et al., 2017). Rather than seeking to explain the 'missing' plastic in the global plastic budget (Koelmans et al., 2017; Lebreton et al., 2019) perhaps we should be refining the models that predict plastic leakage.

Of course, the mass of macro-plastic litter on beaches is highly sensitive to beach cleaning efforts (Ryan et al., 2009). Regular municipal cleaning of an urban beach in Cape Town reduced the mass of surface macro-plastic litter by 99% and buried litter by 85% (Ryan, 2020b). This was one of the main motivations for selecting a remote, uncleaned beach to characterize the number and mass distribution of stranded litter. The combination of the high UV levels and mechanical abrasion makes beaches hotspots for micro-plastic formation (Andrady, 2017; Chubarenko et al., 2020a), and once macro-plastics break down into micro-plastics they are much harder to manage. The collection of large litter items from beaches is therefore a useful stop-gap measure while we formulate effective steps to prevent plastic leakage into the environment.

DATA AVAILABILITY STATEMENT

The raw data supporting the conclusions of this article will be made available by the authors, without undue reservation.

AUTHOR CONTRIBUTIONS

PR: conceptualization, field sampling, data analysis, and writing of first draft. EW and VP: field sampling, lab work, and commenting on draft. CM: conceptualization, field sampling, and commenting on draft. All authors contributed to the article and approved the submitted version.

FUNDING

Funding from the University of Cape Town contributed to this project.

ACKNOWLEDGMENTS

We thank the many students and colleagues who assisted with field sampling, especially Cecile Reed, Deena Pillay, and Mike Lucas, who supervised some sampling teams.

SUPPLEMENTARY MATERIAL

The Supplementary Material for this article can be found online at: https://www.frontiersin.org/articles/10.3389/fmars.2020.575395/full#supplementary-material

REFERENCES

Andrady, A. L. (2017). The plastic in microplastics: a review. *Mar. Pollut. Bull.* 119, 12–22. doi: 10.1016/j.marpolbul.2017.01.082

Barnes, D. K. A., Galgani, F., Thompson, R. C., and Barlaz, M. (2009). Accumulation and fragmentation of plastic debris in global environments. *Philos. Trans. R. Soc. B* 364, 1985–1998. doi: 10.1098/rstb.2008.0205

Bergmann, M., Gutow, L., and Klages, M. (eds) (2015). *Marine Anthropogenic Litter*. Cham: Springer.

Browne, M. A., Chapman, M. G., Thompson, R. C., Amaral Zettler, M. A., Jambeck, J., and Mallos, N. J. (2015). Spatial and temporal patterns of stranded intertidal marine debris: is there a picture of global change? *Environ. Sci. Technol.* 49, 7082–7094. doi: 10.1021/es5060572

Castro-Jiménez, J., Gonzaìlez-Fernaìndez, D., Schmidt, N., and Sempeìreì, R. (2019). Macro-litter in surface waters from the Rhone River: plastic pollution and loading to the NW Mediterranean Sea. *Mar. Pollut. Bull.* 146, 60–66. doi: 10.1016/j.marpolbul.2019.05.067

Chitaka, T. Y., and von Blottnitz, H. (2019). Accumulation and characteristics of plastic debris along five beaches in Cape Town. *Mar. Pollut. Bull.* 138, 451–457. doi: 10.1016/j.marpolbul.2018.11.065

Chubarenko, I., Efimova, I., Bagaeva, M., Bagaev, A., and Isachenko, I. (2020a). On mechanical fragmentation of single-use plastics in the sea swash zone with different types of bottom sediments: insights from laboratory experiments. *Mar. Pollut. Bull.* 150:110726. doi: 10.1016/j.marpolbul.2019.110726

Chubarenko, I., Esiukova, E., Khatmullina, L., Lobchuk, O., Grave, A., Kileso, A., et al. (2020b). From macro to micro, from patchy to uniform: analyzing plastic contamination along and across a sandy tide-less coast. *Mar. Pollut. Bull.* 156:111198. doi: 10.1016/j.marpolbul.2020.111198

Chubarenko, I. P., Esiukova, E. E., Bagaev, A. V., Bagaeva, M. A., and Grave, A. N. (2018). Three-dimensional distribution of anthropogenic microparticles in the body of sandy beaches. *Sci. Total Environ.* 628–629, 1340–1351. doi: 10.1016/j.scitotenv.2018.02.167

Collins, C., and Hermes, J. C. (2019). Modelling the accumulation and transport of floating marine micro-plastics around South Africa. *Mar. Pollut. Bull.* 139, 46–58. doi: 10.1016/j.marpolbul.2018.12.028

Cózar, A., Echevarrìa, F., Gonzaìlez-Gordillo, J. I., Irigoien, X., Ubeda, B., Hernaìndez-Leoìn, S., et al. (2014). Plastic debris in the open ocean. *Proc. Natl. Acad. Sci. U.S.A.* 111, 10239–10244.

de Villiers, S. (2018). Quantification of microfibre levels in South Africa's beach sediments, and evaluation of spatial and temporal variability from 2016 to 2017. *Mar. Pollut. Bull.* 135, 481–489. doi: 10.1016/j.marpolbul.2018.07.058

Dixon, T. J., and Dixon, T. R. (1983). Marine litter distribution and composition in the North Sea. *Mar. Pollut. Bull.* 14, 145–148. doi: 10.1016/0025-326x(83)90068-1

Eriksen, M., Lebreton, L. C. M., Carson, H. S., Thiel, M., Moore, C. J., Borerro, J. C., et al. (2014). Plastic pollution in the world's oceans: more than 5 trillion plastic pieces weighing over 250,000 tons afloat at sea. *PLoS One* 9:e111913. doi: 10.1371/journal.pone.0111913

Fazey, F. M. C., and Ryan, P. G. (2016). Debris size and buoyancy influence the dispersal distance of stranded litter. *Mar. Pollut. Bull.* 110, 371–377. doi: 10.1016/j.marpolbul.2016.06.039

Filella, M. (2015). Questions of size and numbers in environmental research on microplastics: methodological and conceptual aspects. *Environ. Chem.* 12, 527–538. doi: 10.1071/en15012

GESAMP (2019). "Guidelines for the monitoring and assessment of plastic litter and microplastics in the ocean," in *IMO/FAO/UNESCO-IOC/UNIDO/WMO/IAEA/UN/UNEP/UNDP/ISA Joint Group of Experts on the Scientific Aspects of Marine Environmental Protection*, eds P. J. Kershaw, A. Turra, and F. Galgani (London: GESAMP), 1–130.

Gregory, M. R. (1978). Accumulation and distribution of virgin plastic granules on New Zealand beaches. *N. Z. J. Mar. Freshw. Res.* 12, 399–414. doi: 10.1080/00288330.1978.9515768

Hartmann, N. B., Hüffer, T., Thompson, R. C., Hassellöv, M., Verschoor, A., Daugaard, A. E., et al. (2019). Are we speaking the same language? Recommendations for a definition and categorization framework for plastic debris. *Environ. Sci. Technol.* 53, 1039–1047. doi: 10.1021/acs.est.8b05297

Hidalgo-Ruz, V., Gutow, L., Thompson, R. C., and Thiel, M. (2012). Microplastics in the marine environment: a review of the methods used for identification and quantification. *Environ. Sci. Technol.* 46, 3060–3075. doi: 10.1021/es2031505

Hinata, H., Mori, K., Ohno, K., Miyao, Y., and Kataoka, T. (2017). An estimation of the average residence times and onshore-offshore diffusivities of beached microplastics based on the population decay of tagged meso- and macrolitter. *Mar. Pollut. Bull.* 122, 17–26. doi: 10.1016/j.marpolbul.2017.05.012

Horton, A. A., Svendsen, C., Williams, R. J., Spurgeon, D. J., and Lahive, E. (2017). Large microplastic particles in sediments of tributaries of the River Thames, UK – Abundance, sources and methods for effective quantification. *Mar. Pollut. Bull.* 114, 218–226. doi: 10.1016/j.marpolbul.2016.09.004

Jambeck, J. R., Geyer, R., Wilcox, C., Siegler, T. R., Perryman, M., Andrady, A. L., et al. (2015). Plastic waste inputs from land into the ocean. *Science* 347, 768–771. doi: 10.1126/science.1260352

Koelmans, A. A., Kooi, M., Law, K. L., and van Sebille, E. (2017). All is not lost: deriving a top- down mass budget of plastic at sea. *Environ Res Lett.* 12:114028. doi: 10.1088/1748-9326/aa9500

Kusui, T., and Noda, M. (2003). International survey on the distribution of stranded and buried litter on beaches along the Sea of Japan. *Mar. Pollut. Bull.* 47, 175–179. doi: 10.1016/s0025-326x(02)00478-2

Lavers, J. L., and Bond, A. L. (2017). Exceptional and rapid accumulation of anthropogenic debris on one of the world's most remote and pristine islands. *Proc. Natl. Acad. Sci. U.S.A.* 114, 6052–6055. doi: 10.1073/pnas.1619818114

Lebreton, L., Egger, M., and Slat, B. (2019). A global mass budget for positively buoyant macroplastic debris in the ocean. *Sci. Rep.* 9:12922.

Lebreton, L., Slat, B., Ferrari, F., Sainte-Rose, B., Aitken, J., Marthouse, R., et al. (2018). Evidence that the Great Pacific Garbage Patch is rapidly expanding. *Sci. Rep.* 8:4666.

Lebreton, L. C. M., Zwet, J., van der Damsteeg, J.-W., Slat, B., Andrady, A., and Reisser, J. (2017). River plastic emissions to the world's oceans. *Nat. Commun.* 8:ncomms15611.

Lee, J., Hong, S., Song, Y. K., Hong, S. H., Jang, Y. C., Jang, M., et al. (2013). Relationships among the abundances of plastic debris in different size classes on beaches in South Korea. *Mar. Pollut. Bull.* 77, 349–354. doi: 10.1016/j.marpolbul.2013.08.013

Martins, J., and Sobral, P. (2011). Plastic marine debris on the Portuguese coastline: a matter of size? *Mar. Pollut. Bull.* 62, 2649–2653. doi: 10.1016/j.marpolbul.2011.09.028

Mathalon, A., and Hill, P. (2014). Microplastic fibers in the intertidal ecosystem surrounding Halifax Harbor, Nova Scotia. *Mar. Pollut. Bull.* 81, 69–79. doi: 10.1016/j.marpolbul.2014.02.018

Merrell, T. R. Jr. (1984). A decade of change in nets and plastic litter from fisheries off Alaska. *Mar. Pollut. Bull.* 15, 378–384. doi: 10.1016/0025-326x(84)90172-3

Nel, H. A., and Froneman, P. W. (2015). A quantitative analysis of microplastic pollution along the south-eastern coastline of South Africa. *Mar. Pollut. Bull.* 101, 274–279. doi: 10.1016/j.marpolbul.2015.09.043

Nel, H. A., Hean, J. W., Noundou, X. S., and Froneman, P. W. (2017). Do microplastic loads reflect the population demographics along the southern African coastline? *Mar. Pollut. Bull.* 115, 115–119. doi: 10.1016/j.marpolbul.2016.11.056

Olivelli, A., Hardesty, B. D., and Wilcox, C. (2020). Coastal margins and backshores represent a major sink for marine debris: insights from a continental-scale analysis. *Environ. Res. Lett.* 15:074037. doi: 10.1088/1748-9326/ab7836

OSPAR (2010). *Guideline for Monitoring Marine Litter on the Beaches in the OSPAR Maritime Area*. London: OSPAR Commission.

R Core Team (2019). *R: A Language and Environment for Statistical Computing*. Vienna: R Foundation for Statistical Computing.

Rech, S., Macaya-Caquilpán, V., Pantoja, J. F., Rivadeneira, M. M., Madariaga, D. J., and Thiel, M. (2014). Rivers as a source of marine litter – A study from the SE Pacific. *Mar. Pollut. Bull.* 82, 66–75. doi: 10.1016/j.marpolbul.2014.03.019

Ryan, P. G. (2016). "Ingestion of plastics by marine organisms," in *Hazardous Chemicals Associated with Plastics in the Environment*, eds H. Takada and H. K. Karapanagioti (Cham: Springer), 235–266. doi: 10.1007/698_2016_21

Ryan, P. G. (2020a). Land or sea? What bottles tell us about the origins of beach litter in Kenya. *Waste Manage.* 116, 49–57. doi: 10.1016/j.wasman.2020.07.044

Ryan, P. G. (2020b). The transport and fate of marine plastics in South Africa and adjacent oceans. *S. Afr. J. Sci.* 116:7677.

Ryan, P. G., Dilley, B. J., Ronconi, R. A., and Connan, M. (2019). Rapid increase in Asian bottles in the South Atlantic Ocean indicates major debris inputs from ships. *Proc. Natl Acad. Sci. U.S.A.* 116, 20892–20897. doi: 10.1073/pnas.1909816116

Ryan, P. G., and Moloney, C. L. (1990). Plastic and other artefacts on South African beaches: temporal trends in abundance and composition. *S. Afr. J. Sci.* 86, 450–452.

Ryan, P. G., Moore, C. J., van Franeker, J. A., and Moloney, C. L. (2009). Monitoring the abundance of plastic debris in the marine environment. *Philos. Trans. R. Soc. B* 364, 1999–2012.

Ryan, P. G., Perold, V., Osborne, A., and Moloney, C. L. (2018). Consistent patterns of debris on South African beaches indicate that industrial pellets and other mesoplastic items mostly derive from local sources. *Environ. Pollut.* 238, 1008–1016. doi: 10.1016/j.envpol.2018.02.017

Ryan, P. G., Pichegru, L., Perold, V., and Moloney, C. L. (2020). Monitoring marine plastics – will we know if we're making a difference? *S. Afr. J. Sci.* 116:7678.

Schmidt, C., Krauth, T., and Wagner, S. (2017). Export of plastic debris by rivers into the Sea. *Environ. Sci. Technol.* 51, 12246–12253. doi: 10.1021/acs.est.7b02368

Schöneich-Argent, R. I., Dau, K., and Freund, H. (2020). Wasting the North Sea? – A field-based assessment of anthropogenic macrolitter loads and emission rates of three German tributaries. *Environ. Pollut.* 263:114367. doi: 10.1016/j.envpol.2020.114367

Suaria, G., Achtypi, A., Perold, V., Lee, J. R., Pierucci, A., Bornman, T. G., et al. (2020). A global characterization of microfibers in oceanic surface waters. *Sci. Adv.* 6:eaay8493. doi: 10.1126/sciadv.aay8493

Takada, H., and Karapanagioti, H. K. (eds) (2018). "Hazardous chemicals associated with plastics in the environment," in *Handbook of Environmental Chemistry*, (Cham: Springer).

Thompson, R. C., Olsen, Y., Mitchell, R. P., Davis, A., Rowland, S. J., John, A. W. G., et al. (2004). Lost at sea: where is all the plastic? *Science* 304:838. doi: 10.1126/science.1094559

Turra, A., Manzano, A. B., Dias, R. J. S., Mahiques, M. M., Barbosa, L., Balthazar-Silva, D., et al. (2014). Three dimensional distribution of plastic pellets in sandy beaches: shifting paradigms. *Sci. Rep.* 4:4435.

UNEP (2009). *Marine Litter: A Global Challenge*. Nairobi: UNEP.

van Sebille, E., Aliani, S., Law, K. L., Maximenko, N., Alsina, J., Bagaev, A., et al. (2020). The physical oceanography of the transport of floating marine debris. *Environ. Res. Lett.* 15:023003.

van Sebille, E., Wilcox, C., Lebreton, L., Maximenko, N., Hardesty, B. D., van Franeker, J. A., et al. (2015). A global inventory of small floating plastic debris. *Environ. Res. Lett.* 10:124006. doi: 10.1088/1748-9326/10/12/124006

Verster, C., and Bouwman, H. (2020). Land-based sources and pathways of marine plastics in a South African context. *S. Afr. J. Sci.* 116:7700.

Vriend, P., van Calcar, C., Kooi, M., Landman, H., Pikaar, R., and van Emmerik, T. (2020). Rapid assessment of floating macroplastic transport in the Rhine. *Front. Mar. Sci.* 7:10. doi: 10.3389/fmars.2020.00010

Weideman, E. A., Perold, V., Arnold, G., and Ryan, P. G. (2020). Quantifying changes in litter loads in urban stormwater run-off from Cape Town, South Africa, over the last two decades. *Sci. Tot. Environ.* 724:138310. doi: 10.1016/j.scitotenv.2020.138310

Willis, K., Hardesty, B. D., Kriwoken, L., and Wilcox, C. (2017). Differentiating littering, urban runoff and marine transport as sources of marine debris in coastal and estuarine environments. *Sci. Rep.* 7:44479.

Conflict of Interest: The authors declare that the research was conducted in the absence of any commercial or financial relationships that could be construed as a potential conflict of interest.

frontiers in Environmental Science

ORIGINAL RESEARCH
published: 21 December 2020
doi: 10.3389/fenvs.2020.574274

Biogenic Aggregation of Small Microplastics Alters Their Ingestion by a Common Freshwater Micro-Invertebrate

Claudia Drago[1]*, *Julia Pawlak*[1] and *Guntram Weithoff*[1,2]

[1] Department for Ecology and Ecosystem Modeling, University of Potsdam, Potsdam, Germany, [2] Berlin-Brandenburg Institute of Advanced Biodiversity Research (BBIB), Berlin, Germany

In recent years, increasing concerns have been raised about the environmental risk of microplastics in freshwater ecosystems. Small microplastics enter the water either directly or accumulate through disintegration of larger plastic particles. These particles might then be ingested by filter-feeding zooplankton, such as rotifers. Particles released into the water may also interact with the biota through the formation of aggregates, which might alter the uptake by zooplankton. In this study, we tested for size-specific aggregation of polystyrene microspheres and their ingestion by a common freshwater rotifer *Brachionus calyciflorus.* The ingestion of three sizes of polystyrene microspheres (MS) 1-, 3-, and 6-μm was investigated. Each MS size was tested in combination with three different treatments: MS as the sole food intake, MS in association with food algae and MS aggregated with biogenic matter. After 72 h incubation in pre-filtered natural river water, the majority of the 1-μm spheres occurred as aggregates. The larger the particles, the higher the relative number of single particles and the larger the aggregates. All particles were ingested by the rotifer following a Type-II functional response. The presence of algae did not influence the ingestion of the MS for all three sizes. The biogenic aggregation of microspheres led to a significant size-dependent alteration in their ingestion. Rotifers ingested more microspheres (MS) when exposed to aggregated 1- and 3-μm MS as compared to single spheres, whereas fewer aggregated 6-μm spheres were ingested. This indicates that the small particles when aggregated were in an effective size range for *Brachionus*, while the aggregated larger spheres became too large to be efficiently ingested. These observations provide the first evidence of a size- and aggregation-dependent feeding interaction between microplastics and rotifers. Microplastics when aggregated with biogenic particles in a natural environment can rapidly change their size-dependent availability. The aggregation properties of microplastics should be taken into account when performing experiments mimicking the natural environment.

Keywords: microplastics ingestion, *Brachionus calyciflorus*, aggregation, microplastics, polystyrene, functional response

OPEN ACCESS

Edited by:
Andrew Turner,
University of Plymouth,
United Kingdom

Reviewed by:
Ceri Lewis,
University of Exeter, United Kingdom
Ulrike Obertegger,
Fondazione Edmund Mach, Italy

***Correspondence:**
Claudia Drago
drago@uni-potsdam.de

Specialty section:
This article was submitted to Toxicology, Pollution and the Environment, a section of the journal Frontiers in Environmental Science

Received: *19 June 2020*
Accepted: *30 November 2020*
Published: *21 December 2020*

Citation:
Drago C, Pawlak J and Weithoff G (2020) Biogenic Aggregation of Small Microplastics Alters Their Ingestion by a Common Freshwater Micro-Invertebrate. Front. Environ. Sci. 8:574274. doi: 10.3389/fenvs.2020.574274

INTRODUCTION

Plastics have become a universal material due to their numerous properties. The mass production of plastics started in the 1950s at just one million tons per year. Nowadays, production has reached 335 million tons worldwide (Meng et al., 2020). Over 8 million tons of mostly single-use plastics enter the ocean each year (Jambeck et al., 2015), despite increasing recycling efforts and public awareness around the world. According to recent estimates, between 1.15 and 2.41 million tons of plastic are transported from rivers to the sea (Réu et al., 2019). In the past, research on the impact of plastic has focused on marine environments, with comparatively fewer studies conducted in freshwater habitats. Plastics are entering all ecosystems in all sizes, and large pieces disintegrate into smaller particles due to physical or chemical degradation. The resulting small particles below 5 mm are called secondary microplastics (Hartmann et al., 2019). In addition to these secondary microplastics, primary microplastics in the form of beads and pellets are manufactured to be used in personal care products and in industrial cleaning. Nanoplastics (size range from 1 to 1,000 nm) are frequently used in the cosmetics industry, though their use is decreasing (Strungaru et al., 2019). Particles from tire wear and shedding of microfibers from synthetic clothing also pollute aquatic ecosystems (Barboza et al., 2018). Unlike large plastic debris, microplastics are invisible to the naked eye and cannot be removed from the environment for recycling. The estimated number of microplastics smaller than 100 μm is still underestimated also in the marine environment (Lindeque et al., 2020).

Microplastic particles, particularly spheres, can be ingested by numerous zooplankton species (Kögel et al., 2020; Zheng et al., 2020). For example, rotifers, copepods, and cladocerans have the ability to ingest polystyrene microbeads ranging from 1.7 to 30.6 μm (Scherer et al., 2018). Typically, in these studies, microspheres are provided as defined and standardized food particles. Therefore, care is taken to avoid any clumps or aggregates and spheres are sonicated before use to assure that only singular particles are present. However, the plastic's surface serves as a physical substrate for microorganisms such as bacteria, fungi, algae and heterotrophic protists, which altogether form a complex biofilm. When the particles are in the size range of nanoparticles, they become enveloped within a biofilm (Martel et al., 2014; Ikuma et al., 2015; Summers et al., 2018). This conglomerate of plastics and biota is called "plastisphere" (Zettler et al., 2013; Kirstein et al., 2019; Amaral-Zettler et al., 2020). Moreover, extracellular polymeric substances (EPS), particularly transparent exopolymers particles (TEP), produced by microorganisms play a significant role in the formation of nano- and microplastic agglomerates (Cunha et al., 2019). These aggregated particles might be ingested by invertebrates having low feeding selectivity, such as filter-feeders (Scherer et al., 2017). The ingested plastic aggregates might then affect the fitness of the consumers (Vroom et al., 2017). Herbivorous rotifers are filter-feeding metazoans and their feeding behavior and low selectivity allows them to ingest small particles such as microplastics. In the freshwater food web, rotifers play a pivotal role in the energy transfer from primary producers to secondary consumers and potentially also transfer pollutants to higher trophic levels through ingestion and accumulation (Snell and Janssen, 1995). Several studies show that brachionid rotifers can ingest polystyrene microbeads with negative effects on their reproduction and growth rate (Juchelka and Snell, 1994; Baer et al., 2008; Jeong et al., 2016, 2018). Thus, these properties make rotifers very suitable animals for studying microplastics ingestion.

The aim of the present study was to investigate the ingestion of microplastics by the cosmopolitan freshwater planktonic rotifer *Brachionus calyciflorus*. We examined the ingestion of three sizes of polystyrene microspheres as single food particles, in association with a similar-sized food alga and as biogenic aggregated microspheres through bacteria and exopolymers particles. Moreover, we characterized the size of the aggregated microplastics and the number of singles MS.

We tested the following hypotheses: (i) the ingestion of microspheres is size-dependent and influenced by the presence of algal food, and (ii) the biogenic aggregation of microspheres influences their ingestion.

MATERIALS AND METHODS

Polystyrene Microsphere

As microplastic particles, we used polystyrene microspheres (MS) of three different diameters: 1.03, 3.06, and 5.73 μm; for convenience, we refer to them as 1, 3 and 6 MS (Polysciences, Inc. Fluoresbrite® YG Polystyrene Microspheres, USA) (see **Table 1**). A stock solution was prepared with deionized MilliQ water under sterile conditions to minimize bacterial growth. To keep the MS as singular particles, each stock solution was sonicated for 30 min and was mixed using a vortexer.

Organism

Stock cultures of all experimental organisms, algae and rotifers, were kept in glass flasks in a modified Woods Hole WC-medium (Guillard and Lorenzen, 1972) with regular substitution of the medium to sustain the continuous growth phase. Cultures were kept at 20°C in a light-dark cycle of 14:10 h and a light intensity of 35-μM photons s^{-1} m^{-2}. We used the herbivorous monogononta rotifer *Brachionus calyciflorus* s.s. Pallas 1776 [strain IGB (Paraskevopoulou et al., 2018)] as a generalist

TABLE 1 | Characteristics of the phytoplankton: *Synechococcus elongatus*, *Chlorella vulgaris,* and coccal green algae.

Phytoplankton	*S. elongatus*	*C. vulgaris*	Coccal green algae
Diameter (μm)	1.40	2.60	4.30
Shape	oblong	spherical	oblong
Polystyrene MS	1	3	6
Diameter (μm)	1.03	3.06	5.73
Shape	spherical	spherical	spherical

Note: for S. elongatus sizes were taken from Schälicke et al. (2019), for C. vulgaris and coccal green algae the size were taken prior the experiment. Characteristic of polystyrene microspheres from Fluoresbrite® YG Microspheres technical data sheet.

consumer. Stock cultures were maintained with the food alga *Monoraphidium minutum* (SAG 243-1, culture collection of algae, Göttingen, Germany). During the three days prior to the experiment, the rotifers were fed daily with 1×10^6 cells ml^{-1} to assure constant food saturation conditions (Fussmann et al., 2005). For the treatments with additional food algae, we used the phytoplankton species *Synechococcus elongatus* (SAG 89.79), *Chlorella vulgaris* (SAG 211-11b), and an unidentified coccal green alga grown under the same conditions as *M. minutum*.

Aggregation Experiment

To study the effect of a natural bacteria community on potential aggregation of the MS, we incubated the polystyrene MS in a pre-filtered water sample. In May, 2019 we took a natural water sample (1l) from the river Havel in the urban area of Potsdam (Germany). The sample was pre-filtered with a 30-μm mesh and afterwards filtered through a glass fiber filter (Whatman®, GF/C), retaining most microplankton and allowing bacteria to pass through. In order to avoid any differences among the MS sizes the experiment with the natural water was conducted contemporarily and on the same day. After incubating the MS in 3 ml for 72 h in a rocking shaker, the degree of aggregation was quantified in two steps. The concentration used for the experiment are shown in **Table 2** and they were the same used for the ingestion experiment. We first quantified the number of single particles (not aggregated) in a subsample for each concentration using a haemocytometer (Paul Marienfeld GmbH & Co., Germany) and a microscope (Zeiss Axioskop 2, Germany). Because we could not unambiguously determine the number of particles within one aggregate due to the formation of clumps, we filtered 1 ml subsample from each concentrations through 0.2-μm polycarbonate filters and stained them with DAPI (4′,6′-diamidino-2-phenylindole) and alcian blue. DAPI specifically binds to double-stranded DNA and polyphosphate (Zafiriou and Farrington, 1980), and with an aqueous solution of 0.02% alcian blue we could stain the polysaccharides contained in the transparent exopolymer particles (TEP) forming the aggregates. The stained polysaccharides were inspected microscopically on a glass slide, covered with immersion oil and a cover slip (Passow, 2002). From each sample, 30 pictures were randomly taken and the area of each aggregate was quantified using the open-source software ImageJ (Schneider et al., 2012). We quantified the aggregation for each particle size and concentration separately. We tested for differences in the frequency distribution (log2 scaled) among concentrations within each particle size using a test of homogeneity. We found no differences among the concentration in the 3 and 6 μm spheres ($\chi^2 = 9.7$ and 5.2, respectively; $p > 0.6$), but some differences within the 1 μm spheres with smaller aggregates at the lowest concentration ($\chi^2 = 19.9$, $p = 0.035$). We then pooled the data for each particle size and compared the median sizes among the different sizes. These were highly significantly different from each other (Kruskall-Wallis-test, $p = 0.005$).

Ingestion Experiment

We measured the ingestion rate in three treatments: microspheres as the sole food source (MS), microspheres in association with algae (MS + algae) and microspheres incubated with pre-filtered, natural water in the presence of bacteria (MS aggregated) (**Table 2**). For all three treatments we used several particle concentrations (**Table 2**), and for each particle concentration we had three replicates. From these data, the functional response was calculated; see below. Seventy-five randomly chosen adult rotifers from the prepared cultures were transferred into 3-ml particle suspension on a UVA-transparent polystyrene 12-well microtiter plate (Greiner Bio-One). After 2 min of exposure in a rocking shaker, the rotifers were washed with the medium, narcotized with carbonated water and preserved in Lugol's solution. The exposure time of 2 min takes the short gut passage time of <10 min and the practicability of the quantification of the ingested MS into account. At high concentrations, the particles form clumps in the animals' gut and cannot be quantified. The maximum particle concentration was chosen in order to cover the full range of the functional response until saturation (Mohr and Adrian, 2000; Fussmann et al., 2005; Seifert et al., 2014).

The number of ingested MS per individual rotifer was quantified using an epifluorescent microscope (Zeiss Axioskop 2, Germany). Between 30 and 36 rotifers per sample were transferred to a microscope slide and carefully squeezed under a coverslip until the MS were compressed into a single layer (Baer

TABLE 2 | Concentration and (bio) volume of phytoplankton (*Synechococcus elongatus*, *Chlorella vulgaris,* and coccal green algae) and polystyrene MS (1, 3, and 6 μm) used in the aggregation and ingestion experiments.

Concentration	*S. elongatus*	*C. vulgaris*	Coccal green algae
		Phytoplankton (cells/ml)	
1st	5.3×10^5	8.1×10^4	2.5×10^4
2nd	1.2×10^6	2.1×10^5	6.2×10^4
3rd	2.4×10^6	4.1×10^5	1.6×10^5
4th	4.8×10^6	8.2×10^5	8.1×10^5
5th	/	1.6×10^6	1.6×10^6
Concentration	**1**	**3**	**6**
		Polystyrene MS (p/ml)	
1st	1.3×10^6	5.0×10^4	7.7×10^3
2nd	3.0×10^6	1.3×10^5	1.9×10^4
3rd	6.0×10^6	2.5×10^5	5.0×10^4
4th	1.2×10^7	5.0×10^5	2.5×10^5
5th	/	1.0×10^6	5.0×10^5
Concentration	***S. elongatus* and 1 MS**	***C. vulgaris* and 3 MS**	**Coccal green algae and 6 MS**
		Biovolume (μm^3/ml)	
1st	7.6×10^5	7.5×10^5	7.6×10^5
2nd	1.7×10^6	1.9×10^6	1.9×10^6
3rd	3.4×10^6	3.8×10^6	4.9×10^6
4th	6.9×10^6	7.5×10^6	2.5×10^7
5th	/	1.5×10^7	4.9×10^7

et al., 2008). The MS found in the gut and in the trophi of each rotifer were counted either directly or, in some cases, pictures of the gut were taken and the MS number was quantified with ImageJ. All experiments were run in triplicate. To study the effect of algae as an accompanying food source, algae of similar size were added for each size of MS. We used an additive design so that the addition of algae doubled the total volume of MS particles per treatment (**Table 2**). Prior to the addition, the cell number from stock cultures was quantified with a haemocytomer (Paul Marienfeld GmbH & Co., Germany) and the addition was adjusted to equalize the volume of the respective MS.

Statistical Analysis

The resource-dependent consumption of food items by a consumer can be described as functional response curves. The type I functional response has a linear relationship between ingestion and resource concentration until a saturation is reached and ingestion remains constant with increasing resource concentration. The type II functional response exhibits a saturation function where ingestion approaches asymptotically its maximum. The type III functional response has a sigmoidal shape with very low ingestion at low resource concentration. To fit and compare the consumer functional response, we followed the procedure of Pritchard et al. (2017). Type II and III can be characterized by:

$$N_e = N_0(1 - \exp\left(aN_0^q\left(hN_e - T\right)\right)) \quad (1)$$

N_0 is the initial resource concentration; T is the experimental time; a is the instantaneous resource attack rate of the consumer; h represents the time spent subjugating, ingesting and digesting the resource and q is the scaling exponent. Type II and III functional responses differ in their value for q: When $q = 0$ a type II functional response prevails, when $q > 0$ the sigmoidal type III prevails. The number of MS ingested during the experimental period of 2 min was expressed as MS ingested per hour.

For fitting the functional response, we used the r-package FRAIR v0.5.100 (Pritchard et al., 2017). Three steps were involved: (i) model selection, (ii) model fitting, and (iii) comparison of fit and coefficients. The model selection step was used to distinguish between Type-II (saturation function) and Type-III (sigmoidal) functional response. When the evidence for a Type-II response was positive, we fitted a linear functional response Type I and a functional response Type II and compared the models using the Akaike information criterion (AIC). After providing starting estimates and fixed values of the parameters, the model was optimized using maximum likelihood estimation (MLE) with the bbml package and the function ml2 (Bolker, 2008). The last step included comparisons of the fitted coefficients through two approaches: the delta or difference method of Juliano (2001), and non-parametric bootstrapping of the raw data. We compared the fitted coefficients for each MS size separately. The comparison of the fitted coefficients with the delta or difference methods of Juliano (2001) yielded the difference between two fitted coefficients. The functional responses were plotted with empirical approximations of 95% confidence intervals (CI) based on the bootstrapped model fits for the number of MS ingested per rotifer. The lack of overlap between the CIs of the model parameters was considered equivalent to a null hypothesis test (Pritchard et al., 2017). All statistical analyses were carried out using R 3.4.3 (R Core Team, 2017).

RESULTS

Aggregation Experiment

The incubation for 72 h with the natural bacteria community led to significant formations of aggregates that were size-specific. The percentage of single particles was the lowest in the smallest size: 1-μm MS 16 ± 1% (mean ± SE), and increased with the biggest sizes: 42 ± 3% (mean ± SE) for the 3-μm MS and 67 ± 8% (mean ± SE) for the 6-μm (**Figure 1A**). The vast majority of the 1-μm MS occurred in aggregates, whereas the majority of the 6-μm MS were single particles. The area of the aggregates also showed a size-specific pattern. The smaller the MS, the smaller the area of the aggregates: for the 1-μm, the area was 64 ± 16 μm^2 (mean ± SE), for the 3-μm 133 ± 18 μm^2 (mean ± SE), and 245 ± 33 μm^2 (mean ± SE) for the 6-μm spheres (**Figure 1B**). Staining with DAPI revealed the presence of bacteria in the size range of 0.5–2.0 μm (**Figures 2A,B**) and the alcian blue revealed that transparent exopolymer particles were involved in the formation of the aggregate (**Figures 2C–E**).

Functional Response

Ingestion Rate

Brachionus calyciflorus fed on all three tested sizes of polystyrene MS (**Figures 3A,B**), in all combinations: microplastics alone, microplastics in association with food algae and microplastics incubated with bacteria in natural water. For each size and treatment, the number of MS ingested by the rotifers increased with the increasing concentration of MS in suspension, reaching a plateau. The comparison with the different types of functional responses, based on the AIC (**Table 3**), revealed a Type-II functional response (**Figures 4A–C**). Subsequently, all functional response curves were fit by the Type-II functional response and the handling time and attack rate were calculated (**Table 4**).

With regard to the 1- and 3-μm MS, *B. calyciflorus* showed the highest ingestion of MS when these were aggregated with biogenic particles though this was less pronounced for the 3-μm MS (**Table 5**). We found lower ingestion when the MS were provided as the sole food source and in association with algae. The opposite pattern was found for the 6-μm MS, where the ingestion was higher when they were provided as the sole food source and lower when aggregated with biogenic particles (**Table 5**). The maximum number of ingested 1-μm MS occurred at the highest concentration of MS aggregated with biogenic particles, with 3155 MS h^{-1}. The 3-μm MS were ingested at a rate of 895 MS h^{-1} and the maximum ingestion occurred at the highest concentration of MS aggregated with biogenic particles. The maximum ingestion of 1483 MS h^{-1} occurred with the 6-μm MS at the highest concentration as single particles (**Table 5**).

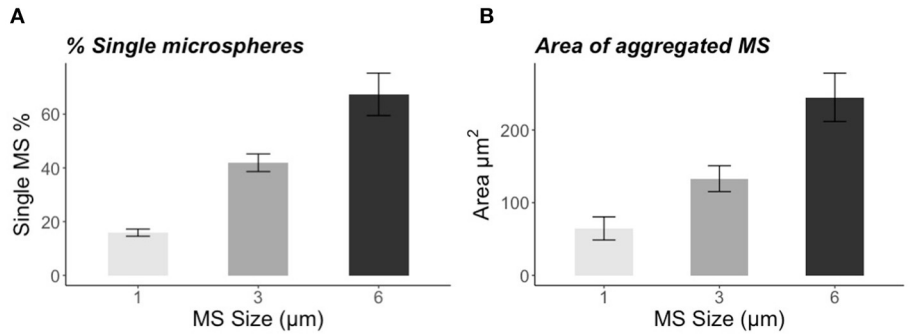

FIGURE 1 | (A) Percentage of single microspheres (1, 3, and 6 μm) found in the sample after 72 h of incubation with natural water and bacteria. **(B)** Area (μm^2) of aggregated microspheres (1, 3, and 6 μm) measured with ImageJ. The error bars represent SE.

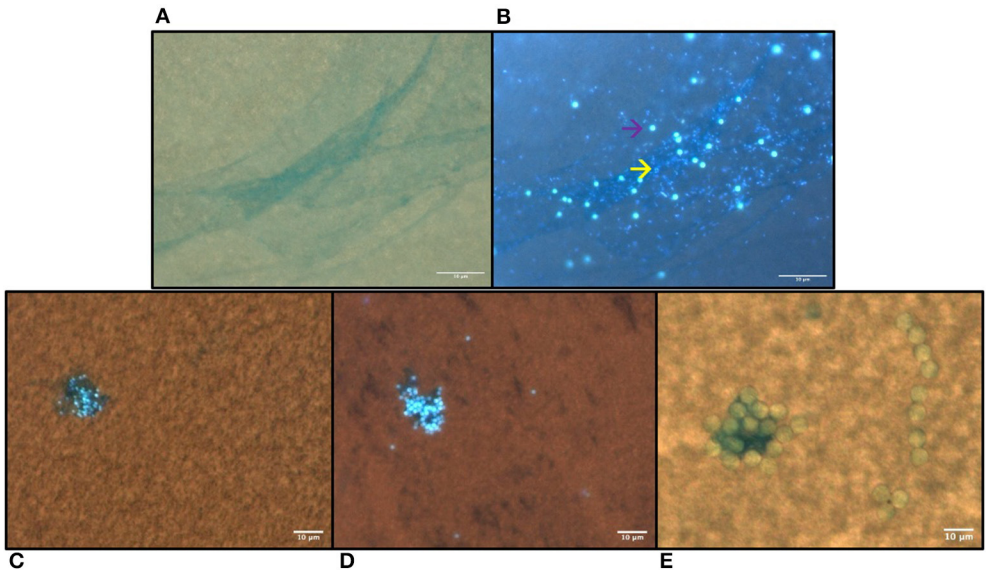

FIGURE 2 | Microplastic aggregation formed after 72 h of incubation in prefiltered natural freshwater stained with alcian blue and DAPI. **(A)** Transparent exopolymer particles (TEP) stained with alcian blue and DAPI in 1 μm MS sample visualized under bright light and **(B)** under UV-light, the yellow arrow indicates the bacteria and the purple arrow indicates the MS; **(C)** 1 μm, **(D)** 3 μm MS aggregation visualized with merged UV-light and bright light **(E)** 6 μm. The microspheres are visible also under the UV light **(B–D)**. The scale bar is 10 μm.

Attack Rate and Handling Time

The differences in the ingestion rates are reflected in the attack rate and the handling time: For the 1-μm MS, the attack rate of the aggregated particles increased by a factor of 6.65 compared to the singular particles (**Table 4**). This effect leveled off for the 3-μm MS with a factor of 1.57 and reversed for the 6-μm MS where the attack rate was 9 times lower for the aggregated MS (**Table 4**). The handling time differed much less between these two treatments.

DISCUSSION

The scope of this study was to investigate the ingestion of microplastics in the rotifer *B. calyciflorus* mediated by biogenic aggregation and in the presence of food algae. The three sizes of polystyrene MS (1, 3, and 6 μm) were ingested in all treatments. Our study has shown that the ingestion of the three sizes as the sole food, in association with algae or aggregated with biogenic particles followed the Holling's type II model and the ingestion can be influenced by the aggregation of MS.

Biogenic Aggregation of Microspheres

We found aggregations of the polystyrene microspheres (MS) in each concentration, after an incubation of 72 h in prefiltered natural freshwater. Staining these aggregates with DAPI and alcian blue revealed that they contained a community of bacteria and transparent exopolymer particles (TEP). The exopolymers are contained in the TEP encapsulated and trapped the microplastic particles to form an amorphous matrix. The presence and persistence of microplastics has been shown to

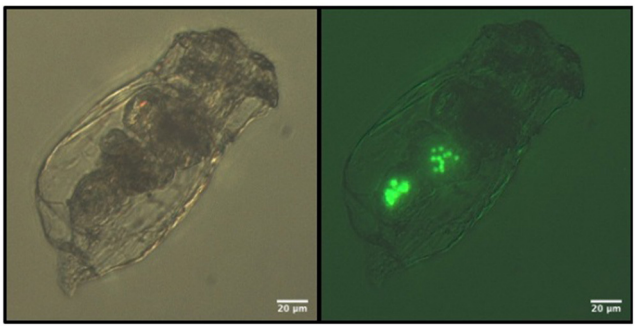

FIGURE 3 | Images of the 3 µm fluorescent polystyrene MS ingested by *B. calyciflorus*: **(A)** bright light, **(B)** fluorescent light.

TABLE 3 | The results of logistic regressions for the selection of type II are shown, together with the Akaike information criterion (AIC) values for fitted type II (see Equation 1 in the text) and type I functional response models for three sizes of MS (1, 3, and 6) and the treatments (MS, MS + algae, and MS aggregated).

		MS	MS + algae	MS aggregated
			1	
Logistic regression type II	**1st term**	-2.19×10^{-8}	-3.35×10^{-8}	-7.48×10^{-8}
	P	<0.001	<0.001	<0.001
AIC type II		**58504**	**79550**	**586746**
AIC type I		60509	84001	658551
			3	
Logistic regression type II	**1st term**	-9.40×10^{-8}	-4.80×10^{-8}	-1.01×10^{-8}
	P	<0.001	<0.001	<0.001
AIC type II		**163607**	**207505**	**182189**
AIC type I		207909	211959	226209
			6	
Logistic regression type II	**1st term**	-1.27×10^{-8}	-3.37×10^{-8}	-2.63×10^{-8}
	P	<0.001	<0.001	<0.001
AIC type II		**156904**	**65376**	**63665**
AIC type I		172702	113776	73698

The bold values indicates the AIC for the choosen model.

enhance the agglomeration of particulate matter and microalgal cells (Kettner et al., 2019). Several studies have shown that bacteria and glycoproteins contribute to the formation of plastic aggregates. This confirms the high aggregation potential of microplastics to rapidly coagulate with biogenic particles, forming pronounced aggregates within a few days (Michels et al., 2018; Summers et al., 2018). Here, we provide further evidence on how fast the formation of aggregates can take place when the pristine plastic MS were exposed to prefiltered natural freshwater. The percentage of aggregated MS after 72 h of incubation with prefiltered natural water was size-specific: The smaller the particles, the higher the number of aggregated particles. In detail, the percentage of single particles was below 20% for the 1-µm spheres and the aggregates were smaller than those from larger spheres. This finding indicates that the small particles were easily trapped by the TEPs, although larger aggregates are not formed. On the contrary, a higher percentage of single MS 3 (>40%) and 6 µm (>60%) was found, but the aggregated MS were larger. This indicates that the larger particles were less efficiently captured by TEPs, but once they were caught, the aggregates grow larger. We did not find differences in the aggregation pattern within the different sphere sizes at different concentrations (except for a slightly higher share of small aggregates in the 1 µm MS at the lowest concentration); however, it should be taken into account that the absolute numbers of the tested particles differed among sizes because of size-specific differences in functional response curves (see **Table 1**).

The process of aggregation might change over the season due to different numbers and composition of bacteria, temperature and water chemistry, however, we believe that the process itself and the resulting pattern does not change much. In general, the aggregation of detritus and living organisms (bacteria, algae, fungi, and microzooplankton) is a common phenomenon in lakes and oceans, known as lake or marine snow (Grossart and Simon, 1993; Silver, 2015) and a substantial incorporation of plastics into these aggregates seems very likely. Another process that alters the properties of MP in the environment is due to aging and the association with colloids which modifies the particles' surface (Alimi et al., 2018). Thus, the environmental conditions together with the specific properties of the particles affects their aggregation behavior in aquatic environments (Wang et al., 2021).

It is still a matter of debate whether the microbial community associated with plastic is specific to that kind of substrate or to an unspecific community from the surrounding water (Amaral-Zettler et al., 2020). Either way, aggregate formation alters the properties of the plastic, leading to higher sedimentation, or altered ingestion by consumers (Besseling et al., 2017; Alimi et al., 2018; Summers et al., 2018).

Ingestion of Microplastics Particles as the Sole Food Source

The ingestion of the MS (1, 3, and 6 µm), even if considered below the optimal size of feeding efficiency (Rothhaupt, 1990a), showed a Type-II functional response model. Previous studies demonstrated that the highest feeding efficiency for *B. calyciflorus* and closely related *Brachionus* species is in the range of a 3.5- to ∼10-µm equivalent spherical diameter (ESD) (Vadstein, 1993; Baer et al., 2008) or even higher (Pagano, 2008). We found a Type-II functional response for the 1-µm MS, considered in the similar size range of (large) bacteria or small algae. In general, very small particles were ingested with lower efficiency, but the presence of aggregated small particles can increase the ingestion efficiency. As in Rothhaupt (1990b), the larger MS (6 µm) are preferably ingested in terms of biovolume than the smaller MS (1 and 3 µm), as the attack rate is higher. Comparing the ingestion rate of 3-µm MS as a sole food source from our study

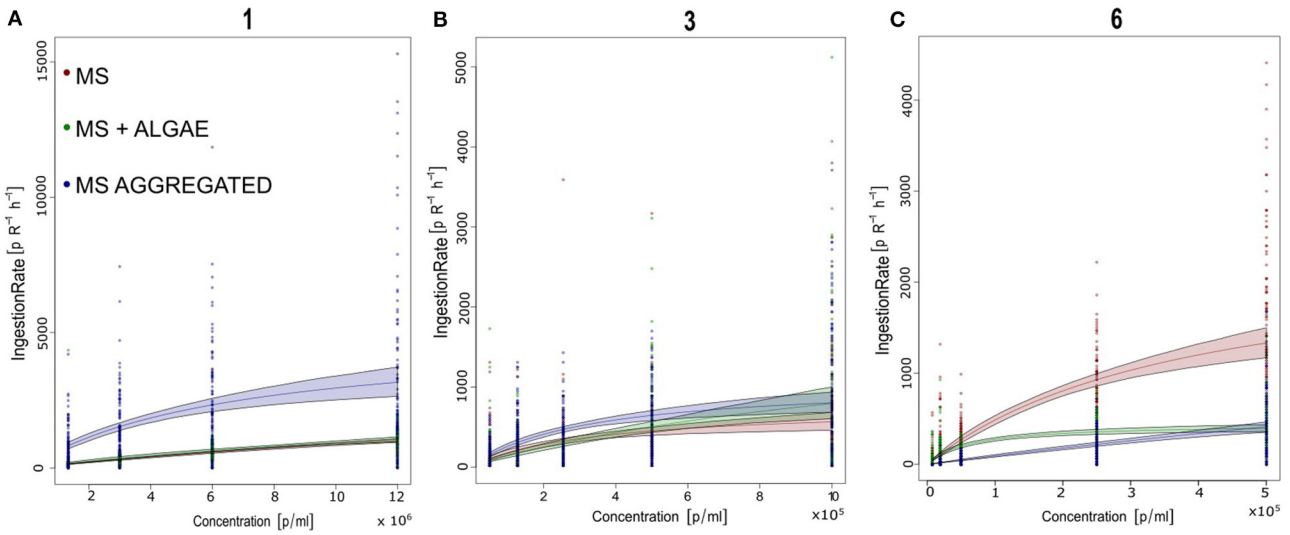

FIGURE 4 | Number of polystyrene microspheres ingested by *Brachionus calyciflorus* (IGB) within 1h at offered microsphere densities of 10^3-10^7 particles / ml. Data from all 3 replicates are shown. The curves represent the best-fitting functional response model (Rogers Type II functional response). Parameter estimated for each treatment and size are given in **Tables 3**, **4**. **(A)** 1 μm; **(B)** 3 μm; and **(C)** 6 μm.

TABLE 4 | Parameter estimates from type II (see Equation 1 in the text) functional responses for three sizes of MS (1, 3, and 6) and the treatments (MS, MS + algae, MS aggregated).

		MS	MS + algae	MS aggregated
			1	
Type II	Attack rate	1.11×10^{-4} $\pm 5.90 \times 10^{-7}$ ($p < 0.001$)	1.36×10^{-4} $\pm 7.41 \times 10^{-7}$ ($p < 0.001$)	7.38×10^{-4} $\pm 2.54 \times 1\,0^{-6}$ ($p < 0.001$)
	Handling time	2.33×10^{-4} $\pm 5.67 \times 10^{-6}$ ($p < 0.001$)	3.35×10^{-4} $\pm 5.02 \times 10^{-6}$ ($p < 0.001$)	2.03×10^{-4} $\pm 7.70 \times 10^{-7}$ ($p < 0.001$)
			3	
Type II	Attack rate	20.62×10^{-4} $\pm 1.63 \times 10^{-5}$ ($p < 0.001$)	13.06×10^{-4} $\pm 8.13 \times 10^{-6}$ ($p < 0.001$)	31.36×10^{-4} $\pm 2.08 \times 10^{-5}$ ($p < 0.001$)
	Handling time	13.44×10^{-4} $\pm 9.54 \times 10^{-5}$ ($p < 0.001$)	5.24×10^{-4} $\pm 7.89 \times 10^{-6}$ ($p < 0.001$)	9.56×10^{-4} $\pm 5.28 \times 10^{-6}$ ($p < 0.001$)
			6	
Type II	Attack rate	61.57×10^{-4} $\pm 3.39 \times 10^{-5}$ ($p < 0.001$)	72.84×10^{-4} $\pm 6.61 \times 10^{-5}$ ($p < 0.001$)	9.46×10^{-4} $\pm 9.17 \times 10^{-6}$ ($p < 0.001$)
	Handling time	4.24×10^{-4} $\pm 3.03 \times 10^{-6}$ ($p < 0.001$)	22.51×10^{-4} $\pm 1.09 \times 10^{-5}$ ($p < 0.001$)	3.06×10^{-4} $\pm 2.58 \times 10^{-5}$ ($p < 0.001$)

Data are the original maximum likelihood estimates ± SE and the p-values.

with the ingestion of the similar-sized food alga *Monoraphidium minutum,* we found a similar maximum ingestion rate as in Fussmann et al. (2005), using the same algal and rotifer strains but applying the radioisotope method. The highest ingestion based on biovolume was found for the 6-μm MS. The volume of one 6-μm MS is eight times larger than one 3 μm in size, and 216 times larger than a 1-μm MS. Thus, the total microplastics uptake of 1-μm MS was lower than for the larger-sized MS. However, toxicity does not necessarily correlate with the total amount of ingested plastic. Mueller et al. (2020), found for freshwater nematodes that the toxicity increased with the surface area-to-volume ratio of the applied microspheres. The absolute

TABLE 5 | The highest ingestion of microspheres per rotifers per hours.

	MS	MS+ algae	MS aggregated
	Maximum ingestion per hours (mean ± SE)		
1	1014 ± 34	1066 ± 44	3155 ± 330
3	639 ± 60	752 ± 107	895 ± 78
6	1483 ± 89	439 ± 27	415 ± 34

The ingested microspheres for each rotifer are multiplied per hours and expressed as mean of all three replicates ± SE.

concentration of microplastics in this study were quite high. However, for this size fraction of 1–6 μm, no reliable data on the distribution and abundance in the field are available and it is suggested that with increasing fragmentation of larger particles the concentration of such small particles strongly increases. Most field studies about microplastics are limited by the sampling methodology and the respective detection limit of the devices that were used (Besseling et al., 2019). A commonly used lower limit of mesh size lies between 300 and 800 μm. Applying smaller mesh sizes would retain a broader fraction of MPs (Wiggin and Holland, 2019) but would be more difficult to handle. A huge amount of microplastics enters the environment via the discharge from waste water treatment plants. Whereas particles larger than 10 μm are relatively efficiently removed, smaller particles likely enter the environment in higher rates (Chen et al., 2018). Once these particles are released to the environment, they might accumulate through sedimentation as aggregates in regions with low flow velocity, for example in reservoirs. Resuspension of plastics from the sediment might then makes it available again for the biota (Besseling et al., 2019).

Ingestion of MS Together With Food Algae

Rotifers are often regarded as unselective filter-feeders; however, some degree of selectivity has been found (Starkweather, 1980). In experiments with flavored polystyrene spheres (Demott, 1986), it was found that *B. calyciflorus* fed preferentially on 12-μm spheres, but did not discriminate against those with adsorbed algal flavors (Snell, 1998). Similarly, large daphnids exhibit no taste discrimination for small beads and smaller daphnids show some degree of taste and acute size discrimination. Contrarily, calanoid copepods can evaluate the resource quality in small and large particles and discriminate accordingly (Scherer et al., 2017). Thus, non-discriminating filter feeders are expected to take up more MP than raptorial feeders which might lead to reduced food intake and population growth and supports selective feeders (Setälä et al., 2016). In our experiment, we added the algae to the tested MS concentrations, leading to an increase in the total number of available particles. Thus, with algae added to low microplastics concentrations when the functional response curve is nearly linear, the uptake of the spheres is not necessarily reduced. Only at high particle concentrations, is the uptake of plastic particles expected to decrease due to algal additions.

Ingestion of MS Aggregated With Biogenic Particles

The biogenic formation of aggregates within 72 h specifically altered the ingestion of smaller and larger microplastics particles.

It is known from previous studies that the diet of *B. calyciflorus* includes not only algae but also bacteria to some extent. Bacteria may be utilized as food (Raatz et al., 2018) and, moreover, it seems likely that *Brachionus* can also ingest larger detrital particles and bacterial aggregates, deriving nutritional benefit from those cells as well (Starkweather et al., 1979).

The difference between the parameters' estimation when the MS are associated with biogenic particles shows us that the ingestion of MS is influenced by their size. Despite the size selectivity of the rotifers *B. calyciflorus*, the presence of aggregated MS increases the feeding efficiency of particles considered below the optimal size, such as 1 and 3 μm, by making them more available when aggregated; ingestion of otherwise edible MS (6 μm) can be prevented through aggregation. These results are reflected in the differences in the calculated attack rates between the experiments with and without aggregation. When the MS were ingested, it was not possible to recognize whether they were ingested as singular or aggregated particles. Nevertheless, the reduction in the attack rate of the 6-μm MS when aggregates were present indicates that the large particles were inedible and interfered with the ingestion of the well-edible singular MS. The high attack rate for the aggregated 1-μm MS indicates that the aggregates were of a well-edible size. However, technically, the effective number of particles was lower and the attack on one aggregate represents the attack on all MS within this aggregate. Zhao et al. (2018) found that the aggregation of small MP (0.5–1 μm) and nanoplastics (30 and 100 nm) facilitated the uptake from mussels. Besides the increase in particle size through aggregation, changes in surface topography and density were found. Once incorporated into aggregates, several transformations can occur, including an increase in the effective particle size and change in surface topography and density as a result of the physical and biological processes in the aggregate microcosm (Zhao et al., 2018).

Once a food item was captured, the calculated handling time varied only little among these two treatments. Thus, the similar handling times of singular MS and aggregated MS indicates that the handling time increases proportionately to the number of MS within the aggregate. This means that the "effective" handling time of an aggregate with 10 MS can be 10 times longer than the handling time of one singular MS in order to end up at the same calculated handling time. Overall, the ingestion and the effect on life history and survival can differ depending on whether microplastics are provided in a pristine state or aged and/or in natural water.

We did not test for toxicity; however, the toxicity of polystyrene nanoplastics to the rotifer *Brachionus plicatilis* was lower when the particles were provided in natural sea water compared to reconstituted sea water (Manfra et al., 2017). A potential reason for that was the interplay between surface charge, aggregation and salt. In a study on marine

copepods, the aging of plastics promoted their uptake by marine zooplankton (Vroom et al., 2017). Even the type of plastic on which a natural biofilm developed influenced the food quality of the biofilm for a freshwater snail (Vosshage et al., 2018). These results underline the importance of experiments under near-natural conditions to better estimate the effect of microplastics on the biota and to complement standardized toxicological tests.

CONCLUSION

Our results demonstrate that the aggregation of MS accelerates the ingestion of smaller MS particles and prevents the ingestion of the largest ones in the freshwater rotifer *B. calyciflorus*. The aggregation potential of microplastics has to be considered in order to recreate the environmental interaction between microplastics and aquatic organisms. The aggregation processes, together with degradation processes, are the cause of physical and chemical alteration of pristine microplastics. These two processes might alter the response of the aquatic organism to microplastics in laboratory and natural environments. In particular, non-selective filter feeders such as crustaceans and rotifers that feed mainly size-specific (Burns, 1968; Geller, 1981; Bern, 1990; Brendelberger, 1991; Baer et al., 2008; Scherer et al., 2017) are affected by aggregation processes. Consequently, the variation in the MS size range might lead to an increased interaction between the smallest particles and aquatic consumers. To test for the response of aquatic organisms to microplastics, the increased or decreased ingestion of microplastics is fundamental to take into account. In order to fill this gap, further studies are needed on the direct and indirect effects of aggregated microplastics on the life cycles of aquatic consumers.

DATA AVAILABILITY STATEMENT

The raw data supporting the conclusions of this article will be made available by the authors, without undue reservation.

AUTHOR CONTRIBUTIONS

CD, JP, and GW designed the experiment. CD conducted the experiment and performed the analysis of the data. CD and GW wrote the manuscript. All authors discussed the results and provided extensive comments on the manuscript concerning the analysis, interpretation, and writing. All authors approved the final version and have accepted accountability for all aspects of the work.

FUNDING

This research was supported by the BMBF project MikroPlaTaS (02WPL1448C).

ACKNOWLEDGMENTS

We thank S. Saumweber and C. Schirmer for providing us with samples and technical support and Dr. P. Colangeli and Dr. T. Klauschies for their valuable advice on the experimental design. We also thank the reviewers for their comments that improved the manuscript.

SUPPLEMENTARY MATERIAL

The Supplementary Material for this article can be found online at: https://www.frontiersin.org/articles/10.3389/fenvs.2020.574274/full#supplementary-material

REFERENCES

Alimi, O. S., Farner Budarz, J., Hernandez, L. M., and Tufenkji, N. (2018). Microplastics and nanoplastics in aquatic environments: aggregation, deposition, and enhanced contaminant transport. *Environ. Sci. Technol.* 52, 1704–1724. doi: 10.1021/acs.est.7b05559

Amaral-Zettler, L. A., Zettler, E. R., and Mincer, T. J. (2020). Ecology of the plastisphere. *Nat. Rev. Microbiol.* 18, 139–151. doi: 10.1038/s41579-019-0308-0

Baer, A., Langdon, C., Mills, S., Schulz, C., and Hamre, K. (2008). Particle size preference, gut filling and evacuation rates of the rotifer *Brachionus* "Cayman" using polystyrene latex beads. *Aquaculture* 282, 75–82. doi: 10.1016/j.aquaculture.2008.06.020

Barboza, L. G. A., Dick Vethaak, A., Lavorante, B. R. B. O., Lundebye, A. K., and Guilhermino, L. (2018). Marine microplastic debris: an emerging issue for food security, food safety and human health. *Mar. Pollut. Bull.* 133, 336–348. doi: 10.1016/j.marpolbul.2018.05.047

Bern, L. (1990). Size-related discrimination of nutritive and inert particles by freshwater zooplankton. *J. Plankton Res.* 12, 1059–1067. doi: 10.1093/plankt/12.5.1059

Besseling, E., Quik, J. T. K., Sun, M., and Koelmans, A. A. (2017). Fate of nano- and microplastic in freshwater systems: a modeling study. *Environ. Pollut.* 220, 540–548. doi: 10.1016/j.envpol.2016.10.001

Besseling, E., Redondo-Hasselerharm, P., Foekema, E. M., and Koelmans, A. A. (2019). Quantifying ecological risks of aquatic micro- and nanoplastic. *Crit. Rev. Environ. Sci. Technol.* 49, 32–80. doi: 10.1080/10643389.2018.1531688

Bolker, B. M. (2008). *Ecological Models and Data in R*. Princeton, NJ: Princeton University Press.

Brendelberger, H. (1991). Filter mesh size of cladocerans predicts retention efficiency for bacteria. *Limnol. Oceanogr.* 36, 884–894. doi: 10.4319/lo.1991.36.5.0884

Burns, W. (1968). Particle size and sedimentation in the feeding behavior of two species of *Daphnia*. *Limnol. Oceanogr.* 14, 392–402. doi: 10.4319/lo.1969.14.3.0392

Chen, J. P., Li, J., Liu, H., and Chen, J. P. (2018). Microplastics in freshwater systems: a review on occurrence, environmental effects, and methods for microplastics detection. *Water Res.* 137, 362–374. doi: 10.1016/j.watres.2017.12.056

Cunha, C., Faria, M., Nogueira, N., Ferreira, A., and Cordeiro, N. (2019). Marine vs freshwater microalgae exopolymers as biosolutions to microplastics pollution. *Environ. Pollut.* 249, 372–380. doi: 10.1016/j.envpol.2019.03.046

Demott, W. R. (1986). The role of taste in food selection by freshwater *zooplankton*. *Oecologia* 69, 334–340. doi: 10.1007/BF00377053

Fussmann, G. F., Weithoff, G., and Yoshida, T. (2005). A direct, experimental test of resource vs. consumer dependence. *Ecology* 86, 2924–2930. doi: 10.1890/04-1107

Geller, W. (1981). The filtration apparatus of cladocera: filter mesh-sizes and their implications on food selectivity. *Oecologia* 49, 316–321. doi: 10.1007/BF00347591

Grossart, H.-P., and Simon, M. (1993). Limnetic macroscopic organic aggregates (lake snow): occurrence, characteristics, and microbial dynamics in

Lake Constance. *Limnol. Oceanogr.* 38, 532–546. doi: 10.4319/lo.1993.38.3.0532

Guillard, R. R. L., and Lorenzen, C. J. (1972). Yellow-green algae with chlorophyllide c. *J. Phycol.* 8, 10–14. doi: 10.1111/j.1529-8817.1972.tb03995.x

Hartmann, N. B., Hu, T., Thompson, R. C., Hassello,M., Verschoor, A., Daugaard, A. E., et al. (2019). Are we speaking the same language? Recommendation for a definition and categorization framework for plastic debris. *Environ. Sci. Technol.* 53, 1039–1047. doi: 10.1021/acs.est.9b02238

Ikuma, K., Decho, A. W., and Lau, B. L. T. (2015). When nanoparticles meet biofilms- interactions guiding the environmental fate and accumulation of nanoparticles. *Front. Microbiol.* 6:591. doi: 10.3389/fmicb.2015.00591

Jambeck, J. R., Geyer, R., Wilcox, C., Siegler, T. R., Perryman, M., Andrady, A., et al. (2015). Plastic waste inputs from land into the ocean. *Science* 347, 768LP—771. doi: 10.1126/science.1260352

Jeong, C. B., Kang, H. M., Lee, Y. H., Kim, M. S., Lee, J. S., Seo, J. S., et al. (2018). Nanoplastic ingestion enhances toxicity of persistent organic pollutants (pops) in the monogonont rotifer *Brachionus koreanus* via multixenobiotic resistance (MXR) disruption. *Environ. Sci. Technol.* 52, 11411–11418. doi: 10.1021/acs.est.8b03211

Jeong, C. B., Won, E. J., Kang, H. M., Lee, M. C., Hwang, D. S., Hwang, U. K., et al. (2016). Microplastic size-dependent toxicity, oxidative stress induction, and p-JNK and p-p38 Activation in the monogonont rotifer (*Brachionus koreanus*). *Environ. Sci. Technol.* 50, 8849–8857. doi: 10.1021/acs.est.6b01441

Juchelka, C. M., and Snell, T. W. (1994). Rapid toxicity assessment using rotifer ingestion rate. *Arch. Environ. Contam. Toxicol.* 26, 549–554. doi: 10.1007/BF00214160

Juliano, S. A. (2001). "Nonlinear curve fitting," in *Design and Analysis of Ecological Experiments*, eds S. M. Scheiner and J. Gurevitch (Oxford: Oxford University Press), 178–196.

Kettner, M. T., Oberbeckmann, S., Labrenz, M., and Grossart, H. P. (2019). The eukaryotic life on microplastics in brackish ecosystems. *Front. Microbiol.* 10:538. doi: 10.3389/fmicb.2019.00538

Kirstein, I. V., Wichels, A., Gullans, E., Krohne, G., and Gerdts, G. (2019). The plastisphere – Uncovering tightly attached plastic "specific" microorganisms. *PLoS ONE* 14:e0215859. doi: 10.1371/journal.pone.0215859

Kögel, T., Bjorøy, Ø., Toto, B., Bienfait, A. M., and Sanden, M. (2020). Micro- and nanoplastic toxicity on aquatic life: determining factors. *Sci. Total Environ.* 709:136050. doi: 10.1016/j.scitotenv.2019.136050

Lindeque, P. K., Cole, M., Coppock, R. L., Lewis, C. N., Miller, R. Z., Watts, A. J. R., et al. (2020). Are we underestimating microplastic abundance in the marine environment? A comparison of microplastic capture with nets of different mesh-size. *Environ. Pollut.* 265:114721. doi: 10.1016/j.envpol.2020.114721

Manfra, L., Rotini, A., Bergami, E., Grassi, G., Faleri, C., and Corsi, I. (2017). Comparative ecotoxicity of polystyrene nanoparticles in natural seawater and reconstituted seawater using the rotifer *Brachionus plicatilis*. *Ecotoxicol. Environ. Saf.* 145, 557–563. doi: 10.1016/j.ecoenv.2017.07.068

Martel, J., Peng, H.-H., Young, D., Wu, C.-Y., and Young, J. D. (2014). Of nanobacteria, nanoparticles, biofilms and their role in health and disease: facts, fancy and future. *Nanomedicine* 9, 483–499. doi: 10.2217/nnm.13.221

Meng, Y., Kelly, F. J., and Wright, S. L. (2020). Advances and challenges of microplastic pollution in freshwater ecosystems: a UK perspective. *Environ. Pollut.* 256:113445. doi: 10.1016/j.envpol.2019.113445

Michels, J., Stippkugel, A., Lenz, M., Wirtz, K., and Engel, A. (2018). Rapid aggregation of biofilm-covered microplastics with marine biogenic particles *Proc. R. Soc. B.* 285:20181203. doi: 10.1098/rspb.2018.1203

Mohr, S., and Adrian, R. (2000). Functional responses of the rotifers *Brachionus calyciflorus* and *Brachionus rubens* feeding on armored and unarmored ciliates. *Limnol. Oceanogr.* 45, 1175–1179. doi: 10.4319/lo.2000.45.5.1175

Mueller, M., Fueser, H., Trac, L. N., Mayer, P., Traunspurger, W., and Ho, S. (2020). Surface-related toxicity of polystyrene beads to nematodes and the role of food availability. *Environ. Sci. Technol.* 54, 1790–1798. doi: 10.1021/acs.est.9b06583

Pagano, M. (2008). Feeding of tropical cladocerans (*Moina micrura*, *Diaphanosoma excisum*) and rotifer (*Brachionus calyciflorus*) on natural phytoplankton : effect of phytoplankton size – structure. *J. Plankton Res.* 30, 401–14. doi: 10.1093/plankt/fbn014

Paraskevopoulou, S., Tiedemann, R., and Weithoff, G. (2018). Differential response to heat stress among evolutionary lineages of an aquatic invertebrate species complex. *Biol. Lett.* 14:20180498. doi: 10.1098/rsbl.2018.0498

Passow, U. (2002). Transparent exopolymer particles (TEP) in aquatic environments. *Prog. Oceanogr.* 55, 287–333. doi: 10.1016/S0079-6611(02)00138-6

Pritchard, D. W., Paterson, R. A., Bovy, H. C., and Barrios-O'Neill, D. (2017). frair: an R package for fitting and comparing consumer functional responses. *Methods Ecol. Evol.* 8, 1528–1534. doi: 10.1111/2041-210X.12784

R Core Team (2017). *R: A Language and Environment for Statistical Computing*. Vienna: R Foundation for Statistical Computing. Available online at: https://www.r-project.org/

Raatz, M., Schälicke, S., Sieber, M., Wacker, A., and Gaedke, U. (2018). One man's trash is another man's treasure—the effect of bacteria on phytoplankton–zooplankton interactions in chemostat systems. *Limnol. Oceanogr. Methods* 16, 629–639. doi: 10.1002/lom3.10269

Réu, P., Svedberg, G., Hässler, L., Möller, B., Svahn, H. A., and Gantelius, J. (2019). A 61% lighter cell culture dish to reduce plastic waste. *PLoS ONE* 14:e0216251. doi: 10.1371/journal.pone.0216251

Rothhaupt, K. O. (1990a). Differences in particle size-dependent feeding efficiencies of closely related rotifer species. *Limnol. Oceanogr.* 35, 16–23. doi: 10.4319/lo.1990.35.1.0016

Rothhaupt, K. O. (1990b). Population growth rates of two closely related rotifer species: effects of food quantity, particle size, and nutritional quality. *Freshw. Biol.* 23, 561–570. doi: 10.1111/j.1365-2427.1990.tb00295.x

Schälicke, S., Teubner, J., Martin-creuzburg, D., and Wacker, A. (2019). Fitness response variation within and among consumer species can be co-mediated by food quantity and biochemical quality. *Sci. Rep.* 9:16126. doi: 10.1038/s41598-019-52538-2

Scherer, C., Brennholt, N., Reifferscheid, G., and Wagner, M. (2017). Feeding type and development drive the ingestion of microplastics by freshwater invertebrates. *Sci. Rep.* 7:17006. doi: 10.1038/s41598-017-17191-7

Scherer, C., Weber, A., Lambert, S., and Wagner, M. (2018). "Interactions of microplastics with freshwater biota," in *Freshwater Microplastics. The Handbook of Environmental Chemistry*, eds M. Wagner and S. Lambert, Vol. 58 (Cham: Springer), 153–180. doi: 10.1007/978-3-319-61615-5_8

Schneider, C. A., Rasband, W. S., and Eliceiri, K. W. (2012). NIH image to imagej: 25 years of image analysis. *Nat. Methods* 9, 671–675. doi: 10.1038/nmeth.2089

Seifert, L. I., de Castro, F., Marquart, A., Gaedke, U., Weithoff, G., and Vos, M. (2014). Heated relations: temperature-mediated shifts in consumption across trophic levels. *PLoS ONE* 9:e95046. doi: 10.1371/journal.pone.0095046

Setälä, O., Norkko, J., and Lehtiniemi, M. (2016). Feeding type affects microplastic ingestion in a coastal invertebrate community. *Mar. Pollut. Bull.* 102, 95–101. doi: 10.1016/j.marpolbul.2015.11.053

Silver, M. (2015). Marine snow: a brief historical sketch. *Limnol. Oceanogr. Bull.* 24, 5–10. doi: 10.1002/lob.10005

Snell, T. W. (1998). "*Review paper*: chemical ecology of rotifers," in *Rotifera VIII: A Comparative Approach. Developments in Hydrobiology, Vol.* 134, eds E. Wurdak, R. Wallace, and H. Segers (Dordrecht: Springer), 267–276. doi: 10.1007/978-94-011-4782-8_34

Snell, T. W., and Janssen, C. R. (1995). Rotifers in ecotoxicology : a *review*. *Hydrobiologia* 313, 231–247. doi: 10.1007/978-94-009-1583-1_32

Starkweather, P. L. (1980). Aspects of the feeding behavior and trophic ecology of suspension-feeding rotifers. *Hydrobiologia* 73, 63–72. doi: 10.1007/BF00019427

Starkweather, P. L., Gilbert, J. J., and Frost, T. M. (1979). Bacterial feeding by the rotifer *Brachionus calyciflorus* clearance and ingestion rates, behavior and population *dynamics*. *Oecologia* 30, 26–30. doi: 10.1007/BF00346392

Strungaru, S. A., Jijie, R., Nicoara, M., Plavan, G., and Faggio, C. (2019). Micro- (nano) plastics in freshwater ecosystems: abundance, toxicological impact and quantification methodology. *Trends Anal. Chem.* 110, 116–128. doi: 10.1016/j.trac.2018.10.025

Summers, S., Henry, T., and Gutierrez, T. (2018). Agglomeration of nano- and microplastic particles in seawater by autochthonous and *de novo*-produced sources of exopolymeric substances. *Mar. Pollut. Bull.* 130, 258–267. doi: 10.1016/j.marpolbul.2018.03.039

Vadstein, O. (1993). Particle size dependent feeding by the rotifer *Brachionus plicatilis*. *Hydrobiologia* 255, 261–267. doi: 10.1007/978-94-011-1606-0_34

Vosshage, A. T. L., Neu, T. R., and Gabel, F. (2018). Plastic alters biofilm quality as food resource of the freshwater gastropod *Radix balthica*. *Environ. Sci. Technol.* 52, 11387–11393. doi: 10.1021/acs.est.8b02470

Vroom, R. J. E., Koelmans, A. A., Besseling, E., and Halsband, C. (2017). Aging of microplastics promotes their ingestion by marine zooplankton. *Environ. Pollut.* 231, 987–996. doi: 10.1016/j.envpol.2017.08.088

Wang, X., Bolan, N., Tsang, D. C. W., Sarkar, B., Bradney, L., and Li, Y. (2021). A review of microplastics aggregation in aquatic environment: influence factors, analytical methods, and environmental implications. *J. Hazard. Mater.* 402:123496. doi: 10.1016/j.jhazmat.2020.123496

Wiggin, K. J., and Holland, E. B. (2019). Validation and application of cost and time effective methods for the detection of 3–500 μm sized microplastics in the urban marine and estuarine environments surrounding Long Beach, California. *Mar. Pollut. Bull.* 143, 152–162. doi: 10.1016/j.marpolbul.2019.03.060

Zafiriou, O. C., and Farrington, J. W. (1980). The use of DAPI for identifying aquatic microfloral. *Limnol. Oceanogr.* 25, 943–948. doi: 10.4319/lo.1980.25.5.0943

Zettler, E. R., Mincer, T. J., and Amaral-Zettler, L. A. (2013). Life in the "plastisphere": Microbial communities on plastic marine debris. *Environ. Sci. Technol.* 47, 7137–7146. doi: 10.1021/es401288x

Zhao, S., Ward, J. E., Danley, M., and Mincer, T. J. (2018). Field-based evidence for microplastic in marine aggregates and mussels: implications for trophic transfer. *Environ. Sci. Technol.* 52, 11038–11048. doi: 10.1021/acs.est.8b03467

Zheng, S., Zhao, Y., Liangwei, W., Liang, J., Liu, T., Zhu, M., et al. (2020). Characteristics of microplastics ingested by zooplankton from the Bohai Sea, China. *Sci. Total Environ.* 713:136357. doi: 10.1016/j.scitotenv.2019.136357

Conflict of Interest: The authors declare that the research was conducted in the absence of any commercial or financial relationships that could be construed as a potential conflict of interest.

frontiers in Environmental Science

ORIGINAL RESEARCH
published: 23 December 2020
doi: 10.3389/fenvs.2020.572424

Various Digestion Protocols Within Microplastic Sample Processing—Evaluating the Resistance of Different Synthetic Polymers and the Efficiency of Biogenic Organic Matter Destruction

*Felix Pfeiffer and Elke Kerstin Fischer**

Department of Earth Sciences, Center for Earth System Research and Sustainability, Universität Hamburg, Hamburg, Germany

OPEN ACCESS

Edited by:
Andrew Turner, University of Plymouth, United Kingdom

Reviewed by:
Dietmar Schlosser, Helmholtz Centre for Environmental Research (UFZ), Germany
Joana Correia Prata, University of Aveiro, Portugal

***Correspondence:**
Elke Kerstin Fischer
elke.fischer@uni-hamburg.de

Specialty section:
This article was submitted to Toxicology, Pollution and the Environment, a section of the journal Frontiers in Environmental Science

Received: *14 June 2020*
Accepted: *30 November 2020*
Published: *23 December 2020*

Citation:
Pfeiffer F and Fischer EK (2020) Various Digestion Protocols Within Microplastic Sample Processing—Evaluating the Resistance of Different Synthetic Polymers and the Efficiency of Biogenic Organic Matter Destruction. Front. Environ. Sci. 8:572424. doi: 10.3389/fenvs.2020.572424

The digestion of biogenic organic matter is an essential step of sample preparation within microplastic analyses. Organic residues hamper the separation of polymer particles especially within density separation or polymer identification via spectroscopic and staining methods. Therefore, a concise literature survey has been undertaken to identify the most commonly applied digestion protocols with a special focus on water and sediments samples. The selected protocols comprise different solutions, concentrations, and reaction temperatures. Within this study we tested acids (nitric acid and hydrochloric acid), bases (sodium hydroxide and potassium hydroxide), and oxidizing agents [hydrogen peroxide, sodium hypochlorite and Fenton's reagent (hydrogen peroxide 30% in combination with iron(II)sulfate 0.27%)] at different concentrations, temperature levels, and reaction times on their efficiency of biogenic organic matter destruction and the resistance of different synthetic polymers against the applied digestion protocols. Tests were carried out in three parallels on organic material (soft tissue—leaves, hard tissue—branches, and calcareous material—shells) and six polymers (low-density polyethylene, high-density polyethylene, polypropylene, polyamide, polystyrene, and polyethylene terephthalate) in two size categories. Before and after the application of different digestion protocols, the material was weighed in order to determine the degree of digestion efficiency and polymer resistance, respectively. The efficiency of organic matter destruction is highly variable. Calcareous shells showed no to very low reaction to oxidizing agents and bases, but were efficiently dissolved with both tested acids at all concentrations and at all temperatures. Soft and hard tissue were most efficiently destroyed by sodium hypochlorite. However, the other reagents can also have good effects, especially by increasing the temperature to 40–50°C. The additional temperature increase to 60–70°C showed a further but less effective improvement, compared to the initial temperature increase. The resistance of tested polymer types can be rated as good except for polyamide and polyethylene terephthalate. Increasing the concentrations and temperatures, however, results in accelerated degradation of all polymers. This is

most evident for polyamide and polyethylene terephthalate, which show losses in weight between 15 and 100% when the digestion temperature is increased. This effect is most pronounced for polyamide in the presence of acids and for polyethylene terephthalate digested with bases. As a concluding recommendation the selection of the appropriate digestion method should be specifically tested within initial pre-tests to account for the specific composition of the sample matrix and the project objectives.

Keywords: microplastics, sample purification, synthetic polymer resistance, digestion efficiency, biogenic organic matter, protocol evaluation

INTRODUCTION

The investigation of environmental pollution by synthetic polymers and its effects is a rapidly developing research discipline. However, especially considering the detection of small particles, the separation of plastic particles from the sample matrix still poses a major challenge. The isolation of plastic particles requires the removal of the natural sample matrix consisting of mineral and biogenic organic substances. The optimal digestion method for the respective samples eliminates the biogenic organic matter as much as possible while preserving the target particles of synthetic polymers. For this purpose chemical digestion with acids, bases and oxidizing agents and enzymes are applied.

A number of studies address a comparison of different digestion methods to optimize the efficiency of biogenic organic matter destruction (Nuelle et al., 2014; Cole et al., 2015; Dehaut et al., 2016; Enders et al., 2017; Karami et al., 2017; Herrera et al., 2018; Hurley et al., 2018; Munno et al., 2018; Prata et al., 2019; Duan et al., 2020).

The efficiency of biogenic organic matter destruction is matrix-dependent. For example, applying strong acids, such as nitric acid (HNO_3) led to very good digestion results regarding biota tissue, mainly consisting of proteins, carbohydrates and fats (Nuelle et al., 2014; Lusher et al., 2017; Naidoo et al., 2017). Karami et al. (2017) confirmed this for HNO_3 and hydrochloric acid (HCl) digestion of fish tissue. Alkaline solutions, such as potassium hydroxide (KOH) also provide good results concerning the digestion of biotic tissue (Foekema et al., 2013; Nuelle et al., 2014; Collard et al., 2015; Dehaut et al., 2016; Karami et al., 2017; Prata et al., 2019). Enders et al. (2017) found highest efficiencies in applying KOH with NaClO (1:1) to fish stomach samples. These protocols are likely to be effective to destroy adhering biofilms that also predominately are composed of polysaccharides, proteins and lipids. Their elimination also is of great relevance since they may influence, e.g., physical behavior within density separation of sediment samples (Rummel et al., 2017; Harrison et al., 2018). However, KOH or sodium hydroxide (NaOH) are less successful when applied to water and sediment samples, as the biogenic organic material in these matrices often originates from plant material (including leafs, woody debris, and algae) and/or contains parts of carapace and shells (Duan et al., 2020). Therefore, in addition to calcareous substances, cellulose, hemicellulose, lignin, tannin, humic substances, and chitin, which are difficult to digest, must be eliminated (Herrera et al., 2018; Möller et al., 2020). For these sample matrices, oxidizing agents, such as hydrogen peroxide (H_2O_2) are increasingly implemented, also as Fenton's reagent and less frequently in combination with sodium hypochlorite (NaClO) (Enders et al., 2017; Karami et al., 2017; Hengstmann et al., 2018; Duan et al., 2020). Oxidizing agents are therefore considered to be promising candidates for a most efficient digestion of a wide range of sample matrices.

Besides efficiently destroying biogenic organic matter, applied protocols need to leave synthetic polymers unaffected concerning their weight, volume, shape, and if required, color. Furthermore, it is possible that the chemical structure or the surface structure and morphology of the polymers is affected and changed by the digestion methods (Enders et al., 2017). In order to detect these changes, further investigations by, e.g., scanning electron microscopy (SEM) or detailed spectroscopic analyses implementing μRaman-spectroscopy or FTIR-spectroscopy are necessary. It has been reported that under the influence of acids, in particular pH-sensitive synthetic polymers are altered. When exposed to HNO_3, the degradation or complete destruction of polyamide (PA) (Dehaut et al., 2016; Roch and Brinker, 2017; Duan et al., 2020), and a critical melting of polystyrene (PS) (Claessens et al., 2013) occurred. Concentrated HNO_3 and HCl may also dissolve nylon and partially degraded polyethylene (PE), polypropylene (PP), polystyrene (PS), polyethylene terephthalate (PET), and polyvinyl chloride (PVC) (Karami et al., 2017; Naidoo et al., 2017). Catarino et al. (2017) further reported that melding of PET and PE particles and complete dissolution of nylon fibers even occurs when using HNO_3 in lower concentrations of 35%. Especially the application of HNO_3 in higher concentrations at high temperatures significantly affects synthetic polymers with complete dissolution of PE and PS (Avio et al., 2015). Furthermore, HNO_3 can cause yellowing of polymers, such as PE, PP, PA, and PS (Dehaut et al., 2016).

Strong bases can also have an influence on synthetic polymers. According to Dehaut et al. (2016) KOH digestion resulted in degradation of cellulose acetate (CA) and caused a significant weight increase for PS and weight decrease for polycarbonate (PC) (Hurley et al., 2018). When temperatures higher than 50°C were additionally applied, PVC also degraded and furthermore, a color alteration of nylon occurred (Karami et al., 2017). Dehaut et al. (2016) and Hurley et al. (2018) tested the application of sodium hydroxide (NaOH) resulting in degradation of CA, PC, and PET.

The use of oxidants, such as H_2O_2 at room temperature has only a minor effect on synthetic polymer weight and size but can lead to discoloration. However, an increase in temperature to 70–100°C is reported to cause a significant loss in weight and size of PA (Hurley et al., 2018; Duan et al., 2020).

The results of these studies are extremely valuable. However, an objective assessment of the actual efficiency of biogenic matter destruction or the resistance of plastics to the various digestion solutions is masked by the use of pre-specified protocols. Different concentrations, temperatures, and application times are used and compared in order to optimize the pre-selected protocols.

For an objective evaluation of chemical digestion methods with a focus on water and sediment samples, the present study examines acids, bases, and oxidizing agents in different concentration ranges at three identical temperature levels using identical methods. Within extensive laboratory tests, a total number of 40 protocols were evaluated with regard to their efficiency of biogenic organic matter destruction and their influence on synthetic polymers. The aim of our study is to provide a toolbox to assist the selection of digestion methods, to minimize the previously described laboratory analytical challenges and to represent a step toward the standardization of laboratory methods.

MATERIALS AND METHODS

Digestion Solutions and Protocols Tested

Within this study, we tested acids (HNO_3 20 and 65%, HCl 10 and 37%), bases (NaOH 2.5, 5, and 10 M or 4.7, 9.4, and 18.8%, respectively, KOH 1 and 4 M or 2.6 and 10.6%, respectively), and oxidizing agents [H_2O_2 30 and 50%, NaClO ∼7.5 and 10%, Fenton's reagent (H_2O_2 30% and iron(II)sulfate 0.27%)]. The digestion protocols were carried out at three different temperature levels (20, 40–50, and 60–70°C) and reaction times (8–24 h or 7 days). For protocols with increased temperature (40–50 or 60–70°C), the samples were heated for 8 h of the overall exposure time of 24 h. The 7 d experiments were performed with H_2O_2 (30 and 50% at room temperature) and KOH (2.6 and 10.6% at room temperature). All experiments were conducted in three parallels. An overview of all tested protocols is provided in **Table 1**.

TABLE 1 | List of the applied digestion solutions with corresponding concentrations, temperatures, and exposure times.

Digestion solution	Concentration (%)	Temperature applied (°C)			Exposure time	
		20	40–50	60–70	24 h	7 days
Hydrogen peroxide (H_2O_2)	30	✦	✦	✦	✦	✦
Hydrogen peroxide (H_2O_2)	50	✦	✦	✦	✦	✦
Sodium hypochlorite (NaClO)	7.5	✦	✦	✦	✦	
Sodium hypochlorite (NaClO)	10	✦	✦	✦	✦	
Hydrogen peroxide (H_2O_2) + Iron(II) sulfate ($FeSO_4$)	30 + 0.27	✦	✦	✦	✦	
Nitric acid (HNO_3)	20	✦	✦	✦	✦	
Nitric acid (HNO_3)	65	✦	✦	✦	✦	
Hydrochloric acid (HCl)	10	✦	✦	✦	✦	
Hydrochloric acid (HCl)	37	✦	✦	✦	✦	
Sodium hydroxide (NaOH)	4.7	✦	✦	✦	✦	
Sodium hydroxide (NaOH)	9.4	✦	✦	✦	✦	
Sodium hydroxide (NaOH)	18.8	✦	✦	✦	✦	
Potassium hydroxide (KOH)	2.6	✦	✦	✦	✦	✦
Potassium hydroxide (KOH)	10.6	✦	✦	✦	✦	✦

Origin and Processing of Synthetic Polymer Reference Particles

All protocols were tested for two size categories in three replicates, each. Virgin pellets of LDPE, HDPE, PP, PA, PS, and PET in nominal granule sizes of 1.0–5.0 mm were purchased from Goodfellow Cambridge Ltd.

For size category 1.0–5.0 mm, the virgin pellets were used as delivered by the manufacturer. Ten particles of each polymer per replicate were weighed to 0.01 mg accuracy (Cubis MSE324P, Sartorius) and transferred into glass test tubes. For size category 0.3–1.0 mm, the pellets were ground using a cutting mill (SM100, Retsch) and subsequent wet sieving in order to rinse off adhering smaller particles. About 150 mg of the respective polymers per replicate were weighed to 0.01 mg accuracy and transferred into glass test tubes. An aliquot of the respective digestion solution was slowly added in order to soak the complete sample material. The volumes applied depended on the incubation temperature (10 ml for room temperature and 20 ml for temperatures of 40–50 and 60–70°C). Test tubes dedicated to protocols with elevated temperatures were placed on sand baths (ST72, Harry Gestigkeit GmbH). For all temperatures, the exposure time was 24 h. Increased temperatures were applied for 8 h using a time-temperature controller. Subsequently, the samples of size category 1.0–5.0 mm were thoroughly rinsed through a stainless steel sieve with a mesh size of 1 mm (Retsch) with MilliQ water and were placed within covered glass petri dishes for subsequent drying at 40°C. Samples containing the smaller size fraction (0.3–1.0 mm) were filtered onto PC filters (Cyclopore, 5 µm, Whatman) by means of a stainless steel filtration device (3-fold Combisart, Sartorius) and were thoroughly rinsed with MilliQ water. Filter residues were immediately transferred into evaporating dishes with small amounts of MilliQ water that were placed into a drying oven at 40°C. After drying, all samples were evacuated within a desiccator until room temperature was

achieved. Samples were then re-weighed to 0.01 mg accuracy. Based on the initial and final weight, the percentage change in weight of the respective synthetic polymer samples were calculated. For the comparability of results for large and small particles, the surface to volume ratio of plastic polymer particles were calculated based on mean dimensions and results were standardized to a surface to volume ratio of 2.

The polymers were photographed before and after the treatment to visually document possible changes in size, shape, or color (**Supplementary Figures 1–5**). Particles with visibly distinct changes in size, shape, or color were further investigated by μRaman spectroscopy (DXR2xi, ThermoFisher Scientific) to determine the potential effects of these visual alterations on the chemical structure of the polymer. For a spectroscopic analysis of possible changes in spectra by the respective application, single particles were placed on a microscope slide with tweezers for verification via μRaman-spectroscopy. Spectra were recorded using a 532 nm laser at 5–10 mW (25 μm confocal pinhole) and 100–10 Hz integrating 1,000 measurements. All spectra were smoothed (7 points) and the baseline was corrected automatically.

Material and Processing of Biogenic Organic Matter

Concerning the efficiency tests of digestion methods a focus was set on biogenic organic matter with high contents in cellulose and lignin typically present in sediment and water samples. Therefore, three different biogenic organic materials were tested: soft plant tissue (leaves, *Fagus sylvatica*), hard plant tissue (branches, *Fagus sylvatica* and *Quercus robus*) and calcareous shells (mussels, various marine species). Samples were shredded using a cutting mill (SM100, Retsch) for soft and hard tissue and a mortar for mussel shells. Subsequently, samples were sieved to gain pieces of 1.0–5.0 mm in longitudinal direction. Biogenic organic matter samples were dried at 40°C for 24 h and incubated in a desiccator until room temperature was achieved. Aliquots of about 150 mg were weighed to 0.01 mg accuracy (Sartorius, Cubis CPA 124S) and transferred to glass test tubes.

The further processing of biogenic samples was done in accordance to synthetic polymer tests described above. Chemical solutions were added and tubes were placed onto a sand bath when the protocol provides an increase in temperature. After the respective incubation time, samples were filtered and carefully rinsed into pre-weighed evaporating dishes with MilliQ water as it was done for the small plastic particles. After drying at 40°C, the loss of weight in biogenic matter was determined and calculated.

Statistical Analyses

Results were statistically analyzed using R statistics (R Core Team, 2017, Version 3.4.2) in an R Studio environment (RStudio Team, 2016, Inc., Version 1.1.383) and SPSS (IBM Version 26) concerning normality (Shapiro-Wilk), equality of variances (Levene's test), and analyses of variances (Mann-Whitney-*U* and Kruskall Wallis tests with subsequent Bonferroni correction and pairwise comparison, $\alpha = 0.05$).

RESULTS

Results on Resistance of Synthetic Polymer Particles

The results concerning the resistance of synthetic polymers against the applied reagents predominantly show good to very good results with weight changes $< \pm 1\%$ (see **Figures 1A,B** providing different y-scale dimensions). **Figures 1A,B** display mean weight differences with strong changes up to 100% standing for most destroying protocols. According to oxidizers, acids and bases the relevant protocols follow the order of different concentrations and then temperature levels.

Oxidizing agents, in this case H_2O_2 and NaClO, marginally affected synthetic polymers except for PA. For PA, the application of H_2O_2 50% at temperatures between 60 and 70°C led to a mean decrease in weight of 8.7%. In contrast, other protocols using H_2O_2 led to an insignificant increase in weight of PA particles. This increase is weakened with rising temperatures but intensified for the 7 d period at room temperature. A slight decrease in weight for PA was further observed when applying NaClO (7.5%) at the temperature levels of 40–50 and 60–70°C (−1.1%, $p = 0.020$). PP might be slightly affected when higher concentrations of NaClO are provided at the highest temperature level of 60–70°C ($p = 0.046$, see **Supplementary Table 1B**).

Acidic digestion protocols showed the greatest influence again on PA. HCl was less aggressive than HNO_3 at almost all concentrations and temperatures. Concerning HCl, the increase of concentration from 10 to 37% at 20°C led to degradation of PA. For low concentrations of HCl (10%), temperature is a major influencing factor. In this case, a temperature increase from 20 to 60–70°C leads to a reduction in weight for PA of up to 50.4% ($p = 0.039$).

The application of HNO_3 at all concentrations and temperatures led to a severe destruction of PA except for concentrations of 20% at 20°C (mean + 5.9%). Even though PA was also dissolved in HNO_3 at 20°C it re-precipitated when adding MilliQ-water and thus, could be reweighed (**Supplementary Figure 2**).

Furthermore, an insignificant increase in weight of PS was detected when applying HNO_3 (65%) and raising the temperature level from 20 to 60–70°C (+0.4 vs. +5.3%). Visually, the generation of PS flakes (for particles of the size category 0.3–1.0 mm) was observed (**Supplementary Figure 5**). An opposite effect, with a significant loss in weight, is detected for PET when increasing the temperature level from 20 to 60–70°C (+0.8 vs. −4.7%, $p = 0.002$).

The protocols including the alkaline reagents NaOH and KOH resulted in good to very good resistances for all tested synthetic polymers except for PET. PET seems to be more affected by NaOH compared to KOH. Due to great variances, these differences are not significant, though. KOH shows an increasing loss in weight for PET with higher concentration (2.6 vs. 10.6%) at 40–50°C (−0.7 vs. −4.7%, $p = 0.039$). As for oxidizing agents, a slight increase in weight of PS particles is observed for alkaline protocols.

The spectroscopic examination of selected particles by μRaman-spectroscopy showed that for some of the particles

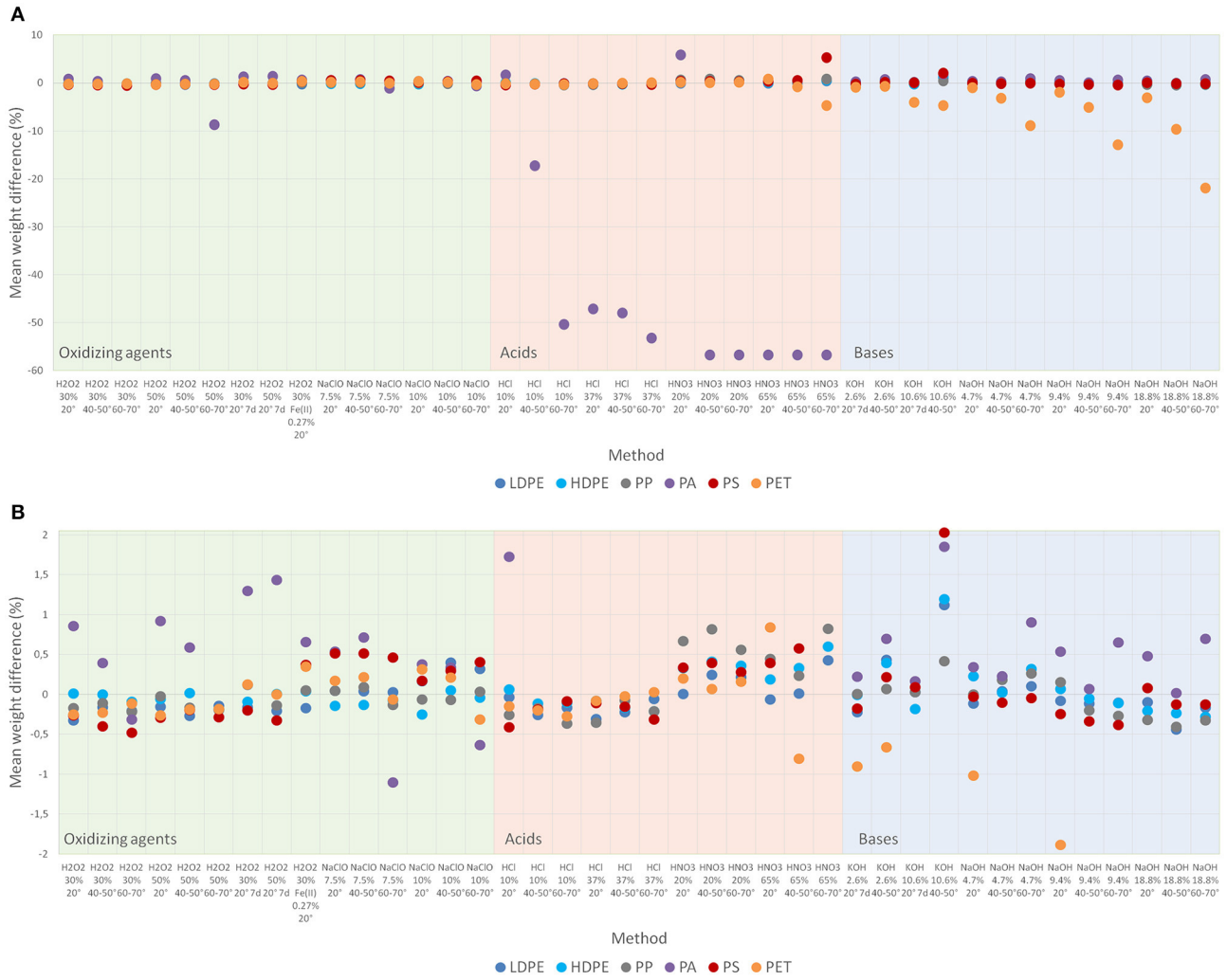

FIGURE 1 | (A) Mean resistance of synthetic polymer particles against applied digestion protocols (expressed as mean difference in weight (%) of size standardized particles, full scale). **(B)** Mean resistance of synthetic polymer particles against applied digestion protocols (expressed as mean difference in weight (%) of size standardized particles, focused scale to values of ±2% difference in weight).

distinct changes in the fingerprint region as well as in the C–H-stretch between the spectra before and after the treatment could be noticed. This was most notably recorded for PA but also PS and PET when HCl was applied at higher temperatures. Nevertheless, in all selected cases the polymer type was correctly identified (**Supplementary Figure 6**).

Results on Digestion Effectiveness of Biogenic Organic Matter

The effectiveness of digestion protocols for biogenic organic matter is highly variable and matrix dependent (**Figure 2**). **Figure 2** displays mean weight differences with strong changes up to 100% standing for most effective protocols. According to oxidizers, acids and bases the relevant protocols follow the order of different concentrations and then temperature levels.

The application of H_2O_2 showed the highest efficiency of biogenic organic matter digestion in soft and hard tissue compared to shells. The digestion efficiency increased with rising concentrations from 30 to 50% and was enhanced even more with rising temperature from 20 to 60–70°C. Concerning soft tissue, this resulted in a maximum weight reduction of 71.1% (30%/20°C −11.0 vs. 50%/60–70°C −71.1%, $p = 0.011$). Similar effects were achieved for hard tissue with a mean weight decrease of 6.4% (30%/20°C) vs. 58.9% (50%/60–70°C, $p = 0.036$).

Adding Fenton's reagent also resulted in digestion of both soft and hard tissue of up to 64.4%. The elongation of the reaction time up to 7 d (20°C) resulted in only minor improvements of the digestion.

The application of NaClO provided even better results than H_2O_2 with loss in weight of up to 88.0% for soft tissue and 92.1% for hard tissue. The increase of the concentration from 7.5 to 10% did not result in a significant improvement. Increasing the temperature from 20 to 40–50°C led to a significantly better digestion result for soft tissue in NaClO (10%) (66.3 vs. 87.4%,

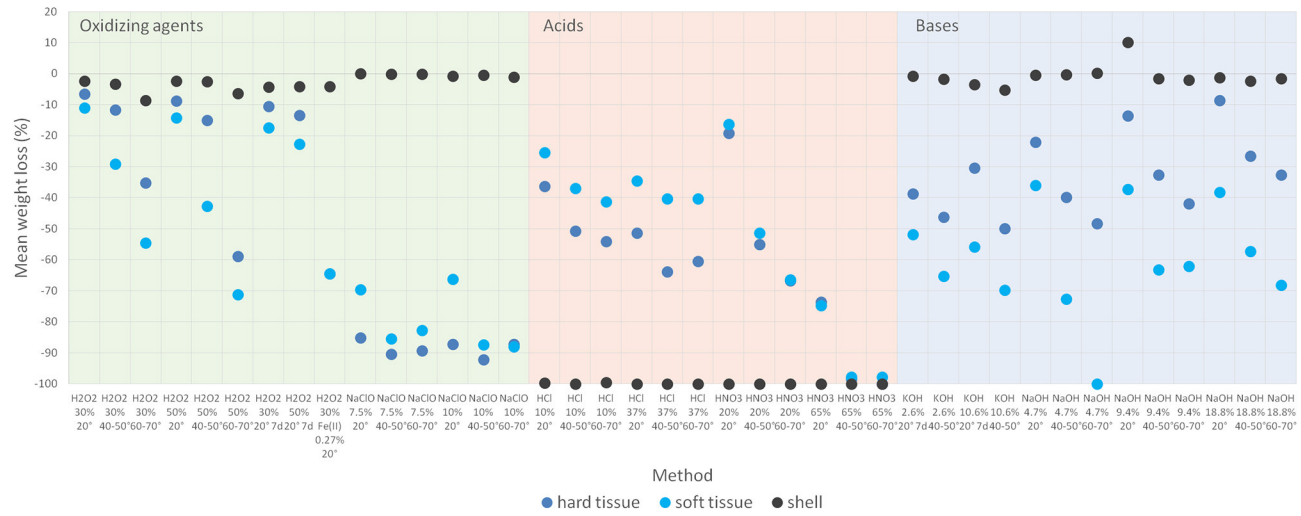

FIGURE 2 | Efficiency of tested protocols concerning biogenic organic matter digestion given as mean loss in weight (%).

$p = 0.043$). Further elevation of temperature did not cause any significant increase in the digestion of soft and hard tissue.

The calcareous material derived from shells was hardly digested by oxidizing agents. Only a slight increase of digestion efficiency with rising temperature can be observed for the H_2O_2 protocol.

The acid protocols with HCl and HNO_3 were the only ones leading to satisfying results concerning digestion of calcareous material. Both reagents led to the dissolution with 99.5–100% loss in weight at all concentrations and applied temperatures. Concerning soft and hard tissue, the digestion efficiencies increase with rising concentrations and rising temperatures to maximum values of 74.7 and 73.5%, respectively. This effect is significant for soft tissue digested in HCl 10% when raising the temperature from 20 to 40–50°C (−25.3 vs. −41.2%, $p = 0.043$). Further increasing the temperature level does not lead to a significant enhancement in the digestion efficiency.

Only when applying HNO_3 at 65% with elevated temperatures >40°C a nearly complete digestion of soft and hard tissue is achieved (97.8–100%).

Digestion protocols using alkaline solutions predominantly did not lead to sufficient results concerning biogenic organic matter destruction and were in a similar range as the protocols using acids except for calcareous material. The maximum values of weight reduction accounted for 49.8% (hard tissue, KOH 10.6%, 40–50°C) and 100% (soft tissue, NaOH, 4.7%, 60–70°C). In general, better results were achieved for both KOH and NaOH with higher temperature levels. Bases had no relevant effects on calcareous substances.

DISCUSSION

Effects of Oxidizers on Synthetic Polymers and Biogenic Organic Matter

With regard to the resistance of polymers exposed to oxidizers, their influence on the tested synthetic polymers is low except for PA when exposed at higher reaction temperatures. The significant loss in weight for PA when exposed to H_2O_2 50% at 60–70°C is comparable to the findings of Hurley et al. (2018) applying a temperature of 70°C and describing a significant loss in weight (26.7%) and size (33.4%).

The application of H_2O_2 at all concentrations did not result in good digestion efficiencies of the tested biogenic organic material when applied at room temperature even with a prolonged reaction time of 7 days. The results could be distinctly improved by raising the temperature up to 70°C. This is in accordance with findings by Duan et al. (2020) who stated good digestion efficiencies of vegetal litter with stepwise addition of H_2O_2 and temperature increase to 100°C. Best digestion results on soft and hard tissue were obtained with NaClO with similar efficiencies for both tested concentrations. Again, an improvement of efficiencies was gained by increasing the temperature to 40–50% while no further progress was found for higher temperatures.

Effects of Acids on Synthetic Polymers and Biogenic Organic Matter

Based on synthetic polymer resistance, the digestion protocols applying acids were suitable at all concentrations and temperature levels except for PA. Digestion with HNO_3 at different concentration levels (20 vs. 65%) even led to a significant degradation of PA ($p = 0.037$). As shown by Dehaut et al. (2016) and Duan et al. (2020) nitric acid may cause complete degradation, which is supported by our data, as well.

Furthermore, HCl only affected polymers when exposed to high concentrations and/or high temperatures. Acids in general have a larger influence on synthetic polymers compared to oxidizers being most pronounced for PA and to a lesser extent for PS and PET. This was also stated by other authors (Dehaut et al., 2016; Karami et al., 2017; Naidoo et al., 2017; Duan et al., 2020), which underlines these results. Other studies furthermore report the partial degradation of other synthetic polymers, such as PE, PP, and PVC by acids HCl and HNO_3 (Karami et al., 2017;

Naidoo et al., 2017). These findings are not confirmed within the present study due to differences in weight of $< \pm 1\%$ documented.

Effects of Bases on Synthetic Polymers and Biogenic Organic Matter

The application of alkaline protocols on the tested biogenic material had no or only very slight effects on calcareous material. The efficiencies on hard and soft tissues could be improved by applying elevated concentrations and temperatures. The protocols implementing bases did not achieve satisfying digestion efficiencies except for NaOH (4.7%) at the highest temperature level where an at least soft tissue was digested efficiently. Here, a maximum digestion efficiency of about 70% of soft tissue and about 50% of hard tissue could be obtained. This finding is underlined by the results of Duan et al. (2020) who digested vegetal litter with a mixture of NaOH 10 M and H_2O_2 at room temperature over 7 days.

NaOH was reported to cause degradation on synthetic polymers. Similar to the study of Hurley et al. (2018) an increase in weight of PS was detectable when applying KOH 10.6% at 40–50°C (Hurley et al., 2018: +12.1 vs. 2.0% this study). The strongest degradation effect of all bases was observed for PET when treated with NaOH. The degradation of mass and size of PET through the application of 10 M NaOH has also been demonstrated within other studies (Dehaut et al., 2016; Hurley et al., 2018).

The alteration of synthetic polymers by digestion chemicals can result not only in a decrease but also in an increase in weight. This is especially given for certain protocols and the polymers PA and PS. Pretests with alkaline protocols revealed that it is of utmost importance to carefully rinse the samples since residues of the respective salts might still be present. This can lead to an overestimation in weight. The present experiments considered this fact, thus, the increase in weight of especially PA and PS is more indicative concerning an alteration due to an initial degradation at the surface and thus an increase in volume (as was also demonstrated by Dehaut et al., 2016 and Hurley et al., 2018) and finally structural changes within the synthetic polymer. Furthermore, the increase in weight also might be a result from the relaxation of the polymer structure and entrapping of water molecules (Lulu et al., 2019).

Effects of Rising Concentration and Temperature Levels

Some of the results are very convincingly demonstrating that both concentration of the agent and temperature level applied are of utmost importance for polymer resistance.

The influence of rising concentrations on the digestion of biogenic organic matter is partly masked by influences due to applied temperatures. Tests on significant differences by concentrations resulted in several tendencies (see **Supplementary Table 1A**). Most significant differences occurred concerning the HNO_3 digestion of hard tissue at temperatures between 60 and 70°C when raising the concentration from 20 to 65% ($p = 0.046$). The digestion of soft tissue is significantly improved when the concentration of NaOH is increased from 4.7 to 9.4% ($p = 0.037$).

Except for PS and PA, effects are detected concerning the alteration of synthetic polymers through increasing the concentration of the digestion solutions (see **Supplementary Table 1B**).

In general, increasing the temperature leads to a significant improvement of the digestion results for soft and hard tissue concerning almost all tested reagents except for KOH (**Supplementary Table 2A**). Acid and alkaline treatments especially in lower concentrations showed a significant influence on hard tissue and soft tissue only when rising the temperature level from 20 to 60–70°C. Concerning oxidative treatment the results with H_2O_2 50% reveal the same temperature related tendency. With NaClO a significant improvement is already achieved when increasing temperatures from 20 to 40–50°C. A further elevation of the temperature to the level of 60–70°C only leads to a minor improvement of the digestion result with NaClO.

Similarly, the resistance of synthetic polymers especially of PA, PS, and PET is affected by increased temperatures at all concentrations applied (**Supplementary Table 2B**). Significant effects predominantly occur when the temperature level is raised from 20 to 60–70°C. Only PS is affected at 40–50°C when treated with H_2O_2 (30%). For example, HCl application on PA reveals that the destruction of the polymer is affected to a comparable extent by increasing the concentration from 10 to 37% as by raising the temperature from 20 to 60–70°C at the 10% HCl solution.

Though, when implementing H_2O_2 or Fenton's reagent for the digestion of organic-rich samples high temperatures might occur without externally supply due to exothermic oxidative reactions (Munno et al., 2018; Wiggin and Holland, 2019). Based on the results, it is recommended not to exceed temperatures of 40 or 50°C. This can either be achieved in reducing the concentrations and/or by placing the sample beakers into a cooling water bath. For better performance, also the application in multiple doses might be considered.

The results of the present study are based on weight changes. Therefore, a potential weight-neutral chemical or biological transformation of the parent polymers through the application of chemical digestion remains undetected. Hence, a possible under- or overestimation of the resistance of the polymers to the applied digestion methods cannot be excluded.

CONCLUSIONS

Taking into account both the resistance of synthetic polymers and the digestion efficiency of biogenic organic matter, our findings reveal that best results are achieved by applying oxidative treatment with NaClO. Both tested concentrations of 7.5 and 10% with further activation by a moderate increase in temperature to 40–50°C are considered to be highly effective for the digestion of soft and hard tissue. For the destruction of calcareous materials oxidizers are not suitable.

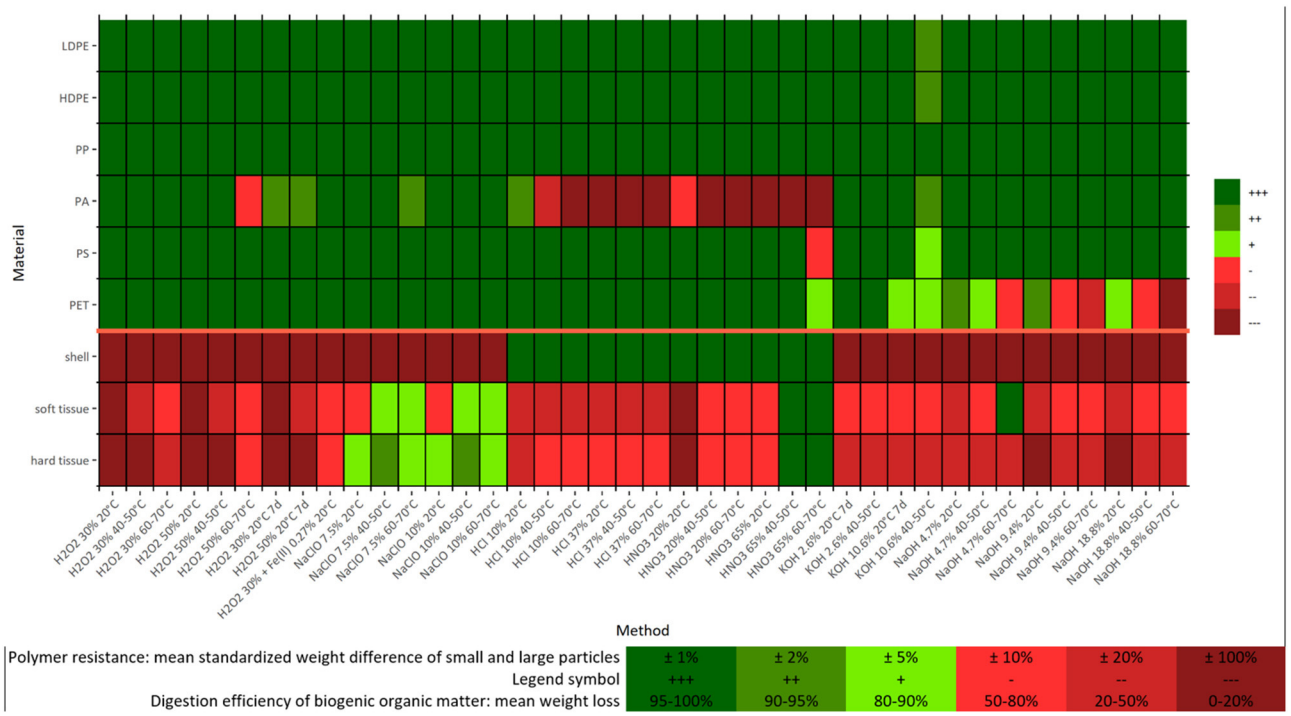

FIGURE 3 | Evaluation of tested digestion protocols on synthetic polymer resistance (mean standardized efficiency of small and large particles) and digestion efficiency of biogenic organic matter.

Acid digestion led to partial or complete degradation of some synthetic polymers, such as PA, PET, and PS. Furthermore, the application of acids on biogenic organic material did not lead to sufficient digestion results. Consequently, concerning biogenic organic material within sediments and water samples the application of acid digestion is not recommended except for sample matrixes with high contents of calcareous substances. In this case, the application of HCl at a maximum concentration of 10% at a reaction temperature of 20°C can be an essential part of the digestion protocol especially since it does not show any distinct effect on any of the synthetic polymers either.

Based on the results, digestion protocols implementing alkaline protocols are considered to be less suitable for their application on sediment and water samples, either. These samples are mainly characterized by higher proportions of cellulose, hemicellulose and lignin of plant residues that are only less affected by alkaline digestion. Furthermore, especially PET is affected by NaOH and to a lesser extent—KOH. PET constitutes the major part of fibers in environmental samples and should thus not be excluded by implementing protocols causing a relevant degradation.

Each sample matrix is different even amongst sediments from different origins or water samples from different marine or freshwater environments. Thus, pre-tests with different digestion protocols are highly recommend to achieve best digestion results with simultaneous consideration of the best possible protection of the targeted plastic particles. This often requires a multi-stage process in which several digestion solutions are applied sequentially. As a rule, intermediate rinsing must be carried out between the respective dosages, which in turn involves the risk of increased contamination.

Nevertheless, in larger-scale studies, e.g., examining an entire ecosystem and different matrices, care should be taken to ensure the greatest possible methodological homogeneity even within sample digestion, so that comparable data sets provide a representative overall picture.

We understand our results as a modular system, which makes it possible to develop a suitable sample-specific protocol (**Figure 3**). The first step in sample preparation should be an evaluation of the composition of the biogenic organic matter. On this basis, the suitable digestion solution(s) can then be selected and the efficiency of the method can be optimized, e.g., by combining several digestion stages and/or slightly increasing the reaction temperature.

DATA AVAILABILITY STATEMENT

The original contributions presented in the study are included in the article/**Supplementary Material**, further inquiries can be directed to the corresponding author/s.

AUTHOR CONTRIBUTIONS

FP and EF contributed equally to the investigation, conception of the experimental setup, conducting laboratory experiments, and equal contribution to the manuscript. FP calculated the

results, standardized values, and developed the included figures. All authors contributed to the article and approved the submitted version.

ACKNOWLEDGMENTS

The authors would like to thank Philip John Mordecai for help on extensive lab experiments on biogenic organic matter samples and Elena Hengstmann and Matthias Tamminga for their useful comments on an earlier version of the manuscript.

SUPPLEMENTARY MATERIAL

The Supplementary Material for this article can be found online at: https://www.frontiersin.org/articles/10.3389/fenvs.2020.572424/full#supplementary-material

REFERENCES

Avio, C. G., Gorbi, S., and Regoli, F. (2015). Experimental development of a new protocol for extraction and characterization of microplastics in fish tissues: first observations in commercial species from Adriatic Sea. *Mar. Environ. Res.* 111, 18–26. doi: 10.1016/j.marenvres.2015.06.014

Catarino, A. I., Thompson, R., Sanderson, W., and Henry, T. B. (2017). Development and optimization of a standard method for extraction of microplastics in mussels by enzyme digestion of soft tissues: standard method for microplastic extraction from mussels. *Environ. Toxicol. Chem.* 36, 947–951. doi: 10.1002/etc.3608

Claessens, M., Van Cauwenberghe, L., Vandegehuchte, M. B., and Janssen, C. R. (2013). New techniques for the detection of microplastics in sediments and field collected organisms. *Mar. Pollut. Bull.* 70, 227–233. doi: 10.1016/j.marpolbul.2013.03.009

Cole, M., Webb, H., Lindeque, P. K., Fileman, E. S., Halsband, C., and Galloway, T. S. (2015). Isolation of microplastics in biota-rich seawater samples and marine organisms. *Sci. Rep.* 4:4528. doi: 10.1038/srep04528

Collard, F., Gilbert, B., Eppe, G., Parmentier, E., and Das, K. (2015). Detection of anthropogenic particles in fish stomachs: an isolation method adapted to identification by Raman spectroscopy. *Archiv. Environ. Contamin. Toxicol.* 69, 331–339. doi: 10.1007/s00244-015-0221-0

Dehaut, A., Cassone, A.-L., Frère, L., Hermabessiere, L., Himber, C., Rinnert, E., et al. (2016). Microplastics in seafood: benchmark protocol for their extraction and characterization. *Environ. Pollut.* 215, 223–233. doi: 10.1016/j.envpol.2016.05.018

Duan, J., Han, J., Zhou, H., Lau, Y. L., An, W., Wei, P., et al. (2020). Development of a digestion method for determining microplastic pollution in vegetal-rich clayey mangrove sediments. *Sci. Total Environ.* 707:136030. doi: 10.1016/j.scitotenv.2019.136030

Enders, K., Lenz, R., Beer, S., and Stedmon, C. A. (2017). Extraction of microplastic from biota: recommended acidic digestion destroys common plastic polymers. *ICES J. Mar. Sci.* 74, 326–331. doi: 10.1093/icesjms/fsw173

Foekema, E. M., Gruijter, C. D., Mergia, M. T., van Franeker, J. A., Murk, A. T. J., and Koelmans, A. A. (2013). Plastic in North Sea Fish. *Environ. Sci. Technol.* 47, 8818–8824. doi: 10.1021/es400931b

Harrison, J. P., Hoellein, T. J., Sapp, M., Tagg, A. S., Ju-Nam, Y., and Ojeda, J. J. (2018). "Microplastic-associated biofilms: a comparison of freshwater and marine environments," in *Freshwater Microplastics*, eds M. Wagner and S. Lambert (Cham: Springer), 181–201.

Hengstmann, E., Tamminga, M., vom Bruch, C., and Fischer, E. K. (2018). Microplastic in beach sediments of the Isle of Rügen (Baltic Sea)–implementing a novel glass elutriation column. *Mar. Pollut. Bull.* 126, 263–274. doi: 10.1016/j.marpolbul.2017.11.010

Herrera, A., Garrido-Amador, P., Martínez, I., Samper, M. D., López-Martínez, J., Gómez, M., et al. (2018). Novel methodology to isolate microplastics from vegetal-rich samples. *Mar. Pollut. Bull.* 129, 61–69. doi: 10.1016/j.marpolbul.2018.02.015

Hurley, R. R., Lusher, A. L., Olsen, M., and Nizzetto, L. (2018). Validation of a method for extracting microplastics from complex, organic-rich, environmental matrices. *Environ. Sci. Technol.* 52, 7409–7417. doi: 10.1021/acs.est.8b01517

Karami, A., Golieskardi, A., Choo, C. K., Romano, N., Ho, Y. B., and Salamatinia, B. (2017). A high-performance protocol for extraction of microplastics in fish. *Sci. Total Environ.* 578, 485–494. doi: 10.1016/j.scitotenv.2016.10.213

Lulu, L., Junhao, Q., Zihua, Y., Daihuan, C., Chunxia, Z., Pengzhi, H., et al. (2019). A simple method for detecting and quantifying microplastics utilizing fluorescent dyes–Safranine T, fluorescein isophosphate, Nile red based on thermal expansion and contraction property. *Environ. Pollut.* 255:113283, doi: 10.1016/j.envpol.2019.113283

Lusher, A. L., Welden, N. A., Sobral, P., and Cole, M. (2017). Sampling, isolating and identifying microplastics ingested by fish and invertebrates. *Anal. Methods* 9, 1346–1360. doi: 10.1039/C6AY02415G

Möller, J. N., Löder, G. J., and Laforsch, C. (2020). Finding microplastics in soils: a review of analytical methods. *Environ. Sci. Technol.* 54, 2078–2090. doi: 10.1021/acs.est.9b04618

Munno, K., Helm, P. A., Jackson, D. A., Rochman, C., and Sims, A. (2018). Impacts of temperature and selected chemical digestion methods on microplastic particles. *Environ. Toxicol. Chem.* 37, 91–98. doi: 10.1002/etc.3935

Naidoo, T., Goordiyal, K., and Glassom, D. (2017). Are nitric acid (HNO_3) digestions efficient in isolating microplastics from juvenile fish? *Water Air Soil Pollut.* 228:470. doi: 10.1007/s11270-017-3654-4

Nuelle, M. T., Dekiff, J. H., Remy, D., and Fries, E. (2014). A new analytical approach for monitoring microplastics in marine sediments. *Environ. Pollut.* 184, 161–169. doi: 10.1016/j.envpol.2013.07.027

Prata, J. C., da Costa, J. P., Duarte, A. C., and Rocha-Santos, T. (2019). Methods for sampling and detection of microplastics in water and sediment: a critical review. *Trends Anal. Chem.* 110, 150–159. doi: 10.1016/j.trac.2018.10.029

R Core Team (2017). *R: A Language and Environment for Statistical Computing*. Available online at: https://www.R-project.org/

Roch, S., and Brinker, A. (2017). Rapid and efficient method for the detection of microplastic in the gastrointestinal tract of fishes. *Environ. Sci. Technol.* 51, 4522–4530. doi: 10.1021/acs.est.7b00364

RStudio Team (2016). *RStudio: Integrated Development for R.* Boston, MA: RStudio, PBC. Available online at: http://www.rstudio.com/

Rummel, C. D., Jahnke, A., Gorokhova, E., Kühnel, D., and Schmitt-Jansen, M. (2017). Impacts of biofilm formation on the fate and potential effects of microplastic in the aquatic environment. *Environ. Sci. Technol. Lett.* 4, 258–267. doi: 10.1021/acs.estlett.7b00164

Wiggin, K. J., and Holland, E. B. (2019). Validation and application of cost and time effective methods for the detection of 3-500 μm sized microplastics in the urban marine and estuarine environments surrounding Long Beach, California. *Mar. Pollut. Bullet.* 143, 152–162. doi: 10.1016/j.marpolbul.2019.03.060

Conflict of Interest: The authors declare that the research was conducted in the absence of any commercial or financial relationships that could be construed as a potential conflict of interest.

frontiers in Marine Science

ORIGINAL RESEARCH
published: 18 January 2021
doi: 10.3389/fmars.2020.578178

Nanofragmentation of Expanded Polystyrene Under Simulated Environmental Weathering (Thermooxidative Degradation and Hydrodynamic Turbulence)

Karin Mattsson, Frida Björkroth, Therese Karlsson and Martin Hassellöv*

Department of Marine Sciences, Kristineberg Marine Research Station, University of Gothenburg, Fiskebäckskil, Sweden

Fragmentation of macroplastics into microplastics in the marine environment is probably one of the processes that have generated most drive for developing the microplastics research field. Thus, it is surprising that the level of scientific knowledge on the combinative effect of oxidative degradation and mechanical stressors on fragmentation is relatively limited. Furthermore, it has been hypothesized that plastic fragmentation continues into the nanoplastic size domains, but environmentally realistic studies are lacking. Here the effects of thermooxidative aging and hydrodynamic conditions relevant for the shoreline environment on the fragmentation of expanded polystyrene (EPS) were tested in laboratory simulations. The pre-degraded EPS was cut into pieces and subjected to mechanical, hydrodynamic simulations during four-day stirring experiments. Subsamples were filtered and subsequently analyzed with light microscopy with automated image analysis particle size distribution determinations, polymer identification with Raman spectroscopy, Scanning Electron Microscopy (SEM) with automated image analysis particle size distribution. The nanoplastic size fraction was measured using nanoparticle tracking analysis. In addition, the degree of polymer oxidation was spectroscopically characterized with Fourier transform infrared (FTIR) spectroscopy. The results illustrate that fragmentation of the mesoplastic objects is observed already after 2 days, but that is more distinct after 4 days, with higher abundances for the smaller size fractions, which imply more release of smaller sizes or fragmentation in several steps. For the nanoplastic fraction, day four shows a higher abundance of released or fragmented particles than day two. The conclusions are that nanofragmentation is an important and understudied process and that standardized test protocols for both thermooxidative degradation and mechanical treatments mimicking realistic environmental conditions are needed. Further testing of the most common macro- and mesoplastic materials to assess the rates and fluxes of fragmenting particles to micro- and nanoplastic fractions should be conducted.

Keywords: nanofragmentation, environmental weathering, polystyrene, thermooxidative aging, hydrodynamic turbulence, Raman spectroscopy, FTIR, SEM

OPEN ACCESS

Edited by:
Andrew Turner,
University of Plymouth,
United Kingdom

Reviewed by:
Ilaria Corsi,
University of Siena, Italy
Christian Laforsch,
University of Bayreuth, Germany

****Correspondence:***
Karin Mattsson
email@uni.edu;
karin.mattsson@gu.se

Specialty section:
This article was submitted to Marine Pollution, a section of the journal Frontiers in Marine Science

Received: *30 June 2020*
Accepted: *28 December 2020*
Published: *18 January 2021*

Citation:
Mattsson K, Björkroth F, Karlsson T and Hassellöv M (2021) Nanofragmentation of Expanded Polystyrene Under Simulated Environmental Weathering (Thermooxidative Degradation and Hydrodynamic Turbulence). Front. Mar. Sci. 7:578178. doi: 10.3389/fmars.2020.578178

INTRODUCTION

Plastic debris in a large variety of sizes can be found in all ecosystems around the world. Plastic particles between 1 and 10 mm are referred to as mesoplastics, while plastic particles between 1 and 1,000 μm are called microplastics, and nanoplastics are plastic particles with a size between 1 and 1,000 nm (Hartmann et al., 2019). Microplastics have been reported to compose the majority of the numerical abundance of the marine debris (Browne et al., 2010; Hidalgo-Ruz et al., 2012; Goldstein et al., 2013). Microplastics are present in the marine environments as primary particles or as secondary particles. Primary particles are plastic particles manufactured in the micrometer size range, such as virgin plastic pellets or powders, whereas secondary particles are fragments from larger ones. Most microplastic particles in the marine environment are secondary particles, i.e., fragments from larger pieces (Brandon et al., 2016; Song et al., 2017) with a higher abundance for the lower size classes (Enders et al., 2015; Ter Halle et al., 2016; Primpke et al., 2017). Moreover, microplastics collected from the environment and analyzed with Scanning Electron Microscopy (SEM) or spectroscopic techniques such as Fourier transform infrared (FTIR) Spectroscopy show that particles can be in an advanced state of weathering (Cooper and Corcoran, 2010).

Plastic particles in the environment are subjected to degradation, a chemically, physically, or biologically introduced process, and one consequence is the creation of smaller particles (Andrady, 2011). One important degradation process for floating plastic particles in the ocean, such as expanded polystyrene (EPS), is photooxidative degradation initiated by UV-radiation (Gewert et al., 2015; Weinstein et al., 2016). The PS absorbs light *via* the aromatic phenyl groups, and the energy is transferred to the nearest C-H bond, where it causes a bond braking, and free radicals are formed. The final products of the polymer radical reaction are the formation of ketones and olefins, while the main products of PS are styrene monomers since end-chain scission is predominant. However, oligomers of styrene can also be formed. The same process occurs when plastic particles are exposed to thermooxidation except that the bond-breaking process is catalyzed by heat instead of light. Mechanical fragmentation occurs when the particles are subject to mechanical stress from waves, rocks, sand, and other forces or substances that the polymer can interact with in the ocean. Biological degradation is when microorganisms such as bacteria and fungi degrade the plastics through extracellular or intracellular enzymes and use the plastics as a substrate for growth. However, biodegradation is complex and not fully understood (Ho et al., 2018).

UV-radiation causes degradation of PS particles and creates particles in the nanometer size range (Lambert and Wagner, 2016a,b) with increasing particle concentration with decreasing size (Lambert and Wagner, 2016b). However, when in the marine environment, this degradation process is slow compared to in air (Kalogerakis et al., 2017; Cai et al., 2018; Julienne et al., 2019) or in pure water (Cai et al., 2018). Moreover, the fragmentation increases for particles when exposed to water compared to in the air (Julienne et al., 2019). Comparing onshore and nearshore conditions show more fragmentation when exposed to nearshore conditions (Kalogerakis et al., 2017). The degree of degradation increases over time (Lambert and Wagner, 2016a; Cai et al., 2018) as well as the creation of cracks and flakes on the particle surface (Weinstein et al., 2016; Cai et al., 2018; Julienne et al., 2019). Extremely ruff mechanical forces, e.g., the force from a kitchen blender has also been shown to create PS nanoplastic particles (Ekvall et al., 2019). More environmentally relevant mechanical forces, e.g., the force from a rotating mixer filled with water and sediment mimicking a breaking wave in the swash zone, shows that EPS particles fragment linear while PS pellets fragmented in a quad dependent size over time (Efimova et al., 2018). There is also a correlation between the sediment particles' size and the fragmentation pattern, where larger sediment particles lead to more fragmentation (Chubarenko et al., 2020). However, both swash zone studies only considered particle sizes down to 0.5 mm (Efimova et al., 2018; Chubarenko et al., 2020). In another study, plastic pellets have been exposed during 3 years to conditions mimicking plastics exposure on beaches, benthic environments, and floating on the sea surface. They report a non-linear aging pattern for the degradation over time when analyzing the chemical bonds with FTIR (Brandon et al., 2016). However, in general, during the first 13 months, the particles mimicking floating plastics showed more degradation than the other treatments (Brandon et al., 2016), while the combination of UV-radiation with mechanical abrasion shows that, in general, the more prolonged exposure to UV-radiation creates more fragments and that the number of fragmented particles increased with decreasing particle size (Song et al., 2017). Biodegradation also occurs in the environment (Zettler et al., 2013), and for PS, it occurs in natural environments but at a prolonged rate (Ho et al., 2018). Moreover, terrestrial insects from polar environments can feed on EPS and ingest small fragments (Bergami et al., 2020).

The weathering of plastics generates smaller particles; however, how these particles fragment and the time scales for weathering plastic in the marine environment is not well studied or known. Moreover, the parameters that affect the fragmentation pattern are not known or the links between the polymer's exposure, nature, and its manufacturing process. We analyze the size distribution of weathering EPS particles under environmentally relevant conditions by using pre-degraded EPS by thermooxidation combined with hydrodynamic turbulence. EPS was chosen since it is commonly found in the environment (Hidalgo-Ruz et al., 2012), and prone to fragment (Efimova et al., 2018).

MATERIALS AND METHODS

Particle Preparation and Thermal Oxidation Analysis

The polystyrene plastics originated from a conventional EPS packaging foam from an insulation box. The EPS was degraded in an oven at 80°C for 20 days. The thermal oxidation of EPS was verified by FTIR using the Thermo Scientific Nicolet iN10

infrared microscope. Three pieces were cut from the surface of the degraded EPS, and from the surface of the original, undegraded EPS and the absorption spectrum were recorded. All spectra were baseline corrected. The absorption spectrum of the degraded EPS was normalized to the peak at 3,028 cm^{-1}, which corresponds to the C-H stretch in the average spectra of the undegraded spectra. The average area of the OH peaks (3,741–3,134 cm^{-1}) for both the undegraded and degraded EPS spectrum was integrated, and the area was compared. Thereafter, the degraded EPS was cut by hand into pieces sized 5 × 5 mm. The thickness of the EPS varied between 1–2 mm and 20 pieces of EPS weighted 0.028 ± 0.0024 g. All plastics were stored in the refrigerator to decrease unwanted further degradation.

Fragmentation

To determine the time needed to create a suitable amount of fragmented particles, four fragmentation experiments with different fragmentation times were performed, 1, 2, 4, and 9.5 days. After evaluating the results, 2 and 4 days were concluded to be sufficient.

Initially, five 1 L-beakers were filled with 750 mL Milli-Q water together with 20 pieces of EPS. Two beakers were kept without plastics, serving as blank controls. The beakers containing plastic were placed in the flocculator, creating circle motion turbulence by paddles spinning at 250 rpm. The speed of 250 rpm was calculated to the Kolmogorov dissipation length scale to about 0.09 mm by using the following equation

$$\eta = \left(\frac{\nu^3}{\varepsilon}\right)^{\frac{1}{4}}$$

where η is the Komogorov dissipation length, ν is the viscosity of the fluid, and ε is the average rate of dissipation energy per mass. The energy dissipation rate (ε) was estimated to be 0.019 mm, calculated from the ε = 0.023 mm at 300 rpm (Sulc et al., 2015), and with Milli-Q water's viscosity 1.004×10^{-6} $m^{2/s}$. All beakers were covered with aluminum foil, and the open side of the flocculator was wrapped in plastic to prevent contamination. The two beakers without plastics were placed beside the flocculator, also covered in aluminum foil and plastic. After 2 days of fragmentation, the paddles were removed from the beakers and rinsed with 50 mL Milli-Q water to release any particles stuck on their surfaces. For the blanks, 50 mL of Milli-Q water was added. All beakers were then covered in aluminum foil and placed in the refrigerator until filtering. Next, the fragmentation was repeated, but the experiment lasted for 4 days. Finally, the fragmentation was repeated for both times, with the control beakers placed inside the flocculator.

Filtration

Initially, the filter set-up had three filters, 1000, 300, and 10 μm. The 1,000 μm metal sieve was chosen to collect the 5 × 5 mm start pieces. The 300 μm mesh was chosen since it is a common size for microplastic sampling, and as an addition, 10 μm polycarbonate filters (Millipore Isopore 1 μm) were used. The remaining water with the smaller sized particles was kept for further analysis with Nanoparticle Tracking Analysis (NTA). However, when the experiment was repeated, two filters were added to the set-up; 1 μm and 200 nm. For the 1 μm, polycarbonate filters (Millipore Isopore 1 μm) were used where half of the number of filters were coated with a 100 nm thick aluminum layer. The 200 nm filters were made of aluminum oxide (Whatman Anopore).

Particle Characterization

Photo Characterization

Photo characterization was used to characterize the formed microplastics' size distributions on the 300 and 10 μm filters. The photo characterization was carried out with a Lecia MZ16 A Stereomicroscope and the software ImageJ (version 1.51j8). All photos were analyzed for each sample, but some were excluded due to blurriness or lack of particles. The Petri dishes containing the samples were put on a dark blue background, and 5–7 photos were taken under the stereomicroscope. The dark background made it easier to distinguish the white microplastics. Firstly, the contrast was enhanced by allowing 0.30% of the pixels to become saturated. Secondly, the color threshold was adjusted, so just the particles were selected. Lastly, the function Analyze Particles was used to measure the area, the major and minor axis, and the maximum Feret diameter of each microplastic. The algorithm used replaced the particle's area with the best fitting two-dimensional ellipse, and the major and minor axis was then measured. Hence the ellipse had the same area as the area measured. The microplastics in contact with the edges of the photo were excluded. The measured microplastics' mask was also controlled to ensure the background and light flicker was fully excluded. The replicates' microplastics were summed for EPS and the blanks each for the 2 and 4-day fragmentation to get enough data in the size bins to create number-based size distributions. For the 300 and 10 μm samples, binwidth 300 and 50 μm were used respectively.

Raman Spectroscopy

The pre-degraded EPS pieces, the particles collected in the 1,000 μm sieve, and on all filters were analyzed with Raman spectroscopy on a WiTec alpha300 R microscope equipped with a 532 nm laser. First, a confocal mosaic image was obtained, and then a Raman spectrum from the particles was recorded. Laser power depending on the size of the particles since different objectives (5x, 20x, and 100x) were used, and 50 accumulations of spectra with an integration time of 0.5 s were recorded. These spectra were baseline corrected and compared to identify any spectral changes. On the 1 μm filter, many particles were analyzed to distinguish between EPS particles and contamination.

Scanning Electron Microscopy

The EPS particles' size present on 1 μm filters was imaged in SEM (Zeiss Sigma VP) in VP mode (30 Pa) using the BSD detector with a magnification of 3.5 kX and EHT 15 kV. With the confocal mosaic image obtained from the Raman microscope and the Raman spectra from the particles, a brightness-contrast

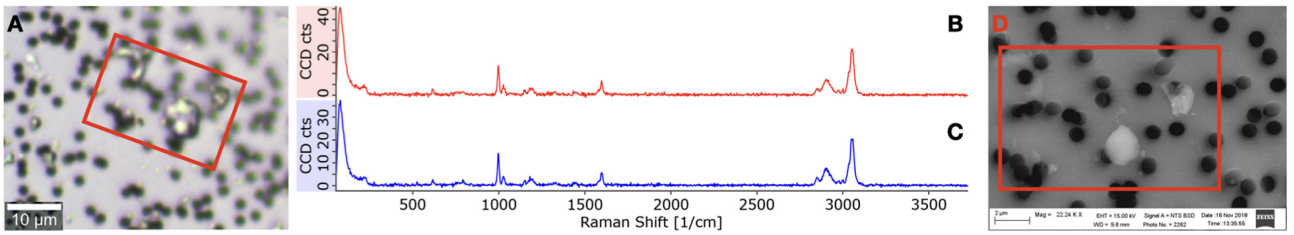

FIGURE 1 | Raman-SEM identification for 1 µm membranes. **(A)** A confocal image of EPS particles obtained with the Raman microscope, **(B)** spectrum from the particles in a **(C)** spectrum from the exposed EPS pieces. **(D)** SEM image of the same particles.

threshold was defined, so only EPS particles were analyzed with SEM (**Figure 1**). The software SmartPI was used to automatically image a mosaic of a defined area of the filter. The size of all particles within the area was measured according to the defined brightness-contrast threshold. For the different fragmentation times, 2 and 4 days, a total of 18,287 and 16,989 EPS particles were measured, respectively.

The 200 nm filters were also analyzed with SEM. However, the fragmented particles on these filters were fluffy, and with blurry edges, it was not possible to measure the particles' exact size, so these filters were neglected.

Nanoparticle Tracking Analysis

The instrument Malvern NanoSight LM10 was used for preforming NTA, measuring diffusion coefficients and hydrodynamic diameter of particles in the size range 10–1,000 nm. It is important to note that this instrument cannot distinguish what type of particles it is measuring. Three sub-samples from the collected water were analyzed. Every sub-sample was injected into the laser module chamber, and five videos were recorded over 1 min each, with a 5-s delay in between. After every recording, the sample temperature was noted. In between every sub-sample, the chamber was rinsed with Milli-Q water. The chamber was taken apart and cleaned with a 10% Hellmanex in Milli-Q solution, rinsed with Milli-Q water and dried with a 50% EtOH in Milli-Q solution and compressed air. After that, the software NanoSight (version 2.3) performed a summary analysis of the video batch. An excel macro was used to calculate the concentration in the size bins (binwidth 5 nm). The results from each 1 min recording were manually checked, and outliers were excluded. The EPS concentrations and the blanks were summed each for the 2 and 4-day fragmentations, and concentration based size distributions were computed.

Contamination

To investigate the contamination from the corrosion of the flocculator and the filter set-up, a test with blank beakers inside vs. outside the flocculator was performed. Three beakers were put in the flocculator, and three beakers were put on the outside, all containing 750 mL Milli-Q water. All beakers were covered with aluminum foil and plastic. After 4 days, the samples were filtered through 1,000, 300, and 10 µm and analyzed.

To exclude any contamination from the Milli-Q water produced by the Millipore Milli-Q Reference Water Purification System, the concentration of nanoparticles in the Milli-Q water was measured with NTA.

RESULTS

Contamination

The contamination from the flocculator and/or the filter set-up was black in color for both treatments. As the black fragments could easily be excluded in the photo characterization performed on the 10 µm filters, the contamination was not quantified.

Particles that were not plastics on the 1 µm filters were identified with Raman spectroscopy and SEM-EDX, e.g., iron-rich particles that most likely originated from one of the holders used for the filtration set-up. However, this was not considered to interfere with the results since the plastic particles on these filters were first sorted through polymer identification with Raman spectroscopy and excluded in the SEM automated analysis with a brightness-contrast threshold.

The concentrations of nanoparticles were similar for both treatments $28.74 \pm 16.63 \times 10^6$ and $29.19 \pm 13.86 \times 10^6$ particles/mL for samples inside the flocculator vs. samples outside the flocculator. This concluded that the experiment set-up did not add any nano-sized particles to the samples.

The concentration of nanoparticles in Milli-Q water was 0 particles/mL. It was concluded that the corrosion from the flocculator and the filter-set up did not contaminate the samples with the contamination that could not be excluded in the sample analysis.

Thermal Aging

The absorption peaks found in the spectra for the undegraded EPS at 3,150–3,000 and 3,000–2,800 cm^{-1} correspond to the phenyl group and C-H backbone stretch, respectively (**Figure 2A**). These peaks can also be found in the spectra for the degraded EPS (**Figure 2B**). Additionally, the degraded EPS show absorption around 3,570–3,200 cm^{-1} corresponding to O-H stretch. In the wavelengths 2,000–400 cm^{-1} there is much disturbance in both spectra due to poorly calibrated measurements, but this range is not crucial for estimating degradation state. The hydroxyl bond's integrated area at 3,741–3,134 cm^{-1} for the undegraded EPS was 7.72 area units, whereas, for the degraded EPS, the area was 16.71. This verifies that the

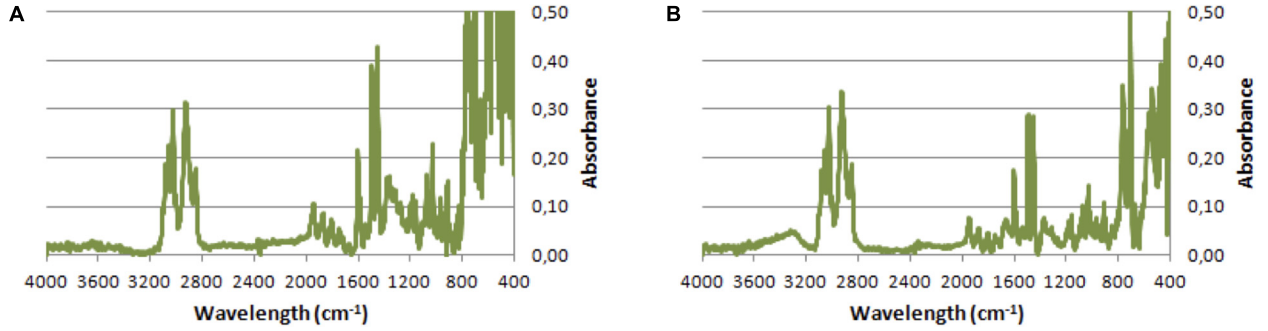

FIGURE 2 | FTIR Absorption spectrum for **(A)** undegraded and **(B)** degraded EPS.

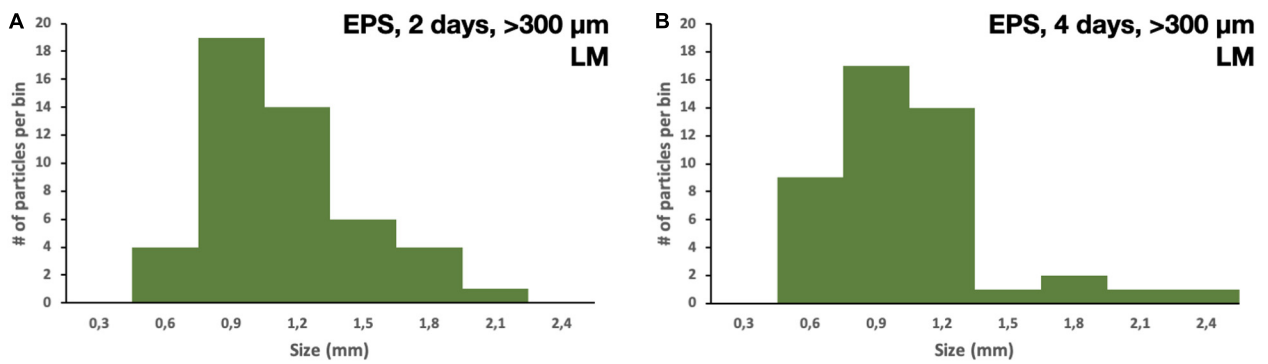

FIGURE 3 | Size distribution of particles collected on the 300 µm filter after **(A)** 2 days of fragmentation and **(B)** 4 days of fragmentation.

degraded EPS was more thermal aged than the undegraded EPS (Andrady, 2017).

Fragmentation

All of the 5 × 5 mm start pieces of EPS were, as expected, collected in the 1,000 µm sieve, and no particles were found in the blanks. On the 300 µm filter, fragments of EPS were collected. After 2 and 4 days of fragmentation, 48 and 45 fragments of microplastics were found, respectively. The particles' size distribution was similar for both times; however, there were more particles of the smaller sizes in the 4 days of fragmentation, 450–750 µm, nine vs. four (**Figures 3A,B**). There were no particles found in the blank samples. More particles were collected on the 10 µm filters, as expected, compared to the 300 µm. The particles' size distribution was similar for both times, with more particles in the smaller size range. However, after 4 days of fragmentation, more particles were present 746 compared to 312 on the 2 days of fragmentation, an increase of 140% (**Figures 4A,B**). There were only 7 and 6 microplastics collected in the blanks after 2 and 4 days of fragmentation, respectively (**Figures 4C,D**). These particles were carried over from the filtration equipment and identified as EPS. The size distribution of the particles on the 1 µm filters was similar for both 2 and 4 days of fragmentation with a higher numerical amount of particles in the smaller size range, where 51% respectively, 49% of the particles were below 3.75 µm (**Figures 5A,B**). Most particles were identified between 2.25 and 4.25 µm, 62%, respectively, 61%. From the water samples, the concentration of EPS particles increased by 114% from 34.35 ± 10.70 × 10^6 to 73.49 ± 23.36 × 10^6 particles/mL (**Figures 6A,B**). The blank samples' concentration was 15.07 ± 9.51 × 10^6 and 9.27 ± 5.92 × 10^6 particles/mL, respectively, a decrease of 38% (**Figures 6C,D**).

DISCUSSION

The degree of weathering can be determined with FTIR and SEM can be used to study the surface structure of the particles and identifying surface changes such as cracks or bacteria growth. We used FTIR to determine the thermal aging degree of the pre-degraded EPS pieces and show that the particles aged when exposed to heat. The size distribution shows a higher abundance for the smaller sized particles; however, for the particles with a size close to the pore size, the number of identified particles was low. On all filters, we measured the particles max ferret value, the longest distance between two parallel tangents on opposite sides of a randomly oriented particle measured for eight different angles. Most of the larger particles had an irregular shape, while for the smaller particles, the shape was more similar to a sphere or elliptical. The irregular sized particles can have one dimension smaller than the pore size and therefore passing through a filter. However, the impact from the particles with a size close to the pore size can be seen in **Figure 7**, where the last measured point

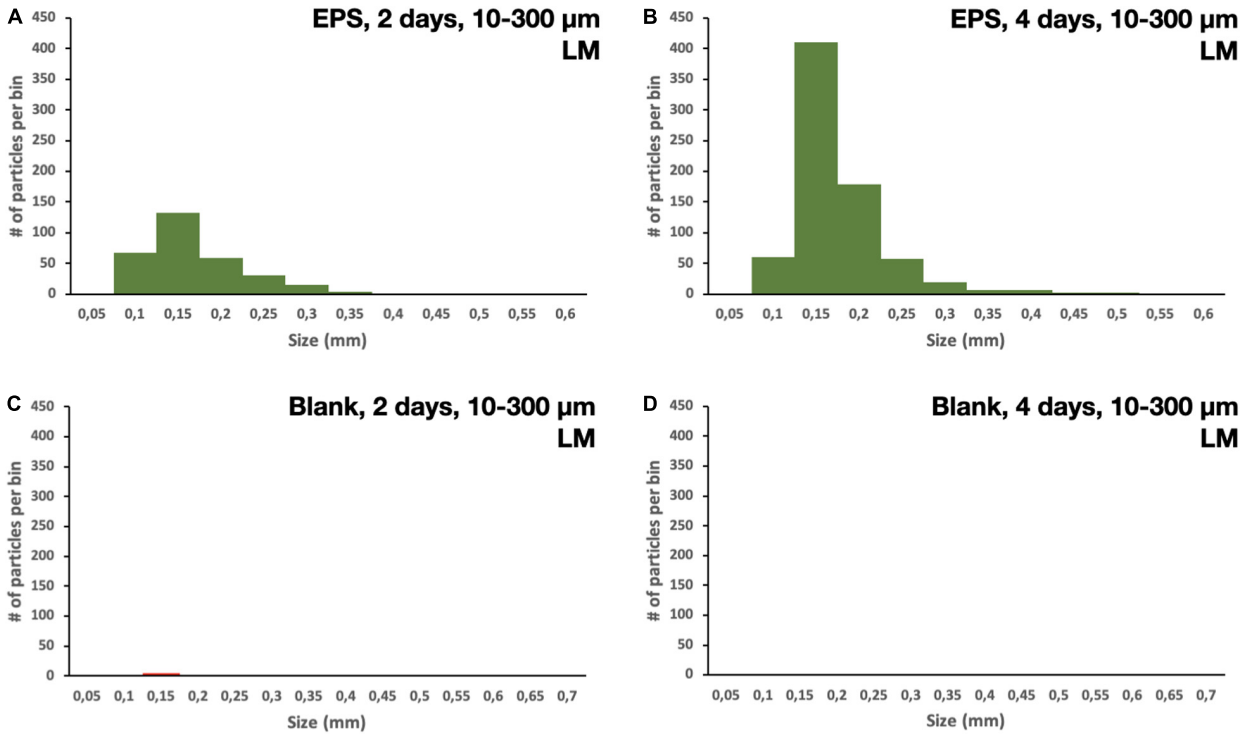

FIGURE 4 | Size distribution of particles collected on the 10 µm filter after **(A)** 2 days of fragmentation, **(B)** 4 days of fragmentation, **(C)** blank samples after 2 days of fragmentation, and **(D)** blank samples after 4 days of fragmentation.

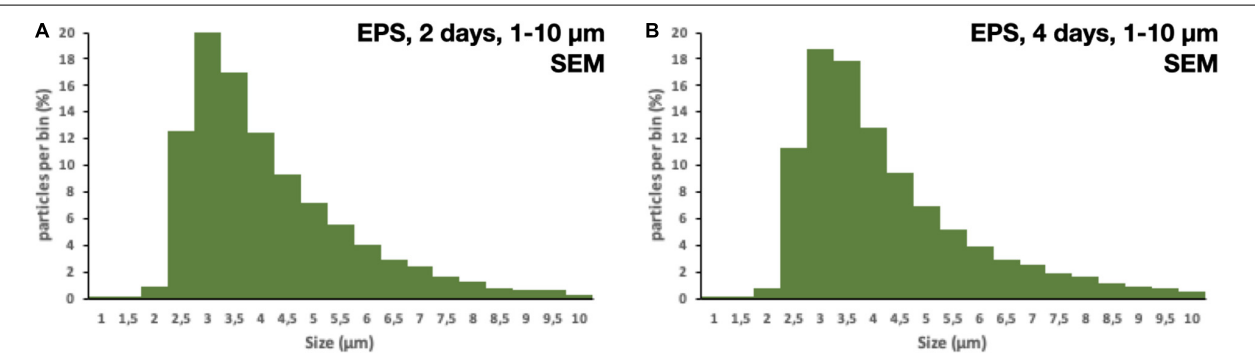

FIGURE 5 | Size distribution of particles collected on the 1 µm filter after **(A)** 2 days of fragmentation and **(B)** 4 days of fragmentation.

on each membrane, i.e., the bin closest to the pore size have a drop in particle amount. For NTA, the hydrodynamic diameter was measured, the diameter of a sphere with the same hydrodynamic behavior as the particle being measured. The size limitations of NTA can be seen in **Figures 6**, **7**, where there are only a few particles measured in the smaller sizes. The NTA data also show a size-dependent fragmentation over time (**Figure 6**).

Even in a controlled laboratory study, contamination from the surroundings poses a threat to interfere with the results. For larger particles, visible through a light microscope, this does not have to interfere with the results. The contamination can be separated from the studied particles by comparing color, size, shape, and other ocular properties. For smaller particles, less than 10 µm, it is more challenging to distinguish between particles and contamination. However, spectroscopic techniques such as Raman or FTIR, which identifies the polymer can be used. For particles in solutions, light scattering techniques such as NTA and Dynamic light scattering (DLS) is widely used which measure the size distribution and concentration of the particles in the solution, but without distinguishing between different types of particles, i.e., the measured concentration can be higher than the actual value. In our experiment, contamination could easily be distinguished from EPS on the 10 µm filter by ocular inspection since the contamination had a different color then what the EPS particles had, black vs. white. The chemical fingerprint of the EPS particles was also confirmed with Raman spectroscopy.

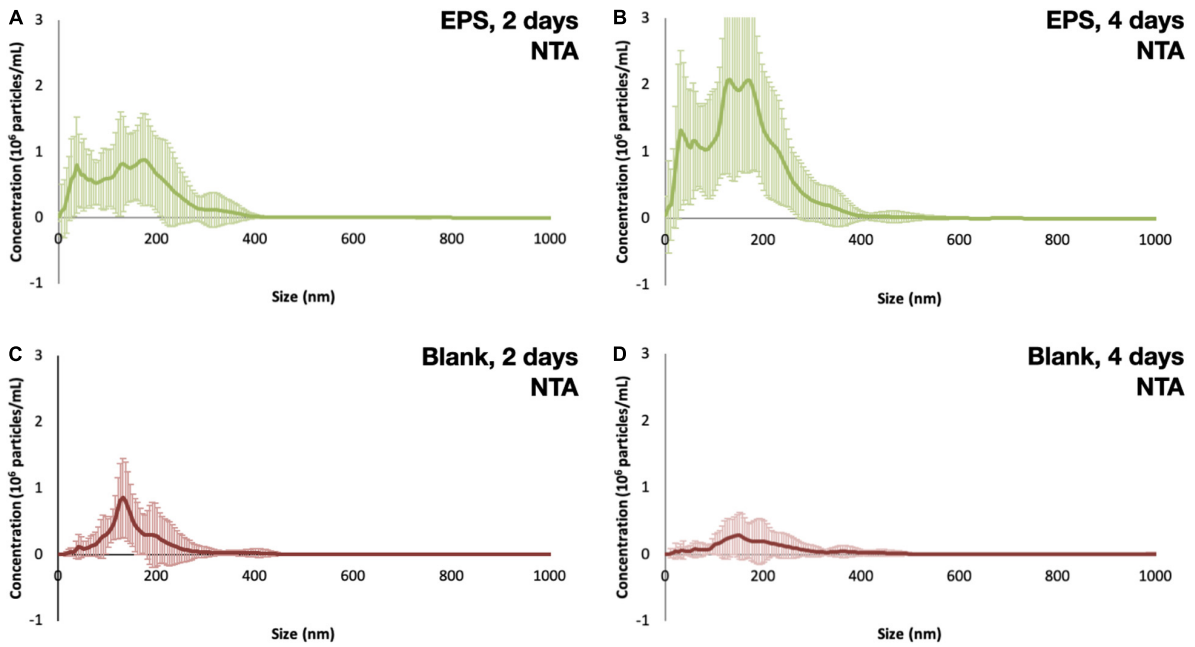

FIGURE 6 | Size distribution of particles measured with NTA after **(A)** 2 days of fragmentation, **(B)** 4 days of fragmentation, **(C)** blank samples after 2 days of fragmentation, and **(D)** blank samples after 4 days of fragmentation.

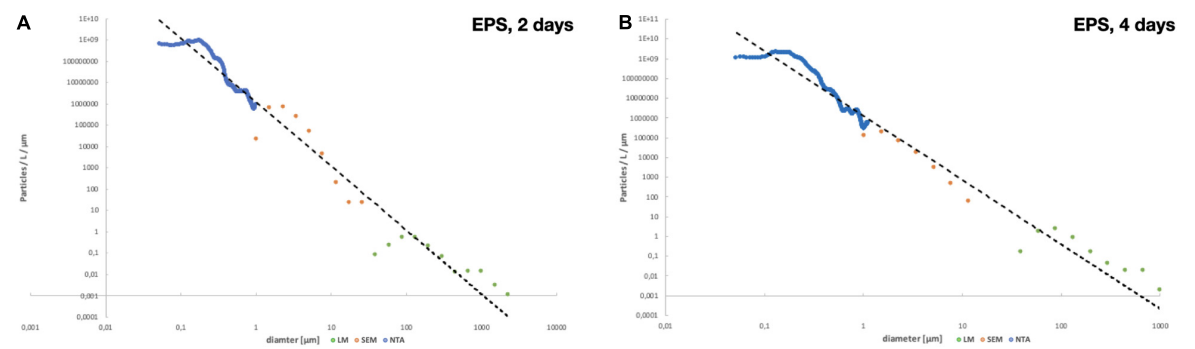

FIGURE 7 | Total size distribution per particles/L/µm after **(A)** 2 days of fragmentation and **(B)** 4 days of fragmentation.

On the 1 µm filter, we first identified the EPS particles with Raman spectroscopy and, together with the confocal image, a threshold in which only registered EPS particles were applied in the SEM to measure the size distribution of the particles on these filters. The nano-sized particles were measured with NTA, and the concentration was compared with blank samples as well as with pure Milli-Q water.

Most studies have only considered one type of degradation; UV (Brandon et al., 2016; Lambert and Wagner, 2016a,b; Cai et al., 2018; Julienne et al., 2019) or mechanical forces (Kalogerakis et al., 2017; Efimova et al., 2018; Ekvall et al., 2019; Chubarenko et al., 2020), and only two has considered a combination of UV and mechanical forces (Weinstein et al., 2016; Song et al., 2017). One has used conditions that are not relevant for the environment (Ekvall et al., 2019); some focus on the characterization of the degree of degradation, and some investigate the fragmentation pattern; however, most studies only consider a small size range (Lambert and Wagner, 2016a,b; Efimova et al., 2018; Ekvall et al., 2019; Julienne et al., 2019; Chubarenko et al., 2020). We have analyzed the thermooxidation, and when exposed to hydrodynamic turbulence. Moreover, the fragmentation pattern was measured for particles larger than 30 nm.

Future developments of more environmentally realistic hydrodynamic reactors would be desirable, that for example, mimics the beach zone under different hydrodynamic and geomorphological conditions.

The insights from these simple simulations of hydrodynamic mixing that can occur in the nearshore environment such as a beach splash zone, illustrate the importance that macro plastic litter such as EPS, is promptly being remediated from the marine environment, e.g., by beach cleaning efforts, in order to minimize

the oxidation-fragmentation reaction chain, that both may inflict more ecosystem impact, but also render the plastic matters virtually impossible to clean-up.

CONCLUSION

For both 2 and 4 days of fragmentation, there was a clear fragmentation pattern with more fragments in the smaller size classes. When comparing what happens over time, the size distribution is similar for both 2 and 4 days of fragmentation for all size classes (**Figures 3–6**). However, the number of particles in size range between 0.025 and 2.7 mm was higher, 993 particles/L for 4 days compared to 446 particles/L after 2 days.

The conclusions are that nanofragmentation is an important and understudied process and that standardized test protocols for both weathering and mechanical treatments mimicking realistic environmental conditions are needed and then further testing of the most common macroplastic materials to assess the rates and fluxes of fragmenting particles to micro- and nanoplastic fractions should be conducted.

DATA AVAILABILITY STATEMENT

The raw data supporting the conclusions of this article will be made available by the authors, without undue reservation.

AUTHOR CONTRIBUTIONS

KM and FB performed the experiment. KM, FB, and MH analyzed the results and wrote the manuscript. All authors designed the experiment.

FUNDING

This research was supported by the Swedish Research Council FORMAS Project Grant #2019-01016, "Nanofragmentation of weathered plastics in marine environment – increased toxicity or biodegradability."

REFERENCES

Andrady, A. L. (2011). Microplastics in the marine environment. *Mar. Pollut. Bull.* 62, 1596–1605. doi: 10.1016/j.marpolbul.2011.05.030

Andrady, A. L. (2017). The plastic in microplastics: a review. *Mar. Pollut. Bull.* 119, 12–22. doi: 10.1016/j.marpolbul.2017.01.082

Bergami, E., Rota, E., Caruso, T., Birarda, G., Vaccari, L., and Corsi, L. (2020). Plastics everywhere: first evidence of polystyrene fragments inside the common Antarctic collembolan *Cryptopygus antarcticus*. *Biol. Lett.* 16:20200093. doi: 10.1098/rsbl.2020.0093

Brandon, J., Goldstein, M., and Ohman, M. D. (2016). Long-term aging and degradation of microplastic particles: comparing in situ oceanic and experimental weathering patterns. *Mar. Pollut. Bull.* 110, 299–308. doi: 10.1016/j.marpolbul.2016.06.048

Browne, M. A., Galloway, T. S., and Thompson, R. C. (2010). Spatial patterns of plastic debris along Estuarine shorelines. *Environ. Sci. Technol.* 44, 3404–3409. doi: 10.1021/es903784e

Cai, L., Wang, J., Peng, J., Wu, Z., and Tan, X. (2018). Observation of the degradation of three types of plastic pellets exposed to UV irradiation in three different environments. *Sci. Total Environ.* 628-629, 740–747. doi: 10.1016/j.scitotenv.2018.02.079

Chubarenko, I., Efimova, I., Bagaeva, M., Bagaev, A., and Isachenko, I. (2020). On mechanical fragmentation of single-use plastics in the sea swash zone with different types of bottom sediments: insights from laboratory experiments. *Mar. Pollut Bull.* 150:110726. doi: 10.1016/j.marpolbul.2019.110726

Cooper, D. A., and Corcoran, P. L. (2010). Effects of mechanical and chemical processes on the degradation of plastic beach debris on the island of Kauai. *Hawaii. Mar. Pollut. Bull.* 60, 650–654. doi: 10.1016/j.marpolbul.2009.12.026

Efimova, I., Bagaeva, M., Bagaev, A., Kileso, A., and Chubarenko, I. P. (2018). Secondary microplastics generation in the sea swash zone with coarse bottom sediments: laboratory experiments. *Front. Mar. Sci.* 5:313. doi: 10.3389/fmars.2018.00313

Ekvall, M. T., Lundqvist, M., Kelpsiene, E., Šileikis, E., Gunnarsson, S. B., Cedervall, T., et al. (2019). Nanoplastics formed during the mechanical breakdown of daily-use polystyrene products. *Nanoscale Adv.* 1, 1055–1061. doi: 10.1039/c8na00210j

Enders, K., Lenz, R., Stedmon, C. A., and Nielsen, T. G. (2015). Abundance, size and polymer composition of marine microplastics >/=10mum in the Atlantic Ocean and their modelled vertical distribution. *Mar. Pollut Bull.* 100, 70–81. doi: 10.1016/j.marpolbul.2015.09.027

Gewert, B., Plassmann, M. M., and MacLeod, M. (2015). Pathways for degradation of plastic polymers floating in the marine environment. *Environ. Sci. Process Impacts.* 17, 1513–1521. doi: 10.1039/c5em00207a

Goldstein, M. C., Titmus, A. J., and Ford, M. (2013). Scales of spatial heterogeneity of plastic marine debris in the northeast pacific ocean. *PLoS One* 8:e80020.doi: 10.1371/journal.pone

Hartmann, N. B., Hüffer, T., Thompson, R. C., Hassellöv, M., Verschoor, A., Daugaard, A. E., et al. (2019). Are we speaking the same language? Recommendations for a definition and categorization framework for plastic debris. *Environ. Sci. Technol.* 53, 1039–1047. doi: 10.1021/acs.est.8b05297

Hidalgo-Ruz, V., Gutow, L., Thompson, R. C., and Thiel, M. (2012). Microplastics in the marine environment: a review of the methods used for identification and quantification. *Environ .Sci. Technol.* 46, 3060–3075. doi: 10.1021/es2031505

Ho, B. T., Roberts, T. K., and Lucas, S. (2018). An overview on biodegradation of polystyrene and modified polystyrene: the microbial approach. *Crit. Rev. Biotechnol.* 38, 308–320. doi: 10.1080/07388551.2017.1355293

Julienne, F., Delorme, N., and Lagarde, F. (2019). From macroplastics to microplastics: role of water in the fragmentation of polyethylene. *Chemosphere* 236:124409. doi: 10.1016/j.chemosphere.2019.124409

Kalogerakis, N., Karkanorachaki, K., Kalogerakis, G. C., Triantafyllidi, E. I., Gotsis, A. D., Partsinevelos, P., et al. (2017). Microplastics generation: onset of fragmentation of polyethylene films in marine environment mesocosms. *Front. Mar. Sci.* 4:84. doi: 10.3389/fmars.2017.00084

Lambert, S., and Wagner, M. (2016a). Characterisation of nanoplastics during the degradation of polystyrene. *Chemosphere* 145, 265–268. doi: 10.1016/j.chemosphere.2015.11.078

Lambert, S., and Wagner, M. (2016b). Formation of microscopic particles during the degradation of different polymers. *Chemosphere* 161, 510–517. doi: 10.1016/j.chemosphere.2016.07.042

Primpke, S., Lorenz, C., Rascher-Friesenhausen, R., and Gerdts, G. (2017). An automated approach for microplastics analysis using focal plane array (FPA) FTIR microscopy and image analysis. *Anal. Methods* 9, 1499–1511. doi: 10.1039/c6ay02476a

Song, Y. K., Hong, S. H., Jang, M., Han, G. M., Jung, S. W., and Shim, W. J. (2017). Combined effects of UV exposure duration and mechanical abrasion on microplastic fragmentation by polymer type. *Environ. Sci. Technol.* 51, 4368–4376. doi: 10.1021/acs.est.6b06155

Sulc, R., Pesava, V., and Ditl, P. (2015). Local turbulent energy dissipation rate in a vessel agitated by a rushton turbine. *Chem. Process Eng.* 36, 135–149. doi: 10.1515/cpe-2015-0011

Ter Halle, A., Ladirat, L., Gendre, X., Goudouneche, D., Pusineri, C., Routaboul, C., et al. (2016). Understanding the fragmentation pattern of marine plastic debris. *Environ. Sci. Technol.* 50, 5668–5675. doi: 10.1021/acs.est.6b00594

Weinstein, J. E., Crocker, B. K., and Gray, A. D. (2016). From macroplastic to microplastic: degradation of high-density polyethylene, polypropylene, and polystyrene in a salt marsh habitat. *Environ. Toxicol. Chem.* 35, 1632–1640. doi: 10.1002/etc.3432

Zettler, E. R., Mincer, T. J., and Amaral-Zettler, L. A. (2013). Life in the "plastisphere": microbial communities on plastic marine debris. *Environ. Sci. Technol.* 47, 7137–7146. doi: 10.1021/es401288x

Conflict of Interest: The authors declare that the research was conducted in the absence of any commercial or financial relationships that could be construed as a potential conflict of interest.

frontiers in Environmental Science

ORIGINAL RESEARCH
published: 21 January 2021
doi: 10.3389/fenvs.2020.560237

Efficiency of Aerial Drones for Macrolitter Monitoring on Baltic Sea Beaches

Gabriela Escobar-Sánchez[1], *Mirco Haseler*[1,2], *Natascha Oppelt*[3] *and Gerald Schernewski*[1,2]*

[1]Coastal Research and Management Group, Leibniz Institute for Baltic Sea Research, Warnemünde, Germany, [2]Marine Research Institute of Klaipėda University, Klaipeda, Lithuania, [3]Department of Geography, Faculty of Mathematics and Natural Sciences, Remote Sensing and Environmental Modelling, Christian-Albrechts Universität zu Kiel, Kiel, Germany

Marine litter is a global problem that requires soon management and design of mitigation strategies. Marine litter monitoring is an essential step to assess the abundances, distributions, sinks and hotspots of pollution as well as the effectiveness of mitigation measures. However, these need to be time and cost-efficient, fit for purpose and context, as well as provide a standardized methodology suitable for comparison among surveys. In Europe, the Marine Strategy Framework Directive (MSFD) provides a structure for the effective implementation of long-term monitoring. For beaches, the well-established 100 m OSPAR macrolitter monitoring exists. However, this method requires a high staff effort and suffers from a high spatio-temporal variability of the results. In this study, we test the potential of aerial drones or Unmanned Aerial Vehicles (UAVs) together with a Geographic Information System approach for semi-automatic classification of meso- (1–25 mm) and macrolitter (>25 mm) at four beaches of the southern Baltic Sea. Visual screening of drone images in recovery experiments (50 m^2 areas) at 10 m height revealed an accuracy of 99%. The total accuracy of classification using object-based classification was 45–90% for the classification with four classes and 50–66% for the classification with six classes, depending on the algorithm and flight height used. On 100 m beach monitoring transects the accuracy was between 39–74% (4 classes) and 25–74% (6 classes), with very low kappa values, indicating that the GIS classification method cannot be regarded as a reliable method for the detection of litter in the Southern Baltic. In terms of cost-efficiency, the drone method showed high reproducibility and moderate accuracy, with much lower flexibility and quality of data than a comparable spatial-OSPAR method. Consequently, our results suggest that drone based monitoring cannot be recommended as a replacement or complement existing methods in southern Baltic beaches. However, drone monitoring could be useful at other sites and other methods for image analysis should be tested to explore this tool for fast-screening of non-accessible sites, fragile ecosystems, floating litter or heavily polluted beaches.

Keywords: cost-efficiency, Image classification, OSPAR, unmanned aerial vehicle, marine litter, marine strategy framework directive, recovery experiment

OPEN ACCESS

Edited by:
Andrew Turner,
University of Plymouth,
United Kingdom

Reviewed by:
Brendan Kelaher,
Southern Cross University, Australia
Corrado Battisti,
Roma Tre University, Italy

***Correspondence:**
Gerald Schernewski
gerald.schernewski@io-warnemuende.de

Specialty section:
This article was submitted to Toxicology, Pollution and the Environment, a section of the journal Frontiers in Environmental Science

Received: *08 May 2020*
Accepted: *11 December 2020*
Published: *21 January 2021*

Citation:
Escobar-Sánchez G, Haseler M, Oppelt N and Schernewski G (2021) Efficiency of Aerial Drones for Macrolitter Monitoring on Baltic Sea Beaches. Front. Environ. Sci. 8:560237. doi: 10.3389/fenvs.2020.560237

INTRODUCTION

The pollution of seas and coasts with marine litter, especially plastics, is a growing global problem (United Nations Environment Programme, 2019). The state of pollution of beaches with macrolitter (>25 mm), and its associated problems are well known and documented for many regions worldwide (Abu-Hilal and Al-Najjar, 2009; Jayasiri et al., 2013; Rosevelt et al., 2013; Topçu et al., 2013; Duhec et al., 2015; Hidalgo-Ruz et al., 2018). In Europe, the pollution of beaches ranges from a few up to more than 1,000 litter items on a 100 m beach stretch, depending on factors such as exposition, accessibility or population density (e.g., Marlin 2013; Gago et al., 2014; Schulz et al., 2015; Schernewski et al., 2017). Here the most common items are plastics, and the main sources of pollution vary between fishing in the North Sea (Schulz et al., 2015) and tourism and recreation in the Mediterranean Sea (Vlachogianni, 2019), Baltic Sea (Schernewski et al., 2017) and North East Atlantic (Schulz et al., 2015).

Marine litter is addressed as one of the UN Sustainable Development Goals (SDG 14.1) aiming at preventing and significantly reducing pollution in the world oceans by 2025 (United Nations, 2019). In order to design mitigation strategies and fulfill SDG 14, as well as national and regional goals timely, managers require monitoring methods that are time and cost-efficient, fit for purpose and context. Although *in-situ* beach litter monitoring is a commonly applied survey worldwide, until today there is no clear consensus on the monitoring strategy to be used and units are difficult to compare (Serra-Gonçalves et al., 2019).

Efforts directed to monitor marine litter and to implement measures for its reduction in Europe have been reflected in the creation of the Marine Strategy Framework Directive (MSFD, 2008/56/EC); a comprehensive legislation to effectively protect the marine environment across Europe, including a detailed implementation procedure. Within this framework, the European Union included marine litter as a descriptor for a Good Environmental Status (GES) to be reached by 2020 (MSFD, 2008/56/EC). The implementation involves an initial assessment of the current environmental status and environmental impact, the determination of the GES, the establishment of environmental targets and associated indicators as well as the development of a monitoring program and cost estimates. Since 2013, a joint, harmonized monitoring strategy is carried out (JRC, 2013) which adapts and further develops the OSPAR Guideline (OSPAR, 2010) and ensures that data is comparable among monitoring surveys. The OSPAR guideline evaluates the trend of abundance of litter over an extended period of time (every 3 months) at sites fulfilling specific criteria, recording the number of items over beach transects of 100 m, from the sea edge to the highest strandline or edge of vegetation, and identifying items according to an item category list (OSPAR, 2010). Although the OSPAR guideline is a flexible and relatively low-cost method that can be carried out with volunteers; it suffers from several weaknesses, being time-intensive, subjective upon litter types, site conditions, frequency of sampling and the training and experience of volunteers and staff (Smith and Markic, 2013; Lavers et al., 2016; Schernewski et al., 2017). This increases the challenge considering the inherent temporal and spatial variability of marine litter subject to beach exposition, winds, currents and distance to pollution sources (Ryan et al., 2009; Critchell and Lambrechts, 2016; Schernewski et al., 2017). As a consequence, Schernewski et al. (2017) conclude for Baltic Sea beaches that the macrolitter beach monitoring method in practice is spatially restricted, does not provide the required reliable data to provide long-term trends and should only serve as a method in combination with others. Optional methods such as the 1 km beach sampling method to monitor marine litter above 50 cm (OSPAR, 2010) or the Rake method (Haseler et al., 2019) focusing on the mesolitter size class, are suitable complementary approaches for Baltic beaches but rarely applied. Therefore, a need for complementary beach litter monitoring methods for macrolitter still exists. Since the MSFD expands the environmental monitoring and reporting requirements, responsible authorities in Europe face the pressure to meet these new demands with limited financial and staff resources (JRC, 2013). Therefore, cost-effectiveness is a pre-condition that additional beach litter monitoring methods must meet.

Aerial drones or Unmanned Aerial Vehicles (UAVs) offer new opportunities for marine litter monitoring and the remote collection of high temporal and spatial resolution data. So far, remote sensing studies have mainly relied on satellite or airplane images to monitor floating marine debris at sea (Veenstra and Churnside, 2012), derelict fishing gear (Moy et al., 2018) and other litter in islands (Kataoka et al., 2018) or after disaster events (Murphy, 2015); however all at much lower spatial resolutions. The higher flexibility and smaller size of UAVs allow capturing images at lower altitudes, obtaining images in cloudy conditions and in narrower areas at higher spatial resolutions, thus collecting more specific information on the surfaces recorded (Pajares, 2015).

Consumer-based drones are nowadays accessible tools used in various environmental purposes, such as monitoring of invasive plant management (Lehmann et al., 2017) or mapping of ecologically sensitive habitats (Ventura et al., 2018). Although their use for scientific purposes is still new and limitations exist, these commercial aerial drones have shown promising results for rapid assessment and mapping of marine litter at beaches. First studies developed abundance and density maps with georeferenced location of specific litter items and hotspots (Hengstmann et al., 2017; Deidun et al., 2018), while most recent studies have tested the potential of machine learning (Atwood et al., 2018; Martin et al., 2018), deep learning approaches (Fallati et al., 2019) and most recently, the combination of photogrammetry, geomorphology, machine learning and hydrodynamic models (Goncalves et al., 2020) for the automatic identification of macrolitter. Based on these findings, drone-based monitoring could have the potential to cover larger spatial scales in less time, provide with standardized units of litter abundance and assess distribution patterns and pollution hotspots. Thus, it already seems reasonable to assess the potential of consumer UAVs for regular and official beach monitoring in practice.

The purpose of this study is to evaluate the applicability of commercial aerial drones for the implementation of long-term

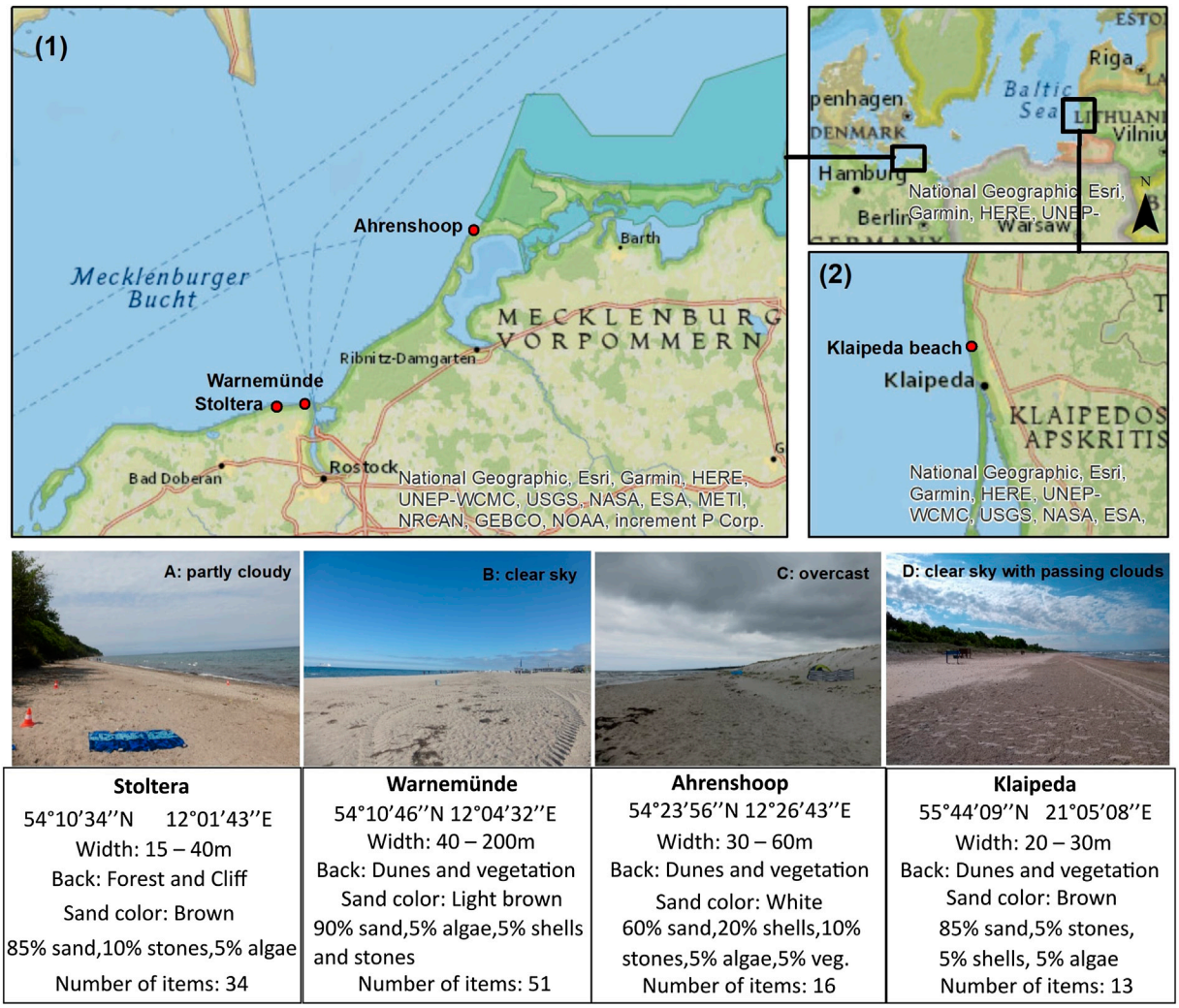

FIGURE 1 | Study sites for drone mapping and *in-situ* data collection of beach litter in the Southern Baltic Sea, specifically Germany (1) **(A)**: Stoltera, **(B)**: Warnemünde, **(C)**: Ahrenshoop) and Lithuania (2) **(D)**: Klaipeda).

monitoring strategies within regional environmental agencies in the Southern Baltic Sea. Nonetheless, this evaluation could also serve as a template for the evaluation of drone-based monitoring for other regions. Here, we intend to answer: could drone-based monitoring complement the 100 m OSPAR method to extend its spatial coverage and provide a pollution pattern over e.g. an entire coastline? We 1) explore and test an UAV approach for marine litter monitoring of meso- (1–25 mm) and macrolitter (>25 mm) with a GIS based semi-automatic object-based classification; 2) apply this methodology at four different southern Baltic beaches and 3) evaluate its suitability and cost-efficiency as a complementary method in monitoring programs.

METHODOLOGY

Study Sites

The Baltic Sea is an enclosed sea with a population of 90 million people and 15 major coastal cities, 10 main rivers (Marlin, 2013) and with an economy that highly focuses on tourism, with cruises and ferries frequently transporting people and goods across the sea, and to a smaller extent on fishing and shipping (HELCOM, 2017). Four beaches in the southern Baltic Sea, three in northeastern Germany and one in Lithuania, were selected for the study (**Figure 1**). Beaches were selected based on their accessibility and for presenting different beach geomorphology, sand color, background substrate (i.e. stones, shells, algae and vegetation) and level of tourism. Two of the sites, Warnemünde and Klaipeda, are urban beaches. Stoltera and Ahrenshoop are peri-urban beaches located close to Nature Conservation Areas. Beach visitors and hikers were present in different quantities at all sites during the sampling time.

Aerial images were captured under different weather conditions (**Figure 1**). At all German beaches, official cleaning activities takes place regularly. In Stoltera and Warnemünde, cleaning occurred every day from 5–9 a.m. during high season and three times per week during low season. This is carried out

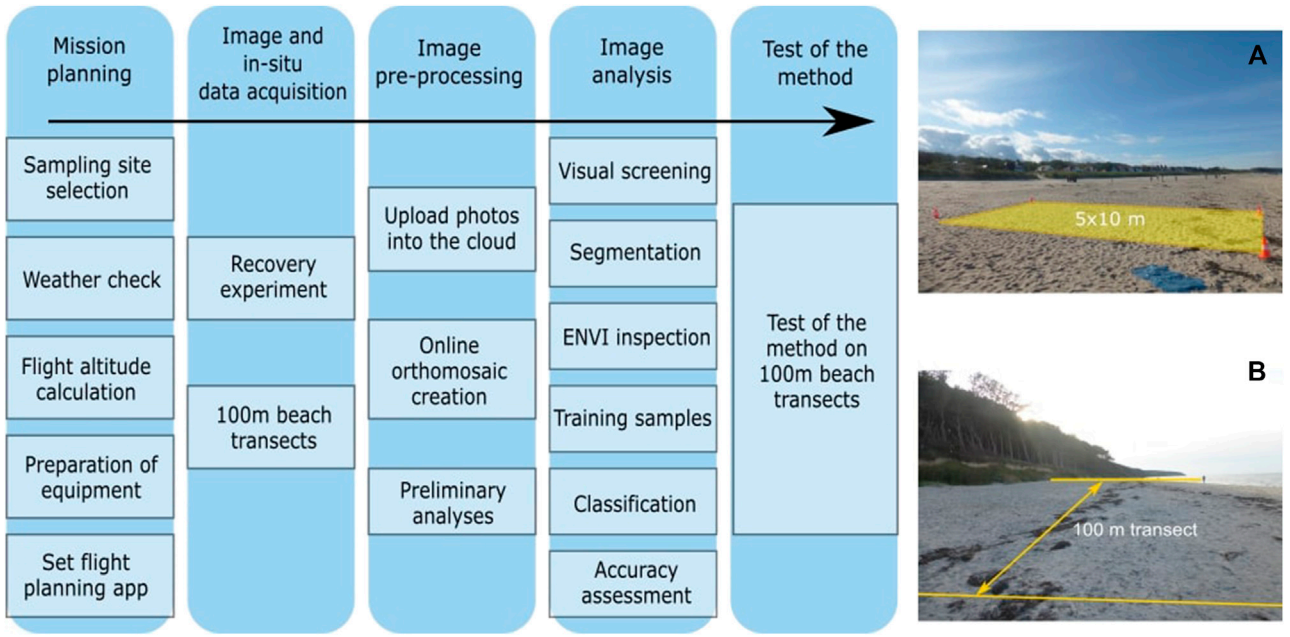

FIGURE 2 | (1) Workflow for drone-based monitoring and object-based supervised classification based on five main steps, each with separate single steps to follow. (2) Set up for sampling of the recovery experiment **(A)** and 100 m beach transects **(B)**. In the recovery experiments, selected items (based on most common items found in the Baltic region) were placed in a cleaned area of 5 × 10 m. The 100 m monitoring was based on OSPAR guidelines. After drone mapping of the zone, litter was collected on the area from the intertidal to the back of the beach with two people and then counted and classified according to the OSPAR list of items.

with a mechanical vehicle ("Beach Tech 2000") which removes litter and seaweed and is able to clean 22,000 m^2 per hour (pers. com. Rostocker Gehwegreinigung, July 2019; Tourismuszentrale, 2019). In Ahrenshoop, regular cleaning takes place by hand two times a week during high season (June–September) and no cleaning the rest of the year (pers. com. Kurverwaltung Ahrenshoop, October 2020). In Klaipeda, the beach belongs to the protected area "Coastal Region Park" and cleaning takes place only after extreme weather events (pers. com. A. Balciunas, 2019). In addition, removal of beach litter is also carried out by NGOs at all sites, serving as environmental awareness raising mechanisms (e.g., Battisti and Gippoliti, 2019).

Equipment and Software

Study areas were mapped with a low cost quadcopter DJI Phantom four Pro V2.0 with an integrated RGB CMOS camera of 20 Megapixels (focal length 8.8 mm) to develop and test an UAV-based approach for marine litter monitoring of meso- (1–25 mm) and macrolitter (>25 mm). The drone had a GPS/GLONASS system with a hover accuracy of ±0.5 m (vertical) and ±1.5 m (horizontal), a gimbal unit to provide near nadir observations and obstacle avoidance, automatic flight and Return To Home (RTH) features. A controller, which uses a smartphone device as display, allows monitoring of battery life and drone status. In this study, two smartphone devices (Android and iOS) were tested to run the flight mapping apps and fly the drone. PolarPro ND filters were used to adjust shutter speed under different light conditions, with ND 8 for cloudy, ND 16 for sunny and ND 32 for very sunny conditions.

For mapping, two apps were tested: DroneDeploy v.3.13.1 and Pix4D Capture v.4.5.0. The apps set the mapping area, flight altitude, speed, field of view (FOV), front and side overlap and create an orthomosaic with the images obtained. Agisoft Metashape was used for image stitching for one orthomosaic where neither of the mapping apps provided satisfactory results, using a standard process of photo alignment which uses images and point cloud data to create mosaics or 3D data (Agisoft, 2020). Moreover, the geospatial analysis software ENVI 5.3 and ArcGIS v.10.5 were used for image analyses. ENVI 5.3 served to explore the spectral signatures of different objects in the image, while ArcGIS v.10.5 was used to carry out supervised object-based classification.

Field Approach and Image Acquisition

The methodology for image acquisition and analysis followed five main steps (**Figure 2**). A total of four flights per beach (three for Klaipeda and Warnemünde) were carried out as one-time sampling in the same day at three different altitudes near the highest sun zenith angle (between 11 a.m and 1 p.m CET) in May, June, July and October 2019. All sampling was carried out under the permission of the Ministry for Energy, Infrastructure and Digitalization in MV, Germany and following the guidelines of the German Air Traffic Control (Deutsche Flugsicherung, DFS). In Lithuania, drone flights for small devices (<25 kg) do not require permission, thus sampling was not restricted but followed regulations (Civil Aviation Administration, CAA, 2020). Care was taken during all surveys to avoid impacts such as crashing on

people or structures (e.g. trees), or cause disturbances to birds by the noise and start/landing of the drone. We carried out sampling away from conglomeration of people and chose a start/land site with sufficient distance from trees and structures. The drone was always kept on sight to maneuver in case of danger. The flight heights used were low and thus more noise was produced, but we kept flights short (3 min for recovery experiments and max. 20 min for one sampling of 100 m beach transect) to minimize disturbance. The sampling was carried out only under good stable weather conditions (noon, clear sky or homogeneous cloud cover, wind speed <20 km/h, no rain). **Supplementary Table S1** shows the settings used for drone-based mapping following Martin et al. (2018) and own experiences. Ground Control Points (GCPs) were not used for georeferencing. The drone gives good positional relative accuracy- that is how points on a map are placed relative to each other- which we suggest is sufficient for image classification, as we are not overlaying different orthomosaics but rather making a comparison of the classification results between different flight altitudes and algorithms.

Previous studies using consumer drones with a camera resolution similar to ours, tested flight altitudes between 5 and 35 m (Deidun et al., 2018; Martin et al., 2018; Fallati et al., 2019) and up to 60 m (Atwood et al., 2018; Goncalves et al., 2020). The flight altitudes chosen for this study were set based on the *Pix4D Ground Sampling Distance (GSD) calculator* to obtain a GSD <5 mm as optimal spatial resolution to detect litter in the meso (5–25 mm) and macro (>25 mm) scale; namely 10, 15, and 18 m, which would give spatial resolutions of 2.7, 4.1, and 4.9 mm, respectively. This is also in accordance with the EU law regulations for drone flights, limited to a range of 10 m to 120 m, based on the aircraft settings and EU law (European Parliament and Council, 2018).

To assess the detection accuracy of litter items at these different flight heights, recovery experiments were carried out on a previously cleaned area of 5 × 10 m (**Figure 2**) where litter items of different colors, shapes and sizes (1–30 cm) were displayed (**Supplementary Figure S1**). These included the most common item categories for the Baltic (Schernewski et al., 2017). The sites mapped had different number of items (14–57 items) and background substrates and were sampled under different weather conditions (**Figure 1**). In addition, beach transects of 100 m (with unknown number and type of litter) were mapped from the intertidal zone to the back of the beach (**Figure 2**) at a flight height of 10 m. After mapping, two people collected the items seen by naked eye and classified them according to the OSPAR list of items (OSPAR, 2010). All captured images were converted into orthomosaics and these were integrated in a Geographic Information System (GIS) for image analyses.

Image Processing and Pre-analyses

A total of 14 orthomosaics were created in GeoTIFF format which presented spatial resolutions of 2.7–8 mm/px, based on flight height and mapping app used. In general, all apps use photogrammetry approaches based on image orthorectification with point clouds and elevation data to produce orthomosaics, however, different image processing may have caused the differing spatial resolutions between the apps (e.g., use of image stitching enhances image spatial resolution). For each site, three orthomosaics (one for each flight height) of recovery experiments (Klaipeda and Warnemünde, only two) and one orthomosaic of a 100 m beach transect taken at 10 m altitude. Image analysis was carried out on ArcGIS, using Digital Numbers (DN) with a radiometric resolution of 8 bit. The projection used was WGS1984 UTM Zone 33N/34N for Germany and Lithuania, respectively.

First, the orthomosaics obtained from the recovery experiments at 10 m height were visually screened to assess and compare the accuracy of litter detection from drone imagery vs. ground truth data. Here, the analyst knew the number and type of items but not their position in the image. The items were counted from left to right, starting at the top of the image towards the bottom, zooming at the objects to mark them. Preliminary analyses were conducted to find the best classification method between pixel-based vs. object-based classification. Similarly, the influence of different number of classes (2, 4, and 6 classes) was tested in ArcGIS and ENVI. The latter was used to inspect the spectral differences of each background material by taking 10–20 samples of objects in each orthomosaic.

Object-Based Supervised Classification

Image classification followed a standard procedure of object-based supervised classification incorporated in ArcGIS including four steps, i.e. segmentation, the selection of training samples, classification and accuracy assessment.

Segmentation groups pixels into "objects" based on homogeneity criteria set by spectral and spatial values and minimum segment size. This aims at reducing noise from the background and highlighting objects of interest for object-based classification. Based on the gained knowledge from the investigated sites, a decision tree for choosing segmentation parameters was created (**Figure 3**). Spectral and spatial values were chosen individually per site. The minimum segment size used here was between 2 and 10 pixels (1–5 cm^2) with the aim to allow recognizing small litter items like cigarette butts (1–2.5 cm). It is important to consider that only four beaches were studied, thus the employment of this decision tree should be further tested for its application in more sites. For an example of the segmentation result, see **Supplementary Figure S2**.

The classification approach used is supervised and therefore requires training data. Training samples were taken as segments to obtain 4–6 distinct classes. The criteria used here were: 1) select >20 samples (if possible), proportional to the class size but not exceeding the number of objects per class in the image, 2) select samples with enough distance from one another to increase variability of the training set, 3) select samples at the center of the item to avoid mixed pixels and 4) include different color tones for each class, i.e. if vegetation was present in different tones of green, training samples included these to provide an accurate classification of the class. Additionally, histograms and scatterplots on ArcGIS were checked to ensure that each class was spectrally distinct from one another. The training samples taken at each recovery experiment were used for classification of the recovery sites and 100 m beach transects.

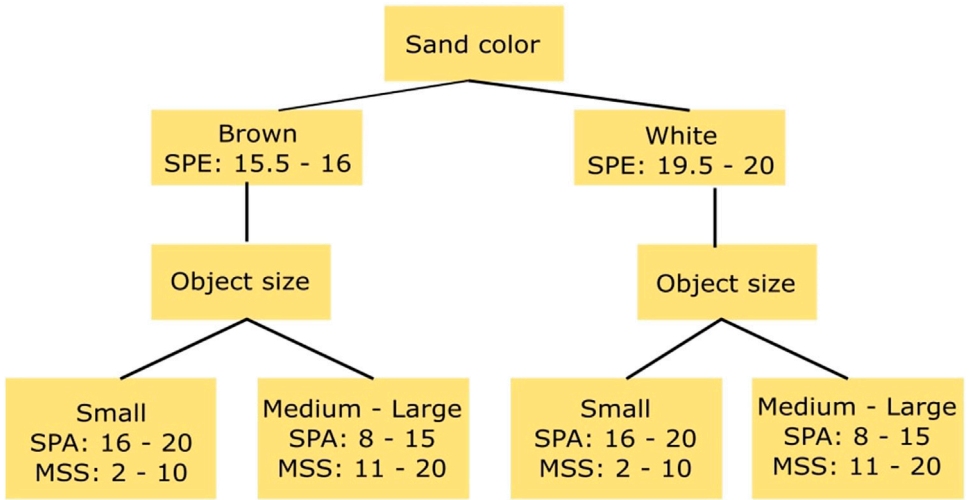

FIGURE 3 | Decision tree for segmentation parameters based on beach characteristics of the four study sites. SPE: Spectral Value, SPA: Spatial Value, MSS: Mean Segment Shift Value.

Three supervised classification algorithms were tested: Maximum Likelihood (ML), Random Forest (RF) and Support Vector Machine (SVM). These algorithms follow different set of rules in respect to the training samples to be used. For the RGB camera used, ML classification in ArcGIS requires a minimum number of 20 training samples per class and assumes normal distribution of the samples, while RF classification and SVM can work with fewer samples, do not assume normal distribution and are less susceptible to noise in the image. The functioning of each algorithm is also different. ML is based on the concept of normal distribution and Bayes theorem of decision making, based on the probability that every pixel in an image belongs to a particular class. The strength of ML is that it considers the variability within each class using the covariance matrix to classify the candidate pixel (Lillesand et al., 2004). RF uses multiple decision trees trained to use small variation of the data, where the majority vote from the trained trees decides the class assignment for each pixel (Berhane et al., 2018). SVM is a non-parametric statistical learning approach and therefore there is no assumption made on the underlying data distribution. SVM maps input data as vectors into a higher dimensional space to separate data into different classes using hyperplanes (Mountrakis et al., 2011). The output of the approaches is a classified image (*.tif*) of a number of classes as defined in the training samples.

Accuracy assessment of the image classifications was carried out with a set of 500 validation points created in an "equalized stratified random" manner, i.e. distributed within each class, each one having the same number of points. A confusion matrix, based on the comparison between the classification and reference data, revealed the accuracy of each algorithm by calculation of commission and omission errors for each class, total accuracy and kappa value of agreement. The total accuracy (TA) is the percentage of correctly classified validation pixels and measures the accuracy of the classified image. The producer's accuracy (PA), also known as recall, indicates the true positive rate or the proportion of true positives in relation to true positives and false negatives in the model classification. It is also a measure of omission error. The user's accuracy (UA), also known as precision, indicates the positive predictive power or the proportion of true positives in relation to true positives and false positives in comparison to the reference data. It is also a measure of commission error (Story and Congalton, 1986; Campbell and Wynne, 2011). Cohen's Kappa gives an overall assessment of accuracy of the classification in respect to randomness, with a value of 0 indicating no better than random, >0 better than random and <0 worse than random (Cohen, 1960).

Because only one replicate classification was carried out per height and algorithm, statistical tests for significant differences were not conducted. Instead, we provide an overview of the accuracy measures obtained from each image classification and a comparison of the mean and standard deviation between the classifications at different flight heights for each sampling site.

Cost-Efficiency Analysis

Official marine litter monitoring methods need to be time and cost efficient. The MSFD requires the comparison of methods for marine litter monitoring to meet the practical demand of cost-efficiency (JRC, 2013) considering implementation and annual running costs to fulfill the MSFD Descriptor 10 and to be implemented by national authorities within their national marine litter monitoring programs. The following approach provides a subjective comparison of a set of two monitoring methods: an UAV monitoring method with a commercial RGB drone and a hypothetical non-established spatial-OSPAR monitoring method to evaluate aspects of costs and efficiency. The evaluation of efficiency was based on four criteria: accuracy, reproducibility, flexibility and quality. Accuracy refers to the

share of items identified at the beach transects vs. ground truth data. Reproducibility reflects the likelihood that, when a method is applied by different persons, drones and software, the same results will be obtained. Flexibility is defined as how flexible the method is with respect to weather conditions, external disturbances, permissions and battery life. Quality refers to how well are items defined and whether sufficient data is provided, i.e. type and number of items, type of material and spatial distribution.

In contrast to the current OSPAR method, spatial-OSPAR considers the spatial distribution of litter items per area, thus comparable to the output of the drone approach, and taking into account 100 m beach transects (or 1 km beach transects for items >50 cm) with smaller transects of 10 m and 3–6 quadrats of 9 m^2, displayed from the tide line, middle and to the back of the beach (an adapted version after Bravo et al., 2009).

Costs of the UAV and the spatial-OSPAR methods were calculated considering implementation costs (equipment, software and testing period) and annual running costs for office and field/lab work to be carried out at four beaches, four times a year, by a minimum of two persons. Our time and costs estimations follow own experiences. These estimations may, therefore, vary based on type of drone used, analysis method and level of training required, as well as currency and salary estimations for the country. The initial costs include equipment costs as well as the costs for a testing period for both methods (6 months for the UAV-method and 3 months for the spatial-OSPAR method). Annual running costs include field/lab (travel, survey and analysis) working time and office (planning, organization and reporting) working time. The total monitoring costs were calculated as the sum of initial costs and annual running costs for field/lab and office work, and were classified as: 5 (very low) < 15,000 €; 4 (low) < 30,000 €; 3 (moderate) < 45,000 €; 2 (high) < 90,000 € and 1 (very high) > 90,000 €.

Each method and criteria was scored separately, evaluated by three experts as: 1 (very low), 2 (low), 3 (moderate), 4 (high) and 5 (very high). The efficiency score is the average of the scores for each criterion. To obtain the final cost-efficiency score, the cost and the efficiency scores were multiplied and classified as: <5 (very low), <10 (low), <15 (moderate), <20 (high) and >20 (very high).

RESULTS

Preliminary Analyses

Accuracy Assessment by Visual Screening

Visual screening carried out on images captured at 10 m flight height revealed a mean recovery rate of 99.4 ± 16.2% for the four beaches (Ahrenshoop 87.5%, Stoltera 97%, Warnemünde 90%, in Klaipeda 16 instead of 13 items were found again, 123%). These results gave the first "green light" towards testing a semi-automatic method for classification with ArcGIS. The objects easier to find by visual screening were larger items (>2.5 cm), items placed close to each other, items of bright colors and shapes normally not found naturally at the beach (e.g. bottle caps in yellow, blue, pink, orange, red, bright green). The objects most difficult to find were mainly in colors white, black, brown and transparent and shapes like string/cord, lines and squares, especially of small sizes and diameters (<2.5 cm).

Pixel Based vs. Object Based Classification

The high spatial resolution of drone images, which is needed for the detection of small litter, also led to noise from shadows, differences in sand color and tread marks, which disturb the classification, and thus needed to be handled accordingly. Pixel-based unsupervized classification (A) resulted in a complex image due to high variations on sand, background substrate (i.e. sand color and amount of stones, shells and vegetation), colors and shades. Using object-based unsupervized classification (B) objects were clearly separated from sand and the "noise" from shadows and differences in sand color were reduced or eliminated (**Supplementary Figure S3**). The results of this test classification also showed that images at 10 m height gave a closer and sharper look into smaller objects than images obtained at 15 and 18 m height (**Supplementary Figure S4**), which reduced the noise of the background but smaller objects were more difficult to identify and classify.

Influence of Different Number of Classes

Unsupervized classification into two classes highlighted all objects from sand (**Supplementary Figure S5A**), whereas classification into four classes (**Supplementary Figure S5B**) showed clustering of the objects, however with high variability in the classification, i.e. one object was classified as three different ones. The classification into six classes showed even higher variability in the classification: objects of white and black color were clustered separately and colorful litter items were highlighted from the sand but classified in non-coherent clusters with single items belonging to more than one class (**Supplementary Figure S5C**).

The analysis of spectral profiles of objects on ENVI 5.3 revealed that each object had a different spectral profile and could therefore be classified separately into a total of maximum six classes: litter, algae, vegetation, shells, stones and sand. For Warnemünde, the class "shadows" was added (**Supplementary Figure S6**). Between all classes present, algae, vegetation and sand presented characteristic and consistent spectral profiles that could allow the differentiation from other classes. However, for the case of litter the high variation in color presented no consistent curve in which classification could be based upon. Lastly, shells, stones and shadows that were present in either white or dark colors had similar spectral profiles with flat DN values at either extreme (0–255).

Like this, four to six classes were chosen for the selection of training samples to carry out object-based supervised classification with three algorithms. For classification with four classes, algae and vegetation as well as stones and shells were considered together as two classes. For classification with six classes, algae and vegetation as well as stones and shells were considered as separate classes. This latter classification was carried out only for the sites where the presence of stones and shells as well as of algae and vegetation was clear, in this case Stoltera and Ahrenshoop. Although these classes are not the object of interest, it was important to understand how white and black objects would be classified.

TABLE 1 | Accuracy of image classification on recovery sites with 4 and 6 classes (litter, vegetation, algae, stones, shells and sand) for each site, algorithm and flight height. The values are presented as percentage from top to bottom: Total Accuracy (TA), Producer's accuracy (PA) of litter class, User's accuracy (UA) of litter class and kappa value of agreement (k).

		Four classes				Six classes			
Site	**Algorithm/Height**	**10 m**	**15 m**	**18 m**	**Mean ± SD**	**10 m**	**15 m**	**18 m**	**Mean ± SD**
Stoltera	ML	0.75 0.85 0.55 0.66	0.76 0.80 0.57 0.68	0.62 0.45 0.18 0.50	0.71 ± 0.06 0.70 ± 0.18 0.43 ± 0.18 0.61 ± 0.08	0.64 0.79 0.70 0.56	0.58 0.70 0.59 0.49	0.56 0.46 0.30 0.47	0.59 ± 0.03 0.65 ± 0.14 0.53 ± 0.17 0.51 ± 0.04
	RF	0.58 0.95 0.39 0.43	—	—	—	0.50 0.35 0.16 0.40	0.51 0.28 0.13 0.42	—	0.51 ± 0.01 0.32 ± 0.03 0.15 ± 0.01 0.41 ± 0.01
	SVM	0.73 0.81 0.42 0.63	0.74 0.72 0.47 0.66	0.73 0.61 0.42 0.64	0.73 ± 0.00 0.71 ± 0.08 0.44 ± 0.02 0.64 ± 0.01	0.62 0.48 0.91 0.54	0.65 0.75 0.99 0.58	0.63 0.59 0.99 0.55	0.63 ± 0.01 0.61 ± 0.11 0.96 ± 0.04 0.56 ± 0.02
Ahrenshoop	ML	0.84 0.97 0.50 0.78	0.82 0.98 0.45 0.76	0.79 0.98 0.36 0.71	0.82 ± 0.02 0.98 ± 0.00 0.44 ± 0.06 0.75 ± 0.03	0.66 0.92 0.28 0.59	0.65 0.92 0.29 0.58	0.61 0.86 0.15 0.53	0.64 ± 0.02 0.90 ± 0.03 0.24 ± 0.06 0.57 ± 0.03
	RF	0.73 0.77 0.08 0.63	0.73 0.73 0.09 0.63	0.73 0.92 0.09 0.64	0.73 ± 0.00 0.81 ± 0.08 0.09 ± 0.00 0.63 ± 0.00	0.56 0.22 0.02 0.47	0.56 0.18 0.04 0.47	0.57 0.18 0.02 0.48	0.56 ± 0.00 0.19 ± 0.02 0.03 ± 0.01 0.47 ± 0.00
	SVM	0.74 0.96 0.19 0.66	0.76 1 0.21 0.68	0.75 0.94 0.14 0.66	0.75 ± 0.01 0.97 ± 0.02 0.18 ± 0.03 0.67 ± 0.01	0.60 0.87 0.16 0.52	0.63 0.44 0.20 0.55	0.64 0.54 0.26 0.56	0.62 ± 0.02 0.62 ± 0.18 0.21 ± 0.04 0.54 ± 0.02
Warnemünde[a]	ML	0.90 1 0.88 0.87	0.75 0.99 0.70 0.66	—	0.83 ± 0.08 1.00 ± 0.01 0.79 ± 0.09 0.77 ± 0.11	[a]drone images taken only at 10 and 15 m. Classification was done only with 4 classes because only 4 features were present			
	RF	0.71 0.93 0.22 0.62	0.61 0.67 0.08 0.48	—	0.66 ± 0.05 0.80 ± 0.13 0.15 ± 0.07 0.55 ± 0.07				
	SVM	0.76 0.97 0.74 0.68	0.62 0.95 0.30 0.49	—	0.69 ± 0.07 0.96 ± 0.01 0.52 ± 0.22 0.59 ± 0.10				
Klaipeda[b]	ML	—	0.69 0.88 0.88 0.59	0.54 0.93 0.79 0.38	0.62 ± 0.07 0.91 ± 0.03 0.84 ± 0.05 0.49 ± 0.11	[b]drone images taken only at 15 and 20 m instead of 18 m. Classification was done only with 4 classes because only 4 features were present			
	RF	—	0.54 0.74 0.11 0.38	—	—				
	SVM	—	0.71 0.89 0.69 0.61	0.44 0.76 0.36 0.25	0.58 ± 0.14 0.83 ± 0.07 0.53 ± 0.17 0.43 ± 0.18				

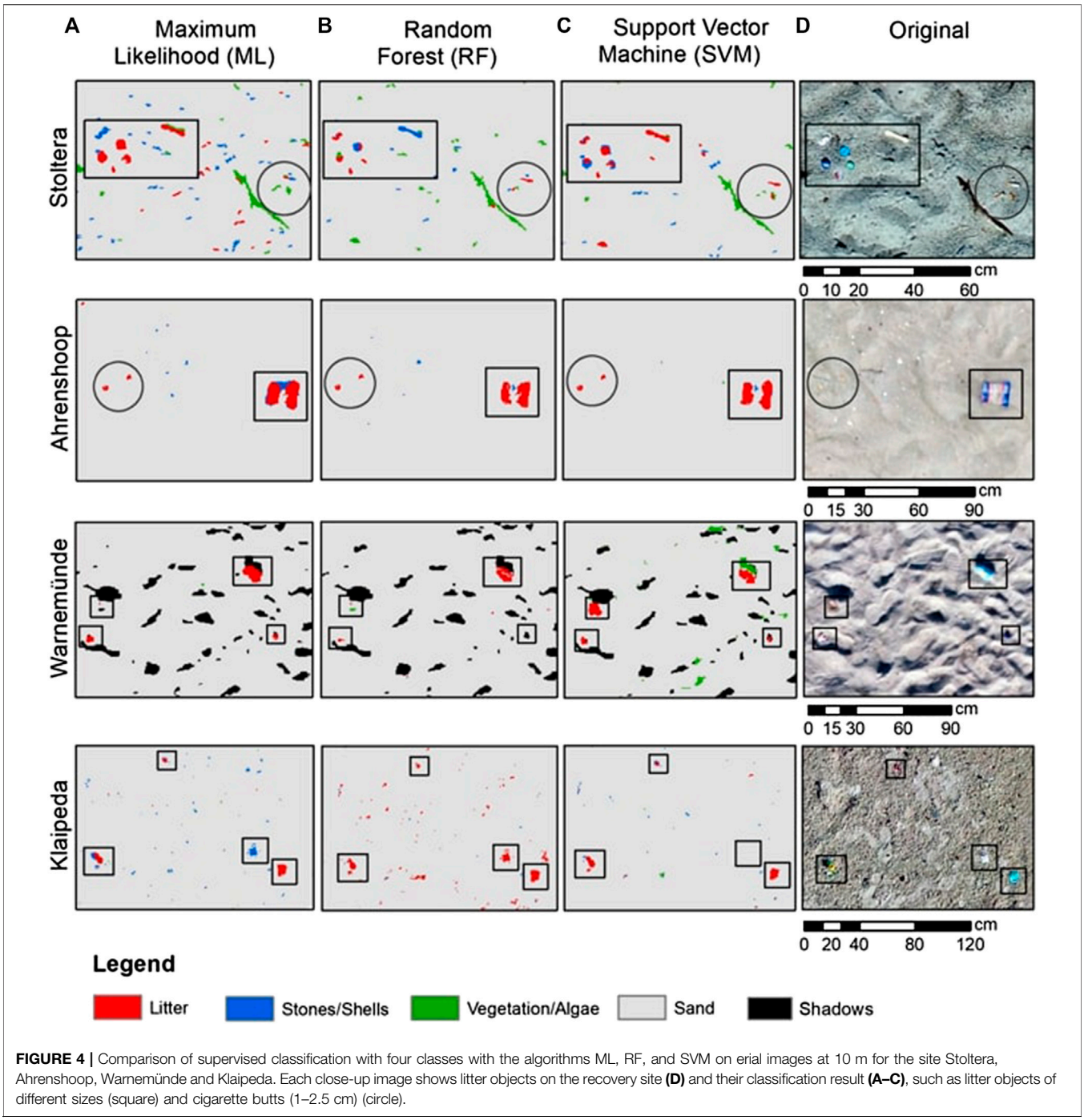

FIGURE 4 | Comparison of supervised classification with four classes with the algorithms ML, RF, and SVM on erial images at 10 m for the site Stoltera, Ahrenshoop, Warnemünde and Klaipeda. Each close-up image shows litter objects on the recovery site **(D)** and their classification result **(A–C)**, such as litter objects of different sizes (square) and cigarette butts (1–2.5 cm) (circle).

The criterion to "select >20 training samples" was not possible to fulfill in all beaches and taking a larger amount of training samples in the small recovery area contradicted the goal of the semi-automatic classification. For the object of interest (i.e. litter), most beaches had at least 20 training samples. For Klaipeda, which had the lowest density of litter in the recovery area, 10 training samples were chosen. Since stones and shells were not easy to distinguish from white or black objects (e.g., litter or algae pieces) from the spectral profiles, only a few samples were taken based on their shape and distance from algae or water, to avoid misclassifications.

Object-Based Classification

The accuracies of image classification for recovery experiment (5 × 10 m) are shown in **Table 1**. The classification with four

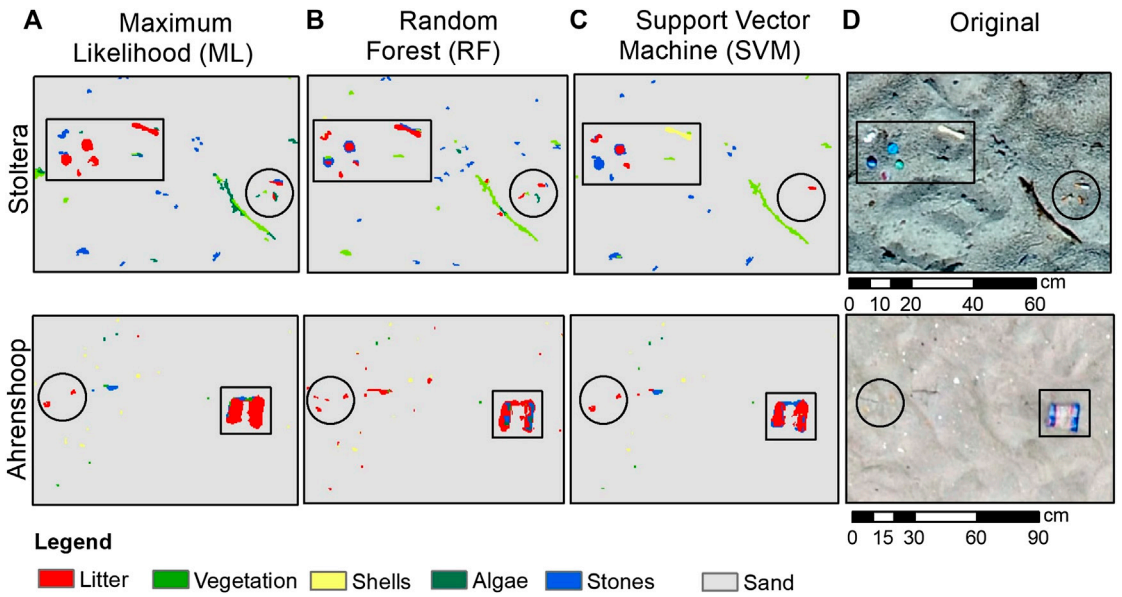

FIGURE 5 | Comparison of supervised classification with six classes with the algorithms ML, RF, and SVM on erial images at 10 m for the site Stoltera and Ahrenshoop. Each close-up image shows the distribution of litter objects on the recovery site **(D)** and their classification result **(A–C)**, such as litter objects of different sizes (square) and cigarette butts (1–2.5 cm) (circle).

classes showed total accuracies (TA) that ranged between 36% and 90% for ML, 54% and 73% for RF and 44% and 76% for SVM, depending on flight height and site. Producer's accuracy (PA) for litter showed similar ranges: 45–100% for ML, 67–95% for RF and 61–100% for SVM. Whereas user's accuracies (UA) for litter were lower. Kappa values were in most cases >0.60 indicating that classification was better than random. Classification with six classes showed in general lower values for TA, PA and UA for all algorithms and sites. Here kappa values were in most cases <0.60 indicating that classification was closer to random.

In most cases, measures of accuracy (TA, PA, and UA) decreased at images taken at higher flight altitudes. Classification of images taken at 10 m showed highest TAs, highest PA for litter classification and highest kappa values in most sites for the three algorithms. In some cases, higher TAs were also seen at images taken at 15 m or 18 m; however, this was mainly due to higher accuracies in classes other than litter. User's Accuracy (UA) for litter was lower for all classification algorithms, with values of 18–88% for ML, 8–39% for RF and 14–75% for SVM with four classes and 15–70% for ML, 2–16% for RF and 16–99% for SVM with six classes, depending on flight height and site (**Table 1**).

Due to a lack of replicates, an assessment of significant differences for measures of accuracy between algorithms was not possible to carry out and thus is not possible to statistically assess if an algorithm performs better than another. Nevertheless, **Table 1** shows that no clear differences were found between algorithms for samples taken at different sites. Similarly, no clear differences were observed between measures of accuracy for images taken at different heights, which in general showed low standard deviations from the mean.

The resulting classified images showed that ML and SVM gave a better representation of litter and background features in contrast to RF (**Figure 4**). In the case of Warnemünde, similar classifications were seen between the three algorithms but SVM showed misclassifications between vegetation/algae and shadows (**Figure 4**). For 6-class classification, these results were similar, but as more classes were used, more detail was defined and misclassifications were seen between shells and white litter objects (**Figure 5**). In general, both ML and SVM were able to classify meso- and macrolitter size with varying accuracies relative to sand color, background substrate, weather conditions and litter objects.

The classification of 100 m beach transects (at 10 m flight height for German sites and 15 m for Klaipeda) showed lower accuracy values than achieved on the recovery experiments, independent from site and image resolution. Classification with four classes showed kappa values between 0.23 and 0.53, which indicated that classification was rather random among different algorithms and no single algorithm could show a good performance in all cases (**Table 2**). Similar patterns were seen for the classification with six classes. The high range of difference for PA and UA for litter is due to how AAPs are placed on the image, sometimes hitting only one or no litter item, which skewed the results to either extreme (0 or 100%).

The classified 100 m beach transects showed similar classification patterns as in the recovery experiments but could not be representative of the litter found on the sites during collection (Stoltera: 174 items, Warnemünde: 167 items,

TABLE 2 | Accuracy of image classification on 100 m beach transects at 10 m flight height with 4 and 6 classes (litter, vegetation, algae, stones, shells and sand) for each site, algorithm and flight height. The values are presented as percentage from top to bottom: Total Accuracy (TA), Producer´s accuracy (PA) of litter class, User´s accuracy (UA) of litter class and kappa value of agreement (k).

Algorithms/Sites	Stoltera		Ahrenshoop		Warnemünde	Klaipeda
	Four classes	Six classes	Four classes	Six classes		
ML	0.44	0.25	0.55	0.64	0.47	0.54
	0	0	1	0	0.25	1
	0	0	0.007	0	0.02	0.02
	0.27	0.11	0.39	0.56	0.31	0.37
RF	0.72	0.39	0.51	0.57	0.74	0.39
	0	0	0	0	0	1
	0	0	0	0	0	0.02
	0.49	0.15	0.35	0.46	0.54	0.23
SVM	0.66	0.36	0.44	0.74	0.73	0.52
	0	0	1	1	0.25	0.75
	0	0	0.01	0.04	0.11	0.03
	0.36	0.13	0.31	0.64	0.52	0.34

TABLE 3 | Cost-efficiency analysis for UAV and spatial-OSPAR for beach litter monitoring methods. The values are based on our experience taking into account the MSFD guidelines (JRC, 2013) and federal state authority staff salaries (37.5 € per hour) for a monitoring of four beaches, four times a year. In bold are shown the scores for cost and efficiency, giving the cost-efficiency score.

Costs	Description	Items >2.5 cm 100 m monitoring		Items >50 cm 1 km monitoring	
		UAV	Spatial-OSPAR	UAV	Spatial-OSPAR
Investment and initial test for implementation[a]	Costs of equipment, software, methodological tests in the field, training for field work and analysis	48,000 €	15,100 €	48,000 €	15,100 €
Annual office costs[b]	Orders, selection of sites, drone permissions and licenses, reporting, annual replacement costs for materials	10,000 €	10,000 €	10,000 €	10,000 €
Annual field/lab costs[b]	Travel to site, survey, analysis of data	10,600 €	5,800 €	16,000 €	4,000 €
Annual running costs		20,600 €	15,800 €	26,000 €	14,000 €
Total annual costs[c]		36,600 €	20,833 €	42,000 €	19,033 €
Person hours/year		1,296	768	1,440	720
Cost score		**3**	**4**	**3**	**4**
Efficiency					
Accuracy		3	4	5	5
Reproducibility		5	3	5	5
Flexibility		1	4	2	4
Quality		3	5	4	4
Efficiency score		**3.0**	**4.0**	**4.0**	**4.5**
Cost—efficiency		**9.0** Low	**16** High	**12** Moderate	**18** High

[a]*One-time investment to be done every 3 years, considering a drone lifetime of 3 years and renewal of training.*
[b]*Considers brutto salary for a federal state authority in Germany (37.50 € per hour).*
[c]*Considers a third of the investment and initial costs added to the annual running costs.*

Ahrenshoop: 77 items and Klaipeda: 214 items) (**Supplementary Figure S7**). **Figure 5** shows the classification results with highest TA, PA for litter and kappa values for each site (seen at **Table 2**). Both images and confusion matrices showed that misclassifications occurred in all algorithms (**Supplementary Table S2**). ML showed misclassification between litter and vegetation in Warnemünde (**Supplementary Figure S12**) and between vegetation, stones and litter in the classification with four classes in Ahrenshoop (**Supplementary Figure S10**). RF showed an overestimation of litter abundance in Klaipeda (**Supplementary Figure S13**) and in the classification with six classes in Ahrenshoop (**Supplementary Figure S11**). SVM misclassified vegetation and litter in Stoltera (**Supplementary Figures S8, S9**) and stones and litter in Klaipeda (**Supplementary**

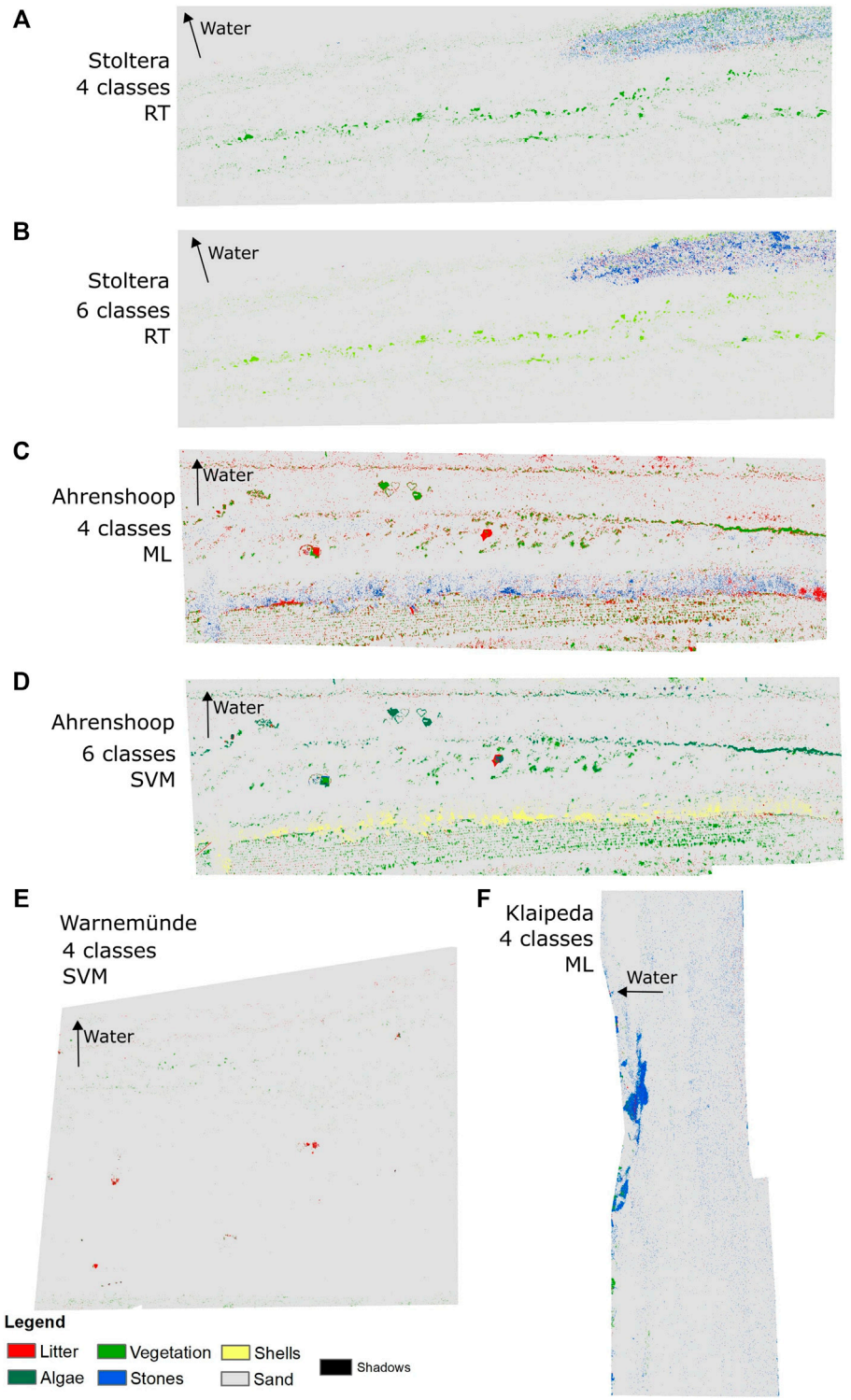

FIGURE 6 | Object-based supervised classification of 100 m beach transects taken at 10 m flight height. Only the results with best total accuracy (TA), producer's accuracy for litter (PA) and kappa value of agreement for with 4 and 6 classes are shown for each site: Stoltera **(A,B)**, Ahrenshoop **(C,D)**, Warnemünde **(E)** and Klaipeda **(F)**.

Figure S13). Objects that were correctly classified were anthropogenic items (beach tents of ca. 2 m in Warnemünde–**Supplementary Figure S12**—and Ahrenshoop–**Supplementary Figures S10, S11** classified as litter), algae and beach wrack in Stoltera (**Supplementary Figure S8**) and Ahrenshoop (**Supplementary Figure S10**), vegetation (**Supplementary Figure S10**) and shells (**Supplementary Figure S11**) in Ahrenshoop, and stones in Klaipeda (**Supplementary Figure S13**).

Time and Cost-Efficiency

As seen on **Table 3**, the UAV spatial method for 100 m and 1 km beach monitoring involves higher initial costs and about two times more costs and time effort for field work and analysis than the spatial-OSPAR method. The higher investment costs for the UAV method are related to software costs, since license software is often required within official federal agencies. If these software costs were not considered, the investment costs would decrease to only 3,000 € for the drone and other materials. Costs for testing period of implementation were higher for the drone method, estimated as 30,000 € for the 100 m and 1 km monitoring vs. 15,000 € for the spatial-OSPAR method. Office costs are the same for both methods. Annual running field costs (survey on site) were lower for the UAV method at 100 m beach transects (1,800 € vs. 2,400 € for the spatial-OSPAR), but higher once spatial extension increased to 1 km (2,400 € vs. 1,800 € for the spatial-OSPAR method). Annual running costs for analysis of the data (lab work) was considerably higher for the UAV method than for the spatial-OSPAR method (4,800 € vs. 2,400 € for 100 m and 9,600 € vs. 1,200 € for 1 km) (**Table 3**).

The overall cost-efficiency score for beach litter monitoring was 9–12 (low to moderate) for the UAV method vs. 16–18 (high) for the spatial-OSPAR method.

DISCUSSION

Lessons Learned From Object-Based Classification

Results from the recovery experiment showed that litter sizes >2.5 cm (i.e. macrolitter size) were the minimum size detectable. PAs for litter for the recovery experiments at different sites were between 77% and 100% with kappa values between 0.43 and 0.87 for images taken at 10 m height. These accuracy values were comparable to those obtained through visual screening of the same images (>87%, mean 99.4% ± 16.2). Even if smaller litter items were detected and classified (e.g., **Figures 4**, **5**, cigarette butts <2.5 cm), in reality many were misclassified. Another study also showed limitations in the detection of smaller items size, where items <4 cm were also most misclassified (Martin et al., 2018). TA was lower for classification into six vs. four classes (**Table 1**), but the PA for litter was in some cases similar, reaching values between 70 and 80%. In the 6-class classification, white and dark litter items were better classified than with the 2-class or 4-class classification (**Supplementary Figure S5**), but at the same time introducing more classes increased the complexity of the image.

The results from visual screening and spectral curves gave an initial indication of misclassification. Objects with a flat spectral curve (e.g. white shells and black stones) in colors white, black, transparent and brown, and litter which did not present any consistent curve (**Supplementary Figure S6**) were most misclassified on RGB images, whereas the objects of bigger size (>2.5 cm) and bright colors were correctly classified as litter (e.g. **Figure 4**). This is because object color, weather, light conditions and background substrate influence DN values and thus classification. In addition, the selection of training samples based on DN values depends on the judgment of the observer, increasing chances of error and misclassifications. Furthermore, it was not possible to establish whether one algorithm can cope better with background complexity than others, since factors like weather conditions differed in each site. We suggest that the higher complexity of sand and background substrate challenges segmentation of the image, which in turn, influences classification results. This was also observed by Martin et al. (2018) where shadows, vegetation and non-uniform background as well as the variability of each item within the same category (different sizes and colors) presented limitations in classification. In our study, as complexity of the background increased, the use of more classes became beneficial (e.g. in Ahrenshoop, **Supplementary Figures S10, S11**). However, in order to derive accurate statistics, the use of replica on each site and condition as well as further explore the influence of litter quantities and background substrate should be explored.

No clear differences of performance accuracy could be assessed between the algorithms; however, in contrast to previous studies, RF was the algorithm that presented most problems in performance in our images (**Table 1**). Martin et al., (2018) used RF classification obtaining an accuracy of 61.8% for detection of litter, 39.5% total accuracy and F-score of 0.13. Their classification presented an overestimation of 5-times due to false positive items, as similarly seen in the classified images with RF in our study. Another study by Goncalves et al. (2020) at beaches in Portugal also used RF, obtaining 75% sensitivity (≈Producer's accuracy) and 73% positive predictive value (≈User's accuracy) with a F-score of 0.75. These studies used approaches related to changes in the color space of spectra (Martin et al., 2018; Goncalves et al., 2020) which were not used in this study.

Observations of the classified images from recovery experiments suggest that ML better highlighted small features (stones or shells) (**Figure 4**, **5**) but did not necessarily classify litter better (**Table 1**), yet bottle caps and larger macrolitter were detected. In contrast, SVM gave less importance to small features leading to less noise from stones, shells or sand heterogeneity within the images. Still, small objects (also litter) were well classified in most cases, up to large mesolitter sizes like cigarette butts (**Figures 4**, **5**). Some studies suggest that a higher litter abundance leads to higher detection of litter by RF and other algorithms (Martin et al., 2018; Atwood et al., 2018), which was not observed in our study.

The image classification used in this study did not provide a distinction of litter composition and only focused on detection of litter items to provide an estimation of abundance and distribution. Based on the litter collected on site, the highest amounts of litter were in the categories plastics and paper (mainly due to cigarette butts), mainly macrolitter size of white or brown color and colorful mesolitter items (**Supplementary Figure S7**). Our results showed, however, that GIS classification based on RGB data was not satisfactory to provide estimations of abundance, since litter items were not possible to identify from the classified images at large spatial scales (100 m beach transect). TAs at the 100 m beach transects were much lower than at recovery experiments and PAs for litter were in most cases 0% (**Table 2**). This may be due to uncertainties in the method, because accuracy assessment depended on whether one or more points hit a litter object or not, bringing accuracy to extreme values of 0 or 100%. Due to the low segment size used for segmentation, large items were constructed with several segments, thus litter "objects" could not be counted as such in the classified images since the number of segments per item would overestimate the real count. Future studies should consider taking the GPS coordinates of litter items as a method to get reference data for larger transects.

Our analysis method did not prove to be sufficiently accurate or time-efficient. It is important to consider other methods for analysis, while following requirements for official beach litter monitoring. As technology develops and advanced equipment becomes more accessible, many of the limitations encountered in our study (mainly related to image resolution and processing time) will be overcome. Other methods including deep learning have demonstrated to be an alternative for the classification of objects on RGB images since it does not rely only on DN values (Fallati et al., 2019). In their study, object recognition reached a sensitivity (≈Producer's accuracy) of 67%, positive predictive value (≈User's accuracy) of 94% and F-score of 0.49, arguing the tool can be well used for the monitoring of litter and detection of hotspots in the study sites.

Strengths and Limitations of Consumer Drones for Beach Litter Monitoring

Taking into account our experiment results and assessment on cost and time efficiency, drones are still a method that needs to be explored and adjusted for efficient monitoring. The images from drones provide high spatial resolution which is required for the detection of small litter items. Our results showed that litter sizes >2.5 cm (i.e. macrolitter size) were the minimum size detectable. Even if smaller litter items were detected and classified (e.g., **Figure 4**, cigarette butts <2.5 cm), in reality many were misclassified. Thus, the accuracy of consumer RGB drones can be regarded as high (**Table 3**) for large particles but decreases with smaller item size and additionally depends on parameters such as item color, shape and weather conditions. These limitations could be overcome with more advanced drone sensors (e.g. multispectral) or the use of other analysis methods (e.g. deep learning) which increase accuracy; however, this would involve higher costs and expertize. In terms of type of data obtained and quality, our results suggest that the drone method (with RGB camera) can only provide data on the number of items and spatial distribution (moderate to high quality), in contrast to the spatial-OSPAR method where litter objects are collected by hand and can be better visualized to define also type of item and material, and give indications of pollution sources (**Table 3**).

A clear strength of drones is reproducibility (**Table 3**). Our results showed that the mapping of sites can be easily carried out after simple training of staff with the help of free mapping apps. These apps automatically map a site of interest at a set height, speed and area, enabling long term monitoring of the same site under consistent conditions. Although our analysis method did not prove to be sufficiently accurate and time-efficient, analysis of data in general would follow a strict protocol, carried out semi-automatically, decreasing chances of human error once the method is set up and sufficiently evaluated. For the 100 m OSPAR beach monitoring it is known that a difference of at least ± 10% is common, depending on who is carrying out the field work (Schernewski et al., 2017). In this respect, the drone method shows very high reproducibility in contrast to moderate reproducibility for the spatial-OSPAR method, and comparable values for 1 km beach transects (**Table 3**). Nevertheless, our own experiences showed that drone and GIS based monitoring is time-intensive (creation of orthomosaics 2–8 h, classification of the images, 3–8 h) and analysis of the images requires higher skills than for data obtained with an adapted spatial-OSPAR method.

Flexibility was the main limitation for monitoring with commercial drones in contrast to current monitoring methods (**Table 3**). The drone method depends on wind, weather and light conditions and can hardly be applied according to a fixed timetable. However, the dependence on weather conditions is a factor that all remote sensing studies need to consider (Murphy, 2015). At our study sites, ideal weather conditions initially involved wind speeds <20 km/h and enough sun light; however, overcast conditions and wind speeds of 27 km/h at Ahrenshoop also demonstrated good results (**Table 1**: **Figures 4**, **5**). Cloudy conditions showed best image outputs to avoid direct sunlight and shadows which led to sun glint and darker areas that disturbed image classification (**Supplementary Figures S8, S9**). ND Filters helped to minimize the reflection from sand under strong sunlight but shadows and sun glint could not be fully corrected. Issues with GPS signal, battery life (max. 20 min) and compatibility between smartphone device and mapping apps were also limitations encountered during our sampling. In addition, drone licenses are nowadays needed for all types of aerial drones and legal permissions are required at most places in Germany and limited to zones outside nature protected areas and of high urban density or conglomerations of people (§ 21a LuftVO, BMVI, 2017). From December 31, 2020, new EU regulations will apply and replace national regulations for each country (European Union Avitation Safety Agency, 2020).

Another important factor to discuss is the common natural trade-off of remote sensing approaches where decreasing flight altitude increases image resolution, but also decreases the area of coverage, increasing post-processing times and costs (Murphy, 2015). The large number of images obtained (44–234 images for recovery experiments and 459–1,247 images for 100 m beach transects) at 10 m led to high processing time for orthomosaic

creation (12–24 h). Drone images in our study had a high spatial resolution (2.7–8 mm, 20 MP camera) and litter objects were possible to see on images taken at all flight heights, but higher flight altitudes (e.g., 18 m) were not enough to classify objects (i.e. stones, shells, vegetation) accurately. Low flight height has also been related to blurry images and vigneting effect especially on sites with homogenous ground, like sand, which hinders orthomosaic construction (DroneDeploy, 2020). Studies that carried out mapping at much higher altitudes, focused on litter patches or much larger litter at the coastline or rivers (Atwood et al., 2018; Deidun et al., 2018) or combined geomorphological and hydrodynamic variables into one model that allowed more specific detection (Goncalves et al., 2020).

Contrarily to our results, a recent study using a similar set up suggests drone survey to be a cost-efficient method for litter quantification, however their study inspects a beach area of 20 × 20 m by visual screening done by people (Lo et al., 2020). The higher costs, and thereby lower cost-efficiency suggested in our study are likely related to the method used for analysis and the larger areas of beach inspected, as required by OSPAR (2010).

The main constraint for remote sensing of plastic litter is the various shapes, dimensions, colors and materials in which litter is present, making its recognition complex. Litter that is partially or completely buried or hidden between the back vegetation are not easily detected (Kataoka et al., 2018), especially with colors white, black, brown and transparent, as seen in our study. NIR spectroscopy with a MicroPhazir hand-held device is used to complement OSPAR studies and obtain more detailed information on material composition of mesolitter (Haseler et al., 2018; 2019); however, to our knowledge there is no published study using multi- or hyperspectral data on drones for the purpose of marine litter monitoring. Methods by Acuña-Ruz et al., (2018) used supervised classification for the detection of Styrofoam and other macrolitter items (>0.5 m^2) on hyperspectral data using Visible and Near Infrared (VNIR), Short Wave InfraRed (SWIR) and Thermal InfraRed (TIR) wavelengths of satellite imagery for the creation of a spectral library of macrolitter items and natural features at the beach (e.g., sand, algae, stones and shells) for classification. The spectral signature of marine plastics has shown to have three absorption features at 1,215 –1732 nm (Garaba et al., 2018) as well as 2,313 nm specifically for PE (Levin et al., 2006) and between the blue and green bands and NIR spectrum for the detection of Styrofoam and other macrolitter items at the beach (Acuña-Ruz et al., 2018). Although the use of multi- and hyperspectral data can provide more detailed data, it also implies higher costs due to equipment and expertize needed.

Application of Aerial Drones as Official Beach Monitoring Methods

The MSFD encourages developing a comprehensive knowledge on the sources and sinks of marine litter to adopt policies that adapt to its current status. In the OSPAR guideline, currently in use at the Baltic, trends on abundance and types of litter are assessed every 3 months (OSPAR, 2010). Fulfilling the requirements from the MSFD and carrying out monitoring for all marine compartments to get a complete overview of the marine litter problem can be challenging in time and cost efforts. The data acquired needs to be reliable and accurate for the design of mitigation strategies. With drone-based monitoring, efforts during sampling can be reduced and the fatigue aspect and visual differences can be eliminated if automatic detection is carried out. However, as it is common when using remote sensing approaches, implementation costs for the drone-based method are higher (Murphy, 2015) in contrast to OSPAR, as also seen in our results. In addition, the skills needed for analysis require prior professional training and longer processing times, leading to higher annual running costs. Furthermore, the drone-based method requires the removal of litter, when carried out within a monitoring program. Thus, despite a shorter time spent at the field and higher reproducibility, the implementation of consumer RGB drones as beach monitoring strategy involves significantly higher costs, lower accuracy and provides less information on the type of litter and material, thus can hardly be regarded as a cost-efficient tool for this purpose in southern Baltic Sea beaches.

Nonetheless, UAV-based monitoring has proven successful at other sites; and comparing our results to previous studies already suggests that accuracy results depend upon the method chosen for image analysis. Drones have been used for the monitoring of litter in the Maldives (Fallati et al., 2019) and Maltese islands (Deidun et al., 2018), showing satisfactory results in countries of comparable pollution levels. These studies also highlight the importance of density and distribution maps (Deidun et al., 2018); data that is not normally obtained from current OSPAR monitoring. UAV-based methods could also become interesting for highly polluted sites like Indonesia (Purba et al., 2019), India (Kaladharan et al., 2017) or the Mediterranean coasts (Vlachogianni, 2019) to give a fast overview of litter abundance and distribution to design fast removal and mitigation strategies.

Although drones did not prove successful at beaches in our study, other sites become of interest to further explore this tool. At the Baltic Sea, many beaches cannot fulfill the OSPAR criteria, with beaches at the north (e.g., Finland, Sweden) having rocky coasts and cliffs not accessible for monitoring (Schernewski et al., 2017) where drones could also become a helpful monitoring tool. Furthermore, drones could also expand our understanding of marine litter pollution by covering the back of the beach, dunes, river mouths, fjords and the sea to monitor floating litter, as these sites have not yet been considered during monitoring approaches or by default require more expensive equipment (e.g., like monitoring at sea, JRC, 2013). Drones could also serve to assess pollution levels of proximate urban areas that work as sources of pollution, as well as after specific weather events, disasters like tsunamis or storms (Murphy 2015; Kataoka et al., 2018), or even social events. Moreover, drone methods allow for storage of data long-term which can take into account physical factors (like weather, light conditions and geomorphology of the beach) for more spatio-temporal analysis (Kataoka et al., 2018). Due to the high initial investment required in remote sensing methods, it becomes necessary decreasing costs through opportunistic research, partnerships and collaborations between members of the state and the research community (Murphy, 2015).

Drone sensors for multi- or hyperspectral data operating in the VNIR and SWIR domain are still expensive, nevertheless, the fast

development of technology and lower costs for drones and software suggest future studies could provide promising results and cover this niche. In this sense, we suggest that monitoring of litter items <50 cm and less polluted areas should continue to occur under current *in-situ* methods, whereas for highly polluted sites with macrolitter and sites with litter items >50 cm, drone monitoring could become an option in the future.

CONCLUSION

Although the results from image acquisition and drone performance at recovery sites were promising, methods for litter detection and classification need to be further tested, especially when applied to larger spatial scales. In frame of the EU Marine Strategy Framework Directive (MSFD), this study showed that drone monitoring with an integrated RGB camera is not suitable to complement 100 m monitoring for Southern Baltic beaches; however, there is potential for improving cost and time efficiency in the 1 km monitoring for litter >50 cm with alternative methods to decrease processing time while increasing accuracy of data. Drone monitoring has the potential to expand spatial coverage to larger areas, monitor fragile or inaccessible sites and provide maps of litter abundance and distribution, especially in the context of hotspots. However, all these alternative methods need to consider cost-efficiency in factors such as type of equipment, processing time, effort and level of expertize needed for the analysis of larger and more complex data for establishing long-term monitoring strategies.

DATA AVAILABILITY STATEMENT

The raw data supporting the conclusions of this article will be made available by the authors, without undue reservation.

AUTHOR CONTRIBUTIONS

G-ES developed the methodology, carried out the field work, took care of data analyses and led the article writing. MH contributed to the research design, acquired the equipment and permissions, supported the field work and commented the article. NO and GS developed the general concept, supervised the work, and supported the article writing.

FUNDING

The work received minor financial support by the projects BONUS MicroPoll (03A0027A) and MicroCatch (03F0788A), both funded by the German Federal Ministry for Education and Research. BONUS MicroPoll has received funding from BONUS (Art 185) funded jointly from the European Union's Seventh Programme for research, technological development and demonstration, and from Baltic Sea national funding institutions.

ACKNOWLEDGMENTS

We would like to thank Amina Baccar Chaabane and Arunas Balciunas for supporting the sampling and Sarah Piehl for reviewing the content. We would also like to thank the feedback from two anonymous reviewers who helped to improve the writing of this manuscript.

SUPPLEMENTARY MATERIAL

The Supplementary Material for this article can be found online at: https://www.frontiersin.org/articles/10.3389/fenvs.2020.560237/full#supplementary-material.

REFERENCES

Abu-Hilal, A., and Al-Najjar, T. (2009). Marine litter in coral reef areas along the Jordan gulf of aqaba, red sea. *J. Environ. Manag.* 90, 1043–1049. doi:10.1016/j.jenvman.2008.03.014

Acuña-Ruz, T., Uribe, D., Taylor, R., Amézquita, L., Guzmán, M. C., Merrill, J., et al. (2018). Anthropogenic marine debris over beaches: spectral characterization for remote sensing applications. *Remote Sens. Environ.* 217, 309–322. doi:10.1016/j.rse.2018.08.008

Agisoft (2020). Tutorial (beginner level): orthomosaic and DEM generation with agisoft PhotoScan Pro 1.2 (with Ground Control Points). Available at: https://www.agisoft.com/pdf/PS_1.2%20-Tutorial%20(BL)%20-%20Orthophoto,%20DEM%20(with%20GCPs).pdf. (Accessed November 6, 2020)

Atwood, E. C., Castaño, S. R., Piehl, S., Cordova, M. R., Bochow, M., Franke, J., et al. (2018). Classification of riverine floating debris based on true color images collected by a low-cost drone system," in Sixth International Marine Debris Conference (6IMDC), Citarum River, Indonesia, March, 2018.

Battisti, C., and Gippoliti, S. (2019). Not just trash! Anthropogenic marine litter as a "charismatic threat" driving citizen-based conservation management actions. *Anim. Conserv.* 22, 311–313. doi:10.1111/acv.12473

Berhane, T. M., Lane, C. R., Wu, Q., Autrey, B. C., Anenkhonov, O. A., Chepinoga, V. V., et al. (2018). Decision-tree, rule-based, and random forest classification of high-resolution multispectral imagery for wetland mapping and inventory. *Rem. Sens.* 10, 580. doi:10.3390/rs10040580

BMVI (2017). Verordnungzur Regelung des Betriebs von unbemannten Fluggeräten. § 21a. Available at: https://www.bmvi.de/SharedDocs/DE/Anlage/LF/verordnung-zur-regelung-des-betriebs-von-unbemannten-fluggeraeten.pdf?__blob=publicationFile. (Accessed November 6, 2020).

Bravo, M., de los Ángeles Gallardo, M., Luna-Jorquera, G., Núñez, P., Vásquez, N., and Thiel, M. (2009). Anthropogenic debris on beaches in the SE Pacific (Chile): results from a national survey supported by volunteers. *Mar. Pollut. Bull.* 58, 1718–1726. doi:10.1016/j.marpolbul.2009.06.017

Campbell, J. B., and Wynne, R. H. (2011). *Introduction to remote sensing*. 5th Edn. New York, NY: Guilford Press.

Civil Aviation Administration (CAA) (2020). Approval of rules for the operation of unmanned aircraft. Available at: https://dronerules.eu/assets/covers/National-Regulation_LIT.pdf. (Accessed November 6, 2020).

Cohen, J. A. (1960). Coefficient of agreement for nominal scales. *Educ. Psychol. Meas.* 20 (1), 37–46. doi:10.1177/001316446002000104

Critchell, K., and Lambrechts, J. (2016). Modelling accumulation of marine plastics in the coastal zone; what are the dominant physical processes? *Estuar. Coast. Shelf Sci.* 171, 111–122. doi:10.1016/j.ecss.2016.01.036

Deidun, A., Gauci, A., Lagorio, S., and Galgani, F (2018). Optimising beached litter monitoring protocols through aerial imagery. *Mar. Pollut. Bull.* 131, 212–217. doi:10.1016/j.marpolbul.2018.04.033

DroneDeploy (2020). *Making successful maps*. San Francisco, CA. DroneDeploy.

Duhec, A. V., Jeanne, R. F., Maximenko, N., and Hafner, J. (2015). Composition and potential origin of marine debris stranded in the Western Indian Ocean on remote Alphonse Island, Seychelles. *Mar. Pollut. Bull.* 96, 76–86. doi:10.1016/j.marpolbul.2015.05.042

European Parliament and Council (2018). Regulation (EU) 2018/1139. Available at: https://eur-lex.europa.eu/legal-content/EN/TXT/PDF/?uri=CELEX:32018R1139&from=EN (Accessed November 6 2020).

European Union Aviation Safety Agency (EASA) (2020). Civil drones (Unmanned aircraft) regulations. Available at: https://www.easa.europa.eu/domains/civil-drones-rpas (Accessed November 6 2020).

Fallati, L., Polidori, A., Salvatore, C., Saponari, L., Savini, A., and Galli, P. (2019). Anthropogenic Marine Debris assessment with Unmanned Aerial Vehicle imagery and deep learning: a case study along the beaches of the Republic of Maldives. *Sci. Total Environ.* 693, 133581. doi:10.1016/j.scitotenv.2019.133581

Gago, J., Lahuerta, F., and Antelo, P. (2014). Características de basuras (abundancia, tipo y origen) en playas de la costa gallega (2001–2010). *Sci. Mar.* 78, 125–134. doi:10.3989/scimar.03883.31B

Garaba, S. P., Aitken, J., Slat, B., Dierssen, H. M., Lebreton, L., Zielinski, O., et al. (2018). Sensing ocean plastics with an airborne hyperspectral shortwave infrared imager. *Environ. Sci. Technol.* 2018, 52, 20, 11699–11707. doi:10.1021/acs.est.8b02855

Goncalves, G., Andriolo, U., Pinto, L., and Bessa, F. (2020). Mapping marine litter using UAS on a beach-dune system: a multidisciplinary approach. *Sci. Total Environ.* 2020 Mar 1; 706, 135742. doi:10.1016/j.scitotenv.2019.135742

Haseler, M., Schernewski, G., Balciunas, A., and Sabaliauskaite, V. (2018). Monitoring methods for large micro- and meso-litter and applications at Baltic beaches. *J. Coast. Conserv.* 22, 27–50. doi:10.1007/s11852-017-0497-5

Haseler, M., Weder, C., Buschbeck, L., Wesnigk, S., and Schernewski, G. (2019). Cost-effective monitoring of large micro- and meso-litter in tidal and flood accumulation zones at south-western Baltic Sea beaches. *Mar. Pollut. Bull.* 149, 110544. doi:10.1016/j.marpolbul.2019.110544

HELCOM (2017). *Economic and social analyses in the Baltic Sea region—supplementary report to the first version of the HELCOM "state of the Baltic Sea" report 2017.* Available at: http://stateofthebalticsea.helcom.fi/about-helcom-and-the-assessment/downloads-and-data. (Accessed June 7, 2020).

Hengstmann, E., Gräwe, D., Tamminga, M., and Fischer, E. K. (2017). Marine litter abundance and distribution on beaches on the Isle of Rügen considering the influence of exposition, morphology and recreational activities. *Mar. Pollut. Bull.* 115, 297–306. doi:10.1016/j.marpolbul.2016.12.026

Hidalgo-Ruz, V., Honorato-Zimmer, D., Gatta-Rosemary, M., Nuñez, P., Hinojosa, I. A., and Thiel, M. (2018). Spatio-temporal variation of anthropogenic marine debris on Chilean beaches. *Mar. Pollut. Bull.* 126, 516–524. doi:10.1016/j.marpolbul.2017.11.014

Jayasiri, H. B., Purushothaman, C. S., and Vennila, A. (2013). Quantitative analysis of plastic debris on recreational beaches in Mumbai, India. *Mar. Pollut. Bull.* 77, 107–112. doi:10.1016/j.marpolbul.2013.10.024

JRC (2013). *Technical recommendations for the implementation of MSFD requirements—Studio*. Brussels, Belgium: JRC, doi:10.2788/99475

Kaladharan, P., Vijayakumaran, K., Singh, V. V., Prema, D., Asha, P. S., Sulochanan, B., et al. (2017). Prevalence of marine litter along the Indian beaches: a preliminary account on its status and composition. *J. Mar. Biol. Assoc. India* 59, 19–24. doi:10.6024/jmbai.2017.59.1.1953-03

Kataoka, T., Murray, C. C., and Isobe, A. (2018). Quantification of marine macro-debris abundance around Vancouver Island, Canada, based on archived aerial photographs processed by projective transformation. *Mar. Pollut. Bull.* 132, 44–51. doi:10.1016/j.marpolbul.2017.08.060

Lavers, J. L., Oppel, S., and Bond, A. L. (2016). Factors influencing the detection of beach plastic debris. *Mar. Environ. Res.* 119, 245–251. doi:10.1016/j.marenvres.2016.06.009

Lehmann, J. R. K., Prinz, T., Ziller, S. R., Thiele, J., Heringer, G., Meira-Neto, J. A. A., et al. (2017). Open-source processing and analysis of aerial imagery acquired with a low-cost Unmanned Aerial System to support invasive plant management. *Front. Environ. Sci.* 5, 1–16. doi:10.3389/fenvs.2017.00044

Levin, N., Lugassi, R., Ben-Dor, E., Ramon, U., and Braun, O. (2006). Remote sensing as a tool for monitoring plasticulture in agricultural landscapes. *Int. J. Rem. Sens.* 28, 183–202. doi:10.1080/01431160600658156

Lillesand, T. M., Kiefer, R. W., and Chipman, J. W. (2004). *Remote sensing and image interpretation*. 5th Edn. New York, NY: John Wiley.

Lo, H. S., Wong, L. C., Kwok, S. H., Lee, Y. K., Po, B. H., Wong, C. Y., et al. (2020). Field test of beach litter assessment by commercial aerial drone. *Mar. Pollut. Bull.* 151, 110823. doi:10.1016/j.marpolbul.2019.110823

Marlin (2013). Final report of baltic marine litter project marlin—litter monitoring and raising awareness. Available at: http://www.cbss.org/wp-content/uploads/2012/08/marlin-baltic-marine-litter-report.pdf (Accessed September, 2011).

Martin, C., Parkes, S., Zhang, Q., Zhang, X., McCabe, M. F., and Duarte, C. M. (2018). Use of unmanned aerial vehicles for efficient beach litter monitoring. *Mar. Pollut. Bull.* 131, 662–673. doi:10.1016/j.marpolbul.2018.04.045

Mountrakis, G., Im, J., and Ogole, C. (2011). Support vector machines in remote sensing: a review. *ISPRS J. Photogrammetry Remote Sens.* 66, 247–259. doi:10.1016/j.isprsjprs.2010.11.001

Moy, K., Neilson, B., Chung, A., Meadows, A., Castrence, M., Ambagis, S., et al. (2018). Mapping coastal marine debris using aerial imagery and spatial analysis. *Mar. Pollut. Bull.* 132, 52–59. doi:10.1016/j.marpolbul.2017.11.045

Murphy, P. (2015). Detecting Japan tsunami marine debris at sea: a synthesis of efforts and lessons learned. Available at: https://marinedebris.noaa.gov/sites/default/files/JTMD_Detection_Report.pdf (Accessed January, 2015).

OSPAR (2010). Guideline for monitoring marine litter on the beaches in the OSPAR maritime area. Available at: https://www.ospar.org/ospar-data/10-02e_beachlitter%20guideline_english%20only.pdf. (Accessed January 7, 2020).

Pajares, G. (2015). Overview and current status of remote sensing applications based on unmanned aerial vehicles (UAVs). *Photogramm. Eng. Rem. Sens.* 81, 281–329. doi:10.14358/PERS.81.4.281

Purba, N. P., Handyman, D. I. W., Pribadi, T. D., Syakti, A. D., Pranowo, W. S., Harvey, A., et al. (2019). Marine debris in Indonesia: a review of research and status. *Mar. Pollut. Bull.* 146, 134–144. doi:10.1016/j.marpolbul.2019.05.057

Rosevelt, C., Los Huertos, M., Garza, C., and Nevins, H. M. (2013). Marine debris in central California: quantifying type and abundance of beach litter in Monterey Bay, CA. *Mar. Pollut. Bull.* 71, 299–306. doi:10.1016/j.marpolbul.2013.01.015

Ryan, P. G., Moore, C. J., Van Franeker, J. A., and Moloney, C. L. (2009). Monitoring the abundance of plastic debris in the marine environment. *Philos. Trans. R. Soc. Lond. B Biol. Sci*. 364, 1999. doi:10.1098/rstb.2008.0207

Schernewski, G., Balciunas, A., Gräwe, D., Gräwe, U., Klesse, K., Schulz, M., et al. (2017). Beach macro-litter monitoring on southern Baltic beaches: results, experiences and recommendations. *J. Coast Conserv.* 22, 5–25. doi:10.1007/s11852-016-0489-x

Schulz, M., Krone, R., Dederer, G., Wätjen, K., and Matthies, M. (2015). Comparative analysis of time series of marine litter surveyed on beaches and the seafloor in the southeastern North Sea. *Mar. Environ. Res.* 106, 61–67. doi:10.1016/j.marenvres.2015.03.005

Serra-Gonçalves, C., Lavers, J. L., and Bond, A. L. (2019). Global review of beach debris monitoring and future recommendations. *Environ. Sci. Technol.* 53, 12158–12167. doi:10.1021/acs.est.9b01424

Smith, S. D, and Markic, A (2013). Estimates of marine debris accumulation on beaches are strongly affected by the temporal scale of sampling. *PLoS One* 8, e83694–13. doi:10.1371/journal.pone.0083694

Story, M., and Congalton, R. G. (1986). Accuracy assessment: a user's perspective. *Photogramm. Eng. Rem. Sens.* 52, 397–399.

Topçu, E. N., Tonay, A. M., Dede, A., Öztürk, A. A., and Öztürk, B. (2013). Origin and abundance of marine litter along sandy beaches of the Turkish Western Black Sea Coast. *Mar. Environ. Res.* 85, 21–28. doi:10.1016/j.marenvres.2012.12.006

Tourismuszentrale (2019). Umweltmanagement am strand. Available at: https://www.rostock.de/aktiv/strand-meer/umweltmanagement-am-strand.html (Accessed November 06, 2020).

United Nations Environment Programme (2019). *Addressing marine plastics: a systemic approach—recommendations for action*. Nairobi, Kenya: United Nations Environment Programme.

United Nations (UN) (2019). Sustainable development goals. Oceans. Available at: https://www.un.org/sustainabledevelopment/oceans/. (Accessed November 06, 2020).

Veenstra, T. S., and Churnside, J. H. (2012). Airborne sensors for detecting large marine debris at sea. *Mar. Pollut. Bull.* 65, 63–68. doi:10.1016/j.marpolbul.2010.11.018

Ventura, D., Bonifazi, A., Gravina, M. F., Belluscio, A., and Ardizzone, G. (2018). Mapping and classification of ecologically sensitive marine habitats using unmanned aerial vehicle (UAV) imagery and object-based image analysis (OBIA). *Rem. Sens.* 10, 1331. doi:10.3390/rs10091331

Vlachogianni, T. (2019). *Marine Litter in the Mediterranean coastal and marine protected areas—how bad is it. A snapshot assessment report on the amounts, composition and sources of marine litter found on beaches*. Athina, Greece: Interreg Med ACT4LITTER & MIO-ECSDE.

Conflict of Interest: The authors declare that the research was conducted in the absence of any commercial or financial relationships that could be construed as a potential conflict of interest.

frontiers in Environmental Science

ORIGINAL RESEARCH
published: 27 January 2021
doi: 10.3389/fenvs.2020.579676

Assessment of Subsampling Strategies in Microspectroscopy of Environmental Microplastic Samples

Josef Brandt[1,2]*, *Franziska Fischer*[1], *Elisavet Kanaki*[1], *Kristina Enders*[3], *Matthias Labrenz*[3] *and Dieter Fischer*[1]*

[1]Leibniz-Institut für Polymerforschung Dresden e. V., Dresden, Germany, [2]Department of Marine Sciences, University of Gothenburg, Gothenburg, Sweden, [3]Leibniz Institute for Baltic Sea Research Warnemünde (IOW), Rostock, Germany

The analysis of environmental occurrence of microplastic (MP) particles has gained notable attention within the past decade. An effective risk assessment of MP litter requires elucidating sources of MP particles, their pathways of distribution and, ultimately, sinks. Therefore, sampling has to be done in high frequency, both spatially and temporally, resulting in a high number of samples to analyze. Microspectroscopy techniques, such as FTIR imaging or Raman particle measurements allow an accurate analysis of MP particles regarding their chemical classification and size. However, these methods are time-consuming, which gives motivation to establish subsampling protocols that require measuring less particles, while still obtaining reliable results. The challenge regarding the subsampling of environmental MP samples lies in the heterogeneity of MP types and the relatively low numbers of target particles. Herein, we present a comprehensive assessment of different proposed subsampling methods on a selection of real-world samples from different environmental compartments. The methods are analyzed and compared with respect to resulting MP count errors, which eventually allows giving recommendations for staying within acceptable error margins. Our results are based on measurements with Raman microspectroscopy, but are applicable to any other analysis technique. We show that the subsampling-errors are mainly due to statistical counting errors (i.e., extrapolation from low numbers) and only in edge cases additionally impacted by inhomogeneous distribution of particles on the filters. Keeping the subsampling-errors low can mainly be realized by increasing the fraction of MP particles in the samples.

Keywords: microplastics, subsampling, microspectroscopy, Raman, Fourier-Transform infrared

OPEN ACCESS

Edited by:
Andrew Turner,
University of Plymouth,
United Kingdom

Reviewed by:
Claudia Lorenz,
Aalborg University, Denmark
Joana Correia Prata,
University of Aveiro, Portugal

***Correspondence:**
Josef Brandt
josef.brandt@gu.se
Dieter Fischer
fisch@ipfdd.de

Specialty section:
This article was submitted to Toxicology, Pollution and the Environment, a section of the journal Frontiers in Environmental Science

Received: *03 July 2020*
Accepted: *15 December 2020*
Published: *27 January 2021*

Citation:
Brandt J, Fischer F, Kanaki E, Enders K, Labrenz M and Fischer D (2021) Assessment of Subsampling Strategies in Microspectroscopy of Environmental Microplastic Samples. Front. Environ. Sci. 8:579676. doi: 10.3389/fenvs.2020.579676

INTRODUCTION

The occurrence of microplastic (MP) particles in environmental compartments has gained notable interest in both scientific and mainstream media, a trend that is predicted to increase in the coming years (Halden 2015). A major cause of concern related to plastic materials is its accumulation potential due to their high persistence in the environment, while production rates further increase and concomitantly the plastic waste (Jambeck et al., 2015; Brandon et al., 2019; Borrelle et al., 2020). Assessments of the abundance of MP particles in various kinds of samples can be found throughout the literature e.g., in water (Lenz and Labrenz 2018; Liu et al., 2019; Karlsson et al., 2020), sediment or

soil (Claessens et al., 2013; Vianello et al., 2013; Bergmann et al., 2017; Enders et al., 2019), wastewater treatment plants (Tagg et al., 2015; Murphy et al., 2016) as well as biota (Lusher et al., 2017). Understanding sources, pathways and sinks of MP particles is key to understand how to effectively limit further spreading of this pollutant (Halle et al., 2016; Geyer et al., 2017; Siegfried et al., 2017). Therefore, large numbers of environmental samples have to be analyzed quantitatively, as not only the *spatial* but also the *temporal* occurrence of MP particles at a given location is of high relevance. Methods suitable for comprehensive monitoring studies need to be fast, quantitative and automated to deal with the high number of samples to process.

The currently used analytical tools can be sorted into two categories: mass and particle-based methods. Mass based methods are pyrolysis gas chromatography and mass spectrometry (Py-GC-MS) (Fischer and Scholz-Böttcher, 2019; Logemann et al., 2018; Dierkes et al., 2019) or thermoextraction and desorption coupled with gas chromatography-mass spectroscopy (TED-GC-MS) (Fischer and Scholz-Böttcher, 2019; Duemichen et al., 2014; Dümichen et al., 2015; Dümichen et al., 2017). Their main advantages are short analysis times and straightforward application. Also challenging environmental samples can be processed in few hours (Fischer and Scholz-Böttcher, 2019; Dümichen et al., 2017), with only relatively little sample preparation. The better the removal of organic matter, however, the more robust the analysis results will be, as organic compounds can hamper the correct data interpretation (Primpke et al., 2020a). As a drawback, only the integral mass fraction of polymer within the sample is obtained, without giving details on particle numbers or size distribution. Furthermore, the techniques are destructive, which makes it impossible to reuse the samples after measurement. Particle-based methods, such as spectroscopic imaging by Fourier-Transform infrared (FTIR) spectroscopy (Löder et al., 2015; Käppler et al., 2016; Primpke et al., 2017; Primpke et al., 2019) or microspectroscopic particle measurement using FTIR (Browne et al., 2010; Vianello et al., 2013; Löder et al., 2015; Tagg et al., 2015; Wagner et al., 2017; Käppler et al., 2018; Poulain et al., 2019) or Raman (Lenz et al., 2015; Käppler et al., 2016; Anger et al., 2018; Schymanski et al., 2018), register size, morphology and chemical classification of each particle (mass fractions can be estimated by applying volume estimates and bulk density values (Simon et al., 2018)). Particles >500 µm are often picked and investigated manually. For particles <500 µm, a purified particle dispersion (i.e., after removal of non-MP particles) is typically filtered onto a suitable filter substrate and then subjected to either imaging or individual particle measurement. The imaging approach entails scanning the entire filter area without a-priori knowledge about particle locations. Each spectrum at each measured pixel is evaluated and particle information is obtained by grouping together adjacent pixels with identical spectral classification (Primpke et al., 2017; Primpke et al., 2019; Primpke et al., 2020b). The particle measurement approach is done in two passes. First, an optical image is acquired with a light microscope (LM) to identify particles. Then, spectra are only acquired where particles were detected. **Figure 1** illustrates both approaches graphically.

Both methods are inherently slower than the mass-based techniques and require elaborate sample purification steps to remove non-plastic particles (Enders et al., 2020). Increasing the fraction of MP particles per sample allows for a faster and more reliable analysis, as less particles have to be processed and overloaded filters are avoided, which can lead to erroneous results. The currently used microspectroscopic techniques cannot compete with mass-based techniques regarding their sample throughput rates. However, to assess the potential toxicological impacts on both biota and humans, knowledge about MP particle size distribution and numbers is critical (Masó et al., 2003; Zettler et al., 2013). Hence, microspectroscopic methods for MP analysis are of high current relevance and the acceleration of sample throughput rates is one of the major challenges.

One approach to speed up imaging and particle measurements is to measure only a certain fraction of any sample and to extrapolate the obtained results. This can be achieved in two ways: i) Subsampling before filtration: only a fraction of the entire sample is filtered onto the sample substrate which will be completely measured. This method requires very careful homogenization of the sample to avoid extrapolation errors. For homogenization, different densities and the fast sedimentation of the particles in aqueous suspensions pose challenges. The success of this splitting before filtration is largely influenced by the method and splitting tools applied. ii) Subsampling during analysis: The entire sample is filtered on one or multiple filters, but only a fraction of each filter is measured. This method circumvents the challenges of prior homogenization and sample splitting, but requires a robust strategy to select which areas or particles to measure. The main statistical problems therein arise from both, the inhomogeneous distribution of the particles on the filter and the low numbers of MP particles, of typically around 1%. The present study focuses on pathway ii) i.e., the statistical subsampling of particles that are already on the filter substrate. The results are applicable to any MP sampling technique probing particles spatially distributed on a filter substrate, irrespective of the exact measurement technique. However, we do not strive to determine hard numbers for potential speed gains, as these are highly dependent on the actually used method and measurement requirements. Speed optimization of each analysis technique is an important, yet difficult endeavor requiring careful balancing the runtime with result quality, which is highly specific for the respective methods.

Subsampling on a Substrate: Challenges

Filtering particles from an environmental sample onto a microscopy filter does not lead to a homogeneous distribution of particles on the filter area. Comprehensive guidelines explain the challenges and recommend strategies for successful filtrations. (Merck, 2018). The stream of water is usually not of a constant flow-rate, leading to different forces on the particles on the filter throughout the filtration process. Air bubbles can be present that

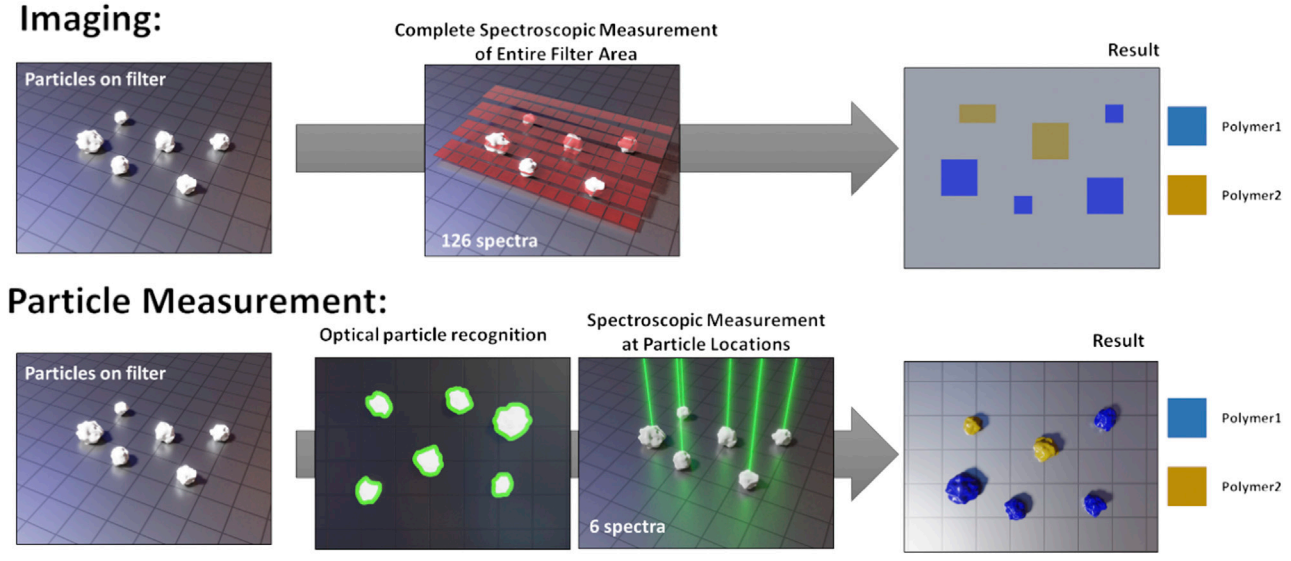

FIGURE 1 | Schematic comparison of spectroscopic imaging and particle measurement. Reproduced from Brandt et al. (2020).

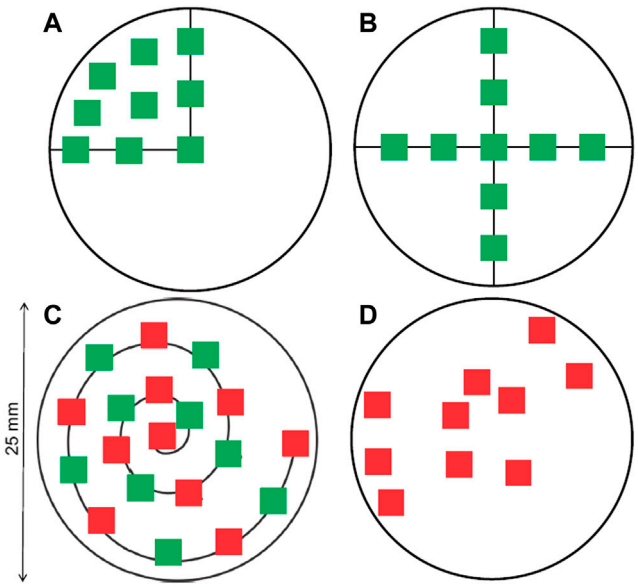

FIGURE 2 | Distribution of measure areas on a circular filter, following different layouts. **(A)** Spreading on a quarter of the filter. **(B)** Forming a cross. **(C)** Following a spiral. **(D)** Random placement. The green squares correspond to 7.3% of the filter area and the red boxes to 8.2%, respectively. Both together represent 15.5% of the filter area (Huppertsberg and Knepper 2018).

introduce additional unpredictable forces. Often, the particle concentration on the filter follows a gradient with low concentrations around the filter center and higher concentrations closer to the filter perimeter (Thaysen et al., 2020). To minimize coagulation of particles on the filter, the flow rate can be reduced or tangential flow filtration can be performed (Buffle and Leppard 1995).

Further inhomogeneity is introduced by the nature of the environmental particles. Depending on the sample origin (e.g., rainwater or wastewater treatment sludge) and given the large range of MP types itself, the samples contain a broad variety of particles different in size, density and shape; properties that have a significant influence on particle distribution dynamics. In addition, particles that tend to aggregate easily clump together and can even incorporate particles of other types. The low fraction of MP particles per sample can lead to low statistical robustness of any deduced conclusions (Anger et al., 2018; Karlsson et al., 2020). All such factors make the selection of a representative subset an especially challenging task and have to be considered during the assessment.

Proposed Subsampling Strategies

The strategies proposed to select a representative subset during analysis can be sorted into two categories, corresponding to two different workflows.

The first category, the "area selection strategy," does not need any *a priori* knowledge and distributes a number of box-shaped areas to measure over the entire filter area. It is mostly suitable for imaging protocols. Different layouts for distributing the measuring boxes can be considered to account for the inhomogeneous distribution of particles on the filter, such as a cross or a spiral layout (refer to **Figure 2**). (Huppertsberg and Knepper, 2018). The number and size of the boxes can be adjusted to cover a desired fraction of the filter. After the spectroscopic measurements within the box areas, the result is then extrapolated according to the fraction of filter area covered by the boxes. It is theoretically possible to design area-based subsampling approaches that do not rely on placing rectangular boxes, for instance dividing the filter in cake-piece shaped sections. Such a section accounts for a radial inhomogeneity by covering central and peripheral area of the filter. Their

TABLE 1 | Summary of origin of analyzed samples (WWTP = wastewater treatment plant).

Compartment	Origin	Number of samples
Rainwater	Weser catchment area, Germany	5
Riverine surface water	Warnow catchment area, Germany	6
Riverine sediment or beach sand	Schlei river, Germany, baltic sea beaches in Germany, Denmark, Sweden	10
Wastewater sludge	Municipal WWTP designed for 50.000 inhabitants, Germany	6

practical application could be limited, however, as most FTIR- or Raman-software packages are restricted to the selection of rectangular areas for measurement. The viability of the different layouts will be assessed practically later in this manuscript.

The second category, the "particle selection strategy," requires some *a priori* knowledge that is gained from first acquiring an overview optical image from the entire filter using a light microscope (LM). That image can be used to determine the number and location of each particle or even characterize the particles further regarding their size, shape and color (thereby decreasing the uncertainty about the particle location) and the actual fraction of particles measured can be adjusted more precisely. If further information per particle is derived, more sophisticated chemometric methods for finding representative subsamples can be engaged (Chaudhuri, 1994; Daszykowski et al., 2002; Rodionova and Pomerantsev, 2008).

It is also possible to combine both approaches. Imhof et al., for instance, chose to manually identify particles larger than 500 µm and to automatically measure all smaller particles based on an "area selection strategy," measuring approx. 1.6% of the filter area (Imhof et al., 2016).

Different subsampling strategies are currently in use that usually measure about 1–10% of the filter area. Their use is in most cases justified by hypothetical considerations, but practical validations of the subsampling strategies are scarce. A recent study by Mintenting et al. assessed the subsampling and errors of riverine water samples and concluded that at least 50% filter coverage is needed for robust particle counts, which is substantially higher than most studies aim for (Mintenig et al., 2020).

With this publication, we revisited 27 MP samples from different environmental compartments that were measured by Raman microspectroscopy, without using any subsampling method. The GEPARD software was used for particle detection and automated Raman measurement, an appropriate tool to reduce analysis time and remove operator-bias (Brandt et al., 2020). As a side effect, all information about the filtered sample (e.g., particle count, coordinates, sizes and spectral identification) is stored in particle datasets. These datasets are used to re-evaluate the sample by simulating a measurement using a dedicated subsampling strategy and determining the subsampled result. Comparing subsampled to original result allowed us to draw quantitative conclusions about the statistical robustness and usability of the investigated subsampling strategies.

MATERIALS AND METHODS

Sample Details and Filtration

27 fully analyzed samples from different environmental compartments were the basis for our analysis (**Table 1**). The samples underwent purification procedures identical to established schemes as presented by Enders et al. (Enders et al., 2020), a study which presents a flow chart of detailed protocols for the different sample conditions. Reproducibility of the applied purification methods is thereby ensured. An exception to the above are the rainwater samples that underwent a combination of oxidation with Fenton's reagent, enzymatic digestion and density separation using $ZnCl_2$ (Löder et al., 2017). The final filtration was done using a tailor-made glass filtration device. After cleaning all glass parts with 3% H_2O_2 and sonication in MilliQ water (3 × 10 min, renewal of the MilliQ water after each 10 min interval), 10 × 10 mm silicon filters with 10 or 50 µm holes were inserted into the filtration device using red PTFE filter holders that also act as seals. During filtration, the flow rate of the water is observed to avoid overloading of the filters. The filtration is done in a laminar flow box (Telstar Aeolus V) to avoid contamination from air-borne particles. Full details about used filters and the filtration setup are already published and can be found elsewhere (Käppler et al., 2015; Brandt et al., 2020). Without prior homogenization, each sample was filtered onto several filters. Only one of these filters per sample was used in the following analyses, so the particle numbers and MP content are not representative for the actual environmental sample. Therefore, further information on the sample origin and the sampling is neglected. The analyzed samples counted between 1,500 and 33,000 particles per filter. In the following, both "sample" and "filter" refer to the single filter representing each environmental sample.

Particle Measurements

Full details about the measurement workflow using the GEPARD software are reported in a separate publication (Brandt et al., 2020); only a short summary is given here.

LM images were acquired directly in the Raman microscope (WITec® alpha 300R), which is also used for the spectroscopic measurements using a 532 nm laser and a 600 L/mm spectroscopic grating. The optical LM images were acquired in dark-field at adjustable focus heights, which allows constructing an image of optimal depth-of-field for both, small and large, particles. A watershed-based image segmentation algorithm was used to localize particles and determine their boundaries. Raman spectra were collected for each particle (typical conditions: 0.5 s

integration time, five accumulations) and the TrueMatch® software (WITec®) was used for spectral evaluation. The results from spectra database matching were combined with the particle information from the particle recognition step to obtain complete information about particle type *and* size distributions.

Data Processing

The datasets generated by the GEPARD software contain all information about particle location, contour and chemical classification. This readily allows revisiting the datasets and selecting particles from the entirety of the particle list according to any desired subsampling strategy. The code for all calculations is realized in form of a *Python* script, the full source code can be found on https://gitlab.ipfdd.de/Brandt/subsampling.

To assess the performance of any considered subsampling model it is necessary to derive quantitative measures of its performance. We calculated the *subsampling-error* according to **Equation 1**. A subsampling model was applied to each fully measured dataset and the subsampled count of MP particles determined (SI chapter "Application of Subsampling Methods"). To estimate the total MP particle count, the subsampled count was extrapolated by dividing by the subsampling fraction. That estimated MP particle count was then divided by the original MP particle count.

$$\textit{subsamplingError} = \frac{\textit{mpCount}_{\textit{subsampled}} \big/ \textit{fraction}}{\textit{mpCount}_{\textit{original}}} \cdot 100\% \quad (1)$$

To reduce statistical deviations, each filter was processed 10 times. For each iteration, the filter was rotated about 36° around the filter center and then the subsampling is repeated. This increases the number of performed tests by 10-fold and reduces noise in the results, making data interpretation more robust.

Implemented Subsampling Methods

Hereafter, we describe the implemented subsampling methods. The first two followed the particle selection strategy, *i.e.*, rely on knowledge about particle location, and the remaining methods follow the area selection strategy, i.e., they represent different approaches for placing rectangular areas (boxes) for conducting measurements. To test practically relevant fractions, we tested fractions from 2 to 90% in terms of particle count fractions, and from 2% to the maximum achievable fraction in terms of filter area coverage for the individual box selection methods.

Random Particle Subsampling

The method is based on a prior particle recognition step. Out of the list of detected particles, a given number is selected on a completely random basis to represent the desired fraction of particles measured.

SizeBin Particle Subsampling

The concept is the same as in the random particle subsampling with additional accounting for size distribution bias to reduce the uncertainty related to low number size fractions (as usually the case for larger particles). Therefore, the detected particles are first grouped into size bins. The chosen size limits in between the bins are 5 µm, 10 µm, 20 µm, 50 µm, 100 µm, 200 µm, and 500 µm. After sorting the particles into the bins, a certain number of particles is randomly drawn from each bin so that the measured fraction of particles is equal for all bins. At least one particle is taken from each bin (given, that the bin is not empty). For example, when 10% of all particles have to be measured, the algorithm will select 5 particles out of a bin with 50 particles, 20 out of a bin with 200 particles and 1 out of a bin with only 4 particles.

TABLE 2 | Highest achievable filter coverage for the implemented patterns. By its pattern, the cross layout is only feasible with five or 9 boxes (3 or five boxes across, respectively). The other patterns were arbitrarily set to have either 5, 10 or 20 boxes.

Number of boxes	Cross	Spiral	Random	Random quarter
5	54%	26%	46%	21%
9	38%	n.a.	n.a.	n.a.
10	n.a.	29%	47%	17%
20	n.a.	25%	43%	14%

Box Selection Subsampling

Four different layouts were implemented for placing measuring boxes on the circular filter:

i. Cross layout with either 3 or 5 boxes across, respectively (**Figure 2B**)
ii. Spiral layout with 5, 10 or 20 boxes. The first box is located in the center and the last one touches the perimeter of the filter area. (**Figure 2C**).
iii. Random layout with 5, 10 or 20 boxes. The boxes are placed randomly on the filter area. Given this random character, the highest achievable fractions can vary slightly, also depending on how many tries the algorithm was allowed to perform to find a valid solution. The implemented algorithm sets the random number generator to a fixed seed prior to calculation to yield the same random pattern for each run (**Figure 2D**).
iv. Random layout on a quarter of the filter with 5, 10 or 20 boxes. Same as iii), but box placement is restricted to only a quarter of the filter (**Figure 2A**).

In all box selection approaches, the size of the (square) boxes is adjusted so that the desired fraction of filter area is covered, without having the individual boxes overlap or range over the filter perimeter. The maximum achievable fraction of filter to be covered is summarized in **Table 2** (More details about box placement and the link to the code for interactive visualization can be found in SI chapter 1).

Figure 3 shows a graphic user interface (gui) to visualize the implemented methods on real samples, measured by GEPARD. All the subsampling methods in **Figure 3** are configured to select 10% of the sample i.e., 10% of the particles are measured by the "random" and the "size bin" selection, whereas 10% of the filter area is covered by the respective box selection methods. The gui

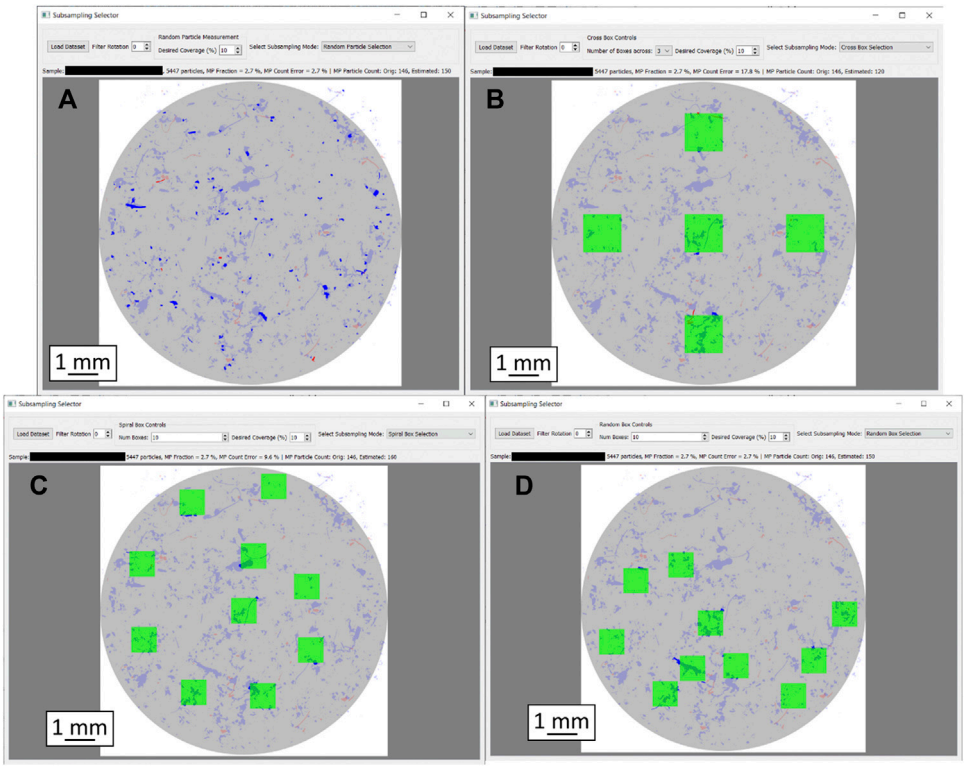

FIGURE 3 | Graphic representation of the particle distribution heterogeneity as well as different subsampling approaches with 10% filter coverage each. Filter diameter is 10 mm in each case. **(A)**: Random subsampling, **(B)**: Box selection, cross layout, **(C)**: Box selection, spiral layout, **(D)**: Box selection, random layout. MP particles are shown in red, others in blue. Particles missed by the respective subsampling method are displayed in pale colors; only the particles in strong colors were captured.

allows adjusting the measured fraction of each method, as well as the number of boxes for the box sampling methods. Furthermore, the loaded sample can be rotated about a given angle. A text box above the filter scheme summarizes sample details (particle count, MP percentage) and displays the results from the respective subsampling method.

RESULTS AND DISCUSSION

Particle-Based Subsampling

At first, we investigated the subsampling-error (%) as a function of the measured fraction of particles (%) for the four respective sample categories (**Figure 4**), see SI chapter "Selected Images of Filters" for example images. We chose grouping the samples by their environmental origin because a sample's origin is always known. Sorting samples into categories allows deduction of parameters influencing subsampling efficiency and, vice versa, allows estimating subsampling efficiency if a sample's category was known. Hence, any correlation between environmental compartment and subsampling performance would allow for a better planning of the subsampling strategy without any further sample characterization. The averaged particle numbers per filter are given in the plot titles for each category, as well as the average MP percentage within these particles. Each data point in **Figure 4** represents the average over all filters from the respective group of sample types (number of filters is given in plot title), where each filter was evaluated 10 times. The resulting subsampling-error exponentially decreases with increasing measured fraction and approaches 0 at 100% (note the logarithmic *x*-axis in **Figure 4**). Comparing the two different particle based subsampling methods shows that sorting particles into size bins (**Figure 4**, green) or not (**Figure 4**, orange) does not seem to have a systematic advantage across sample types.

The results illustrate that measuring only small filter fractions (both in terms of particle count or covered filter area) can lead to large counting errors. Measuring less than 5% of the entire particle population leads to errors exceeding 50%. Even worse, also the error margins increase with decreasing fraction measured in the plots in **Figure 4**. For example, at 5% measured fraction, the subsampling-error could be 20% or 80%. This large range of potential errors of a particular filter demonstrates that measuring such small fractions does not allow a sensible extrapolation of MP occurrences.

Comparing the results from the different compartments shows that the subsampling-errors are generally lower when the sample has more particles (i.e., higher number of particles is measured at a given fraction) or the sample has a higher content of MP particles. Especially the MP content is critical: The high MP content of the rainwater samples compensates the low particle

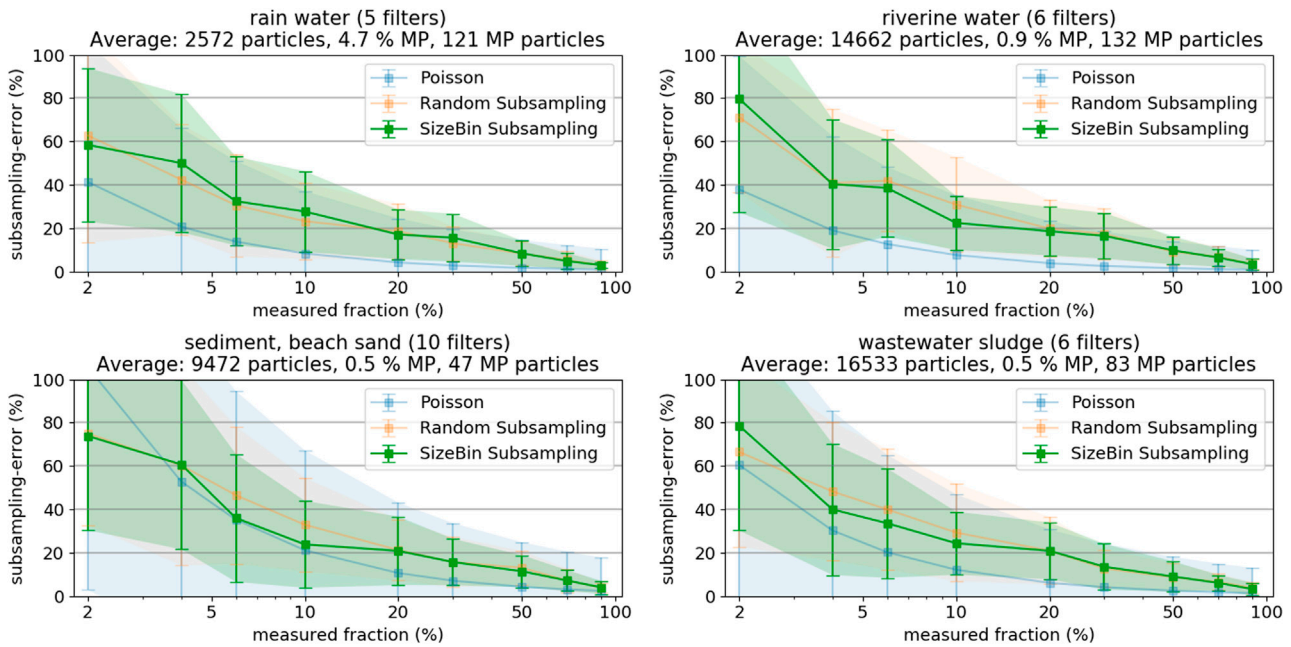

FIGURE 4 | Subsampling-errors and their standard deviation of Random and SizeBin Subsampling, as derived from the different sample types (rainwater, river water, sediment, and sludge). As reference, the theoretical subsampling-error derived from the Poisson distribution.

count (at 10%, only about 300 particles are measured!) and the subsampling-errors are comparable to the sludge samples with a substantially higher particle count (at 10%, about 1,700 particles have to be measured) but low MP content.

Reliably predicting magnitude and standard deviation of the subsampling-error is a complicated task. Anger et al. used the normal distribution to estimate the number of particles to achieve a certain error, but applying the formula requires knowing MP fraction and the prediction interval (Anger et al., 2018). Karlsson et al. used the Poisson distribution to model the probability density functions of MP occurrence observations (Karlsson et al., 2020). The Poisson distribution is better suitable for smaller sample sizes and, for application to the present study results, only requires an estimate of the MP fraction (mean equals variance in the Poisson distribution). **Figure 4** also shows the theoretically expected errors and error margins for the Poisson distribution, assuming the average MP count indicated in the plot titles. The agreement of theoretical and experimental subsampling-errors is good for the samples from sediment and beach sand, having the lowest absolute number of MP particles. However, the Poisson distribution more and more underestimates the subsampling-error with increasing number of MP particles. A more in-depth statistical discussion of the topic should be the scope of a separate study.

The estimation of the present MP content on a particular filter is difficult, but vital for the determination of the minimum subsampling fraction to measure. Based on the divers set of different sample types and applying the random particle subsampling, we found, that if we accept a maximum subsampling-error of 20%, the minimum fraction of particles to measure is either 50% of all particles, or a total of 7,000 particles (**Figure 5**). These thresholds are valid even for MP fractions approaching as low values as 0.1%. Note, the set of filters herein analyzed was characterized with relatively low total particle counts (maximum of 33,000), which hinders applying our findings to larger filters with substantially higher particle counts. These results furthermore show decreasing subsampling-errors with increasing MP content. This, in turn, highlights the tremendous importance of effective sample purification measures to increase the MP fraction. As a result, not only analysis times shorten by reducing the total number of particles to consider, but also the extrapolation of results becomes more reliable when applying subsampling methods.

Measuring at least 5,000 particles per filter might be a realistic target for scientific purposes, but might also be impractical for monitoring applications with substantially higher sample counts. Measurement times can vary greatly depending on the exact parameters for optical scan and spectroscopic measurement. Our Raman microspectroscopy approach would require approximately 6 to 8 h for such a measurement, including optical scan (1–3 h), particle detection (several minutes) and spectroscopic measurement (approximately 5 h, a more comprehensive review of commonly used analysis times for Raman microspectroscopy is given by Anger et al. (2018)). The particle-based methods allow exploiting information from the optical microscope image to decrease the subsampling-errors at very low measured fractions. The image of the filter not only allows to precisely count and locate the particles, but also to analyze each particle in terms of its characteristics regarding shape, color, size and texture. A classifier that allows distinguishing MP from non-MP particles (with a certain level of confidence) based on these characteristics can be trained by

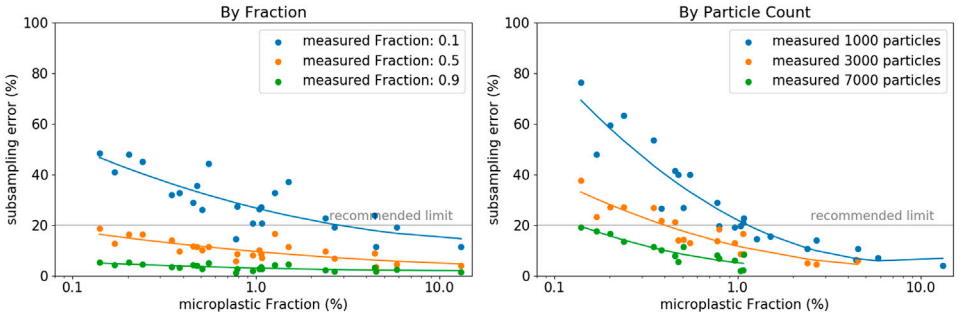

FIGURE 5 | Compilation of the individual errors of each sample (each representing an average of 10 iterations per sample) as a function of the MP fraction with a color-coding representing **(A)** the measured fraction of particles or **(B)** a distinct particle count, respectively (random particle subsampling).

running a feature extraction on a large number of particles of known type (i.e., MP and non-MP, respectively). This "artificial" up-concentration of MP particles post purification reduces the error-margins in subsampling and is especially useful when only low percentages of particles can be measured. Procedures for the classification of particles from microscopy can be found throughout literature and give valuable information about what kind of particle features to exploit (Xu et al., 1997; Xu et al., 2018; Peng and Kirk, 1998). Developing a machine-learning model for effective MP classification from microscopy images goes beyond the scope of this manuscript, due to the complexity of such an endeavor, especially due to the low content of MP particles i.e., the highly imbalanced datasets (Batista et al., 2004; Wei and Dunbrack 2013). Instead, we decided to assess the final reduction in subsampling-errors, given a classifier with a certain accuracy score would exist. That helps deciding on whether to actually start the efforts of developing a real classifier. As our datasets where already fully analyzed, a dummy classifier can be readily set up yielding any desired score from 0.5 (i.e., no actual knowledge, sampling is completely random) to 1.0 (i.e., perfect classifier). Three dummy classifiers with scores of 0.6, 0.7, and 0.8 were tested, respectively. The concept is to use the classifier to extract a subsample of all particles, which will have a higher MP fraction than the original set of particles. As discussed above, a higher fraction of MP has the highest potential to increase subsampling accuracy. Then, the desired number of particles is chosen on a random base from the subset with increased MP fraction. Details about the dummy classifier and the exact calculations can be found in SI chapter "Details on Trained Random Particle Subsampling". **Figure 6** shows the results of the three classifiers, as compared to the purely random particle subsampling.

The subsampling-errors at low measured fractions decrease significantly when the score of the used classifier increases. The results clearly show that the application of a classifier substantially decreases the very high subsampling-errors below 10% measured fraction, even if their classification score is not higher than 0.6 to 0.8. The effect gets less pronounced at higher measured fractions wherefore it is most sensible to apply the methods if the measured fractions are lower than 10%. It is important to keep in mind that the final particle assignment is done according to the results of the spectroscopy measurement, regardless of the used classifier's initial guess. Subsampling based on a classifier, however, complicates the step of extrapolation as the sample measured is no longer a random representative of the statistical universe of the filter. Refer to SI chapter 5 for more details on the calculations. The obtained findings are good reason for engaging in development of a real classifier suitable for MP classification on LM images. However, also other techniques, such as particle staining with fluorescent dyes, could be exploited for an according pre-selection of a subset with increased MP content (Shim et al., 2016).

Box-Based Subsampling

A closer investigation on distribution of the particles on the filters is necessary before reviewing the box-based subsampling method. The patchy and inhomogeneous distribution of the particles on the filter exemplifies the difficulty to design a pattern for a box selection subsampling (**Figure 3**, MP particles in red, others in blue). Analyzing the impact of particle distribution heterogeneity on the subsampling-error of the box-placement methods requires quantification of the heterogeneity, which is a difficult endeavor. Comparable literature studies are scarce but, fortunately, a recent study investigated the distribution of particles on filters (Thaysen et al., 2020). However, only examples from artificially produced model samples were included. They proposed plotting particle count as a function of particle distance to filter center to observe particle distribution patterns. They exhibited "starburst" particle distributions with highest particle density around the filter center. To compare our results of real environmental samples to their results we did the same calculations for filters from different environmental compartments. However, we converted "particle count" into "particle density". Particle density is obtained by dividing particle count by the area of the filter section that is represented by the respective distances (intuitively, the section from 1 to 2 mm away from filter center is smaller than the section from 4 to 5 mm). Thereby, the differences in area of the filter sections is taken into account and patterns emerge more clearly (the original plots with particle count as function of distance from filter center (i.e., without correction for filter increasing area of filter sections) can be found in supporting information **Supplementary Figure S1**). However, the distance from the filter center distribution alone does not fully capture particle distribution inhomogeneity. For instance, the method would be insensitive to particles distributed only on one half, or quarter, of the filter. To overcome this potential error we developed and

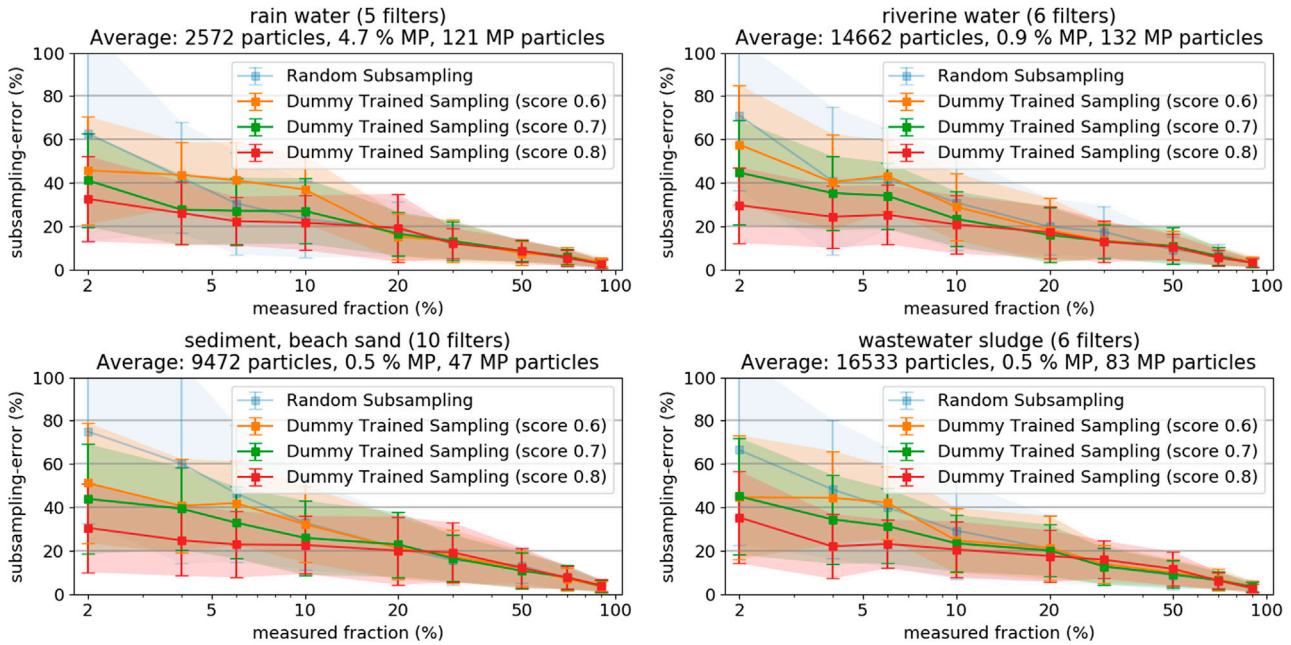

FIGURE 6 | Resulting subsampling-errors and their standard deviation from random sampling based on trained classifiers with different scoring, as derived from samples from rainwater, river water, sediment, and sludge, respectively.

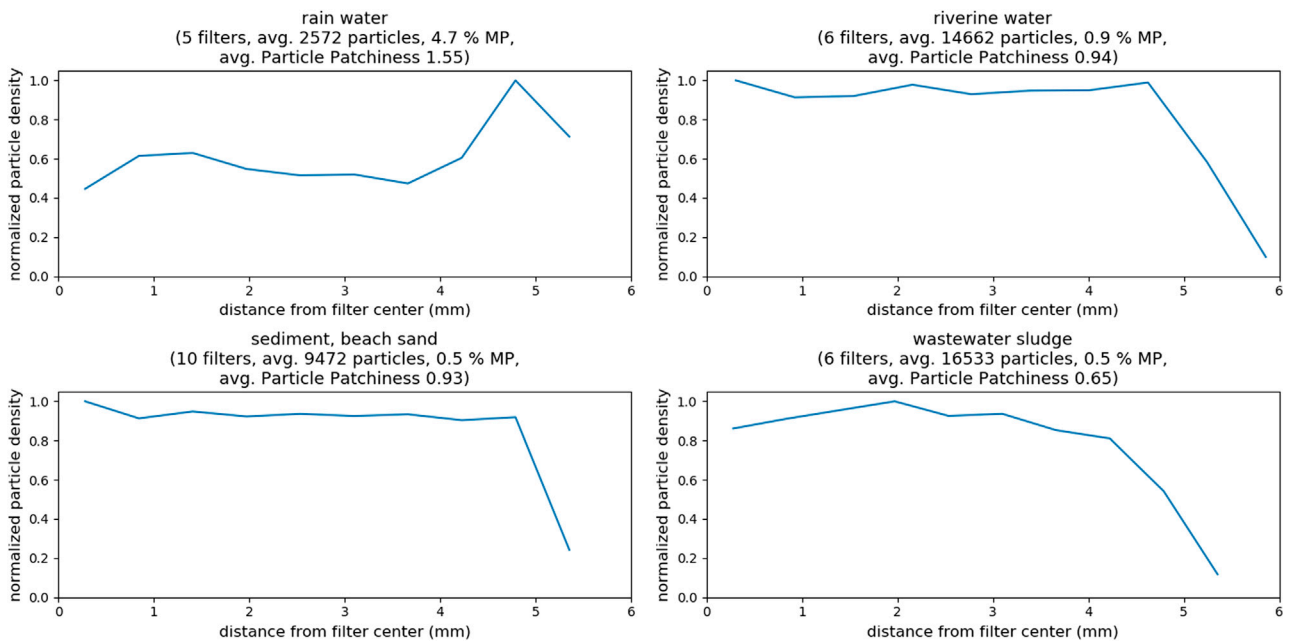

FIGURE 7 | Total particle density as function of distance from filter center for samples of different compartments, as well as determined particle patchiness. All filtrations were done on 10 × 10 mm silicon filters.

implemented an orthogonal approach to calculate the "average particle patchiness" value. The approach entails dividing the filter area in cells (e.g., 50 × 50), and calculating the number of particles in each cell. The average particle patchiness is then obtained by dividing standard deviation of the particle number per cell by its mean value. **Supplementary Figure S2** in the SI shows example images of filters with low, medium and high particle patchiness and the respective (increasing) values.

In **Figure 7**, the filters are grouped again according to their environmental origin. Again, knowing if there was any

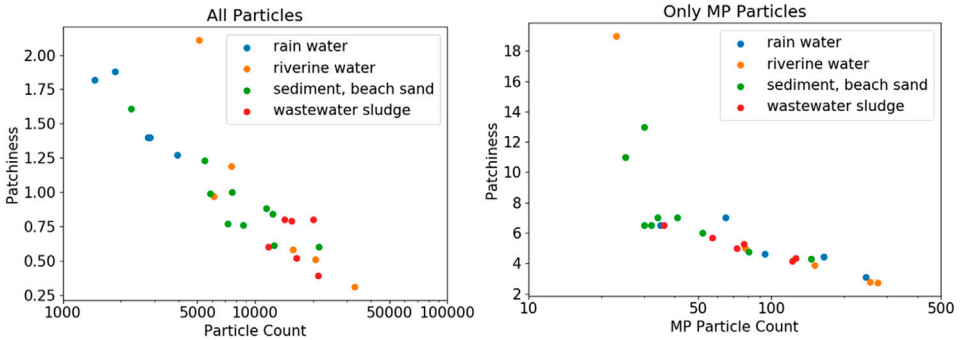

FIGURE 8 | Particle patchiness as a function of total particle count and MP particle count, respectively. Note the logarithmic scale of the particle count. The patchiness is generally lower at higher particle counts.

correlation between particle distribution homogeneity and sample compartment would be useful (see SI chapter "Selected Images of Filters" for example images). In case of the rainwater filters, particle density on the filters peaks at around 5 mm, indicating a ring formation of particles at the perimeter of the filter (refer to **Supplementary Figure S3**); inhomogeneous particle distribution is also indicated by the high patchiness value of about 1.5. The samples from all other compartments show a similar pattern with almost constant particle density from center to the border of the filter, where particle density eventually decreases (refer to **Supplementary Figures 4 - 6**). The analyzed examples did not reveal any "starburst" pattern as to be expected from model samples (Thaysen et al., 2020), but drawing any conclusions is difficult, without taking into account details about sample workup and filtration procedures (Merck, 2018). Conversely, observing the averaged particle counts and the corresponding patchiness values indicates a correlation. Higher overall particle counts lead to a more homogeneous distribution of the particles on the filter. In fact, the observed patchiness of all investigated samples correlates well with the particle count, as shown in the left panel of **Figure 8**. It is important not to misunderstand that finding! The goal should not be to maximize the absolute particle count, but to increase the number of MP particles on a filter. The right panel of **Figure 8** shows that the correlation between patchiness and particle count is the same if only MP particles on the filter are considered. The trend is the same, although the absolute values of the patchiness increase substantially. Refer to **Supplementary Figure S2** in the SI for a visualization of different levels of patchiness.

Reviewing the subsampling-errors of the box subsampling methods, our investigations showed that the obtained subsampling-errors are very similar for the individual layouts when applied to the filters grouped according to their environmental origin (refer to **Supplementary Figure S7–Supplementary Figure S10**). The number of boxes to create the individual layouts does not seem to have a notable effect, although the cross layout shows slightly lower errors when using five, instead of three boxes across. Only in case of the rainwater samples with low particle counts and inhomogeneous particle distribution (resulting in many empty spaces on the filter i.e., high patchiness), the errors from box measurement subsampling exceed the errors from the random particle subsampling. Otherwise, the observed subsampling is dominated by the counting error, rather than an additional error resulting from inhomogeneous particle distribution.

Figure 9 shows the subsampling-error of the box-placement methods when sorting the filters into categories with different particle counts. Including the random particle subsampling-error, which is not affected by particle patchiness, allows distinguishing the pure counting error from errors resulting from inhomogeneous particle distribution on the filter. In case of very low particle numbers (≤2000) the subsampling-error from the box-based methods is substantially higher than for the random particle subsampling, which indicates an additional contribution of particle distribution inhomogeneity to the subsampling-error. At higher particle counts, the subsampling-errors from random particle subsampling and the box-placement methods come closer together, indicating a decreasing influence of the particle distribution inhomogeneity. At around 5,000 particles (corresponding to a patchiness of approximately 1.0, see **Figure 8**) the box-based sampling methods do not perform worse than the random particle subsampling.

In order to keep the subsampling-error and its deviation within one sigma below a 20% error margin, the covered area of the filter should be at least 50%. A 50% filter area coverage could only be fully realized with the cross layout with three boxes across and, near enough, the random box layout (with 47% coverage at 10 boxes, **Table 2**). In contrast to the particle-based subsampling, the box placement methods do not bear opportunities for exploiting machine-learning methods to increase accuracy at low measured fractions.

Counting all MP vs. Counting Particular MP Types

To simplify the quantitative assessment, herein only the integral MP particle numbers were considered without discrimination into different polymer types or morphological features. Most studies, however, require information of MP species such as chemical classification, color, size and shape. There are no standard categorization methods in place as it depends on the research question and the precise analytical tasks chosen. However, the issue shall be addressed with some general reflections.

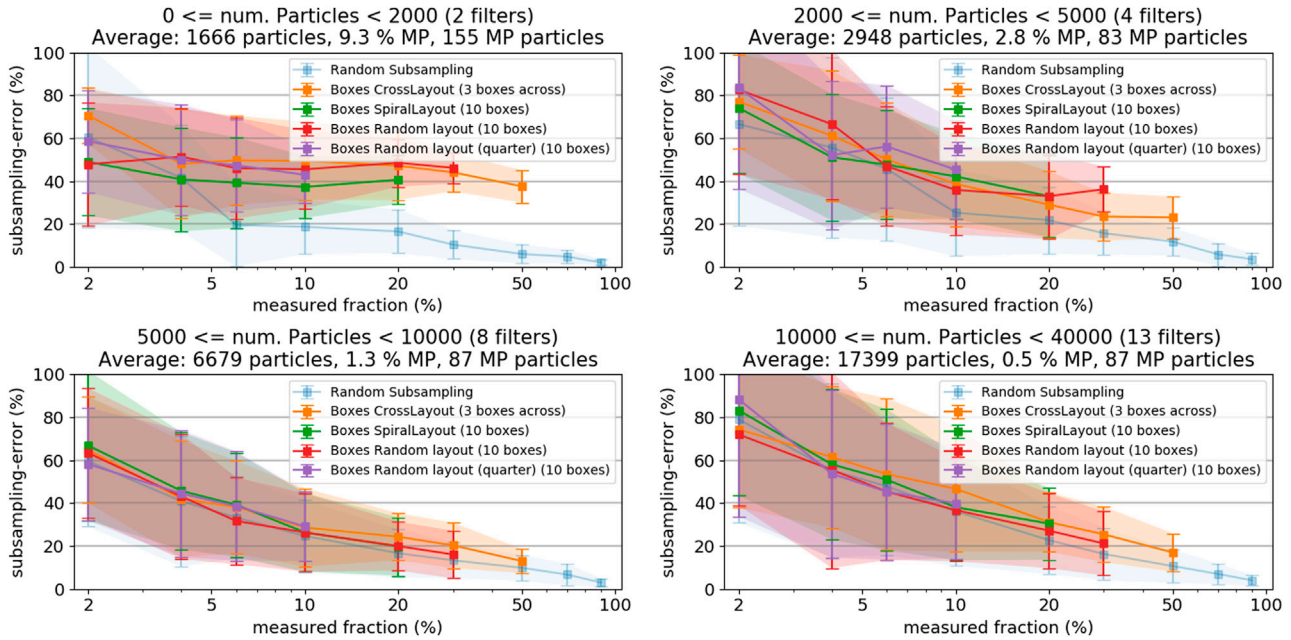

FIGURE 9 | Subsampling-error of the box placement methods for filters with low **(A)** and high **(B)** particle patchiness, respectively. Both plots also show the random particle subsampling method, representing the count error, as reference.

Our study demonstrated the occurrence of high subsampling-errors and high error margins when measuring low fractions of particles on a filter. As a differentiation of different particle types would decrease the individual particle numbers, the subsampling-errors would increase accordingly. In other words, if particle types have to be distinguished, the overall number of particles to measure has to be increased. Thus, predicting which MP particle classes are present in a sample results in even larger uncertainties than estimating the integral MP content. A general recommendation about required particle numbers cannot be reliably given for such cases. A practical approach should entail measuring a certain fraction of all particles, counting the particles in all categories of interest and deciding if more particles need to be measured. As a consequence, already reducing the initial sample volumes prior to the purification steps can limit the final robustness of the results i.e., when yielding to small numbers of the target particles. Treated sample volumes should therefore be generously calculated. Karlsson et al. discussed how many particles have to be measured for having a statistically robust number (Karlsson et al., 2020). Their study concluded a reasonable number would be of about 30 particles per class. This is in agreement with the results of our analysis that revealed an error of about 20% (**Figure 4**) when having measured about 30 MP particles. Nevertheless, exceptions have to be made for "very rare" categories.

CONCLUSION AND OUTLOOK

Spectroscopic particle measurements are of high importance when it comes to MP analysis in environmental samples but need to be sped up to be established as monitoring tools. We compared the performance of different subsampling approaches, based on two different method categories: 1) particle-based methods and 2) measure box placement methods on 27 environmental samples from different compartments, such as rainwater, river water, sediment and wastewater sludge.

The results can be summarized in three general findings. First, none of the tested subsampling methods was identified to clearly outperform the others. The dependency of the subsampling-errors on the fraction measured was very similar for all methods; differences could only be seen in edge scenarios, as for instance in the case of filters with relatively low particle counts and inhomogeneous particle distribution on the filter. There, the particle-based subsampling proved to be more accurate than the box-based methods. In the majority of samples however, the observed subsampling-error was due to the counting error (i.e., extrapolating from a low number of measured particles) and particle distribution inhomogeneity is negligible.

Second, the magnitude of the averaged subsampling-error easily exceeded 50% if only 5% or less of the filter was measured. More critically, the standard deviation of the subsampling-error strongly increases when decreasing the measured fraction. If reliable particle counts with an error of less than 20% are required, the measured fraction should be at least 50% or, in the case of particle-based subsampling, at least 7,000 particles. However, if exact counts of particular types of MP particles are of interest, the measured fraction would have to be increased even further, thus reducing the time saving from the subsampling. It might be advisable to measure the entire filter in these cases.

Third, the best way to increase accuracy at low particle counts is to increase the fraction of MP particles in the sample. This can be done by further optimization of sample preprocessing steps or by

implementing methods to identify possible MP particles prior to spectroscopic measurement (by specifically trained classification models or fluorescent staining). That finding seems trivial, but is important to keep in mind when designing workflows for workup and analysis of certain sample types. If only qualitative results are required (i.e., are MP particles present or not), higher error margins can be tolerated. Vice versa, if robust particle numbers are required, sample preprocessing should be optimized or, if not possible, higher fractions of the sample have to be measured.

To increase the validity of the herein gathered results to a larger diversity of filters, especially with higher particle counts, we encourage scientists in the field to critically reassess their measurements similarly as described here. Deeper statistical considerations would be beneficial for underpinning the observed effects.

The decision on the most appropriate subsampling strategy for a fast and proper quantification of specific objects from different environmental compartments is important for several scientific disciplines, going far beyond microplastic research. Only one example would be the microscopic quantification of specific prokaryotic groups via phylogenetic staining of cells e.g., by Fluorescence *in situ* hybridization (FISH). Therefore, we also understand this study as a general stimulus for a more extensive and interdisciplinary research on statistically relevant counting of small and less abundant objects in the environment.

DATA AVAILABILITY STATEMENT

The datasets and calculations presented in this study can be found in online repositories. The repositories can be found under: https://gitlab.ipfdd.de/Brandt/subsampling.

AUTHOR CONTRIBUTIONS

All authors listed have made a substantial, direct, and intellectual contribution to the work and approved it for publication.

FUNDING

This research was funded by the projects MicroCatch_Balt (03F0788A), PLASTRAT (02WPL1446 I) and PLAWES (03F0789A) supported by the Federal Ministry of Education and Research (BMBF Germany) and the BONUS MICROPOLL project supported by BONUS (Art 185), funded jointly by the European Union and BMBF (03F0775A).

ACKNOWLEDGMENTS

We thank Robin Lenz, Dr. Alexander Tagg and Juliana Ivar do Sul (IOW), Dr. Sarmite Kernchen, Dr. Martin Löder, and Prof. Christian Laforsch (University of Bayreuth), as well as Annett Mundane, Natalie Wick, and Prof. Christian Schaum (Universität der Bundeswehr München) for obtaining, treating and providing the samples.

SUPPLEMENTARY MATERIAL

The Supplementary Material for this article can be found online at: https://www.frontiersin.org/articles/10.3389/fenvs.2020.579676/full#supplementary-material.

REFERENCES

Anger, P. M., Esch, E., Baumann, T., Elsner, M., Niessner, R., Ivleva, N. P., et al. (2018). Raman microspectroscopy as a tool for microplastic particle analysis. *TrAC Trends Anal. Chem.* 109, 214–226. doi:10.1016/j.trac.2018.10.010

Batista, G. E. A. P. A., Prati, R. C., and Monard, M. C. (2004). A study of the behavior of several methods for balancing machine learning training data. *ACM SIGKDD Explor. Newsl.* 6, 20–29. doi:10.1145/1007730.1007735

Bergmann, M., Wirzberger, V., Krumpen, T., Lorenz, C., Primpke, S., Tekman, M. B., et al. (2017). High quantities of microplastic in arctic deep-sea sediments from the HAUSGARTEN observatory. *Environ. Sci. Technol.* 51, 11000–11010. doi:10.1021/acs.est.7b03331

Borrelle, S. B., Ringma, J., Law, K. L., Monnahan, C. C., Lebreton, L., McGivern, A., et al. (2020). Predicted growth in plastic waste exceeds efforts to mitigate plastic pollution, *Science.* 369: 1515–1518. doi:10.1126/science.aba3656

Brandon, J. A., Jones, W., and Ohman, M. D. (2019). Multidecadal increase in plastic particles in coastal ocean sediments. *Sci. Adv.* 5, eaax0587. doi:10.1126/sciadv.aax0587

Brandt, J., Bittrich, L., Fischer, F., Kanaki, E., Tagg, A., Lenz, R., et al. (2020). High-throughput analyses of microplastic samples using fourier transform infrared and Raman spectrometry. *Appl. Spectrosc.* 74 (9), 1185–1197. doi:10.1177/0003702820932926

Browne, M. A., Galloway, T. S., and Thompson, R. C. (2010). Spatial patterns of plastic debris along estuarine shorelines. *Environ. Sci. Technol.* 44, 3404–3409. doi:10.1021/es903784e

Buffle, J., and Leppard, G. G. (1995). Characterization of aquatic colloids and macromolecules. 2. Key role of physical structures on analytical results. *Environ. Sci. Technol.* 29, 2176–2184. doi:10.1021/es00009a005

Chaudhuri, B. B. (1994). How to choose a representative subset from a set of data in multi-dimensional space. *Pattern Recogn. Lett.* 15, 893–899. doi:10.1016/0167-8655(94)90151-1

Claessens, M., Van Cauwenberghe, L., Vandegehuchte, M. B., and Janssen, C. R. (2013). New techniques for the detection of microplastics in sediments and field collected organisms. *Mar. Pollut. Bull.* 70, 227–233. doi:10.1016/j.marpolbul.2013.03.009

Daszykowski, M., Walczak, B., and Massart, D. L. (2002). Representative subset selection. *Anal. Chim. Acta.* 468, 91–103. doi:10.1016/S0003-2670(02)00651-7

Dierkes, G., Lauschke, T., Becher, S., Schumacher, H., Földi, C., and Ternes, T. (2019). Quantification of microplastics in environmental samples via pressurized liqudslbid extraction and pyrolysis-gas chromatography. *Anal. Bioanal. Chem.* 411, 6959–6968. doi:10.1007/s00216-019-02066-9

Duemichen, E., Braun, U., Senz, R., Fabian, G., and Sturm, H. (2014). Assessment of a new method for the analysis of decomposition gases of polymers by a combining thermogravimetric solid-phase extraction and thermal desorption gas chromatography mass spectrometry. *J. Chromatogr. A.* 1354, 117–128. doi:10.1016/j.chroma.2014.05.057

Dümichen, E., Barthel, A.-K., Braun, U., Bannick, C. G., Brand, K., Jekel, M., et al. (2015). Analysis of polyethylene microplastics in environmental samples, using a thermal decomposition method. *Water Res.* 85, 451–457. doi:10.1016/j.watres.2015.09.002

Dümichen, E., Eisentraut, P., Bannick, C. G., Barthel, A.-K., Senz, R., Brau, U., et al. (2017). Fast identification of microplastics in complex environmental samples by a thermal degradation method. *Chemosphere.* 174, 572–584. doi:10.1016/j.chemosphere.2017.02.010

Enders, K., Käppler, A., Biniasch, O., Feldens, P., Stollberg, N., Lange, X., et al. (2019). Tracing microplastics in aquatic environments based on sediment analogies. *Sci. Rep.* 9, 15207. doi:10.1038/s41598-019-50508-2

Enders, K., Lenz, R., Ivar do Sul, J. A., Tagg, A. S., and Labrenz, M. (2020). When every particle matters: a QuEChERS approach to extract microplastics from environmental samples. *Methods.* 7, 100784. doi:10.1016/j.mex.2020.100784

Fischer, M., and Scholz-Böttcher, B. M. (2019). Microplastics analysis in environmental samples-recent pyrolysis-gas chromatography-mass spectrometry method improvements to increase the reliability of mass-related data. *Anal. Methods.* 11: 2489–2497. doi:10.1039/C9AY00600A

Geyer, R., Jambeck, J. R., and Law, K. L. (2017). Production, use, and fate of all plastics ever made. *Sci. Adv.* 3, e1700782. doi:10.1126/sciadv.1700782

Halden, R. U. (2015). Epistemology of contaminants of emerging concern and literature meta-analysis. *J. Hazard Mater.* 282, 2–9. doi:10.1016/j.jhazmat.2014.08.074

Halle, A. T., Ladirat, L., Gendre, X., Goudouneche, D., Pusineri, C., Routaboul, C., et al. (2016). Understanding the fragmentation pattern of marine plastic debris. *Environ. Sci. Technol.* 50, 5668–5675. doi:10.1021/acs.est.6b00594

Logemann, J., Oveland, E., Bjorøy, Ø., Peters, W., Cojocariu, C., and Kögel, T. (2018). "Pyrolysis-GC-Orbitrap MS-a powerful analytical tool for identification and quantification of microplastics in a biological matrix". (2018), application note 10643.

Huppertsberg, S., and Knepper, T. P. (2018). Instrumental analysis of microplastics-benefits and challenges. *Anal. Bioanal. Chem.* 410, 6343–6352. doi:10.1007/s00216-018-1210-8

Imhof, H. K., Laforsch, C., Wiesheu, A. C., Schmid, J., Anger, P. M., Niessner, R., et al. (2016). Pigments and plastic in limnetic ecosystems: a qualitative and quantitative study on microparticles of different size classes. *Water Res.* 98, 64–74. doi:10.1016/j.watres.2016.03.015

Jambeck, J. R., Geyer, R., Wilcox, C., Siegler, T. R., Perryman, M., Andrady, A., et al. (2015). Marine pollution. Plastic waste inputs from land into the ocean. *Science.* 347, 768–771. doi:10.1126/science.1260352

Käppler, A., Fischer, D., Oberbeckmann, S., Schernewsk, G., Labrenz, M., Eichhorn, K.- J., et al. (2016). Analysis of environmental microplastics by vibrational microspectroscopy: FTIR, Raman or both?. *Anal. Bioanal. Chem.* 408, 8377–8391. doi:10.1007/s00216-016-9956-3

Käppler, A., Fischer, M., Scholz-Böttcher, B. M., Oberbeckmann, S., Labrenz, M., Fischer, D., et al. (2018). Comparison of μ-ATR-FTIR spectroscopy and py-GCMS as identification tools for microplastic particles and fibers isolated from river sediments. *Anal. Bioanal. Chem.* 410, 5313–5327. doi:10.1007/s00216-018-1185-5

Käppler, A., Windrich, F., Löder, M. G. J., Malanin, M., Fischer, D., Labrenz, M., et al. (2015). Identification of microplastics by FTIR and Raman microscopy: a novel silicon filter substrate opens the important spectral range below 1300 cm^{-1} for FTIR transmission measurements. *Anal. Bioanal. Chem.* 407, 6791–6801. doi:10.1007/s00216-015-8850-8

Karlsson, T. M., Kärrman, A., Rotander, A., and Hassellöv, M. (2020). Comparison between manta trawl and *in situ* pump filtration methods, and guidance for visual identification of microplastics in surface waters. *Environ. Sci. Pollut. Res. Int.* 27, 5559–5571. doi:10.1007/s11356-019-07274-5

Lenz, R., Enders, K., Stedmon, C. A., Mackenzie, D. M., and Nielsen, T. G. (2015). A critical assessment of visual identification of marine microplastic using Raman spectroscopy for analysis improvement. *Mar. Pollut. Bull.* 100, 82–91. doi:10.1016/j.marpolbul.2015.09.026

Lenz, R., and Labrenz, M. (2018). Small microplastic sampling in water: development of an encapsulated filtration device. *Water.* 10, 1055. doi:10.3390/w10081055

Liu, F., Olesen, K. B., Borregaard, A. R., and Vollertsen, J. (2019). Microplastics in urban and highway stormwater retention ponds. *Sci. Total Environ.* 671, 992–1000. doi:10.1016/j.scitotenv.2019.03.416

Löder, M. G. J., Imhof, H. K., Ladehoff, M., Löschel, L. A., Lorenz, C., Mintenig, S., et al. (2017). Enzymatic purification of microplastics in environmental samples. *Environ. Sci. Technol.* 51, 14283–14292. doi:10.1021/acs.est.7b03055

Löder, M. G. J., Kuczera, M., Mintenig, S., Lorenz, C., and Gerdts, G. (2015). Focal plane array detector-based micro-Fourier-transform infrared imaging for the analysis of microplastics in environmental samples. *Environ. Chem.* 12, 563–581. doi:10.1071/en14205

Lusher, A. L., Welden, N. A., Sobral, P., and Cole, M. (2017). Sampling, isolating and identifying microplastics ingested by fish and invertebrates. *Anal. Methods.* 9, 1346–1360. doi:10.1039/c6ay02415g

Masó, M., Garcés, E., Pagès, F., and Camp, J. (2003). Drifting plastic debris as a potential vector for dispersing Harmful Algal Bloom (HAB) species. *Sci. Mar.* 67, 107–111. doi:10.3989/scimar.2003.67n1107

Merck (2018). *AD030 Air and fluid particle monitoring guide*, Darstamdt, Germany: MerckKGaA.

Mintenig, S. M., Kooi, M., Erich, M. W., Primpke, S., Redondo-Hasselerharm, P. E., Dekker, S. C., et al. (2020). A systems approach to understand microplastic occurrence and variability in Dutch riverine surface waters. *Water Res.* 176, 115723. doi:10.1016/j.watres.2020.115723

Murphy, F., Ewins, C., Carbonnier, F., and Quinn, B. (2016). Wastewater Treatment Works (WwTW) as a source of microplastics in the aquatic environment. *Environ. Sci. Technol.* 50, 5800–5808. doi:10.1021/acs.est.5b05416

Peng, Z., and Kirk, T. B. (1998). Automatic wear-particle classification using neural networks. *Tribol. Lett.* 5, 249–257. doi:10.1023/A:1019126732337

Poulain, M., Mercier, M. J., Brach, L., Martignac, M., Routaboul, C., Perez, E., et al. (2019). Small microplastics as a main contributor to plastic mass balance in the North Atlantic subtropical Gyre. *Environ. Sci. Technol.* 53, 1157–1164. doi:10.1021/acs.est.8b05458

Primpke, S., Christiansen, S. H., Cowger, W., Frond, H. D., Deshpande, A., Fischer, M., et al. (2020a). Critical assessment of analytical methods for the harmonized and cost-efficient analysis of microplastics. *Appl. Spectrosc.* 74, 1012–1047. doi:10.1177/0003702820921465

Primpke, S., Cross, R. K., Mintenig, S. M., Simon, M., Vianello, A., Gerdts, G., et al. (2020b). Toward the systematic identification of microplastics in the environment: evaluation of a new Independent software tool (siMPle) for spectroscopic analysis. *Appl. Spectrosc.* 74 (9), 1127–1138. doi:10.1177/0003702820917760

Primpke, S., Dias, P. A., and Gerdts, G. (2019). Automated identification and quantification of microfibres and microplastics. *Anal. Methods.* 11, 2138–2147. doi:10.1039/C9AY00126C

Primpke, S., Lorenz, C., Rascher-Friesenhausen, R., and Gerdts, G. (2017). An automated approach for microplastics analysis using focal plane array (FPA) FTIR microscopy and image analysis. *Anal. Methods.* 9, 1499–1511. doi:10.1039/c6ay02476a

Rodionova, O. Y., and Pomerantsev, A. L. (2008). Subset selection strategy. *J. Chemom.* 22, 674–685. doi:10.1002/cem.1103

Schymanski, D., Goldbeck, C., Humpf, H. U., and Fürst, P. (2018). Analysis of microplastics in water by micro-Raman spectroscopy: release of plastic particles from different packaging into mineral water. *Water Res.* 129, 154–162. doi:10.1016/j.watres.2017.11.011

Shim, W. J., Song, Y. K., Hong, S. H., and Jang, M. (2016). Identification and quantification of microplastics using Nile Red staining. *Mar. Pollut. Bull.* 113, 469–476. doi:10.1016/j.marpolbul.2016.10.049

Siegfried, M., Koelmans, A. A., Besseling, E., and Kroeze, C. (2017). Export of microplastics from land to sea. A modelling approach. *Water Res.* 127, 249–257. doi:10.1016/j.watres.2017.10.011

Simon, M., van Alst, N., and Vollertsen, J. (2018). Quantification of microplastic mass and removal rates at wastewater treatment plants applying Focal Plane Array (FPA)-based Fourier Transform Infrared (FT-IR) imaging. *Water Res.* 142, 1–9. doi:10.1016/j.watres.2018.05.019

Tagg, A. S., Sapp, M., Harrison, J. P., and Ojeda, J. J. (2015). Identification and quantification of microplastics in wastewater using focal plane array-based reflectance micro-FT-IR imaging. *Anal. Chem.* 87, 6032–6040. doi:10.1021/acs.analchem.5b00495

Thaysen, C., Munno, K., Hermabessiere, L., and Rochman, C. (2020). EXPRESS: toward Raman automation for microplastics: developing strategies for particle adhesion and filter subsampling. *Appl. Spectrosc.* 74, 000370282092290. doi:10.1177/0003702820922900

Vianello, A., Boldrin, A., Guerriero, P., Moschino, V., Rella, R., Sturaro, A., et al. (2013). Microplastic particles in sediments of Lagoon of Venice, Italy: first observations on occurrence, spatial patterns and identification. *Estuar. Coast. Shelf Sci.* 130, 54–61. doi:10.1016/j.ecss.2013.03.022

Wagner, J., Wang, Z. M., Ghosal, S., Rochman, C., Gassel, M., and Wall, S. (2017). Novel method for the extraction and identification of microplastics in ocean trawl and fish gut matrices. *Anal. Methods.* 9, 1479–1490. doi:10.1039/C6AY02396G

Wei, Q., and Dunbrack, R. L. (2013). The role of balanced training and testing data sets for binary classifiers in bioinformatics. *PLoS One.* 8, e67863. doi:10.1371/journal.pone.0067863

Xu, B., Wen, G., Zhang, Z., and Chen, F. (2018). Wear particle classification using genetic programming evolved features. *Lubric. Sci.* 30, 229–246. 10.1002/ls.1411

Xu, K., Luxmoore, A. R., and Deravi, F. (1997). Comparison of shape features for the classification of wear particles. *Eng. Appl. Artif. Intell.* 10, 485–493. doi:10.1016/S0952-1976(97)00017-1

Zettler, E. R., Mincer, T. J., and Amaral-Zettler, L. A. (2013). Life in the "plastisphere": microbial communities on plastic marine debris. *Environ. Sci. Technol.* 47, 7137–7146. doi:10.1021/es401288x

Conflict of Interest: The authors declare that there the research was conducted in the absence of any commercial or financial relationships that could be construed as a potential conflict of interest.

frontiers in Environmental Science

SYSTEMATIC REVIEW
published: 16 February 2021
doi: 10.3389/fenvs.2020.575614

Microplastics in Sea Turtles, Marine Mammals and Humans: A One Environmental Health Perspective

*Idoia Meaza, Jennifer H Toyoda and John Pierce Wise Sr**

Wise Laboratory of Environmental and Genetic Toxicology, Department of Pharmacology and Toxicology, University of Louisville, Louisville, KY, United States

Microplastics are ubiquitous pollutants in the marine environment and a health concern. They are generated directly for commercial purposes or indirectly from the breakdown of larger plastics. Examining a toxicological profile for microplastics is a challenge due to their large variety of physico-chemical properties and toxicological behavior. In addition to their concentration, other parameters such as polymer type, size, shape and color are important to consider in their potential toxicity. Microplastics can adsorb pollutants such as polycyclic aromatic hydrocarbons (PAHs) or metals on their surface and are likely to contain plastic additives that add to their toxicity. The observations of microplastics in seafood increased concern for potential human exposure. Since literature considering microplastics in humans is scarce, using a One Environmental Health approach can help better inform about potential human exposures. Marine mammals and sea turtles are long-lived sentinel species regularly used for biomonitoring the health status of the ocean and share trophic chain and habitat with humans. This review considers the available research regarding microplastic and plastic fiber exposures in humans, marine mammals and turtles. Overall, across the literature, the concentration of microplastics, size, color, shape and polymer types found in GI tract and feces from sea turtles, marine mammals and humans are similar, showing that they might be exposed to the same microplastics profile. Additionally, even if ingestion is a major route of exposure due to contaminated food and water, dermal and inhalation studies in humans have provided data showing that these exposures are also health concerns and more effort on these routes of exposures is needed. *In vitro* studies looked at a variety of endpoints showing that microplastics can induce immune response, oxidative stress, cytotoxicity, alter membrane integrity and cause differential expression of genes. However, these studies only considered three polymer types and short-term exposures, whereas, due to physiological relevance, prolonged exposures might be more informative.

Keywords: microplastics, marine mammals, sea turtles, human, one health

OPEN ACCESS

Edited by:
Montserrat Filella, Université de Genève, Switzerland

Reviewed by:
Sylvain De Guise, University of Connecticut, United States
Hans Peter Heinrich Arp, Norwegian Geotechnical Institute, Norway

****Correspondence:***
John Pierce Wise
John.Wise@louisville.edu

Specialty section:
This article was submitted to Toxicology, Pollution and the Environment, a section of the journal Frontiers in Environmental Science

Received: *23 June 2020*
Accepted: *23 December 2020*
Published: *16 February 2021*

Citation:
Meaza I, Toyoda JH and Wise Sr JP (2021) Microplastics in Sea Turtles, Marine Mammals and Humans: A One Environmental Health Perspective. Front. Environ. Sci. 8:575614. doi: 10.3389/fenvs.2020.575614

INTRODUCTION

Plastics are typically composed of a variety of polymers and additives used to impart unique properties, such as lightweight, thermal and electrical insulation, durability, corrosion-resistance, and tensile strength (Andrady and Neal, 2009). The usefulness and low cost of these materials for diverse applications is responsible for the increase in worldwide plastics production from two million

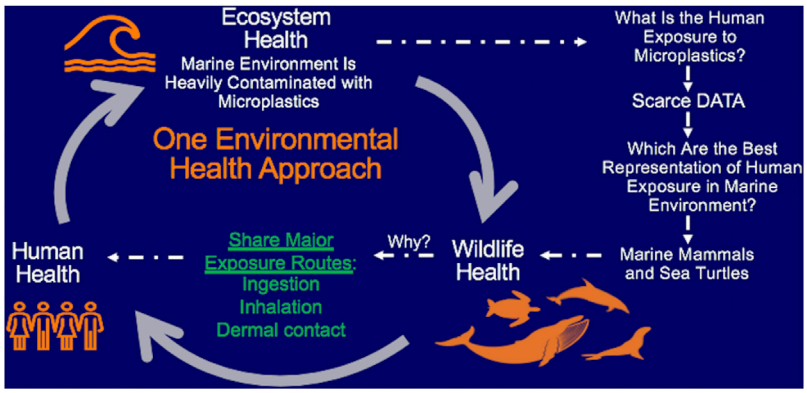

GRAPHICAL ABSTRACT |

tonnes in 1950 (Geyer et al., 2017) to 359 million tonnes in 2018 (PlasticEurope, 2019). Microplastics originate from breakdown of larger plastics or are specially manufactured for use in products, such as toothpaste or skincare products. Microplastics are defined as "any synthetic solid particle or polymeric matrix, with regular or irregular shape and with size ranging from 1 um to 5 mm" (Frias and Nash, 2018). Their small size and durability have allowed them to become ubiquitous. Physical and chemical properties of microplastics could determine their toxicity (Wright and Kelly, 2017). Physical properties including size, shape and particle density influence the transport and fate of particles (Chubarenko et al., 2016). Chemical composition, including manufacturing materials such as polymers, colorizers (e.g., chromium), UV stabilizers (e.g., lead and cadmium) and flame retardants (e.g., aluminum oxide), as well as contaminants from the environment that attach to the surface through sorption (e.g., metals and persistent organic pollutants) can include hazardous compounds (Campanale et al., 2020).

The marine environment is a major sink for microplastics. These microplastic particles can enter the ocean through a variety of land and sea sources and have been found from the sea surface all the way to the seafloor and along the shoreline (GESAMP 2016; FAO 2018). River runoff is considered one of the major sources of plastic pollution in seawater. Indeed, Lebreton et al. (2017) estimated 67% of the plastic pollution in the ocean started in twenty rivers, mainly located in Asia. Another important source contributing to marine microplastic pollution is the widespread use of plastics in fisheries and aquaculture such as disposable fishing gear, plastic cages, packages and buoys. Consequently, Lusher et al. (2017) found that over 220 species of marine animals (excluding birds, turtles and mammals) ingested microplastic, of which half of them are considered relevant for commercial purposes and increase the risk of human consumption of microplastics.

In particular, large marine vertebrates, such as marine mammals and sea turtles, are key species for microplastic biomonitoring (Galgani et al., 2014). Exposure to environmental microplastics can occur though ingestion, inhalation and dermal contact though most research so far has focused on inhalation and ingestion (Revel et al., 2018, Prata et al., 2020). Marine mammals and sea turtles integrate all three exposure routes, a feature they share with humans, which makes them more representative of human exposures in the marine environment. Ingestion of these particles has received the most attention due to the presence of microplastics in commonly used products, such as sugar (0.44 microplastic/g), honey (0.1 microplastic/g), salt (0.11 microplastic/g), alcohol (32.27 microplastics/l), bottled water (94.37 microplastic/g), tap water (4.23 microplastic/l) and seafood (1.48 microplastic/g) (Cox et al., 2019). The presence of microplastics in seafood raises concern about potential bioaccumulation and biomagnification of microplastics in the trophic chain (van Raamsdonk et al., 2020). Marine mammals and sea turtles are likely to ingest similar microplastics as humans because they share similar marine trophic chains, and therefore can reveal valuable information on trophic transfer of microplastics (Carbery et al., 2018). One might argue that humans have a more diverse diet that may include things like alcohol or beverages that contain microplastics (Cox et al., 2019); however, marine mammals and sea turtles, are the best animal representation of humans in the marine environment, which is the major sink of microplastics and thus, important insights may still be gleaned from these comparisons.

Marine mammals, sea turtles and humans are all air breathers, which makes them susceptible for particle inhalation. The presence of microplastics in air have been extensively studied in the past years (Zhang et al., 2020). These studies show that atmospheric deposition transports microplastic particles to the ocean surface air (Liu et al., 2019; Wang et al., 2020; Szewc et al., 2021), therefore, making marine air breathers highly susceptible to microplastic inhalation. Currently, there is no literature on microplastic inhalation, however it is clear they do inhale airborne particles as several studies reported the inhalation of HgSe particles in *Tursiops truncatus* and *Globicephala macrohynchus* (Rawson et al., 1995) and presence of accumulation of macrophages loaded with fine carbon particles in *Tursiops truncatus* resulting in anthracosis (Rawson et al., 1991), which is commonly reported in human autopsies, suggesting that the inhalation exposure of air-breathers is similar. Additionally, marine mammals and sea turtles are extremely vulnerable to inhaling airborne microplastics because they rapidly exchange big masses of air before diving and hold

TABLE 1 | Microplastics presence in the gastrointestinal tract of 7 species of sea turtles.

Location	Species	*n*	No of Microplastics	Size	Shape	Color	Polymer type	Ref.
Pacific Ocean (Cairns)	*Chelonia mydas*	2	3.5 microplastics/turtle	Particles in juvenile ranged from 0.45 to 2.51 mm. Particle in the adult female ranged from 0.76 to 2.95 mm	Particles and a microfilm (in adult female)	Out of 7 items, 3 clear particles, 1 clear film, 1 dark green particle, 1 black particle and 1 white particle	EAA, PVA, a particle composed of cotton: Olefin: PES and one mixed yarn synthetic fabric	Caron et al. (2018)
Pacific Ocean (Queensland)	*Chelonia mydas*	7	11 particles/turtle[a]	Average fiber size 2.85 ± 0.23 mm. Fragment and bead average diameter 0.26 ± 0.01 mm	Fibres 64.8%, fragments 20.2% and microbead 4.8%	Blue 44.9%, black 39.1%, red 8.6% and clear 2.9%	Elastomers 3.4% (e.g., EPDM rubber), synthetic regenerated CL fibres 68.9%, PE, EP, PET, PAM 27.7%	Duncan et al. (2019)
	Caretta caretta	3	6 particles/turtle[a]					
	Natator depressus	4	6 particles/turtle[a]					
	Eretmochelys imbricata	1	5 particles/turtle[a]					
	Lepidochelys olivacea	1	4 particles/turtle[a]					
Mediterranean Sea (Northern Cyprus)	*Chelonia mydas*	34	10 particles/turtle[a]	Average fiber size 1.40 ± 0.54 mm (mean ± S.E). Fragment and bead average diameter 0.07 ± 0.01 mm	Fibres 85.3%, Fragments 14.7%	Blue 34.4%, black 31.3%, red 18.2% and clear 9.9%	Elastomers 61.2% (e.g., EPDM rubber), woven synthetics 4.9%, synthetic regenerated CL fibres 5.8% and PE, EP, PET, PAM (total 20.7%)	Duncan et al. (2019)
	Caretta caretta	22	12.5 particles/turtle[a]					
Atlantic Ocean (North Carolina)	*Chelonia mydas*	10	5 particles/turtle[a]	Average fiber size 2.87 ± 0.20 mm. Fragment and bead average diameter 0.31 ± 0.04 mm	Fibres 77.1% Fragments 22.9%	Blue 36.3%, black 43.7%, red 17.5% and clear 2.5%	Synthetic regenerated CL fibres 63.2%, PE, EP, PET and PAM (total 36.8%)	Duncan et al. (2019)
	Caretta caretta	8	2.5 particles/turtle[a]					
	Lepidochelys kempii	10	3 particles/turtle[a]					
	Dermochelys coriacea	2	4 particles/turtle[a]					
Atlantic Ocean (Azores islands)	*Caretta caretta*	24	95 microplastics total in 58% of the turtles. 3.95 items/turtle	1–5 mm	Fragments (87%), sheets (8%) and pellets (5%)	Blue, green, and white most predominant	PE (60%), PP (20%) and different polymer mixtures (12%)^	Pham et al. (2017)
Atlantic Ocean and Indian Ocean (Sourthern Cape)	*Caretta caretta*	16	Fragments 12.2 ± 14.9/ turtle (range 0–50). Pellets 0.6 ± 1.3/turtle (range 0–5). In total 229 fragment and 10 pellets	Average fragment size 4.7 ± 2.4 × 3.0 ± 1.4×1.0 ± 0.5 mm and average pellet size 3.9 ± 0.5×3.4 ± 0.8 × 1.4 ± 0.7 mm	Among all items: Fragments 76%. Pellets 3%	Fragments mostly white/cream, clear or blue/purple and pellets mostly black/ grey/brown, white/ cream and clear	NA	Ryan et al. (2016)

[a]*Extrapolated from Figure 2 in Duncan et al., 2019; ^Authors took into account all the items (macro, meso and microplastics) found; Abbreviations: polyethylene acrylic acid EAA, polyvinyl acrylic PVA Polyethylene PE, Ethylene propylene EP, Polyester PES, Polyacrylamide PAM, Polypropylene PP, Polystyrene PS, Polyamide (nylon) PA, Cellulose CL.*

their breath during prolonged dives, resulting in a larger magnitude and exposure of the inhaled contaminant (Takeshita et al., 2017). Furthermore, marine mammals lack nasal turbinate structures responsible for filtering the air and trapping particles, enabling them to sneeze out the particles (Takeshita et al., 2017). Similarly, sea turtles lack turbinate structure except for *Dermochelys*, which is an exemption within reptiles (Davenport et al., 2009). Yet, despite their vulnerability, inhalation of airborne contaminants by marine mammals and sea turtles is often overlooked. Given the health concerns about marine microplastics and the importance of these sentinel species, this review considers the available research regarding microplastic and plastic fiber exposures in humans, marine mammals and turtles.

METHODS

Search Strategy

International databases including PubMed and ScienceDirect were searched for articles published up to the date of search. First search was carried out on 3/23/2020 for marine mammals and human related articles in PubMed and ScienceDirect databases. Searches included: 1) ((microplastics) and human) and epidemiology, 2) ((plastic fibers) and human) and epidemiology 3) (microplastics) and (the word of interest) 4) (plastic fibers) and (word of interest). The words of interest were the following: *Pinnipedia*, pinnipeds, *Otariidae*, sea lion, fur seal, *Phocidae*, true seal, seal, *Odobenidae*, walrus, *Mustelidae*, sea otter, *Ursidae*, polar bear, *Cetacea*, *Odontoceti*, *Physeteridae*, sperm whale, *Kogiidae*, pigmy sperm

whale, dwarf sperm whale, *Ziphiidae*, beaked whale, *Platanistidae*, south Asian river dolphin, Ganges river dolphin, bhulan, Iniidae, amazon river dolphin, Bolivian bufeo, common boto, *Lipotidae*, Yangtze river dolphin, *Pontoporiidae*, franciscana, toninha, *Monodontidae*, beluga, narwhal, *Delphinidae*, dolphin, killer whale, pilot whale, grampus, Tucuxi, *Phocoenidae*, porpoise, *Mysticeti*, *Neobalaenidae*, pigmy right whale, *Balaenidae*, bowhead whale, North Atlantic right whale, North Pacific right whale, *Eschrichtiidae*, gray whale, *Balaenopteridae*, rorqual, *Sineria*, *Trichechidae*, manatee, *Dugongidae*, dugong, whale, marine mammals and human. Additionally, all the words of interest were searched for plural and singular forms when possible in order to avoid missing papers.

The literature searches for sea turtles were performed on April 15, 2020. PubMed and ScienceDirect databases were explored for searches including (Microplastics) AND (the word of interest) and (plastic fibers) AND (word of interest). The words of interest were the following: *Cheloniidae, Dermochelyidae*, green sea turtle, *Chelonia mydas mydas, Chelonia, mydas agassizii,* loggerhead sea turtle, *Caretta caretta*, Kemp´s ridley sea turtle, *Lepidochelys kempii,* Olive ridley sea turtle, *Lepidochelys olivacea,* hawksbill sea turtle, *Eretmochelys imbricate,* flatback sea turtle, *Natator depressor,* Leatherback sea turtle, *Dermochelys coriacea* and sea turtle. Additionally, all the words of interest were searched for plural and singular forms when possible in order to avoid missing papers.

We further considered relevant articles found referenced by the articles under consideration in the review.

Exclusion Criteria

From all the results obtained we excluded: 1) Articles not related to the review topic, 2) Review articles, 3) Articles not containing primary data, such as articles based on prediction models. Due to the uniqueness of marine mammal samples, variation in methodology and data reporting criteria was to be expected and, therefore, no further exclusion criteria were applied.

RESULTS

Microplastics in Sea Turtles

Five studies considered microplastics in sea turtles (**Table 1**). Microplastics were found in all seven sea turtle species: green sea turtle *(Chelonia mydas),* loggerhead sea turtle *(Caretta caretta)*, Kemp's ridley sea turtle *(Lepidochelys kempii)*, olive ridley sea turtle *(Lepidochelys olivacea),* hawksbill sea turtle *(Eretmochelys imbricate),* flatback sea turtle *(Natator depressus),* and leatherback sea turtle *(Dermochelys coriacea)* (**Table 1**). Each study focused on characterizing microplastic particles in the GI tract with four studies characterizing environmental levels of microparticles found in 144 wild sea turtles from 7 species, while the fifth administered microplastic particles to study gut passage time. The data are insufficient to consider any species-specific patterns.

The four studies of environmental levels of gut microparticles each documented microplastic particles in the digestive contents of the gut and characterized the physico-chemical aspects of the particles (**Table 1**). Particle size ranged from 0.1 to 5 mm, with mean sizes ranging from 1.4–4.7 mm, depending on the study. The average particle concentrations from the GI tract in sea turtles ranged from 2.5 to 12.5 particles per turtle (**Figure 1**). Particle shapes were predominately fibers and fragments and the most prevalent colors were blue, black, clear and white. Three studies (Pham et al., 2017; Caron et al., 2018; Duncan et al., 2019) reported polymer composition with polyethylene, ethylene propylene, polypropylene, polyester, polyacrylamide, polystyrene, polyamide, cellulose and elastomers most frequently found. One study (Duncan

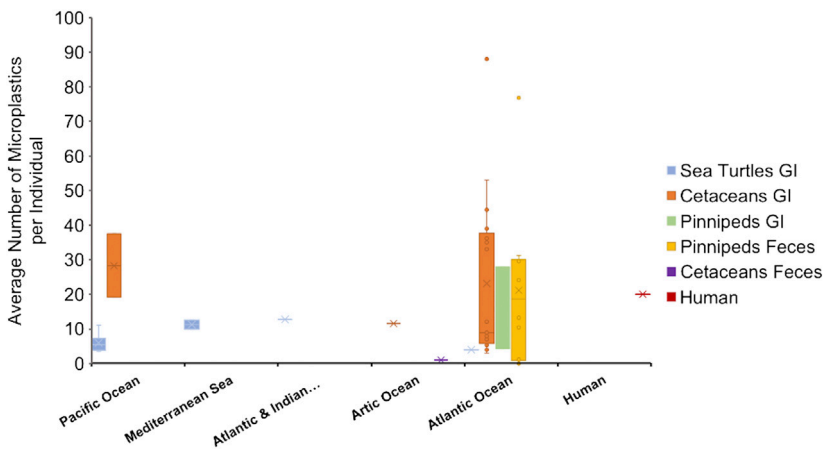

FIGURE 1 | Average number of microplastics per individual based on animal groups and location, represented in a boxplot-chart. Data were extracted from Tables 1–4, representing the average number of microplastics per individual in each species. When the number of microplastics was given in the original article by shape (for example, number of pellets per individual and number of fragments per individual) the numbers were summed (Ryan et al., 2016; Donohue et al., 2019; Perez-Venegas et al., 2020). Only the information from the adult individuals in Zhu et al. (2019) were considered. Articles only reporting a range were not plotted on the boxplot (Nelms et al., 2018; Perez-Venegas et al., 2018). Human data (value of 20 microplastics/individual) represent the median value reported by Schwabl et al. (2019), with a range of 18–172 microplastics per individual.

et al., 2019) compared different polymer types and turtles found in three different bodies of water but found no correlation between polymer type and the location of the turtles.

The fifth study (Amorocho and Reina, 2008) administered microplastic beads to wild juvenile East Pacific green turtles (*Chelonia mydas agassizii*) kept in captivity during the experiment for over 30 days and measured passage time of the microparticles. They administered different diets to the turtles together with microplastic beads and measured recovery of the beads. Cylindrical yellow beads of 2–3 x 1 mm size were packaged at a concentration of 20 beads per capsule. 3–5 capsules were introduced into the sea turtle lower esophagus by pushing them through a plastic hose. The average ingesta passage time in 6 turtles was 23.3 ± 6.6 days (559 h). Turtles fed with protein-based diet seemed to have longer ingesta passage time than turtles fed with mixed or plant-based diets, showing that diet might affect the retention time in the gut and therefore exposing the turtles to more prolonged exposures. Unexpectedly, 12 days after the initiation of the experiment one turtle died due to a hook ingested prior to the study and its necropsy showed microplastic beads were localized within boluses distributed along the midgut (Amorocho and Reina, 2008). This outcome further suggests food interacts with the microplastic particles and diet likely alters ingesta passage time of the beads. However, this study does not investigate such interaction or the potential breakdown of the microplastics.

Passage time was also noted in Pharm et al. (2017). In this study the color of macroplastics and microplastics in the GI tract did not match in some turtles. While microplastics can arise from breakdown of macroplastics, in this case the localization of microplastics with unique colors suggests that either they were ingested in the microplastic form or that they have a longer passage time through the gut than their microplastic source. Additionally, Pharm et al. (2017) not only identified macro, meso and microplastic ingestion in loggerhead sea turtles, but also showed that microplastics were mostly localized in the intestine, compared to the esophagus and stomach, suggesting a longer retention time in the intestine.

Microplastics in Marine Mammals

16 articles regarding marine mammals met our selection criteria. From those, 9 studies analyzed presence of microplastics in the GI content of 15 cetaceans and 2 pinniped species from Atlantic, Pacific and Arctic Oceans (**Table 2**). From those 15 cetacean species, only one was mysticetes (*Megaptera novaeangliae*) and 14 were odontocetes. Additionally, 7 articles analyzed microplastics from fecal samples of 8 pinniped species and one odontocete (**Table 3**).

The average number of microplastics found in the GI tracts of large odontocetes ranged from 9 to 88 microplastics/individual, small odontocetes ranged 3 to 45 microplastics/individual and the only mysticete analyzed contained 6 items (**Figure 1**, **Table 2**). Lusher et al. (2018) found microplastic quantities in small odontocetes from Ireland, such as *Delphinus delphis, Stenella coeruleoalba, Phocoena phocoena* and *Tursiops truncatus,* that are comparable to the levels observed in bigger odontocetes, such as *Ziphius cavirostris* and *Orcinus orca,* analyzed in the same study. High levels of microplastics in small cetaceans could be reflective of coastal behavior, which puts them at higher risk of plastic ingestion.

The average number of microplastics per individual in the GI tracts of two pinniped species (*Phoca vitulina* and *Halichoerus grypus)* ranged between 4 and 27.9 microplastics/individual (**Figure 1**, **Table 2**). These values are similar to the number found in feces of pinniped species. However, one study showed alarmingly high presence of microplastics in *Arctocephalus australis* with values ranging from 0 to up to 180 microfibers per scat (Perez Venegas et al., 2018) (**Figure 1**, **Table 3**). Additionally, half of scat sub-samples from grey seals living in a sanctuary contained microplastics, where anthropogenic contamination is low. This evidence shows the ubiquity of microplastics even in controlled or less polluted areas (Nelms et al., 2018).

The size range of the microplastics found in the GI contents and feces were highly heterogenous ranging from 0.1 to 5 mm. Fibers were the most abundant shape of microplastics (Lusher et al., 2015; Hernandez-Gonzalez et al., 2018; Lusher et al., 2018; Xiong et al., 2018; Nelms et al., 2019; Zhu et al., 2019) in the GI tract content (**Table 2**), whereas fragments were more ubiquitous in the feces from 5 out of the 7 selected studies (Eriksson and Burton, 2003; Nelms et al., 2018; Donohue et al., 2019; Hudak et al., 2019; Moore et al., 2020) (**Table 3**). Among the selected studies in this review, one study looking at GI tract content and another study looking at the feces were unable to measure fibers due to the lack of procedural blanks (Besseling et al., 2015; Hudak et al., 2019).

Color and polymer type are two additional characteristics often reported in articles regarding microplastics. Among all the colors found, blue, black, white/clear/transparent and green are the most commonly observed in GI tract contents (Hernandez-Gonzalez et al., 2018; Lusher et al., 2018; Xiong et al., 2018; Nelms et al., 2019; Zhu et al., 2019) (**Table 2**) and fecal samples (**Table 3**). Additionally, fecal samples often contained red, purple, brown, green and yellow (**Table 3**). The spectrum of polymers observed is heterogeneous in the GI tract and fecal samples. Most common polymers were ethylene propylene, polypropylene, polyethylene, polyester, cotton, nylon and polyether sulfone (**Tables 2,3**). However, others such as polystyrene, polycarbonate, cellulose, polyolefin, polyvinyl chloride, acrylic, polyamide resin, low density polyethylene, poly(ethylene:prolypene:diene) rubber, alkyd resin and cellophane have been also found (**Tables 2, 3**). Most studies that analyzed the polymer type used FTIR (**Tables 2, 3**) and only one used Raman spectroscopy (Xiong et al., 2018) (**Table 3**). However, in some cases authors only analyzed a subsample of the fragments and fibers, due to the large quantity (Lusher et al., 2015; Donohue, 2019; Nelms, 2019; Perez Venegas, 2020).

Procedural blanks are extremely important to control for contamination during isolation of microplastics, especially fibers, since they are ubiquitous in the laboratory. From **Table 2**, 6 studies out of 9 (Lusher et al., 2015; Xiong et al., 2018; Hernandez-Millan et al., 2019; Nelms et al., 2019; Zhu et al., 2019; Moore et al., 2020) and in **Table 3**, only 3 studies mentioned specifically using procedural blanks to control for contamination (Nelms et al., 2018; Perez-Venegas et al., 2018; Donohue et al.,

TABLE 2 | Microplastic Presence in the Gastrointestinal Tract of 15 Cetacean and two Pinniped Species (in grey).

Location	Species	n	Microplastics/ Individual	Size	Shape	Color	Polymer type	References
Pacific Ocean (China)	*Neophocaena asiaeorientalis sunameri*	7	19.1 ± 7.2	NA	Fibers (70.1%). Sheets (14.9%), fragments (13.4%), and foam (1.5%)	Most were blue. Red, transparent, yellow, green	Most abundant: PP. Others found: PE, PA, PS, PC, and PET	Xiong et al. (2018)
	Sousa chinensis	3	2 adults (total 30 and 45)[a] and the calf (2)	Average size 2.2 mm ± 0.4 (0.1 to 4.8 mm)	Fibers (70.3%). Fragments and flakes were also found	Most were white and blue	Most abundant: PES, Others found: PP, CL, PE, PA and PBT.	Zhu et al. (2019)
Arctic Ocean (Canada)	*Delphinapterus leucas*	7	11.6 ± 6.6 (total 97 ± 47)[a]	Size range 0–5 mm >1 mm most abundant	Fibers (49%) and fragments (51%)	NA	Most abundant: 44% PET (85% fibers). Others found: PVC, PO, PA, acrylic, PP, PS, PE.	Moore et al. (2020)
Atlantic Ocean (Netherland, Spain, Ireland, Scotland, England, Wales)	*Megaptera novaeangliae*	1	6 (total 167)[a]	Average size 1.1–4.7 mm by 0.4–2.4 mm	Sheets and fragments were found. Fibers not counted due to lack of blanks	NA	Most abundant: PE, PA. Others found: PP, PVC and PET.	Besseling et al. (2015)
	Delphinus delphis	35	12 ± 8 (range 3 to 41)	Fibers 2.11 ± 1.26 mm. Fragments 1.29 ± 0.93 mm. Beads 0.95 mm	Fibers (96.59%), fragments (3.16%), beads (0.24%)	Blue (45.26%), black (24.57%), green (15.58%), red (14.36%)	NA	Hernandez-Gonzalez., et al. (2018)
	Ziphius cavirostris	1	53	Most abundant sizes 1 to 5 mm. Size range 0.3 to 16.7 mm	Fibers (83.6%) and fragments (16.4%)	Blue (29.2%), grey (18.2%), black (16.8%) and orange (15.05%)	NA	Lusher et al. (2018)
	Delphinus delphis	9 (4)[+]	36.25 ± 19.36[b]					
	Stenella coeruleoalba	2	44.5 ± 16.26[b]					
	Phocoena phocoena	5 (3)[+]	33 ± 23.07[b]					
	Orcinus orca	1	39					
	Tursiops truncatus	2 (1)[+]	35 ± 21.92[b]					
	Mesoplodon mirus	1	88	Mean length 2.16 mm ± 1.39 (0.3 to 7 mm)	Most were fibers and fragments. Film was also found	NA	Most abundant: Rayon (53%) Others found: PET, acrylic, PP, PE.	Lusher et al. (2015)
	Phocoena phocoena	21	5.23 ± 2.53[b]	Average fiber size 2 mm ± 2.3 mm (2 cm to 0.1 mm). Average fragments size 0.9 mm ± 1.1 (4 × 2 mm to 100 × 100 um)	Fibers (84%) and fragments (16%)	Most were blue (42.5%), black (26.4%), clear (12.8%)	Most abundant: Nylon 60%. Others found: PE, PET, PES, phenoxy resin, PE, PP and rayon, PA and LDPE.	Nelms et al. (2019)
	Stenella coeruleoalba	1	7					
	Tursiops truncatus	1	6					
	Delphinus delphis	16	5.69 ± 3.34[b]					
	Grampus griseus	1	9					
	Kogia breviceps	1	4					
	Lagenorhynchus albirostris	1	3					
	Lagenorhynchus acutus	1	8					
	Phoca vitulina	4	4.25 ± 2.5[b]					
	Halichoerus grypus.	3	6 ± 2[b]					
	Halichoerus grypus	13	27.9 ± 14.7	NA	Fibers (86%), fragments (14%) and films (1%)	NA	NA	Hernandez-Millan et al. (2019)

[a]*estimated from the analysis of a section. Abbreviations: Polyethylene PE, Low density polyethylene LDPE, Ethylene propylene EP, Polyester PET, Polyacrylamide PAM, Polypropylene PP, Polystyrene PS, Polyamide (nylon) PA, Polycarbonate PC, Polybutylene terephthalate PBT, Polyvinyl chloride PVC, Polyether sulfone PES, Cellulose CL, Polyolefin PO.*
[b]*average calculated from supplementary data; + number individual where intestines were analyzed.*

TABLE 3 | Microplastic content in feces from 8 pinniped species and 1 odontocete species (in grey).

Location	Species	n	No of microplastics	Size	Shape	Color	Polymer type	Ref
Atlantic Ocean (Cornish Seal sanctuary and Massachusetts)	*Halichoerus grypus*^	31 from 4 resident seals	48% of scats contained microplastics. Ranging 0 to 4 particles/scat.[a]	Fragments size from 0.4 × 0.3 mm to 5.5 × 0.4 mm. Fibers from 0.6 to 3.5 mm	Fragments (69%) and fibers (31%)	Black (27%), transparent and red (23% both), blue (15%), and orange (12%)	EP (27%), PP (27%), PE (12%). Other polymers were also found	Nelms et al. (2018)
	Phoca vitulina vitulina	32	2 fragments in 32 scats	Size ranged 1.2 to 3.5 mm	Fragments	Tan, red, purple and white	Alkyd resin (1), celophane (2), EPDM rubber(1)	Hudak et al. (2019)
	Halichoerus grypus atlantica	129	2 fragments in 129 scats					
Pacific Ocean (Australia, Alaska, California, Peru, Chile)	*Arctocephalus tropicalis* *Arctocephalus gazella*	145	164 plastic items in total. Mean 1.13 particle/scat*	Mean length 4.1 mm. Mean width 1.9 mm. Range 2 mm to 5 mm	Most were fragments with irregular shapes	White, brown, blue green and yellow were most common	PE 93%, PP 4% Other polymers were found	Eriksson and Burton (2003)
	Callorhinus ursinus	44	398 fragments and 186 fibers in total. 9.05 fragments/scat and 4.22 fibers/scat	82% of microplastics below 1 mm and 72% fibers below 2 mm	Fragments and fibers. Fibers were also present in the laboratory blanks and sediment samples	Fragments were white. Fibers were black, white, purple, blue, red, yellow and clear	Fragments were low density PE. Only two fragments tested and fibers were NA.	Donohue et al. (2019)
	Arctocephalus australis	50	8.84 ± 11.01 fibers/scat and 1.5 ± 5.78 fragments/scat*	NA	Fibers more abundant. Fragments were also present	Most abundant color was blue and white	81.5% of fragments or fibers were anthropogenic in origin. 51.5% were cotton and 30% were polymers (PET and PA), the rest did not match any spectra	Perez-Venegas et al. (2020)
	Arctocephalus philippii	40	29.75 ± 49.1 fibers/scat and 1.5 ± 6.36 fragments/scat*					
	Otaria byronia	14	75.57 ± 81.46 fibers/scat and 1.28 ± 4.8 fragments/scat*					
		12	23.08 ± 16.18 fibers/scat and 1.25 ± 3.1 fragments/scat*					
		10	29.2 ± 26 fibers/scat and 0.4 ± 1.26 fragments/scat*					
	Arctocephalus australis	79	23.97 ± 34 fibers/scat and 0.16 ± 1.46 fragments/scat*					
	Arctocephalus australis	51	Microfibers in 67% of examined samples. Ranging from 0 to 180/scat	>0.1 mm	Microfibers	Blue (45%), white (24%), black(16%), red (15%)	NA	Perez-Venegas et al. (2018)
Arctic Ocean (Canada)	*Delphinapterus leucas*[a]	2	2 and 0 items	Range was 0–5 mm. Most were <1 mm	Fragments (51%) and fibres (49%)	NA	Most abundant 44% PES (85% fibres). Others: PVC, PO, PA, acrylic, PP, PS, PE.	Moore et al. (2020)

** calculated from data in the paper.^ Seals from Cornish Seal Sanctuary, UK[a] results are outcomes from GI tract and feces content; [a] subsample analyzed. Abbreviations: Polyethylene PE, Ethylene propylene EP, Polyester PET, Polypropylene PP, Polystyrene PS, Polyamide (nylon) PA, Polyvinyl chloride PVC, poly(ethylene:prolypene:diene) EPDM, Polyolefin PO.*

2019). The size, shape, color and polymer type of microplastics isolated from GI tract content is highly limited by the methods used during the isolation and characterization process.

Non-dietary ingestion of microplastics might account for a high percentage of total ingestion. Hernandez Millan et al. (2019) analyzed microplastics in grey seals and estimated

TABLE 4 | Presence of microplastics in human samples: Feces and lungs.

Endpoint	n	Method	No of microplastics	Size and shape	Polymer type	Ref
Microplastics isolation from human stool	8	*Chemical digestion of organic material. *Filtration through a 50 um metal sieve. *Resuspended in ultrapure water, filtered via vacuum system and dried.*Polymer composition by FTIR.	100% samples had microplastic. Median: 20 microplastics/10 g (range 18 to 172)	Size range from 50 to 500 um sizes. Most were fragments or films. Rarely spheres and fibers	9 types: PP, PET, PS, PE, POM, PC, PA, PVC, PU The most abundant PP and PET (present in all samples)	Schwabl et al., (2019)
	10	*Fenton´s reagent and nitric acid digestion* vacumm filtration steps in between digestions* polymer composition by Raman spectra	40% samples had microplastic	>1 um	The microplastics were identified as PBT and PVB particles	Yan et al., (2020)
Presence of plastic fibers in human lung tissue	114	*Fresh lung specimens were analyzed in dual-slide chambers under white light, fluorescent light, polarizing light and phase contrast light. *Paraffin embedded lung tissue histopathological slides were analyzed	87% samples had fibers. 83% of nonneoplastic lung specimens and 97% of malignant lung specimens contained inhaled fibers		The histopathological slides confirmed the presence of cellulosic and plastic fibers in the lungs identified by polarized light	Pauly et al., (1998)

Abbreviations: Polyethylene PE, Polyester PET, Polypropylene PP, Polystyrene PS, Polyamide (nylon) PA, Polyvinyl chloride PVC, Polyoxymethylene POM, Polybutylene terephthalate PBT, Polyvinyl ether PVE, Polycarbonate PC, Polyurethane PU.

theoretical ingestion of microplastics using the estimation by Lusher et al. (2013) of 1.9 microplastics ingestion per fish consumed. According to their results, 67% of the total amount of particles they observed were from dietary origin, therefore suggesting non-dietary ingestion occurs. Interestingly, Xiong et al. (2018) observed presence of microplastics in neonatal porpoise at levels that were comparable to the adults, suggesting a high rate of non-dietary ingestion. Moreover, Zhu et al. (2019) found microplastics in a newborn calf of a coastal delphinid species (*Sousa chinensis*), although at lower quantities.

Multiple studies analyzed the concentration of microplastics across different sections of the GI tract. Nelms et al. (2019) showed higher concentrations of microplastics in stomachs compared to intestines and Lusher et al. (2018) showed no correlation between number of microplastics and section of GI tract. In both studies, the majority of the microplastics were fibers. Lusher et al. (2015) showed that out of 88 particles isolated from a *Mesoplodon mirus* individual, 29 were located in the stomachs and 59 in the intestines, of which 89% were fibers. Xiong et al. (2018) showed similar results, a retention of fibers in the first sections of the intestine.

Microplastics in Humans

22 articles regarding human exposure to microplastics were further reviewed. From those, 7 papers were based on *in vitro* studies using human cells, two used artificial digestion to understand the effects of human digestive fluids on the microplastics, 3 analyzed microplastics in human samples and 10 studied the effect of different toxicants involved in plastic manufacturing and associated risk of developing pathologies.

Microplastics in Human Samples: Lung and Feces

Three articles analyzed microplastics in human samples and all of them show presence of microplastics in human body (Pauly, 1998; Schwabl et al., 2019; Yan et al., 2020) (**Table 4**). Each of the studies had rigorous procedural blanks showing lack of contamination throughout the analysis. Two studies out of three investigated the presence of microplastics in human feces (Schwabl et al., 2019; Yan et al., 2019). Schwabl et al. (2019) and Yan et al. (2020) showed microplastics present in 100% and 40% of the fecal samples respectively. Schwabl et al. (2020) reported a median of 20 microplastics per 10 g of stool, with a range of 18–172 per 10 g of stool (**Figure 1**, **Table 4**). From those microplastics most were fragments or films with a size range of 50 um to 500 um. This study observed 9 polymer types by FTIR (polyethylene, polyester, polypropylene, polystyrene, polyamide (nylon), polyvinyl chloride, polyoxymethylene, polycarbonate, polyurethane) although polypropylene and polyester were most ubiquitous. On the contrary, Yan et al. (2020) identified polybutylene terephthalate and polyvinyl ether by Rama spectroscopy. Yan et al. (2020) did not provide information on size range or shape of microplastics found.

The third study, Pauly et al. (1998), for the first time identified patient tissue samples of nonneoplastic lung and malignant lung specimens contained inhaled plastic fibers. The authors suggest that fibers might increase the risk of developing lung disease.

Artificial Digestion System

Stock et al. (2020) and Liao and Yang (2020) studied the changes in microplastics during artificial digestions by whole digestive system *in vitro* method (WDSM). Both papers used synthetic gastric juices with different pHs and included shaking steps to mimic digestion steps. Saliva juices were shaken for 5 min, gastric

juices for 1 h (Liao and Yang 2020) or 2 h (Stock et al., 2020). Intestinal juice was then shaken for 2 h (Stock et al., 2020) or 4 h (Liao and Yang, 2020), and finally Liao and Yang (2020) added an additional step of large intestinal phase of 18 h.

Stock et al. (2020) investigated polyethylene, polyester, polyvinyl chloride, polypropylene and polystyrene microplastic polymers and observed that polystyrene particles showed changes in size and shape. These particles developed an irregular surface after the digestive steps and diameters increased up to 20 um through the different digestion steps. The rest of the polymer types were less affected by the digestive processes.

Interestingly, Liao and Yang (2020) analyzed polyester, polyvinyl chloride, polypropylene, polystyrene and polylactic acid polymers loaded with chromium (Cr), which simulates the release of toxicants that are attached to the microplastics throughout digestion. Oral bioaccessibility of Cr(VI) and Cr(III) was negligible in the mouth phase. However, the bioaccessibility of Cr(VI) in the gastric phase was significantly higher than those in the intestinal phases (small and large). For Cr(III) the highest bioaccessibility was on the small intestine. However, the levels were smaller to those found for Cr(VI) in gastric phase. Comparing between microplastic types, polylactic acid showed a higher release of Cr(VI) in each digestive phase.

In vitro Studies in Human Cells

In vitro studies looked at a variety of endpoints: cell viability, intracellular localization, oxidative stress, membrane integrity and immune response are summarized in **Table 5** and **Table 6**. Overall, these *in vitro* studies assessed exposure to polystyrene, polyethylene and polypropylene polymer type microplastics.

Cell viability was reduced after exposure to microplastics in 4 studies (Helser et al., 2019; Hwang et al., 2019; Stock et al., 2019; Dong et al., 2020), but was not affected in other 3 studies (Schirinzi et al., 2017; Wu et al., 2019; Wu et al., 2020) (**Table 5**). No effects were found when cells were exposed to polystyrene for 12 h (0.1 or 5 um), 24 h or 48 h (5 um) and 24 h (10 um) or to polyethylene for 24 h (3–16 um). However, smaller particles of polystyrene (1, 1.72 or 4 um) induced a reduction in cell viability after 24 h, which was further decreased after prolonged (48 h) exposure to human epithelial colorectal adenocarcinoma cells (Caco-2) and human lung bronchial epithelial (BEAS-2B) cells (Stock et al., 2019; Dong et al., 2020). Moreover, COOH-modified polystyrene particles (0.5 um) exposure for 24 h also induced cytotoxicity in intestinal, placental and embryonic cells (Helser et al., 2019). Finally, 20 um polypropylene particles reduced cell viability after 48 h exposure in human dermal fibroblast (HDF) (Hwang et al., 2019).

Cellular uptake of microplastics was observed in 3 studies under different conditions (**Table 5**). (Helser et al., 2019; Stock et al., 2019; Wu et al., 2019). Stock et al. (2019) showed that 4 um polystyrene particles were preferentially internalized and among all the cell types tested (mucus co-culture, M model and Caco-2 cells), macrophages had the highest ability to internalize the particles. Additionally, prolonged exposures resulted in an increase in intracellular particles. Moreover, COOH-modified polystyrene of 0.5 um were also observed intracellularly in intestinal and placental cells (Helser et al., 2019). Fluorescent polystyrene (0.1 um) particles were found colocalized with lysosomes in Caco-2 cells (Wu et al., 2019).

One study (Wu et al., 2019) showed that polystyrene particles might be exerting their toxicity through ABC transporters. 0.1 um size polystyrene particles greatly inhibited ABC transporters in Caco-2 cells (Wu et al., 2019) and larger (5 um) polystyrene particles were only able to inhibit the transporter at higher concentrations. Moreover, co-exposure of microplastics and arsenic showed that the intracellular concentration of arsenic in cells exposed to arsenic-coated polystyrene increased compared to the arsenic-only exposure. Additionally, when artificial ABC inhibitors were added, 0.1 um particles accumulated intracellularly. Therefore, the authors suggested that 0.1 um size polystyrene particles might exacerbate other contaminant-induced toxicity by acting as substrates of ABC transporters and reducing the transport capacity of other substrates. However, since 5 um particles did not act as a substrate, they suggested that they could inhibit ABC transporter activity by mitochondrial depolarization and subsequent depletion of ATP (**Table 5**).

Oxidative stress was exacerbated at different experimental conditions in 5 studies (Schirinzi et al., 2017; Hwang et al., 2019; Wu et al., 2019; Dong et al., 2020; Wu et al., 2020) (**Table 6**). Direct measurement of ROS showed an increase after exposure to polystyrene (0.1 and 0.5 um) for 12 h, polystyrene (10 um) for 24 h, polyethylene (3–16 um) for 24 h and polypropylene for 6 h (20 um when administered in DMSO). Polystyrene particles increased heme oxygenase-1 (HO-1) enzyme levels, which is directly involved in oxidative degradation (Dong et al., 2020), and inhibited catalase activity (Wu et al., 2020). Additionally, polystyrene-arsenic co-exposure increased ROS levels compared to arsenic-only exposure (Wu et al., 2019).

Membrane integrity was compromised after 12 and 24 h polystyrene exposure in two studies (Wu et al., 2019 and Dong et al., 2020) (**Table 6**). Polystyrene exposure also induced mitochondrial membrane depolarization (Wu et al., 2019), TEER value decrease (Dong et al., 2020), Zonula Occludens-1 (ZO-1) expression decrease (Dong et al., 2020) and ATT (Dong et al., 2020) level increase, further suggesting membrane destabilization. However, COOH-modified polystyrene particles did not cause any effect in the cellular membranes of the gastrointestinal tract (GIT) or placental barrier co-culture models (Hesler et al., 2019).

Immune response was assessed by four studies and results greatly varied depending on the experimental conditions (**Table 6**). 24 h exposure to polystyrene particles of 5 um size upregulated 4 inflammation genes (Wu et al., 2020) and 1.72 ± 0.26 um particle size polystyrene increased IL-6 and IL-8 levels (Dong et al., 2020). However, small size (20 um) polypropylene particles only increased IL-6 levels at high concentrations (100–1,000 ug/ml) and TNF-α increased after 100 ug/ml after 20 um size exposure in peripheral blood mononuclear (PBMC) cells (Hwang et al., 2019). Polypropylene particles (20 um, 25–200 um) induced histamine release in mast (HMC-1) cells (Hwang et al., 2019). However, polystyrene particles exposure for 24 and 72 h time points did not induce differentiation of macrophages (Stock et al., 2019).

TABLE 5 | Effects of microplastics in cell viability and uptake.

End-point	Polymer type	Exposure time	Size	Concentration range	Assay	Cell type	Outcome	Ref
Cell viability	Polystyrene (PS)	12 h	0.1 and 5 um	1–200 ug/ml	CCK-8 kit	Caco-2 cells	No effect was observed	Wu et al. (2019)
		24 h, 48 h	1.72 ± 0.26 um	1–1,000 ug/cm^2	Trypan blue	BEAS-2B	Viability decreased to 60–70% at 1,000 ug/cm2 after 24 h exposure and all the concentrations above 10ug/cm2 after 48 h exposure	Dong et al. (2020)
			1, 4 and 10 um	1–1,000 ug/ml	CTB and MTT	Caco-2 cells	CTB: 24 h 48 h exposures decrease the viability to 0% only after 1um PS exposure. MTT: Showed the same, results and additionally cell viability decreased to 80% and 70% after 24h and 48 h exposure to 4um	Stock et al. (2019)
			5 um	0.00001–100 ug/ml	MTT	Caco-2 cells	No effect was observed	Wu et al., (2020)
		24 h	10 um	0.05–10 mg/L	Hoechst 33258	T98G and HeLa cells	No effect was observed	Schirinzi et al., (2017)
	COOH-modified polystyrene (PS)	24 h	0.5 um	0.01–100 ug/ml	WST-1	GIT co culture model	Intestinal cells: PS decreased the metabolic activity only at 0.01 μg/ml. Placental cells: PS increased mitochondrial activity only at concentrations from 0.01–10 μg/ml	Helser et al., (2019)
					MTS	BeWo b30 cells		
	Polyethylene (PE)	24 h	3–16 um	0.05–10 mg/L	Hoechst 33258	T98G and HeLa cells	No effect was observed	Schirinzi et al., (2017)
	Polypropylene (PP)	48 h	20 and 25–200 um	In DMSO 10–1000 ug/ml and in powder 0.1–4.5 mg	CCK-8 colorimetric kit	HDF	HDF cells: only the 20 um PP (in DMSO) caused a reduction in viability (20%) at the highest concentration 1000 ug/ml	Hwang et al., (2019)
Intra-cellular locali-zation	Polystyrene (PS)	12 h	0.1 and 5 um	1–80 ug/ml	ABC transporter activity (CAM cell probe)	Caco-2 cells	Inhibition of ABC transporter was observed for 0.1 um PS concentrations >20 ug/ml and 5 um PS only at 80 ug/ml	Wu et al., (2019)
		24 h	1, 4 and 10 um	10^8/ml (1 and 4 um), 3×10^6/ml (10 um)	Fluorescence microscopy	Caco-2 cells, mucus co-culture[1] model and M-cell model[2]	4 um PS were absorbed the most in Caco-2 cells (3.8%), M cell model and mucus model 4.8%). 1 um PS were significantly absorbed by the M cell mode (5.8%)*	Stock et al., (2019)
		24 h, 72 h	1, 4 and 10 um	100,000/ml (1 um), 250,000/ml (4 um), 60,000/ml (10 um)	Fluorescence microscopy	THP-1 cells derived macrophages	Macrophages contained intracellular 4 um PS (40–80%) and 1 um and 10 um in lower extent	Stock et al., (2019)
	COOH-modified polystyrene (PS)	24 h	0.5 um	100 ug/ml	Confocal microscopy	GIT barrier[3] and placental barrier coculture[4] models	In the GIT barrier coculture, PS were internalized by intestinal cells and in the placental barrier model the placental cells	Hesler et al., (2019)
	Fluorescent polystyrene (PS)	12 h	0.1 um and 5 um	20 ug/ml	Confocal microscopy	Caco-2 cells	Overlap between lysosomes and microplastics. Level of 5 um entering into cells lower than 1 um	Wu et al., (2019)
	Polystyrene (PS) and arsenic (As)	12 h	0.1 and 5 um	PS: 20 ug/ml (0.1 um), 80 ug/ml (0.5 um). As: 150 mg/L	Intracellular arsenic by ICP-MS	Caco-2 cells	0.1 um PSs at 20 ug/ml increased the intracellular concentration of As	Wu et al., (2019)

**extrapolated from the graph. Abbreviations: Polystyrene PS, Polyethylene PE, Polypropylene PP.*

[1]*Caco-2 cells and HT29-MTX-E12 cells*

[2]*Caco-2 and RajiB transwell coculture*

[3]*Caco-2 and HT29-MTX-E12 cells*

[4]*BeWo b30 and HPEC-A2 cells.*

TABLE 6 | Effects of microplastics in oxidative stress and membrane integrity.

End-point	Polymer type	Exposure time	Size	Concentration range	Assay	Cell type	Outcome	Ref
Oxidative stress	Polystyrene (PS) and arsenic (As)	12 h	0.1 and 5 um	20 ug/ml (0.1 um), 80 ug/ml (0.5 um) As:75 and 150 ug/l	DCFH-DA kit assay	Caco-2 cells	ROS increased after the co-exposure (PS + As), comparing to just arsenic exposure	Wu et al. (2019)
	Polystyrene (PS)	12 h	0.1 and 5 um	1–200 ug/ml	DCFH-DA kit assay	Caco-2 cells	ROS production only increased after 200 ug/ml exposure to 0.1 um and 5 um PS.	Wu et al. (2019)
		24 h	1.72 ± 0.26 um	10–1000 ug/cm^2	Western blot (HO-1) DCFH-DA kit assay	BEAS-2B cells	HO-1 protein level significantly increased after 10 and 1000 ug/cm^2 DCFH-DA increased at 1000 ug/cm^2	Dong et al. (2020)
			10 um	0.05–10 mg/L	DHE solution	T98G and HeLa cells	ROS increased in both cell lines. EC50 9.6 mg/L in T98G and EC50 13.56 mg/L in HeLa cells	Schirinz et al. (2017)
		24 h, 48 h	5 um	12.5–50 mg/L	SOD, GSH, MDA detection and CAT activity	Caco-2 cells	No effect on SOD, GSH and MDA levels. Activity of catalase was inhibited only after 24 and 48 h exposure to 50 mg/L of 5 um PS	Wu et al. (2020)
	Polyethylene (PE)	24 h	3–16 um	0.05–10 mg/L	DHE solution	T98G and HeLa cells	ROS increased only in T98G cells. EC50 41.22 mg/L	Schirinzi et al. (2017)
	Polypropylene (PP)	6 h	20 and 25–200 um	50–1,000 ug/ml in powder and DMSO	DCFH-DA kit assay	HDF cells	ROS increased after exposure to 20 um PP (in DMSO) at 1000 ug/mL. When administered in powder, ROS did not increase	Hwan et al. (2019)
Membrane integrity	Polystyrene (PS)	12 h	0.1 and 5 um	1–80 ug/mL	JC1 assay, LDH assay and TMA-DPH	Caco-2 cells	Mitochondrial membrane depolarization occurred after 20 to 80 ug/mL for 0.1 um PS and after all the concentrations of 5 um. No effects on LDH leakage or polarization	Wu et al. (2019)
		24 h	1.72 ± 0.26 um	10–1000 ug/cm^2	TEER, ELISA (ZO-1 and AAT) and Western blot (ZO-1)	BEAS-2B cells	TEER value decreased in the epithelial barrier after 10 and 1,000 ug/cm^2 exposure. ZO-1 levels decreased after exposure to 10 and 1000 ug/cm^2. AAT level decreased after exposure to 1,000 ug/cm^2	Dong et al. (2020)
	COOH-modified polystyrene (PS)	24 h	5 um	10–100 μg/ml	TEER	GIT barrier and placental barrier coculture model	No effect in GIT or placental barrier were observed	Hesler et al. (2019)
Immune response	Polystyrene (PS)	24 h	1.72 ± 0.26 um	10–1000 ug/cm^2	ELISA (IL-6, IL-8)	BEAS-2B cells	IL-6 significantly increased at 10 and 1000 ug/cm^2 exposure. 1000 ug/cm^2 exposure increased IL-8 expression	Dong et al. (2020)
		24 h, 48 h	5 um	12.5–50 mg/L	RT-PCR	Caco-2 cells	Four inflammation related genes (TRPV1, iNOS, IL-1β, IL-8) were up-regulated	Wu et al. (2020)
		24 h, 72 h	1, 4 and 10 um	100,000/ml (1 um), 250,000/ml (4 um), 60,000/ml (10 um)	Macrophage polarization (Western Blot and RT-PCR)	THP-1 cells	No macrophage differentiation	Stock et al. (2019)
	Polypropylene (PP)	4 h, 72 h, 4 days	20 and 25–200 um	10–1,000 ug/ml	ELISA (IL-2, IL-6, IL-10, TNF-α)	PBMC	PBMC: IL-6 increased after 20 um PP at 1,000 and 100 ug/ml and TNF-α increased after 100 ug/mL after 20 um size exposure	Hwang et al., (2019)
		48 h	20 and 25–200 um	100 ug/ml and 500 ug/ml (20 um and 25–200 um)	Histamine by ELISA kit	HMC-1 cells	Histamine was released after exposure to 500 ug/ml 20 um PP in HMC-1 cells	Hwang et al., (2019)

Abbreviations: PS, Polystyrene; PE, Polyethylene; PP, Polypropylene.

Other endpoints, such as, genotoxicity, gene expression, embryotoxicity and hemolysis, were also investigated to a lesser degree in some of these studies. Hwang et al. (2019) showed that polypropylene particles of 20 um and 25–200 um sizes can induce hemolysis in sheep red blood cells. Hesler et al. (2019) showed no genotoxic potential of COOH-modified polystyrene particles (0.5 um) by a p53 reporter assay in HepG2CDKN1A-DsRed and micronucleus assay in CHO-KI cells after 24 h exposure. Moreover, their study also showed that 0.5 um polystyrene are weakly embryotoxic after 24 h exposure.

Wu et al. (2020) carried out expression analysis on Caco-2 cells exposed for 24 h or 48 h to 5 um polystyrene particles at concentrations of 12.5 or 50 mg/L. RNA-Seq analysis after 24 h showed 80 upregulated differentially expressed genes (DEGs) and 94 downregulated genes. The GO terms after 12.5 mg/ml compared to 50 mg/ml shows a shift from enriched metabolism pathways to cancer pathways, which was consistently observed after 48 h exposure, where 210 DEGs were observed. RT-PCR on cells exposed for 24 h to polystyrene showed five proliferation related genes (Ras, ERK, MER, CDK4, Cyclin 1D) were downregulated and four inflammation related genes (TRPV1, iNOS, IL-1β, IL-8) were up-regulated.

Workers in Plastic Factories Develop Dermatoses

Search results showed 10 epidemiological studies that investigated the effect of different toxicants involved in plastic manufacturing and associated risk of developing pathologies. Those studies analyzed health records from workers occupationally exposed to nylon fibers (Kern et al., 1998), poly(vinyl acetate) fibers (Morinaga et al., 1999), epoxy resin (Jolanki et al., 1996), fiberglass reinforced plastic (Minamoto et al., 2002a and Minamoto et al., 2002b), acrylonitrile (Felter et al., 1997; Wood et al., 1998), glycidyl ether (Lanes et al., 1994), styrene (Sass-Kortsak et al., 1995) and glycerol polyclycidyl ether (Watkins et al., 2001).

Four studies showed that not only chemical additives but also plastic dust causes mechanical and contact dermatitis in workers. Briefly, Kern et al. (1998) studied 165 workers from a nylon flocking industry and showed increased risk interstitial lung diseases. Moreover, from 150 workers of a ski factory occupationally exposed to epoxy resin, 22 developed skin diseases such as allergic contact dermatitis (Jolanki et al., 1996). From 149 workers of fiberglass-reinforced plastics factories studied for skin diseases, 22 developed skin dermatoses, 7 were diagnosed with allergic contact dermatitis due to exposure to chemical, 3 developed irritant contact dermatitis and interestingly, 3 developed dermatitis due to mechanical irritation from glass fibers or dust and 9 developed allergic contact dermatitis and/or mechanical irritation dermatitis. Diagnosis was carried by sticking patches to the workers (Minamoto et al., 2002a). Minamoto et al. (2002b) further investigated the increased risk of developing skin diseases in workers from fiberglass-reinforced plastics. From 148 workers of fiberglass reinforced plastics factories studied, 87 (58.8%) developed skin problems.

The other 6 studies from our search showed no clear associations between the selected parameters (Lanes et al., 1994; Sass-Kortsak et al., 1995; Felter et al., 1997; Wood et al., 1998; Morinaga et al., 1999; Watkins et al., 2001).

DISCUSSION

This review provides an opportunity to look at different fields of research that work towards the same objective, isolation and characterization of microplastic exposure and the identification of toxicological effects in different species and models, allowing us to identify the data gaps and weaknesses. Moreover, this review aimed to include wildlife species relevant to humans by using the One Environmental Health approach (Perez and Wise, 2018). Sea turtles and marine mammals include long-lived species that share a great variety with food sources and habitat with humans. While chronic exposures of over 10 years seem unfeasible under laboratory conditions, sampling these two groups of species provide insightful data on whole life exposures. However, a limitation that we faced on this review is the term microplastic is practically new, first used by Thompson et al. (2004), and therefore previous literature observing small size plastic debris could not be included.

Most observed data on microplastics exposure in sea turtles, marine mammals and humans concern ingestion. Nevertheless, as shown in human epidemiological studies, inhalation and dermal contact exposure are important routes of exposure that are overlooked by literature to date, forming a knowledge gap in the field. From the studies available, however, we identified 5 key parameters that any studies investigating microplastic exposure, no matter which route, should consider reporting: 1) concentration of microplastics, 2) average size, 3) shape, 4) color and 5) polymer type.

The concentration of microplastics found in each sample highly depends on the method of isolation. Overall, comparing the amount of microplastics per individual, marine mammal GI tracts contained more microparticles per individual. Specifically, the levels reported by Lusher et al. (2018) in small odontocetes from Atlantic Ocean were extraordinarily high for their body size. Scats from pinnipeds in the Pacific Ocean and fecal samples from human volunteers showed levels comparable to those found in the GI tract of odontocetes (**Figure 1**). Sea turtles overall contained lower levels of microplastics in the GI tract. The average size of the microplastics were between 0.1 and 5 um, however, more studies reported average sizes at the lower end of the range.

With respect to shape, GI tracts from sea turtles and marine mammals contained more fibers than fragments, while pinniped scat and human feces showed a higher proportion of fragments. These findings might suggest fibers have a longer residence time in the intestine. Fibers could be retained in the gut papillae due to shape plasticity and, therefore, might have a higher potential of toxicological effect due to a longer residence time in the gut. Such possibilities remain to be tested.

Blue, black, green and white/clear plastics are preferentially found in sea turtles and marine mammals, which is consistent with observations that they are the most frequent colors of microfibers in marine sediments (Gago et al., 2018). These same colors were found in pinniped feces along with red,

purple, brown and yellow. Whereas, black and blue color plastic might be highly ingested due to their ubiquity in fishing gear, white/clear plastic has been hypothesized to be ingested by marine fauna because they mimic prey such as jellyfish (da Silva Mendes et al., 2015). Studies considering microplastics in humans did not report the color.

The polymer profiles found in sea turtles, marine mammals and human samples are similar. Polyethylene, polypropylene, ethylene propylene, polystyrene and polyester are found at high percentages in GI and fecal samples. However, other polymers such as poly(ethylene:prolypene:diene) rubber, polyamide (nylon), polyacrylamide, synthetic cellulose, polyoxymethylene, polycarbonate, polyvinyl chloride, polyurethane, polyvinyl ether, polybutylene terephthalate and polyether sulfone were also frequently observed. Those results correlate with the composition of microfibers and microplastics found in marine sediment and water column (Gago et al., 2018; Guo and Wang, 2019; Ajith et al., 2020). Among all, polyethylene and polypropylene are commonly found floating in the water column due to their low densities, which makes them more available for wildlife to ingest (Guo and Wang, 2019). It should not come as surprise the ubiquity of polyethylene polymer since it is extensively used in fishing gear (Chen et al., 2018) as well as packing food, plastic bags and bottles, among others. Interestingly, a review by Koelmans et al. (2019) showed that polyethylene, polypropylene, polyvinyl chloride, polyester and polystyrene are the most abundant polymers in drinking water. These outcomes suggest sea turtles, marine mammals and humans are being exposed to the same polymer types.

Microplastics are able to carry pollutants such as metals and organic pollutants through sorption, due to their distinct properties. Levels of organic pollutants have been measured across the globe indicating that PAH levels in microplastics are of special concern in East Asia and South America (Guo and Wang, 2019). However, in comparison fewer studies considered metals in microplastics from the marine environment (Guo and Wang, 2019), which is of special concern since laboratory and field studies have demonstrated that microplastics act as vectors for metals. Moreover, whole digestive system *in vitro* method (WDSM) have shown changes in bioavailability of metals adsorbed onto microplastics such as Cr(VI) through the digestive process and changes in shape and size of the particles.

Toxicity data on marine plastics in sea turtles, marine mammals and humans are limited. Cell culture studies indicate microplastics may cause cytotoxicity, oxidative stress, intracellular uptake, produce immune response, induce changes in the membrane, alter gene expression, cause weak embryotoxicity and hemolysis. Notably, most studies treated the cells only for acute (24 h) exposures, whereas for the investigation of effects of microplastics in the gut, a more prolonged exposure is more relevant. In humans a normal transit time is between 24 h and 48 h, or even 96 h depending on the diet (de Vries et al., 2015). The gut passage time and excretion time of microplastics in marine mammal species are largely unknown, and likely depend on the anatomical features of the GI tract of each species, the diet and the type of the plastic ingested. However, gut passage time in seals was calculated to be around 6 days (Grellier et al., 2006), whereas in turtles the ingesta passage time was 23 days. Therefore, data from prolonged exposures are essential. Additionally, unified reporting of units is also needed. As suggested by Karami (2017) in a review on the gaps in aquatic toxicological studies of microplastics, and as routinely used in particles toxicology, the best units to report concentration of microplastic in laboratory-based experiments is weight per unit of the surface area (example g/cm^2).

In this review, variability in data collection made it challenging to compare number of microplastics, size and polymer types between studies. More standardization of sample preparation, digestion and isolation, characterization and quality control procedures will be key for the field to advance and allow more consistent reporting of data to allow for clearer comparisons. For example, in the wildlife research we found that, an important factor to take into consideration is the percentage of sample analyzed. Not analyzing the whole GI tract introduces variability in the results, since the occurrence of microplastics across the gut is not homogeneous (Lusher et al., 2015; Nelms et al., 2019). Digestion is another critical step in microplastic isolation and can lead to their destruction. Other sources of biases are mesh or filter sizes and the techniques used for polymer identification such as FITR, which directly influence the types of microplastics that are detected. Additionally, we found that using blank controls through the sample preparation, microplastic identification and characterization steps is necessary to account for external contamination.

CONCLUSIONS

The characterization of physico-chemical properties of microplastics in sea turtles, marine mammals and human have shown that both wildlife and humans are likely being exposed to the same microplastics profiles. This conclusion is consistent with these three groups having similar major routes of exposure; inhalation, dermal contact and ingestion. From the available literature, we found that the five key parameters mentioned above: concentration, average size, shape, color and polymer type seem to be similar across the literature reviewed here.

Most of the studies regarding microplastics study the presence and characterization of microplastics in the GI tract and fecal samples. However, although ingestion in a major route of exposure, dermal and inhalation exposures are also a health concern. Epidemiological studies have linked exposure to toxicants involved in plastic manufacturing, such as additives and fiber dust, with contact and mechanical dermatitis and fibers localized in lung tissues have been suggested to increase risk of lung disease. However, those routes of exposure are largely unexplored in humans as well as marine mammals and sea turtles, indicating a significant knowledge gap in the field. Although data on human exposure to microplastics is currently limited, this field is rapidly developing and it is expected that in the future, new datasets and methodologies might allow for a better understanding of the exposure.

Additionally, even if the full toxicological profile of microplastics is largely unknown due to their complexity, *in vitro* studies have shown the ability of microplastics to

induce immune response, oxidative stress, cytotoxicity, alter membrane integrity and cause differential expression of genes. However, these studies only investigated exposure to polystyrene, polyethylene and polypropylene polymer type microplastics and short-term exposures. Due to physiological relevance, more effort on prolonged exposures is needed.

DATA AVAILABILITY STATEMENT

The original contributions presented in the study are included in the article/Supplementary Material, further inquiries can be directed to the corresponding author.

AUTHOR CONTRIBUTIONS

IM contributions included literature search, data curation, validation, visualization and writing the original draft and writing both reviewing and editing. JT contributions were literature search validation, data validation and writing both reviewing and editing. JW contributions included conceptualization, supervision, validation, visualization and writing both reviewing and editing.

FUNDING

This work was supported by two grants from the National Institute of Environmental Health Sciences (R01ES016893 to JPW) and T32ES011564 to JPW and JHT). Publication costs were supported by Parley for the Oceans and Ocean Alliance.

ACKNOWLEDGMENTS

The content is solely the responsibility of the authors and does not necessarily represent the official views of the National Institute of Environmental Health Sciences. Work was conducted under National Marine Fisheries Service permit # 21329 (J. Wise Sr., PI).

REFERENCES

Ajith, N., Arumugam, S., Parthasarathy, S., Manupoori, S., and Janakiraman, S. (2020). Global distribution of microplastics and its impact on marine environment-a review. *Environ. Sci. Pollut. Res. Int.* 27 (21), 25970–25986. doi:10.1007/s11356-020-09015-5

Amorocho, D. F., and Reina, R. D. (2008). Intake passage time, digesta composition and digestibility in East Pacific green turtles (*Chelonia mydas agassizii*) at Gorgona National Park, Colombian Pacific. *J. Exp. Mar. Biol. Ecol.* 360 (2), 117–124. doi:10.1016/j.jembe.2008.04.009

Andrady, A. L., and Neal, M. A. (2009). Applications and societal benefits of plastics. *Philos. Trans. R. Soc. Lond. B Biol. Sci.* 364, 1977–1984. doi:10.1098/rstb.2008.0304

Besseling, E., Foekema, E. M., Van Franeker, J. A., Leopold, M. F., Kühn, S., Bravo Rebolledo, E. L., et al. (2015). Microplastic in a macro filter feeder: humpback whale *Megaptera novaeangliae*. *Mar. Pollut. Bull.* 95 (1), 248–252. doi:10.1016/j.marpolbul.2015.04.007

Campanale, C., Massarelli, C., Savino, I., Locaputo, V., and Uricchio, V. F. (2020). A detailed review study on potential effects of microplastics and additives of concern on human health. *Int. J. Environ. Res. Publ. Health* 17 (4), 1212. doi:10.3390/ijerph17041212

Carbery, M., O'Connor, W., and Palanisami, T. (2018). Trophic transfer of microplastics and mixed contaminants in the marine food web and implications for human health. *Environ. Int.* 115, 400–409. doi:10.1016/j.envint.2018.03.007

Caron, A. G. M., Thomas, C. R., Berry, K. L. E., Motti, C. A., Ariel, E., and Brodie, J. E. (2018). Ingestion of microplastic debris by green sea turtles (*Chelonia mydas*) in the Great Barrier Reef: validation of a sequential extraction protocol. *Mar. Pollut. Bull.* 127, 743–751. doi:10.1016/j.marpolbul.2017.12.062

Chen, M., Jin, M., Tao, P., Wang, Z., Xie, W., Yu, X., et al. (2018). Assessment of microplastics derived from mariculture in Xiangshan Bay, China. *Environ. Pollut.* 242, 1146–1156. doi:10.1016/j.envpol.2018.07.133

Chubarenko, I., Bagaev, A., Zobkov, M., and Esiukova, E. (2016). On some physical and dynamical properties of microplastic particles in marine environment. *Mar. Pollut. Bull.* 108 (1–2), 105–112. doi:10.1016/j.marpolbul.2016.04.048

Cox, K. D., Covernton, G. A., Davies, H. L., Dower, J. F., Juanes, F., and Dudas, S. E. (2019). Human consumption of microplastics. *Environ. Sci. Technol.* 53, 7068–7074. doi:10.1021/acs.est.9b01517

da Silva Mendes, S., de Carvalho, R. H., de Faria, A. F., and de Sousa, B. M. (2015). Marine debris ingestion by *Chelonia mydas* (Testudines: Cheloniidae) on the Brazilian coast. *Mar. Pollut. Bull.* 92 (1-2), 8–10. doi:10.1016/j.marpolbul.2015.01.010

Davenport, J., Fraher, J., Fitzgerald, E., McLaughlin, P., Doyle, T., Harman, L., et al. (2009). Ontogenetic changes in tracheal structure facilitate deep dives and cold water foraging in adult leatherback sea turtles. *J. Exp. Biol.* 212 (21), 3440–3447. doi:10.1242/jeb.034991

de Vries, J., Miller, P. E., and Verbeke, K. (2015). Effects of cereal fiber on bowel function: a systematic review of intervention trials. *World J. Gastroenterol.* 21 (29), 8952–8963. doi:10.3748/wjg.v21.i29.8952

Dong, C. D., Chen, C. W., Chen, Y. C., Chen, H. H., Lee, J. S., and Lin, C. H. (2020). Polystyrene microplastic particles: in vitro pulmonary toxicity assessment. *J. Hazard Mater.* 385, 121575. doi:10.1016/j.jhazmat.2019.121575

Donohue, M. J., Masura, J., Gelatt, T., Ream, R., Baker, J. D., Faulhaber, K., et al. (2019). Evaluating exposure of northern Fur seals, *Callorhinus ursinus*, to microplastic pollution through fecal analysis. *Mar. Pollut. Bull.* 138, 213–221. doi:10.1016/j.marpolbul.2018.11.0310.1016/j.marpolbul.2018.11.036

Duncan, E. M., Broderick, A. C., Fuller, W. J., Galloway, T. S., Godfrey, M. H., Hamann, M., et al. (2019). Microplastic ingestion ubiquitous in marine turtles. *Global Change Biol.* 25 (2), 744–752. doi:10.1111/gcb.14519

Eriksson, C., and Burton, H. (2003). Origins and biological accumulation of small plastic particles in Fur seals from Macquarie Island. *Ambio* 32 (6), 380–384. doi:10.1579/0044-7447-32.6.380

FAO (2018). *The state of world fisheries and aquaculture 2018–meeting the sustainable development goals*. Rome, Italy: IGO

Felter, S. P., and Dollarhide, J. S. (1997). Acrylonitrile: a reevaluation of the database to support an inhalation cancer risk assessment. *Regul. Toxicol. Pharmacol.* 26 (3), 281–287. doi:10.1006/rtph.1997.1174

Frias, J. P. G. L., and Nash, R. (2019). Microplastics: finding a consensus on the definition. *Mar. Pollut. Bull.* 138, 145–147. doi:10.1016/j.marpolbul.2018.11.022

Gago, J., Carretero, O., Filgueiras, A. V., and Viñas, L. (2018). Synthetic microfibers in the marine environment: a review on their occurrence in seawater and sediments. *Mar. Pollut. Bull.* 127, 365–376. doi:10.1016/j.marpolbul.2017.11.070

Galgani, F., Claro, F., Depledge, M., and Fossi, C. (2014). Monitoring the impact of litter in large vertebrates in the Mediterranean Sea within the European Marine Strategy Framework Directive (MSFD): constraints, specificities and recommendations. *Mar. Environ. Res.* 100, 3–9. doi:10.1016/j.marenvres.2014.02.003

GESAMP (2016). "Sources, fate and effects of microplastics in the marine environment: Part 2 of a global assessment," in *GESAMP reports and studies No. 93*. Editors P. J. Kershaw and C. M. Rochman (London, UK: IMO).

Geyer, R., Jambeck, J. R., and Law, K. L. (2017). Production, use, and fate of all plastics ever made. *Sci Adv* 3 (7), e1700782. doi:10.1126/sciadv.1700782

Grellier, K., and Hammond, P. S. (2006). Robust digestion and passage rate estimates for hard parts of grey seal *(Halichoerus grypus)* prey. *Can. J. Fish. Aquat. Sci.* 63, 1982–1998. doi:10.1139/f06-092

Guo, X., and Wang, J. (2019). The chemical behaviors of microplastics in marine environment: a review. *Mar. Pollut. Bull.* 142, 1–14. doi:10.1016/j.marpolbul.2019.03.019

Hernandez-Gonzalez, A., Saavedra, C., Gago, J., Covelo, P., Santos, M. B., and Pierce, G. J. (2018). Microplastics in the stomach contents of common dolphin *(Delphinus delphis)* stranded on the Galician coasts (NW Spain, 2005–2010). *Mar. Pollut. Bull.* 137, 526–532. doi:10.1016/j.marpolbul.2018.10.026

Hernandez-Milian, G., Lusher, A., MacGabban, S., and Rogan, E. (2019). Microplastics in grey seal *(Halichoerus grypus)* intestines: are they associated with parasite aggregations?. *Mar. Pollut. Bull.* 146, 349–354. doi:10.1016/j.marpolbul.2019.06.014

Hesler, M., Aengenheister, L., Ellinger, B., Drexel, R., Straskraba, S., Jost, C., et al. (2019). Multi-endpoint toxicological assessment of polystyrene nano- and microparticles in different biological models *in vitro*. *Toxicol. In Vitro* 61, 104610. doi:10.1016/j.tiv.2019.104610

Hudak, C. A., and Sette, L. (2019). Opportunistic detection of anthropogenic micro debris in harbor seal *(Phoca vitulina vitulina)* and gray seal (*Halichoerus grypus atlantica*) fecal samples from haul-outs in southeastern Massachusetts, USA. *Mar. Pollut. Bull.* 145, 390–395. doi:10.1016/j.marpolbul.2019.06.020

Hwang, J., Choi, D., Han, S., Choi, J., and Hong, J. (2019). An assessment of the toxicity of polypropylene microplastics in human derived cells. *Sci. Total Environ.* 684, 657–669. doi:10.1016/j.scitotenv.2019.05.071

Jolanki, R., Tarvainen, K., Tatar, T., Estlander, T., Henriks-Eckerman, M. L., Mustakallio, K. K., et al. (1996). Occupational dermatoses from exposure to epoxy resin compounds in a ski factory. *Contact Dermatitis* 34 (6), 390–396. doi:10.1111/j.1600-0536.1996.tb02239.x

Karami, A. (2017). Gaps in aquatic toxicological studies of microplastics. *Chemosphere* 184, 841. doi:10.1016/j.chemosphere.2017.06.048

Kern, D. G., Crausman, R. S., Durand, K. T., Nayer, A., and Kuhn, C. (1998). Flock worker's lung: chronic interstitial lung disease in the nylon flocking industry. *Ann. Intern. Med.* 129 (4), 261–272. doi:10.7326/0003-4819-129-4-199808150-00001

Koelmans, A. A., Mohamed Nor, N. H., Hermsen, E., Kooi, M., Mintenig, S. M., and De France, J. (2019). Microplastics in freshwaters and drinking water: critical review and assessment of data quality. *Water Res.* 155, 410–422. doi:10.1016/j.watres.2019.02.054

Lanes, S. F., Rothman, K. J., Soden, K. J., Amsel, J., and Dreyer, N. A. (1994). Mortality among synthetic fiber workers exposed to glycerol polyglycidyl ether. *Am. J. Ind. Med.* 25 (5), 689–696. doi:10.1002/ajim.4700250508

Lebreton, L. C. M., van der Zwet, J., Damsteeg, J. W., Slat, B., Andrady, A., and Reisser, J. (2017). River plastic emissions to the world's oceans. *Nat. Commun.* 8, 15611. doi:10.1038/ncomms15611

Liao, Y. L., and Yang, J. Y. (2020). Microplastic serves as a potential vector for Cr in an in-vitro human digestive model. *Sci. Total Environ.* 703, 134805. doi:10.1016/j.scitotenv.2019.134805

Liu, K., Wu, T., Wang, X., Song, Z., Zong, C., Wei, N., et al. (2019). Consistent transport of terrestrial microplastics to the ocean through atmosphere. *ES T (Environ. Sci. Technol.)* 53 (18), 10612–10619. doi:10.1021/acs.est.9b03427

Lusher, A., Hollman, P., and Mendoza-Hill, J. (2017). *Microplastics in fisheries and aquaculture – Status of knowledge on their occurrence and implications for aquatic organisms and food safety*. Rome, Italy: FAO. Technical Paper 615.

Lusher, A. L., Hernandez-Milian, G., Berrow, S., Rogan, E., and O'Connor, I. (2018). Incidence of marine debris in cetaceans stranded and bycaught in Ireland: recent findings and a review of historical knowledge. *Environ. Pollut.* 232, 467–476. doi:10.1016/j.envpol.2017.09.070

Lusher, A. L., Hernandez-Milian, G., O'Brien, J., Berrow, S., O'Connor, I., and Officer, R. (2015). Microplastic and macroplastic ingestion by a deep diving, oceanic cetacean: the True's beaked whale *Mesoplodon mirus*. *Environ. Pollut.* 199, 185–191. doi:10.1016/j.envpol.2015.01.023

Lusher, A. L., McHugh, M., and Thompson, R. C. (2013). Occurrence of microplastics in the gastrointestinal tract of pelagic and demersal fish from the English channel. *Mar. Pollut. Bull.* 67 (1–2), 94–99. doi:10.1016/j.marpolbul.2012.11.028

Minamoto, K., Nagano, M., Inaoka, T., and Futatsuka, M. (2002a). Occupational dermatoses among fibreglass-reinforced plastics factory workers. *Contact Dermatitis* 46 (6), 339–347. doi:10.1034/j.1600-0536.2002.460604.x

Minamoto, K., Nagano, M., Inaoka, T., Kitano, T., Ushijima, K., Fukuda, Y., et al. (2002b). Skin problems among fiber-glass reinforced plastics factory workers in Japan. *Ind. Health* 40 (1), 42–50. doi:10.2486/indhealth.40.42

Moore, R. C., Loseto, L., Noel, M., Etemadifar, A., Brewster, J. D., MacPhee, S., et al. (2020). Microplastics in beluga whales *(Delphinapterus leucas)* from the eastern beaufort sea. *Mar. Pollut. Bull.* 150, 110723. doi:10.1016/j.marpolbul.2019.110723

Morinaga, K., Nakamura, K., Kohyama, N., and Kishimoto, T. (1999). A retrospective cohort study of male workers exposed to PVA fibers. *Ind. Health* 37 (1), 18–21. doi:10.2486/indhealth.37.18

Nelms, S. E., Barnett, J., Brownlow, A., Davison, N. J., Deaville, R., Galloway, T. S., et al. (2019). Microplastics in marine mammals stranded around the British coast: ubiquitous but transitory?. *Sci. Rep.* 9 (1), 1075. doi:10.1038/s41598-018-37428-3

Nelms, S. E., Galloway, T. S., Godley, B. J., Jarvis, D. S., and Lindeque, P. K. (2018). Investigating microplastic trophic transfer in marine top predators. *Environ. Pollut.* 238, 999–1007. doi:10.1016/j.envpol.2018.02.016

Pauly, J. L., Stegmeier, S. J., Allaart, H. A., Cheney, R. T., Zhang, P. J., Mayer, A. G., et al. (1998). Inhaled cellulosic and plastic fibers found in human lung tissue. *Cancer Epidemiol. Biomark. Prev.* 7 (5), 419–428

Pérez, A., and Wise, S. J. P. (2008). One environmental health: an emerging perspective in toxicology. *F1000Res* 7, 918. doi:10.12688/f1000research.14233.1

Perez-Venegas, D. J., Seguel, M., Pavés, H., Pulgar, J., Urbina, M., Ahrendt, C., et al. (2018). First detection of plastic microfibers in a wild population of South American Fur seals (*Arctocephalus australis*) in the Chilean Northern Patagonia. *Mar. Pollut. Bull.* 136, 50–54. doi:10.1016/j.marpolbul.2018.08.065

Perez-Venegas, D. J., Toro-Valdivieso, C., Ayala, F., Brito, B., Iturra, L., Arriagada, M., et al. (2020). Monitoring the occurrence of microplastic ingestion in Otariids along the Peruvian and Chilean coasts. *Mar. Pollut. Bull.* 153, 110966. doi:10.1016/j.marpolbul.2020.110966

Pham, C. K., Rodríguez, Y., Dauphin, A., Carriço, R., Frias, J. P. G. L., Vandeperre, F., et al. (2017). Plastic ingestion in oceanic-stage loggerhead sea turtles (*Caretta caretta*) off the North Atlantic subtropical gyre. *Mar. Pollut. Bull.* 121 (1–2), 222–229. doi:10.1016/j.marpolbul.2017.06.008

PlasticEurope Plastics (2019). *The facts 2019: a analysis of European plastics production*. Demand and Waste Data, 1–42.

Prata, J. C., da Costa, J. P., Lopes, I., Duarte, A. C., and Rocha-Santos, T. (2020). Environmental exposure to microplastics: an overview on possible human health effects. *Sci. Total Environ.* 702, 134455. doi:10.1016/j.scitotenv.2019.134455

Rawson, A. J., Bradley, J. P., Teetsov, A., Rice, S. B., Haller, E. M., and Patton, G. W. (1995). A role for airborne particulates in high mercury levels of some cetaceans. *Ecotoxicol. Environ. Saf.* 30 (3), 309–314. doi:10.1006/eesa.1995.1035

Rawson, A. J., Anderson, H. F., Patton, G. W., and Beecher, T. (1991). Anthracosis in the Atlantic bottlenose dolphin. *Mar. Mamm. Sci.* 7 (4), 413–416. doi:10.1111/j.1748-7692.1991.tb00117.x

Revel, M., Châtel, A., and Mouneyrac, C. (2018). Micro(nano)plastics: a threat to human health?. *Curr. Opin. Environ. Sci. Health.* 1, 17–23. doi:10.1016/j.coesh.2017.10.003

Ryan, P. G., Cole, G., Spiby, K., Nel, R., Osborne, A., and Perold, V. (2016). Impacts of plastic ingestion on post-hatchling loggerhead turtles off South Africa. *Mar. Pollut. Bull.* 107 (1), 155–160. doi:10.1016/j.marpolbul.2016.04.005

Sass-Kortsak, A. M., Corey, P. N., and Robertson, J. M. (1995). An investigation of the association between exposure to styrene and hearing loss. *Ann. Epidemiol.* 5 (1), 15–24. doi:10.1016/1047-2797(94)00036-s

Schirinzi, G. F., Pérez-Pomeda, I., Sanchís, J., Rossini, C., Farré, M., and Barceló, D. (2017). Cytotoxic effects of commonly used nanomaterials and microplastics on cerebral and epithelial human cells. *Environ. Res.* 159, 579–587. doi:10.1016/j.envres.2017.08.043

Schwabl, P., Koppel, S., Konigshofer, P., Bucsics, T., Trauner, M., Reiberger, T., et al. (2019). Detection of various microplastics in human stool: a prospective case series. *Ann. Intern. Med.* 171, 453–457. doi:10.7326/m19-0618

Stock, V., Böhmert, L., Lisicki, E., Block, R., Cara-Carmona, J., Pack, L. K., et al. (2019). Uptake and effects of orally ingested polystyrene microplastic particles *in vitro* and *in vivo*. *Arch. Toxicol.* 93 (7), 1817–1833. doi:10.1007/s00204-019-02478-7

Stock, V., Fahrenson, C., Thuenemann, A., Dönmez, M. H., Voss, L., Böhmert, L., et al. (2020). Impact of artificial digestion on the sizes and shapes of microplastic particles. *Food Chem. Toxicol.* 135, 111010. doi:10.1016/j.fct.2019.111010

Szewc, K., Graca, B., and Dołęga, A. (2021). Atmospheric deposition of microplastics in the coastal zone: characteristics and relationship with meteorological factors. *Sci. Total Environ.* 761, 143272. doi:10.1016/j.scitotenv.2020.143272

Takeshita, R., Sullivan, L., Smith, C., Collier, T., Hall, A., Brosnan, T., et al. (2017). The Deepwater Horizon oil spill marine mammal injury assessment. *ESR (Eur. Surg. Res.)* 33, 95–106. doi:10.3354/esr00808

Thompson, R. C., Olsen, Y., Mitchell, R. P., Davis, A., Rowland, S. J., John, A. W., et al. (2004). Lost at sea: where is all the plastic?. *Science* 304, 838. doi:10.1126/science.1094559

van Raamsdonk, L., van der Zande, M., Koelmans, A. A., Hoogenboom, R., Peters, R., Groot, M. J., et al. (2020). Current insights into monitoring, bioaccumulation, and potential health effects of microplastics present in the food chain. *Foods* 9 (1), 72. doi:10.3390/foods9010072

Wang, X., Li, C., Liu, K., Zhu, L., Song, Z., and Li, D. (2020). Atmospheric microplastic over the south China sea and East Indian ocean: abundance, distribution and source. *J. Hazard Mater.* 389, 121846. doi:10.1016/j.jhazmat.2019.121846

Watkins, D. K., Chiazze, L., Fryar, C. D., and Amsel, J. (2001). An historical cohort mortality study of synthetic fiber workers potentially exposed to glycerol polyglycidyl ether. *J. Occup. Environ. Med.* 43 (11), 984–988. doi:10.1097/00043764-200111000-00009

Wood, S. M., Buffler, P. A., Burau, K., and Krivanek, N. (1998). Mortality and morbidity of workers exposed to acrylonitrile in fiber production. *Scand. J. Work. Environ. Health* 24 (Suppl. 2), 54–62

Wright, S. L., and Kelly, F. J. (2017). Plastic and human health: a micro issue?. *Environ. Sci. Technol.* 51 (12), 6634–6647. doi:10.1021/acs.est.7b00423

Wu, B., Wu, X., Liu, S., Wang, Z., and Chen, L. (2019). Size-dependent effects of polystyrene microplastics on cytotoxicity and efflux pump inhibition in human Caco-2 cells. *Chemosphere* 221, 333–341. doi:10.1016/j.chemosphere.2019.01.056

Wu, S., Wu, M., Tian, D., Qiu, L., and Li, T. (2020). Effects of polystyrene microbeads on cytotoxicity and transcriptomic profiles in human Caco-2 cells. *Environ. Toxicol.* 35 (4), 495–506. doi:10.1002/tox.22885

Xiong, X., Chen, X., Zhang, K., Mei, Z., Hao, Y., Zheng, J., et al. (2018). Microplastics in the intestinal tracts of East asian finless porpoises (*Neophocaena asiaeorientalis sunameri*) from yellow sea and bohai sea of China. *Mar. Pollut. Bull.* 136, 55–60. doi:10.1016/j.marpolbul.2018.09.006

Yan, Z., Zhao, H., Zhao, Y., Zhu, Q., Qiao, R., Ren, H., et al. (2020). An efficient method for extracting microplastics from feces of different species. *J. Hazard Mater.* 384, 121489. doi:10.1016/j.jhazmat.2019.121489

Zhang, Y., Kang, S., Allen, S., Allen, D., Gao, T., and Sillanpää, M. (2020). Atmospheric microplastics: a review on current status and perspectives. *Earth Sci. Rev.* 203, 103118. doi:10.1016/j.earscirev.2020.103118

Zhu, J., Yu, X., Zhang, Q., Li, Y., Tan, S., Li, D., et al. (2019). Cetaceans and microplastics: first report of microplastic ingestion by a coastal delphinid, *Sousa chinensis*. *Sci. Total Environ.* 659, 649–654. doi:10.1016/j.scitotenv.2018.12.389

frontiers in Marine Science

ORIGINAL RESEARCH
published: 05 March 2021
doi: 10.3389/fmars.2021.579913

Rapid Landscape Changes in Plastic Bays Along the Norwegian Coastline

Eivind Bastesen[1], Marte Haave[1,2], Gidske L. Andersen[3], Gaute Velle[1,4], Gunhild Bødtker[1] and Charlotte Gannefors Krafft[1,5]*

[1] NORCE Norwegian Research Centre, Bergen, Norway, [2] Department of Chemistry, University of Bergen, Bergen, Norway, [3] Department of Geography, University of Bergen, Bergen, Norway, [4] Department of Biological Sciences, University of Bergen, Bergen Norway, [5] Faculty of Mathematics and Natural Sciences, University of Bergen, Bergen, Norway

The Norwegian Coastal Current transports natural debris and plastic waste along the Norwegian coastline. Deposition occurs in so-called wreck-bays and includes floating debris, such as seaweed, driftwood and volcanic pumice, and increasing amounts of plastics during the last decades. Deposition in these bays is controlled by ocean currents, tidal movements, prevailing winds and coastal morphology. We have compared soil profiles, analyzed the vegetation and inspected aerial photos back to 1950 in wreck-bays and defined three zones in the wreck-bays, where accumulation follows distinct physical processes. Zone 1 includes the foreshore deposition and consists of recent deposits that are frequently reworked by high tides and wave erosion. Thus, there is no accumulation in Zone 1. Zone 2 is situated above the high tide mark and includes storm embankments. Here, there is an archive of accumulated debris potentially deposited decades ago. Zone 3 starts above the storm embankments. The debris of Zone 3 is transported by wind from Zone 1 and Zone 2, and the zone continues onshore until the debris meets natural obstacles. Plastic accumulation seems to escalate soil formation as plastic is entangled within the organic debris Mapping and characterizing the soil layers indicates that deep soils have been formed by 50 or more years' accumulation, while the pre-plastic soil layers are thin. The plastic soil forms dams in rivers and wetlands, changing the shape and properties of the coastal landscape, also altering the microhabitat for plants. This case-study describes an ongoing landscape and vegetation change, evidently co-occurring with the onset of plastic accumulation. Such processes are not limited to the Norwegian coastline but are likely to occur wherever there is accumulation of plastic and organic materials. If this is allowed to continue, we may witness a continued and escalating change in the shape and function of coastal landscapes and ecosystems globally.

Keywords: macroplastic, Norwegian coastline, landscape changes, wreck bays, sea current

OPEN ACCESS

Edited by:
Montserrat Filella, Université de Genève, Switzerland

Reviewed by:
Christian Joshua Sanders, Southern Cross University, Australia
Conrad Sparks, Cape Peninsula University of Technology, South Africa

****Correspondence:***
Eivind Bastesen
Eiba@norceresearch.no

Specialty section:
This article was submitted to Marine Pollution, a section of the journal Frontiers in Marine Science

Received: *03 July 2020*
Accepted: *09 February 2021*
Published: *05 March 2021*

Citation:
Bastesen E, Haave M, Andersen GL, Velle G, Bødtker G and Krafft CG (2021) Rapid Landscape Changes in Plastic Bays Along the Norwegian Coastline. Front. Mar. Sci. 8:579913. doi: 10.3389/fmars.2021.579913

INTRODUCTION

Plastics are lightweight, durable materials made of synthetic polymers, and have become an integrated part of modern society. Since mass-production of plastics began in the 1950s, the production has increased rapidly and has now reached over 360 million metric tons per year (Plastics Europe.com). Due to poor waste management, plastics are now omnipresent in the marine

environment and have become of increasing scientific and public concern. The occurrence of plastic in the oceans and consequences for marine life have been reported since industrial production commenced in the 1960s (e.g., Heyerdahl, 1971; Kartar et al., 1973; Laist, 1987; Thompson et al., 2004, Thompson et al., 2009; Pham et al., 2014). Plastic in beach sediments was first reported by Merrell (1980) who observed the vast amount of fishery related waste along a section of the Alaskan coast from 1972 to 1974 and remarked how the plastic was encapsulated into the beach sediments and thereby covered by vegetation. Now, approximately 70 years after the onset of industrial plastic production, waste management is still unable to prevent plastic from entering the marine environment (Thompson et al., 2004; Ivar et al., 2009; Jambeck et al., 2015; Lebreton et al., 2017; Borrelle et al., 2020; Napper and Thompson, 2020).

The Norwegian Coastal Current transports natural debris and plastic waste from the North Sea region and Norwegian waters northward along the Norwegian coastline (OSPAR, 2007; Thiel et al., 2011; Cózar et al., 2017). Deposition of floating debris typically occurs in so-called "wreck bays" (Eriksson et al., 2013). These bays are largely unchanged over centuries, controlled by ocean currents, prevailing winds, tidal movements and coastal morphology. Originally, the floating debris included seaweed, kelp, driftwood and volcanic pumice. Nowadays, plastic is a substantial part of the debris. Plastic, as opposed to organic materials, does not decompose and can therefore accumulate where it is deposited. Thus, plastic accumulates along shorelines that are not regularly cleaned, such as in remote and uninhabited regions. The Norwegian coastline is more than 100 000 km long and is sparsely populated, with the implication that cleaning operations along the Norwegian coast until recently have focused on inhabited areas, such as near settlements, in recreational areas and near infrastructure. However, less accessible distal coves and bays at uninhabited islands and on the mainland are rarely cleaned and have accumulated debris for several decades.

We recently mapped a 70 km stretch of sparsely inhabited coastline in southwestern Norway and found plastic in over 800 accumulation sites (Bastesen et al., 2020), suggesting that remote areas along the southwestern coast of Norway are heavily polluted with plastic. Here, we argue that plastic accumulation is not only a concern for the affected wildlife that risk entanglement and death by contact with macroplastic, or the generation of microplastic that enters the ecosystem (Barnes et al., 2009). Based on our observations, the plastic accumulation also changes the physical properties of the soil and landscape, and thereby may alter the physicochemical properties and the function of the coastal ecosystems.

In this study, we focus on two locations that illustrate how landscape changes may occur because of long-term accumulation of marine plastic litter. This study aims to increase our understanding of the ongoing and potential landscape changes resulting from at least 50 years of plastic accumulation in coastal regions. Our investigation of the soil and vegetation aims to elucidate and describe the processes that started at the onset of plastic production and accumulation. If the accumulation continues, effects on soil and vegetation will be irreversible without a severe and costly human effort. The cleaning process itself may also be detrimental to the stability and resilience of the ecosystem. In order to mitigate detrimental effects of plastic accumulation, we need to understand the processes and speed at which they operate and their biological effects (e.g., Laist, 1987).

Our investigation of the plastic accumulation and coastal morphological changes encompassed three primary tasks. First to document the geomorphic character of two wreck bays of different physical properties; second to qualitatively map the distribution of plastic litter on the surface, in the soil and sediments according to a suggested accumulation/deposition zone framework. And third, to describe and qualitatively analyze the effects of plastic accumulation on the landscape development.

MATERIALS AND METHODS

Physical Factors Controlling Plastic Accumulation in Western Norway

The coastline along Western Norway can be referred to as rocky (Storlazzi and Field, 2000; Trenhaile, 2016) and consists of glacially eroded crystalline rocks forming a rugged landscape with a vast number of bays, coves and beaches. Sediments are mostly glacial deposits and are under erosion (Mangerud et al., 2011).

Onshore accumulation of marine plastic is controlled by ocean currents, tidal movements, wind and coastal shape. Important geographical properties that control deposition include shape and orientation of the bay, shoreline slope and substratum (Haarr et al., 2019). Plastic accumulation in western Norway is localized into bays and coves (Bastesen et al., 2020). Most plastic waste accumulates in bays that are oriented toward the sea and prevailing wind and current directions, and commonly above the high tide mark. This is often a result of winter storm events. Historical wind data from the period 2005-2018 (see[1]) shows that, there were on average more than 25 events with moderate gale ($>$ 15 m/s), 8 events with severe gale (21–24 m/s), and 1.5 storm events ($>$ 25 m/s) annually. Winds are mostly from the SW, W or NW direction.

Case Study of Two Wreck Bays in Western Norway

Two sites (**Figure 1**) representing so called hot spots for accumulation of marine waste were selected for the case study. Case 1 is facing the open sea, whereas case 2 is facing a large fjord basin that is open toward the outer coastline. The two sites are somewhat different in terms of the energy-level that directs the physical processes; however, both represent examples of exposed and semi-exposed locations where plastic waste accumulates.

Case 1: Lisle Lyngøyna Island

Lisle Lyngøyna is an island located at the northern extent of Øygarden municipality at the southwestern exterior coast of Norway facing the North Sea (**Figure 1**). The area of the island is 0.3 km^2 (0.5 $\times$ 0.5 km). It has a narrow cove with a lateral length of 100 m and width of 30 m facing the sea to the S-SW. A freshwater pond is in the N-NE continuation of the cove. The

[1]https://klimaservicesenter.no/observations/

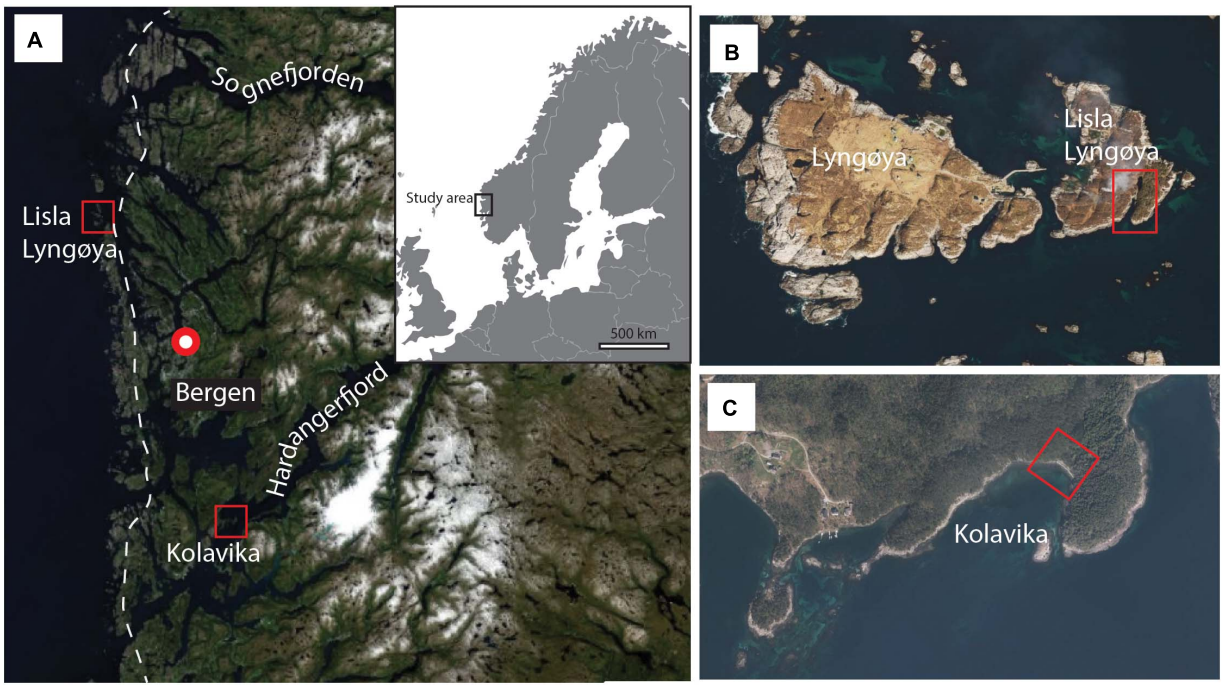

FIGURE 1 | (A) Location of the two study sites in the NW part of the North Sea basin. **(B)** Lisle Lyngøyna aerial photo from (Norway in pictures). **(C)** Kolavika (aerial photo from Norway in pictures).

bedrock in the archipelago consists of felsic gneiss (acidic). The vegetation is classified as coastal heathland (Fremstad et al., 1991; Hjelle et al., 2010), consisting of a mosaic of heather (*Calluna vulgaris*) dominated vegetation, nutrient poor peatbogs and areas of barren rocks. In some areas there is regrowth with shrubs and trees. Coastal heathlands are cultural landscapes created and managed through regular burning and mowing of heather, and by grazing and browsing by sheep throughout the year. Historically, the area has also been used for peat extraction (until the 1950s), and remnants of peat carvings and irrigation channels are still visible in the landscape.

Case 2: Kolavika Bay

Kolavika is a SW facing bay located at the northern shores of the outer Hardangerfjord system. The bay is a pebble beach that is 50 m wide and consists of reworked moraine material. The sediment depth is unknown, and basement rocks crop out in the middle of the bay. The valley is bordered by small hills and has two small streams running toward the sea. Kolavika is part of a nature reserve[2], and is protected because of its characteristic geology, nature types and biodiversity. The vegetation in the area is coastal forest; both rich deciduous and pine forest types are found there. They bay is surrounded by these vegetation types but was itself until recently a plantation forest of *Picea sitchensis*. Kolavika (kol = coal) was historically a location for charcoal production from pine. Remnants of the coal production can be observed in the substratum as a coal layer.

[2]https://lovdata.no/dokument/LF/forskrift/2014-12-12-1669

Equipment and Sampling

Pictures and Historical Images to Investigate Landscape Changes

A DJI Phantom 4 pro drone was used to collect high resolution images from flight heights of 20 m and 70 m using pre-programed flight routes (DroneDeploy version 2018). Images was collected during clear days in May and November 2018 for the Lisle Lyngøy site and in November 2019 for the Kolavika site. Images were processed by photogrammetric methods (Agisoft Photoscan 1.6.2 (Metashape); Westoby et al., 2012). Detailed orthomosaics and digital terrain models were subsequently generated and used in detailed mapping of the bays using the 3D visualization software Lime (version 2.2.2) (Buckley et al., 2019), for detecting plastic polluted areas, mapping of vegetation and analyzing plastic-modified terrain morphology. In order to analyze the evolution of the landscape, aerial images pre-dating the onset of the plastic pollution was compared with images from the present. This analysis was only performed at the Lisle Lyngøyna since historical images was not accessible over the Kolavika location. Aerial photos were provided by Norway digital and included the series, Midthordland 2019 (orthophoto resolution 0.08 m); Midthordland 2004 (orthophoto resolution 0.08 m) and Sotra-Fedje 1962 (orthophoto resolution 0.2 m) (©Kartverket, Geovekst, Øygarden; Tysnes). The georeferenced images were interpreted in ArcGIS (Esri version 10.1) by comparing the coastline, and the shoreline of ponds and other recognizable features. Observed landscape changes, such as increase in soil thickness due to plastic accumulation were quantified by area and volumetric measurement of the plastic waste using the 3D

visualization software. An estimate of litter types and the amount of litter on surface was given mostly within per cent ranges based on inspections of drone photos. To quantify volumes of the plastic contaminated soil in field, measurements such as average depth of soil was multiplied with the surface area.

Sediment and Soil Stratigraphy

The soil layers were investigated first by using a metal rod for measuring the thickness of the soil down to the bedrock or sediment substrate. To characterize the 3D distribution of plastic, and to elucidate the formation process of the plastic soils, we retrieved full-length cores from the soil where possible. It was challenging to retrieve cores from this substratum as the plastic items and ropes were entangled and layered within the soil. We attempted to core using a Russian Peat Corer and cylinders with sharpened ends without success. Instead, we dug small transects (soil profiles of ∼1 × 1 m) with shovels and knives to describe the composition and layering of the substrate. Soil cores (**Tables 1**, **2**) were retrieved using serrated knives (**Figure 2E**). The cores were wrapped in aluminum foil and transported to the laboratory for detailed investigation of plastic fragments. The bottom sediments in the pond at Lisle Lyngøyna were sampled by a hand-held van Veen grab, deployed from a small rubber boat. Also, we snorkeled the pond to describe plastic distribution and littering at the bottom. At Lisle Lyngøyna 10 locations were studied whereas 6 samples were collected for laboratory studies (**Table 1**). At Kolavika 5 locations were studied and 2 full cores were successfully retrieved for laboratory analysis (**Table 2**).

Vegetation Types

Mapping of vegetation in zones 2 and 3 was done in field with a GPS-receiver in combination with aerial imagery. Dominant and characteristic species were noted within each vegetation type. We counted annual growth rings (dendrochronology) of ash trees that grew in the plastic infused soil on the beach in Kolavika. The age of the oldest trees can be an indicator of when the plastic accumulation started.

TABLE 1 | Samples collected at Case1 Lisla Lyngøya.

Sample	Location type	Zone	Depth of plastic*	Soil and plastic type
LL1	Soil core	2	70 cm	Large plastic pieces, organic rich nutritious soil
LL2	Inspection	3	No plastic	peat/heather
LL3	Inspection	3	No plastic	peat/heather
LL4	Inspection	3	No plastic	peat/heather
LL5A	Soil core	3	No plastic	peat/Heather
LL5B	Soil core	3	10 cm	Small pieces (1–2 mm only found at 10 upper cm)
LL6	Soil core	3	25 cm	Various plastic, tar lump in upper part of sample, peat moss matrix
LL7	Soil core	3	60 cm	Fragmented plastic found in entire sample peat moss matrix
LL8	inspection	3	No plastic	Fragmented plastic found in entire sample peat moss matrix
LL9	Van Ween grab	3	No plastic	Sample bottom of pond silt and clay (no visible plastic)
LL10	Soil core	3	35 cm	Fragmented plastic found in entire sample, peat moss matrix

TABLE 2 | Samples collected at case 2 Kolavika.

Sample	Location type	Zone	Depth of plastic	Soil and plastic type
KL1	Soil core	2	70 cm	Mixture of macro plastic pieces, beach pebbles and three roots
KL2	Inspection	2	40 cm	Mixture of macro plastic pieces, beach pebbles and three roots
KL3	Inspection	2	50 cm	Mixture of macro plastic pieces, beach pebbles and three roots
KL4	Inspection	3	No plastic	20 cm soil over beach pepple deposit scattered plastic found on surface
KL5	Soil core	3	20 cm	Fragmented plastic found in upper soil layer
KL6	Inspection	3	30 cm	Fragmented wind blown plastic (bags and flakes) found down to pebble base

RESULTS

General Deposition Zones in the Studied Beaches

Based on our qualitative analysis and on the results of Bastesen et al. (2020) and Haarr et al. (2019), we suggest a general division of deposition zones at beaches (**Figure 3**). We adhere to this division when describing our results. We here define three zones that can be recognized in wreck-bays, based on the natural processes that impact the accumulation and deposition of debris. These zones, although of varying shape and size among locations, can be used to describe and understand their physical properties.

Zone 1 includes the upper littoral zone or foreshore, placed at or immediately above the high tide mark; an area affected by high energy, such as waves and tidal movements. The zone comprises mostly non-vegetated to sparsely vegetated beach or bare rock faces. The materials that deposit include seaweed, driftwood and plastic debris. Characteristic for these zones is that materials are only temporarily placed there and may be washed away or blown to another location during storms or high tides.

Zone 2 is situated above the high tide mark and includes more permanent deposits, or storm embankments. Deposits may often comprise large items that only can be transported and deposited by severe storms and storm surges. These embankments are common morphological features in coastal bays of Norway and may be referred to as so-called drift embankments (Carlsen and Bär, 2016). During calm periods, such as the summer seasons, the vegetation thrives on the nutritious substratum (decomposed seaweed and kelp). The vegetation cover inhibit erosion during storm seasons. This annual cycle of winter storm deposition and summertime vegetation may form growth of

FIGURE 2 | (A) Drone photo of the Zone 2 embankment that limits the pond from Zone 1. The profile that was used for measuring depth to basement rocks is denoted. **(B)** Close up image showing the type and amount of marine litter on the surface. Note the water saturated surface and water protruding from the pond in Zone 3. **(C)** Illustration of the depth profile through the embankment. Colored items illustrate plastic fragments of various sizes and types. **(D)** Photo of core taken in central part of the storm embankment. Various items observed on the surface are denoted. Upper part comprises small fragmented plastic pieces embedded in black organic rich soil, middle part consists of large and preserved marine litter, lower part consists of a base soil layer free from plastic. Colored pieces represent pumice that may be of volcanic origin. **(E)** Coring technique by using a serrated knife. **(F)** Pieces of preserved packaging plastic found in the middle part of the core. The Kellogg's cornflakes packaging is dated 1973.

deposits accumulated over several decades. Soil profiles of Zone 2 may therefore constitute a chronological archive of accumulation, which can be used for dating and stratigraphic investigation of long-term plastic accumulation.

Zone 3 is defined as the zone above (and around) Zone 2. Zone 3 accumulates wind-transported debris, and continues onshore until the debris meets natural obstacles, such as trees or boulders. This debris represents a scattered selection of materials and is to a lesser degree a chronological and layered archive of accumulation. The extent of Zone 3 depends on the morphology and physical properties of the area, such as ponds, vegetation, rocks, coves or other shapes that either facilitate or prevent wind transportation.

Case 1 – The Lisle Lyngøyna Island

At Lisle Lyngøyna, plastic litter covered a large area from the inner part of the cove to approximately 120 m inland (**Figure 4**). Large amounts of plastic items of considerable

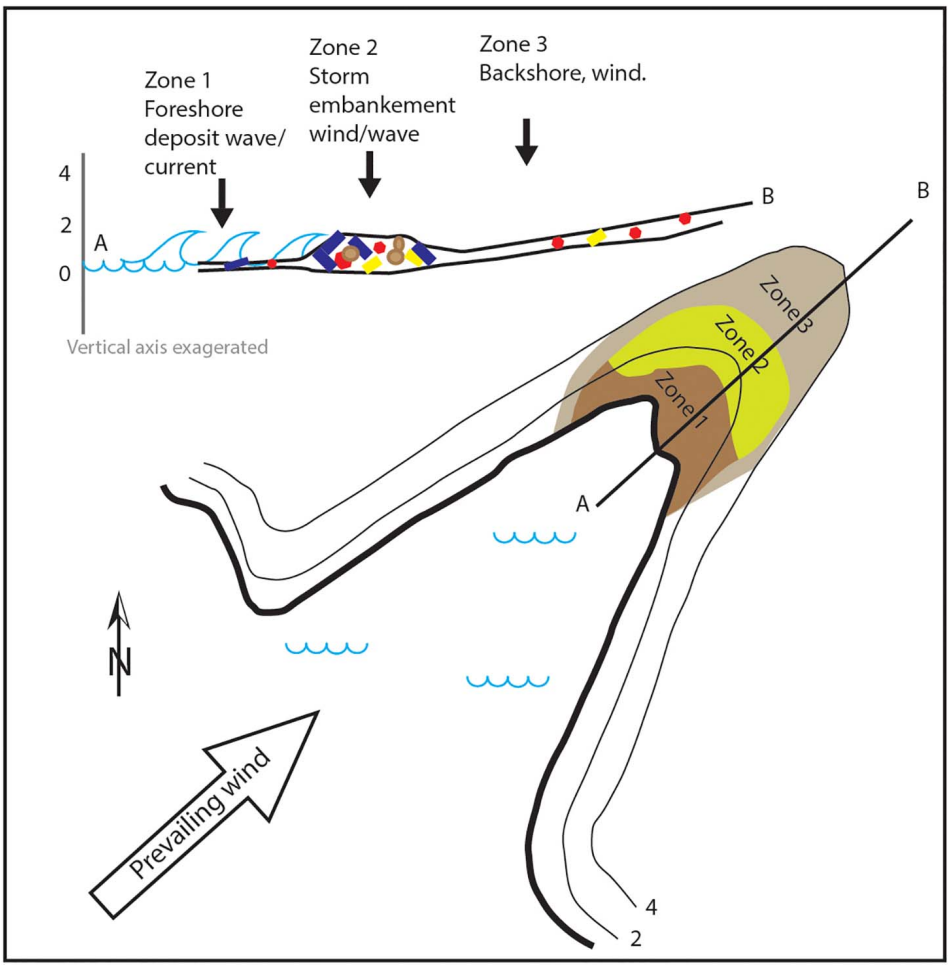

FIGURE 3 | Conceptual sketch of wreck bays based on observation in the two localities. Zone 1 foreshore deposition. Zone 2 backshore/storm embankment, Zone 3 area of dominantly wind deposited plastic.

size were also found in and along the shores of the pond, demonstrating the high energy events that occur here and lead to the deposition of plastic waste. Evidence of long-term plastic accumulation was observed, and in some places the entire edge of the pond was comprised of plastic entangled into or overgrown with vegetation. In the following, landscape characteristics and sediment stratigraphy are described in each of the accumulation zones.

Lisle Lyngøyna Zone 1

Zone 1 was comprised of the shore and inner part of the cove up to about 20 m inland from the high tide mark (**Figure 5**). The area consisted mostly of barren rock faces, small tidal ponds and small patches of grass (**Figure 5**). Plastic intermixed with seaweed was accumulated into small depressions within Zone 1. The two drone images in **Figure 5** illustrate the dynamics of these depositions. The images were retrieved at different times, May (**Figure 5A**) and November (**Figure 5B**) 2018. In November the near shore part of Zone 1 was filled with plastic items dominated by bottles. In May earlier the same year this same spot was completely cleared. This gives an indication of the accumulation rate and it also shows the dynamics of the lower foreshore area and that more plastic is observed at winter season compared to summer season. Plastic covered below 10% of the surface. Several lumps of tar originating from bitumen/oil, were attached to the rocks immediately above the high tide mark. In some cases, plastic pellets were embedded in the tar. The thin layer of soil beneath the scattered grass patches (**Figure 5A**), were investigated by digging, revealing only a thin soil layer without plastic.

Lisle Lyngøyna Zone 2

Zone 2 was adjacent to Zone 1, covering the area until the beginning of the pond located approximately 30 meters from the high tide mark. It was comprised of an 11 × 11 m (approx. 50–60 m^3) storm embankment (**Figures 2**, **4**), The embankment surface was on average elevated 1.9–2.3 m above mean sea level and had a characteristic flat surface.

Zone 2 typically had more and larger plastic items than Zone 1, such as buckets, containers, bottles, fishnets, ropes, pipes and

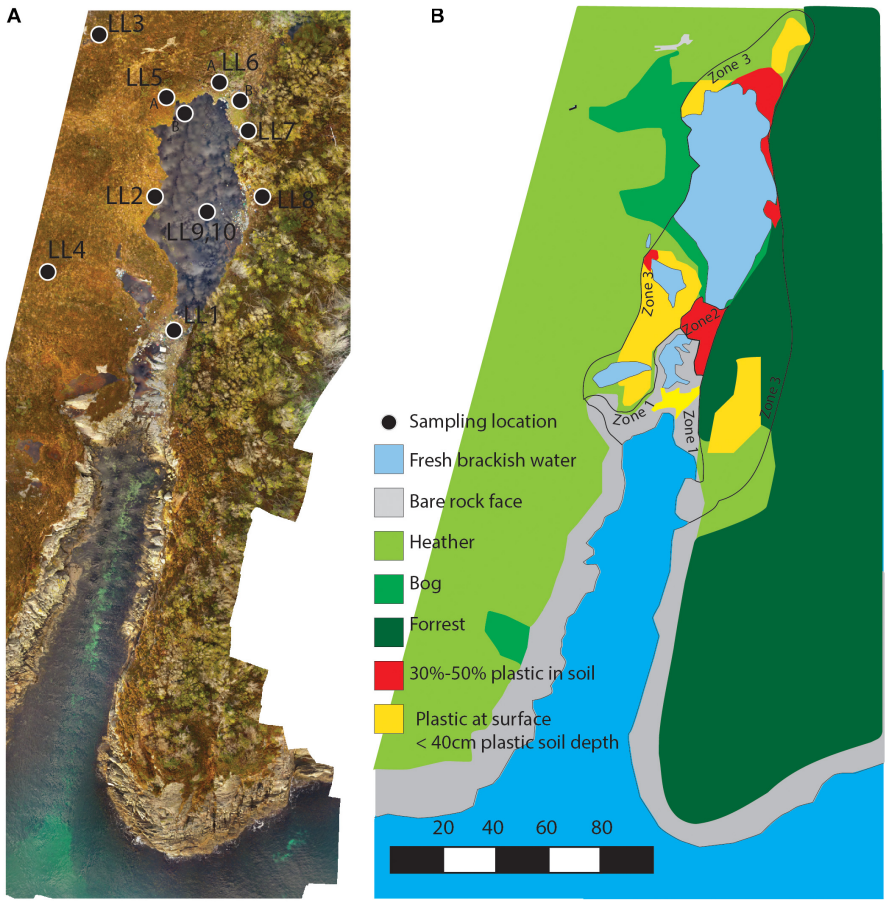

FIGURE 4 | Map showing the plastic pollution in Lisle Lyngøyna and typical vegetation types. **(A)** Drone orthomosaic. **(B)** Map based on field work and image interpretation.

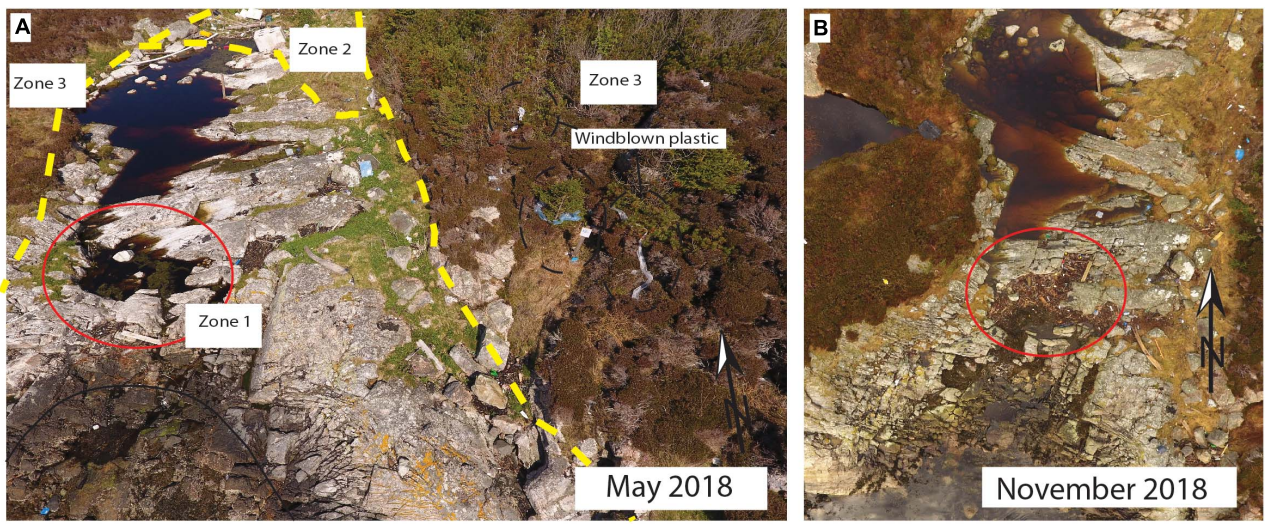

FIGURE 5 | Zone 1 Drone photo of the cove area representative of Zone 1. **(A)** Photo taken in May 2018, note the clear area (red circle) **(B)** drone photo acquired in November (winter) with a substantial increase in deposited waste. No cleaning had been performed in the area.

plastic films (**Figure 2B**). Compared to zone 1, drone images and ground investigations shows that in places more than 50% of the surface are covered by visible plastic (**Figure 2A**). Plastics were also embedded deeper in the soil and fully or partly overgrown by vegetation, thus plastics were in fact covering close to 100% of the surface, although not visible from aerial photos. In places this resulted in a lumpy surface. We documented plants, such as *Hydrocotyle vulgaris, Scutellaria galericulata, Lychnis flos-cuculi*, and more nutrient-demanding species such as *Iris pseudocarus, Galeopsis* sp., and *Argentina anserine.* The soil was between 0.3 to 0.7 m thick down to bedrock. Transects revealed an irregular bedrock topography (**Figure 2C**). The embankment thus smooths out depressions in the landscape. The water level of the pond was at the same level as the embankment. There was no visible outlet/stream from the pond, however channels protruding from the pond extend into the embankment (**Figure 2A**). During excavations of the embankment, the ditches that were dug were filled rapidly with water.

Excavations, soil coring and steel probe profiling showed that the soil from the embankment consisted of three main layers (Soil core LL1, **Figures 2D,E**). The upper 5 cm consisted of organic rich soil intermixed with macro plastic items that were partly buried into the ground. The soil immediately underneath (5–35 cm depth) was composed of dark brown soil with roots and mostly fragmented plastics, small rope pieces and pellets. In this section the soil to plastic ratio was around 80/20. Immediately under this layer was a thick layer of water-saturated, soft mass comprised of large plastic items and organic rich dark brown soil. Litter included fishnets, ropes, plastic bags and packaging, bottles, glass and pieces of wood, as well as smaller fragments of plastic, pellets and expanded polystyrene beads. Characteristic for this layer is the large amount of well-preserved plastic items, such as food packaging from thick plastic film, containers of detergents and personal care products. The packaging design could be recognized on the items, indicating the production-period (**Figure 2F**). Most of the items found had a typical design belonging to the 1970-1990 period. This layer also contained half-burned and melted plastics and some pumice rocks. This layer consisted of a soil to plastic ratio of 30/70. Throughout Zone 2 this layer had thicknesses of 30–70 cm. The base-layer of the embankment consisted of a black soil layer about 10 cm thick, densely packed with roots, driftwood and pumice rocks. This layer rests immediately on the basement rocks. In cores and in samples investigated in field there was no plastic observed in this layer (**Figure 2D**). This may be the original surface layer before the onset of plastic accumulation that formed the embankment.

Lisle Lyngøyna Zone 3

Zone 3 was comprised of areas covered by windblown plastic. The zone included the freshwater pond, its northern shores, the bog surrounding the pond and the hills to the east and west of the pond and bay, where windblown plastic items were found in and among the heather and trees (**Figures 4–6**). The bog in Zone 3 is a nutrient poor type and was dominated by various peat mosses (*Sphagnum sp.*) and *Trichophorum cespitosum, Calluna vulgaris, Erica tetralix, Vaccinum uligonosum, Oxycoccus palustris, Chamaepericlymenum suecicum* and *Potentilla erecta.*

The drone photo in **Figure 6a** illustrates that the distribution of plastic at the surface of the bog in the northern shore varies considerably. From west to east there was a visible increase in surface plastic debris. From 0-5% cover at the western side up to 50–100% cover on the eastern side. The litter was accumulated in shelters/bays/edges facing SW, typically controlled by the prevailing wind directions from the SW (**Figure 6b**). Items were for example 10–50 L industrial containers, fish boxes, pieces and objects of expanded polystyrene, baskets, bottles, and a litterbin with labeling showing that it was of United Kingdom origin (long transported). Larger pieces of plastic were also scattered on the bottom of the pond.

Soil cores (**Figure 6c**) that were retrieved at the shores of the pond revealed a large amount of plastic found deep into the bog at the northern and eastern shores of the pond (LL6 and LL7), whereas there was little to no plastic found in the deep section at the western shore of the pond (LL5 A and B). The organic content of the soil was dominated by peat moss (sphagnum), on average about 40–50 cm thick and resting on a flat bedrock surface (**Figure 6d**). The bedrock surface deepened at the NE part of the pond to a depth of 70–100 cm.

The profiles from soil cores around the lake indicate that plastics are present in the substratum whenever plastic is also present on the surface. Cores retrieved at the western side of the pond, LL5 A and B, were dominated by a thick layer of peat and only 1 small visible plastic fragment was observed in LL5B. With prevailing winds from the W-SW, no plastic litter had accumulated on the western side of the pond but instead accumulated at NE side of the pond. The LL5A core was 50 cm deep from surface to bedrock and consisted of three peat layers, where the upper 20 cm consisted of green sphagnum. The middle part consisted of a lighter green, more large leaved sphagnum. The lower part consisted of a 10 cm dark brown soil with roots of wooden plants (heather). At the bottom, pieces of angular pebble sized rock fragments were found. LL5B was retrieved 1 m from the edge of the pond and 5 m from LL5A. The core was 48 cm deep and included green sphagnum in the upper 10 cm. At 10–30 cm below the surface there was a darker moss-like sphagnum with abundant wooden roots throughout (heather). Presence of such roots indicates that this site may previously have been drier and covered by heather. The lower 10 cm consisted of dark peat.

LL6 and LL7 were both collected near the NE part of the shore (**Figure 6c**) where there was a high amount of plastic on the surface. Sample LL6 (**Figures 6c,d**) was retrieved in an area with mostly smaller plastic particles on the surface. The LL6 core had a 5 cm layer of sphagnum at the top followed by a 15 cm layer of brown moss and heather roots (**Figure 6c**). Plastics in the top 5 cm consisted of small pieces (< 1 cm) including nylon threads, colored hard plastic, clear plastic foil and pellets. A tar lump was observed at 15 cm from the top of core. The subsequent layer was dark brown moss (17 cm to 38 cm in the core) with green sphagnum and no plastic. The bottom 10 cm layer consisted of dark soil without plastic.

The sampling site LL7 was at the deepest part of the bog where there was a depression in the bedrock, and the core sampled was 60 cm deep. Plastic was found in the upper 50 cm in a

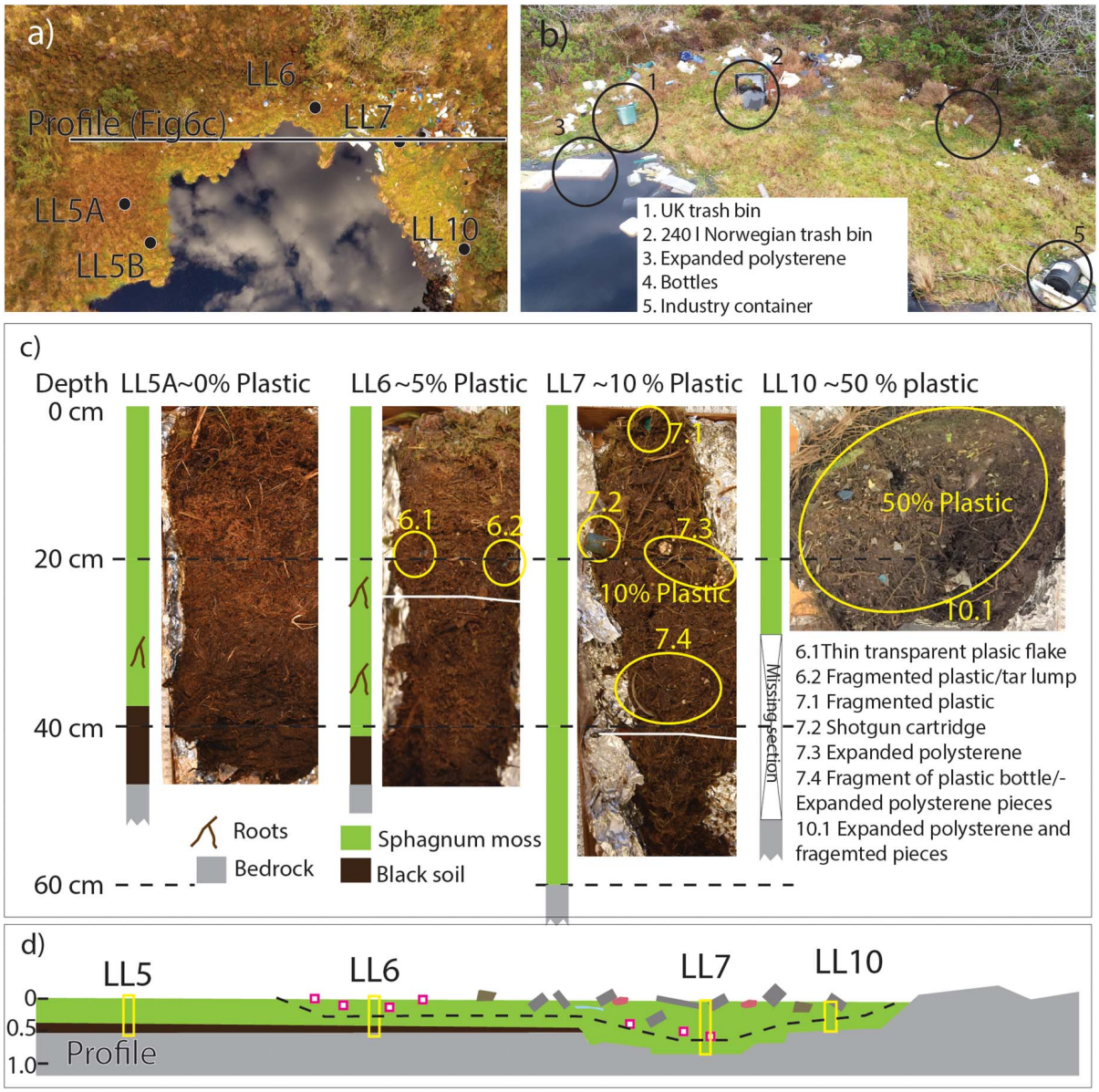

FIGURE 6 | Samples and field work in northern part of pond Zone 3. **(a)** Drone photo of a bog in the northern part of the pond. Note decreasing amount of surface litter from east to west (the image is oriented NNW-SSE), subsurface soil core sample sites and profile (**c** and **d**) are denoted. **(b)** Close up drone photo of the NE part of pond displaying the high amount of litter observed on surface. **(c)** Cores LL5, LL6, LL7 and LL10. Samples display clearly how plastic is incorporated into the soil. **(d)** Profile based on the soil profiles and steel probe measurement.

matrix of large-leaved moss with a well-preserved green color. The deeper layers of moss had no visible plastics. The base layer consisted of a 10 cm thick layer of dark soil with the presence of pumice rocks.

In the samples from LL10 (**Figures 6c,d**) on the eastern shore, plastic was observed in the entire core, except for a gravel layer at the base. The gravel was not possible to retrieve for lab inspection. Several other shorter cores in the surrounding 5–10 m radius had top layers containing plastic embedded in the moss, and lower layers without plastic. However, it was difficult to retrieve the cores from the bog due to the water content, depth and abundant plastic litter. Most of these cores included plastic down to 30–40 cm depth and had an underlying layer of black soil or gravel with pumice rocks. Large macroplastic items were found down to 40 cm depths at several places.

The Pond in Zone 3

The prevailing south westerly winds have over time caused aggregates of plastic in the inner northwestern part and at the western side of the pond (**Figures 6**, **7**). On the pond surface, plastics were concentrated at the eastern and northern bank, whereas on the western and northwestern bank, no plastic

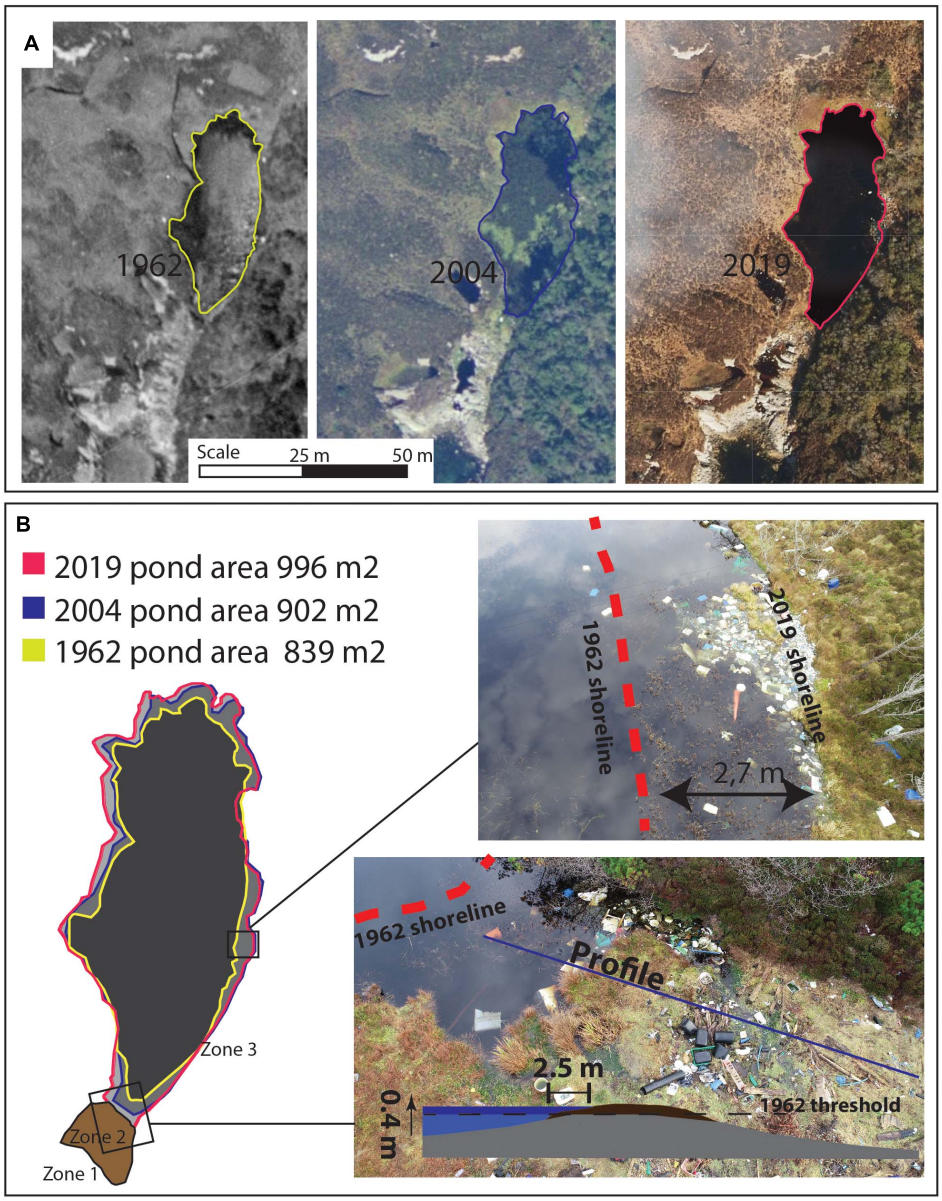

FIGURE 7 | (A) Comparing landscape features from historical images from 1962 and 2004 to current situation in 2019. **(B)** Shoreline comparison shows a pond increase from 1962 to today. The increase is observed as 2–3 meter horizontal extension? along the eastern and northern shores. At western shores the horizontal increase is less due to steep shore gradient. In Zone 2 where the pond is dammed by the embankment, shoreline has moved toward pond, indicating that the embankment has increased in size since 1962.

was seen on the surface. A gradual increase in surface plastic concentration was observed toward the east, where plastics were gradually entangled and incorporated into the macrophytes and peat moss, fully or in part covering the floating items (**Figure 7B**). These "Green Plastic islands" behave as buoyant floats of vegetation and plastic, and are clearly not attached to the ground, but are thick and were in some cases stable enough to carry an adult human.

The bottom sediments of the pond consisted of mineral clay and coarse sand, probably a result of surface weathering and marine deposits (sample LL9, **Table 1**). No plastic fragments could be observed, and no large plastic items were caught in the grab. The sediment layer was thin and was not sampled for further core description. Divers observed large pieces of well-preserved plastic sheets and tarpaulins on the bottom of the pond, mainly in areas of macrophytic vegetation that trapped the plastic among the stems. The species recorded in the pond included: *Menyanthes trifoliata, Comarum palustre, Sparganium angustifolium, Hipporus vulgaris, Juncus articulatis, Nymphaea alba,* and *Myriophyllum alterniflorum*. Most of these species grow in nutrient poor lakes, but the latter two also grow under nutrient-rich conditions.

Evidence of Landscape Changes

At Lisle Lyngøyna, aerial images show plastic debris on the island dating back to 2004. The comparison of pond size and outline on imagery from 1962 with later imagery (2004 and 2019) showed a change in pond shape and size from 1962 to 2004 and 2019 (**Figure 7A**). The 1962 image is black and white, which challenge the discriminations between vegetated areas, bedrocks and reflection from the sun. The resolution is too low to identify marine litter/debris from 1962 (which normally would be mainly driftwood). The shoreline of the pond was however clearly detectable in the images, facilitating a detailed interpretation. These images also indicated that a substantial part of the soil/peat was extracted at the location north of the pond, this is seen as sharp cuttings in the landscape (see **Figure 7A**). In the 2004 and 2019 images it is possible to observe plastic in the images, even though it is vague in the 2004 images due to the resolution. The shoreline trace of the three images shows an increase in pond size from 1962 to 2004 and 2019. The increase is largest at the flat bogs at the north and eastern shores showing a move of the shoreline by 2.5–3 meters (**Figure 7B**). There is also an apparent change in Zone 2 from 1962 to modern time. Although the image quality in the 1962 images is not sufficient to conclude, there seems to be a barren rock surface where the storm deposit (Zone 2) is placed today.

Case 2 - Kolavika Bay

Kolavika Zone 1

The gravel and pebble beach (1–10 cm pebble diameter) in Kolavika made up Zone 1 (**Figures 8**, **9**). It was dominated by a belt of fresh seaweed at the high tide mark. The seaweed was mixed with plastic items of recent date, such as plastic tobacco (snus) containers, ropes, lids, plastic films, corks and smaller items, such as packaging film. As is typical for Zone 1, the sediment is mobile and shifts from season to season similar to what was observed in Lisle Lyngøyna.

Kolavika Zone 2

This zone was made up of a 0.5 m high (on average), 48 m long and 2 to 8 m wide embankment consisting of large quantities of plastic, soil and driftwood that lined the entire width of the bay (**Figures 8**, **9**). The embankment was terrace shaped with a flat top and steeper (20°) slope down toward

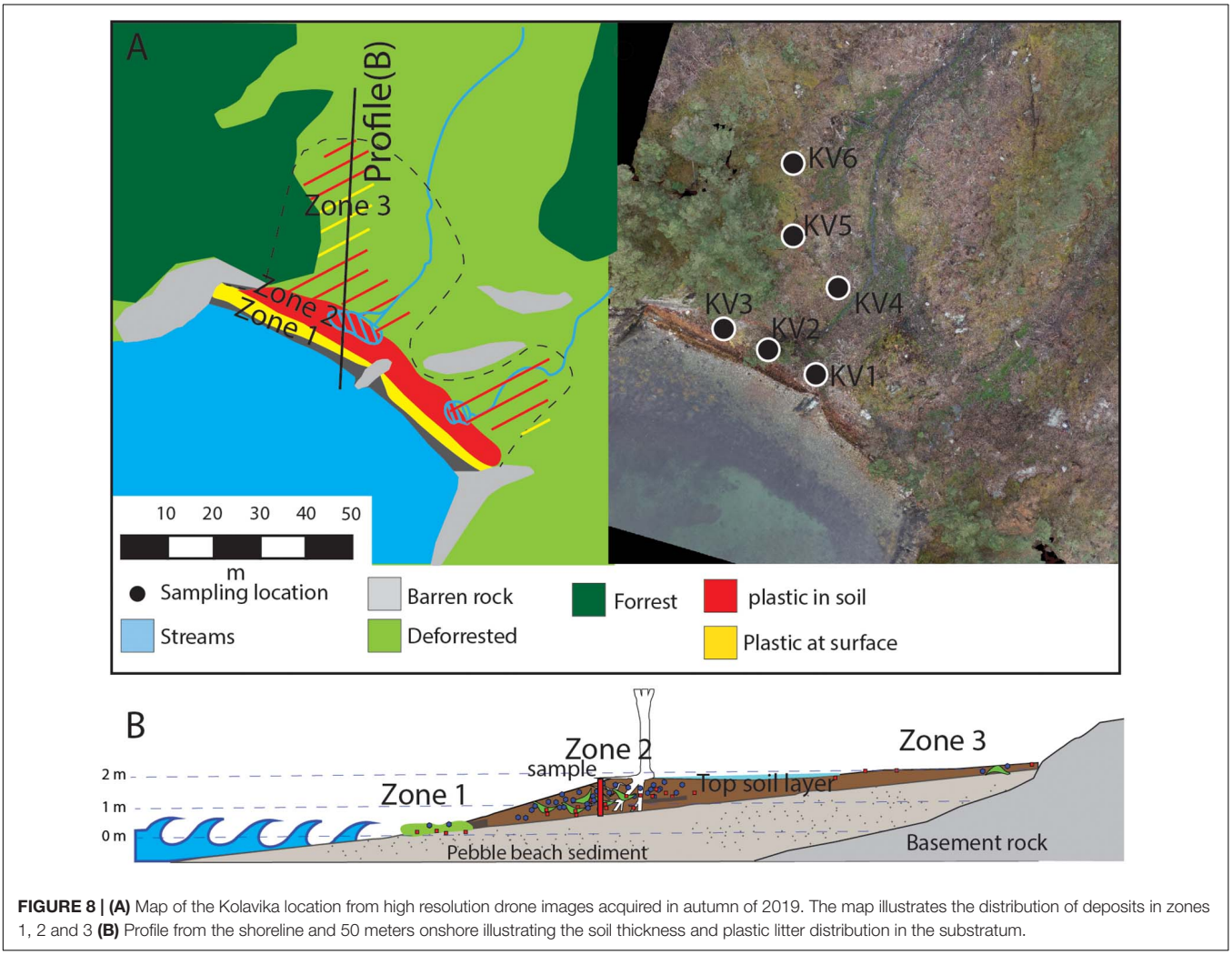

FIGURE 8 | (A) Map of the Kolavika location from high resolution drone images acquired in autumn of 2019. The map illustrates the distribution of deposits in zones 1, 2 and 3 **(B)** Profile from the shoreline and 50 meters onshore illustrating the soil thickness and plastic litter distribution in the substratum.

FIGURE 9 | (A) Field photo of pebble beach and Zone 1 and Zone 2 deposits at Kolavika location. **(B)** profile section (sample KV 2), **(C)** typical well-preserved items found in the storm embankment (Zone 2), **(D)** Sketch displaying the soil in Zone 2 with an ash tree growing in the plastic polluted soil.

the sea. The upper layer was comprised of organic matter with a 5 cm layer of sand and clay, mixed with pieces of bark on top. The sediment composition of this layer was similar to the composition of sediments in the stream, which indicates that it was deposited by the stream during a recent flood event. The middle layer consisted of soil rich in roots, driftwood, beach pebbles (rip-up clasts) and plastic fragments. Plastic was present down to 90 cm depth in the embankment. We estimated that the storm embankment consisted of 50/50 soil to plastic ratio by volume. The pieces of plastic were often well preserved and could be recognized in terms of purpose of use, labels and prints (**Figure 9B**). In the bottom layer at 40-60 cm below the surface, there were brittle, but well-preserved plastic toys with a typical 1960's design (**Figure 9C**), plastic perfume containers, bottles for liquid dishwashing detergent and candy wrappings with a 1960-1970 design.

The vegetation was dominated by a group of young European ash trees (*Fraxinus excelsior*) (**Figure 9A**), a few specimens of *Alnus glutinosa* in the eastern part and *Plantago lanceolata*, *Lotus corniculatus, Rubus nemoralis* and *Geranium robertianum* in the field layer. The moister parts of the upper, flat embankment were dominated by *Juncus bufonius, Cardamine amara* and *Triglochin maritima.*

The ash trees grew in the plastic soil, with roots surrounding and penetrating plastic fragments. The tree diameter at breast height varied between 17 and 57 cm. Based on tree ring counts, many were under 20 years old and one was 55 years old. These observations indicate that the trees started growing in the plastic infused substrate after the onset of plastic accumulation.

Kolavika, Zone 3

Zone 3 in Kolavika started behind the storm embankment (Zone 2) and extended inland toward the NE to about 60 m from the high tide mark (**Figure 8**). In general, a 30-50 cm thick layer of soil covered a base layer of beach pebbles. The post glacial rebound after the last ice age caused the beach zone to have gradually been uplifted. The shoreline has consequently moved gradually toward the SW, and beach sediments can therefore be found under the soil some distance from the present shoreline. The map in **Figure 8** (dashed black line) illustrates where we can

assume to find beach sediments under the soil layer, based on the assumption that areas with a consistent 5–6° slope gradient are remnant beaches. Zone 3 consisted mainly of a recently clear-cut area. It was dominated by different species of herbs and moss, such as *Veronica officinalis, Mercurialis perennis, Hylocomium splendens* and *Pleurozium schreberi* on the drier parts and *Juncus bufonius*, *Cardamine amara* and *Triglochin maritima* on the moister parts and along the stream. Pieces of plastic were scattered on the surface in Zone 3. Soil samples (sample KL 5 and 6) contained about 90/10 soil plastic ratio. Plastic was also found at a land-tongue of about 35 m in length and 20 meter in width in a NE direction. The soil profile in Zone 3, 25 m from the high tide mark indicated that the upper 10 cm mostly consisted of organic matter and included also clear and colored plastic flakes from plastic bags, and expanded polystyrene beads, all of which could easily be windblown to this position. Fragmented hard plastics were also observed and could stem from larger pieces that could be windblown, and later break up or degrade into smaller pieces. Below this upper vegetated layer pieces of plastic were found within the thin soil down to 20 cm above the base layer of pebbles and gravel.

TABLE 3 | Quantification of landscape changes at the two case studies.

Changes in landscape	Lisle Lyngøyna	Kolavika
Bay shape	Narrow rocky cove, open sea setting, high wave wind energy	Straight pepple beach in an open cove, moderate wind and wave
Width of bay	10 m	50 m (beach width) 150 m (bay width)
Volume of plastic debris	100–125 m3	50–75 m3
Estimated thickness incease in storm embankment	0,7 m	0,5 m
Change in water level/damming	Damming of Pond - 40cm increase	Damming of streams forming wetland
Soil-plastic ratio/area of zone		
Zonel	90/10 465 m^2	90/10 150 m^2
Zone 2	50/50 100 m^2	50/50 100 m^2
Zone 3	90/10 to 50/50 2000 m^2	90/10 to 50/50 1350 m^2

DISCUSSION

The sites described in this paper include two accumulation sites for marine debris that have not been cleaned for several decades. A general mapping of parts of the Norwegian archipelago (Bastesen et al., 2020) indicates that such sites are common along the outer archipelago, and likely all along the Norwegian coastline where conditions are favorable for accumulation of debris. Similar observations are also reported elsewhere in the world (Merrell, 1980; Andrady, 2003), and likely share some common features. To our knowledge no other studies have investigated the potential long-term effect of plastic accumulation on the development of the coastal landscape, soil and vegetation, and the corresponding consequences for coastal ecosystems.

Signs of Landscape Changes Due to Plastic Accumulation

Table 3 summarizes the quantifiable landscape changes observed at the two localities based on estimation from the field work and from 3D model interpretation. Accumulation of plastic soil is evident at both study sites. The accumulation has had a profound impact on the surrounding soil generation, vegetation and landscape, although with somewhat different consequences for the landscape development at the two sites. At Lisle Lyngøyna the historical images show that the pond increased in size, which may coincide with the increased accumulation of plastic in the storm embankment (Zone 2). At Kolavika, increased plastic pollution caused the formation of an oversized drift embankment. We estimated an increase in soil volume of 100–125 m^3 at Lisle Lyngøyna and about 75 m^3 at Kolavika (**Table 3**). Both places can be described as typical hot spots where ocean current, wind and landscape shapes are favorable for accumulation of marine debris.

Landscape Changes in Lisle Lyngøyna

Based on the observations, a two staged evolutionary model of the landscape changes at Lisle Lyngøyna can be sketched (**Figure 10**).

Stage 1 before1960: the landscape was managed heathland (Fremstad et al., 1991). Peat was extracted from the northern shores of the pond leaving a thin soil layer above the bedrock. The pond level was below the flat bedrock surface leaving this area mostly dry. The storm embankment at the cove (Zone 2) consisted of driftwood and other organic materials. The deposit level was about 5–10 cm thick and was kept stable by a balance between deposition through storms, erosion and biodegradation. Furthermore, driftwood may also have been harvested by local farmers for firewood, reducing the amount of accumulation.

Stage 2 1960 to the present: A visible growth of the storm embankment took place, and our hypothesis is that this was due to an increasing proportion of plastic waste in the marine debris. Plastic waste accumulated in the storm embankment, in the pond, and at the shores of the pond. The plastic within the embankment was not subjected to extensive fragmentation or degradation and protected the organic material from erosion. Consequently, there was an escalating growth of the storm embankment. Deposition of plastic debris on high grounds took place during major storms. An increased height of the embankment caused an elevation of the threshold at the outlet of the pond and consequently the pond level rose.

The cores and profiles at the northern shore (LL5, LL6, LL7, **Figure 6**) of the pond showed that plastic is entangled into the vegetation down to 40 cm below the surface. These plastic fragments were found below the present pond water level (down to 40 cm). Some items, such as pellets and tar were found at 20–30 cm depth (**Figure 6**), these materials that are buoyant and compact are less likely to be deposited by wind and more likely deposited by water. Hence, the material must have been deposited at the water surface of the pond. Since it is now present 20-30 cm

below surface it indicates that the water level has risen gradually during the period with accumulation of plastic. The assumed bare land north of the pond was gradually flooded and overgrown with peat moss (**Figures 7**, **10**). The increased area of the pond is opposite to a natural succession where ponds grow in with vegetation and over time develop into bogs and finally forest.

The lack of aerial images from 1970 until 2000 makes some uncertainties to the model, however observation of items in the soil profile with the deepest items dating back to the 1970's, support the idea that soil has been formed at least from this time onward.

Landscape Changes in Kolavika

In Kolavika, the storm embankment consists of plastic, soil and vegetation, and has formed a semi-impermeable plastic filled barrier for the small streams running through the area toward the sea. Although the streams percolated in part through the pebbles at the base of the embankment, the area behind the embankment was still saturated with water. This area experiences heavy rains throughout all seasons, and poor drainage will therefore easily lead to an increased water saturation. Plastic is causing an increased barrier to ground water flow.

Soil Formation/Microhabitats

Observations of the deposits in the two locations also support the impression that plastic debris increases soil formation by forming a scaffold that binds the organic material and protects the decomposing seaweed from being washed away during the subsequent winter storms. The plastic will also prevent evaporation and retain moisture in the soil and reduce the exchange of gases through impermeable layers of plastic. Together this may alter or change soil formation and soil properties compared to plastic free conditions.

At Lisle Lyngøyna the soil layer is thicker in areas with plastic than in areas without plastic. Moreover, the organic rich and humid plastic soil may provide a favorable microhabitat for some plants. Experiments have shown that microplastic alters the structure and biophysical properties of soils with various effects on plant growth, e.g., biomass above and below ground, and changed growth (Boots et al., 2019; Rillig et al., 2019; Rillig and Lehmann, 2020). Changing growth conditions in plastic polluted soils can lead to change in competition among plant species and eventually in their composition (Lozano and Rillig, 2020). In the vicinity of the Lisle Lyngøyna storm embankment, we found some nutrient demanding species in an otherwise nutrient poor environment (**Figure 2**). However, we cannot exclude that their presence is due to natural nutrient rich conditions caused by the accumulation of seaweeds in this zone. In Kolavika, a similar build-up of a plastic-soil embankment seems to be the main reason that ash trees have managed to establish in an environment that otherwise would have been unstable (**Figure 9**). The group of ash trees growing on the storm embankments are evidently all younger than 55 years, indicating that the trees started growing in the plastic infused substrate after the onset of plastic accumulation. In this case plastic contamination can have facilitated growth of trees that normally would not have survived due to lack of soil for nutrients and root attachment. In other words, seedlings and saplings growing in a more permeable embankment on the pebble beach would be vulnerable to droughts and erosion. We hypothesize that the plastic accumulation has created sufficient stable, humid soil masses and protective shelter for seeds to germinate and permanently establish in the storm embankment.

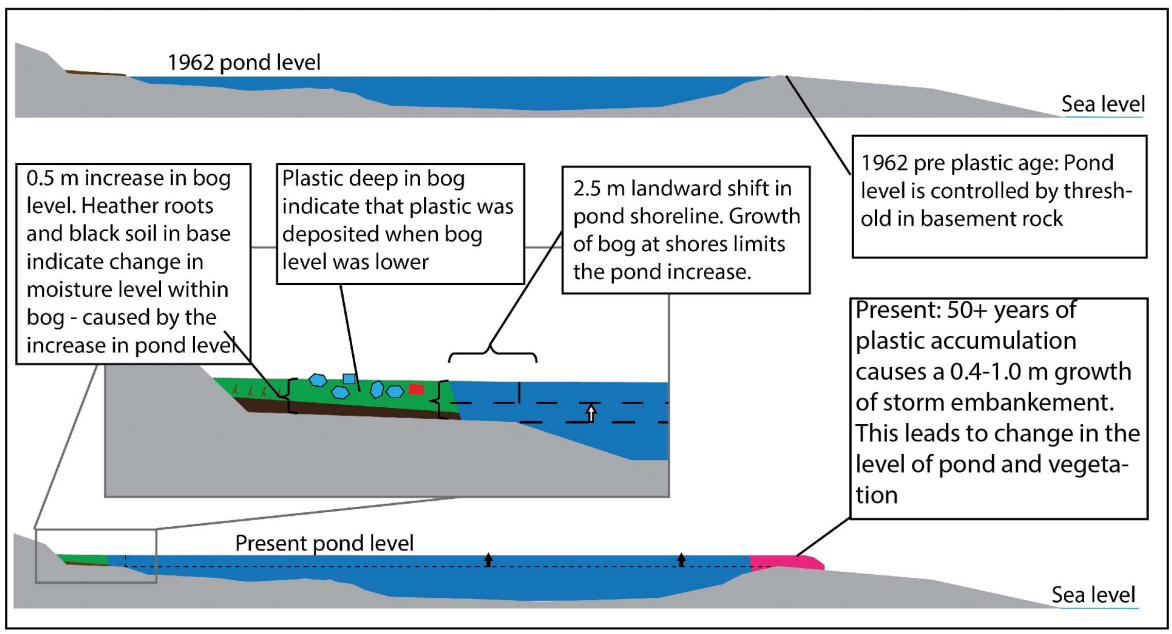

FIGURE 10 | Model displaying the evolution of the Lisle Lyngøyna from the onset of plastic in the 1960s. See insets and text for explanation.

Trends of waste in the soil profiles may reflect the amounts of plastic and the historical development of plastic use and waste generation. Investigation of the plastic layers may reveal sources, as well as consumer patterns from the time of accumulation. In this study we have tried to keep the location untouched and we have therefore not removed enough to conclude if there is a stratigraphic deposition following the principles of the law of superposition. This law states that within a sequence of sediments the oldest layer is at the base and the layers are progressively younger upward in the sequence. At the storm embankments a base layer pre-dates the plastic deposit should be found in the base and gradually younger plastic pieces should be found upward. Some trends can however be observed. At Lisle Lyngøyna as well as in Kolavika, base layer of the storm deposit (zone 2) seems to be plastic free, marine debris is wooden pieces and pumice fragments. The latter would be the most persistent to degradation. Volcanic pumice from nearby sources (Iceland) is however Holocene age (older than 4000 years), pumice fragments of this age is found scattered along the entire north Atlantic (Newton, 2000; Larsen et al., 2014). It will therefore be of great importance to geochemically compare the pumice found in and below the plastic deposits, are these pumices redeposited Holocene pumices or do they represent modern pumice from a far distance source for instance the South Sandwich Island eruption in 1962 (Risso et al., 2002)? Other similarities were the common debris from the fishing and boat industry are represented by ropes, fish nets, containers, aquaculture feed-tubes and fish crates. The plastic industry is also represented, as plastic resin pellets are commonly observed in all soil layers.

Physical fragmentation of the plastic litter is a severe problem for the environment as this process generates microplastic and such sites could therefore be considered sources of microplastic (Thompson et al., 2004; Barnes et al., 2009). In some areas of the field sites fragmented plastic is quite common, typically in Zone 3 (sample LL7 **Figure 6**). After deposition, the plastic will be exposed to UV-light and frost degradation at the surface, that speeds up the degradation rate (Andrady et al., 2003). Some items will be degraded quickly into smaller fragments, especially thinner plastic items, such as plastic from bags or foil. In Zone 2 a substantial part of the plastic observed in the soil was nevertheless well preserved (**Figures 2**, **9**). For example, the mid layer down to 60 cm in the soil in the storm deposit at Lisle Lyngøyna and Kolavika was composed of well-preserved plastic pieces from the 1970s and 1980s (**Figures 2**, **9**). The good preservation could be due to the polymer types used in plastic materials in the 1970's and 1980's, or that the thicker plastic we find is more resilient to weathering in the low intensity sunlight of Norway, while the thinner plastics from the same time may already have fragmented. The fast accumulation and burial in these zones may also protect these plastic items from further physical degradation processes.

Man-Made Landscape Changes and Restoration

It is important to consider the changes that have occurred over the last decades in the coastal cultural landscape and how humans use the coast. The coastal areas have been cultivated and populated for centuries, and the resources offered by the areas were valuable for the coastal population. It was common to exploit driftwood for firewood and seaweed for fertilizer or food for livestock. Peat was cut from bogs and burned for heating (see example from Lisle Lyngøyna in **Figure 7**). We can assume that Lisle Lyngøyna, Kolavika and many other wreck bays were cleaned regularly to exploit these resources. This may have influenced the way the storm deposits evolved, as some bays may have been cleared annually for most loose material. After 1960 modernization caused a change in the way people lived and these resources from the sea were left behind and allowed to accumulate or degrade.

Cleaning operations are rarely complete when it comes to the plastic buried in the soil after decades of accumulation as it would require intensive efforts and resource. So far, we lack knowledge about the effects of the plastic as well as from disturbances caused by cleaning operations. Removing all the plastic soil to restore the landscape to its "natural" state may potentially cause more damage to the aquatic life in the pond, the vegetation and inhabitants at the plastic contaminated sites, and cause more immediate harm than if we were to leave it and perform regular clean-ups to gradually remove emerging debris and allow the changes to take place slowly. In cases when the plastic has negligible impact on the ecosystem, we can remove visible debris on the surface and restore recreational value for humans. However, we should not automatically assume that the plastic in the soil profile is of pressing concern to conservation of ecological integrity. Decisions on abatement measures that are not knowledge-based can lead to a waste of conservation resources and in the worst case be harmful for the ecosystem, e.g., by remobilization of buried contaminants or by disturbing the ecosystem.

CONCLUSION

We have made the following observations that support the hypotheses of landscape changes due to plastic accumulation:

(1) Plastic accumulation accelerates the formation of a thick storm embankment by acting as a scaffolding for organic deposits. This observation is supported by transects in the deposition zone showing a 5–10 cm bottom layer of compact and plastic-free soil with dense roots under a 40–70 cm layer of organic rich and wet soil mixed with plastic items. The soil and plastic items are distributed throughout the soil, indicating that the soil was generated alongside the accumulation of plastic.
(2) Aerial photos of Lisle Lyngøyna, indicate that the pond has increased in size from 1960 to 2015, as opposed to the natural succession where ponds grow in with vegetation and over time develop into bogs and finally forest over time. This suggests that plastic deposits and newly generated plastic-rich soil can form dams and prevent natural drainage of near shore wetlands and ponds.
(3) Our observation indicates that plastic accumulation caused changes in the vegetation. This is supported by the soil

profiles around the ponds and bogs including a base layer with peat moss and heather overlain by a layer of peat moss with incorporation of plastic fragments. This finding indicates that the wet conditions leading to growth of peat moss instead of heather co-occurred with the deposition of plastic fragments. In support of this, we also see that plastic fragments float in the pond before they are trapped and deposited in the vegetation around the pond. The current bog vegetation grows around the plastic fragments, and over time, peat soil will overlay the plastic.

The observed accumulation and distribution patterns of marine plastic debris and long-term changes to the structure of soils, and the associated morphological development/changes of the landscape should not be assumed to occur only along the Norwegian coastline. This is likely a global phenomenon. Wherever there is debris, tidal movement, wind and a potential for accumulation it is likely that similar processes occur, potentially leading to large changes to costal ecosystems around the globe. The remedy is, first and foremost, to prevent and mitigate plastic waste accumulation by better waste management systems and frequent beach cleans. Such measures are likely far more realistic and desirable than the complete cessation of the use and release of plastic, although it is an enormous cleaning job that will go on for decades, long after the input of plastic to the ocean has stopped. Simply exchanging non-biodegradable plastic with biodegradable polymers is not recommended by the recent SAPEA report (Science Advice for Policy by European Academies (SAPEA), 2020) due to risk of continuation of the waste problem. However, biodegradable plastics may be a solution for some applications with high risk of loss to the open environment and where it is difficult or expensive to remove it from the environment. Sound application of biodegradable plastics designed for industrial composting is dependent on a working waste management system, in the same manner as conventional plastics.

Our results support that we have entered the Anthropocene/Plastocene period whereupon layers of mismanaged plastic debris is influencing the landscape, the vegetation and geological processes and one day will be evident in sedimentary records of the future.

DATA AVAILABILITY STATEMENT

The original contributions presented in the study are included in the article/supplementary material, further inquiries can be directed to the corresponding author/s.

AUTHOR CONTRIBUTIONS

EB did the idea and project leader and field work and manuscript writing. MH did the field work and initiative to the study. GA did the field work on bothanics. GV did the Field work biology and lake and contributed with ideas. GB did the field work biology. CK did the field work. All authors contributed to the article and approved the submitted version.

ACKNOWLEDGMENTS

Special thanks to Rune Gaasø (Clean Shores Global) and Kenneth Bruvik (Norwegian Hunter- and Anglers' Association) for making us aware of the plastic accumulation at Lisle Lyngøyna and for their engagement in developing the Lisle Lyngøyna project into a scientific study. Cato Lyngøy, representative of the landowners, is thanked for letting us work at the location and for providing valuable historical input. Sveinung Toppe and Gudrun Fatland from Bergen Recreational Council (Bergen Omland Friluftsråd) for financial support, aiding in boat transport to the Kolavika bay and for fruitful discussions regarding plastic accumulation in western Norway. The Retailers' Environment Fund (Handelens Miljøfond) for supporting the project "Plastrent Tysnes." Bergen and Øygarden municipalities for financing several small projects regarding plastic mapping leading up to this project. Christoph Postler, Benjamin Dolva, Tobias Kurz, and Simon Buckley are thanked for photogrammetric work and drone image collection. Jan Tveranger is thanked for providing knowledge and discussion around coastal sedimentary systems. Emily Lyng is thanked for proofreading and language correction. Two reviewers are thanked for comments and suggestions that significantly improved the manuscript.

REFERENCES

Andrady, A. L. (ed.). (2003). *Plastics and the Environment*. Hoboken, NJ: John Wiley & Sons.

Andrady, A. L., Hamid, H. S., and Torikai, A. (2003). Effects of climate change and UV-B on materials. *Photochem. Photobiol. Sci*. 2, 68–72.

Barnes, D. K., Galgani, F., Thompson, R. C., and Barlaz, M. (2009). Accumulation and fragmentation of plastic debris in global environments. *Philos. Trans. R. Soc. Lond. B Biol. Sci*. 364, 1985–1998. doi: 10.1098/rstb.2008.0205

Bastesen, E., Haave, M., Avlesen, H., and Neby, S. (2020). *Utvikling av Kartleggingsmetoder og Estimat for Oppryddingskostnader for Makroplast i Strandsonen.* NORCE Report nr 4, (Bergen, BC: NORCE Research), doi: 10.1098/rstb.2008.0205

Boots, B., Russell, C. W., and Green, D. S. (2019). Effects of microplastics in soil ecosystems: above and below ground. *Environ. Sci. Technol*. 53, 11496–11506. doi: 10.1021/acs.est.9b03304

Borrelle, S. B., Ringma, J., Law, K. L., Monnahan, C. C., Lebreton, L., McGivern, A., et al., (2020). Predicted growth in plastic waste exceeds efforts to mitigate plastic pollution. *Science* 369, 1515–1518. doi: 10.1126/science.aba3656

Buckley, S. J., Ringdal, K., Naumann, N., Dolva, B., Kurz, T. H., Howell, J. A., et al., (2019). LIME: software for 3-D visualization, interpretation, and communication of virtual geoscience models. *Geosphere* 15, 222–235. doi: 10.1130/ges02002.1

Carlsen, T., and Bär, A. (2016). *Skjøtselsplan for beiteområde for beiteområde på Bliksvær i Bodø kommune, Nordland*. Nord-Trøndelag: NIBIO.

Cózar, A., Martí, E., Duarte, C. M., García-de-Lomas, J., Van Sebille, E., Ballatore, T. J., et al., (2017). The Arctic Ocean as a dead end for floating plastics in the North Atlantic branch of the Thermohaline circulation. *Sci. Adv*. 3:e1600582. doi: 10.1126/sciadv.1600582

Eriksson, C., Burton, H., Fitch, S., Schulz, M., and van den Hoff, J. (2013). Daily accumulation rates of marine debris on sub-Antarctic island beaches. *Mar. Pollut. Bull*. 66, 199–208. doi: 10.1016/j.marpolbul.2012.08.026

Fremstad, E., Aarrestad, P. A., and Skogen, A. (1991). *Kystlynghei på Vestlandet og i Trøndelag: Naturtype og Vegetasjon i Fare*, Vol. 029. Trondheim: Norsk institutt for naturforskning.

Haarr, M. L., Westerveld, L., Fabres, J., Iversen, K. R., and Busch, K. E. T. (2019). A novel GIS-based tool for predicting coastal litter accumulation and optimising coastal cleanup actions. *Mar. Pollut. Bull.* 139, 117–126. doi: 10.1016/j.marpolbul.2018.12.025

Heyerdahl, T. (1971). Atlantic Ocean pollution and biota observed by the "Ra" expeditions. *Biol. Conserv.* 3, 164–167. doi: 10.1016/0006-3207(71)90158-3

Hjelle, K. L., Halvorsen, L. S., and Overland, A. (2010). Heathland development and relationship between humans and environment along the coast of western Norway through time. *Quat. Int.* 220, 133–146. doi: 10.1016/j.quaint.2009.09.023

Ivar, D. S. J., Spengler, Â, and Costa, M. F. (2009). Here, there and everywhere. small plastic fragments and pellets on beaches of Fernando de Noronha (equatorial western Atlantic). *Mar. Pollut. Bull.* 58:1236. doi: 10.1016/j.marpolbul.2009.05.004

Jambeck, J. R., Geyer, R., Wilcox, C., Siegler, T. R., Perryman, M., Andrady, A., et al., (2015). Marine pollution. plastic waste inputs from land into the ocean. *Science* 347, 768–771. doi: 10.1126/science.1260352

Kartar, S., Milne, R. A., and Sainsbury, M. (1973). Polystyrene waste in the Severn Estuary. *Mar. Pollut. Bull.* 4:144. doi: 10.1016/0025-326x(73)90010-6

Laist, D. W. (1987). Overview of the biological effects of lost and discarded plastic debris in the marine environment. *Mar. Pollut. Bull.* 18, 319–326. doi: 10.1016/s0025-326x(87)80019-x

Larsen, G., Eiríksson, J., and Gudmundsdóttir, E. R. (2014). Last millennium dispersal of air-fall tephra and ocean-rafted pumice towards the north Icelandic shelf and the Nordic seas. *Geol. Soc. Lond. Spec. Publ.* 398, 113–140. doi: 10.1144/sp398.4

Lebreton, L. C. M., van der Zwet, J., Damsteeg, J. W., Slat, B., Andrady, A., and Reisser, J. (2017). River plastic emissions to the world's oceans. *Nat. Commun.* 8:15611.

Lozano, Y. M., and Rillig, M. C. (2020). Effects of microplastic fibers and drought on plant communities. *Environ. Sci. Technol.* 54, 6166–6173. doi: 10.1021/acs.est.0c01051

Mangerud, J., Gyllencreutz, R., Lohne, Ø, and Svendsen, J. I. (2011). "Glacial history of Norway. *Dev. Quat. Sci.* 15, 279–298.

Merrell, T. R. Jr. (1980). Accumulation of plastic litter on beaches of Amchitka Island. *Alaska Mar. Environ. Res.* 3, 171–184. doi: 10.1016/0141-1136(80)90025-2

Napper, I. E., and Thompson, R. C. (2020). Plastic debris in the marine environment: history and future challenges. *Glob. Chall.* 4:1900081. doi: 10.1002/gch2.201900081

Newton, A. (2000). *Ocean-Transported Pumice in the North Atlantic*. Doctoral dissertation, University of Edinburgh, Edinburgh.

OSPAR (2007). *OSPAR Pilot Project on Monitoring Marine Beach Litter – Monitoring of Marine Litter in the OSPAR Region. OSPAR Commission (2007)*. London: OSPAR

Pham, C. K., Ramirez-Llodra, E., Alt, C. H. S., Amaro, T., Bergmann, M., Canals, M., et al., (2014). Marine litter distribution and density in European Seas, from the shelves to deep basins. *PLoS One* 9:e95839. doi: 10.1371/journal.pone.0095839

Rillig, M. C., and Lehmann, A. (2020). Microplastic in terrestrial ecosystems. *Science* 368, 1430–1431. doi: 10.1126/science.abb5979

Rillig, M. C., Lehmann, A., de Souza Machado, A. A., and Yang, G. (2019). Microplastic effects on plants. *New Phytol.* 223, 1066–1070. doi: 10.1111/nph.15794

Risso, C., Scasso, R. A., and Aparicio, A. (2002). Presence of large pumice blocks on Tierra del Fuego and South Shetland Islands shorelines, from 1962 South Sandwich Islands eruption. *Mar. Geol.* 186, 413–422. doi: 10.1016/s0025-3227(02)00190-1

Science Advice for Policy by European Academies (SAPEA) (2020). *Biodegradability of Plastics in the Open Environment*. Berlin: SAPEA. doi: 10.26356/biodegradabilityplastics

Storlazzi, C. D., and Field, M. E. (2000). Sediment distribution and transport along a rocky, embayed coast: Monterey Peninsula and Carmel Bay. *Calif. Mar. Geol.* 170, 289–316. doi: 10.1016/s0025-3227(00)00100-6

Thiel, M., Hinojosa, I. A., Joschko, T., and Gutow, L. (2011). Spatio-temporal distribution of floating objects in the German Bight (North Sea). *J. Sea Res.* 65, 368–379. doi: 10.1016/j.seares.2011.03.002

Thompson, R. C., Olsen, Y., Mitchell, R. P., Davis, A., Rowland, S. J., John, A. W., et al., (2004). Lost at sea: where is all the plastic? *Science* 304:838. doi: 10.1126/science.1094559

Thompson, R. C., Swan, S. H., Moore, C. J., and Vom Saal, F. S. (2009). Our plastic age. *Philos. Trans. R. Soc. Lond. B Biol. Sci.* 364, 1973–1976. doi: 10.1098/rstb.2009.0054

Trenhaile, A. (2016). Rocky coasts—their role as depositional environments. *Earth Sci. Rev.* 159, 1–13.

Westoby, M. J., Brasington, J., Glasser, N. F., Hambrey, M. J., and Reynolds, J. M. (2012). 'Structure-from-motion" photogrammetry: a low-cost, effective tool for geoscience applications'. *Geomorphology* 179, 300–314. doi: 10.1016/j.geomorph.2012.08.021

Conflict of Interest: The authors declare that the research was conducted in the absence of any commercial or financial relationships that could be construed as a potential conflict of interest.

frontiers in Environmental Science

ORIGINAL RESEARCH
published: 15 March 2021
doi: 10.3389/fenvs.2021.575058

Documentation of Microplastics in Tissues of Wild Coastal Animals

Marte Haave[1]*, *Alessio Gomiero*[1], *Jürgen Schönheit*[2], *Hanne Nilsen*[2] and *Anne Berit Olsen*[2]

[1]NORCE Norwegian Research Centre, Environment, Bergen, Norway, [2]Norwegian Veterinary Institute, Bergen, Norway

Microplastic pollution is omnipresent in biota around the globe, and concerns are rising that humans are exposed to microplastics (MP) through food. Investigations of MP in wild animals relevant for human consumption and the effects in exposed birds and mammals is warranted. We investigated the concentrations of MP in organs and tissues of fish, seabirds, terrestrial and marine mammals from a plastic polluted area near Bergen, Norway. A standardized autopsy included evaluation of condition, bacteriological and histopathological analyzes. Tissues were analyzed for MP (>10 µm) by pyrolysis Gas Chromatography Mass Spectrometry (py-GCMS) and inspected by polarized light microscopy. We analyzed samples of stomach and intestinal wall, liver and muscle/fillet from three flounders, three cod, three seabirds, three otters and one seal, kidneys from seabirds, otters and the seal, and gills from the fishes. No large plastic items were observed in the gastrointestinal tracts. Eight of 13 animals had MP in one or several tissues. MP was found in intestine (5), stomach (4), liver (3), muscle (3). No MP was found in the seal, and only in the stomach wall of one otter. In seabirds, MP was found in the intestine, stomach and liver, but not muscle. The highest concentration was 3.4 µg/g wet weight in cod liver. Three of the nine investigated polymers were found above the Limit of Quantification (LOQ): Polyvinylchloride>polystyrene>>polyethylene terephthalate. MP was quantified in one of four replicates of cod muscle and one of two replicates of cod liver. No MP was observed by microscopy. The results show levels under or close to the current LOQ. Replicates indicate uneven MP distribution in tissues and resulted in higher prevalence of MP for cod. No adverse effects could be related to MP. The sample size was small, and conclusions cannot be drawn regarding effects or risks. The animals were by-catch, and mostly in good condition when caught. Procedural blanks and air-controls showed very low MP, and support that the MP come from environmental sources. Further studies are needed to determine levels of microplastic in edible tissues and the current wildlife exposure through the food web.

Keywords: microplastics, tissue, uptake, wildlife, food web, polarization microscopy, histopathology

LSID: Harbor seal (*Phoca vitulina*), LSID: urn:lsid:zoobank.org:act:064A76C7-49C4-4231-842D-67C82DACD58E; Eurasian otter (*Lutra lutra*), LSID: urn:lsid:zoobank.org:pub:E1B2A866-06A0-4687-A18D-482D27424816; Red breasted merganser (*Mergus serrator*), LSID: urn:lsid:zoobank.org:act:7723FFD6-5FBF-4134-AE15-4B7728D78DD4; Common guillemot, common murre or thin billed murre (*Uria aalge*), LSID: unknown; Cod (*Gadus morhua*), LSID: urn:lsid:zoobank.org:act:389BE401-2718-4CF2-BBAE-2E13A97A5E7B; Flounder (*Limanda limanda*), LSID: urn:lsid:zoobank.org:act:A9350141-7463-4878-85E4-4629F310F317.

OPEN ACCESS

Edited by:
Andrew Turner, University of Plymouth, United Kingdom

Reviewed by:
Sutapa Ghosal, California Department of Public Health, United States
Mario Barletta, Independent Researcher, Recife, Brazil

***Correspondence:**
Marte Haave
marte.haave@norceresearch.no

Specialty section:
This article was submitted to Toxicology, Pollution and the Environment, a section of the journal Frontiers in Environmental Science

Received: *22 June 2020*
Accepted: *25 January 2021*
Published: *15 March 2021*

Citation:
Haave M, Gomiero A, Schönheit J, Nilsen H and Olsen AB (2021) Documentation of Microplastics in Tissues of Wild Coastal Animals. Front. Environ. Sci. 9:575058. doi: 10.3389/fenvs.2021.575058

INTRODUCTION

The increasing amounts of plastic pollution in the ocean is a global concern, yet the distribution, environmental fate and detrimental effects of microplastic (MP) (<1000 µm, (Hartmann et al. 2019) in the ocean is still poorly understood. Evidence from the past years have documented the omnipresence of microplastic pollution in deep oceans, in Antarctica and the Arctic, on land, and in air and atmospheric fallout (Dris et al. 2016; Bergmann et al. 2017; Courtene-Jones et al. 2017; Munari et al. 2017; Bergmann et al. 2019; Wright et al. 2020). Recent expert group opinions state that current knowledge is insufficient to evaluate the risks from human or ecosystem exposure to MP (Skåre et al., 2019). It has also been noted that global ecosystem effects are hard to document at this stage, but that the lack of documentation should not be taken as evidence of no risk (SAPEA 2019). A recent, systematic literature review and resulting Species Sensitivity Distribution concluded that the lowest Hazard concentration or Predicted No Effect Concentration was within the range that can be considered environmentally relevant in some regions (Skåre et al., 2019), thus effects of MP may already be detrimental to populations of vulnerable species in some highly polluted regions. Moreover, this indicates that effects will become increasingly evident if general levels continue to rise. Prospective studies and models report that levels high enough to cause detrimental effects of sedimented and beached plastics are expected before the end of the century, and that such levels have already been reported in different ecosystem compartments (Everaert et al. 2018). MP fragments in the ocean likely end up on the ocean floor (Barnes et al. 2009; Woodall et al. 2014) while macroplastic items either sink or are deposited along the shorelines, depending on their density and buoyancy (Jambeck et al. 2015; Lebreton et al. 2017; Lebreton and Andrady 2019). Along shorelines, macroplastics degrade and generate MP by a number of processes such as UV-radiation, temperature changes, microbial degradation, abrasion and leaching of plasticizers (Andrady et al. 2003; Andrady 2011; Andrady 2017; Urbanek et al. 2018). The MP generated from degradation on land may potentially re-enter the coastal waters by wind and wave-erosion and increase microplastic exposure of marine ecosystems in the water column and on the sea floor along the coastline.

The Norwegian coastline is over 100 000 km long, where the shoreline with uninhabited islands and inlets accumulates floating debris brought by the Norwegian Coastal Current and the predominant winds from the south-west (Bastesen et al. 2020). Models have shown how the Norwegian coastline is a trap for floating debris (Onink et al. 2019). Mammals, seabirds and fish that live in these coastal habitats are in this way exposed to a high volume of deposited and/or floating plastic debris despite the scarce human population. The coastline is also the site for coastal fisheries and hosts a high number of fish farms that use, lose and discard plastic equipment. Although the concentrations and distribution of MP along the Norwegian coastline are not yet fully mapped and understood, recent publications document the occurrence, levels and variation of MP in sediments and waters in urban areas (Gomiero et al., 2019b; Haave et al., 2019) and even on the Norwegian continental shelf (Jensen and Cramer, 2017). Ingestion and uptake of plastic fragments by a range of marine species have also been documented over the past decade (Browne et al., 2008; Andrady, 2011; Bravo Rebolledo et al., 2013; Lusher et al., 2013; Van Cauwenberghe and Janssen, 2014; Watts et al., 2014; Van Cauwenberghe et al., 2015; Brate et al., 2016; Lusher et al., 2016), and the implications are that humans are exposed through consumption of seafood (Andrady, 2011; Lusher et al., 2017). Although uptake and transfer of micro and nanoplastics through the food web have been proven experimentally (Mattsson et al., 2015; Mattsson et al., 2017) the environmental relevance of such transfer for ecosystem and human health at current concentrations is still poorly understood (Smith et al., 2018; Ribeiro et al., 2019). A knowledge base on the levels of MP contamination in edible tissues and the associated health risks in exposed animals and humans is needed in order to perform relevant Environmental Risk Assessments (ERA), now and with predicted future increases in plastic pollution and release.

By investigating wild animals living in a plastic polluted area we aimed to elucidate whether MP are present at quantifiable levels in tissues of exposed wildlife at current environmental levels. This will also add to knowledge about MP potentially reaching humans through dietary intake of wild caught species. This is a necessary step to evaluate relevant exposure scenarios and provide long- term risk assessment for human consumers. The aim of this study was 1) to investigate the occurrence and levels of MP in tissues of wild animals from a plastic polluted area, 2) to perform a qualitative assessment of health, investigating a standardized battery of health parameters 3) Assess the relation between microplastic analyses and observed health parameters

MATERIALS AND METHODS

We investigated the concentrations of MP in tissues of fish, seabirds, terrestrial and marine mammals from a highly plastic polluted area on the west-coast of Norway, at the Sotra archipelago outside the city of Bergen (**Figure 1**). Preliminary studies done by NORCE in a regional project (RFFV #277264) found that the volumes of accumulated plastic debris at Sotra was approximately eight metric tons per kilometer (in 2018). The estimated global average has been estimated to a little over a metric ton per kilometer coastline (Smith and Markic, 2013; Ryan et al., 2014).

Investigated Wildlife

Fresh or frozen birds and mammals were donated to the study by local fishermen (**Table 1**). The samples were caught from December 25. 2017 to March 15. 2019. The animals were mainly taken as by-catch in fishing nets and crab-boxes. The animals obtained for investigation of both microplastic and health parameters were three otters (*Lutra lutra*), two sawbill ducks (red breasted merganser) (*Mergus serrator)* and one common guillemot (common murre; *Uria aalge*) that were delivered to the Norwegian Veterinary Institute (NVI) in Bergen. One

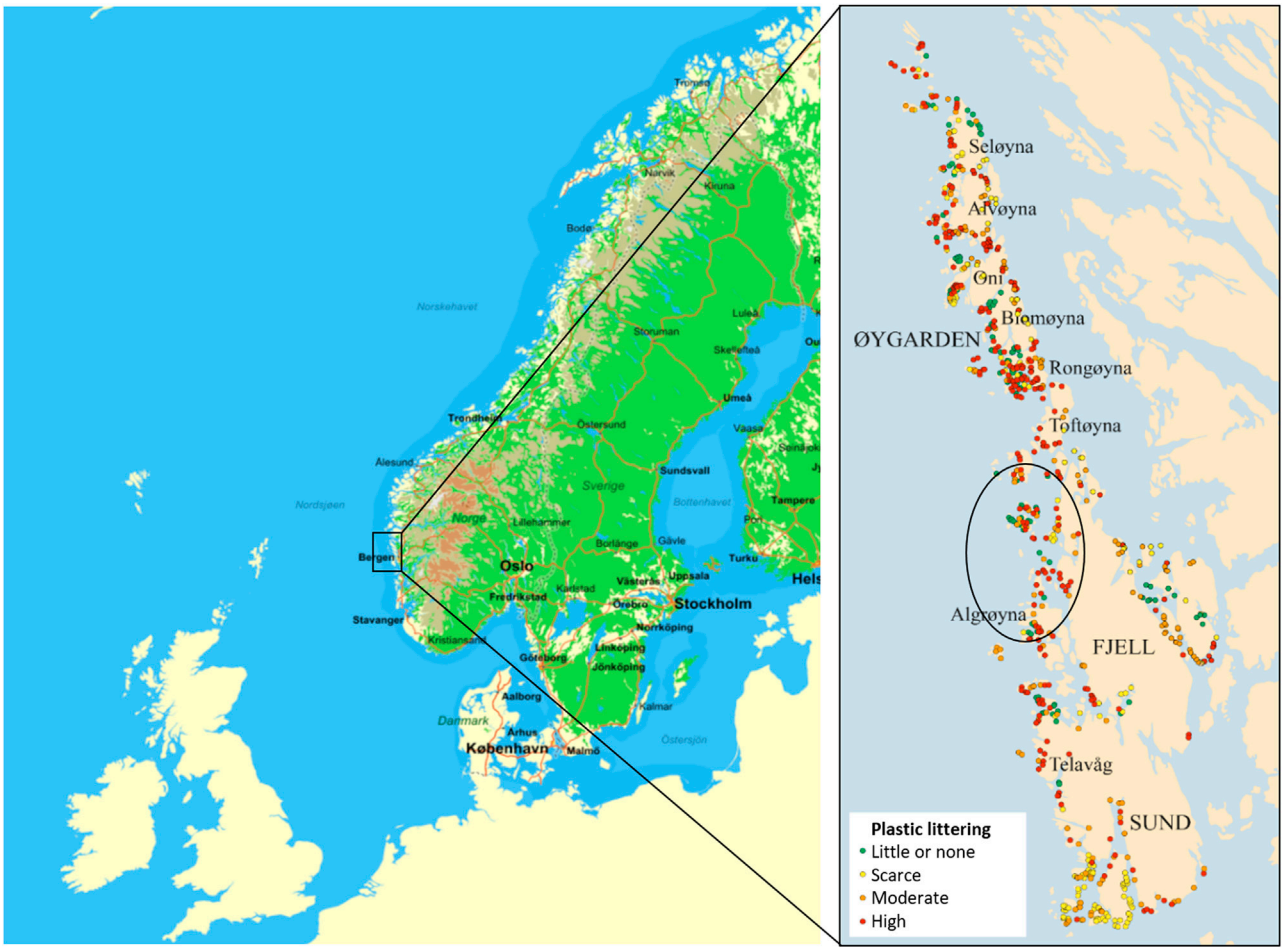

FIGURE 1 | Map of Norway with the Sotra Achipelago to the West, and the plastic exposed area (circled) where the samples were caught. Map of plastic littered bays from Bastesen et al. (2020).

Harbor seal (*Phoca vitulina*) was autopsied outdoors. Three cod (*Gadus morhua*) and three flounders (*Limanda limanda*) were caught specifically for the project by collaborating volunteers from the Norwegian Hunter and Anglers Association and delivered fresh to NVI. Another three otters were sampled for health parameters, but not included for chemical MP investigation. Five of the otters and one bird were frozen at −20°C for up to ten months before sampling, as not enough fresh animals were obtained during the duration of the project.

Gross and Histopathological Examination and Bacteriology

All animals were subject to autopsy according to guidelines at the NVI (http://kvalitet/eknet/docs/pub/dok01304.htm). In addition to a general gross pathological investigation of the animal, the gastrointestinal tract was examined for presence of large pieces of plastic materials. Tissue samples for histopathological examination from most organs including tissues with visible lesions were fixed in 10% neutral buffered formalin, embedded in paraffin and routinely processed into sections of 3–4 µm thickness (**Supplementary Table S1**). Tissues were stained with haematoxylin and eosin (H&E) following standard procedures and examined by light microscopy. Autopsy and histopathological examination were performed by trained pathologists.

Bacteriological examination for pathogens was performed according to procedures at the NVI. For all animals, samples from an internal organ (kidney or spleen) were sampled. From otters and birds, samples for bacteriology were also collected from lungs and intestines.

Polarization Microscopy for Microplastics in Tissues

All H&E stained histopathological sections (**Supplementary Table S1**) were examined by polarized light microscopy (PLM) in order to assess occurrence and localisation of possible plastic particles in the tissues. A Leica DM 2500 LED microscope with analyser and polarizer filter was used. This method may enlarge structures by 1000 x and allows the detection of very small birefringent particles including the size limit for the chemical analysis used in this study of 10 µm.

TABLE 1 | Details of the sampled animals, results of the autopsies, general health, histopathological observations and chemical analyses of MP in tissues from wildlife from Sotra 2018–2019.

Species	Date of capture/Date of sampling	Gender/age group	Weight (kg)/ Length (cm)	Likely cause of death	Health related obs.	Chemical analyses of MP in tissues (Py-GCMS) (µg/g wet weight)			Occurrence and effects of MP (HP and PLM)
						PVC	PS	PET	
Otter	2018.03.19/2018.03.19	F/juv	5.1/53	Drowned	NO	-	St: 1.7	-	NO
Otter	2018 unkn/2018.10.24^{F}	M/juv	3.6/50	Road-kill	NO	-	-	-	NO
Otter	2017.12.25/2018.10.24^{F}	M/ad	>6/56	Drowned	NO	-	-	-	NO
Otter	2018 unkn/2018.10.24^{F}	M/ad	4.8/46	Drowned	NO	NT	NT	NT	NO
Otter	2018 unkn/2018.10.24^{F}	M/ad	4.9/50	Drowned	NO	NT	NT	NT	NO
Otter	2018 unkn/2018.10.24^{F}	M/ad	>6/58	Drowned	NO	NT	NT	NT	NO
Harbor seal	2019.03.11/2019.03.13	M/juv	45/130	Drowned	NO	-	-	-	NO
Sawbill duck	2018.03.21/2018.03.22	F/ad	1/42 (72)	Drowned	NO	I: 1.0	I: 1.2	-	NO
Sawbill duck	2019.01.01/2019.08.05^{F}	F/ad	0.9/48 (70)	Drowned	NO	I: 1.0	I: 1.2	-	NO
Common guillemot	2019.15.03/2019.15.03	F/juv	0.95/43 (62)	Drowned	Emac., muscle degen.	S: 1.7	-	L: 1.0	NO
Cod	2019.05.08/2019.05.08	F/ad	2.9/77	Caught	P	L: 3.4 S: 2.6 I: 2.5	M: 1.0	-	NO
Cod	2019.05.08/2019.05.08	F/ad	2.7/66	Caught	P	L: 1.7 S: 2.0 I: 2.1	M: 1.0	-	NO
Cod	2019.05.08/2019.05.08	unkn./juv	3.2/70	Caught	P	I: 1.2	-	-	NO
Flounder	2019.13.03/2019.13.03	F/ad	1.3/44	Caught	P	M: 1.5	-	-	NO
Flounder	2019.13.03/2019.13.03	M/ad	0.8/42	Caught	NO	-	-	-	NO
Flounder	2019.13.03/2019.13.03	F/ad	0.8/41	Caught	P	-	-	-	NO

Superscript ^{F}: indicates frozen at −20°C from date of capture until dissection. Juv = juvenile, Ad = Adult, Length = from forehead to tail base (bird wingspan in brackets); Health related observations: NO = No specific illness observed, P = Parasites and/or parasitic lesions; chemical analyses of MP in tissues - abbreviations: I = Intestine, L = Liver, M = Muscle, S = Stomach; Polymers: PVC = polyvinyl chloride, PS = polystyrene, PET = polyethylene terephthalate; NT = Not tested for MP; NO = not observed; - = The concentration is under the Limit of Quantification for all polymers.

Tissue and Organ Sampling for Chemical Analysis

During autopsy, the stomach and intestinal contents were examined for visible macro plastics and blockage of the intestines. A chemical analysis aimed to detect presence of MP within tissues of internal organs was performed. Samples were taken for chemical analyses of the liver, stomach wall and intestines, as well as a piece of a large muscle from all the animals (**Table 1**). In mammals an internal muscle of the back (*M. iliopsoas*) was taken, in birds a cut from the thickest part of the large pectoral muscle (*M. pectoralis major*) and in fish a piece of the central dorsal fillet behind the dorsal fin was taken. The kidneys were also sampled in birds and mammals, the spleen in otters, and the gills of fish. From the harbor seal we also analyzed a piece of the lung. The stomachs were opened, and the intestines were emptied and inspected for large plastics that might influence the plastic uptake, health and wellbeing of the animals. The intestines were rinsed through with 50–100 ml saline using a small glass funnel. Samples were weighed, packed in aluminum foil and frozen at −20°C until analysis.

Chemical Analysis of Microplastics in Tissues

The surfaces of gills and intestines were rinsed again before further analyses, to minimize the potential to have particles attached to the surface that might be considered to be within the tissues. A sample size of 6–30 g of tissue was used for chemical analyzes of MP, limited by availability of tissue and the efficiency of enzymatic degradation. Due to relevance as human food source, four replicate samples of muscle and two replicates of liver were analyzed from the two first cods. Budget constraints allowed only single replicates in the remaining samples.

Extraction of particles was based on previous published methods (Gomiero et al., 2019a). To extract microplastic particles (MP > 10 µm), samples were placed in microplastic free (burned at 500°C), 125 ml volume D4 borosilicate sintered glass filtration funnels (crucibles, with porosity 4, ROBU, VWR Cat.no 511-1322) and placed in a 600 ml glass beaker for support during treatment. The beaker was covered with aluminium foil to prevent airborne contamination. Samples were first incubated overnight (50°C) in 70 ml 5% SDS solution, then placed on a vacuum filtration assembly and the SDS gently vacuumed off. The residual material was rinsed with 30 ml Milli-Q water, 70 ml of protease (1:5) in glycine buffer was added, the sample sonicated and incubated for 36 h at 50°C. Digestates were then vacuumed off and residual material rinsed again with 30 ml of Milli-Q, incubated for 48 h at 30°C with 50 ml of lipase (Sigma, Germany) in PBS (1:5) at pH 7.4 , vacuumed off and rinsed with Milli-Q. A final strong oxidative digestion was performed using 50 ml hydrogen peroxide

(H_2O_2, 30%, VWR International, Germany) at 50°C for 12 h. After removal of the H_2O_2, the residual material in the crucibles was quantitatively transferred into a in a separation funnel with zinc chloride solution (final density 1.70–1.75 g/cm^3) by gently scratching the sintered glass filter surface. The mixture was stirred for 30 min before being left to settle for 72 h in pre cleaned separator funnels. The supernatant containing the floating plastic particles was collected by filtration on a glass fiber filter GF/A (Gomiero et al., 2019b) before packing into a pyrolytic tin cup. 10 ml of tetramethylammonium hydroxide (TMAH, 25% in water) was added to the tin cups pre-loaded with samples and allowed to dry at 40°C prior to py-GCMS. Py-GCMS measurements were performed by a Shimadzu Optima 2010C GCMS controlled by GCMS solution V 4.45, equipped with a Rxi-5ms column (RESTEC, Bellefonte, PA) and coupled with Frontiers lab's Multi-Shot Pyrolizer EGA/PY-3030D with auto-shot sampler (BioNordika, Norway). Pyrolysis is performed at 590°C, according to (Fischer and Scholz-Bottcher, 2017; Gomiero et al., 2019b) Eight of the most commonly used plastic polymers (polyethylene - PE, polypropylene - PP, polystyrene - PS, polyvinyl chloride - PVC, polyamide - PA, polymethyl methacrylate - PMMA, Polycarbonate - PC and polyethylene terephthalate-PET) of purity >99% were used to set up the calibration and quantification curves. In order to identify single polymers unambiguously in complex environmental samples, specific indicator compounds were chosen by pyrolyzing polymer standards. The obtained pyrograms were compared with a customized database and cross-checked with literature data following recommendations and selecting criteria from Fischer and Scholz-Bottcher (2017) and Gomiero et al. (2019b). To obtain calibration curves for quantification, standards between 10 and 360 mg of polymer were weighed directly into the pyrolysis tin cups using a XPE205 DeltaRange Mettler Toledo balance coupled with an Anti-Static Electricity Discharger tool (Sartorius, Germany). Individual polymers are identified by means of preselected combination of retention time and mass markers and quantified by integrating the chromatograms of their associated indicator ions. The limit of quantification (LOQ) was calculated according to Hermabessiere et al., (2018).

Contamination Control and Quality Assurance

To prevent contamination during and after sampling, the autopsies were performed on a steel bench using steel scalpels, scissors and plyers, placing the tissues on steel trays or aluminum foil, avoiding plastic materials as far as possible. Sterile containers and cups for formaldehyde fixation were of plastics, but these were not used for tissues for chemical analyses of microplastics. Surfaces in the dissection lab were wiped with tissue paper and water before start, and tissues were placed on pre-rinsed steel trays and clean tin foil for weighing and packaging. Nitrile gloves and semi-synthetic lab-coats were worn, and the lab did not have specialized air filtration, thus the surface of the samples were considered potentially contaminated after sampling. Before further chemical analysis in the dedicated MP lab at NORCE Stavanger, samples were rinsed with Milli-Q, and the surface layer of tissue was removed to avoid potentially contaminated surface layers of tissues. Removal of external layers was however not possible for delicate structures such as gills and intestines or stomachs. All liquid reagents for the chemical analyses, including Milli-Q water, were prefiltered over glass fiber filter (GF/A, 1.2 µm, Whatman). All glassware and equipment for the chemical analyses were heated to 550°C in a muffle oven before use, wet traps for air-contamination and blank procedure controls for reagents were applied (**Supplementary Table S2**).

The LOQ for target polymers was as low as 1 µg/g wet weight (ww) for all the investigated polymers except PMMA that had a LOQ of 5 µg/g ww.

Data Treatment

SPSS v25 for Windows (IBM Statistics, United States) was used for statistical investigations and to create graphs.

RESULTS

Animal Health and Condition–Pathological and Bacteriological Examination

Four of the animals were juveniles around the age of maturation, while the majority were adults. Most of the animals were in normal condition with food in their stomach. The birds and mammals were found dead, caught as bycatch in fishing nets and crab-boxes. The pathological investigation supported death by drowning for the birds and five of six otters (**Table 1**). One otter was found by the road, probably hit by a car. No bacteriological pathogens were isolated from the investigated animals. Details of size/weight, health status, likely cause of death, concentrations of microplastics and health observations can be seen in **Table 1**.

Mammals: One otter had multiple trauma with crushings and bleedings indicating that it was hit by a car. In five of six otters and the seal, findings were consistent with drowning, such as fluid, froth and congestion of the respiratory tract. No specific illnesses were detected. The young seal was in good condition but had nematodes in the lungs and stomach.

Birds: Gross pathology revealed circulatory disturbances of the respiratory tract indicated drowning. The sawbill ducks were in normal or mildly reduced condition. No specific diseases were observed. The guillemot had muscle degeneration of unknown cause and was emaciated.

Fish: Two cods and all three flounders were matured or in maturing. One matured cod was emaciated. In the cods and in one of the flounders we made observations common to adult fish, such as parasitic nodules in mesenterium and organs, some of them containing nematodes identified as *Anisakis* sp. One cod had a few small areas of chronic skin inflammation and one had a parasitic inflammation in an eye. Inflammation of gill and epicardium of unknown cause was seen in one flounder.

Ingestion of Non-food Items

No macroplastic items were observed in the stomachs or intestines of any mammal, fish or bird. Organic debris other than prey items, such as small rocks and sticks were observed in birds and fish stomachs.

Histological Examination for Microplastics and Tissue Effects

No particles or structures consistent with plastics were observed by either PLM or histopathology. In tissues positive for MP by the chemical analysis, no tissue reaction like thickening of intestinal epithelium, inflammation or necrosis that could be associated with MP were observed.

Polarization Microscopy

Polarization microscopy of the histological sections did not reveal particles or structures consistent with plastics.

Chemical Analysis for Microplastics

Analyses for microplastic particles of (theoretically) >10 µm (MP) were performed on tissues from five organs of each of the 13 animals, when organ sizes permitted both microplastic and histological analyses. Results are given in **Table 1**.

Microplastics in Animal Species

MP were not observed above LOQ in any tissue sample from the seal. MP was quantified in the stomach tissue sample of one of three otters (**Table 1**), while the other tissues from otters were negative. In seabirds, MP of the PVC and PS of the same concentrations were found in the intestines of the two sawbill ducks, while the guillemot had quantifiable levels of MP in the stomach (PVC) and liver (PET), but no MP in the intestinal tissue. The cods had the highest frequency and tissue concentrations of MP of all the animals (**Figure 2**), but cod was also the only species where replicate samples were analyzed. It is noteworthy that MP was only observed in muscle tissue from fish, not in birds or mammals, although this may have been influenced by the higher number of replicate analyses of cod tissues. Two of three cods had MP in all three tissues; intestines, liver and muscle. Among the flounders, MP was found in only one muscle sample, and in no other tissues (**Table 1**).

Microplastics in Different Tissues

Eight of the 13 investigated animals had quantifiable levels of MP in at least one of the tissue samples. Seven of the eight animals had MP in the stomach wall or intestines, while four different individuals had detectable levels of MP in muscles and/or liver (**Table 1**). In falling order, MP was most frequently found in tissue samples from intestines (5), stomachs (4), livers (3) and muscles (3). The highest single MP concentration found in any tissue was 3.4 µg/g wet weight (ww) found in cod liver (**Table 1**). No MP were found in samples of gill, lung, spleen or kidney after one replicate analysis of each tissue sample.

Polymer Types

Three of the nine investigated polymers were found in tissues: PVC was the most common polymer and was detected in seven animals in samples of intestine (5), stomach (3), liver (2) and muscle (1). PS was found in five animals, in intestines (2), muscle (2) and stomach (1). PET was found in one sample from the liver of a seabird, but not in any other samples or animals. All the polymers PE, PC, PP, PMMA, PA-66 were below the Limit of Quantification (LOQ) in all samples.

BLANK CONTROLS

Two of the 40 blank analyses from the extraction procedure room showed a measurable concentration of two the eight synthetic polymers (PE and PS) in the air contamination control in two separate weeks (**Supplementary Table S2**). The forty blank analyses of prefiltered reagents and the 40 blanks from the analysis room air controls showed no polymer contamination above the LOD (for liquid LOD, see **Supplementary Table S3**).

DISCUSSION

General Observations and Tissue Distribution

This study focused on presence of microplastic in tissues of naturally exposed wild animals. Analyses of microplastics in stomach and intestinal contents and within ingested prey items were not within the scope of this work. The intestines are per definition external to the body, and MP in the intestinal lumen thus demonstrates ingestion, not uptake. Efficient egestion has been shown in several species (Frydkjaer et al., 2017; Ory et al., 2018; Woods et al., 2018), and the content of MP in stomach and intestines at any point in time is not necessarily representative for the long-term exposure, but shows the momentary status.

Microplastics Uptake and Transport

The findings of MP in internal organs above the background contamination suggests that translocation of MP to tissues of wildlife vertebrate species exposed in their natural habitats occurs. Uptake of MP after experimental exposure has previously been observed (Avio et al., 2015; Deng et al., 2017), but this is one of very few studies that have demonstrated MP uptake in vertebrates under natural exposure. Previous publications have shown MP in liver of anchovies (Collard et al., 2017), but to our knowledge this is the first study showing uptake of MP in tissues of wild birds. Previous studies indicate that the mode of uptake and translocation is through intestinal wall and transport of particles may occur via the portal system and chyle to the liver and other organs (Volkheimer, 1975; Volkheimer, 1993; Volkheimer, 2001) (Volkheimer, 1975). Transport was believed to happen also between cells, as peristaltic movement increased the uptake.

Uptake by the specialized epithelial M-cells of the gut associated lymphoid tissues like the Peyer's patches has previously been discussed as a means of entry of MP in mammals for subsequent dissemination by lymph, blood and macrophages (Cannon and Swanson, 1992; Florence, 1997). Enterocytes with M-cell-like characteristics with capacity to absorb intact macromolecules are also reported in teleost fish (Fuglem et al., 2010). However, uptake by regular enterocytes is also emphasized (Carr et al., 2012), as well as entry between the enterocytes for larger particles and a spread from the

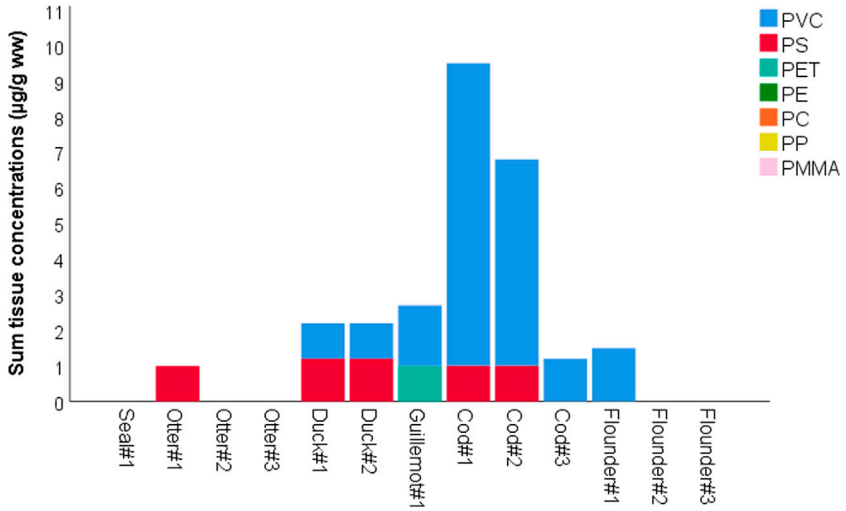

FIGURE 2 | Sum of tissue concentrations (µg/g ww) of detected microplastic polymer types in coastal animals from Sotra in 2018–2019.

digestive tract through the portal vein (Volkheimer, 1975; Volkheimer, 1993; Volkheimer, 2001). Hematogenous dissemination through the portal system would explain the presence of MP in liver, as the primary target for the blood from the digestive tract. Further hematogenous dissemination throughout the body is also likely, as MP was also detected in muscle of fish. Whether the secondary vascular system of fish might also play a role for such transport is, however, not known (Rummer et al., 2014).

Target Tissues

The highest single observed concentration of any polymer was found in a liver sample of cod (**Table 1**; **Figure 3**). The single observation is not evidence of liver as a target organ for plastic accumulation, however, it may seem that the liver is an important part of the process of uptake and/or excretion, as a high prevalence of MP in livers was also observed by Collard et al., (2017) studying European anchovies (*Engraulis encrasicolus, L.*). Another study of MP in wild and farmed salmon showed that MP was found in liver and muscle in equally high concentrations, and that muscle tissue may be just as suitable for monitoring as liver (Gomiero et al., 2020a). Another possible route of uptake and transfer to internal organs of fish could be via the gills, but no MP was found in the gill samples in our study. In recent studies we have observed PE particles in gill samples of farmed and wild salmon (Gomiero et al., 2020b).

Microplastic Localization Within Tissues

The observation of MP in samples of stomach and intestines has been observed by a number of previous studies (reviewed in Lusher et al., 2017). Although intestines were rinsed with saline during sampling, and all samples were rinsed again before enzymatic degradation, MP may still have been attached to the surface of the mucosal layer or trapped between folds and invaginations. For the liver and muscle, the findings indicate the presence of MP inside these organs and cannot be explained by potential surface contamination, as the surface layers were removed prior to enzymatic digestion. It is therefore not unlikely that the MP may also have been present within the tissue layers of the intestines. The study cannot dismiss the possibility that the observed MP is localized within blood or lymph vessels in the investigated tissues. The absence of MP in blanks and a range of other investigated tissues, such as spleen, kidney and lungs suggest that the method is able to discriminate between absence and presence of MP. Absence could also be explained by low concentrations (under the LOQ) or patchy distribution where a small sample of <30 g may have missed occasional MP in the tissues.

It was not within the scope of this study to investigate the localization of plastic particles within the tissue, or the mode of uptake and transport of MP through the tissues. Our results document, however, that transfer of MP over external barriers into tissues and between organs may occur for both fishes and birds under natural conditions, and that closer investigation of uptake and translocation are warranted.

Food Web-Transfer, Bioaccumulation and Biomagnification

Most of the investigated animals were adults, and there were a number of negative findings per species (**Table 1**). With only three specimen per species, the data is not sufficient to comment on potential bioaccumulation (uptake and retention of MP leading to increasing levels of MP from the environment to biota) or biomagnification (increase of MP with trophic level). The animals are mainly predators in the same ecosystem but are not directly linked themselves as prey/predators.

In the stomach of the sawbill ducks we observed only small fish (2–5 cm), although they can also take larger fishes. The bottom-dwelling flatfish eat polychaetes and benthic invertebrates. The cod is a generalist and an opportunist that takes a range of prey from the benthic sediments such as polychaetes, crabs and other crustaceans,

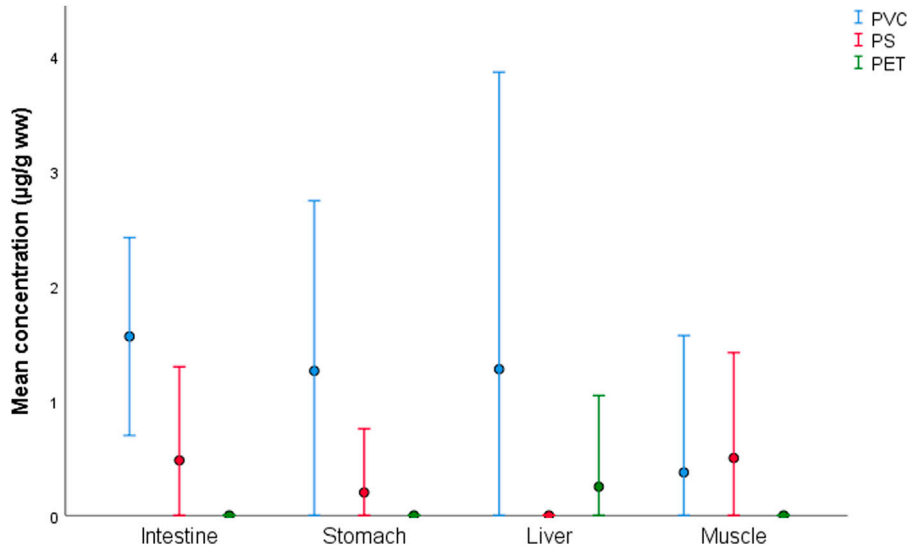

FIGURE 3 | Mean and 95% confidence intervals of concentrations (µg/g ww) of microplastic polymers quantified in tissues of coastal animals from Sotra in 2018–2019.

but also take fish on the bottom and in the water column. Cod from western Norway have also been caught with large plastic items in their stomach. Documented in the media is a large plastic bottle (www.dagbladet.no/nyheter/jeg-fikk-vondt-av-a-oppdage-dette/69687244), and even a sex-toy (www.nrk.no/mr/torsk-hadde-dildo-i-magen-1.11663195). The cod, as a generalist is more likely to try ingesting anything that looks edible, including plastic. Such generalist feeding habits have previously been correlated with higher plastic ingestion (Silva et al. 2018). The coastal cod in this study is a resident type of the Atlantic cod, and individuals therefore live their entire life-cycle in the same region, and do not go on oceanic foraging trips, unlike the migrating stocks of Atlantic cod ("skrei") that spend most of their life in the open Atlantic waters. With its opportunistic foraging and small home-range, the coastal cod may be a good candidate as a fish species for coastal monitoring of microplastics.

The seal and otters also move between the surface and deep waters to breath and hunt for a range of fish, mussels and crabs. Otters sleep and nest on land in inlets and sheltered areas where the shoreline is often heavily polluted with accumulated macro and mega-plastics. Otter dens have been observed under remnants of boat wrecks, and their trails are commonly seen between the masses of stranded debris that are abundant in this unpopulated area. It is obvious that otters, seals and birds are likely to have many daily encounters with floating and beached plastic debris in this region. It is therefore interesting to observe the low levels or absence of detectable microplastics in the mammals, both old and young, living surrounded by large and smaller plastic debris. It may be speculated that the mammals are able to discriminate plastic from prey and do not ingest as much plastic items as the heavily polluted habitat should imply. Otters sometimes eat only parts of their prey, and possibly avoid the GI tract, but smaller fish can be eaten whole. Eating the prey whole, which the seal does, would expose the mammals to MP in the GI-tract of the prey items, and therefore, potential intestinal uptake and transport into mammalian tissues as well. Although we did not observe MP in liver and muscle of the mammals, we cannot exclude that such uptake also occurs in mammals.

The distribution patterns and polymer types detected in the tissues were similar in individuals of the same species, such as the cods and sawbill ducks. Such coherent findings of similar polymers and concentrations in the same species, indicate that the observation represents a pattern of exposure and uptake and may suggest that similar sources of MP and similar feeding behavior and exposure routes is reflected in the tissue levels. Similarly, it has previously been reported that foraging behavior and different habitat use during different life stages influences the levels of MP fibers in the GI tract of three species of snooks (*Centropomidae* spp, (Silva et al. 2018; Ferreira et al. 2019) However, a higher number of specimen, and a higher number of positive findings are needed to elucidate the distribution patterns and range of MP within and between species to correlate to foraging behavior.

Good contamination controls with no observed PVC in the blank controls support that the findings represent actual presence of MP in tissues. We can however not say anything about the residence time of the MP in the tissues, and whether the MP is in the process of being excreted, or by which mechanisms uptake and excretion occurs. The results we observe of MP in tissues may well represent a snapshot of the situation, and may reflect MP in blood vessels running through the tissues. The observation is in itself not evidence of bioaccumulation or biomagnification. To elucidate bioaccumulation or biomagnification it is necessary to perform a study with larger sample volumes per tissue and/or several parallels per sample in order to determine the concentration of MP in muscle and tissues of individuals related to age, size and trophic level. The current study identifies the presence of MP in tissues and indicates strongly that such investigations are warranted. It is also necessary to perform controlled studies to elucidate the mechanisms of uptake, translocation, excretion, and the localization of MP within tissues, to ultimately understand the excretion and half-life of MP.

Observed Polymers in Samples of Wild Animals

The most prevalent polymer found in tissues was PVC, which is a versatile and much used polymer in anything from building materials, pipes and constructions to electronics and hygienic materials in health care. The polymer has a density of 1.38 kg/L, thus it is heavier than Atlantic Seawater (1.02–1.03 kg/L). PS was the other detected polymer type, which is used for clear plastics (packaging, cutlery) or colored and used for a range of utensils (toys, household items) as well as electronics and car parts. PS has a density of 1.03–1.06 kg/L. However, expanded Polystyrene (EPS) can frequently be found on the beaches of this area, with a density of only 10–30% that of water. EPS is much used as insulating fish-boxes and for buoyancy devices at sea. Exposure to PS in the form of EPS is therefore likely. PET was observed in only one sample. PET is often used for drinking bottles. PET is also in the polyester family, often used for textiles, and the most common synthetic textile produced. Data are lacking on the prevalence and distribution of plastic polymers in sediments and water along most of the Norwegian coastline, and only a few quantitative analyses of sediments have been performed in Western Norway (Gomiero et al., 2019b; Haave et al., 2019). PVC, PS and PET were observed in most of the sediment samples of these studies but were not dominant. However, polymer composition in sediments shows great variations (Haave et al., 2019), and one cannot generalize to occurrence of polymers based on two studies from different regions. The general polymer contamination of sediments in the study area has not yet been investigated. Mapping the occurrence and levels of microplastics along the coastline is necessary in order to understand potential wildlife exposure to MP.

Tissue Effect

The histopathological investigations did not reveal any tissue reaction that could be related to the presence of MP. Only low levels of MP, close to the Limit of Quantification were observed in this study, in contrast to high doses used in experimental studies that report histopathological reactions in zebrafish and mice respectively (Lu et al., 2016; Deng et al., 2017). However, histopathological studies that claim to observe effects have been criticized for poor quality (Baumann et al., 2016), or histopathology has revealed no tissue effect (Karami et al., 2017). This study is too small to conclude on the impact of MP on animal health, but the confirmation of MP in tissues of animals exposed under natural conditions is a strong indication that tissue uptake, residence and health effects of MP should be carefully followed in a long-term perspective.

It is considered plausible that MP uptake into tissues may have long term effects due to plastic-associated chemicals. For this study it is unlikely that we will be able to correlate such effects with the observable and momentary presence of MP in the tissue, in part due to low levels of MP and a too low number of samples to see correlations. Also, if the MP is not accumulating but is excreted after a short residence time in the tissue, attempting to demonstrate long-term effects based on a snapshot of momentary presence of MP is not advisable. Moreover, the mode of action for MP and the level of biological organization at which effects will appear (biochemical, cellular, tissue, organ, individual) are not yet properly elucidated. More research into the modes of action is needed to understand the long-term effects of MP in wildlife.

Method Limitations

Cost and Time for Extraction and Preparation

Analysis of MP by py-GCMS in biological samples demands complete removal of proteins and fats while maintaining the integrity of the plastic polymers, as remnants of organic material, proteins and fats will hamper the chemical characterization. Currently recommended methods (Loder et al., 2017; Gomiero et al., 2019b; Gomiero et al., 2020b) use gentle enzymatic digestion and oxidizing agents, which is time consuming and costly. This leads to small volumes of tissue used (≤30 g), resulting in high LOQs. Larger samples or a higher number of replicates would mean a better representation of the organ sampled, but require more time and reagents, increasing costs. The current enzymatic digestion and preparation thus makes the analyses time consuming and expensive and the high costs are an obstacle to perform large studies with a sufficiently high number of samples or replicates for a better resolution of the data. The low sensitivity and low number of samples with quantified microplastic concentrations in this study hampers statistical analyses.

Are Samples Representative?

In this study we performed replicate analysis of the cod muscle and livers, to investigate how representative a small sample is. Our results showed that concentrations of MP were above LOQ in one of four replicates of cod muscle and one of two parallel liver samples, performed in two cod. This means that small sample volumes and limitations of cost and time to single replicates in all the other samples may have led to false negatives.

Sensitivity

The LOQ for py-GCMS corresponds to the plastic mass of one spherical particle of about 10 μm in size. The 10 μm filters used theoretically limit the size to >10 μm, but smaller particles can also be trapped on the filters. In support of the suspected uneven MP distribution in tissues, no MP in any sample was observed by PLM. The finding of concentrations close to LOQ, at the same time as no observations were made of MP by PLM, may also indicate that MP are present as very small particles that may evade detection by PLM. The indications of a patchy distribution of MP also implies that a thin section of tissue is likely to miss the MPs when present at low concentrations, and that a higher number of samples would be needed to observe MP embedded in the tissues. High exposure concentrations have been used to investigate modes of uptake and excretion, and to determine target organs for MP (Volkheimer et al., 1968; Deng et al., 2017), and so far current environmental levels of microplastics are far from these high-exposure conditions.

Reliability, Quality Control

Neither PVC nor PET were observed in the control samples, whereas PS was observed in one control sample throughout the lab work (**Supplementary Table S2**). Evidence of polymers in tissues that were not present in the lab or in contamination controls, indicate that MP observed in tissues from internal organs is not contamination from the lab environment but represent actual uptake of PVC into wildlife.

Potential Human Exposure Through Food

This study is not sufficient to draw conclusions on human exposure through ingestion of wild caught fish or birds. To conclude on human exposure through ingestion of food, a larger sample size would be needed. The current study documents the presence of MP, but results indicate that positive findings are correlated with a higher number of replicate analyses, or a higher sample volume. Due to the indication of patchy distribution of MP in organs, it may, moreover, be inaccurate to extrapolate from the concentrations in a tissue sample to the entire organ. Thus, the concentrations cannot be considered representative of the average and the few replicates from cod fillet or cod liver are insufficient to draw conclusions on human exposure through consumption of these tissues. Presence in the alimentary tract is moreover not an indication of harm caused to the animal, but is an evidence of oral intake, indicating likely uptake of MP over the intestine.

CONCLUSION

This novel study demonstrates that low levels of MP in tissues of wild animals can be detected and quantified by current methods. This is to our knowledge the first study to demonstrate MP in tissues of birds exposed to relevant environmental concentrations of plastics and microplastics in their natural habitat.

Presence of MP does not document bioaccumulation or biomagnification but may represent recently absorbed particles in blood vessels, absorbed into tissues or in the process of being excreted. Observations of higher levels in the liver may suggest that the liver is involved in uptake or excretion of MP.

The concentrations in tissues are currently close to, and sometimes below the Limit of Quantification, and it is likely that there are several false negatives due to a limited number of replicates. The study, however, does not demonstrate that analytical methods are sufficiently sensitive to detect current levels of MP in wildlife, and that it is now possible to start investigating baseline levels of MP in environmentally exposed animals.

The contamination control shows low levels of contamination and no evidence of the most frequently observed polymer in tissues, PVC. The number of false positives is expected to be low, and we believe the methods are more likely to underestimate than over-estimate the concentrations.

Although the levels are currently low, the presence indicates uptake into biota and a potential transfer throughout the food web, including humans, through ingestion of muscle tissue or liver from wild fish and birds. The study does not permit conclusions at this stage on human exposure through wild caught food.

No detrimental effects of current levels of MP are observed. However, the current study, with a low number of positive findings of MP in tissues, is too small to conclude on detrimental or non-detrimental effects of MP.

Method development is needed to map MP distribution and potential accumulation in tissues in a cost-efficient manner. The sensitivity of current methods for MP quantification is not comparable to the analytical sensitivity for other environmental contaminants. It is expected that the sensitivity of the analyses will improve in the years to come, and that lower concentrations can be detected with small sample volumes. This will give highly desired data for potential human exposure through food. It is of the highest interest to elucidate the mechanisms of uptake, transport and excretion following realistic exposure levels in wildlife, and the following potential for human exposure through food. Data from a higher number of species, individuals and investigated areas is needed to provide relevant Environmental Risk Assessments for coastal regions.

This study documents MP throughout different tissues from several wild species exposed through their natural habitat. In combination with the evidence of patchiness of MP within tissues and likely false negatives, this warrants more studies with a higher number of species, individuals and replicates from several regions, highly plastic polluted or clean, to increase the understanding of current microplastic pollution in the coastal ecosystem and the potential harm to the ecosystem health and human exposure through edible tissues.

DATA AVAILABILITY STATEMENT

The raw data supporting the conclusions of this article will be made available by the authors, without undue reservation.

ETHICS STATEMENT

Ethical review and approval was not required because the studies did not involve tests on live animals but analyzed tissues of dead animals accidentally caught as bycatch in fishing nets and delivered to us by local fishermen. The fish caught for analyses were caught by recreational fishermen and were lawful harvest of sustainable fish-stocks.

AUTHOR CONTRIBUTIONS

MH, AG, AO, HN, and JS contributed conception and design of the study. MH had the main responsibility for application and project organization. MH, JS, AO, and HN performed the autopsies and sampling. AG developed the method and performed the chemical analyses for microplastics, JS and AO performed histopathology and pathogen analysis. MH organized the data, wrote the first draft of the manuscript. AO, JS, and AG wrote sections of the manuscript. All authors contributed to manuscript revision, read and approved the submitted version.

FUNDING

Funded by Plastreturs Miljøprosjekt. In-kind funding by The Norwegian Veterinary Institute, Norwegian Association of Hunters and Anglers and Norwegian Research Centre (NORCE).

ACKNOWLEDGMENTS

Thanks to Kenneth Bruvik and Rune Gaasø for essential contributions to the initialization and realization of the project, for delivery of bycatch of birds and mammals, and thanks to pupils from TAM for catching fish for the project. Thanks to involved personnel: Kjell-Birger Øysæd at NORCE PlastLab for assistance in the py-GCMS analyses, Eivind Bastesen for creating maps, and the technical staff at NVI and students at the University of Bergen for laboratory assistance during autopsies.

SUPPLEMENTARY MATERIAL

The Supplementary Material for this article can be found online at: https://www.frontiersin.org/articles/10.3389/fenvs.2021.575058/full#supplementary-material.

REFERENCES

Andrady, A. L., Hamid, H. S., and Torikai, A. (2003). Effects of climate change and UV-B on materials. *Photochem. Photobiol. Sci.* 2 (1), 68–72. doi:10.1039/b211085g

Andrady, A. L. (2011). Microplastics in the marine environment. *Mar. Pollut. Bull.* 62 (8), 1596–1605. doi:10.1016/j.marpolbul.2011.05.030

Andrady, A. L. (2017). The plastic in microplastics: a review. *Mar. Pollut. Bull.* 119 (1), 12–22. doi:10.1016/j.marpolbul.2017.01.082

Avio, C. G., Gorbi, S., and Regoli, F. (2015). Experimental development of a new protocol for extraction and characterization of microplastics in fish tissues: first observations in commercial species from Adriatic Sea. *Mar. Environ. Res.* 111, 18–26. doi:10.1016/j.marenvres.2015.06.014

Barnes, D. K., Galgani, F., Thompson, R. C., and Barlaz, M. (2009). Accumulation and fragmentation of plastic debris in global environments. *Philos. Trans. R. Soc. Lond. B, Biol. Sci.* 364 (1526), 1985–1998. doi:10.1098/rstb.2008.0205

Bastesen, E., Haave, M. H. A., and Neby, S. (2020). Utvikling av kartleggingsmetoder og estimat for oppryddingskostnader for makroplast i strandsonen. NORCE report 4-2020, 9.

Baumann, L., Schmidt-Posthaus, H., Segner, H., and Wolf, J. C. (2016). Comment on "uptake and accumulation of polystyrene microplastics in zebrafish (Danio rerio) and toxic effects in liver". *Environ. Sci. Technol.* 50 (22), 12521–12522. doi:10.1021/acs.est.6b04193

Bergmann, M., Mützel, S., Primpke, S., Tekman, M. B., Trachsel, J., and Gerdts, G. (2019). White and wonderful? Microplastics prevail in snow from the alps to the arctic. *Sci. Adv.* 5 (8), eaax1157. doi:10.1126/sciadv.aax1157

Bergmann, M., Wirzberger, V., Krumpen, T., Lorenz, C., Primpke, S., Tekman, M. B., et al. (2017). High quantities of microplastic in arctic deep-sea sediments from the HAUSGARTEN observatory. *Environ. Sci. Technol.* 51 (19), 11000–11010. doi:10.1021/acs.est.7b03331

Bråte, I. L. N., Eidsvoll, D. P., Steindal, C. C., and Thomas, K. V. (2016). Plastic ingestion by Atlantic cod (Gadus morhua) from the Norwegian coast. *Mar. Pollut. Bull.* 112 (1–2), 105–110. doi:10.1016/j.marpolbul.2016.08.034

Bravo Rebolledo, E. L., Van Franeker, J. A., Jansen, O. E., and Brasseur, S. M. (2013). Plastic ingestion by harbour seals (Phoca vitulina) in The Netherlands. *Mar. Pollut. Bull.* 67 (1–2), 200–202. doi:10.1016/j.marpolbul.2012.11.035

Browne, M. A., Dissanayake, A., Galloway, T. S., Lowe, D. M., and Thompson, R. C. (2008). Ingested microscopic plastic translocates to the circulatory system of the mussel, Mytilus edulis (L). *Environ. Sci. Technol.* 42 (13), 5026–5031. doi:10.1021/es800249a

Cannon, G. J., and Swanson, J. A. (1992). The macrophage capacity for phagocytosis. *J. Cell Sci.* 101 (Pt 4), 907–913.

Carr, K. E., Smyth, S. H., McCullough, M. T., Morris, J. F., and Moyes, S. M. (2012). Morphological aspects of interactions between microparticles and mammalian cells: intestinal uptake and onward movement. *Prog. Histochem. Cytochem.* 46 (4), 185–252. doi:10.1016/j.proghi.2011.11.001

Collard, F., Gilbert, B., Compère, P., Eppe, G., Das, K., Jauniaux, T., et al. (2017). Microplastics in livers of European anchovies (Engraulis encrasicolus, L). *Environ. Pollut.* 229, 1000–1005. doi:10.1016/j.envpol.2017.07.089

Courtene-Jones, W., Quinn, B., Gary, S. F., Mogg, A. O. M., and Narayanaswamy, B. E. (2017). Microplastic pollution identified in deep-sea water and ingested by benthic invertebrates in the Rockall Trough, North Atlantic Ocean. *Environ. Pollut.* 231 (Pt 1), 271–280. doi:10.1016/j.envpol.2017.08.026

Deng, Y., Zhang, Y., Lemos, B., and Ren, H. (2017). Tissue accumulation of microplastics in mice and biomarker responses suggest widespread health risks of exposure. *Sci. Rep.* 7, 46687. doi:10.1038/srep46687

Dris, R., Gasperi, J., Saad, M., Mirande, C., and Tassin, B. (2016). Synthetic fibers in atmospheric fallout: a source of microplastics in the environment? *Mar. Pollut. Bull.* 104 (1–2), 290–293. doi:10.1016/j.marpolbul.2016.01.006

Everaert, G., Van Cauwenberghe, L., De Rijcke, M., Koelmans, A. A., Mees, J., Vandegehuchte, M., et al. (2018). Risk assessment of microplastics in the ocean: modelling approach and first conclusions. *Environ. Pollut.* 242 (Pt B), 1930–1938. doi:10.1016/j.envpol.2018.07.069

Ferreira, G. V. B., Barletta, M., Lima, A. R. A., Morley, S. A., and Costa, M. F. (2019). Dynamics of marine debris ingestion by profitable fishes along the estuarine ecocline. *Sci. Rep.* 9 (1), 13514. doi:10.1038/s41598-019-49992-3

Fischer, M., and Scholz-Böttcher, B. M. (2017). Simultaneous trace identification and quantification of common types of microplastics in environmental samples by pyrolysis-gas chromatography-mass Spectrometry. *Environ. Sci. Technol.* 51 (9), 5052–5060. doi:10.1021/acs.est.6b06362

Florence, A. T. (1997). The oral absorption of micro- and nanoparticulates: neither exceptional nor unusual. *Pharm. Res.* 14 (3), 259–266. doi:10.1023/a:1012029517394

Frydkjaer, C. K., Iversen, N., and Roslev, P. (2017). Ingestion and egestion of microplastics by the cladoceran Daphnia magna: effects of regular and irregular shaped plastic and sorbed phenanthrene. *Bull. Environ. Contam. Toxicol.* 99 (6), 655–661. doi:10.1007/s00128-017-2186-3

Fuglem, B., Jirillo, E., Bjerkås, I., Kiyono, H., Nochi, T., Yuki, Y., et al. (2010). Antigen-sampling cells in the salmonid intestinal epithelium. *Dev. Comp. Immunol.* 34 (7), 768–774. doi:10.1016/j.dci.2010.02.007

Gomiero, A., Strafella, P., Øysæd, K. B., and Fabi, G. (2019a). First occurrence and composition assessment of microplastics in native mussels collected from coastal and offshore areas of the northern and central Adriatic Sea. *Environ. Sci. Pollut. Res. Int.* 26 (24), 24407–24416. doi:10.1007/s11356-019-05693-y

Gomiero, A., Øysæd, K. B., Agustsson, T., van Hoytema, N., van Thiel, T., and Grati, F. (2019b). First record of characterization, concentration and distribution of microplastics in coastal sediments of an urban fjord in south west Norway using a thermal degradation method. *Chemosphere* 227, 705–714. doi:10.1016/j.chemosphere.2019.04.096

Gomiero, A., Haave, M., Bjørøy, Ø., Herzke, D., Kögel, T., Nikiforov, V., et al. (2020a). Quantification of microplastic in fillet and organs of farmed and wild salmonids-a comparison of methods for detection and quantification (SALMODETECT). NORCE report 8-2020, 43.

Gomiero, A., Marte, H., Tanja, K., Ørjan, B., Mona, G., Trygve, B. L., et al. (2020b). Tracking of Plastic emissions from aquaculture industry (TrackPlast). NORCE report 4-2020 NORCE, 71.

Haave, M., Lorenz, C., Primpke, S., and Gerdts, G. (2019). Different stories told by small and large microplastics in sediment - first report of microplastic concentrations in an urban recipient in Norway. *Mar. Pollut. Bull.* 141, 501–513. doi:10.1016/j.marpolbul.2019.02.015

Hartmann, N. B., Hüffer, T., Thompson, R. C., Hassellöv, M., Verschoor, A., Daugaard, A. E., et al. (2019). Are we speaking the same language? Recommendations for a definition and categorization framework for plastic debris. *Environ. Sci. Technol.* 53 (3), 1039–1047. doi:10.1021/acs.est.8b05297

Hermabessiere, L., Himber, C., Boricaud, B., Kazour, M., Amara, R., Cassone, A. L., et al. (2018). Optimization, performance, and application of a pyrolysis-GC/MS

method for the identification of microplastics. *Anal Bioanal. Chem.* 410 (25), 6663–6676. doi:10.1007/s00216-018-1279-0

Jambeck, J. R., Geyer, R., Wilcox, C., Siegler, T. R., Perryman, M., Andrady, A., et al. (2015). Marine pollution. Plastic waste inputs from land into the ocean. *Science* 347 (6223), 768–771. doi:10.1126/science.1260352

Jensen, H. K. B., and Cramer, J. (2017). *MAREANOs pilotprosjekt på mikroplast-resultater og forslag til videre arbeid*. NGU 2017.043.

Karami, A., Groman, D. B., Wilson, S. P., Ismail, P., and Neela, V. K. (2017). Biomarker responses in zebrafish (Danio rerio) larvae exposed to pristine low-density polyethylene fragments. *Environ. Pollut.* 223, 466–475. doi:10.1016/j.envpol.2017.01.047

Lebreton, L., and Andrady, A. (2019). Future scenarios of global plastic waste generation and disposal. *Palgrave Commun.* 5 (1), 6. doi:10.1057/s41599-018-0212-7

Lebreton, L. C. M., van der Zwet, J., Damsteeg, J. W., Slat, B., Andrady, A., and Reisser, J. (2017). River plastic emissions to the world's oceans. *Nat. Commun.* 8, 15611. doi:10.1038/ncomms15611

Löder, M. G. J., Imhof, H. K., Ladehoff, M., Löschel, L. A., Lorenz, C., Mintenig, S., et al. (2017). Enzymatic purification of microplastics in environmental samples. *Environ. Sci. Technol.* 51 (24), 14283–14292. doi:10.1021/acs.est.7b03055

Lu, Y., Zhang, Y., Deng, Y., Jiang, W., Zhao, Y., Geng, J., et al. (2016). Uptake and accumulation of polystyrene microplastics in Zebrafish (Danio rerio) and toxic effects in liver. *Environ. Sci. Technol.* 50 (7), 4054–4060. doi:10.1021/acs.est.6b00183

Lusher, A., Hollman, P., and Mendoza-Hill, J. (2017). *Microplastics in fisheries and aquaculture- Status of knowledge on their occurrence and implications for aquatic organisms and food safety*. FAO Fisheries and Aquaculture, Technical Paper 615(147).

Lusher, A. L., McHugh, M., and Thompson, R. C. (2013). Occurrence of microplastics in the gastrointestinal tract of pelagic and demersal fish from the English Channel. *Mar. Pollut. Bull.* 67 (1–2), 94–99. doi:10.1016/j.marpolbul.2012.11.028

Lusher, A. L., O'Donnell, C., Officer, R., and O'Connor, I. (2016). Microplastic interactions with North Atlantic mesopelagic fish. *Ices J. Mar. Sci.* 73 (4), 1214–1225. doi:10.1093/icesjms/fsv241

Mattsson, K., Ekvall, M. T., Hansson, L. A., Linse, S., Malmendal, A., and Cedervall, T. (2015). Altered behavior, physiology, and metabolism in fish exposed to polystyrene nanoparticles. *Environ. Sci. Technol.* 49 (1), 553–561. doi:10.1021/es5053655

Mattsson, K., Johnson, E. V., Malmendal, A., Linse, S., Hansson, L. A., and Cedervall, T. (2017). Brain damage and behavioural disorders in fish induced by plastic nanoparticles delivered through the food chain. *Sci. Rep.* 7 (1), 11452. doi:10.1038/s41598-017-10813-0

Munari, C., Infantini, V., Scoponi, M., Rastelli, E., Corinaldesi, C., and Mistri, M. (2017). Microplastics in the sediments of terra nova bay (ross sea, Antarctica). *Mar. Pollut. Bull.* 122 (1–2), 161–165. doi:10.1016/j.marpolbul.2017.06.039

Onink, V., Wichmann, D., Delandmeter, P., and van Sebille, E. (2019). The role of ekman currents, geostrophy, and Stokes drift in the accumulation of floating microplastic. *J. Geophys. Res. Oceans* 124 (3), 1474–1490. doi:10.1029/2018JC014547

Ory, N. C., Gallardo, C., Lenz, M., and Thiel, M. (2018). Capture, swallowing, and egestion of microplastics by a planktivorous juvenile fish. *Environ. Pollut.* 240, 566–573. doi:10.1016/j.envpol.2018.04.093

Ribeiro, F., O'Brien, J. W., Galloway, T., and Thomas, K. V. (2019). Accumulation and fate of nano- and micro-plastics and associated contaminants in organisms. *Trac Trends Anal. Chem.* 111, 139–147. doi:10.1016/j.trac.2018.12.010

Rummer, J. L., Wang, S., Steffensen, J. F., and Randall, D. J. (2014). Function and control of the fish secondary vascular system, a contrast to mammalian lymphatic systems. *J. Exp. Biol.* 217 (Pt 5), 751–757. doi:10.1242/jeb.086348

Ryan, P. G., Lamprecht, A., Swanepoel, D., and Moloney, C. L. (2014). The effect of fine-scale sampling frequency on estimates of beach litter accumulation. *Mar. Pollut. Bull.* 88 (1–2), 249–254. doi:10.1016/j.marpolbul.2014.08.036

SAPEA (2019). A scientific perspective on microplastics in nature and society. *SAPEA Evid. Rev. Rep.* 4, 173. doi:10.26356/microplastics

Silva, J. D. B., Barletta, M., Lima, A. R. A., and Ferreira, G. V. B. (2018). Use of resources and microplastic contamination throughout the life cycle of grunts (Haemulidae) in a tropical estuary. *Environ. Pollut.* 242: 1010–1021. doi:10.1016/j.envpol.2018.07.038

Skåre, J. U., Alexander, J., Haave, M., Jakubowicz, I., Knutsen, H. K., Lusher, A., et al. (2019). Microplastics; occurrence, levels and implications for environment and human health related to food. Scientific opinion of the Scientific Steering Committee of the Norwegian Scientific Committee for Food and Environment. Oslo, Norway: Norwegian Scientific Committee for Food and Environment (VKM), 16.

Smith, M., Love, D. C., Rochman, C. M., and Neff, R. A. (2018). Microplastics in seafood and the implications for human health. *Curr. Environ. Health Rep.* 5 (3), 375–386. doi:10.1007/s40572-018-0206-z

Smith, S. D. A., and Markic, A. (2013). Estimates of marine debris accumulation on beaches are strongly affected by the temporal scale of sampling. *PLoS One* 8 (12), e83694. doi:10.1371/journal.pone.0083694

Urbanek, A. K., Rymowicz, W., and Mirończuk, A. M. (2018). Degradation of plastics and plastic-degrading bacteria in cold marine habitats. *Appl. Microbiol. Biotechnol.* 102 (18), 7669–7678. doi:10.1007/s00253-018-9195-y

Van Cauwenberghe, L., Claessens, M., Vandegehuchte, M. B., and Janssen, C. R. (2015). Microplastics are taken up by mussels (Mytilus edulis) and lugworms (Arenicola marina) living in natural habitats. *Environ. Pollut.* 199, 10–17. doi:10.1016/j.envpol.2015.01.008

Van Cauwenberghe, L., and Janssen, C. R. (2014). Microplastics in bivalves cultured for human consumption. *Environ. Pollut.* 193, 65–70. doi:10.1016/j.envpol.2014.06.010

Volkheimer, G., Schulz, F. H., Lehmann, H., Aurich, I., Hübner, R., Hübner, M., et al. (1968). Primary portal transport of persorbed starch granules from the intestinal wall. *Med. Exp. Int. J. Exp. Med.* 18 (2), 103–108. doi:10.1159/000137143

Volkheimer, G. (1975). Hematogenous dissemination of ingested polyvinyl chloride particles. *Ann. N. Y Acad. Sci.* 246, 164–171. doi:10.1111/j.1749-6632.1975.tb51092.x

Volkheimer, G. (1993). [Persorption of microparticles]. *Pathologe* 14 (5), 247–252.

Volkheimer, G. (2001). The phenomenon of persorption: persorption, dissemination, and elimination of microparticles. in *Old Herborn University Seminar Monograph*. Herborn: Herborn Litterae, 14, 7–18.

Watts, A. J., Lewis, C., Goodhead, R. M., Beckett, S. J., Moger, J., Tyler, C. R., et al. (2014). Uptake and retention of microplastics by the shore crab Carcinus maenas. *Environ. Sci. Technol.* 48 (15), 8823–8830. doi:10.1021/es501090e

Woodall, L. C., Sanchez-Vidal, A., Canals, M., Paterson, G. L., Coppock, R., Sleight, V., et al. (2014). The deep sea is a major sink for microplastic debris. *R. Soc. Open Sci.* 1 (4), 140317. doi:10.1098/rsos.140317

Woods, M. N., Stack, M. E., Fields, D. M., Shaw, S. D., and Matrai, P. A. (2018). Microplastic fiber uptake, ingestion, and egestion rates in the blue mussel (Mytilus edulis). *Mar. Pollut. Bull.* 137, 638–645. doi:10.1016/j.marpolbul.2018.10.061

Wright, S. L., Ulke, J., Font, A., Chan, K. L. A., and Kelly, F. J. (2020). Atmospheric microplastic deposition in an urban environment and an evaluation of transport. *Environ. Int.* 136, 105411. doi:10.1016/j.envint.2019.105411

Conflict of Interest: The authors declare that the research was conducted in the absence of any commercial or financial relationships that could be construed as a potential conflict of interest.

frontiers in Marine Science

ORIGINAL RESEARCH
published: 08 April 2021
doi: 10.3389/fmars.2021.594415

Urban Microplastics Emissions: Effectiveness of Retention Measures and Consequences for the Baltic Sea

Gerald Schernewski[1,2], Hagen Radtke[1], Rahel Hauk[1], Christian Baresel[3], Mikael Olshammar[3] and Sonja Oberbeckmann[1]*

[1] Leibniz Institute for Baltic Sea Research, Rostock, Germany, [2] Marine Research Institute, Klaipëda University, Klaipëda, Lithuania, [3] IVL Swedish Environmental Research Institute, Stockholm, Sweden

OPEN ACCESS

Edited by:
Montserrat Filella, Université de Genève, Switzerland

Reviewed by:
Britta Denise Hardesty, Commonwealth Scientific and Industrial Research Organisation (CSIRO), Australia
Begoña Jiménez, Consejo Superior de Investigaciones Científicas (CSIC), Spain

***Correspondence:**
Gerald Schernewski
gerald.schernewski@io-warnemuende.de;
schernewski@eucc-d.de

Specialty section:
This article was submitted to Marine Pollution, a section of the journal Frontiers in Marine Science

Received: *13 August 2020*
Accepted: *17 February 2021*
Published: *08 April 2021*

Citation:
Schernewski G, Radtke H, Hauk R, Baresel C, Olshammar M and Oberbeckmann S (2021) Urban Microplastics Emissions: Effectiveness of Retention Measures and Consequences for the Baltic Sea. Front. Mar. Sci. 8:594415. doi: 10.3389/fmars.2021.594415

Urban sewage water pathways seem most important for microplastics emissions to the Baltic Sea. We use microplastics emission data for the entire Baltic Sea region, calculate emissions for three sewage water related urban pathways and develop emission scenarios for the majority of microplastics particles. All plastics are divided into potentially floating (density 0.8–1.0 g/cm³) and sinking (1.1–1.5 g/cm³) polymers and we address the size class of 20–500 μm. 6.7×10^{13} microplastics particles enter the Baltic Sea annually from urban pathways. 62% result from stormwater runoff including sewer overflow, 25% from wastewater treatment plants (WWTPs) and 13% from untreated wastewater. The emission scenarios serve as input for 3D-model simulations, which allow estimating transport, behaviour and deposition in the Baltic Sea environment. Our model approach suggests average annual microplastics concentrations in the water body of the central Baltic Sea of 1–4 particles/m^2 sea surface and 1 particle/m^3 in the upper 2 m sea surface layer. The majority of the particles is accumulated in upper sea surface layers. The model suggests that only between 6% (Arcona Basin) and 21% (Gotland Basin) of the particles are below a depth of 25 m. In coastal waters, the concentrations can exceed 10 particles/m^3 in the upper 2 m surface water layer (e.g., Gulf of Riga, Gulf of Gdansk) and 1 particle/m^2 on the sediment surface. Usually within weeks, emitted microplastics are washed ashore causing annual coastal accumulations of up to 10^9 particles/m coastline within a few kilometres distance to emission sources. On average, above 10^6 particles/m are annually accumulated and trapped at coasts around the Baltic Sea. The reduction of the annual sewer overflow from presently 1.5% of the annual wastewater loads to 0.3% would reduce the total emissions to the Baltic Sea by 50%. If all sewage water would be connected to WWTPs and undergo a tertiary treatment, a reduction of 14.5% of the total emissions could be achieved. The effect of retention in rivers seems limited in the Baltic Sea region, because near coast emissions contribute around 50% of the total microplastics emissions.

Keywords: wastewater, stormwater, sewer overflow, hydrodynamics, beach, retention, sediment

INTRODUCTION

Microplastic covers the size class below 5 mm. The overwhelming majority of microplastics losses (98%) are generated during land-based activities (Boucher and Friot, 2017). With 66%, road runoff is the main pathway, followed by wastewater treatment systems with 25%. River discharge plays a major role for marine plastic pollution (Bergmann et al., 2015; Schmidt et al., 2020). The top 20 polluting rivers, mostly located in Asia, account for 67% of the global total emissions (Boucher and Friot, 2017; Lebreton et al., 2017).

The Baltic Sea is one of the largest brackish water bodies in the world and, with respect to eutrophication and organic chemicals, a pollution hot-spot (HELCOM, 2018b). The Baltic Sea catchment is about four times larger than the surface area (420,000 km^2) and it is inhabited by about 85 million people living in nine countries. The mean annual riverine runoff to the Baltic Sea is 14,425 mł/s (HELCOM, 2018c) and comparable to rivers such as the Mississippi, the Mekong or the Ganges. Therefore, it can be expected that the Baltic is an emission hot-spot for plastics, as well, and that emissions with rivers play the dominating role.

Siegfried et al. (2017) calculated a microplastics load to the Baltic Sea of about 1,000 t/a, including personal care products, laundry textiles, household dust and car tyre wear. Bollmann et al. (2019) assume a total annual microplastics load of 0.2 t/a from urban pathways and a resulting concentration of 0.2 ng/l microplastics in the Baltic Sea. These existing calculations for the Baltic Sea are conceptual, utilize only limited and aggregated data and possess a very high uncertainty. Further, these values differ strongly, do not address particle numbers, but masses and do not allow a comparison with field data. The knowledge about pathways is still very limited (Wagner et al., 2018).

Since human activities are the source for microplastics, wastewater is considered as a major emission pathway (e.g., Mintenig et al., 2016; Ziajahromi et al., 2016; Kay et al., 2018; Prata, 2018). For untreated wastewater, high microplastic concentrations between 10^1 and10^4 particles/L are reported (Gatidou et al., 2019; Sun et al., 2019), but municipal wastewater treatment plants (WWTPs) are efficient in removing microplastics (Carr et al., 2016; Talvitie et al., 2017; Gies et al., 2018). For WWTPs in the Baltic Sea region, Baresel and Olshammar (2019) assumed a microplastics retention between 85 and 98%. The mostly efficient sewage treatment is one explanation for the relatively low estimated microplastic emissions to the Baltic Sea (Siegfried et al., 2017). On the other hand, microplastic emissions with sewer overflow water seems to be an underestimated pathway. Sewer overflow water consists of stormwater and untreated wastewater. In the Baltic, overflow events happen rarely. Despite that, Baresel and Olshammar (2019) conclude that the annual discharge of microplastics from sewer overflows can be in the same magnitude as from treated wastewater.

Another uncertainty and largely unknown factor with high relevance for the total microplastics emissions to seas, is the retention in river systems. Several publications show that the retention in rivers depends on particle size, shape and density (e.g., Nizzetto et al., 2016; Besseling et al., 2017 Kooi et al., 2018). Besseling et al. (2017) carried out scenario studies with a hydrological model and conclude that in 40 km river practically all particles (>100 μm, spherical polystyrene) are kept back. But it remains uncertain whether this retention is permanent or only temporary. As a consequence, some studies take retention into account in emission calculations (e.g., Siegfried et al., 2017) and others do not (e.g., Nizzetto et al., 2016; van Wijnen et al., 2019). Windsor et al. (2019) conclude that still little is known about the residence time of plastics in rivers and the role of rivers as temporary sinks.

The lack of knowledge about microplastics emission quantities and pathways is contrasted by a high societal demand (GESAMP, 2016). HELCOM (2018a) still state that an assessment of the state of pollution with respect to marine litter is still not possible for the Baltic Sea, because operational indicators are lacking. This is especially true for microplastics and indicates urgent research needs. The European Union (EU) is well aware of the plastic problem, too. The EU Marine Strategy Framework Directive (MSFD 2008/56/EC) addresses this problem and requires identifying and quantifying major emission sources and pathways as well as the assessment of effective measures to reduce marine litter pollution in general, and microplastics pollution in specific (JRC, 2011).

In a previous study, we calculated the emissions of two selected microplastic polymers from all urban pathways in the Baltic Sea basin and simulated their transport and behaviour in the Baltic Sea. Focus was on the behaviour of different size classes and particle shapes (Schernewski et al., 2020). In this study our objectives are to (a) expand this approach and take into account all floating and sinking microplastics and the majority of all urban microplastic emissions; (b) calculate the spatial emission pattern from all urban pathways in the Baltic Sea catchment (including Kattegatt), namely wastewater treatment plants (WWTP), combined sewer overflow systems (CSS) including urban stormwater runoff as well as untreated wastewater (not connected to WWTPs); (c) perform 3D-model simulations on transport, behaviour, deposition and concentrations in the Baltic Sea environment (neglecting separate size classes and shapes); (d) calculate the consequences of spatially differentiated retention factors in rivers on the total emissions and (e) assess the effectiveness of emission reduction measures with focus on sanitary sewer overflows and WWTPs.

MATERIALS AND METHODS

Microplastics in Raw Waste- and Stormwater

The density of plastics (artificial polymers) is an important parameter that determines its transport, behaviour and deposition in the aquatic environment. According to the density, we separated two groups, floating and sinking polymer types. The first group covers floating polymers, such as low and high density polyethylene (PE, 0.915–0.97 g/cmł density), polypropylene (PP, 0.89–0.92 g/cmł density) and polystyrene (PS, 0.96–1.05 g/cm^3) or polymers that have a density close to saline

water such as acrylic and polystyrene (1,05 g/cmł density). The group of sinking polymers covers rigid polyvinyl chloride (PVC, 1.3–1.45 g/cmł density), the polyester polyethylene terephthalate (PET, 1.38 g/cmł density), polyamide (PA, 1.14 g/cmł density), polyethersulfone (PES, 1.37 g/cmł density) and polyurethane (PU 1.2 g/cmł). According to Liu et al. (2019) and Olesen et al. (2019) all these polymers cover over 95% of all polymers found in stormwater ponds in Baltic countries. The share of polymers in wastewater varies in a wide range (e.g., Kang et al., 2018). However, Sun et al. (2019) considers PP, PE and PET as the most abundant polymers in WWTPs. Lv et al. (2019) analysed raw wastewater and found 47% PET, 20% PS, 18% PE and 15% PP. Kooi and Koelmans (2019) regard PE (25%), PET (16.5%) and PP (14%) as the most common microplastic polymer types in the aquatic environment. Another indication which plastic polymers can be expected in the aquatic environment provide the production volumes: PE, PP, PVC, PS, and PET belong to the six most commonly produced polymers worldwide (Vermeiren et al., 2016; Geyer et al., 2017; Kooi et al., 2018). Based on this literature, we assume that both polymer groups, floating and sinking, have a share of about 50% each. Further, we assume that our two polymer groups are in general representative and cover the vast majority of all plastics in urban pathways. In the model simulations, a density of 0.9 g/cmł is assumed for the floating and 1.4 for g/cmł for the sinking polymer group.

Microplastics Retention and Emission Calculations

Based on a comprehensive literature survey (Magnusson and Norén, 2014; Talvitie et al., 2015; Magnusson et al., 2016; Murphy et al., 2016; Gies et al., 2018; Kang et al., 2018; Lares et al., 2018; Simon et al., 2018; Long et al., 2019; Sun et al., 2019; Wolff et al., 2019), we calculated an average number of microplastics in raw wastewater (WWTPs influents) of 134,000 particles/mł and a median of 85,000 particles/mł. We applied the median concentration, because it better reflects the results found in northern and central European studies.

Combined sewer systems (CSS), which are common in urban areas of the Baltic Sea region, collect surface water runoff, domestic sewage and industrial wastewater. Baresel and Olshammar (2019) compiled the data for all known 3525 WWTPs in the Baltic Sea region and quantified the amount of sewage water (**Figure 1a**). Further the authors calculated the average MP removal efficiency in WWTPs depending on the treatment technology for primary treatment (85%), secondary treatment (90%), tertiary treatment (N and P removal) (95%), sand filtration (97%) and microfiltration (98%). The MP concentration in influent sewage water and the removal efficiency of each WWTP allowed the quantification of the annual MP-discharge from WWTPs into the river systems of the Baltic Sea region. For details see Baresel and Olshammar (2019). We complemented missing data for single WWTPs based on country specific average amounts of wastewater per person and day as well as taking into account the country specific percentage of the population connected to WWTPs.

In CSS, sanitary sewer overflows take place, where untreated wastewater is discharged from a sanitary sewer into the aquatic environment. Usually this happens due to a temporary insufficient hydraulic capacity after heavy precipitation. Baresel and Olshammar (2019) assumed that in the Baltic Sea region, weather related sanitary sewer overflow accounts for 1.5% of the total WWTP inflow. Separated sewer systems (SSS) collect storm water and wastewater in separated systems. In these systems storm water is often released into the aquatic environment without treatment. For the Baltic Sea region reliable numbers about the water discharge from SSS are lacking. We assumed that SSS have a share of 50% in the Baltic Sea region. We did not treat SSS as separate pathway but are integrated stormwater it into CSS emissions.

Model simulations on transport, behaviour and deposition of MP in the marine environment require the spatially resolved concentrations of MP in and the amount of discharge water at the land/sea interface as model input. The microplastics emissions from every WWTP were calculated, taking into account the specific microplastics removal efficiency (treatment technology), the WWTPs were allocated in and assigned to the river basins. Since the retention in river basins is crucial for the total emitted number of particles to the sea and varies depending on the length of the river basin and the location of the WWTPs in the basin, we used an Excel-based tool to enable a flexible pre-processing of the emission data used as model input. In this tool, the distance of every WWTP to the river mouth was calculated, which generally allowed to enter specific retention factors (% particle retention/km) for different plastic types and size classes. We assumed that coastal cities discharge directly into the sea without any retention. However, the calculation of specific river retention rates is linked to a very high uncertainty. Including river retention in the scenarios would overlay the results and uncertainties of the mitigation measures. Therefore, the role of river retention was analysed separately and in scenarios dealing with mitigation measures no microplastics retention during the transport in the river was taken into account.

Model Approach

The modelling approach followed Osinski and Radtke (2020). We used the UERRA high-resolution atmospheric reconstruction, provided by SMHI, to drive both a third-generation wave model (WAVEWATCH 3) and a hydrodynamic model for the Baltic Sea (GETM). Both models have a horizontal resolution of one nautical mile. A microplastics transport module is added integrated online into the hydrodynamic model following Osinski et al. (2020). The wave model provides wave properties required for the calculation of bottom shear stress, and the hydrodynamic model provides the current field used for the passive transport of the particles, which are represented in a Eulerian framework as a concentration per grid cell. The size, density and shape of the particles determine the vertical velocity relative to the ambient water and the critical shear stress for the resuspension. The actual shear stress at each time step was calculated from the bottom current velocity and the significant wave height which was provided by the wave model.

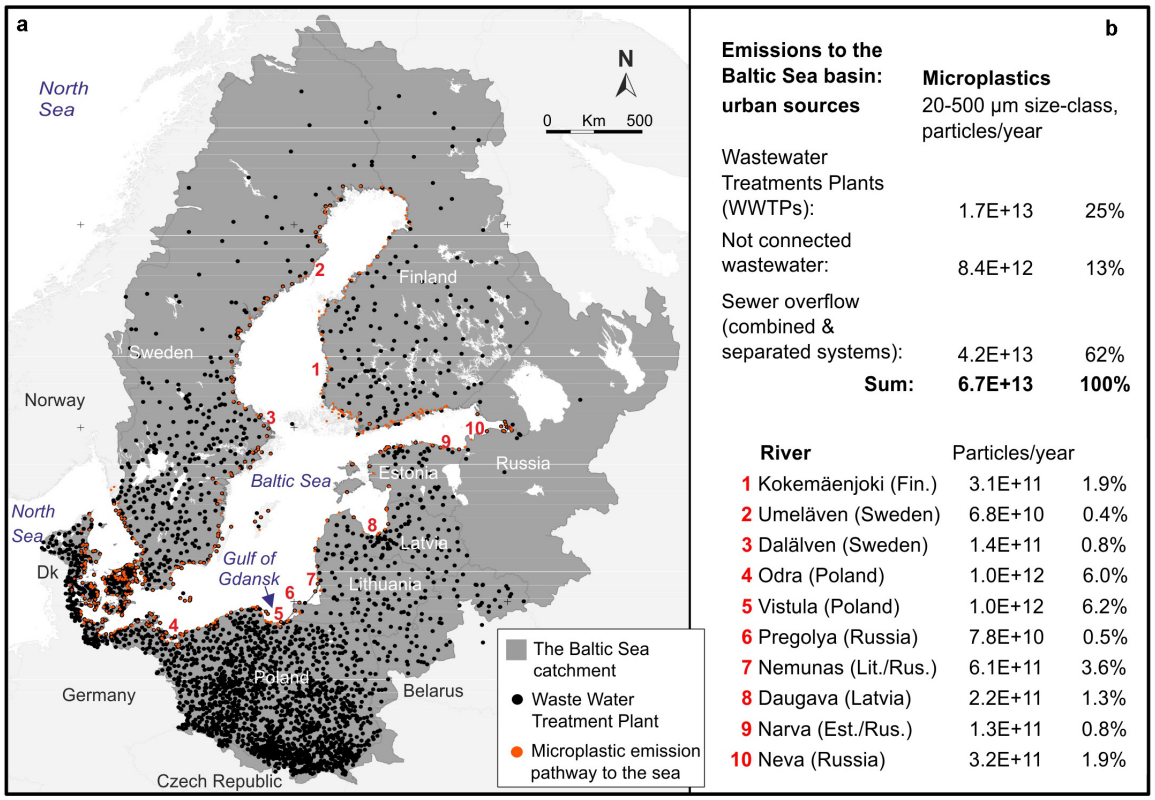

b

Emissions to the Baltic Sea basin: urban sources	Microplastics 20-500 µm size-class, particles/year	
Wastewater Treatments Plants (WWTPs):	1.7E+13	25%
Not connected wastewater:	8.4E+12	13%
Sewer overflow (combined & separated systems):	4.2E+13	62%
Sum:	**6.7E+13**	**100%**

River	Particles/year	
1 Kokemäenjoki (Fin.)	3.1E+11	1.9%
2 Umeläven (Sweden)	6.8E+10	0.4%
3 Dalälven (Sweden)	1.4E+11	0.8%
4 Odra (Poland)	1.0E+12	6.0%
5 Vistula (Poland)	1.0E+12	6.2%
6 Pregolya (Russia)	7.8E+10	0.5%
7 Nemunas (Lit./Rus.)	6.1E+11	3.6%
8 Daugava (Latvia)	2.2E+11	1.3%
9 Narva (Est./Rus.)	1.3E+11	0.8%
10 Neva (Russia)	3.2E+11	1.9%

FIGURE 1 | (a) Location of the 3525 wastewater treatment plants in the Baltic Sea catchment (black dots), micro-plastics emission points (rivers and direct discharge) to the Baltic Sea, including Kattegatt (red dots), and location of 10 selected rivers (red numbers). **(b)** total micro-plastic (floating and sinking fraction, size class 20–500 µm) emissions to the Baltic Sea from all three urban sources and emissions from selected rivers as well as the share of every river of the total emissions.

Settled particles were re-suspended, when the actual shear stress exceeded the critical value.

Shape is a factor that determines the behaviour of particles in the aquatic environment (e.g., Kowalski et al., 2016; Kooi and Koelmans, 2019). However, we did not distinguish between fragments, beads, spheres, flakes and films but partly separated fibers. Our previous study (Schernewski et al., 2020) did show that differences in shape and size have only a limited effect on our simulation results, because of the temporal and spatial resolution of our model approach. Sinking velocities were determined from the Stokes parameterization assuming a spherical shape. The critical shear stress was calculated from the Shields curve (Shields, 1936). Both sinking velocities and critical shear stresses for microplastics particles depend on viscosity and vary with temperature. For example, at 10°C water temperature and particles with 20 µm size, we applied for a vertical velocity of 2.32E-05 (m/s) for the floating fraction and −4.48E-04 (m/s) for the sinking fraction. While the floating fraction is not accumulated at the sediment surface, the sinking fraction (20 µm) is re-suspended at a critical shear stress of 1.63E-02 (N/m^3). For more details, see the supplementary material in Schernewski et al., 2020). The restriction of our approach to the 20–500 µm size class resulted from model limitations. Large particles with a density of 1.4 or above show a higher sinking velocity and the faster transfer from one vertical model layer to the next one, could not be resolved with the applied model calculation time steps and would have caused model instability.

Particles entering a grid cell (1 nm) adjacent to a land cell were immediately removed from the model and counted as washed ashore. The particles washed ashore were accumulated over time to provide numbers of the total amount of particles washed ashore. An exception are those grid cells serving as an emission source, such as rivers, here we did not assume beach accumulation. A possible resuspension and further transport of the particles that were previously washed ashore was neglected. We did not distinguish between different coast types, such as cliffs, sandy beaches or rocky shores. The model simulations covered altogether 2 years, the period from March 2016 until December 2017. Additional 2 months before were used for model spin-up.

In general, our model approach allows a scaling of the microplastics concentrations in the environment, by post-processing the simulation results. This means the absolute concentrations emitted via each pathway and size class potentially can be adjusted if new insights or better field data are available. This is possible as long as the relative spatio-temporal emission pattern remains the same. However, this has no consequences for the presented results.

RESULTS

Emissions and Behaviour of Microplastics in the Baltic Sea

Our calculated total annual emission of all floating and sinking microplastics from all urban sources to the Baltic Sea is 6.7×10^{13} particles (size class 20–100 μm) (**Figure 1b**). The most important urban pathway is stormwater runoff and sewer overflow, from combined (CSS) and separated (SSS) systems with 4.2×10^{13} particles or 62% of the total annual emissions. WWWTs contribute 1.7×10^{13} particles per year or 25% of the total emissions and not connected wastewater 8.4×10^{12} or 13% of the total emissions. **Figure 1b** also shows the absolute emissions of floating and sinking microplastics from all urban sources from 10 selected important rivers and their relative share of the total emissions to the Baltic Sea. The spatial allocation of these rivers and the emission hot-spots are shown in **Figure 2a** and, in detail, **Figure 3a**. The high emissions of the Odra and Vistula result from the large size of the river basins and, most important, the high number of population. The Vistula catchment covers 183,000 km^2 with 20.8 million inhabitants, and the Odra catchment 118,000 km^2 with 14.5 million inhabitants (HELCOM, 2018a). With 282.000 km^2, the Neva river, entering the Baltic Sea in St. Petersburg, has the largest river basin in the Baltic but hosts only a population of 6.1 million inhabitants, resulting in a very low population density of 22 people per km^2. Other important rivers are the Nemunas (98,000 km^2, 4.9 million people), Daugava (88,000 km^2, 2.8 million people and Göta älv (Gota, 50.000 km^2, 1.0 million people) (HELCOM, 2018a). These six river basins alone host 60% of the entire population of the Baltic Sea basin.

Other important emission points are large coastal cities such as St. Petersburg (5.3 million inhabitants) or Stockholm, Copenhagen and Helsinki with a population above one million each. Not all emissions from St. Petersburg enter via the Neva river. According to our calculations, the total emissions from St. Petersburg together with the emissions from the Neva river are 1.12×10^{13} or nearly 17% of the total emissions to the Baltic Sea. A major reason is that 24% of the population are not connected to WWTPs. Therefore, St. Petersburg area is the major pollution hot-spot for microplastics from urban sources in the Baltic Sea region.

According to our model, the average residence time for microplastics entering the Baltic Sea water body is about 14 days. This is true for both, the floating and the sinking microplastics fraction. While the floating fraction stays in the water column before it is washed ashore, the sinking fraction first accumulates on the sediment surface. During storms the sinking fraction is resuspended and washed ashore within a year, as well. The total annual average concentrations in the water column of both fractions together is between 1 and 4 particles/m^2 in entire water column in the central Baltic Sea (**Figure 2b**). In central parts of the Arcona, Bornholm and Gotland Basins as well as the Gulf of Finland, the Kattegat and the Bay of Mecklenburg the concentrations in the upper 2 m water layer are around 1 particle/mł. For the Gulfs of Gdansk and Riga, the model suggests 10 particles/mł in the upper 2 m water layer (**Figure 2f**). These high concentrations are restricted to near shore areas with high emissions. In the immediate surrounding of major rivers, such as the Vistula, Nemunas or Pregolja (**Figure 3b**) the concentrations in the water column can exceed 100 particles/m^2.

Microplastic is accumulated near the sea surface. The model suggests that the relative share decreases fast with increasing water depth of an area. The deeper an area is, the higher is the relative share of microplastics in greater water depths (**Figure 2e**). In the deep Gotland Basin 21% of the microplastic in the water column is below 25 m and 8% are below 50 m. In the relatively shallow Arcona Basin, only 6% of the microplastics are below 25 m and 0.5% below 50 m. For the Gulf of Finland (and the Gulf of Gdank) 16% (resp. 9%) are below 25 m and 4% (resp. 2.5%) are below 50 m.

The total annual average concentrations at the sediment surface of the central Baltic is below 0.0001 particles/m^2 or 1 particle/ha and rarely exceeds 1 particle per m^2 in areas close to the coast. In shallow and sheltered coastal areas near major emission spots, the concentrations can be much higher (**Figures 2c**, **3c**). The model also suggests higher concentrations in deeper, central parts of sub-basins, such as the Arcona Basin (western Baltic Sea) and the Gulf of Finland. The Gulf of Gdansk clearly reflects the role of coast-parallel transport with dominating currents and the decreasing concentrations with increasing distance from the shore (**Figure 3d**). 50 km offshore the microplastics concentrations hardly exceed 0.01 particle/m^2 or 100 particles/ha.

According to our model approach, the vast majority of emitted microplastics is washed ashore within the first few kilometres around the emission source (**Figure 2d**). At the coasts around St. Petersburg and near major rivers and cities, above 10^9 particles/m are washed ashore every year. The Gulf of Gdansk (**Figure 3d**) provides a detailed impression of how strong the accumulation pattern of microplastics at beaches depend on prevailing currents, bottom morphometry, coastline structure, shelter and exposition. Within 50 km coastline, east of the Vistula mouth the number of particles decreases from 10^9 particles/m down to 10^6 particles/m. The consequence of the ragged Baltic coastline is a strong and small scale spatial patchiness of microplastic accumulations at shores.

Figure 4 provides a more detailed insight into the behaviour of the two fractions, floating and sinking microplastics, in the water column. While floating microplastics is generally transported over longer distances and spread in the entire Baltic Sea, the heavier microplastics fraction can be found in the water body only near coast, before it is temporary accumulated in sediments and later washed ashore.

Increased Microplastic Retention in Wastewater Treatment Plants

Based on our data, the total microplastics load to the Baltic Sea could be reduced by 10.6% if all wastewater would be connected to WWTPs and undergo a primary treatment (**Figure 5a**). We assume that a primary treatment would remove 85% of all entering microplastics. This relatively low load reduction reflects that in the Baltic Sea region, the vast majority of wastewater is already treated. If all wastewater would undergo at least a secondary treatment, with a microplastics removal rate of 90%,

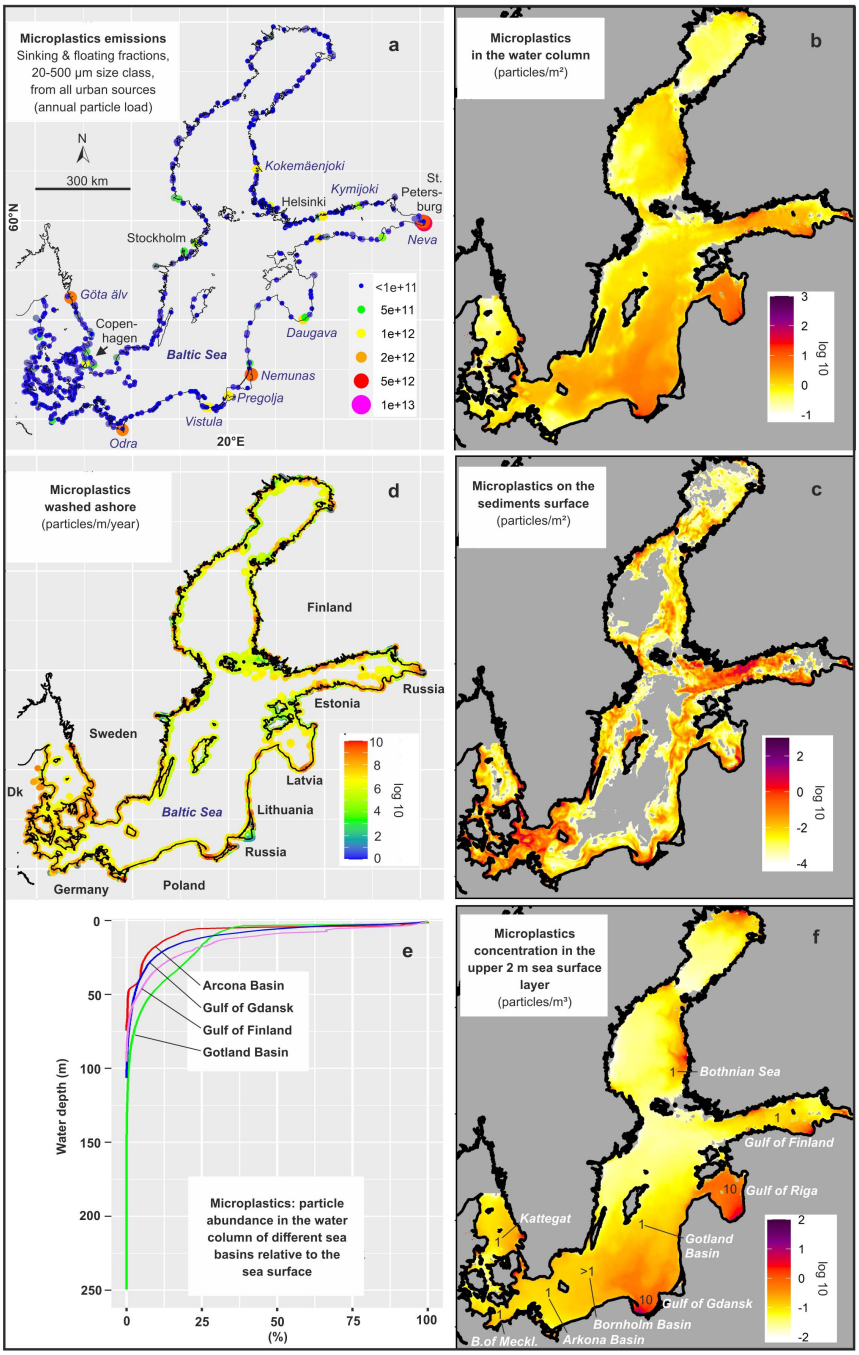

FIGURE 2 | Baltic Sea: **(a)** emissions of microplastic particles from all three urban sources to the Baltic Sea assuming no retention in rivers; **(b)** average annual spatial concentration of microplastic particles (20–500µm size fraction) in the water column; **(c)** at the sediment surface and **(d)** accumulation of micro-plastics microplastic particles (20–500 µm size fraction) at Baltic Sea shores based on simulations with a 3D hydrodynamic model. Grey areas in the sea indicate concentration below the colour scale. Panel **(f)** shows average particle concentrations per m³ in the upper 2 m of the water column and provides concrete values for major sea areas. Panel **(e)** visualizes the relative decreasing particle abundance (compared to the sea surface) with increasing water depth in different sea basins.

the total emissions would be reduced by 12.5% and a tertiary treatment (denitrification and phosphorus-precipitation) would cause a total load reduction of 14.5%. The relatively small load reductions of 3.9%, assuming a tertiary instead of a primary treatment shows that most WWTPs in the Baltic Sea already carry out a tertiary treatment. Related to the present emissions from WWTPs (and presently untreated wastewater) this would mean a loads reduction of 38.7%. Sand-filtration and micro-filtration, as further advanced treatment steps are presently rarely implemented. Despite removing only additional 2% resp. 3%

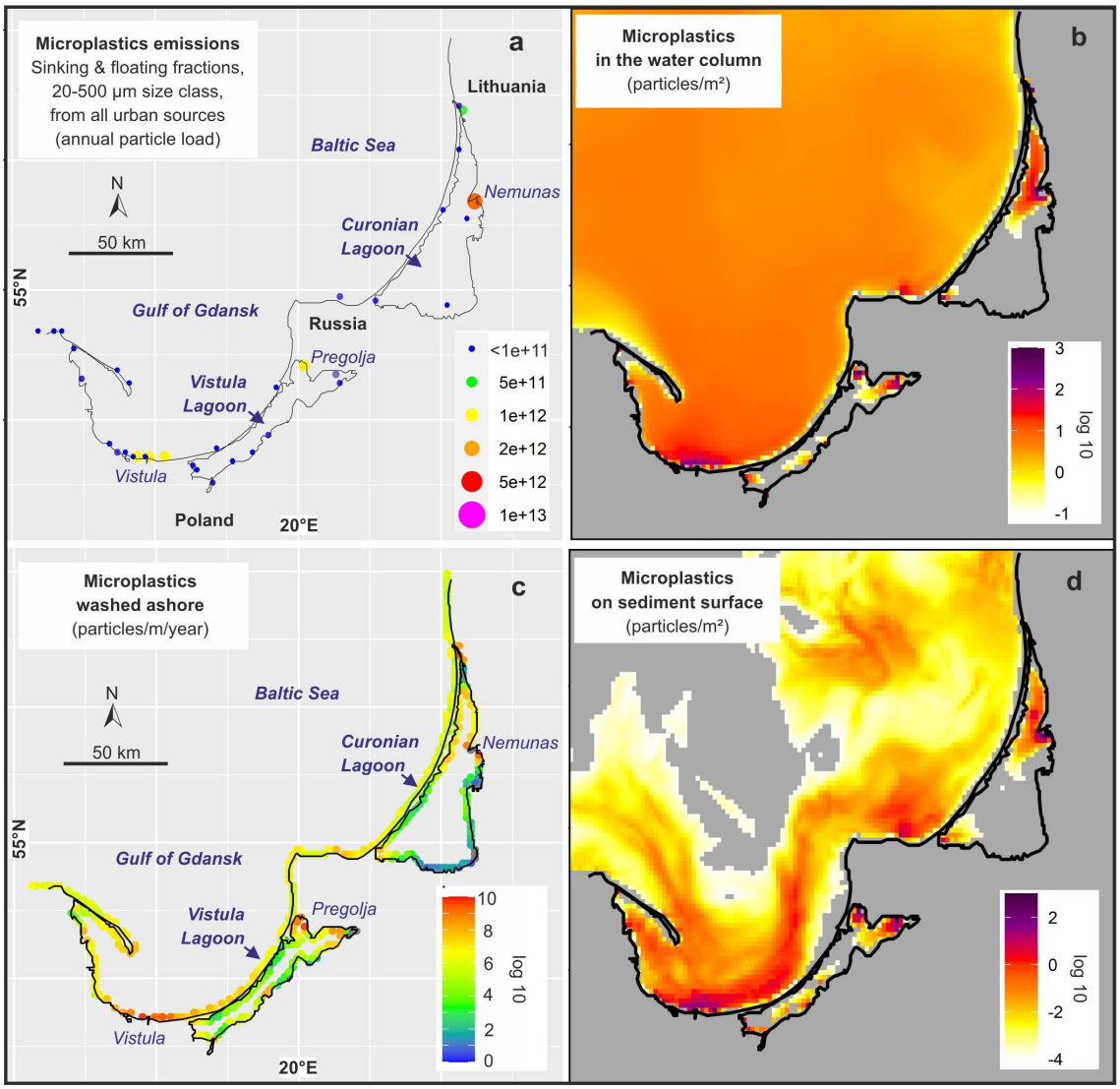

FIGURE 3 | Wider Gulf of Gdansk area: **(a)** emissions of microplastic particles from all three urban pathways to the Baltic Sea assuming no retention in rivers; **(b)** average annual spatial concentration of microplastic particles (20–500µm size fraction) in the water column of the Baltic Sea; **(c)** concentrations at the sediment surface and **(d)** accumulation of micro-plastics particles (20–500µm size fraction) at the shore and based on simulations with a 3D hydrodynamic model. Grey areas in the sea indicate concentration below the colour scale.

microplastics, the effects on the total loads are with 21.7 and 26.9% significant. This strong effect results from the fact that today, hardy any WWWT has this technology implemented and an implementation would reduce the loads from practically all WWTPs around the Baltic Sea. Reason for the low acceptance of these additional treatment steps are the very high costs. Related to the present emissions from WWTPs (and presently untreated wastewater) this would mean a load reduction of 57.9% resp. 71.6%. Altogether, the potential to reduce microplastic emissions with improved treatment technique is relatively limited and beyond a reduction of about 15% of the total emissions (tertiary treatment) becomes very costly.

Figure 5b provides a river basin differentiated picture of microplastics emission reductions resulting from improved WWTP technique. In the river basins of the Kokemäenjoki in Finland and the Umeälven, a tertiary treatment technique is implemented in all WWTPs. Therefore, only additional sand-filtration and/or micro-filtration can potentially reduce the emissions from WWTPs. This is different for the Odra and the Vistula, whose river basins are mainly located in Poland. The implementation of a primary (secondary) treatment could reduce loads by 10% resp. 15% and a tertiary treatment (N/P removal) by 37%. In the Pregolja (Russia) and Daugava (the basin is shared by Russia, Belasus and Lativa) a tertiary treatment can reduce the microplastic emissions by 63% resp. 58%. Regionally, in eastern European states, especially in Russia and Belarus, the improvement of WWTPs can still be regarded as an effective measure to reduce microplastic emissions to the Baltic Sea.

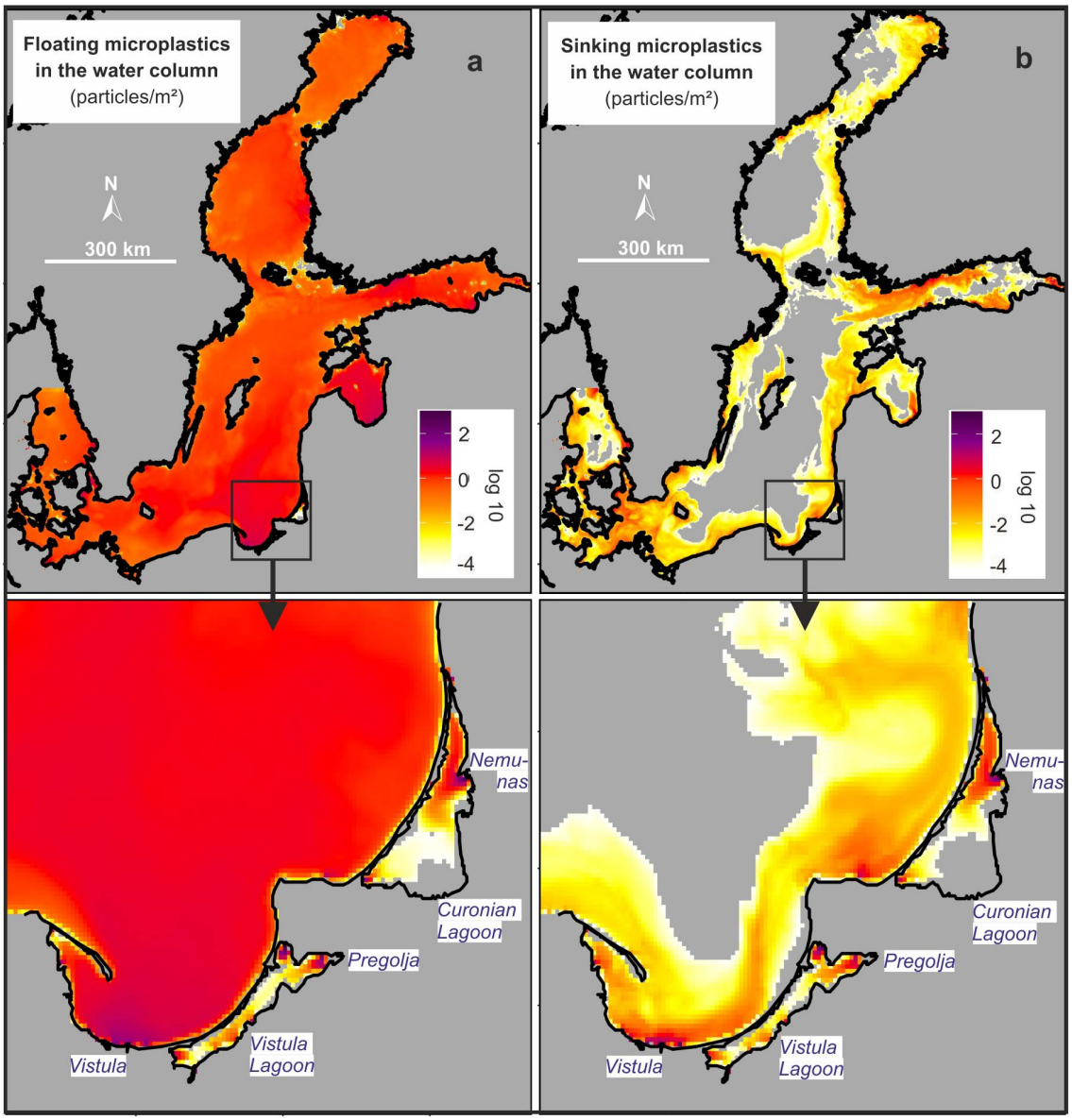

FIGURE 4 | Average annual spatial concentration of **(a)** floating and **(b)** sinking microplastic particles (20–500 μm size fraction) in the water column in the Baltic Sea and the wider Bay of Gdansk based on simulations with a 3D hydrodynamic model. Grey areas in the sea indicate concentration below the colour scale.

Since most WWTPs are located in river basins, rivers cumulate the emitted microplastic loads and are major emission spots to the sea (**Figures 6a,c**). When assuming that all WWTPs have a retention efficiency of 97% (sand filtration) the relevance of rivers as emission pathways strongly decline (**Figures 6b,d**).

Reduction of Sanitary Sewer Overflow Emissions

For the present situation in the Baltic region, we assume that 1.5% of wastewater enters the Baltic Sea without treatment during sanitary sewer overflow events. This includes emissions from stormwater. If technical measures such as stormwater treatment techniques, technical filters, green roofs, bio-retention and infiltrations paths, permeable surfaces, infiltration trenches, stormwater ponds or artificial wetlands would reduce the overflow events by only 0.2%, the total microplastics emissions would be reduced by 8.3% (**Figure 7**). To reduce the total emissions to the Baltic Sea by 50% would require that only 0.3% of the wastewater enters during sanitary sewer overflow events. Because of the relative importance of emissions during sanitary overflow, measures to reduce sewer overflow are effective in reducing total microplastics loads to the Baltic Sea. Implementing sustainable drainage systems would reduce sanitary sewer overflows, but more important reduce the stormwater volume and microplastic particles concentration in the water.

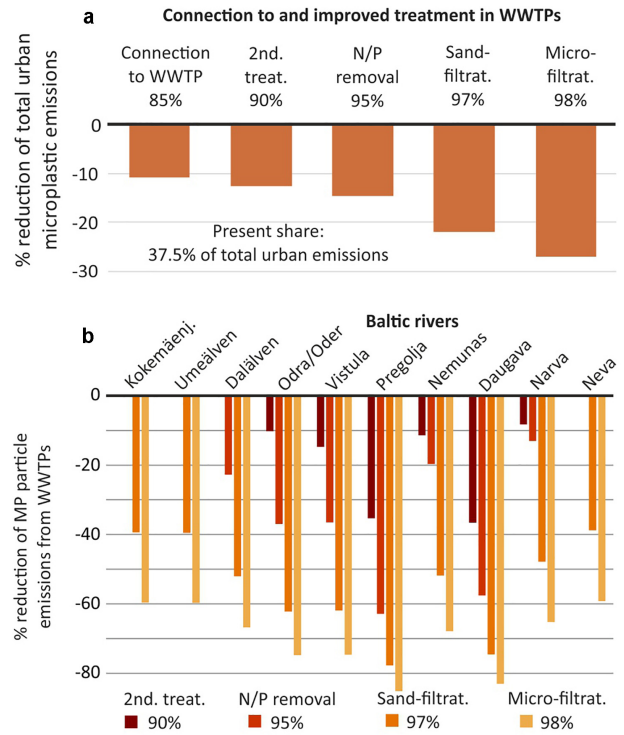

FIGURE 5 | (a) Relative micro-plastic particle emission reductions (floating and sinking fraction, size class 20–500 μm) resulting from the assumption that all sewage water in the Baltic catchment is processed in a basic treatment plant (WWTP) with a micro-plastics cleaning efficiency of 85%, that all are connected and the WWTPs possess a secondary treatment with a 90% cleaning efficiency and that a better treatment is applied, reducing the micro-plastics loads by 95, 97, and 98%. **(b)** Relative micro-plastic particle emission reductions from WWTPs (floating and sinking fraction, size class 20–500 μm) in 10 different Baltic river basins.

Microplastics Retention in Rivers

The retention of microplastics in rivers, resulting from processes such as sedimentation or trapping, can potentially have a strong effect on the microplastic emissions to the Baltic Sea. **Figure 8a** shows the effect of different retention rates on the calculated emissions for the 10 selected rivers. Our simplified approach assumes that the effect on the emissions depends on the distance of the WWTPs to the coast, or a simplified transport distance of a particle in the river. Shorter rivers such as the Umeälven (470 km length) and/or rivers where the WWTPs are mainly located near the coast, such as the Neva, do not show a strong impact of increasing retention factors on the microplastic loads. This is different for large rivers such as Odra, Vistula, Nemunas, or Daugava. In these rivers, a relatively low retention factor of 0.1%/km already causes a microplastics load reduction above 20% and a factor of 0.5%/km a reduction of around 70%.

If these retention factors are applied to all rivers in the Baltic catchment, a factor of 0.1%/km would reduce the loads by 6 and 0.5%/km by 20%. A very high factor of 10%/km would reduce the loads by 47%. This relatively low value indicates the importance of emissions from coastal towns and cities and that especially larger WWTPs are located close to the sea. Taking into account microplastics retention in rivers in emissions calculation to the entire Baltic Sea is relevant, but compared to all other uncertainties associated with microplastic emission calculations seems not to be of highest importance.

However, the application of retention factors affects the importance of rivers for the total microplastic loads to the Baltic Sea (**Figure 8b**). The calculated share of the 10 selected rivers of the total loads is 21.6%. Assuming a retention factor of 0.5%/km his share drops to around half of it, 10.1%. Already a factor of 2%/km would reduce the share to 3.2%. In case new data and field studies would prove that a factor of 2%/km would reflect the reality, emission calculations could be strongly simplified. In this case, calculations could largely neglect the river basins and focus on emissions from a 10 km coastal strip around the Baltic Sea.

DISCUSSION

Approach and Assumptions

A previous study (Schernewski et al., 2020) focussed on single polymer types namely PE, PP as well as PET and their behaviour in the marine environment. It did show that the results for floating PE/PP and sinking PET can be transferred to other polymer types with comparable densities, at least on our spatial model resolution and when aggregating or averaging the results over a year. The two fractions considered in our model approach represent plastic polymers with a density between about 0.8 g/cm³ and 1.5 g/cm³. According to Kang et al. (2018), Lv et al. (2019), Olesen et al. (2019), and Sun et al. (2019) we can assume that our two polymer groups cover above 90–95% of all plastics from urban pathways, at least when neglecting road runoff (tyres).

Based on a literature survey (Talvitie et al., 2015; Murphy et al., 2016; Lares et al., 2018; Simon et al., 2018; Long et al., 2019; Wolff et al., 2019), review papers (Kang et al., 2018; Gatidou et al., 2019; Koelmans et al., 2019; Sun et al., 2019), we calculated average concentrations of the floating and sinking plastic polymers in raw wastewater, used the median concentration of 85,000 particles/m³ shared among both polymer groups with 50% each. Alternatively, the average number of microplastics in raw wastewater (WWTPs influents) of 134,000 particles/m³ could have been applied. Single studies even show much higher concentrations: Talvitie et al. (2015) report extreme values above 600,000 and Simon et al. (2018) even above 7,000,000 microplastics particles/m³. The difference between these values give an idea about the uncertainties associated to our calculated microplastic particle emissions, which possibly exceed +/− one order of magnitude.

Size and shape of particle, such as fibers, fragments, beads, spheres, flakes and films play an important role for the sinking velocity (e.g., Kowalski et al., 2016; Kooi and Koelmans, 2019; Waldschläger and Schüttrumpf, 2019a,b). In this study, we do not distinguish between different sizes and shapes. Further we do not assume that during the relatively short transport time of weeks in the environment, plastic particles are significantly modified in their properties. These simplifications seem justified, because our previous study (Schernewski et al., 2020) showed that size and shape do not play an important role for the behaviour in the

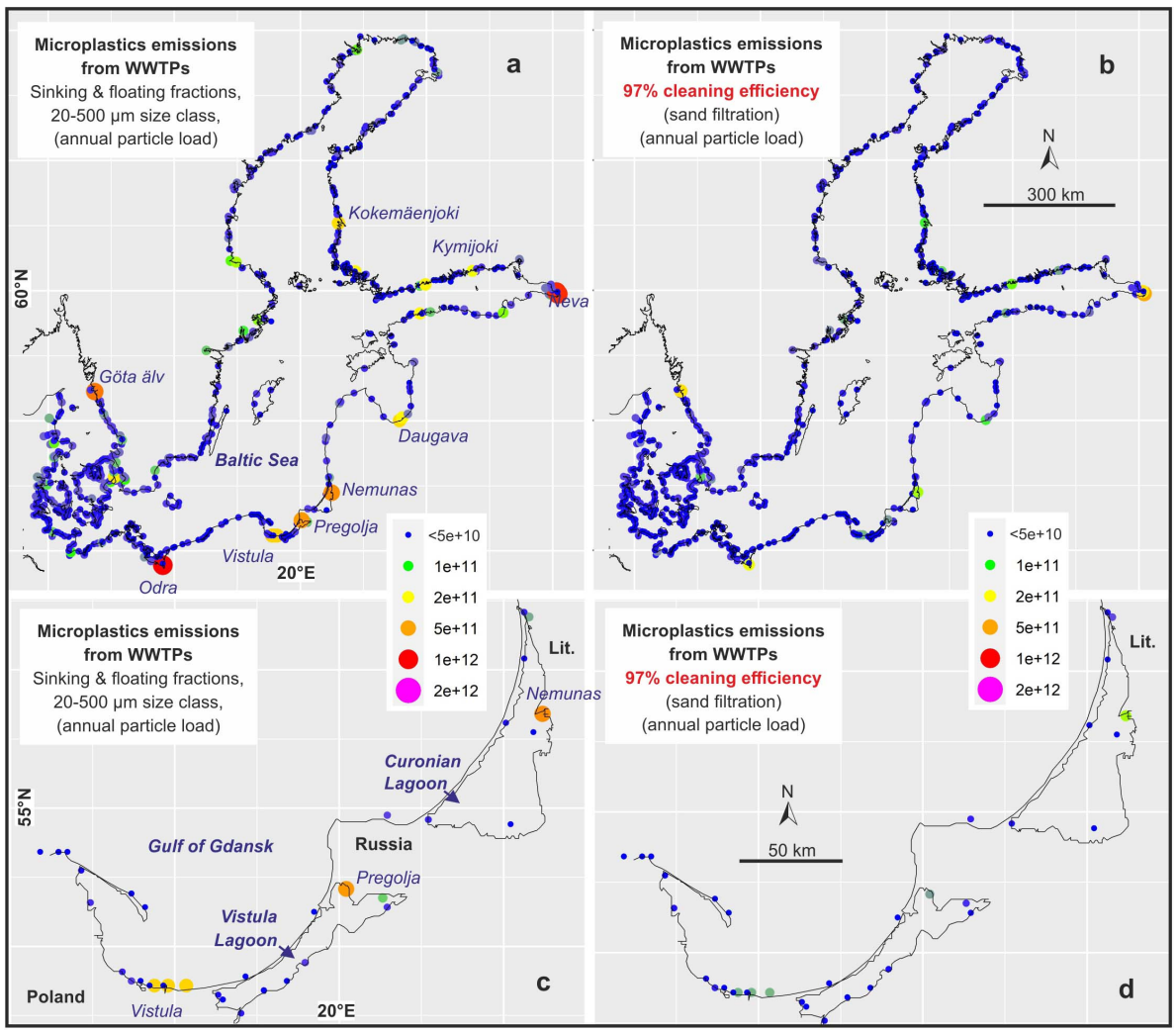

FIGURE 6 | Annual spatial emission pattern of micro-plastic particles only from wastewater treatment plants (WWTPs) to the Baltic Sea, **(a)** assuming no micro-plastics retention in rivers and **(b)** spatial emission pattern emissions into the Baltic Sea assuming that all WWTPs have a 97% cleaning efficiency. Panels **(c,d)** show the same data focussed on the Gulf of Gdansk.

environment, when focussing on time scales of at least weeks and our spatial model resolution.

We calculated the emissions based on aw wastewater microplastic particle concentrations taking into account the treatment efficiency of each WWTP. For this purpose, we used the database by Baresel and Olshammar (2019) including location and emissions from WWTPs, CSS systems including stormwater and untreated wastewater (not connected to WWTPs) in the entire Baltic Sea region. The uncertainties are discussed in Baresel and Olshammar (2019).

Model approaches and simulations always provide a simplified picture of the reality. In general, the spatial transport pattern in the open sea are much more reliable compared to the microplastics accumulation pattern at the coast. The uncertainties associated to the model are discussed in Schernewski et al. (2020). In general, we can conclude that the uncertainties resulting from the model approach are relatively low compared to the high uncertainties related to microplastic particle numbers in raw wastewater and follow-up assumptions on emissions. However, we need to point out one important simplifying assumption in the model. Particles that enter a grid cell adjacent to land are assumed to be washed ashore immediately. This means that near-shore processes such as resuspension from beaches are neglected. Further, the model assumes that particles can be washed ashore at all kinds of coasts.

With an average depth of 55 m, the Baltic Sea is relatively shallow. It is known that in the Baltic Sea a wave induced resuspension of soft sediments takes place down to a depth of about 80 m. Therefore, large areas are subject to frequent resuspension and material with a density around 1 g/cm³ can be transported in the water column over long distances. The likelihood that it ends-up at the coast is high. Material with a higher density already settles near the coast and after resuspension is accumulated at the coast, as well. Therefore, the

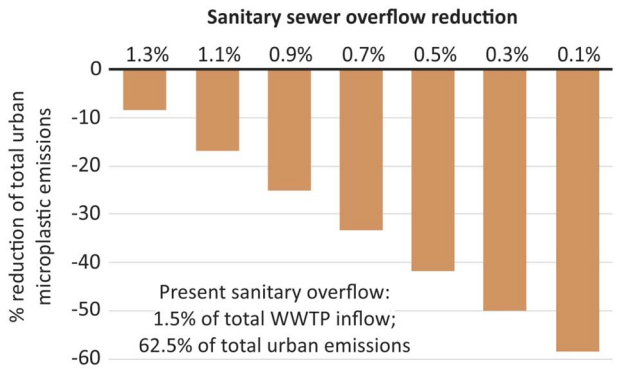

FIGURE 7 | Micro-plastic particle emission reductions (floating and sinking fraction, size class 20–500 μm) resulting from the assumption that instead of todays 1.5% sanitary sewer overflow (of the total annual WWTP inflow) in the Baltic catchment, technical retention measures reduce the overflow share stepwise to 0.1% of the total wastewater amount.

relative shallowness of the Baltic Sea explains why our model suggests that only a small share of microplastics are deposited in deep basins and the vast majority at the coast. The result supported by studies e.g., on N-isotopes or using eutrophication models, indicating that river-borne nutrients are accumulated in coastal areas.

Retention in Rivers

The knowledge about the retention of microplastics in rivers is still scarce. It is known that it depends on particle size, shape and density (e.g., Nizzetto et al., 2016; Besseling et al., 2017; Kooi et al., 2018) and biofilm colonization plays an important modifying role (Hoellein et al., 2019). Hoellein et al. (2019) conclude that current models of microplastic transport underestimate microplastic retention in rivers. This view is supported by results of Besseling et al. (2017) who carried out scenario studies with a hydrological model and conclude that in 40 km river practically all particles (>100 μm spherical polystyrene) are kept back. As a consequence, Siegfried et al. (2017) take into account retention fractions for each microplastics source and the length of the rivers in their microplastic export calculation to seas. On the other hand, Nizzetto et al. (2016) assume that microplastics larger than 200 μm are generally not retained in the Thames river, regardless of their density and that other microplastics can be retained in the sediment until it is remobilized during floods.

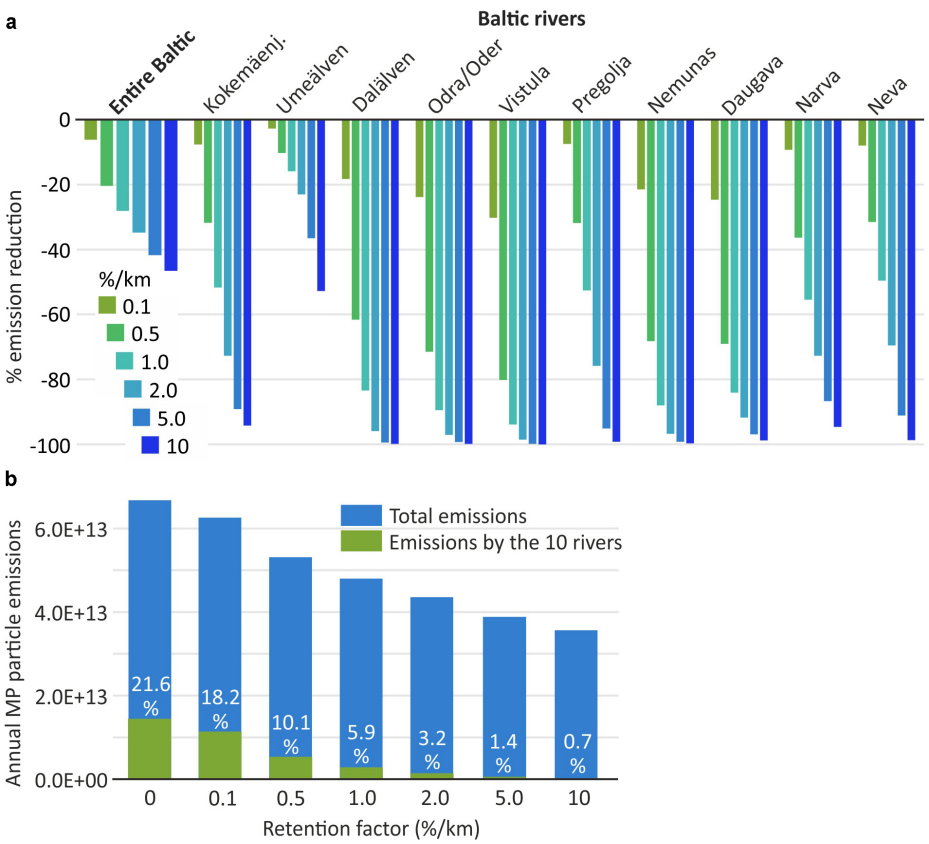

FIGURE 8 | (a) Relative reduction of annual micro-plastic particle emissions reductions (floating and sinking fraction, size class 20–500 μm) to the Baltic Sea assuming different micro-plastics retention factors (%/km) in rivers, calculated for the entire Baltic Sea catchment and 10 selected rivers. The reduction is related to the present load of every river. **(b)** Absolute annual micro-plastics particle emissions resulting from increasing micro-plastic retention factors (%/km) in rivers as well as relative share of the 10 rivers compared to the total emissions to the Baltic Sea.

Other microplastic export calculations do not take into account retention in rivers. (e.g., van Wijnen et al., 2019) and Windsor et al. (2019) state that still little is known about the residence time of plastics in rivers and their role as temporary sinks. The major question is, whether microplastic retention is only temporary since permanent sinks in rivers are lacking. This could be the case at least as long as the rivers do not pass lakes, reservoirs and major wetlands. A consequence is that the retention rate may strongly vary between different rivers. The Warnow river in northern Germany can be regarded as a representative southern Baltic lowland river. Microplastics concentrations and water discharge were sampled on 5 locations along the river. This unpublished data from the MicroCatch project does not indicate a significant retention in the river system.

However, as a consequence of these contradicting views and results we did not apply defined retention factors, but carried out scenario simulations using a range of retention factors. In these calculations we took into account the distance of each WWTP to the sea. A retention factor of 1%/km would reduce the total loads to the Baltic by 28%. Compared to other potential errors still associated to microplastic emission calculations, it seems that the potential error resulting from retention in rivers does not play the major role for emissions to the Baltic Sea. However, retention in rivers has practical implications, because the higher the retention rate, the less important are emissions by rivers. As a practical consequence microplastics mitigation and load reduction measures should preferably address near coast emission sources. With the present scarce knowledge, we think the application of retention factors in rivers would add uncertainties to emission calculations and open the door for manipulations of total emission data to the sea.

Comparison to Data

Our approach refines existing microplastics emission approaches for the Baltic Sea. Instead of calculating mass flows, like Siegfried et al. (2017) or Bollmann et al. (2019) we focus on particle numbers. Disadvantage is that the uncertainties of our approach are very high. Potential advantage is that our results can be directly compared to existing field data and provide concrete microplastics concentrations for the marine environment, that can be assessed with field studies.

For the Swedish river Dalälven, GESAMP (2016), provides estimated total annual emissions of microplastics items of 4×10^{10}, while our calculation results in 1.15×10^{9} particles, but restricted to the 20–500 μm size class and for urban sources only. For the Baltic Sea, HELCOM (2018a) states that an assessment of the state of pollution with respect to marine litter is still not possible. However, some data exists: Setälä et al. (2016) found 0.3–2.1 particles/mł in the Gulf of Finland and Tamminga et al. (2018) 0.04–0.09 particles/mł in the South Funen Archipelago. Both studies only address particle sizes above 333 μm. The differences in the considered size fractions and emission pathways do not allow a direct comparison to our concentrations. However, the order of magnitude is similar and the concentration gradients between the Gulf of Finland and the Archipelago is well reflected in and can be explained with our model simulations.

Our model approach suggests a high annual accumulation of microplastics particles close to the emission pathways, usually around river mouths, cities as well as in enclosed and semi-enclosed coastal waters. Generally, this is well supported by literature. Gewert et al. (2017) found nearly ten times higher abundance of plastics in surface water near central Stockholm than in offshore areas. Yonkos et al. (2014) reported the highest microplastics concentrations near densely populated areas of Chesapeake Bay and comparable results exist for other estuaries and lagoons (Vianello et al., 2013; Song et al., 2015; Vermeiren et al., 2016; Gray et al., 2018; McEachern et al., 2019).

Microplastic is found in many sediments and highest concentrations are observed near populated areas, near emission sources, especially in semi- and enclosed systems (Claessens et al., 2011; Vianello et al., 2013; Gray et al., 2018) and on exposed beaches (Wessel et al., 2016). Whether sediments serve as permanent sink for microplastics (Vianello et al., 2013; Boucher and Friot, 2017) or only as a temporary storage, depends on the system. Our results indicate that the heavier microplastics fraction is accumulating during the summer months in coastal waters, but is re-suspended by wave induced turbulence during frequent autumn and winter storms and washed ashore. Our results do not suggest a permanent accumulation in the Baltic Sea over years. The consequence is an ongoing accumulation at beaches which presently cannot be supported by field data.

Effectiveness of Measures and Policies

Already in 2013, the European Technical Subgroup on Marine Litter asked to "develop common indicators and associated targets related to quantities, composition, sources and pathway of marine litter, including riverine inputs, in order to gain information on long-term trends, and carry out the monitoring of the progress toward achieving the agreed goals and to gain an inventory of marine litter in the Baltic Sea as well as scientific sound evaluation of its sources" JRC (2013). The Baltic Marine Environment Protection Commission (HELCOM) is an intergovernmental organization with the aim to protect the marine environment of the Baltic Sea. HELCOM implements the European Union environmental policies on a regional sea level. An important action is the HELCOM Action Plan on Marine Litter (HELCOM, 2015). It recognizes that especially microplastics is a potential risk for the organisms in the Baltic Sea and that the amounts of marine litter emitted to the Baltic Sea need to be reduced significantly. At the same time, major shortcomings in knowledge are indicated, for example that the establishment of a coordinated regular monitoring with unified methods is still missing. Further, the HELCOM Action Plan on Marine Litter calls for cost-effective actions to reduce the pollution.

The HELCOM action plan mentions the improvement of WWTPs only as voluntary national action. Our calculations suggest that the total microplastics emissions could be reduced by 12.5% if all wastewater in the Baltic catchment would be connected to WWTPs and undergo a secondary treatment with a microplastics retention efficiency of 90%. Especially in eastern Baltic countries this can efficiently reduce microplastic loads to the sea. In rivers such as the Pregolja and the Daugava a

full secondary treatment would already reduce the microplastics emissions from WWTPs by 35–37% and a tertiary treatment even by 58–63%. Therefore, it is recommendable to foster a further improvement of WWTPs at least up to a tertiary cleaning level. The costs of a further treatment using sand-filtration or micro-filtration cannot be evaluated. It depends on many factors such as the implemented technical solution or the size of a WWTP. Further, calculations on its cost-effectiveness have to take into account nutrients and other pollutants, which are kept back as well, when a better treatment technology is applied.

One action defined by HELCOM (2015) is to improve the stormwater management in order to prevent microplastics emissions to the Baltic Sea during heavy weather events. The necessity to tackle stormwater and to reduce sewer overflow especially, is strongly supported by our results. A wide range of measures is possible to implement an emission reduction, such as technical filters, stormwater ponds and artificial wetlands, overland flow systems, green roofs, bio-retention and infiltration paths, permeable surfaces etc. (Coalition Clean Baltic, 2019). The cost-efficiency of these measures is intensively assessed (e.g., Joksimovic and Alam, 2014; Liu et al., 2016; Nobles et al., 2017; Bixler et al., 2020). However, the costs of each single measure and the optimal set of measures to reach a defined stormwater retention depend on the site specific situation (Bixler et al., 2020). A reliable cost estimation for the Baltic region in general is hardly possible. However, the high number of measures ensures flexibility in finding suitable, site specific and cost-effective stormwater retention management approaches.

For Europe, observations and climate model projections show an increase in extreme precipitation (Madsen et al., 2014) and a climate signal in flood observations is already visible (Blöschl et al., 2017). In the Baltic, the future average precipitation amounts are projected to be larger than today and precipitation extremes are expected to increase (Christensen and Kjellström, 2018). Therefore, the amount and importance of stormwater as a pathway for microplastics is likely to increases in the future (Olsson and Foster, 2014). According to our calculations, an increase of sewer overflow from 1.5 to 3.0% resulting from climate change would increase the annual microplastics loads by more than 60% and could not be compensated by other measures such as improvement of WWTPs. The assumed increase in sewer overflow to 3% as a consequence of climate change is speculative, but visualizes the importance and urgency to tackle stormwater and resulting sanitary sewer overflow as emission pathways for microplastics.

CONCLUSION

The aggregation of most plastic polymers based on their density into a floating and a sinking fraction, provides an insight into the behaviour spectrum of microplastics in the marine environment. Further, it covers the majority of all microplastics emitted to the aquatic environment (in the size class between 20 and 500μm), because urban source can be regarded as most important, apart from tyre wear. Our results provide concrete particle concentrations for the water column, sediments and beaches, that have to be verified with field studies. Possibly most important is that the model simulations can explain observed spatial gradients in microplastics concentrations and provide a consistent spatial pollution pattern for the water column, sediments and beaches in the Baltic Sea region, including Kattegatt. It enables the design of spatial monitoring programmes, the optimization of sampling strategies and allows an assessment and extrapolation of field data taken at few locations.

Our results indicate that stormwater runoff and sanitary sewer overflow is the most important urban emission pathway. It seems realistic, that an implementation of retention measures can reduce the total microplastics emissions to the Baltic Sea by more than 30%. Since nutrients and other pollutants would benefit from reduced sewer overflow, as well, and taking into account that the amount and frequency of stormwater is likely to increase as a consequence of climate change, urgent action is recommended. In eastern European river basins and countries, the connection of all wastewater to WWTPs and the implementation of a tertiary treatment can reduce the total microplastics by 15% and is recommendable.

The retention of microplastics during the transport in rivers is largely unknown and requires further research. However, for the Baltic, the error by not applying a retention factor is limited because near coast emissions contribute around 50% of the total microplastics emissions the Baltic Sea. One consequence is that microplastics emission reduction measures should, from a Baltic Sea protection perspective, preferably be implemented near the coast, especially in coastal urban areas.

DATA AVAILABILITY STATEMENT

The raw data supporting the conclusions of this article will be made available by the authors, without undue reservation.

AUTHOR CONTRIBUTIONS

GS developed the article concept, developed the emission scenarios, took care of data analyses, and did the article writing. HR carried out the model simulation and the data processing. RH prepared the input data, carried out a literature analysis and provided complementary calculations for the model emission scenarios. CB and MO compiled and provided all data about the sewage treatment plants and emission calculations. SO coordinated the overall work within project MicroPoll and contributed comments and proof-reading.

FUNDING

The work was financially supported by the project BONUS MicroPoll (03A0027A) and to a small degree by project MicroCatch (03F0788A) as well as ERA.Net RUS Plus project BalticLitter (01DJ19001), all funded by the German Federal Ministry for Education and Research. BONUS MicroPoll has received funding from BONUS (Art 185) funded jointly from the European Union's Seventh Programme for research, technological development and demonstration, and from Baltic Sea national funding institutions.

ACKNOWLEDGMENTS

We like to thank Robert Osinski for providing the model setup, Arunas Balciunas for technical support in preparing **Figure 1** and Mirco Haseler for comments on the draft manuscript. The simulations were performed with resources provided by the North-German Supercomputing Alliance (HLRN). All authors contributed to the article and approved the submitted version.

REFERENCES

Baresel, C., and Olshammar, M. (2019). On the importance of sanitary sewer overflow on the total discharge of Microplastics from sewage water. *J. Environ. Protect.* 10, 1105–1118. doi: 10.4236/jep.2019.109065

Bergmann, M., Gutow, L., and Klages, M. (eds) (2015). *Marine Anthropogenic Litter*. Berlin: Springer. doi: 10.1007/978-3-319-16510-3

Besseling, E., Quik, J. T. K., Sun, M., and Koelmans, A. A. (2017). Fate of Nano- and microplastic in freshwater systems: a modeling study. *ICES J. Mar. Sci.* 220, 540–548. doi: 10.1016/j.envpol.2016.10.001

Bixler, T. S., Houle, J., Ballestero, T. P., and Mo, W. (2020). A spatial life cycle cost assessment of stormwater management systems. *Sci. Total Environ.* 728:138787. doi: 10.1016/j.scitotenv.2020.138787

Blöschl, G., Hall, J., Parajka, J., Perdigão, R. A. P., Merz, B., Arheimer, B., et al. (2017). Changing climate shifts timing of European floods. *Science* 357, 588–590. doi: 10.1126/science.aan2506

Bollmann, U. E., Simon, M., Vollertsen, J., and Bester, K. (2019). Assessment of input of organic micropollutants and microplastics into the Baltic Sea by urban waters. *Mar. Pollut. Bull.* 148, 149–155. doi: 10.1016/j.marpolbul.2019.07.014

Boucher, J., and Friot, D. (2017). *Primary Microplastics in the Oceans: A Global Evaluation of Sources*. Gland: IUCN. doi: 10.2305/IUCN.CH.2017.01.en

Carr, S. A., Liu, J., and Arnold, G. T. (2016). Transport and fate of Microplastic particles in wastewater treatment plants. *Water Res.* 91, 174–182. doi: 10.1016/j.watres.2016.01.002

Christensen, O., and Kjellström, E. (2018). Projections for temperature, precipitation, wind, and snow in the Baltic Sea Region until 2100. *Oxford Res. Encyclop. Clim. Sci.* Available online at: https://oxfordre.com/climatescience/view/10.1093/acrefore/9780190228620.001.0001/acrefore-9780190228620-e-695 doi: 10.1093/acrefore/9780190228620.013.695

Claessens, M., De Meester, S., Van Landuyt, L., De Clerck, K., and Janssen, C. R. (2011). Occurrence and distribution of microplastics in marine sediments along the Belgian coast. *Mar. Pollut. Bull.* 62, 2199–2204. doi: 10.1016/j.marpolbul.2011.06.030

Coalition Clean Baltic (2019). *Recommendations on Improving Helcom Recommendation 23/5 – Including a Brief Identification of Major Stormwater Issues, Stormwater Pollutants and Stormwater Treatment Methods*. REPORT NUMBER 2019-1393-A. Helsinki: Coalition Clean Baltic.

Gatidou, G., Arvaniti, O. S., and Stasinakis, A. S. (2019). Review on the occurrence and fate of microplastics in sewage treatment plants. *J. Hazard. Mater.* 367, 504–512. doi: 10.1016/j.jhazmat.2018.12.081

GESAMP (2016). "Sources, fate and effects of microplastics in the marine environment: part two of a global assessment," in *IMO/FAO/UNESCO-IOC/UNIDO/WMO/IAEA/UN/UNEP/UNDP Joint Group of Experts on the Scientific Aspects of Marine Environmental Protection). Rep. Stud. GESAMP No. 93*, eds P. J. Kershaw and C. M. Rochman (Madrid: GESAMP), 220.

Gewert, B., Ogonowski, M., Barth, A., and MacLeod, M. (2017). Abundance and composition of near surface microplastics and plastic debris in the Stockholm Archipelago, Baltic Sea. *Mar. Pollut. Bull.* 120, 292–302. doi: 10.1016/j.marpolbul.2017.04.062

Geyer, R., Jambeck, J. R., and Law, K. L. (2017). Production, use, and fate of all plastics ever made. *Sci. Adv.* 3:1700782. doi: 10.1126/sciadv.1700782

Gies, E. A., LeNoble, J. L., Noël, M., Etemadifar, A., Bishay, F., Hall, E. R., et al. (2018). Retention of Microplastics in a major secondary wastewater treatment plant in Vancouver, Canada. *Mar. Pollut. Bull.* 133, 553–561. doi: 10.1016/j.marpolbul.2018.06.006

Gray, A. D., Wertz, H., Leads, R. R., and Weinstein, J. E. (2018). Microplastic in two South carolina estuaries: occurrence, distribution, and composition. *Mar. Pollut. Bull.* 128, 223–233. doi: 10.1016/j.marpolbul.2018.01.030

HELCOM (2015). *Regional Action Plan for Marine Litter in the Baltic Sea. 20 pp*. Available online at: https://helcom.fi/media/publications/Regional-Action-Plan-for-Marine-Litter.pdf (assessed June 8, 2020).

HELCOM (2018a). "Input of nutrients by the seven biggest rivers in the Baltic Sea region," in *Proceedings of the Baltic Sea Environment Proceedings No.161*, New York, NY.

HELCOM (2018b). "State of the Baltic Sea – Second HELCOM holistic assessment 2011–2016," in *Proceedings of the Baltic Sea Environment Proceedings 155*, Cambridge.

HELCOM (2018c). *Total and Regional Runoff to the Baltic Sea Baltic Sea Environment Fact Sheet 2016*. Available online at: https://helcom.fi/baltic-sea-trends/environment-fact-sheets/hydrography/total-and-regional-runoff-to-the-baltic-sea/ (assessed June 8, 2020).

Hoellein, T. J., Shogren, A. J., Tank, J. L., Risteca, P., and Kelly, J. J. (2019). Microplastic deposition velocity in streams follows patterns for naturally occurring allochthonous particles. *Sci. Rep.* 9:3740. doi: 10.1038/s41598-019-40126-3

Joksimovic, D., and Alam, Z. (2014). Cost efficiency of Low Impact Development (LID) stormwater management practices. *Proc. Eng.* 89, 734–741. doi: 10.1016/j.proeng.2014.11.501

JRC (2011). *Marine Litter – Technical Recommendations for the Implementation of MSFD Requirements*. Available online at: https://mcc.jrc.ec.europa.eu/documents/201702071118.pdf (assessed June 8, 2020).

JRC (2013). *Guidance on Monitoring of Marine Litter in European Seas*. Available online at: https://mcc.jrc.ec.europa.eu/documents/201702074014.pdf (assessed June 8, 2020).

Kang, H.-J., Park, H.-J., Kwon, O.-K., Lee, W.-S., Jeong, D.-H., Ju, B.-K., et al. (2018). Occurrence of Microplastics in municipal sewage treatment plants: a review. *Environ. Health Toxicol.* 33:2018013. doi: 10.5620/eht.e2018013

Kay, P., Hiscoe, R., Moberley, I., Bajic, L., and McKenna, N. (2018). Wastewater treatment plants as a source of Microplastics in river catchments. *Environ. Sci. Pollut. Res.* 25, 20264–20267. doi: 10.1007/s11356-018-2070-7

Koelmans, A. A., Nor, N. H. M., Hermsen, E., Kooi, M., Mintenig, S. M., and De France, J. (2019). Microplastics in freshwaters and drinking water: critical review and assessment of data quality. *Water Res.* 155, 410–422. doi: 10.1016/j.watres.2019.02.054

Kooi, M., Besseling, E., Kroeze, C., van Wezel, A. P., and Koelmans, A. A. (2018). "Modeling the fate and transport of plastic debris in freshwaters: review and guidance," in *Freshwater Microplastics. The Handbook of Environmental Chemistry*, Vol. 58, eds L. Wagner and U. Lambert (Cham: Springer), 125–152. doi: 10.1007/978-3-319-61615-5_7

Kooi, M., and Koelmans, A. A. (2019). Simplifying Microplastic via continuous probability distributions for size, shape, and density. *Environ. Sci. Technol. Lett.* 6, 551–557. doi: 10.1021/acs.estlett.9b00379

Kowalski, N., Reichardt, A. M., and Waniek, J. J. (2016). Sinking rates of Microplastics and potential implications of their alteration by physical, biological, and chemical factors. *Mar. Pollut. Bull.* 109, 310–319. doi: 10.1016/j.marpolbul.2016.05.064

Lares, M., Ncibi, M. C., Sillanpää, M., and Sillanpää, M. (2018). Occurrence, identification and removal of Microplastic particles and fibers in conventional activated sludge process and advanced MBR technology. *Water Res.* 133, 236–246. doi: 10.1016/j.watres.2018.01.049

Lebreton, L., van der Zwet, J., Damsteeg, J., Slat, B., Andrady, A., Reisser, J., et al. (2017). River plastic emissions to the world's oceans. *Nat. Commun.* 8:15611. doi: 10.1038/ncomms15611

Liu, F., Olesen, K. B., Borregaard, A. R., and Vollertsen, J. (2019). Microplastics in urban and highway stormwater retention ponds. *Sci. Total Environ.* 671, 992–1000. doi: 10.1016/j.scitotenv.2019.03.416

Liu, W., Chen, W., Feng, Q., Peng, C., and Kang, P. (2016). Cost-benefit analysis of green infrastructures on community Stormwater reduction and utilization: a case of Beijing, China. *Environ. Manag.* 58, 1015–1026. doi: 10.1007/s00267-016-0765-4

Long, Z., Pan, Z., Wang, W., Ren, J., Yu, X., Lin, L., et al. (2019). Microplastic abundance, characteristics, and removal in wastewater treatment plants in a

coastal City of China. *Water Res.* 155, 255–265. doi: 10.1016/j.watres.2019.02.028

Lv, X., Dong, Q., Zuo, Z., Liu, Y., Huang, X., and Wu, W.-M. (2019). Microplastics in a municipal wastewater treatment plant: fate, dynamic distribution, removal efficiencies, and control strategies. *J. Clean. Product.* 225, 579–586. doi: 10.1016/j.jclepro.2019.03.321

Madsen, H., Lawrence, D., Lang, M., Martinkova, M., and Kjeldsen, T. R. (2014). Review of trend analysis and climate change projections of extreme precipitation and floods in Europe. *J. Hydrol.* 519, 3634–3650. doi: 10.1016/j.jhydrol.2014.11.003

Magnusson, K., Jörundsdóttir, H., Norén, F., Lloyd, H., Talvitie, J., and Setälä, O. (2016). *Microlitter in Sewage Treatment Systems*. Copenhagen: TemaNord. Nordic Council of Ministers. doi: 10.6027/TN2016-510

Magnusson, K., and Norén, F. (2014). *Screening of Microplastic Particles in and Down-Stream a Wastewater Treatment Plant*. Stockholm: IVL Swedish Environmental Research Institute. Report C55.

McEachern, K., Alegria, H., Kalagher, A. L., Hansen, C., Morrison, S., and Hastings, D. (2019). Microplastics in Tampa Bay, Florida: abundance and variability in estuarine waters and sediments. *Mar. Pollut. Bull.* 148, 97–106. doi: 10.1016/j.marpolbul.2019.07.068

Mintenig, S. M., Int-Veen, I., Löder, M. G. J., Primpke, S., and Gerdts, G. (2016). Identification of Microplastic in effluents of waste water treatment plants using focal plane array-based micro-fourier-transform infrared imaging. *Water Res.* 108, 365–372. doi: 10.1016/j.watres.2016.11.015

Murphy, F., Ewins, C., Carbonnier, F., and Quinn, B. (2016). Wastewater treatment works (WwTW) as a source of Microplastics in the aquatic environment. *Environ. Sci. Technol.* 50, 5800–5808. doi: 10.1021/acs.est.5b05416

Nizzetto, L., Bussi, G., Futter, M. N., Butterfield, D., and Whitehead, P. G. (2016). A theoretical assessment of Microplastic transport in river catchments and their retention by soils and River sediments. *Environ. Sci. Process. Impacts* 18, 1050–1059. doi: 10.1039/C6EM00206D

Nobles, A. L., Goodall, J. L., and Fitch, G. M. (2017). Comparing costs of onsite best management practices to nutrient credits for Stormwater management: a case study in Virginia. *J. Am. Water Resourc. Assoc.* 53, 131–143. doi: 10.1111/1752-1688.12487

Olesen, K. B., Stephansen, D., van Alst, N., and Vollertsen, J. (2019). Microplastics in a Stormwater pond. *Water* 11:1466. doi: 10.3390/w11071466

Olsson, J., and Foster, K. (2014). Short-term precipitation extremes in regional climate simulations for Sweden. *Hydrol. Res.* 45, 479–489. doi: 10.2166/nh.2013.206

Osinski, R. D., Enders, K., Gräwe, U., Klingbeil, K., and Radtke, H. (2020). Model uncertainties of a storm and their influence on microplastics/sediment transport in the Baltic Sea. 1–21. *Ocean Sci. Discuss.* doi: 10.5194/os-2020-28

Osinski, R. D., and Radtke, H. (2020). Ensemble hindcasting of wind and wave conditions with WRF and Wavewatch III® driven by ERA5. *Ocean Sci.* 16, 355–371. doi: 10.5194/os-16-355-2020

Prata, J. C. (2018). Microplastics in wastewater: state of the knowledge on sources, fate and solutions. *Mar. Pollut. Bull.* 129, 262–265. doi: 10.1016/j.marpolbul.2018.02.046

Schernewski, G., Radtke, H., Hauk, R., Baresel, C., Olshammar, M., Osinski, R., et al. (2020). Transport and behavior of microplastics emissions from urban sources in the Baltic Sea. *Front. Mar. Sci.* 8:579361. doi: 10.3389/fenvs.2020.579361

Schmidt, C., Kumar, R., Yang, S., and Büttner, O. (2020). Microplastic particle emission from wastewater treatment plant effluents into river networks in Germany: loads, spatial patterns of concentrations and potential toxicity. *Sci. Total Environ.* 737:139544. doi: 10.1016/j.scitotenv.2020.139544

Setälä, O., Magnusson, K., Lehtiniemi, M., and Norén, F. (2016). Distribution and abundance of surface water microlitter in the Baltic Sea: a comparison of two sampling methods. *Mar. Pollut. Bull.* 110, 177–183. doi: 10.1016/j.marpolbul.2016.06.065

Shields, A. R. (1936). *Application of Similarity Principles and Turbulence Research to Bed-Load Movement*. London: Mitteilungen der Preussischen Versuchsanstalt für Wasserbau und Schiffbau.

Siegfried, M., Koelmans, A. A., Besseling, E., and Kroeze, C. (2017). Export of microplastics from land to sea. A modelling approach. *Water Res.* 127, 249–257. doi: 10.1016/j.watres.2017.10.011

Simon, M., van Alst, N., and Vollertsen, J. (2018). Quantification of Microplastic mass and removal rates at wastewater treatment plants applying Focal Plane Array (FPA)-Based Fourier Transform Infrared (FT-IR) imaging. *Water Res.* 142, 1–9. doi: 10.1016/j.watres.2018.05.019

Song, Y. K., Hong, S. H., Jang, M., Han, G. M., and Shim, W. J. (2015). Occurrence and distribution of Microplastics in the Sea surface Microlayer in Jinhae Bay, South Korea. *Arch. Environ. Contam. Toxicol.* 69, 279–287. doi: 10.1007/s00244-015-0209-9

Sun, J., Dai, X., Wang, Q., van Loosdrecht, M. C. M., and Ni, B.-J. (2019). Microplastics in wastewater treatment plants: detection, occurrence and removal. *Water Res.* 152, 21–37. doi: 10.1016/j.watres.2018.12.050

Talvitie, J., Heinonen, M., Pääkkönen, J.-P., Vahtera, E., Mikola, A., Setälä, O., et al. (2015). Do wastewater treatment plants act as a potential point source of Microplastics? Preliminary study in the coastal Gulf of Finland, Baltic Sea. *Water Sci. Technol.* 72, 1495–1504. doi: 10.2166/wst.2015.360

Talvitie, J., Mikola, A., Koistinen, A., and Setälä, O. (2017). Solutions to Microplastic pollution – removal of microplastics from wastewater effluent with advanced wastewater treatment technologies. *Water Res.* 123, 401–407. doi: 10.1016/j.watres.2017.07.005

Tamminga, M., Hengstmann, E., and Fischer, E. K. (2018). Microplastic analysis in the South Funen Archipelago, Baltic Sea. *Mar. Pollut. Bull.* 208, 601–608. doi: 10.1016/j.marpolbul.2018.01.066

van Wijnen, J., Ragas, A. M. J., and Kroeze, C. (2019). Modelling global river export of microplastics to the marine environment: Sources and future trends. *Sci. Total Environ.* 673, 392–401. doi: 10.1016/j.scitotenv.2019.04.078

Vermeiren, P., Muñoz, C. C., and Ikejima, K. (2016). Sources and sinks of plastic debris in estuaries: a conceptual model integrating biological, physical and chemical distribution mechanisms. *Mar. Pollut. Bull.* 113, 7–16. doi: 10.1016/j.marpolbul.2016.10.002

Vianello, A., Boldrin, A., Guerriero, P., Moschino, V., Rella, R., Sturaro, A., et al. (2013). Microplastic particles in sediments of Lagoon of Venice, Italy: first observations on occurrence, spatial patterns and identification. *Estuar. Coast. Shelf Sci.* 130, 54–61. doi: 10.1016/j.ecss.2013.03.022

Wagner, M., Lambert, S., and Lambert, M. W. (2018). *Freshwater Microplastics*. Berlin: Springer International Publishing. doi: 10.1007/978-3-319-61615-5

Waldschläger, K., and Schüttrumpf, H. (2019a). Effects of particle properties on the settling and rise velocities of Microplastics in freshwater under laboratory conditions. *Environ. Sci. Technol.* 53, 1958–1966. doi: 10.1021/acs.est.8b06794

Waldschläger, K., and Schüttrumpf, H. (2019b). Erosion behavior of different microplastic particles in comparison to natural sediments. *Environ. Sci. Technol.* 53, 13219–13227. doi: 10.1021/acs.est.9b05394

Wessel, C. C., Lockridge, G. R., Battiste, D., and Cebrian, J. (2016). Abundance and characteristics of microplastics in beach sediments: insights into microplastic accumulation in northern Gulf of Mexico estuaries. *Mar. Pollut. Bull.* 109, 178–183. doi: 10.1016/j.marpolbul.2016.06.002

Windsor, F. M., Durance, I., Horton, A. A., Thompson, R. C., Tyler, C. R., and Ormerod, S. J. (2019). A catchment-scale perspective of plastic pollution. *Glob. Chang. Biol.* 25, 1207–1221. doi: 10.1111/gcb.14572

Wolff, S., Kerpen, J., Prediger, J., Barkmann, L., and Müller, L. (2019). Determination of the Microplastics emission in the effluent of a municipal waste water treatment plant using raman microspectroscopy. *Water Res.* 2:100014. doi: 10.1016/j.wroa.2018.100014

Yonkos, L. T., Friedel, E. A., Perez-Reyes, A. C., Ghosal, S., and Arthur, C. D. (2014). Microplastics in four estuarine rivers in the Chesapeake Bay U.S.A. *Environ. Sci. Tech.* 48, 14195–14202. doi: 10.1021/es5036317

Ziajahromi, S., Neale, P. A., and Leusch, F. D. L. (2016). Wastewater treatment plant effluent as a source of microplastics: review of the fate, chemical interactions and potential risks to aquatic organisms. *Water Sci. Technol.* 74, 2253–2269. doi: 10.2166/wst.2016.414

Conflict of Interest: The authors declare that the research was conducted in the absence of any commercial or financial relationships that could be construed as a potential conflict of interest.

frontiers in Environmental Science

ORIGINAL RESEARCH
published: 14 May 2021
doi: 10.3389/fenvs.2021.583454

Human Population Density is a Poor Predictor of Debris in the Environment

Qamar Schuyler[1], Chris Wilcox[1], T. J. Lawson[1], R. R. M. K. P. Ranatunga[2], Chieh-Shen Hu[3], Global Plastics Project Partners[4,5,6,7,8] and Britta Denise Hardesty[1]*

[1]Commonwealth Scientific and Research Organisation, Oceans and Atmosphere, Hobart, TAS, Australia, [2]Center for Marine Science and Technology, University of Sri Jayewardenepura, Nugegoda, Sri Lanka, [3]IndigoWaters Institute, Kaohsiung, Taiwan, [4]Earthwatch Institute Australia, Melbourne, VIC, Australia, [5]GreenHub, Hanoi, Vietnam, [6]Our Sea of East Asia Network, Tongyeong, South Korea, [7]The Society of Wilderness, Taipei, Taiwan, [8]United Nations Environment Programme, Mombasa, Kenya

There have been a variety of attempts to model and quantify the amount of land-based waste entering the world's oceans, most of which rely heavily on global estimates of population density as the key driving factor. Using empirical data collected in seven different countries/territories (China, Kenya, South Africa, South Korea, Sri Lanka, Taiwan and Vietnam), we assessed a variety of different factors that may drive plastic leakage to the environment. These factors included both globally available GIS data as well as observations made at a site level. While the driving factors that appear in the best models varied from country to country, it is clear from our analyses that population density is not the best predictor of plastic leakage to the environment. Factors such as land use, infrastructure and socio-economics, as well as local site-level variables (e.g., visible humans, vegetation height, site type) were more strongly correlated with plastic in the environment than was population density. This work highlights the importance of gathering empirical data and establishing regular monitoring programs not only to form accurate estimates of land-based waste entering the ocean, but also to be able to evaluate the effectiveness of land-based interventions.

Keywords: debris, litter, plastic pollution, socioeconomics, infrastructure, population

OPEN ACCESS

Edited by:
Hans Peter Heinrich Arp, Norwegian Geotechnical Institute, Norway

Reviewed by:
Yong Liu, Tianjin University, China
Lingzhi Deng, East China Normal University, China

****Correspondence:***
Qamar Schuyler
Qamar.Schuyler@csiro.au

Specialty section:
This article was submitted to Toxicology, Pollution and the Environment, a section of the journal Frontiers in Environmental Science

Received: *15 July 2020*
Accepted: *13 April 2021*
Published: *14 May 2021*

Citation:
Schuyler Q, Wilcox C, Lawson TJ, Ranatunga RRMKP, Hu C-S, Global Plastics Project Partners and Hardesty BD (2021) Human Population Density is a Poor Predictor of Debris in the Environment. Front. Environ. Sci. 9:583454. doi: 10.3389/fenvs.2021.583454

INTRODUCTION

The impacts from marine plastic pollution to wildlife, human health, and the economy are well documented (Gall and Thompson, 2015; Beaumont et al., 2019) and are likely to continue to increase as global plastic production rises (Geyer et al., 2017). Because an estimated 80% of marine plastic pollution has land-based origins (Derraik, 2002), the most efficient way to address the problem is by stopping plastic waste leakage from land to the sea. Plastics typically enter the ocean from land as mismanaged waste transported via rivers or wind (Kershaw and Rochman, 2015), though local human deposition in coastal areas also contributes (Hardesty et al., 2016). While debris on land is found ubiquitously and has been reported from the most remote to the most densely populated corners of the earth, it is not equally distributed (Barnes et al., 2009; Martins et al., 2020; Napper et al., 2020).

Many studies have investigated debris at local or regional scales (e.g., Wessel et al., 2019; Miladinova et al., 2020; Vidyasakar et al., 2020) These studies are predominately carried out along the coastal margin (Serra-Gonçalves et al., 2019) though studies along rivers and at river outlets are becoming more common (e.g., Battulga et al., 2019; Cordova and Nurhati, 2019; Van Calcar and Van Emmerik, 2019). However, these empirical studies are, by necessity, restricted to a limited area, so in order to understand debris distribution on a broader scale, modeling and predictions are critical. For

the most part, these studies use globally available data sources as proxies for the amount of mismanaged waste entering the environment (but see Lebreton et al., 2017).

Jambeck and colleagues used global data sets to predict mismanaged waste and calculated that an estimated 4.8–12.7 million MT of plastic entered the ocean in 2010 (2015). They hypothesized that population size and the quality of waste management systems in a country were most important predictors of the amount of debris lost to the marine environment. Lebreton et al. (2017) similarly relied predominately on global estimates of population density and mismanaged plastic waste, but additionally factored in runoff to estimated that between 1.15 and 2.41 MT of plastic is transported to the ocean via rivers. This research also relied on published empirical studies to calibrate the models. Models of floating plastic distribution in the ocean used coastal population density to seed the models (e.g., Van Sebille et al., 2012; Van Sebille, 2014), with (in instances) the addition of impervious surface area (Lebreton et al., 2012) and mismanaged waste (Van Sebille et al., 2015).

More recent studies have acknowledged the fact that mismanaged waste varies not only with population density, but also with factors such as socio-economic status (Borrelle et al., 2020; Lau et al., 2020). Gross Domestic Product (GDP) is positively correlated with reported per capita waste generation, but negatively correlated with the proportion of mismanaged waste, and these relationships can vary between rural and urban areas (Lebreton and Andrady, 2019).

If we are to make accurate predictions, it is critical to test the foundational assumptions that are being made when modeling waste leakage. To date, studies have predominately used global population density estimates without the addition of empirical data, and many of these studies have presumed that population density is an adequate proxy for debris leakage (e.g., Van Sebille et al., 2012). To test these assumptions, we gathered empirical data on debris in the environment in 7 countries/territories (hereafter referred to as countries for simplicity): mainland China, Kenya, South Africa, South Korea, Sri Lanka, Taiwan, and Vietnam. We asked three key questions:

1) What drives the distribution of debris in inland areas?
2) How similar (or different) are these drivers among the seven countries studied?
3) Do models based on population density accurately represent debris observed in the local environment?

To address these questions we assessed a number of potential drivers, including land use, survey type, infrastructure, environmental and socio-economic factors, local population density, and site level information such as steepness and vegetation height (**Table 1**).

MATERIALS AND METHODS

What Drives the Distribution of Debris in Inland Areas?

This research was undertaken as part of the CSIRO global plastics losses project (https://research.csiro.au/marinedebris/projects/globalplasticsleakageproject/), which is aimed at understanding the amount of plastic that is lost from land to the marine environment. The goal is to use empirical data to quantify and better understand debris leakage rates globally, based on locally collected data across an array of countries. We selected countries based on a combination of factors, including the country's ranking in estimated mismanaged waste generated annually (per Jambeck et al., 2015). Between 2017–2019 we worked with local partners in each country to select an urban area within a major watershed. The urban areas selected were Shanghai, China; Mombasa, Kenya; Capetown, South Africa; Yeongsan, South Korea; Negombo/Colombo, Sri Lanka; Kaohsiung, Taiwan, and Haiphong, Vietnam. Inland survey sites were then chosen within a 200 km radius of the central point (with the exception of Shanghai, China, where sites were chosen within 100 km due to excessively long travel time between sites). Sites were selected using a stratified random sampling design, taking into account a variety of environmental and socio-economic factors [population density, distance to infrastructure (roads and rail), distance to coast and river, proxies for socio-economic status, and land use]. For each country we pre-selected approximately 40 inland sites, but due to accessibility constraints and the variability in capacity of our local partners, the total number of sites surveyed varied between 23 and 47 (**Table 2**).

At each site we conducted between 3–6 transects of 25 m^2, distributed in proportion to the site uses present within 200 m of the central site point (e.g., walkways, natural vegetation, roadways, etc.). Transects were usually 12.5 m × 2 m, except in the case of roadsides,

TABLE 1 | Local (recorded at site or transect level), and global (determined from global GIS layers) covariates investigated in the study.

	Local	Global
Physical/environmental	Steepness of land	Distance to the coast
	Vegetation height	Distance to the nearest river
	Substrate color	Landuse
	Percent of bare ground	
	Survey type	
Population or population proxies	Number of people visible	Population density within 1 km^2
		Mean nightlights within 1 km^2
Infrastructure		Distance to the nearest rail station
		Distance to the nearest road
Socio-economic		Total value of the built environment (rural, urban, and total)
		Land use
		Nightlight/population residuals

TABLE 2 | Range, mean, and median items per meter squared found on inland surveys in each country/territory.

Country/territory (urban center)	# Transects (survey sites) in total	Range debris items/m^2	Mean debris items/m^2	Median debris items/m^2
Mainland China (Shanghai)	84 (28)	0–52.4	1.51	0.36
Kenya (Mombasa)	159 (44)	0–10.9	0.59	0.04
South Korea (Yeongsan)	107 (34)	0–3.84	0.40	0.12
South Africa (Capetown)	74 (23)	0–30.4	2.05	0.46
Sri Lanka (Negombo)	118 (36)	0—40.0	1.18	0.14
Taiwan (Kaohsiung)	142 (47)	0–16.0	1.33	0.58
Vietnam (Haiphong)	80 (26)	0–10.7	1.21	0.54
ALL COUNTRIES	764 (238)	0–52.4	1.10	0.24

where they were 25 m × 1 m to ensure the safety of the participants. Observers walked the length of the transect, and categorized any anthropogenic debris within the transect that could be seen from standing height. Debris was placed into one of 84 categories, labeled as either fragment or whole (for a complete methodology, see Schuyler et al., 2018b). At each transect, data were also collected on local conditions that could influence the amount of debris found, including the number of people visible at the site, the steepness of the land, the height of the vegetation, substrate color (dark/light), and percent of bare ground in the transect. Both the methods for the survey as well as the local variables to consider were selected based on previous published studies conducted at large scales (Hardesty et al., 2017a; Hardesty et al., 2017c).

Because one of the goals of this project is to estimate the amount of debris leakage on a global scale, we identified covariates for which global datasets existed, that might influence debris levels on a larger scale. In our previous work, land use, infrastructure, and socio-economic factors were among the most important influencers of debris levels (Hardesty et al., 2016). We identified the following environmental and socio-economic variables at each site: population density within 1km^2, total value of the built environment (rural, urban, and total) identified from the United Nations Global Exposure dataset (GAR15) (UNISDR, 2015), distance to the coast, distance to the nearest rail line, road, and river, mean nightlights within 1 km^2, and land use. We wanted to incorporate a globally available, socio-economic GIS layer at the finest resolution possible in our analysis, so we explored two potential options. While most socio-economic indicators are national, the GAR15 dataset, developed for assessing economic risk from disasters, is one of the only socio-economic datasets with near-global coverage and sub-national resolution. GAR-15 includes several indicators, including the value of the urban environment, the value of the rural environment, and the total value of assets in a given area, all of which we included in our analyses. Our second option was to use the relationship between lighting at night and population density. In general, the higher the population density, the more nightlights you would expect in a given area. However, in areas with higher income or resources, we would assume a disproportionally higher level of lights than would be predicted by population density alone. Therefore, we used the residual deviation around the linear relationship of nightlights regressed on population density as a second proxy for socio-economic status.

We combined the data from all seven and used model selection on generalized additive models (GAMs) with a Tweedie distribution (mgcv package) in the R statistical environment to find the models with the lowest AIC score (Burnham and Anderson, 2002; Wood, 2011; Bartoń, 2018; R Core Team, 2018). We chose GAMs so that we could experiment with smooths of different factors, though ultimately we settled on parametric terms to be able to predict debris outside of our study area. We used a Tweedie distribution because debris is measured as count data, and the distribution gives the flexibility for the model to range between gamma to Poisson. Because there were a number of factors that could potentially influence the debris in the environment, we used dredge (MuMin package) to determine which factors explained the greatest variability in the data. To avoid collinearity, we restricted the analysis to ensure that no two variables with a correlation factor greater than 0.7 could be included in the same model. We also restricted dredge from including both nightlights and population density in the same model, as nightlights, to some extent, could act as a proxy for population.

The dredge process yielded a range of models which were within 2 AICc points of the best model. Because these models are within the 95% confidence set around the best model in terms of AIC model selection, we used model averaging techniques (**Table 3**). To determine which factors best explained the variability in the averaged model, we calculated the effect size by multiplying the median value of the factor (assuming 1 for categorical variables), by the coefficient from the model (**Figures 1**, **2**). We also calculated the variable importance score, which represents the proportion of the total models in which each term appears. For example, if land use appeared in 8 out of the 10 models within 2 AIC points, it would receive a variable importance score of 0.8. The variable importance indicates how consistently a given term is included in the models (**Table 4**).

How Similar (or Different) are the Drivers Between Countries?

For each country individually, we used the same analyses as above to identify the covariates that best described the variability in debris, with the same restrictions as above (**Figure 2**).

Do Models Based on Population Density Accurately Predict Debris?

To determine whether population density is an accurate proxy for debris, we ran a GAM using total debris counts as the response variable, and population density (within 1 km^2) as the predictor variable. We compared the deviance explained and AIC with the null model, and with our full model (**Table 3**).

TABLE 3 | Description of models used in the model averaging (all within 2 AIC values). Lowest AIC indicates the lowest AIC value for the models within each of the countries. Models in the model averaging are all within 2 AIC points of the lowest. Null AIC is the AIC of a regression with no covariates included. Note that the AIC values cannot be compared between countries, because they are using different data sets. AIC values can be compared between all countries, and all countries with population density only because they are using the same data set.

Country/territory	Number of models in model average	Lowest AIC	Null AIC	Range dev. Expl.
China	12	627.4	699.6	66.0–72.2
South Korea	65	1417	1457	23.4–30.4
Taiwan	34	1279.4	1300.2	11.7–15.4
Vietnam	16	675	723	44.3–55.5
Sri Lanka	12	791.32	883.25	56.3–58.5
South Africa	35	681.06	708.66	29.65–41.54
Kenya	10	905.78	979.69	45.4–50.8
All countries, best model	23	4141.6	8799.83	35.9–36.9
All countries population density only	1	8792.33	8799.83	1.24

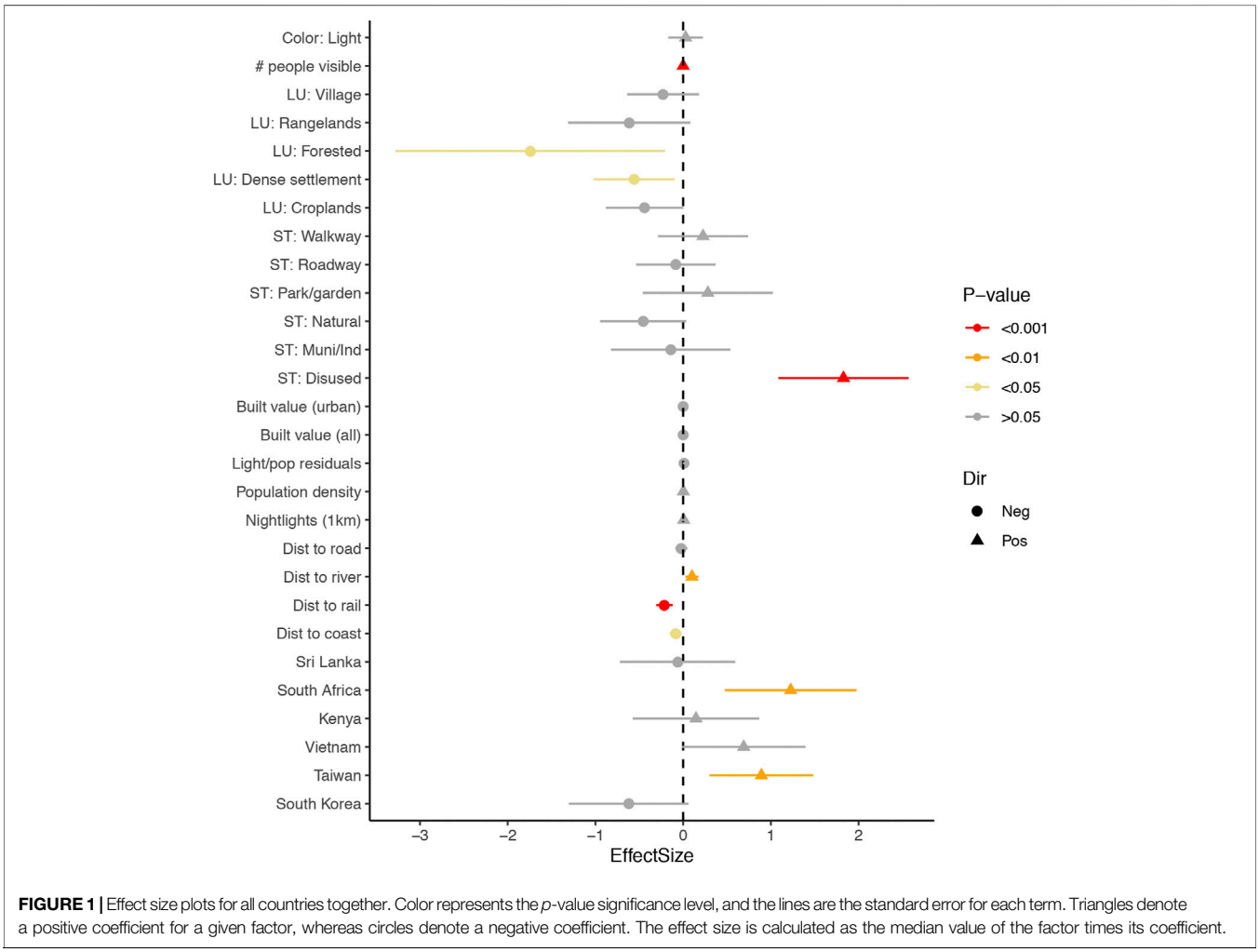

FIGURE 1 | Effect size plots for all countries together. Color represents the *p*-value significance level, and the lines are the standard error for each term. Triangles denote a positive coefficient for a given factor, whereas circles denote a negative coefficient. The effect size is calculated as the median value of the factor times its coefficient.

RESULTS

The total number of items on each transect varied from 0–242 items. South Korea had the overall lowest average debris density (0.4 items/m^2), while South Africa, had the highest (2.05 items/m^2) based on inland surveys (**Table 2**).

What Drives the Distribution of Debris in Inland Areas?

For the combined models, significant terms included visible humans (positively correlated), landuse (forested and dense settlements lower than urban settlements), survey type (disused significantly greater than agriculture), distance to river (positively correlated), rail

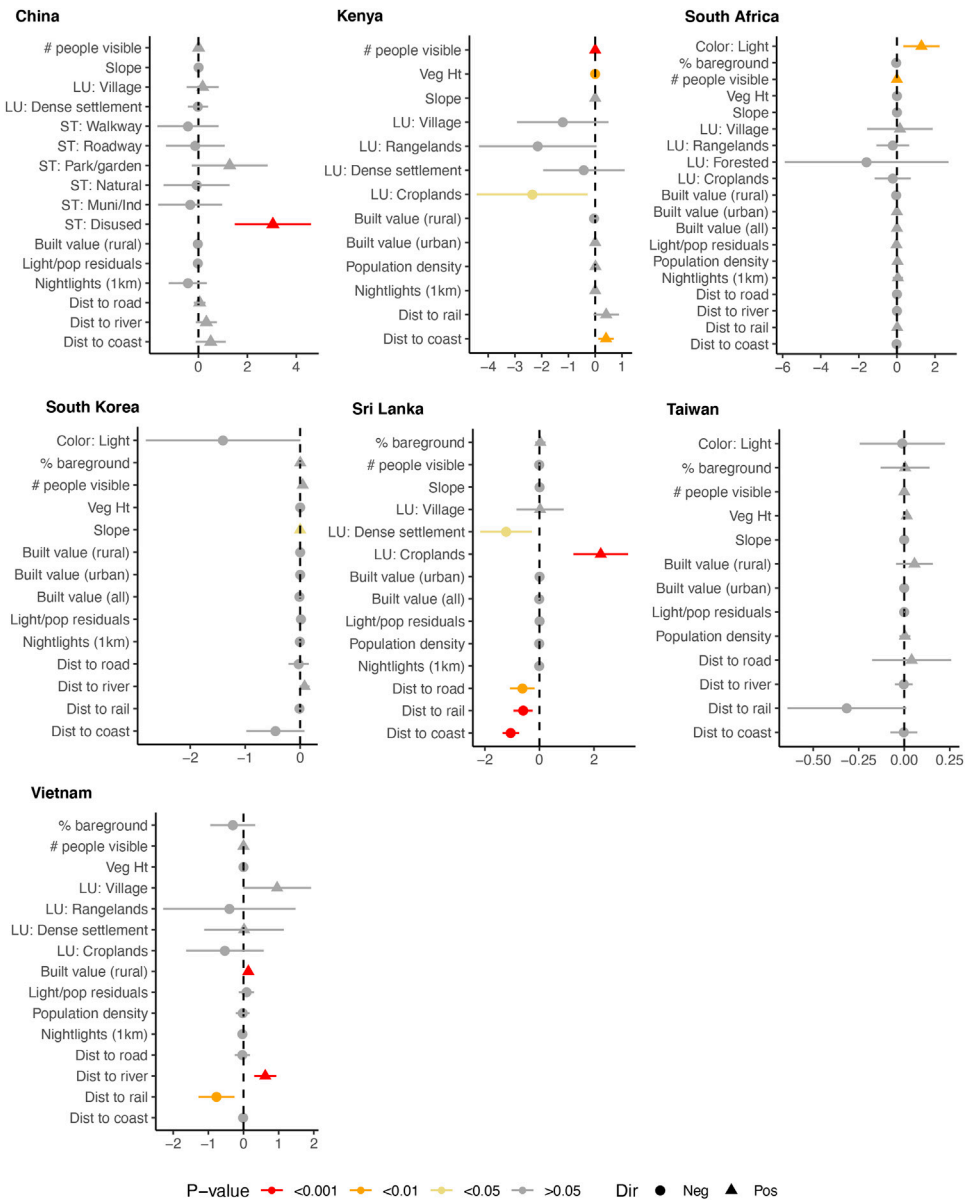

FIGURE 2 | Effect size plots for China, Kenya, South Africa, South Korea, Sri Lanka, Taiwan, and Vietnam. Color represents the *p*-value significance level, and the lines are the standard error for each term. Triangles denote a positive coefficient for a given factor, whereas circles denote a negative coefficient. The effect size is calculated as the median value of the factor times its coefficient.

and coast (negatively correlated), and country (**Figure 1**). All of these terms appeared in all models, with a resulting effect size of 1.0 (**Table 4**). Population/nightlight residuals appeared in 90% of all models, while the other terms appeared in fewer than half of the models. It is worth nothing though, that either nightlights or population density did appear in 62% of the models.

How Similar (or Different) are the Drivers Between Countries?

Drivers were not completely consistent among countries. The best models for each country individually varied both in the terms included, as well as the directions of those terms (e.g., whether they were positively or negatively correlated with observed debris densities) (**Figure 2**; **Table 4**). Two terms appeared in all models: visible humans (positive correlation in all countries except Sri Lanka), and distance to the coast (negative correlation in all countries except mainland China and Kenya). A further six terms occurred in all but one country: slope (all but Vietnam), distance to the nearest rail (all but mainland China), light/population residuals (all but Kenya), total built value of the rural environment (all but Sri Lanka), mean nightlights (all but Taiwan) and distance to the nearest road (all but Kenya).

For individual country models, significant terms included visible humans (South Africa, Kenya), slope of land (South

TABLE 4 | Variable importance scores. Blank cells indicate that the driver was not present in the top models. Importance scores are calculated as the proportion of the models within the model averaging in which the driver appears.

Driver	All countries	Mainland China	Kenya	South Africa	South Korea	Sri Lanka	Taiwan	Vietnam
Physical/environmental								
Steepness		0.05	0.17	0.02	1.00	0.12	0.07	
Vegetation height			1.00	0.02	0.23		0.88	0.67
% bare ground on transect				0.14	0.02	0.20	0.03	0.60
Substrate color	0.16			1.00	0.98		0.04	
Distance to coast	1.00	0.89	1.00	0.22	0.91	1.00	0.03	0.07
Distance to river	1.00	0.83		0.04	0.96		0.04	1.00
Land use	1.00	0.29	0.91	0.37		1.00		1.00
Survey type	1.00	1.00						
Population/population proxies								
Visible humans	1.00	0.04	1.00	0.98	0.90	0.06	0.29	0.18
Population density	0.32		0.31	0.77		0.06	0.11	0.10
Mean nightlights	0.30	0.65	0.32	0.18	0.21	0.09		0.38
Infrastructure								
Distance to rail	1.00		0.91	0.02	0.12	1.00	0.97	1.00
Distance to road	0.45	0.23		0.10	0.14	1.00	0.21	0.14
Socioeconomic								
Pop/nightlight residuals	0.90	0.24		0.16	0.24	0.06	0.16	0.44
Tot CR		0.12	0.25	0.20	0.02		0.81	1.00
Tot val	0.22			0.14	0.24	0.28		
Tot CU	0.40		0.21	0.43	0.20	0.19	0.07	
Country	1.00	NA	NA	NA	NA	NA	NA	NA

Korea), vegetation height (Kenya), substrate color (South Africa), distance to the coast (Sri Lanka, Kenya), distance to the nearest rail (Vietnam, Sri Lanka), distance to the nearest road (Sri Lanka), total built value (rural) (Vietnam), landuse (Sri Lanka, Kenya), and distance to the nearest river (Vietnam) (**Figure 1**).

Variable importance scores were similarly diverse, with different terms appearing more frequently in different countries (**Table 4**).

Do Models Based on Population Density Accurately Predict Debris?

The relationship between population density alone and total debris was significant and positive ($p < 0.001$). The deviance explained was 1.25%. The deviance explained of the 23 full models contributing to the model averaging was between 35.9–36.9.

DISCUSSION

To date, most studies of plastic leakage rates consist either of surveys conducted predominately at coastal or beach locations in a single region or country (e.g., Hardesty et al., 2017a; Schöneich-Argent et al., 2019), or rely on globally available proxy data to model predicted debris on a global or regional scale, without incorporating empirical data (e.g., Jambeck et al., 2015; Lebreton and Andrady, 2019; Borrelle et al., 2020; Lau et al., 2020). Here we combine the two approaches, using survey data to test the utility of a variety of local and global proxy layers.

What Drives the Distribution of Debris in Inland Areas?

Studies of debris on the open ocean and along coastlines have found that physical factors such as currents, waves, wind and tides have an important effect on the distribution and accumulation of debris (Olivelli et al., 2020; Van Sebille et al., 2020), but the drivers of inland debris distribution are less well understood.

When the data were pooled, land use (a globally measured covariate) survey type (a locally determined covariate), and Country, explained a significant amount of the variability in the data. The significant influence of survey type was driven in large part by the elevated levels of litter found in disused areas. Both land use and survey type were also found to be significant in studies conducted in both the United States and Australia (Hardesty et al., 2017b; Hardesty et al., 2017c). Other factors that contributed to the patterns observed included distance to coast, distance to railroad station, and distance to river. However, their effect sizes were considerably lower than land use, survey type, and country.

Previous work has shown that socio-economic status is one of the most influential factors in predicting debris, with higher socio-economic indicators associated with reduced debris loads (Schuyler et al., 2018a). This is likely due to a combination of influences including income, education, infrastructure, access to social structures, and behavioral norms (Ajzen, 1991). For the combined seven country model, three socio-economic indicators appeared among the best models; light/population residuals, the built value (urban), and the built value (all) (**Figure 1**). While none were statistically significant, they all contributed to explaining the variability in the data (and were thus included in the best models).

The values for all three indicators trended toward a negative relationship with debris density, indicating that as an area was higher in socio-economic status, the debris loads were lower/reduced. This finding reflects the negative correlation between GDP and per capita mismanaged waste that has been reported in other work (Lebreton and Andrady, 2019). While richer countries tend to generate more waste per capita, they also tend to have better waste management systems, which ultimately results in a lower proportion of mismanaged waste. Here we showed that the trend reported on a county-wide scale, also holds on a sub-national level.

How Similar (or Different) are the Drivers Between Countries?

Overall, the individual models were quite good at explaining the variability in the debris data, with deviance explained values of up to 72% (**Table 3**). These models generally incorporated factors measured at the site level, such as local land use, vegetation height, survey type, and substrate color.

We found high heterogeneity between countries, both in terms of the magnitude of debris, and the most relevant drivers for the patterns observed. In fact, in the combined model, country is one of the strongest predictors of the total amount of debris reported. The differences observed between the countries remained present even after accounting for the driving factors measured, and may be a result of other underlying factors including political/social differences, legislation, and geography. This reveals another challenge in predicting debris leakage rates on a global level. Each country demonstrated different baseline quantities of debris, with substantial variability observed among survey sites, both within and among countries. This demonstrates the importance of establishing baselines and monitoring programs on a local and regional scale, rather than relying solely on large-scale, global model-based predictions.

Do Models Based on Population Density Accurately Predict Debris?

One goal of both land and ocean-based debris research is to understand and quantify the distribution of debris, which can inform efforts to both prevent waste leaking and to remove litter than has already arrived in the environment. Because it is impossible to sample ubiquitously, researchers rely on globally available data sets to provide proxy measures for the amount of waste or leakage in a given area. Loss rates are often based on population density (e.g., Van Sebille et al., 2012), and, increasingly, the proportion of mismanaged waste (e.g., Lebreton and Andrady, 2019) though occasionally factors such as runoff and artificial barriers may be incorporated into estimates (e.g., Lebreton et al., 2017). These predictions assume that debris leakage rates are proportional to population density, though there is little empirical evidence to support this hypothesis. In the United States, research showed that while land-based debris did increase with population where population densities are low, this relationship did not hold at higher population densities (Ribic et al., 2010). Cities, even in less developed countries, can leverage economies of scale, and may have better systems for managing waste. Thus, the relationship between population and mismanaged waste is not necessarily linear.

In our modeling of empirical data from seven different countries, neither local population density nor one proxy for population (nightlights) were among the most critical factors to explain the variability in the data. Many of the top models did not include either term, and their effect was never significant, whether looking at individual countries or at all countries combined. Moreover, population density was negatively correlated with debris in two of the five individual models in which it appears, and nightlights were negatively correlated with debris density in four of the six countries. In our model regressing population density alone against the total amount of debris across all survey sites, while the relationship was significant and positive, the deviance explained was only 1.25% of the pattern observed.

The distribution of sampling sites in individual countries is quite wide ranging, both geographically as well across the suite of social and environmental factors, land use and human activities (e.g., incorporating urban and rural sites). If population density is not a critical factor at this scale, it is unlikely that the pattern will be reversed at international or continental scales.

The results of the this work indicate that it is critical to develop a more nuanced approach for estimating debris levels, if we are to develop accurate predictive models. Debris densities are extremely heterogeneous, and vary depending on a range of factors, including broad scale characteristics such as land use, finer scale details such as survey type, socio-economic patterns, existing infrastructure and environmental factors. The underlying drivers of debris distribution are complex, and difficult to capture accurately. What is clear, though, is that in all of the models, population density alone did not adequately explain the observed debris distribution. Relying on population density as a primary (or sole!) proxy, as has been done previously, will lead to an inaccurate characterization of debris distributions, and potentially to flawed policy responses based accordingly.

We ranked the seven countries surveyed based on empirical data collected by our teams according to the total debris load. We compared these counts to the per capita rank presented in Jambeck et al. (2015). Our ranking is based on the country coefficient in the model with all countries, and therefore considers population and the other debris drivers in the model. We found very little similarity in rank between our empirical estimates and those reported by Jambeck et al. (2015) (**Table 5**). This is likely due to a combination of factors. First, our analyses included local variables, as well as additional global scale variables that the Jambeck paper did not incorporate. Second, our analyses were based on empirical data. Finally, our surveys took place at a city or watershed scale rather than at a country level. The differences between the relative rankings only serves to highlight the importance of accurate models based on empirical data, so that limited resources for addressing the problems of litter and mismanaged waste can be most effectively deployed.

Many studies that empirically quantify debris leakage are conducted along beaches and coastlines (Serra-Gonçalves

TABLE 5 | Relative rankings of countries surveyed in this study as compared to relative rankings in Jambeck et al. (2015). Highest debris load = 1, lowest = 7.

Country/territory	Rank, this study (based on country coefficient in model)	Rank, Jambeck et al. (2015) based on per capita debris generation with respect to countries in this study (rank overall)
South Africa	1	2 (11)
Taiwan	2	6 (145)
Vietnam	3	4 (25)
Kenya	4	5 (104)
Mainland China	5	3 (22)
Sri Lanka	6	1 (1)
South Korea	7	7 (190)

et al., 2019). However, it is of critical importance to also measure inland debris if we are to fully understand loss rates to the environment. Debris from inland areas is transported to the sea via rivers, along roadways and by wind transport. Measuring debris in non-coastal areas helps to contextualize the factors that influence where debris originates in the environment, before it moves along various pathways, potentially arriving in the coastal or marine environment. Because of the high heterogeneity of inland areas, and the idiosyncratic nature of waste generation, it is crucial to design sampling that takes into account the inherent variability not only in the physical landscape, but also in the suite of factors that influence debris distribution.

Summary/Conclusion

Efforts to remove or prevent debris from entering the environment would be facilitated by a better understanding of the variability in its distribution, and the factors that affect debris density in the environment. The models presented here can also be used to derive large scale predictions of debris hotspots based not only on global data layers, but also on empirical data. These predictions could inform local and regional waste management policies and decisions on waste infrastructure. The results of this study demonstrate that the environmental context (e.g., landuse, site type) is critical in understanding and predicting the amount of debris in the environment. Importantly, population density is not the driving force behind debris distribution, and there is significant variability in the drivers of inland debris across countries. It is of critical importance to establish monitoring programs to understand the baseline levels of debris, not only in order to have accurate estimates of ocean debris inputs, but also so that the effectiveness of land-based interventions can be assessed.

DATA AVAILABILITY STATEMENT

The raw data supporting the conclusions of this article will be made available by the authors, without undue reservation.

AUTHOR CONTRIBUTIONS

QS, BH, and CW developed the methods. All authors contributed to data collection and logistics. QS and CW developed the analytical techniques. TL prepared GIS covariates. QS wrote the manuscript, with editing by BH, CW, RR, and JH.

FUNDING

This work has been funded by CSIRO Oceans and Atmosphere, Oak Family Foundation, Schmidt Marine Technology, the PM Angell Foundation and Earthwatch Institute Australia.

ACKNOWLEDGMENTS

We would like to extend our deepest gratitude to the tireless efforts of volunteers, students, and staff members who helped to collect data in the field. Also thank you to the two reviewers for their constructive comments.

REFERENCES

Ajzen, I. (1991). The Theory of Planned Behavior. *Organizational Behav. Hum. Decis. Process.* 50, 179–211. doi:10.1016/0749-5978(91)90020-t

Barnes, D. K. A., Galgani, F., Thompson, R. C., and Barlaz, M. (2009). Accumulation and Fragmentation of Plastic Debris in Global Environments. *Phil. Trans. R. Soc. B* 364, 1985–1998. doi:10.1098/rstb.2008.0205

Bartoń, K. (2018). MuMIn: Multi-Model Inference. R package version 1.42.1. https://CRAN.R-project.org/package=MuMIn.

Battulga, B., Kawahigashi, M., and Oyuntsetseg, B. (2019). Distribution and Composition of Plastic Debris along the River Shore in the Selenga River Basin in Mongolia. *Environ. Sci. Pollut. Res.* 26, 14059–14072. doi:10.1007/s11356-019-04632-1

Beaumont, N. J., Aanesen, M., Austen, M. C., Börger, T., Clark, J. R., Cole, M., et al. (2019). Global Ecological, Social and Economic Impacts of Marine Plastic. *Mar. Pollut. Bull.* 142, 189–195. doi:10.1016/j.marpolbul.2019.03.022

Borrelle, S. B., Ringma, J., Law, K. L., Monnahan, C. C., Lebreton, L., Mcgivern, A., et al. (2020). Predicted Growth in Plastic Waste Exceeds Efforts to Mitigate Plastic Pollution. *Science* 369, 1515–1518. doi:10.1126/science.aba3656

Burnham, K. P., and Anderson, D. R. (2002). *Model Selection and Multi-Model Inference: A Practical Information-Theoretic Approach*. New York, NY: Springer-Verlag

Cordova, M. R., and Nurhati, I. S. (2019). Major Sources and Monthly Variations in the Release of Land-Derived Marine Debris from the Greater Jakarta Area, Indonesia. *Scientific Rep.* 9, 1–8. doi:10.1038/s41598-019-55065-2

Derraik, J. G. B. (2002). The Pollution of the Marine Environment by Plastic Debris: a Review. *Mar. Pollut. Bull.* 44, 842–852. doi:10.1016/s0025-326x(02)00220-5

Gall, S. C., and Thompson, R. C. (2015). The Impact of Debris on Marine Life. *Mar. Pollut. Bull.* 92, 170–179. doi:10.1016/j.marpolbul.2014.12.041

Geyer, R., Jambeck, J. R., and Law, K. L. (2017). Production, Use, and Fate of All Plastics Ever Made. *Sci. Adv.* 3, e1700782. doi:10.1126/sciadv.1700782

Hardesty, B. D., Lawson, T., Van Der Velde, T., Lansdell, M., and Wilcox, C. (2017a). Estimating Quantities and Sources of Marine Debris at a Continental Scale. *Front. Ecol. Environ.* 15, 18–25. doi:10.1002/fee.1447

Hardesty, B. D., Schuyler, Q., Lawson, T. J., Opie, K., and Wilcox, C. (2016). Understanding Debris Sources and Transport from the Coastal Margin to the

Ocean, in *Final Report to the National Packaging Covenant Industry Association*. (Hobart, TS: CSIRO)

Hardesty, B. D., Schuyler, Q., Willis, K., Lawson, T. J., and Wilcox, C. (2017b). Policy and Practices Analysis to Reduce Debris Inputs to the Environment. A Final Report to the National Packaging Covenant Industry Association, in *Final Report to the National Packaging Covenant Industry Association*. (Hobart, TS: CSIRO)

Hardesty, B. D., Wilcox, C., Schuyler, Q., Lawson, T. J., and Opie, K. (2017c). *Developing a Baseline Estimate of Amounts, Types, Soures, and Distribution of Coastal Litter - an Analysis of US Marine Debris Data. Version 1.2*. (Hobart, TS: CSIRO)

Jambeck, J. R., Geyer, R., Wilcox, C., Siegler, T. R., Perryman, M., Andrady, A., et al. (2015). Plastic Waste Inputs from Land into the Ocean. *Science* 347, 768–771. doi:10.1126/science.1260352

Kershaw, P., and Rochman, C. (2015). Sources, Fate and Effects of Microplastics in the Marine Environment: Part 2 of a Global Assessment. *Reports and studies-IMO/FAO/Unesco-IOC/WMO/IAEA/UN/UNEP Joint* Group of Experts on the Scientific Aspects of Marine Environmental Protection (GESAMP) eng no. 93.

Lau, W. W. Y., Shiran, Y., Bailey, R. M., Cook, E., Stuchtey, M. R., Koskella, J., et al. (2020). Evaluating Scenarios toward Zero Plastic Pollution. *Science* 369, 1455–1461. doi:10.1126/science.aba9475

Lebreton, L., and Andrady, A. (2019). Future Scenarios of Global Plastic Waste Generation and Disposal. *Palgrave Commun.* 5, 1–11. doi:10.1057/s41599-018-0212-7

Lebreton, L. C.-M., Greer, S. D., and Borrero, J. C. (2012). Numerical Modelling of Floating Debris in the World's Oceans. *Mar. Pollut. Bull.* 64, 653–661. doi:10.1016/j.marpolbul.2011.10.027

Lebreton, L. C. M., Van Der Zwet, J., Damsteeg, J.-W., Slat, B., Andrady, A., and Reisser, J. (2017). River Plastic Emissions to the World's Oceans. *Nat. Commun.* 8, 15611. doi:10.1038/ncomms15611

Martins, I., Rodríguez, Y., and Pham, C. K. (2020). Trace Elements in Microplastics Stranded on Beaches of Remote Islands in the NE Atlantic. *Mar. Pollut. Bull.* 156, 111270. doi:10.1016/j.marpolbul.2020.111270

Miladinova, S., Macias, D., Stips, A., and Garcia-Gorriz, E. (2020). Identifying Distribution and Accumulation Patterns of Floating Marine Debris in the Black Sea. *Mar. Pollut. Bull.* 153, 110964. doi:10.1016/j.marpolbul.2020.110964

Napper, I. E., Davies, B. F. R., Clifford, H., Elvin, S., Koldewey, H. J., Mayewski, P. A., et al. (2020). Reaching New Heights in Plastic Pollution-Preliminary Findings of Microplastics on Mount Everest. *One Earth* 3, 621–630. doi:10.1016/j.oneear.2020.10.020

Olivelli, A., Hardesty, D., and Wilcox, C. (2020). Coastal Margins and Backshores Represent a Major Sink for Marine Debris: Insights from a Continental-Scale Analysis. *Environ. Res. Lett.* 15. doi:10.1088/1748-9326/ab7836

R Core Team (2018). *R: A Language and Environment for Statistical Computing*. Vienna, Austria: R foundation for statistical computing.

Ribic, C. A., Sheavly, S. B., Rugg, D. J., and Erdmann, E. S. (2010). Trends and Drivers of Marine Debris on the Atlantic Coast of the United States 1997-2007. *Mar. Pollut. Bull.* 60, 1231–1242. doi:10.1016/j.marpolbul.2010.03.021

Schöneich-Argent, R. I., Hillmann, F., Cordes, D., Wansing, R. A. D., Merder, J., Freund, J. A., et al. (2019). Wind, Waves, Tides, and Human Error? - Influences on Litter Abundance and Composition on German North Sea Coastlines: An Exploratory Analysis. *Mar. Pollut. Bull.* 146, 155–172. doi:10.1016/j.marpolbul.2019.05.062

Schuyler, Q., Hardesty, B. D., Lawson, T., Opie, K., and Wilcox, C. (2018a). Economic Incentives Reduce Plastic Inputs to the Ocean. *Mar. Pol.* 96, 250-255. doi:10.1016/j.marpol.2018.02.009

Schuyler, Q., Willis, K., Mann, V., Wilcox, C., and Hardesty, B. D. (2018b). *Handbook of Survey Methodology – Plastics Leakage*. Australia: CSIRO.

Serra-Gonçalves, C., Lavers, J. L., and Bond, A. L. (2019). Global Review of Beach Debris Monitoring and Future Recommendations. *Environ. Sci. Technol.* 53, 12158–12167. doi:10.1021/acs.est.9b01424

UNISDR (2015). *Making Development Sustainable: The Future of Disaster Risk Management. Global Assessment Report on Disaster Risk Reduction*. Geneva, Switzerland: United Nations Office for Disaster Risk Reduction (UNISDR)

Van Calcar, C. J., and Van Emmerik, T. H. M. (2019). Abundance of Plastic Debris across European and Asian Rivers. *Environ. Res. Lett.* 14, 124051. doi:10.1088/1748-9326/ab5468

Van Sebille, E. (2014). Adrift.org.au - A free, quick and easy tool to quantitatively study planktonic surface drift in the global ocean. *J. Exp. Mar. Biol. Ecol.* 461, 317–322. doi:10.1016/j.jembe.2014.09.002

Van Sebille, E., Aliani, S., Law, K. L., Maximenko, N., Alsina, J. M., Bagaev, A., et al. (2020). The Physical Oceanography of the Transport of Floating Marine Debris. *Environ. Res. Lett.* 15–023003. doi:10.1088/1748-9326/ab6d7d

Van Sebille, E., England, M. H., and Froyland, G. (2012). Origin, Dynamics and Evolution of Ocean Garbage Patches from Observed Surface Drifters. *Environ. Res. Lett.* 7, 044040. doi:10.1088/1748-9326/7/4/044040

Van Sebille, E., Wilcox, C., Lebreton, L., Maximenko, N., Hardesty, B. D., Van Franeker, J. A., et al. (2015). A Global Inventory of Small Floating Plastic Debris. *Environ. Res. Lett.* 10, 124006. doi:10.1088/1748-9326/10/12/124006

Vidyasakar, A., Krishnakumar, S., Kasilingam, K., Neelavannan, K., Bharathi, V. A., Godson, P. S., et al. (2020). Characterization and Distribution of Microplastics and Plastic Debris along Silver Beach, Southern India. *Mar. Pollut. Bull.* 158, 111421. doi:10.1016/j.marpolbul.2020.111421

Wessel, C., Swanson, K., Weatherall, T., and Cebrian, J. (2019). Accumulation and Distribution of Marine Debris on Barrier Islands across the Northern Gulf of Mexico. *Mar. Pollut. Bull.* 139, 14–22. doi:10.1016/j.marpolbul.2018.12.023

Wood, S. N. (2011). Fast Stable Restricted Maximum Likelihood and Marginal Likelihood Estimation of Semiparametric Generalized Linear Models. *J. R. Stat. Scoieety (B)* 73, 3–36. doi:10.1111/j.1467-9868.2010.00749.x

Conflict of Interest: The authors declare that the research was conducted in the absence of any commercial or financial relationships that could be construed as a potential conflict of interest.

Advantages of publishing in Frontiers

OPEN ACCESS
Articles are free to read for greatest visibility and readership

FAST PUBLICATION
Around 90 days from submission to decision

HIGH QUALITY PEER-REVIEW
Rigorous, collaborative, and constructive peer-review

TRANSPARENT PEER-REVIEW
Editors and reviewers acknowledged by name on published articles

Frontiers
Avenue du Tribunal-Fédéral 34
1005 Lausanne | Switzerland

Visit us: www.frontiersin.org
Contact us: frontiersin.org/about/contact

REPRODUCIBILITY OF RESEARCH
Support open data and methods to enhance research reproducibility

DIGITAL PUBLISHING
Articles designed for optimal readership across devices

FOLLOW US
@frontiersin

IMPACT METRICS
Advanced article metrics track visibility across digital media

EXTENSIVE PROMOTION
Marketing and promotion of impactful research

LOOP RESEARCH NETWORK
Our network increases your article's readership